Nano-in-nano containing curcumin and benzydamine hydrochloride for the treatment of Vulvovaginal Candidiasis:

from development to biological application in *vitro and in vivo*

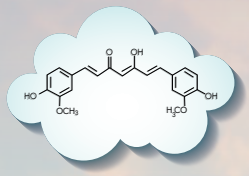

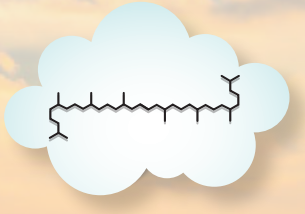

Gabriela Corrêa Carvalho

Nano-in-nano containing curcumin and benzydamine hydrochloride for the treatment of vulvovaginal candidiasis: from development to biological application *in vitro* and *in vivo*

Gabriela Corrêa Carvalho

Copyright © 2024 by Gabriela Corrêa Carvalho

Cover: Gabriela Corrêa Carvalho, Maria Clara Ribeiro Maciel and Dr. Ana Silvia Sartori Barraviera Seabra Ferreira

Printed by Gilderprint

ISBN: 978-94-6496-148-5

university of groningen

unesp

Nano-in-nano containing curcumin and benzydamine hydrochloride for the treatment of vulvovaginal candidiasis: from development to biological application *in vitro* and *in vivo*

PhD thesis

to obtain the degree of PhD at the
University of Groningen
on the authority of the
Rector Magnificus Prof. J.M.A. Scherpen
and in accordance with
the decision by the College of Deans

and

to obtain the degree of PhD at the
São Paulo State University
on the authority of the
Rector Magnificus Prof. P. Barretti
and in accordance with
the decision by the Pro-Rectory of Post-Graduation

Double PhD degree

This thesis will be defended in public on
Wednesday 17 July 2024 at 14:30 hours
by

Gabriela Corrêa Carvalho

born on 3 May 1994
in Botucatu, Brazil

Carvalho, Gabriela Corrêa.
C331n Nano-in-nano containing curcumin and benzydamine hydrochloride for the treatment of vulvovaginal candidiasis: from development to biological application *in vitro* and *in vivo* = Nano-in-nano contendo curcumina e cloridrato de benzidamina para tratamento de Candidíase Vulvovaginal: do desenvolvimento à aplicação biológica *in vitro* e *in vivo* / Gabriela Corrêa Carvalho. – Groningen; Araraquara, 2024.
468 f. : il.

Thesis (Doctorate with double degree) – Universidade Estadual Paulista "Júlio de Mesquita Filho". Faculdade de Ciências Farmacêuticas. Programa de Pós-Graduação em Ciências Farmacêuticas – University Medical Center Groningen. NANOBIOMED: Nanotechnology & Biophysics in Medicine Program.

Advisor: Marlus Chorilli (UNESP).
Advisor: Hélder Almeida Santos (UMCG).
Co-advisor: Taís Maria Bauab (UNESP).
Co-advisor: Brandon W. Peterson (UMCG).
Co-advisor: Rafael Miguel Sábio (UNESP).

1. Nanoparticles. 2. Candidiasis - Vulvovaginal. 3. Curcumin. 4. Drug resistance - Fungal. 5. Hydrogels. I. Chorilli, Marlus, orient. II. Santos, Hélder Almeida, orient. III. Bauab, Taís Maria, coorient. IV. Peterson, Brandon W., coorient. V. Sábio, Rafael Miguel, coorient. VI. Title.

Diretoria do Serviço Técnico de Biblioteca e Documentação - Faculdade de Ciências Farmacêuticas
UNESP - Campus de Araraquara

CAPES: 33004030078P6
The Cataloging in Publication data cannot be altered

CERTIFICADO DE APROVAÇÃO

TÍTULO DA TESE: Nano-in-nano containing curcumin and benzydamine hydrochloride for the treatment of vulvovaginal candidiasis: from development to biological application in vitro and in vivo

AUTORA: GABRIELA CORREA CARVALHO

ORIENTADOR: MARLUS CHORILLI
ORIENTADOR: HÉLDER ALMEIDA SANTOS
COORIENTADOR: RAFAEL MIGUEL SÁBIO
COORIENTADORA: TAIS MARIA BAUAB
COORIENTADOR: BRANDON W PETERSON

Aprovada como parte das exigências para obtenção do Título de Doutora em Ciências Farmacêuticas, área: Pesquisa e Desenvolvimento de Fármacos e Medicamentos, em regime de Cotutela entre a Universidade Estadual Paulista "Julio de Mesquita Filho" e a University of Groningen, Netherlands.

Comissão Examinadora:

Prof. Dr. MARLUS CHORILLI (Participação Virtual)
Departamento de Farmacos e Medicamentos / Faculdade de Ciencias Farmaceuticas do Campus de Araraquara da Unesp

Prof. Dr. HÉLDER ALMEIDA SANTOS (Participação Presencial)
Department of Biomedical Engineering / University Medical Center Groningen - University of Groningen (Netherlands)

Prof. Dr. BRUNO FILIPE CARMELINO CARDOSO SARMENTO (Participação Virtual)
Instituto de Investigação e Inovação em Saúde (i3S) / Universidade do Porto (Portugal)

Prof. Dr. CHRISTIAN CELIA (Participação Presencial)
Dipartimento di Farmacia / Università degli Studi G. d'Annunzio Chieti (Itália)

Profa. Dra. TEREZINHA DE JESUS ANDREOLI PINTO (Participação Virtual)

Departamento de Farmácia / Faculdade de Ciências Farmacêuticas da Universidade de São Paulo (USP)

Profa. Dra. INGE ZUHORN (Participação Presencial)

Department of Biomedical Engineering / University Medical Center Groningen - University of Groningen (Netherlands)

Prof. Dr. JAN MAARTEN VAN DIJL (Participação Presencial)

Department of Medical Microbiology / University Medical Center Groningen - University of Groningen (Netherlands)

Profa.Dra. SANDRA HELENA PULCINELLI (Participação Virtual)

Departamento de Química Analítica, Físico-Química e Inorgânica / Instituto de Química do Campus de Araraquara da Unesp

Araraquara, 17 de julho de 2024

Supervisors
Prof. H. Almeida Santos
Prof. M. Chorilli

Co-supervisors
Prof. T.M. Bauab
Dr. B.W. Peterson

Daily supervisor
Dr. R.M. Sábio

Assessment Committee
Prof. I. Zuhorn
Prof. J.M. van Dijl
Prof. S.H. Pulcinelli
Prof. T.J. Andreoli Pinto

Paranymphs

Gésinda Geertsema-Doornbusch
Jiachen Li

I dedicate this work to Prof. Ione Corrêa, my mom, for always being an example for me, love you!

Table of contents

ABBREVIATIONS AND SYMBOLS LIST		2
CHAPTER 1	Introduction and objective of the thesis	11
CHAPTER 2	Prevalence of vulvovaginal candidiasis in Brazil: A systematic review	21
CHAPTER 3	Infection caused by *Candida auris*: State of the art	45
CHAPTER 4	Lycopene: From tomato to its nutraceutical use and its association with nanotechnology	99
CHAPTER 5	An overview of properties and analytical methods for lycopene in organic nanocarriers	129
CHAPTER 6	Highlights in mesoporous silica nanoparticles as a multifunctional controlled drug delivery nanoplatform for infectious diseases treatment	155
CHAPTER 7	Physicochemical characterization of a lycopene-loaded mesoporous silica nanoparticle formulation	215
CHAPTER 8	Lycopene, mesoporous silica nanoparticles and their Association: a possible alternative against vulvovaginal candidiasis?	249
CHAPTER 9	Cetyltrimethylammonium bromide in the synthesis of mesoporous silica nanoparticles: general aspects and *in vitro* toxicity	269
CHAPTER 10	From curcuma longa to its nutraceutic use and its association with nanotechnology	307
CHAPTER 11	Nano-in-nano particles dual-loaded with curcumin and benzydamine hydrochloride for the treatment of vulvovaginal candidiasis: From development to biological application *in vitro* and *in vivo*	365
CHAPTER 12	Highlights in poloxamer-based drug delivery systems as strategy at local application for vaginal infections	403
CHAPTER 13:	General discussion	435
CHAPTER 14	Conclusions and future perspectives	441
ABSTRACT		443
RESUMO		444
SAMENVATTING		445
APPENDIX 1		447
ACKNOWLEDGMENTS		451
ABOUT THE AUTHOR		455

Abbreviations and symbols list

%	Percentage
~	Approximately
±	Plus–minus
Δm_{MSN}	Empty silica mass variation
ΔmS	Sample mass variation
Δm_T	Total mass variation
°	Degree
µg	Microgram
µL	Microliter
µm	Micrometre
µM	Micromolar
µmol	Micromole
10T1/2	Clonal cell line
$^1O_2$	Singlet oxygen
2D	Two dimensional
3CL	3-chymotrypsin-like
3D	Three dimensional
^{99}mTc	Technetium-99m
A549	Human lung cancer cell line
Ab	Antibody
ABC	Adenosine triphosphate binding cassette
ABCA1	Adenosine triphosphate -binding cassette 1
ACV	Acyclovir
AFLP	Amplified fragment length polymorphism
AgNPs	Silver nanoparticles
AIBA	Sodium dihydrochloride 2,2'- Azobis (2-methylproprylnamide)
AIDS	Acquired immunodeficiency syndrome
AKT	Protein kinase B
AL	Alagoas State
ALT	Alanine aminotransferase
ANOVA	Analysis of variance
AP	Acetophenone
APP/PS1	Transgenic mice that overexpress human mutant amyloid precursor protein and presenilin -1
APTES	3-Aminopropyltriethoxysilane
ARE	Antioxidant response element
ARs	Aspect ratios
AST	Aspartate transaminase
ATCC	American Type Culture Collection
ATP	Adenosine triphosphate
ATR	Attenuated total reflectance
AuNPs	Gold nanoparticles
AuNTs	Gold nanotubes
BA	Bahia State
BAL	Bronchoalveolar lavage
BALB	A portmanteau of "Bagg" and "Albino"
Bax	B-cell lymphoma 2-associated X-protein
BCID	Blood Culture Identification
Bcl-2	B-cell lymphoma 2
Bcl-xL	B-cell lymphoma-extra large
BDNF	Brain-derived neurotrophic factor
BES	Benzenesulfonyl

BET	Brunauer–Emmett–Teller
BHK-21	Baby Hamster Kidney cell line
BLT	Bone marrow, liver, thymus - humanized mice
bMECs	Bovine mammary epithelial cells
BMSCs	Bone mesenchymal stem cells
BNZ	Benzydamine hydrochloride
BNZ@NIN	Benzydamine hydrochloride loaded in the nano-in-nano
BV	Bacterial vaginosis
BZ	Benznidazole
C_{14}TAB	Tetradecyltrimethylammonium bromide
ca.	Approximately
CaCo-2	Cell line derived from a colorectal adenocarcinoma patient
Caco-2/TC7	A Caco-2 cell line subclones
CaSki	Cervical cancer cell line
CAT	Catalase
CCL-119	Human acute lymphoblastic leucemia cell line
CD-1	Outbred mice derived from outbred Swiss mice developed at the Anti-Cancer Center in Lausanne, Switzerland
CDC	Center of Disease Control and Prevention
CDR1	Candida drug resistance 1
CE	Ceará State
CFU	Colony forming units
CFZ	Clofazimine
CG-MS	Gas chromatography/Mass spectrometry
CI	Confidence interval
CINAHL	Cumulative Index to Nursing, and Allied Health Literature
CIP	Ciprofloxacin
CLSI	Clinical and Laboratory Standards Institute
cm^{-1}	Wavenumber
cm^2	Square centimetre
cm^3	Cubic centimetre
CMC	Critical micelle concentration
CMT	critical micellar temperature
COK-12	Centrum Voor Oppervlaktechemie en Katalyse/Centre for Research Chemistry and Catalysis
ConA	Concanavalin A
COVID 19	Coronavirus disease 2019
CP/MAS	Cross-polarization/ Magic-Angle-Spinning
CQDs	Carbon quantum-dots
cRGDY	Cyclic arginine-glycine-aspartic acid-tyrosine
CRL-1490	Human lung fibroblast cell line
CRL-1596	Human Burkitt's lymphoma cell line
CryoTEM	Transmission electron cryomicroscopy
CS	Chitosan succinate
CT-26	Mouse colon carcinoma cell line
CTAB	Cetyltrimethylammonium bromide
CUR	Curcumin
CUR@MSN	Curcumin incorporated in mesoporous silica nanoparticle
CUR+BNZ@HG	Curcumin and benzydamine dispersed in hydrogel
CUR+BNZ@NIN	Curcumin and benzydamine hydrochloride dual loaded in the nano-in-nano
CUR+BNZ@NIN@HG	Curcumin and benzydamine hydrochloride dual loaded in the nano-in-nano dispersed in hydrogel
CVC	Central venous catheter
Da	Dalton

DAD	Diode array detector
DAMO	[3-(2-aminoethylamino) propyl]trimethoxysilane
DC	Dendritic cells
DFO	Desferrioxamine
DHA	Drug: H^+ antiporter
dL	Deciliter
DL	Detection limit
DLS	Dynamic light scattering
DMEM	Dulbecco's modified Eagle medium
DMPC	1,2-Dimyristoyl-sn-glycero-3-phosphocholine
DMSO	Dimethylsulfoxide
DNA	Deoxyribonucleic acid
DNase	Deoxyribonuclease
DOXY	Doxycycline
DPPH	2,2-Diphenyl-1-picrylhydrazyl
DSC	Differential scanning calorimetry
DSPC	1,2-Distearoyl-sn-glycero-3-phosphocholine
DTPA	Diethylenetriaminepentaacetic acid
DW	Dry weight
EA	Ethyl acetate
EAE	Enzyme-assisted extraction
EC	Ethyl cellulose
ECDC	European Center for Disease Prevention and Control
ECO	Econazole
EDTA	Trypsin-ethylenediaminetetraacetic acid
EDX	Energy dispersive X-ray
EE	Encapsulation efficiency
EMA	European Medicines Agency
End1/E6E7	Human endometriosis cell line
EPS	Extracellular polymeric matrix
ERG11	Lanosterol 14 α-demethylase gene
ERK	Extracellular Signal-Regulated Kinase
ES	Espírito Santo State
ETGFA	Expansible thermal gelling foam aerosol
ETH	Ethionamide
EUCAST	European Committee on Antimicrobial Susceptibility Testing
F	Freeze
f	Flake
FA	Formic acid
FB11	*Francisella tularensis* LPS antibody
FBS	Fetal bovine serum
FDA	Food and Drug Administration
FICI	Fractional inhibitory concentration index
FKS1	1.3-Beta-glucan synthase gene
FL	Fluorescein
FMB-01	Clinical strain resistant to azoles provided by the Medical School of São Paulo State University
FP	Fungal pathogen
FSM	Folded sheets of mesoporous materials
FTIR	Fourier-transform infrared spectroscopy
FtsZ	Filamenting temperature-sensitive mutant Z
g	Gram
GAGs	Glycosaminoglycans
GEN	Gentamicin
GFP	Green fluorescent protein

GPI	Glycophosphatidylinositol or glycosylphosphatidylinositol
GPTMS	(3-Glycidoxypropy) trimethoxysilane
GQDs	Graphene quantum-dots
GSH-Px	Glutathione peroxidase
GST	Recombinant Hepatitis E Virus ORF2 Protein
Gwt1	Fungal enzyme inositol acylase
h	Hour
H9c2	Cardiac myofibroblast cells
HA	Hydroxyapatite
HaCaT	Human epidermal keratinocyte cell line
HDL	High-density lipoprotein
HEC-1-A	Human Endometrial cancer cell line
HEK-293T	Human embryonic kidney 293 cells
HeLa	Human epithelial cell
Hep-2	Human larynx epithelioma cancer cell line
HEPES buffer	4-(2-Hydroxyethyl)-1-piperazineethanesulfonic acid buffer
HepG2	Human liver hepatocellular carcinoma cell line
HIV	Human immunodeficiency virus
HLB	Hydrophilic-lipophilic balance
HMG-CoA	3-Hydroxy-3-methylglutaryl coenzyme A
HMM-33	Hiroshima Mesoporous Material-33
HMSNs	Hollow MSNs
HO-1	Heme oxidase
HOMSNs	Hollow oblate mesoporous silica nanoparticle
HOS	Human osteosarcoma
HPLC	High-performance liquid chromatography
HPMC	Hydroxypropyl Methylcellulose
HPV	Human papillomavirus
HR-TEM	High-resolution transmission electron microscopy
HSP	Heat shock protein
HSV	Herpes simplex virus
HT-29 and HT29/MTX	Human colon carcinoma cell line
HTLV	Human T cell lymphotropic virus
Hyal	Hyaluronidase
i.d	Internal Diameter
IC50	Half-maximal inhibitory concentration
ICR	Institute of Cancer Research
ICU	Intensive Care Unit
IE	Impregnation efficiency
IFN	Interferons
IGF-1R	Insulin-like growth factor 1
IgG	Immunoglobulin G
IL	Interleukin
INH	Isoniazid
IP	Intraperitoneally
IR	Infrared
ITS	Internal transcribed spacer
IUDs	Intrauterine Devices
IUPAC	International Union of Pure and Applied Chemistry
IV	Intravenous
J	Joule
JAK	Janus kinase
JNK	c-Jun NH_2-terminal kinase
K	Retention factor
kcal	Kilocalories

KeV	Kilo Electron Volts
kg	Kilogram
kHz	Kilohertz
kJ	Kilojoule
km^{-1}	Kilometre power^{-1}
km^2	Square kilometre
L	Liter
L	Liquid
L0-2	Human hepatocyte cell line
LAMP	loop-mediated isothermal amplification
LC	Loading (or load) capacity
LC-MSNs	Lipid-coated mesoporous silica nanoparticles
LD	Loading degree
LD50	Lethal dose 50
LDH	Lactate dehydrogenase
LDL	Low-density lipoprotein
LED	Light Emitting Diode
LEVO	Levofloxacin
LILACS	Latin American and Caribbean Literature in Health Sciences
Log	Logarithm
LP	Liposomes
LPS	Lipopolisaccharide
LU	Ubiquicidin onto lipid bilayer
LVS	Live vaccine strain
LXRα	Liver X receptor α
LYC	Lycopene
LYC@MSN	Mesoporous silica nanoparticle incorporated with lycopene
LYZ	Lysozyme
M	Mitotic phase
M	Moles per liter
m^2	Square meter
m^3	Cubic metre
MALDI-TOF	Matrix-assisted laser desorption/ionization time-of-flight
MAPK	Mitogen-activated protein kinase
MBI	1-Methyl-1H-benzimidazole
MCF-7	Human breast adenocarcinoma cell line
MCM	Mobil Crystalline Materials or Mobil Composition of Matter
MDA	Malondialdehyde
MDCK	Madin-Darby Canine Kidney cells
MFC	Minimum fungicide concentration
MFS	Major Facilitator Superfamily
MFX	Moxifloxacin
mg	Milligram
MG-63	Human osteoblast cell line
MGCE	Magnetic glassy carbon electrode
MHB	Mueller Hinton Broth
MIC	Minimum Inhibitory Concentration
min	Minutes
miR	MicroRNA
mL	Millilitre
ML-336	A quinazolinone-based compound
mM	Millimolar
mm	Millimeter
mm^3	Cubic millimetre
MMC	Minimum microbicide concentration

mmol	Millimole
MMP	Matrix metalloproteinase
MNZ	Metronidazole
mol	Mole
MONPs	Metal oxide nanoparticles
MPA	Multiplex Probe Amplification
MPO	Myeloperoxidase
MPP+	1-Methyl-4-phenylpyridinium
mRNA	Messenger ribonucleic acid
MRSA	Methicillin-resistant *S. Aureus*
MSN	Mesoporous silica nanoparticles
MSN-C	Calcined mesoporous silica nanoparticle
MSN-R	Refluxed mesoporous silica nanoparticle
MSTO	Human mesothelioma cell line
MTBE	Methyl tert-butyl ether
mTOR	Mammalian target of rapamycin
MTT	Thiazolyl Blue Tetrazolium romide
MTZ	Metronidazole
mV	Millivolt
mW	Milliwatt
MXF	Moxifloxacin
n	Total number of observations or population size
n.a.	Not available
N3	3-[2-(2-Aminoethylamino)ethylamino]propyltrimethoxysilane
NA	No activity in the tested range
NaDC	Sodium deoxycholate
NADH	Nicotinamide adenine dinucleotide hydrogen
NADPH	Nicotinamide adenine dinucleotide phosphate hydrogen
NE	Nanoemulsions
NET	Trapping extracellular neutrophils
NFE2L2	Nuclear factor E2-related factor 2
NF-kB	Nuclear factor kappa B
NFX	Norfloxacin
ng	Nanogram
NHDF	Normal Human Dermal Fibroblasts
NI	Niosomes
NIH/3T3	Mouse fibroblast cell line
NIN	Nano-in-nano
NIR	Near-infrared
NLC	Nanostructured lipid carriers
nm	Nanometer
nM	Nanomolar
NMR	Nuclear Magnetic Resonance
NPs	Nanoparticles
o	Oven
O/W	Oil-in-Water
ºC	Celsius
ORF2	Open reading frames
P	Paste
p/p0	Equilibrium pressure divided by the saturation pressure
PA	Pará State
PAMPs	Pathogen-associated molecular patterns
Panc1	Human pancreatic ductal adenocarcinoma cell line
PAS	Periodic acid-Schiff
PBMCs	Peripheral blood mononuclear cells

PBS	Phosphate-buffered saline
PCR	Polymerase chain reaction
PCV2	Porcine circovirus type 2
PDA	Photodiode arrays
PDI	Polydispersity index
PDMAEMA	Poly(2-(dimethylamino)ethyl methacrylate)
PDT	Photodynamic therapy
PEG	Polyethylene glycol
PEI	Poly(ethylene imine)
PEO	Poly(ethylene oxide)
PI3K	Phosphoinositide 3-kinase
PICO	Population; intervention; comparation and outcome
PK15	Pig kidney cell line
PLGA	Poly(lactic-co-glycolic acid)
PLLA	Poly(L-lactide)
PLMA	Poly(lauryl methacrylate)
PMWS	Post-weaning multi-systemic wasting syndrome
PN	Polymeric nanoparticles
PPARγ	Peroxisome proliferator-activated receptor gamma
ppm	Parts per million
PPO	Poly(p-phenylene oxide)
PPRs	Pattern recognition receptors
PPTT	Plasmonic photothermal therapy
PRISMA	Preferred Reporting Items for Systematic Reviews and Meta-Analyzes
PROSPERO	Prospective Register of Systematic Reviews
PtBA	Poly tert-butyl acrylate
PTT	Photothermal therapy
PUBMED	International database produced by the National Center for Biotechnology information
PVP	Polyvinylpyrrolidone
PZQ	Praziquantel
QL	Quantification limit
qRT-PCR	Real-Time Quantitative Reverse Transcription Polymerase Chain Reaction
R^2	Correlation coefficient
RAW 264.7	Mouse macrophage cell line
RB	Rose Bengal
RECK	Reversion-inducing-cysteine-rich protein with kazal motifs
RIF	Rifampicin
RN	Rio Grande do Norte State
RNA	Ribonucleic acid
ROS	Reactive oxygen species
rpm	Revolutions per minute
RPMI 1640	Roswell Park Memorial Institute
RS	Rio Grande do Sul State
RSD	Relative standard deviation
RT-PCR	Reverse transcription polymerase chain reaction
RVVC	Recurrent vulvovaginal candidiasis
S	South latitude
s	Seconds
SAOS-2	Human osteoblast-like cell line
SARS-CoV-2	Severe acute respiratory syndrome coronavirus 2
SB	Synthetic Broth
SBA	Santa Barbara Amorphous materials
S_{BET}	Specific surface area

SBF	Simulated body fluid
SCFE	Supercritical CO_2 Extraction
Scielo	Scientific Eletronic Online
Scopus	International database produced by Elsevier
SD	Standard deviation
SDA	Sabouraud Dextrose Agar
SDB	Sabouraud Dextrose Broth
SE	Solvent extraction
SEM	Scanning electron microscopy
SHI-1	Acute myelocytic leukemia cell line
SIF	Simulated intestinal fluid
SLN	Solid lipid nanoparticles
SOD	Superoxide dismutase
SP	São Paulo State
SS	Solid-state
STAT	Signal transducer and activator of transcription
SV-80	Human lung fibroblast cell line
SVF	Simulated vaginal fluid
SWAP	Soluble adult worm antigen preparation
TA	Tannic acid
TAC1	Zinc cluster transcription
TBHP	Tert-butyl hydroperoxide
TEB	Tebuconazole
TEM	Transmission electron microscopy
TEOS	Tetraethyl orthosilicate
TG	Thermogravimetric
TG/DTA	Thermogravimetry differential thermal analysis
TGA	Thermogravimetry analysis
TH1	T helper 1
TMPES	Trimethoxy-(2-phenylethyl)silane
TMS	Transmembrane spans
TPP	Tripolyphosphate pentasodium
TSB	Tryptic soy broth
TTC	Triphenyltetrazolium chloride
TUD-1	Technical Delft University
TUNEL	Terminal deoxynucleotidyl transferase dUTP nick end labeling
TZM-bl	Cell line derived from a HeLa cell clone
U251MG	Human glioblastoma cell line
UAE	Ultrasound-assisted extraction
UBI_{29-41}	Ubiquicidin
UDCA	Ursodeoxycholic acid
UnTHCPSi NPs	Carboxylic acid functionalized thermally hydrocarbonized porous silicon nanoparticles
USP	United States Pharmacopeia
UV	Ultraviolet
UV-Vis	Ultraviolet-Visible
v	Vacuum
VAN	Vancomycin
VEEV	Venezuelan equine encephalitis virus
Vero cells	Kidney epithelial cells extracted from an African green monkey
Vk2/E6E7	Human vaginal epithelial cell line
VSV	Vesicular stomatitis virus
VVC	Vulvovaginal candidiasis
W	West longitude
W	Watts

W/O	Water-in-oil
w/w	Weight in weight
WHO	World Health Organization
Wnt	Wingless-related integration site
wt.	Weight
XTT	2,3-Bis(2-methoxy-4-nitro-5-sulfophenyl)-5-[carbonyl(phenylamino)]-2H-tetrazolium-hydroxide
Y-79	Human retinoblastoma cell linem
ZnO@MSNs	Zinc oxide nanoparticles into MSNs
β	Beta
β-CD	β-cyclodextrin
μL	Microliter

CHAPTER 1

Introduction and aim of the thesis

1.Introduction

As a result of the great global concern regarding the scarcity of research and political interventions to combat fungal infections and their growing problem about resistance to antifungal drugs currently used in therapy, the World Health Organization (WHO) recently made public a list of priority fungal pathogens. This list is divided into critical, high and medium priority, and it is observed that the genus *Candida spp*. is a threat to public health. *Candida auris* and *Candida albicans* were classified as critical priority, while *Candida parapsilosis* and *Candida tropicalis* were classified as medium priority (WHO, 2022). Candidiasis, the term used to refer to infections caused by this genus, can be superficial, cutaneous, mucosal or systemic (Mba & Nweze, 2020). Among the types of candidiasis, vulvovaginal candidiasis (VVC) must be highlighted, as is one of the most common causes of gynecological care nowadays, affecting at least once in life 75% of the world's female population (Conte et al., 2023; Żyrek et al., 2021).

Although this genus of fungus is commonly found in the vaginal mucosa microbiota of most healthy women, in a condition of commensalism, factors inherent to the host (*e.g.*, microbiota changes and decreased production of endogenous estrogen), or even to the pathogen (like genetic and phenotypic variation), can break this balance, causing this fungus to become pathogenic (Becker & Sobel, 2023; Gaziano et al., 2023; Sun et al., 2023). When candida becomes pathogenic, it changes from the yeast to hyphae form, which invade the vaginal mucosa, triggering an immune response from the host mainly by inducing signaling cascades that lead to the production of pro-inflammatory cytokines and antimicrobial proteins by epithelial cells, macrophages and polymorphonuclear cells causing discomfort to the patient due to the symptoms of inflammation (Mahalingam et al., 2022). Among the main symptoms can be mentioned pruritus, edema, fissures and dysuria (Conte et al., 2023).

Although different countries have their own protocols for the treatment of this disease, the common point between them is the use of the azoles class as one of the first therapeutic options of choice (British Association for Sexual Health and HIV, 2020; Farr et al., 2021; Hazra et al., 2022; Ministério da Saúde, 2022).Are some examples of drugs belonging to this class that are widely used in the treatment of VVC include: fluconazole, clotrimazole, miconazole, tioconazole, butoconazole and terconazole (Hazra et al., 2022). In addition to drugs derived from this class, such as benzydamine hydrochloride, an anti-inflammatory with antifungal properties as it is derived from indazole (Bossi et al., 2023). However, in the literature it is possible to observe several reports about Candida strains resistant to this class of drug, which appears as a challenge to be faced nowadays (Arrieta-Aguirre et al., 2023; Benhadj et al., 2024; Gerges et al., 2023). Therefore, despite seeking medical assistance, many women continue to have the infection despite have been treated, due to this issue of resistance, which can cause serious

complications such as menstrual disorders, pelvic abscess, pelvic inflammatory disease, infertility, ectopic pregnancy and miscarriage (Gonçalves et al., 2016).

In this context, the need to develop new therapeutic options is a growing trend and several strategies have been studied. Firstly, we can mention the development of new synthetic antifungals such as ibrexafungerp and oteseconazole. As oteseconazole belongs to the azoles class, is susceptible to the same mechanisms of fungal resistance as its class, however, once it is a new therapeutic option, there are still no clinical reports about it being therefore an option for the treatment of this disease (Sobel, 2023a). Another interesting alternative is the use of innovative pharmaceutical forms, such as chitosan-based sponges (biodegradable/dissolvable) containing clotrimazole and sprayable thermosensitive benzydamine hydrogel (an anti-inflammatory with known antifungal activity) (Arpa et al., 2023; Martins et al., 2023).

The association of drugs is already well established in the therapy (azoles and other classes of antifungal) with nanotechnology in order to increase their therapeutic activity, bypassing the resistance issue is also an alternative that has been widely used like itraconazole-based nanosuspension, clotrimazole-loaded cationic *N*-(2-hydroxy)-propyl-3-trimethylammonium, *O*-palmitoyl chitosan nanoparticles and amphotericin B-loaded nanoemulsion (Facchinatto et al., 2021; Marena et al., 2022; Parsana et al., 2023).

Although there are other options nowadays, the last strategy that needs to be highlighted is the use of products of natural origin, like lycopene and curcumin, (alone or in association) as they generally have effectiveness, considerable biocompatibility and low toxicity; however, many of them have limitations (*e.g.*, low aqueous solubility and low absorption) that limit their use in therapy. For this reason, nanotechnology is often also a protagonist when talking about natural products for biological applications (Marena et al., 2022). As example, can be cited fluconazole and propolis co-encapsulated in chitosan nanoparticles; hypericin-loaded nanostructured lipid carriers and chitosan-based system with *Scutellariae baicalensis radix* extract (Chanaj-Kaczmarek et al., 2022; da Silva et al., 2023; Sato et al., 2023).

As a result of this scenario, this thesis sought to develop an ideal formulation based on natural products and nanotechnology in order to combat this growing issue of resistance. However, it is important to highlight that the process of developing a formulation goes through several stages, from the process of conceiving the study hypothesis to the obtainment of a final product, which may or may not prove promising for the purpose studied. To reach the top of the trajectory, that is, to obtain a promising formulation to treat VVC, several steps must be completed. In this case, to develop a nano-in-nano system dual-loaded with curcumin and benzydamine hydrochloride dispersed in a thermoresponsive hydrogel, it was necessary to go through several prior steps, such as the production

of review articles to learn more about the topics and the production of a preliminary nanotechnological system, because that's what science is about: attempts based on scientific knowledge.

2. Summary of the thesis content

According to the Dutch Institute for Healthcare Research, in 2022 urogenital candidiasis in women showed a prevalence of 19.2 per 1000 inhabitants (Dutch Institute for Research in Health Care, 2022). In Brazil, both official data and those published in the literature are obsolete and incomplete, which makes it difficult to understand the epidemiological profile of this disease throughout the Brazilian territory, information that is essential for establishing public policy plans for disease prevention and combat. Due to this shortcoming, a systematic review with meta-analysis (registered in the International Prospective Register of Systematic Reviews: PROSPERO 2020 CRD42020181695) was carried out in **Chapter 2**.

Although *Candida albicans* is the specie most frequently isolated from vulvovaginal candidiasis samples, non-albicans species can also be isolated, with *C. glabrata* and *C. tropicalis* being the most prevalent ones (Chen et al., 2023; Seck et al., 2023). Although not prevalent, emphasis needs to be placed on cases of VVC caused by *C. auris*, since this new emerging yeast is already multidrug-resistant and difficult to eradicate (Krishnasamy et al., 2021; Kumar et al., 2015; Mesini et al., 2021). Despite being considered a great challenge, little is still known about this specie in the scientific literature, which is why **Chapter 3** addresses the state of the art of what is known so far about this new specie.

Turning the attention to the most prevalent one, *C. albicans* is a fungus that inhabits the vulvovaginal mucosa as a commensal microorganism, in the form of yeast; however, as it is a dimorphic fungus, it can change to its pathogenic state in host situations, such as elevation of vaginal pH, microbiota disruption (due the use of antibiotics for example), use of high-estrogen oral contraceptives and hormone replacement, diabetes mellitus and impairment of the immune system (Czechowicz et al., 2022; Peters et al., 2014). This transition to the pathogenic form begins with the change from yeast to hyphae (which does not occur in other species such as *C. glabrata* for example), which invade and damage the host tissue. The fungal components are then recognized by the presenting cells of innate antigens, which triggers the activation of nuclear factor kappa B (NF-kB) resulting in the release of pro-inflammatory cytokines and reactive oxygen species (ROS), that is, the pathogenicity of *C. albicans* leads to an inflammatory response in the host organism (Mahalingam et al., 2022; Peters et al., 2014).

In view of the emergence of *C. albicans* strains resistant to currently available therapies, mainly azoles, and that the inflammation generated by the infiltration of fungal hyphae in the vulvovaginal mucosa leads to the appearance of symptoms, so painful and uncomfortable for the patient, the study of new therapeutic options is increasingly necessary, especially combining antifungal and anti-inflammatory actions (Sobel, 2023b; Sobel et al., 2022). In this context, drugs of natural origin have been explored as promising options to overcome the problem of fungal resistance (Marena et al., 2022).

Among the various natural molecules explored today, lycopene stands out, a carotenoid extracted mainly from tomatoes that has several therapeutic activities, such as antifungal and anti-inflammatory, being therefore desirable for the treatment of VVC (Amorim et al., 2022). However, in addition to low aqueous solubility, this compound has other characteristics that limit its application in therapy, such as sensitivity to light, temperature and oxygen, factors that can lead to isomerism of the molecule, which is not desirable since the different lycopene isomers have different bioavailability and bioaccessibility (Falsafi et al., 2022; Li et al., 2023). This highlights the importance of knowing its physicochemical characteristics and preserving it from extraction until the moment of its application to ensure the maintenance of its biological properties. Thus, **Chapter 4** highlights the entire route that lycopene takes from its cultivation and extraction to its use as a nutraceutical and possible association with nanotechnology.

Lycopene association with nanotechnology, like nanoparticles, is an interesting strategy to not only preserve its physicochemical characteristics but also increase its aqueous solubility. The small size of nanoparticles associated with their large surface area-to-volume make them an interesting strategy for drug delivery. It is also worth highlighting that this association also provides increased biological efficacy, reduced dosage and fewer adverse effects of the active molecule (Falsafi et al., 2022; Manocha et al., 2022). According to their composition, nanoparticles are generally categorized into four classes, inorganic, organic, carbon-based and hybrid (Joudeh & Linke, 2022). For the process of developing a nanoformulation, it is essential to study and define the desirable characteristics for the appropriate choice of the nanocarrier. Hence, **Chapter 5** reinforces the lack of work exploring the association of lycopene with inorganic nanoparticles, highlighting a new topic for study. This chapter also highlights what is in the literature regarding analytical methods for detecting this drug, a key topic for the development of a formulation as it makes it possible to know the amount of drug incorporated and released by the system, thus allowing dose adjustment.

Despite the various inorganic materials used as nanocarriers, it is worth highlighting the silica-based ones, more specifically mesoporous silica nanoparticles (MSN), suitable for biological applications as they have low immunogenicity and good biocompatibility. Furthermore, its large surface area and pore volume give to this nanocarrier not only a high carrying capacity for small or large molecules,

contributing positively to its behavior in the biological environment, but also increase its cellular absorption (Miguel Sábio et al., 2023; Parra-Nieto et al., 2021; Yang et al., 2020). To highlight whether this type of nanoparticle could be an intelligent strategy to combat infectious diseases, such as VVC, specially caused by multidrug resistant microorganisms, **Chapter 6** seeks to explore this topic further.

The abovementioned desirable characteristics, associated with the growing trend of using this type of nanoparticle to combat infectious diseases, made it the choice to be associated with lycopene. The development and characterization process of lycopene-loaded MSN are described in **Chapters 7** and **8**. An important detail that needs to be considered during the MSN synthesis is the availability of the mesopores for drug loading. It is possible to observe studies in the literature where physicochemical characterization analyzes point to residues of organic matter (*e.g.*, cetyltrimethylammonium bromide, CTAB) even after MSNs have undergone removal processes, which can compromise the drug incorporation process (Javdani et al., 2020; Joyce et al., 2020; Pongchaikul et al., 2023; Prem et al., 2023; Wu et al., 2021). In this regard, **Chapter 9** provides an extensive and unprecedented discussion about the use of this surfactant in the synthesis of MSN and its toxicity in eukaryotic and prokaryotic cells, since CTAB is a quaternary ammonium compound (Li et al., 2023). Additionally, the issue of the CTAB residues in MSN led to the execution of the toxicity assessment in *Galleria mellonella,* addressed in **Chapter 8**. Chapter 8 also addresses the antifungal activity of loaded and free lycopene (see **Appendix 1** for lycopene anti-inflammatory activity).

In addition to lycopene, another product of natural origin that has increasingly receiving considerable attention due to its biological activities, like anti-inflammatory and antifungal, is curcumin (Gayathri et al., 2023; Obeid et al., 2023). Diferuloylmethane, or curcumin as it is more widely known, is a yellow-colored polyphenol found primarily in the rhizome of *Curcuma longa* (L) and other *Curcuma* spp (Sharifi-Rad et al., 2020). Like lycopene, this compound also has limitations that hinder its application in therapy, such as limited water solubility, poor absorption and low bioavailability, rapid metabolism and sensitivity to light (Obeid et al., 2023). **Chapter 10** highlights the importance to know and preserve curcumin physicochemical characteristics from its cultivation and extraction towards its biological application and association with nanotechnology, crucial to overcome the cited limitations.

The association of this molecule, with consolidated antifungal activity, with an anti-inflammatory already consolidated in therapy, especially when dealing with gynecological inflammations, such as benzydamine hydrochloride, in a nanosystem that allows the simultaneous incorporation of both drugs proves to be an interesting strategy (Araujo et al., 2020; Di Stefano et al., 2020; Hussain et al., 2022). From this perspective, **Chapter 11** describes the development of a hybrid nanoparticle (nano-in-nano) by microfluidics composed of MSN and a lipid-coating. Lipids were chosen for the manufacture of

this hybrid nanoparticle because they are highly biocompatible, biodegradable, has low immunogenicity and are known to increase the aqueous solubility of hydrophobic drugs. In addition to being clinically approved by the European Medicines Agency (EMA) and Food and Drug Administration (FDA) for therapeutic applications (Giordani et al., 2023; Nsairat et al., 2022). To synthesize this particle, microfluidics was the technique of choice because it is highly controllable, reproducible (maintaining homogeneity), can improve the drug encapsulation efficiency and is scalable (Fontana et al., 2019; Liu et al., 2020; Martins & Santos, 2023). It is worth highlighting that in this chapter, a thermoresponsive hydrogel was also used as an intelligent strategy to enable the topical application of the hybrid nanoparticle *in vivo*, since it is liquid at room temperature, making it easy to apply, and gel at body temperature which associated with the mucoadhesive character of chitosan enables the maintenance of the formulation in the target site (Araujo et al., 2021; dos Santos et al., 2020; Kolawole & Cook, 2023). Due to its thermoresponsive characteristic, poloxamer has been increasingly used for topical formulations where this behavior is desirable, such as the vaginal environment (Su et al., 2023; Sukmawaty et al., 2023).

Finally, **Chapter 12** provides an overview of the general aspects and biological behavior of this polymer as well as its application for controlled drug release in the vaginal environment.

3. Aim of this thesis

Given the high prevalence of VVC and the growing problem of resistance to antifungals commonly used in the clinical practice, it is urgent to develop new therapeutic options to not only combat its causative agent but also to bring better living conditions to the affected patients. In this regard, the aim of this thesis was to a develop drug delivery nanoformulation, associating natural product with nanotechnology to treat, VVC caused by resistant fungi strains. To achieve this, an in-depth study of the literature was necessary to, based on scientific knowledge, choose, and associate the best strategies in order to produce an innovative formulation. As the first hypothesis is not always ideal one to reach the ideal innovative formulation, two nanosystems with different strategies but with some points in common were developed and evaluated *in vitro* and *in vivo*.

4. References

Amorim, A. das G. N., Vasconcelos, A. G., Souza, J., Oliveira, A., Gullón, B., de Souza de Almeida Leite, J. R., & Pintado, M. (2022). Bio-Availability, Anticancer Potential, and Chemical Data of Lycopene: An Overview and Technological Prospecting. *Antioxidants*, *11*(2), Article 360. https://doi.org/10.3390/antiox11020360

Araujo, V. H. S., de Souza, M. P. C., Carvalho, G. C., Duarte, J. L., & Chorilli, M. (2021). Chitosan-based systems aimed at local applications for vaginal infections. *Carbohydrate Polymers*, *261*, Article 117919. https://doi.org/10.1016/j.carbpol.2021.117919

Araujo, V. H. S., Duarte, J. L., Carvalho, G. C., Silvestre, A. L. P., Fonseca-Santos, B., Marena, G. D., Ribeiro, T. de C., dos Santos Ramos, M. A., Bauab, T. M., & Chorilli, M. (2020). Nanosystems against candidiasis: a review of studies performed over the last two decades. *Critical Reviews in Microbiology*, 46(5), 508-547. https://doi.org/10.1080/1040841X.2020.1803208

Arpa, M. D., Kesmen, E. E., & Biltekin, S. N. (2023). Novel Sprayable Thermosensitive Benzydamine Hydrogels for Topical Application: Development, Characterization, and In Vitro Biological Activities. *AAPS PharmSciTech*, *24*(8), Article 214. https://doi.org/10.1208/s12249-023-02674-w

Arrieta-Aguirre, I., Menéndez-Manjón, P., Carrano, G., Diez, A., Fernandez-de-Larrinoa, Í., & Moragues, M.-D. (2023). Molecular Identification of Fungal Species through Multiplex-qPCR to Determine Candidal Vulvovaginitis and Antifungal Susceptibility. *Journal of Fungi*, *9*(12), Article 1145. https://doi.org/10.3390/jof9121145

Becker, M., & Sobel, R. (2023). Vulvovaginal Candidiasis in Postmenopausal Women. *Current Infectious Disease Reports*, *25*(4), 61–66. https://doi.org/10.1007/s11908-023-00801-z

Benhadj, M., Menasria, T., & Ranque, S. (2024). MALDI-TOF mass spectrometry identification and antifungal susceptibility testing of yeasts causing vulvovaginal candidiasis (VVC) in Tebessa (Northeastern Algeria). *Annales de Biologie Clinique*, *81*(6), 576-584. https://doi.org/10.1684/abc.2023.1852

Bossi, P., Gurizzan, C., Guntinas-Lichius, O., Hainarosie, R., & Lancini, D. (2023). The present and the future of benzydamine: expert opinion paper. *Frontiers in Oral Health*, 4, Article 1191319. https://doi.org/10.3389/froh.2023.1191319

British Association for Sexual Health and HIV. (2020). British Association for Sexual Health and HIV national guideline for the management of vulvovaginal candidiasis (2019). *International Journal of STD & AIDS*, *31*(12), 1124–1144. https://doi.org/10.1177/0956462420943034

Chanaj-Kaczmarek, J., Rosiak, N., Szymanowska, D., Rajewski, M., Wender-Ozegowska, E., & Cielecka-Piontek, J. (2022). The Chitosan-Based System with Scutellariae baicalensis radix Extract for the Local Treatment of Vaginal Infections. *Pharmaceutics*, *14*(4), Article 740. https://doi.org/10.3390/pharmaceutics14040740

Chen, Z., Jin, J., Chen, H., Chen, Y., & Feng, S. (2023). The bacterial communities in vagina of different Candida species-associated vulvovaginal candidiasis. *Microbial Pathogenesis*, *177*, Article 106037. https://doi.org/10.1016/j.micpath.2023.106037

Conte, J., Parize, A. L., & Caon, T. (2023). Advanced Solid Formulations For Vulvovaginal Candidiasis. *Pharmaceutical Research*, *40*(2), 593–610. https://doi.org/10.1007/s11095-022-03441-5

Czechowicz, P., Nowicka, J., & Gościniak, G. (2022). Virulence Factors of Candida spp. and Host Immune Response Important in the Pathogenesis of Vulvovaginal Candidiasis. *International Journal of Molecular Sciences*, *23*(11), Article 5895. https://doi.org/10.3390/ijms23115895

da Silva, J. T., Dantas de Sousa, P. H., Costa, A. F., de Menezes, L. B., Alves, S. F., Pellegrini, F., & Amaral, A. C. (2023). Fluconazole and propolis co-encapsulated in chitosan nanoparticles for the treatment of vulvovaginal candidiasis in a murine model. *Medical Mycology*, *61*(11), Article myad113. https://doi.org/10.1093/mmy/myad113

Di Stefano, A. F. D., Radicioni, M. M., Vaccani, A., Caccia, G., Focanti, F., Salvatori, E., Pelacchi, F., Picollo, R., Rosignoli, M. T., Olivieri, S., & others. (2020). Phase I Study in Healthy Women of a Novel Antimycotic Vaginal Ovule Combining Econazole and Benzydamine. *Infectious Diseases in Obstetrics and Gynecology*, *2020*, 1–11. https://doi.org/10.1155/2020/7201840

dos Santos, A. M., Carvalho, S. G., Araujo, V. H. S., Carvalho, G. C., Gremião, M. P. D., & Chorilli, M. (2020). Recent advances in hydrogels as strategy for drug delivery intended to vaginal infections. *International Journal of Pharmaceutics*, *590*, Article 119867. https://doi.org/10.1016/j.ijpharm.2020.119867

Dutch Institute for Research in Health Care. (2022). *Jaarcijfers aandoeningen - Huisartsenregistraties*. Nivel. https://www.nivel.nl/nl/nivel-zorgregistraties-eerste-lijn/cijfers-over-aandoeningen/jaarcijfers-aandoeningen-huisartsenregistraties

Facchinatto, W. M., Galante, J., Mesquita, L., Silva, D. S., Martins dos Santos, D., Moraes, T. B., Campana-Filho, S. P., Colnago, L. A., Sarmento, B., & das Neves, J. (2021). Clotrimazole-loaded N-(2-hydroxy)-propyl-3-trimethylammonium, O-palmitoyl chitosan nanoparticles for topical treatment of vulvovaginal candidiasis. *Acta Biomaterialia*, *125*, 312–321. https://doi.org/10.1016/j.actbio.2021.02.029

Falsafi, S. R., Rostamabadi, H., Babazadeh, A., Tarhan, Ö., Rashidinejad, A., Boostani, S., Khoshnoudi-Nia, S., Akbari-Alavijeh, S., Shaddel, R., & Jafari, S. M. (2022). Lycopene nanodelivery systems; recent advances. *Trends in Food Science & Technology*, *119*, 378–399. https://doi.org/10.1016/j.tifs.2021.12.016

Farr, A., Effendy, I., Frey Tirri, B., Hof, H., Mayser, P., Petricevic, L., Ruhnke, M., Schaller, M., Schaefer, A. P. A., Sustr, V., & others. (2021). Guideline: Vulvovaginal candidosis (AWMF 015/072, level S2k). *Mycoses*, *64*(6), 583–602. https://doi.org/10.1111/myc.13248

Fontana, F., Martins, J. P., Torrieri, G., & Santos, H. A. (2019). Nuts and Bolts: Microfluidics for the Production of Biomaterials. *Advanced Materials Technologies*, *4*(6), Article 1800611. https://doi.org/10.1002/admt.201800611

Gayathri, K., Bhaskaran, M., Selvam, C., & Thilagavathi, R. (2023). Nano formulation approaches for curcumin delivery- a review. *Journal of Drug Delivery Science and Technology*, *82*, Article 104326. https://doi.org/10.1016/j.jddst.2023.104326

Gaziano, R., Sabbatini, S., & Monari, C. (2023). The Interplay between Candida albicans, Vaginal Mucosa, Host Immunity and Resident Microbiota in Health and Disease: An Overview and Future Perspectives. *Microorganisms*, *11*(5), Article 1211. https://doi.org/10.3390/microorganisms11051211

Gerges, M. A., Fahmy, Y. A., Hosny, T., Gandor, N. H., Mohammed, S. Y., Mohamed, T. M. A., Abdelmoteleb, N. E. M., & Esmaeel, N. E. (2023). Biofilm Formation and Aspartyl Proteinase Activity and Their Association with Azole Resistance Among Candida albicans Causing Vulvovaginal Candidiasis, Egypt. *Infection and Drug Resistance*, *16*, 5283–5293. https://doi.org/10.2147/IDR.S420580

Giordani, S., Marassi, V., Zattoni, A., Roda, B., & Reschiglian, P. (2023). Liposomes characterization for market approval as pharmaceutical products: Analytical methods, guidelines and standardized protocols. *Journal of Pharmaceutical and Biomedical Analysis*, *236*, Article 115751. https://doi.org/10.1016/j.jpba.2023.115751

Gonçalves, B., Ferreira, C., Alves, C. T., Henriques, M., Azeredo, J., & Silva, S. (2016). Vulvovaginal candidiasis: Epidemiology, microbiology and risk factors. *Critical Reviews in Microbiology*, *42*(6), 905–927. https://doi.org/10.3109/1040841X.2015.1091805

Hazra, A., Collison, M. W., & Davis, A. M. (2022). CDC Sexually Transmitted Infections Treatment Guidelines, 2021. *Jama* 327(9), 870-871. https://doi.org/10.1001/jama.2022.1246

Hussain, Y., Alam, W., Ullah, H., Dacrema, M., Daglia, M., Khan, H., & Arciola, C. R. (2022). Antimicrobial Potential of Curcumin: Therapeutic Potential and Challenges to Clinical Applications. *Antibiotics*, *11*(3), Article 322. https://doi.org/10.3390/antibiotics11030322

Javdani, H., Khosravi, R., Etemad, L., Moshiri, M., Zarban, A., & Hanafi-Bojd, M. Y. (2020). Tannic acid-templated mesoporous silica nanoparticles as an effective treatment in acute ferrous sulfate poisoning. *Microporous and Mesoporous Materials*, *307*, Article 110486. https://doi.org/10.1016/j.micromeso.2020.110486

Joudeh, N., & Linke, D. (2022). Nanoparticle classification, physicochemical properties, characterization, and applications: a comprehensive review for biologists. *Journal of Nanobiotechnology*, *20*(1), Article 262. https://doi.org/10.1186/s12951-022-01477-8

Joyce, P., Ulmefors, H., Maghrebi, S., Subramaniam, S., Wignall, A., Jõemetsa, S., Höök, F., & Prestidge, C. A. (2020). Enhancing the Cellular Uptake and Antibacterial Activity of Rifampicin through Encapsulation in Mesoporous Silica Nanoparticles. *Nanomaterials*, *10*(4), Article 815. https://doi.org/10.3390/nano10040815

Kolawole, O. M., & Cook, M. T. (2023). In situ gelling drug delivery systems for topical drug delivery. *European Journal of Pharmaceutics and Biopharmaceutics*, *184*, 36–49. https://doi.org/10.1016/j.ejpb.2023.01.007

Krishnasamy, L., Senthilganesh, J., Saikumar, C., & Nithyanand, P. (2021). Biofilm-forming fluconazole-resistant Candida auris causing vulvovaginal candidiasis in an immunocompetent patient: A case report. *Asian Pacific Journal of Tropical Medicine*, *14*(2), 94-96. https://doi.org/10.4103/1995-7645.306768

Kumar, D., Banerjee, T., Pratap, C. B., & Tilak, R. (2015). Itraconazole-resistant Candida auris with phospholipase, proteinase and hemolysin activity from a case of vulvovaginitis. *The Journal of Infection in Developing Countries*, *9*(4), 435–437. https://doi.org/10.3855/jidc.4582

Li, Y., Cui, Z., & Hu, L. (2023). Recent technological strategies for enhancing the stability of lycopene in processing and production. *Food Chemistry*, *405*, Article 134799. https://doi.org/10.1016/j.foodchem.2022.134799

Li, Y., Li, B., Guo, X., Wang, H., & Cheng, L. (2023). Applications of quaternary ammonium compounds in the prevention and treatment of oral diseases: State-of-the-art and future directions. *Journal of Dentistry*, *137*, Article 104678. https://doi.org/10.1016/j.jdent.2023.104678

Liu, Z., Fontana, F., Python, A., Hirvonen, J. T., & Santos, H. A. (2020). Microfluidics for Production of Particles: Mechanism, Methodology, and Applications. *Small*, *16*(9), Article 1904673. https://doi.org/10.1002/smll.201904673

Mahalingam, S. S., Jayaraman, S., & Pandiyan, P. (2022). Fungal Colonization and Infections—Interactions with Other Human Diseases. *Pathogens*, *11*(2), Article 212. https://doi.org/10.3390/pathogens11020212

Manocha, S., Dhiman, S., Grewal, A. S., & Guarve, K. (2022). Nanotechnology: An approach to overcome bioavailability challenges of nutraceuticals. *Journal of Drug Delivery Science and Technology*, *72*, Article 103418. https://doi.org/10.1016/j.jddst.2022.103418

Marena, G. D., Ramos, M. A. dos S., Carvalho, G. C., de Lima, L. C., Nascimento, A. L. C. S. do, Sábio, R. M., Rodero, C. F., Spósito, L., Bauab, T. M., & Chorilli, M. (2022). Development and characterization of an amphotericin B - loaded nanoemulsion applied to Candida auris biofilms control. *Journal of Drug Delivery Science and Technology*, *74*, Article 103566. https://doi.org/10.1016/j.jddst.2022.103566

Marena, G. D., Ramos, M. A. dos S., Carvalho, G. C., Junior, J. A. P., Resende, F. A., Corrêa, I., Ono, G. Y. B., Sousa Araujo, V. H., de Camargo, B. A. F., Bauab, T. M., & Chorilli, M. (2022). Natural product-based nanomedicine applied to fungal infection treatment: A review of the last 4 years. *Phytotherapy Research*, *36*(7), 2710–2745. https://doi.org/10.1002/ptr.7460

Martins, F., Morgado, D. L., Sarmento, B., de Camargo, E. R., & das Neves, J. (2023). Chitosan-based sponges containing clotrimazole for the topical management of vulvovaginal candidiasis. *International Journal of Pharmaceutics*, *647*, Article 123508. https://doi.org/10.1016/j.ijpharm.2023.123508

Martins, J. P., & Santos, H. A. (2023). *Microfluidics as a Tool for the Synthesis of Advanced Drug Delivery Systems*. In Lamprou, D. (Ed.), *Nano- and Microfabrication Techniques in Drug Delivery* (pp. 321–364). Springer. https://doi.org/10.1007/978-3-031-26908-0_13

Mba, I. E., & Nweze, E. I. (2020). Mechanism of Candida pathogenesis: revisiting the vital drivers. *European Journal of Clinical Microbiology & Infectious Diseases*, *39*(10), 1797–1819. https://doi.org/10.1007/s10096-020-03912-w

Mesini, A., Saffioti, C., Mariani, M., Florio, A., Medici, C., Moscatelli, A., & Castagnola, E. (2021). First Case of Candida auris Colonization in a Preterm, Extremely Low-Birth-Weight Newborn after Vaginal Delivery. *Journal of Fungi*, *7*(8), Article 649. https://doi.org/10.3390/jof7080649

Miguel Sábio, R., Corrêa Carvalho, G., Li, J., Chorilli, M., & Santos, H. A. (2023). Advanced porous materials for antimicrobial treatment. *Nano Select,* 1-20. https://doi.org/10.1002/nano.202300114

Ministério da Saúde. (2022). *Protocolo clínico e diretrizes terapêuticas para atenção integral às pessoas com infecções sexualmente transmissíveis (IST)*. Ministério da Saúde. https://bvsms.saude.gov.br/bvs/publicacoes/protocolo_clinico_atecao_integral_ist.pdf

Nsairat, H., Khater, D., Sayed, U., Odeh, F., Al Bawab, A., & Alshaer, W. (2022). Liposomes: structure, composition, types, and clinical applications. *Heliyon*, *8*(5), Article e09394. https://doi.org/10.1016/j.heliyon.2022.e09394

Obeid, M. A., Alsaadi, M., & Aljabali, A. A. (2023). Recent updates in curcumin delivery. *Journal of Liposome Research*, *33*(1), 53–64. https://doi.org/10.1080/08982104.2022.2086567

Parra-Nieto, J., del Cid, M. A. G., Cárcer, I. A., & Baeza, A. (2021). Inorganic Porous Nanoparticles for Drug Delivery in Antitumoral Therapy. *Biotechnology Journal*, *16*(2), Article 2000150. https://doi.org/10.1002/biot.202000150

Parsana, H., Chotaliya, M., & Dudhat, K. (2023). Formulation and Evaluation of Itraconazole Novel Nanosuspension-Based In Situ Gelling System for Vaginal Candidiasis Using 24 Factorial Design. *BioNanoScience*, *13*(4), 1870–1884. https://doi.org/10.1007/s12668-023-01169-z

Peters, B. M., Yano, J., Noverr, M. C., & Fidel, P. L. (2014). Candida Vaginitis: When Opportunism Knocks, the Host Responds. *PLoS Pathogens*, *10*(4), Article e1003965. https://doi.org/10.1371/journal.ppat.1003965

Pongchaikul, P., Hajidariyor, T., Khetlai, N., Yu, Y.-S., Arjfuk, P., Khemthong, P., Wanmolee, W., Posoknistakul, P., Laosiripojana, N., Wu, K. C.-W., & Sakdaronnarong, C. (2023). Nanostructured N/S doped carbon dots/mesoporous silica nanoparticles and PVA composite hydrogel fabrication for anti-microbial and anti-biofilm application. *International Journal of Pharmaceutics: X*, *6*, Article 100209. https://doi.org/10.1016/j.ijpx.2023.100209

Prem, P. N., Balu, K. K., Gandhi, S., & Kurian, G. A. (2023). Preparation of fisetin loaded mesoporous silica nanocarrier to attenuate ischemia reperfusion injury. *Journal of Materials Research*, *38*(19), 4441–4453. https://doi.org/10.1557/s43578-023-01157-9

Sato, M. R., Oshiro-Junior, J. A., Rodero, C. F., Boni, F. I., Araújo, V. H. S., Bauab, T. M., Nicholas, D., Callan, J. F., & Chorilli, M. (2023). Enhancing Antifungal Treatment of Candida albicans with Hypericin-Loaded Nanostructured Lipid Carriers in Hydrogels: Characterization, In Vitro, and In Vivo Photodynamic Evaluation. *Pharmaceuticals*, *16*(8), Article 1094. https://doi.org/10.3390/ph16081094

Seck, M. C., Engo, P. E., Gueye, P. A. T., Faye, C., Mbow, M., Diongue, K., Diallo, M. A., Ndiaye, M., Badiane, A. S., & others. (2023). Identification and antifungal susceptibility of Candida species isolated from vulvovaginal candidiasis in Dakar. *Journal of Yeast and Fungal Research*, *14*(1), 1–7.

Sharifi-Rad, J., Rayess, Y. El, Rizk, A. A., Sadaka, C., Zgheib, R., Zam, W., Sestito, S., Rapposelli, S., & others. (2020). Turmeric and Its Major Compound Curcumin on Health: Bioactive Effects and Safety Profiles for Food, Pharmaceutical, Biotechnological and Medicinal Applications. *Frontiers in Pharmacology*, *11,* Article 01021. https://doi.org/10.3389/fphar.2020.01021

Sobel, J. D. (2023a). New Antifungals for Vulvovaginal Candidiasis: What Is Their Role? *Clinical Infectious Diseases*, *76*(5), 783–785. https://doi.org/10.1093/cid/ciad002

Sobel, J. D. (2023b). Role of Antifungal Susceptibility Tests in the Treatment of Vulvovaginal Candidiasis. *Current Infectious Disease Reports*, *25*(3), 29–32. https://doi.org/10.1007/s11908-023-00797-6

Sobel, R., Nyirjesy, P., Ghannoum, M., Delchev, D., Azie, N., Angulo, D., Harriott, I., Borroto-Esoda, K., & Sobel, J. (2022). Efficacy and safety of oral ibrexafungerp for the treatment of acute vulvovaginal candidiasis: a global phase 3, randomised, placebo-controlled superiority study (VANISH 306). *BJOG: An International Journal of Obstetrics & Gynaecology*, *129*(3), 412–420. https://doi.org/10.1111/1471-0528.16972

Su, R., Li, P., Zhang, Y., Lv, Y., Wen, F., & Su, W. (2023). Polydopamine/tannic acid/chitosan/poloxamer 407/188 thermosensitive hydrogel for antibacterial and wound healing. *Carbohydrate Polymers*, *302*, Article 120349. https://doi.org/10.1016/j.carbpol.2022.120349

Sukmawaty, M., Sartini, Permana, A. D., Mudjahid, M., Roska, T. P., & Rahman, L. (2023). Lipid Complex-Itraconazole in Thermosensitive Mucoadhesive Vaginal Gel to Enhance the Effectiveness of Therapy for Vulvovaginal Candidiasis: Formulation, Optimization, Characterization, and Ex vivo Evaluation. *Journal of Pharmaceutical Innovation, 18,* 1546-1559. https://doi.org/10.1007/s12247-023-09738-1

Sun, Z., Ge, X., Qiu, B., Xiang, Z., Jiang, C., Wu, J., & Li, Y. (2023). Vulvovaginal candidiasis and vaginal microflora interaction: Microflora changes and probiotic therapy. *Frontiers in Cellular and Infection Microbiology*, *13,* Article 1123026. https://doi.org/10.3389/fcimb.2023.1123026

WHO. (2022). *WHO fungal priority pathogens list to guide research, development and public health action* (World Health Organization (WHO). https://www.who.int/publications/i/item/9789240060241

Wu, L., Gou, K., Guo, X., Guo, Y., Chen, M., Hou, J., Li, S., & Li, H. (2021). Dual response to pH and chiral microenvironments for the release of a flurbiprofen-loaded chiral self-assembled mesoporous silica drug delivery system. *Colloids and Surfaces B: Biointerfaces*, *199*, Article 111501. https://doi.org/10.1016/j.colsurfb.2020.111501

Yang, H., Cui, X., Li, S., Cen, Y., Deng, T., Wang, J., Olsbye, U., & Fan, W. (2020). Developing a general method for encapsulation of metal oxide nanoparticles in mesoporous silica shell by unraveling its formation mechanism. *Microporous and Mesoporous Materials*, *305*, Article 110381. https://doi.org/10.1016/j.micromeso.2020.110381

Żyrek, D., Wajda, A., Czechowicz, P., Nowicka, J., Jaśkiewicz, M., Neubauer, D., & Kamysz, W. (2021). The Antimicrobial Activity of Omiganan Alone and In Combination against Candida Isolated from Vulvovaginal Candidiasis and Bloodstream Infections. *Antibiotics*, *10*(8), Article 1001. https://doi.org/10.3390/antibiotics10081001

CHAPTER 2

Prevalence of vulvovaginal candidiasis in Brazil: A systematic review

Gabriela Corrêa Carvalho, Rafaela Aparecida Prata de Oliveira, Victor Hugo Sousa Araújo, Rafael Miguel Sábio, Lídia Raquel de Carvalho, Taís Maria Bauab, Ione Corrêa, Marlus Chorilli*

Medical Mycology, v. 59, n. 10, pp. 946-957, 2021.

Reprinted with permission from Oxford University Press

Abstract

Vulvovaginal candidiasis (CVV) is a condition whose signs and symptoms are related to inflammation caused by *Candida* spp infection. It is the second leading cause of vaginitis in the world, representing a public health problem. The present systematic review comes with the proposal of analyze and identify the available evidence on CVV prevalence in Brazil, pointing out its variability by regions. For this, a systematic literature review was carried out with meta-analysis of cross-sectional and cohort studies, following the Preferred Reporting Items for Systematic Reviews and Meta-Analyzes (PRISMA) guide recommendations, and was registered in the International Prospective Register of Systematic Reviews (PROSPERO 2020 CRD42020181695). The databases used for survey were LILACS, Scielo, Scopus, PUBMED, Web of Science and CINAHL. Fifteen studies were selected to estimate CVV prevalence in the Brazilian territory. South and Southeast regions have higher prevalences than the North and Northeast regions, no data were found for the Midwest region. The estimated prevalence for Brazil is 18%, however, it is suggested that this number is higher due to underreporting and the presence of asymptomatic cases. Therefore, new epidemiological studies are recommended throughout Brazil, to elucidate the profile of this disease in the country, in addition to assisting in the elaboration of an appropriate prevention plan by state.

1. Introduction

Vulvovaginal Candidiasis (VVC) is a disease which signs and symptoms are related to inflammation resulting from infection by *Candida spp.* (Bonifácio et al., 2015; dos Santos Ramos et al., 2016; Sangamithra et al., 2013). After bacterial vaginosis, VVC is the most common cause of vaginitis and it is estimated that about 70-75% of women will present this pathology at some point in their lives (Anderson et al., 1989; Donders & Sobel, 2017; Sobel, 2007). According to Gonçalves and collaborators (2016), the incidence of VVC in different countries varies from 12.1% to 57.3%, where Brazil has the third highest index, behind only Nigeria and Tunisia (Amouri et al., 2011; Okungbowa et al., 2003). These data are reinforced by several other studies carried out in other countries such as Burkina Faso (Sangaré et al., 2018), Argentina (Mucci et al., 2017), Lebanon (Ghaddar et al., 2020), India (Krishnasamy et al., 2020), Saudi Arabia (Venugopal et al., 2020), Ghana (Konadu et al., 2019; Waikhom et al., 2020) and India (RANI et al., 2020), where the prevalence values obtained were within this range.

Despite VVC prevalence, in Brazil there is a lack and an out datedness of epidemiological data on this disease, what leads to VVC underestimation (Brandão et al., 2018). Which can be attributed not only to the fact that it is not a notifiable disease, but also due its asymptomatic cases (Brandão et al., 2018). This lack of information can be detected in other countries like India (Rani et al., 2020), Ethiopia (Tufa & Denning, 2019), Namibia (Dunaiski & Denning, 2019) Saudi Arabia (Venugopal et al., 2020) and Greece (Gamaletsou et al., 2016), where this lack of data motivated epidemiological studies to be carried out. In a study conducted in Mumbai, India, it was observed that 30.7% of women without VVC symptoms had Candida sp. in their vaginal microbiota (Pramanick et al., 2019). Although the prevalence of this disease varies according to the different regions (Farr et al., 2021) a similar value, 33.83%, was also observed by work carried out by researchers from Turkey on asymptomatic women (Cengiz et al., 2020).

It also stands out that as it is a local infection, not associated with mortality, patients sometimes do not look for a health service, leading to a self-medication, this fact also corroborates with underestimation data (Czechowicz et al., 2021; Venugopal et al., 2020; Yano et al., 2019). In a study conducted in the United States of America, 24.1% of women were self-diagnosed with VVC, which is worrying when thinking about self-medication and resistance to antifungals (Araujo et al., 2020; Yano et al., 2019).

Due to the fact that the data found in the literature regarding the epidemiological profile of VVC in Brazil are obsolete and incomplete, a new assessment about the behavior of this pathology is necessary. Considering the previous aspects, the present systematic review comes with the proposal to analyze and identify the available evidence on the prevalence of VVC in Brazil, pointing out its

variability in different regions and updating the data related to the epidemiological profile to assist in a better understanding about this pathology in the Brazilian territory.

2. Methodology

2.1. Protocol design and registration

A systematic literature review was carried out with a meta-analysis of cross-sectional and cohort studies. The study protocol was registered with the International Prospective Register of Systematic Reviews (PROSPERO) under the identification: PROSPERO 2020 CRD42020181695. This review followed the recommendations of the Preferred Reporting Items for Systematic Reviews and Meta-Analyzes guide (PRISMA) (Altman et al., 2015).

2.2. Defining the problem and establishing the guiding question

To perform the guiding question, it was used the PICO anagram (population; intervention; comparation and outcome), according to **Table 1**. It is worth mentioning that depending on the review method, not all elements of the PICO strategy are employed. In this review, the third element, the comparison, was not used (Santos et al., 2007).

Table 1: Description of the PICO strategy.

PICO strategy	Elaboration of the Study Strategy
Population	Women in any age group in Brazil diagnosed with vulvovaginal candidiasis
Intervention	Prevalence of vulvovaginal candidiasis
Comparation	Not applicable in this study
Outcome	Vulvovaginal candidiasis

Thus, the guiding question of this research was: "What is the estimated prevalence of vulvovaginal candidiasis in Brazil?"

2.3. Eligibility criteria

Cross-sectional studies conducted in Brazil that evaluated the prevalence of vulvovaginal candidiasis in women were considered eligible. To be included, the studies needed to present the prevalence or data that would make possible to calculate it. Inclusion criteria were established as primary studies whose sampling was carried out in Brazil that investigated the prevalence of VVC throughout life as a primary or secondary outcome in women of any age group, together with the population number at the time of the study. There was no time limitation or language restriction. Studies with a cohort design (incident cases) were not excluded because they present data from the

reference population and VVC prevalence data, making it possible to calculate the prevalence during the study period. Articles whose data did not favor the prevalence calculation, which had some type of intervention, books or book chapters, letters to the editor, dissertations, theses, opinions, essays, editorials, abstracts in annals, previous notes and review articles were excluded.

2.4. Information sources and search strategies

The search was carried out in the following databases: Latin American and Caribbean Literature in Health Sciences (LILACS), Scientific Eletronic Online (Scielo), Scopus (international database produced by Elsevier), PUBMED (international database produced by the National Center for Biotechnology information), Web of Science, Cumulative Index to Nursing, and Allied Health Literature (CINAHL). The descriptors used for the search, carried out in August 23, 2020, were: (epidemiology) and (Prevalence OR Prevalences) and (Incidence OR Incidences) and (Candidiasis, Vulvovaginal OR Vulvovaginal Candidiasis OR Vulvovaginal Moniliasis OR Genital Vulvovaginal Candidiasis OR Monilial Vaginitis OR Genital Candidiasis OR Vaginal Yeast Infections OR Vaginal Yeast Infection) and (Brazil). As an example, one of the search strategy in WebScience: (epidemiology) and ((Prevalence) OR (Prevalences)) and ((Incidence) OR (Incidences)) and ((Candidiasis, Vulvovaginal) OR (Vulvovaginal Candidiasis) OR (Vulvovaginal Moniliasis)OR (Genital Vulvovaginal Candidiasis) OR (Monilial Vaginitis) OR (Genital Candidiasis) OR (Vaginal Yeast Infections) OR (Vaginal Yeast Infection)) and (Brazil)

2.5. Selection of studies and data extraction

After searching the databases, the articles were selected in three stages. The first stage was performed by the title reading. Then, the second stage is the summary reading, highlighting those who responded to the objective proposed by this study, and finally the third stage was reading the full article, obeying the pre-defined inclusion and exclusion criteria (Moralejo et al., 2018). Aiming to minimize bias in the selection of articles, an open review process was carried out, where the article was evaluated by two researchers (Conterno et al., 2020; Higgins et al., 2019; Moralejo et al., 2018; Tacconelli, 2010). Articles selection was carried out independently, based on the eligibility criteria of the review, based on the guiding question. This is a scientific process that facilitates the improvement of the quality, accuracy, reading, and credibility of the content to be published (Nayak et al., 2005).

In the screening phase of the articles, each researcher registered the agreement or disagreement of the article in a screening program, Rayyan (Ouzzani et al., 2016). A form prepared by the authors was used to extract data from the selected studies with information about study period, city/state, study population, study population characteristic, study type, number of cases and prevalence 95%

confidence interval (CI). In this form was added information about latitude and longitude, population in the last census (2010) and estimated population (2020) and manuscript. For those articles where there was disagreement between the researchers, a third researcher made the decision to include or not (Corrêa et al., 2013; Munn et al., 2014, 2015).

2.6. Data analysis

Proportions and 95% confidence intervals (CIs) for each study in each region were calculated and the pooled proportion and 95% CI either. This pooled proportion was calculated based on the DerSimonian weights for the random effects model. The Cochran Q statistic and I^2 test was used to test heterogeneity (Andrade et al., 2019; Carvalho et al., 2017; Corrêa et al., 2013).

3. Results and discussion

In the searched databases 56 articles were found, of these, 5 were excluded for being duplicate. Of the remaining 51 articles, it was performed a pre-selection based on the reading of the title and abstract, where 28 articles were selected for reading in full. Only 15 articles met all inclusion criteria and were selected for analysis and data tabulation (**Figure 1**), being that three studies were carried out in pregnant women, one in patients with VVC symptoms and one conducted in women using intrauterine devices (IUDs). The other studies were carried out with women from a specific region or from a specific health unit. For the localization, a study was conducted in a northern city, four in northeastern cities, two in southern cities and six in southeastern cities and two studies neither identify the city nor state, not being used only for qualitative synthesis. No study was found in the Midwest region. **Table 2** highlights the main points of the studies in publication chronological order.

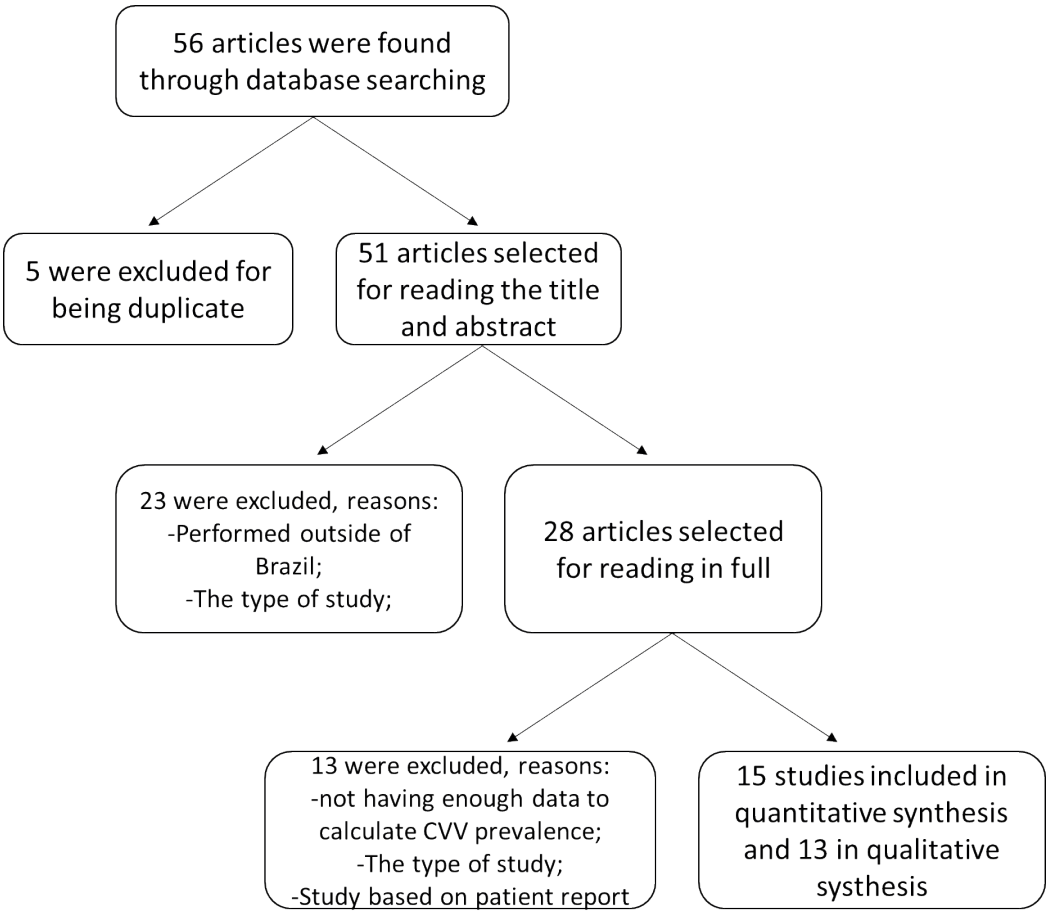

Figure 1: Search diagram.

Table 2: Articles about prevalence of vulvovaginal candidiasis in Brazil.

Study period	City/State	Study population	Study population characteristic	Study type	Number of cases	Prevalence	95% CI	Latitude/ Longitude *	Population in the last census (2010)**	Estimated population (2020)**	Reference
January to April 2016	Natal/ Rio Grande do Norte	41 samples	Pregnant patients	Cross-sectional	-	48.78%	-	5° 46' 45.3252" S 35° 12' 3.2976" W	803,739	890,480	(Brandão et al., 2018)
April 2013 to October 2014	Rio Grande/ Rio Grande do Sul	263 patients	Women assisted in Gynecology clinic of the University Hospital of the FURG	Cross-sectional	71	15%	-	32° 2' 43.368" S 52° 6' 57.096" W	197,228	211,965	(Brandolt et al., 2017)
September 2012, to January 2013	Botucatu/ São Paulo	1519 patients	Women aged 14–54 years attending 18 primary healthcare units	Cross-sectional	75	4.9%	0,3-0,9	22° 53' 9.3876" S 48° 26' 38.8248" W	127,328	148,130	(Marconi et al., 2015)
September 2008 to August 2010	Salvador/ Bahia	100 patients	Sexually active adolescents followed at an adolescent gynecology clinic	Cross-sectional	-	22%	14–30	12° 58' 39.8964" S 38° 30' 5.8644" W	2,675,656	2,886,698	(Mascarenhas et al., 2012)
September 2006 to February 2007	Botucatu/ São Paulo	245 patients	Low-risk pregnant women attending 8 Family Health	Cross-sectional	25	10.2%	-	22° 53' 9.3876" S 48° 26' 38.8248" W	127,328	148,130	(Gondo et al., 2011)

			Strategy of the Primary Care Services								
2006 to 2008	Botucatu/ São Paulo	289 patients	Low-risk pregnant women attending in the public Primary Care Service	Cross-sectional	34	11.8%	-	22° 53' 9.3876" S 48° 26' 38.8248" W	127,328	148,130	(Gondo et al., 2010)
March 2004	Serra Pelada/ Pará	209 patients	Women attended in the clinic	Cross-sectional	-	5.70%	2.6-8.8	20° 0' 16.596" S 41° 1' 47.352" W	-	-	(Miranda et al., 2009)
August 2003 to March 2004	Vitória/ Espírito Santo	299 patients	Women aged 15 to 49, assisted in an area served by the Family Health Program (PSF)	Cross-sectional	28	9.3%	1.3-5.3	20° 19' 0.6204" S 40° 18' 35.7156" W	327,801	365,855	(Barcelos et al., 2008)
-	Pacoti/ Ceará	592 patients	Women from seven hamlets and the center of the municipality, aged 12 to 49 years	Cross-sectional	74	12.50%	10.0-15.5	4° 13' 31.98" S 38° 55' 13.764" W	11,607	12,288	(Oliveira et al., 2007)
Septemb er 2002 to March 2004	-	130 patients	Patients with vulvovaginal candidiasis symptoms	Cross-sectional	-	63%	-	-	-	-	(Moreira & Paula, 2006)
October 2000 to	-	250 patients	Patients (regardless of symptoms)	Cross-sectional	69	27.60%	-	-	-	-	(Galle & Gianinni, 2004)

September 2001											
April to August 2002	Maringá/ Paraná	161 patients	Females who visited the laboratory for examinations of vaginal secretion	Cross-sectional	32	-	-	23° 25' 15.6" S 51° 55' 59.0016" W	35,.077	430,157	(Consolaro et al., 2004)
-	União dos Palmares/ Alagoas	341 patients	Women of reproductive age in rural Alagoas	Cross-sectional	20	5.8%	3.7–9.1	9° 9' 23.904" S 36° 1' 35.868" W	62,358	65,790	(Soares et al., 2003)
May to November 2001	Campinas/ São Paulo	223 patients	New users of IUD (TCu-380A IUD) in a family planning clinic	cohort study	12	5.40%	-	22° 55' 58.5264" S 47° 4' 25.842" W	1,080, 113	1,213,792	(Ferraz do Lago et al., 2003)
January 1998 to December 1999	-/Espírito Santo	205 patients	Women attending the Gynecology and Obstetric Ambulatory Clinic of the University of Espírito Santo	cohort study	78	-	-	-	-	-	(Ribeiro et al., 2001)

* Source: (*Latitude and Longitude Finder*, 2020); ** Source: (IBGE, 2020)

3.1. Southern and Southeast region

The Southern region of Brazil is composed of three states, having a territorial area of 576,783,781 km^2 (Garlet et al., 2019). Large part of this territory is in the South Temperate Climate Zone and the population is mostly composed of Caucasians (Pereira et al., 2015). Only two studies were found in this region, both performed on women attending a particular health service, with only one bringing the prevalence value of VVC in the study population, which was 15% (Brandolt et al., 2017; Consolaro et al., 2004). Consolaro at al. (2004) conducted a study in the city of Maringá, state of Paraná, and among their objectives sought to establish the correlation of colonies number and isolated species with VVC symptoms. It was observed that *C. albicans* was the most isolated in symptomatic women, while non-*C albicans* species were more isolated in asymptomatic women. It is also noted that the disease severity increases as a function of the increasing of isolated *C. albicans*. Additionally, in women with recurrent CVV (RVVC), *C. albicans* was the most isolated species. The correlation between the isolated species and the type of symptom was not statistically relevant.

In addition to RVVC being a cause of morbidity, its main problem is related to the resistance to conventional treatment (Sobel, 2016). Despite the study carried out in Maringá does not specify the age of the studied group in another study carried out in Brazil, it was observed that the most common age group is women with 24 years with RVVC patients. The authors justify by the occurrence of emotional stresses and the use of contraceptives, common at this age, both RVVC predisposing factors (Consolaro et al., 2004; Muniz, 2018). The increase in hormones, such as β-estradiol and progesterone, a common situation in the use of oral contraceptives and during pregnancy, favor the development of VVC because they positively influence both the fungus adhesion to epithelial cells and their resistance to drugs commonly used in therapy (Gonçalves et al., 2020; Luan et al., 2020).

Unlike the article carried out in Maringá, the other study conducted in the southern region, Rio Grande do Sul state, it was observed that *C. albicans* was the most isolated species in both groups, symptomatic and asymptomatic, 74.3 and 62.9%, respectively (Brandolt et al., 2017; Consolaro et al., 2004).

The Southeastern region, which has the highest number of studies, is the most populous in the country and an important economic hub for Brazil and South America. On the other hand, it is the second smallest Brazilian region having an area of approximately 1,000,000 km^2, consisting of four states, with a predominantly tropical climate. With a predominantly Caucasian population, its territory extends between 15 ° and 25 ° south latitude (Neto, 2005; Penna et al., 2020). Of the six studies carried out in this region, four were carried out in the state of São Paulo, of these one in the city of Campinas and three in the city of Botucatu. The rest were conducted in the state of Espírito Santo, one in the city of Vitória and the other not had the city identified.

Two of the three studies carried out in Botucatu were in low-risk pregnant women and the prevalence of VVC found was 10.2 and 11.8% (Gondo et al., 2010; Gondo et al., 2011). While Gondo et al. (2011) observed in his research that 92% of patients with VVC had symptoms, Gondo et al. (2010) realized that the prevalence had little association with symptoms, highlighting the importance of routine diagnosis. Asymptomatic VVC is known to be a risk factor for the patient as it may indicate previous therapeutic failure, resistance of the organism to complete eradication of the fungus and recolonization (Giraldo, 2000; Watson et al., 2013). VVC is a very common disease in women of reproductive age. It is worth mentioning that in the case of pregnant women, the risk becomes greater as this disease can be associated with complications such as premature rupture of membranes, chorioamnionitis, premature birth, and congenital cutaneous candidiasis (Aguin & Sobel, 2015).

The other study, also carried out in this city, has as a study group women of reproductive age (14–54 years) and the prevalence of VVC found was 4.9%. In this study it was observed that the detection of *Candida sp*. in the samples was inversely associated with the presence of bacterial vaginosis, 5.6 and 3.5% in patients with and without bacterial vaginosis, respectively (Marconi et al., 2015). This correlation pattern is in line with the literature where candidiasis showed a protective behavior against bacterial vaginosis (Guédou et al., 2013).

Finally, the other study carried out in the state of São Paulo was performed in the city of Campinas in women using TCu-380A IUDs. The prevalence observed in the study was 5.4%. Although this study also assessed the prevalence of bacterial vaginosis, the correlation between both illness was not determined. The authors pointed out that candidiasis was more significantly acquired after 6 months of using the device, but was significantly ceased without treatment (Lago et al., 2003). Due to the fact that Candida species have the ability to adhere to inert surfaces, tissue or at the air-liquid interface, IUD presence increases the chance of biofilm formation, favoring the occurrence of VVC. This virulence factor increases the pathogenicity of this fungus because biofilm consists of microorganisms' community, previously planktonic, highly organized attached to a surface. As a safe haven, it provides less susceptibility to drugs, increasing microbial resistance making it difficult to treat the patient (Borges et al., 2018; de Barros et al., 2020; Rodríguez-Cerdeira et al., 2019; Silva et al., 2012).

Due to the number of studies found in the literature for this State, it was possible to calculate the estimated prevalence of VVC. The data in **Figure 2** shows the general state prevalence and the 95% CIs for each selected study, based on a random effects model. Thus, it is possible to observe that the estimated prevalence of VVC for the state of São Paulo is 8%.

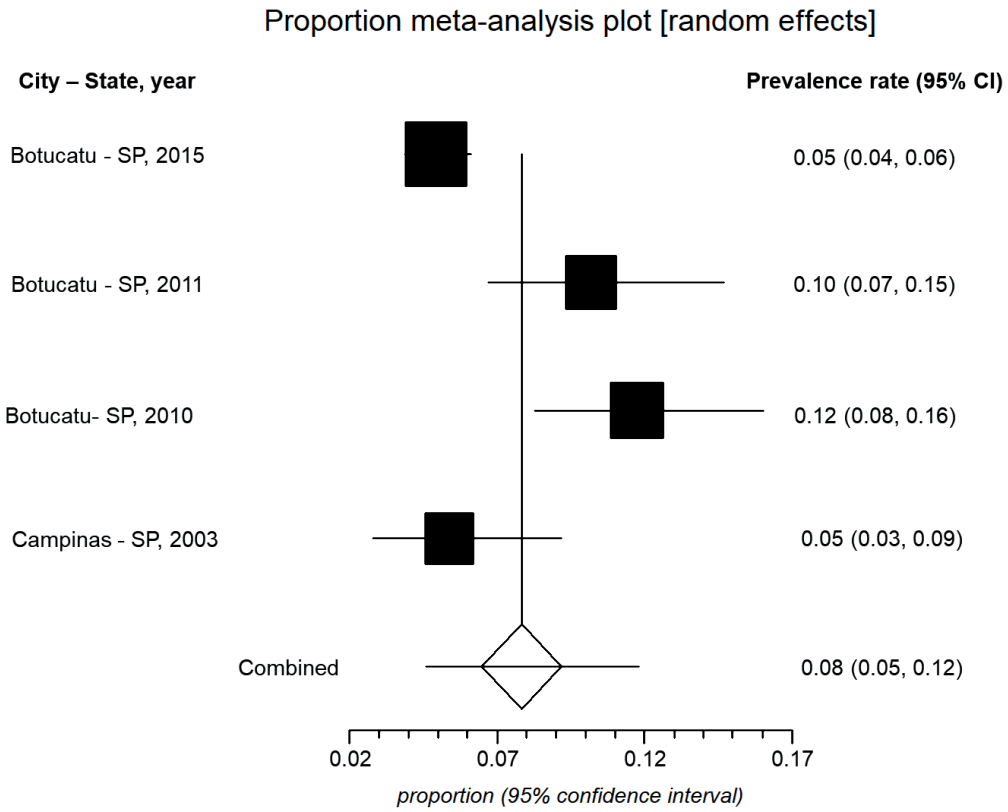

Figure 2: VVC prevalence in São Paulo state with 95% confidence interval. Legend: SP: São Paulo

For the state of Espírito Santo, the two selected studies targeted women served at a specific health service. The first study was carried out in the city of Vitória and had a VVC prevalence of 9.3%, while the other one had neither its city identified nor the calculated prevalence (Barcelos et al., 2008; Ribeiro et al., 2001). The study carried out in Vitória aimed to describe the prevalence and behavioral profile for genital infections in women seen at a local health service. Although it is not considered a sexually transmitted disease, the authors included it in the study because it is a frequent cause of demand for the health system by patients. It was noticed that the factors associated with genital infection were abnormal cervical mucus, previous human immunodeficiency virus (HIV) testing, having had more than one partner in the past year and having had more than a partner in life (Barcelos et al., 2008). Although it can be sexually transmitted, VVC is not considered a sexually transmitted disease because in addition to being part of the vaginal microbiota, it also affects celibate women (Davis, 2020).

The other study carried out in the state of Espírito Santo also focused on women attended by a health service. It is worth noting that the prevalence of this disease was higher in symptomatic patients than in asymptomatic patients, being 60 and 25%, respectively. It should also be noted that *C. albicans* was the most isolated species in both groups, 90 and 46%, respectively. The second most frequently isolated species was *C. glabrata*, 6 and 13%, respectively (Ribeiro et al., 2001). Several articles in the literature report *C. albicans* as the most prevalent species (El-Houssaini et al., 2019; Farahyar et al., 2020; Gerwien et al., 2020; Ghaddar et al., 2020; Krishnasamy et al., 2020; Maraki et al., 2019).

Based on the studies found for the Southern (except studies related to the state of São Paulo) and Southeast region, the estimated prevalence of VVC was calculated. The data in **Figure 3** shows the prevalence of these regions and the 95% CIs for each selected study, based on a random effects model. Therefore, the estimated prevalence of VVC for these regions is 23 %.

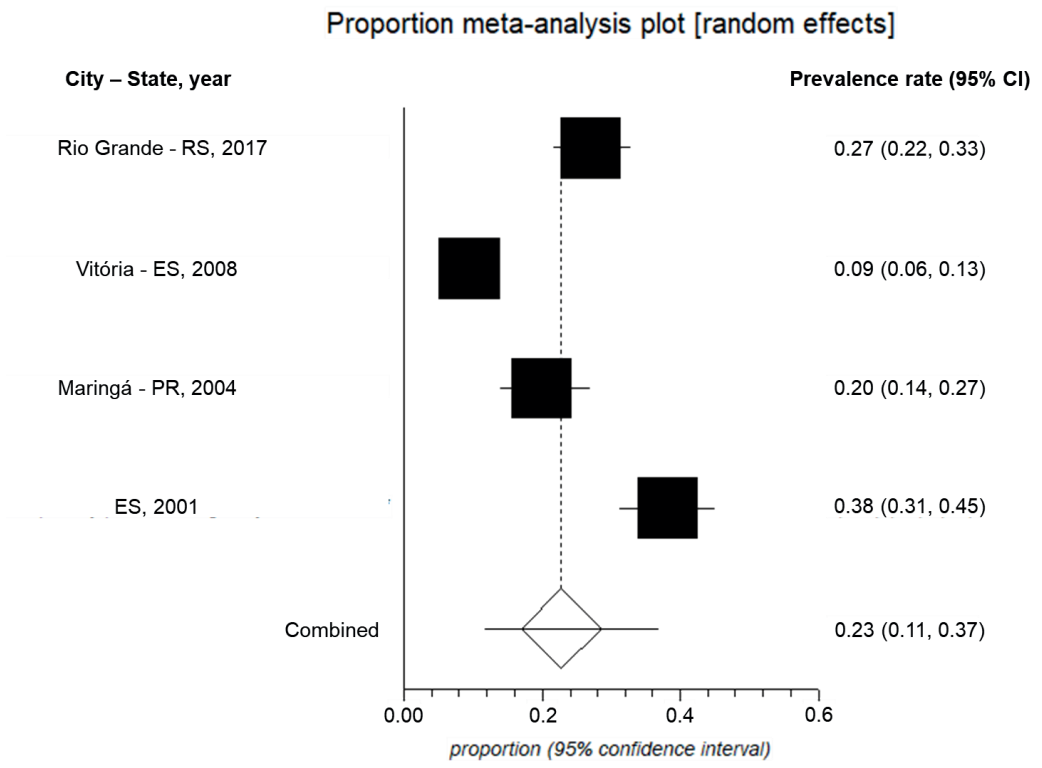

Figure 3: VVC prevalence in Southern and Southeast region with 95% confidence interval. Legend: RS: Rio Grande do Sul; ES: Espírito Santo; PR: Paraná.

3.2. Northern and Northeast Region

These two regions are the poorest in the country as they have the highest proportion of people living on ¼ of the minimum wage per capita (IBGE, 2015). The Northern region, made up of seven states, the Equator line passes in this region so the climate is predominantly tropical (Júnior et al., 2015). Despite being the largest region in the country, comprising 45% of the entire national territory, it has the lowest demographic density, attributable to the Amazon Forest that makes human habitation difficult. This region has a predominantly black and brown population (Cunha et al., 2017; IBGE, 2015).

In this region only one study was found which aims to describe the frequency of genital infections and the reproductive profile in women living in Serra Pelada, a mining region in the state of Pará. In the studied population, the prevalence rate for VVC was 5.7%. Although samples were collected to carry out this study, the authors highlighted that due to the low socioeconomic condition of the region, women do not have access to the clinical laboratory under normal primary care conditions and therefore the diagnosis of VVC is based on signs symptoms. Additionally, the rate of patients' adherence to the study, 14 % of local adult female population, considered high by the authors, reflects the lack of health services in the community, highlighting the need and the success that would be achieved with the implementation of the same (Miranda et al., 2009).

A diagnosis based only on signs and symptoms is not recommended because, besides being variable among patients, they are still nonspecific and can be confused with other pathologies leading to a misdiagnosis and wrong treatment. The use of laboratory tests to confirm the diagnosis is desirable because it avoids delays in the diagnosis, investigation of simultaneous infections and long-term complications. As later initialize the treatment, more severe the symptoms for the patients (Anderson et al., 2004; Mitchell, 2004; Sanches et al., 2020; Venugopal et al., 2020).

The Northeastern region, composed of nine states, has a territorial area of 1,588,196 km^2, approximately 18% of the entire Brazilian territory. Despite being located in a tropical region, it does not show the rainfall pattern, characteristic of this area, showing in some years to be an extremely dry area and others extremely rainy. It also presents three sub-climates, humid coastal climate, tropical climate, and semi-arid tropical climate (Costa et al., 2020; Lacerda et al., 2015). This region has a predominantly black and brown population (IBGE, 2015).

Four studies were found in this region. In the first study carried out in Rio Grande do Norte, the prevalence of VVC in symptomatic pregnant patients was 48.78%. The authors warned of the possibility of misdiagnosis and ineffective treatments, which elevate this disease as an economic public health problem. They also emphasized that because VCC is not a notifiable disease, it causes a shortage of epidemiological data (Brandão et al., 2018).

Another study also carried out in the northeast region, in Salvador, Bahia, was also motivated by the lack of epidemiological information, in this case in adolescent patients. The authors observed that the prevalence of VVC for the studied group was 22%. Although the association of this disease with risk factors (such as family income, education, ethnic groups, conjugal status, tobacco, alcohol and illegal drug use, age at first sexual intercourse, age at menarche, sexual abuse, condom and contraceptives use and number of sexual partners) was studied, no significant correlation was observed with any of them (Mascarenhas et al., 2012). On the other hand, in the study carried out in Maringá, the authors concluded that emotional stresses and the use of contraceptives are risk factors (Consolaro et al., 2004). In the study carried out in Campinas, IUD use was also considered a risk factor (Lago et al., 2003).

In a study carried out in Pacoti in Ceará, also in the Northeastern region of Brazil, the authors point out that population studies more accurately reflect a particular characteristic of a population than studies with a specific population, but these data are lacking in Brazil. In their study, the authors evaluated women of reproductive age who started the sexual life of seven hamlets in the municipality of Pacoti, and observed that the prevalence of VVC was 12.5%. In parallel, the authors assessed the prevalence of symptoms, and the most prevalent for this disease was abnormal vaginal discharge (56.8%) followed by Lower abdominal pain (50%) (Oliveira et al., 2007). However, in a study carried out in Botucatu, Southeast region, another pattern of prevalence of symptoms was observed, discharge (80,5%) followed by itching (56,1%) (Gondo et al., 2010). Evidencing the non-specificity of symptoms and the difficulty of obtaining precision in a diagnosis based only on signs and symptoms. In the last study carried out in the Northeast region, the authors determined the prevalence of sexually transmitted diseases in rural communities in the municipality of União dos Palmares, Alagoas. VVC had a prevalence of 5.8%, in addition vaginal pruritus had a significant association with VVC (Soares et al., 2003).

It was possible to calculate the prevalence of CVV for Northern and Northeast region based on the studies found. The data in **Figure 4** shows the prevalence and 95% CIs for each selected study in these regions, based on a random effects model. Thereby, remark was made that 16% is the estimated prevalence of CVV for these regions.

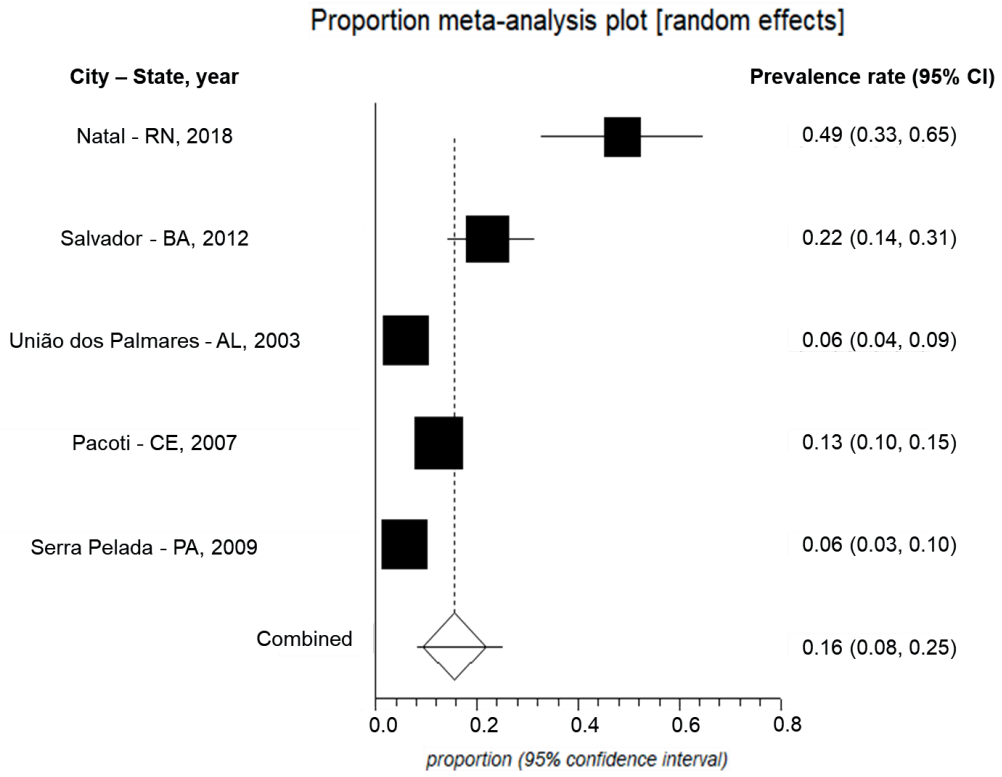

Figure 4: VVC prevalence in Northern and Northeast region with 95% confidence interval. Legend: RN: Rio Grande do Norte; BA: Bahia; AL: Alagoas; CE: Ceará; PA: Pará.

3.3. Midwest Region

This region has five states and covers an area of 1,606,371.5 km^2, with a predominance of brown population with a predominantly tropical climate (Castro et al., 2020; Pereira et al., 2015; IBGE, 2015). It should also be noted that the country's federal capital is located in this region (IBGE, 2020). No study was found in this region.

3.4. Brazilian territory

Brazil is the fifth largest country on the planet, with a territorial area of 8,510,295.914 km², and a population of 211,755,692 people (Castro et al., 2020; IBGE, 2020). From the 15 studies found, it was possible to calculate the estimated prevalence of CVV for Brazil. The prevalence of and the 95% CIs for each study, following a random effects model, is shown in **Figure 5**. Accordingly, it has been identified that the estimated prevalence of CVV for Brazil is 18%. The fact of the low prevalence for

a disease considered a public health issue worldwide, may be due to the fact that few studies have been found, showing the underreporting of this disease. This observation can be attributed to the lack of health services in the country, or to the cases of asymptomatic VVC (Brandão et al., 2018; Miranda et al., 2009; Venugopal et al., 2020).

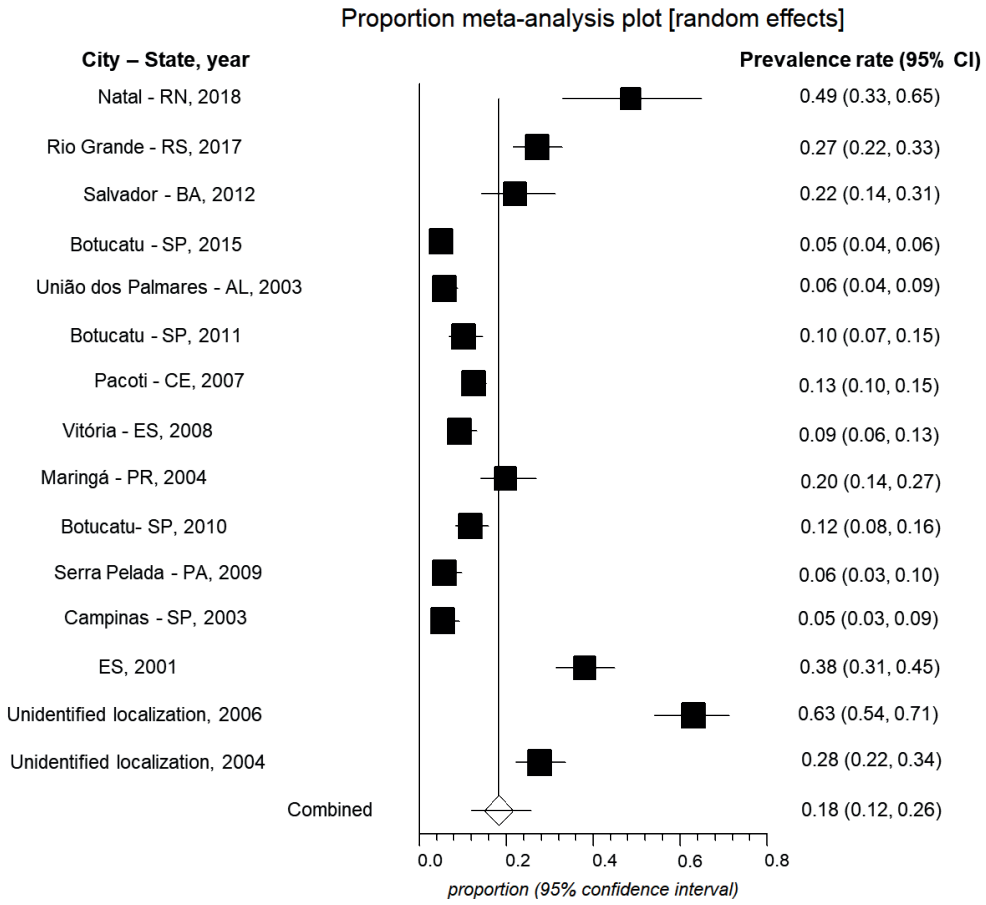

Figure 5: VVC prevalence in the Brazilian territory with 95% confidence interval. Legend: RN: Rio Grande do Norte; RS: Rio Grande do Sul; BA: Bahia; SP: São Paulo; AL: Alagoas; CE: Ceará; ES: Espírito Santo; PR: Paraná; PA: Pará

Due to the number of studies per state, it was possible to calculate the prevalence of VVC only for the state of São Paulo, whereas for the others it was necessary to group the regions. In the case of Brazilian regions, the South and Southeast regions have a higher prevalence than the north and northeast regions, as illustrated in **Figure 6**. On the other hand, it is worth noting that in spite of the

North and Northeast regions having a more favorable climate (the tropical one) for the growth of this fungi, due the relative humid environment, the low prevalence can be attributed the smaller number of articles recovered in these areas (Dou et al., 2015; Jackson et al., 2019).

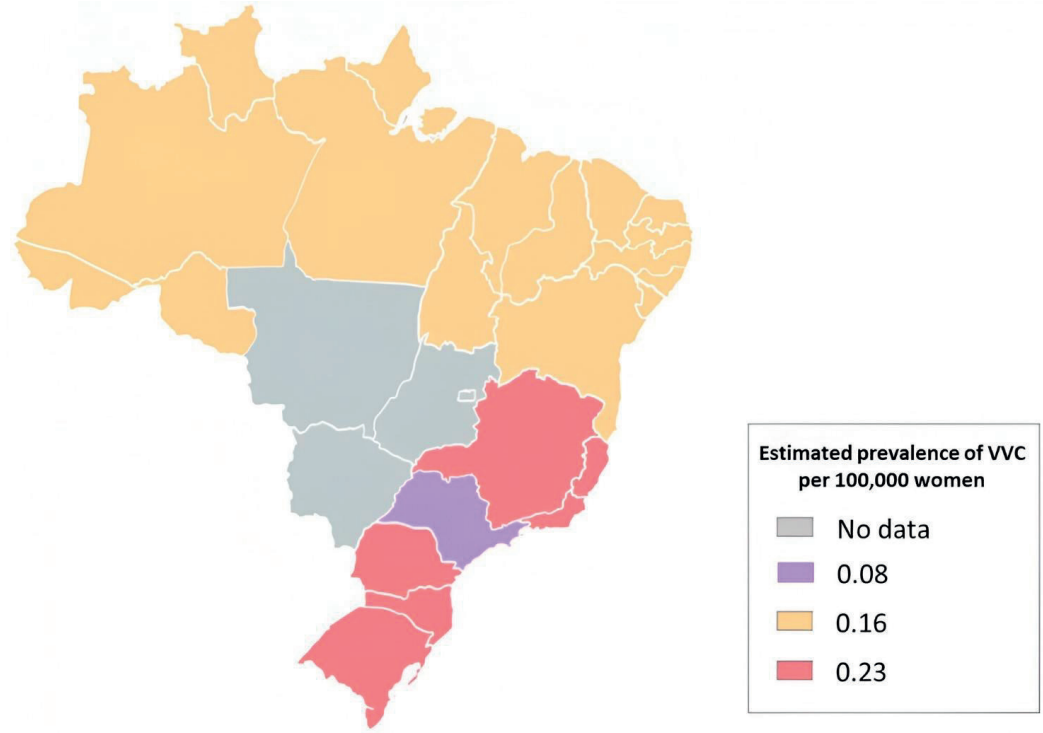

Figure 6: Brazil Regional Division and their estimated VVC prevalence

4. Conclusions

VVC is a worldwide public health problem. Although VVC is not considered a sexually transmitted disease, it can be transmitted sexually and, is therefore, prevalent in women of childbearing age. After the evaluation of a systematic literature review with a meta-analysis of cross-sectional and cohort studies the estimated prevalence of VVC in Brazil is 18%. Our studies suggest that this value may be higher in the Brazilian territory, due to the underreporting of this disease and asymptomatic cases. It is also noteworthy that if a greater number of studies were found by state, it would be possible to estimate the prevalence by state, a limiting factor of this review. Thus, the conduction of further epidemiological studies throughout Brazil is recommended to improve the knowledge of its real

prevalence, as well as that of each state. It would assist in elucidation of a better profile of this disease in Brazil, beyond the development of an adequate plan for its prevention by state.

5. Acknowledgments

This study was financed in part by the Coordenação de Aperfeiçoamento de Pessoal de Ensino Superior – Brasil (CAPES) – Finance code – 001.

6. References

Aguin, T. J., & Sobel, J. D. (2015). Vulvovaginal Candidiasis in Pregnancy. *Current Infectious Disease Reports*, *17*(6), Article 30. https://doi.org/10.1007/s11908-015-0462-0

Altman, D., Antes, G., Atkins, D., Barbour, V., Barrowman, N., Berlin, J. A., Clark, J., Clarke, M., Cook, D., D'Amico, R., & others. (2015). Main items to report Systematic reviews and Meta-analysis: The PRISMA recommendation. *Epidemiologia e Serviços de Saúde*, 24(2), 335-342.

Amouri, I., Sellami, H., Borji, N., Abbes, S., Sellami, A., Cheikhrouhou, F., Maazoun, L., Khaled, S., Khrouf, S., Boujelben, Y., & Ayadi, A. (2011). Epidemiological survey of vulvovaginal candidosis in Sfax, Tunisia. *Mycoses*, *54*(5), 499–505. https://doi.org/10.1111/j.1439-0507.2010.01965.x

Anderson, J., Cundiff, L., Schnars, B., Gao, M., Mackenzie, I., & Soll, D. R. (1989). Hypha formation in the white-opaque transition of Candida albicans. *Infection and Immunity*, *57*(2), 458–467.

Anderson, M. R., Klink, K., & Cohrssen, A. (2004). Clinician's Corner Evaluation of Vaginal Complaints clinical scenarios. *Jama*, *291*(11), 1368–1379. https://doi.org/10.1001/jama.291.11.1368

Andrade, U. V., Oliveira, S. M. do V. L. de, Chang, M. R., Pereira, E. F., Marques, A. P. da C., Carvalho, L. R. de, Mendes, R. P., & Paniago, A. M. M. (2019). Treatment compliance of patients with paracoccidioidomycosis in Central-West Brazil. *Jornal Brasileiro de Pneumologia*, *45*(2) Article e20180167. https://doi.org/10.1590/1806-3713/e20180167.

Araujo, V. H. S., Duarte, J. L., Carvalho, G. C., Silvestre, A. L. P., Fonseca-Santos, B., Marena, G. D., Ribeiro, T. de C., dos Santos Ramos, M. A., Bauab, T. M., & Chorilli, M. (2020). Nanosystems against candidiasis: a review of studies performed over the last two decades. *Critical Reviews in Microbiology*, *46*(5), 508–547. https://doi.org/10.1080/1040841X.2020.1803208

Barcelos, M. R. B., Vargas, P. R. M. de, Baroni, C., & Miranda, A. E. (2008). Infecções genitais em mulheres atendidas em Unidade Básica de Saúde: prevalência e fatores de risco. *Revista Brasileira de Ginecologia e Obstetrícia*, *30*(7). https://doi.org/10.1590/S0100-72032008000700005

Bonifácio, B. V., dos Santos Ramos, M. A., da Silva, P. B., Negri, K. M. S., de Oliveira Lopes, É., de Souza, L. P., Vilegas, W., Pavan, F. R., Chorilli, M., & Bauab, T. M. (2015). Nanostructured lipid system as a strategy to improve the anti-Candida albicans activity of Astronium sp. *International Journal of Nanomedicine*, *10*, 5081-5092. https://doi.org/10.2147/IJN.S79684.

Borges, K. R. A., Pimentel, I. V., Lucena, L. C. L. dos S., Silva, M. A. C. N. da, Monteiro, S. G., Monteiro, C. A., Nascimento, M. do D. S. B., & Bezerra, G. F. de B. (2018). Adhesion and biofilm formation of Candida parapsilosis isolated from vaginal secretions to copper intrauterine devices. *Revista Do Instituto de Medicina Tropical de São Paulo*, *60,* Article e59. https://doi.org/10.1590/s1678-9946201860059

Brandão, L. D. S., Boniek, D., Resende Stoianoff, M. A., da Mata, F. M. R., de Azevedo, P. R. M., Fernandes, J. V., & Andrade, V. S. (2018). Prevalence and antifungal susceptibility of Candida species among pregnant women attending a school maternity at Natal, Brazil. *Letters in Applied Microbiology*, *67*(3), 285–291. https://doi.org/10.1111/lam.13034

Brandolt, T. M., Klafke, G. B., Gonçalves, C. V., Bitencourt, L. R., Martinez, A. M. B. de, Mendes, J. F., Meireles, M. C. A., & Xavier, M. O. (2017). Prevalence of Candida spp. in cervical-vaginal samples and the in vitro susceptibility of isolates. *Brazilian Journal of Microbiology*, *48*(1), 145–150. https://doi.org/10.1016/j.bjm.2016.09.006

Carvalho, L. P., Agarwal, A., Kashiwagi, F. T., Corrêa, I., Pereira, J. E. G., & El Dib, R. (2017). Commonly-used versus less commonly-used methods in the loss of resistance technique for identification of the epidural space: A systematic review and meta-analysis of randomized controlled trials. *Journal of Clinical Anesthesia*, *38*, 41–51. https://doi.org/10.1016/j.jclinane.2017.01.017

Castro, I. A., Costa, L. D. C., Oliveira, A. C. R., Souza, M., Cardoso, D. D. P., Camargos, P. A. M., Costa, P. S. S., & Fiaccadori, F. S. (2020). Circulation profile of respiratory viruses in symptomatic and asymptomatic children from Midwest Brazil. *Brazilian Journal of Microbiology*, *51*(4), 1729–1735. https://doi.org/10.1007/s42770-020-00368-0

Cengiz, T., Özer, T. T., Kılınç, F., Selimoğlu, R., & Yılmaz, H. (2020). Candida albicans infection of cervix and comparison of Pap smear and culture in diagnosis. *Clinical and Experimental Obstetrics & Gynecology*, *47*(2), 253-256. https://doi.org/10.31083/j.ceog.2020.02.5193

Consolaro, M. E. L., Albertoni, T. A., Yoshida, C. S., Mazucheli, J., Peralta, R. M., & Svidzinski, T. I. E. (2004). Correlation of Candida species and symptoms among patients with vulvovaginal candidiasis in Maringá, Paraná, Brazil. *Rev Iberoam Micol*, *21*(4), 202–205.

Conterno, L. O., Turchi, M. D., Corrêa, I., & Monteiro de Barros Almeida, R. A. (2020). Anthelmintic drugs for treating ascariasis. *Cochrane Database of Systematic Reviews,* (4), Article CD010599. https://doi.org/10.1002/14651858.CD010599.pub2

Corrêa, I., Moralejo, D., Barretti, P., & El Dib, R. P. (2013). Interventions to improve adherence to guidelines on "Standard Precautions" for the control of healthcare-associated infections. *Cochrane Database of Systematic Reviews, (10),* Article CD010768. https://doi.org/10.1002/14651858.CD010768

Costa, R. L., Macedo de Mello Baptista, G., Gomes, H. B., Daniel dos Santos Silva, F., Lins da Rocha Júnior, R., de Araújo Salvador, M., & Herdies, D. L. (2020). Analysis of climate extremes indices over northeast Brazil from 1961 to 2014. *Weather and Climate Extremes*, *28*, Article 100254. https://doi.org/10.1016/j.wace.2020.100254

Cunha, M., Marques, R., & Dórea, J. (2017). Child Nutritional Status in the Changing Socioeconomic Region of the Northern Amazon, Brazil. *International Journal of Environmental Research and Public Health*, *15*(1), Article 15. https://doi.org/10.3390/ijerph15010015

Czechowicz, P., Neubauer, D., Nowicka, J., Kamysz, W., & Gościniak, G. (2021). *Antifungal Activity of Linear and Disulfide-Cyclized Ultrashort Cationic Lipopeptides Alone and in Combination with Fluconazole Against Vulvovaginal Candida spp., 13(10),* Article 1589. https://doi.org/10.3390/pharmaceutics13101589

da Gama Pereira, A. B. C. N., Sampaio Lacativa, M. C., da Costa Pereira, F. F. C., & Papais Alvarenga, R. M. (2015). Prevalence of multiple sclerosis in Brazil: A systematic review. *Multiple Sclerosis and Related Disorders*, *4*(6), 572–579. https://doi.org/10.1016/j.msard.2015.08.004

Davis, S. (2020). Bacterial vaginosis and Candida vulvovaginitis. *Professional Nursing Today*, *24*(3), 17–20.

de Barros, P. P., Rossoni, R. D., de Souza, C. M., Scorzoni, L., Fenley, J. C., & Junqueira, J. C. (2020). Candida Biofilms: An Update on Developmental Mechanisms and Therapeutic Challenges. *Mycopathologia*, 185 (3), 415-424. http://doi.org/10.1007/s11046-020-00445-w

Donders, G. G. G., & Sobel, J. D. (2017). *Candida vulvovaginitis: A store with a buttery and a show window*. *Mycoses, 60*, 70–72. https://doi.org/10.1111/myc.12572

Dou, N., Li, W., Zhou, E., Wang, C., Xiao, Z., & Zhou, H. (2015). Risk factors for candida infection of the genital tract in the tropics. *African Health Sciences*, *14*(4), 835. https://doi.org/10.4314/ahs.v14i4.10

Dunaiski, & Denning. (2019). Estimated Burden of Fungal Infections in Namibia. *Journal of Fungi*, *5*(3), Article 75. https://doi.org/10.3390/jof5030075

El-Houssaini, H. H., Elnabawy, O. M., Nasser, H. A., & Elkhatib, W. F. (2019). Correlation between antifungal resistance and virulence factors in *Candida albicans* recovered from vaginal specimens. *Microbial Pathogenesis*, *128*, 13–19. https://doi.org/10.1016/j.micpath.2018.12.028

Farahyar, S., Izadi, S., Razmjou, E., Falahati, M., Roudbary, M., Ashrafi-Khozani, M., Ansari, S., Fattahi, A., Ghahri-Mobaser, Z., & Rahimi, M. (2020). Low prevalence of antifungal resistant Candida africana, in the C. albicans complex causing vulvovaginal candidiasis. *Heliyon*, *6*(3), Article e03619. https://doi.org/10.1016/j.heliyon.2020.e03619

Farr, A., Effendy, I., Frey Tirri, B., Hof, H., Mayser, P., Petricevic, L., Ruhnke, M., Schaller, M., Schaefer, A. P. A., Sustr, & others. (2021). Guideline: Vulvovaginal candidosis (AWMF 015/072, level S2k). *Mycoses*, *64*(6), 583–602. https://doi.org/10.1111/myc.13248

Galle, L. C., & Gianinni, M. J. S. M. (2004). Prevalência e susceptibilidade de leveduras vaginais. *Jornal Brasileiro de Patologia e Medicina Laboratorial*, *40*(4). https://doi.org/10.1590/S1676-24442004000400004

Gamaletsou, M. N., Drogari-Apiranthitou, M., Denning, D. W., & Sipsas, N. V. (2016). An estimate of the burden of serious fungal diseases in Greece. *European Journal of Clinical Microbiology & Infectious Diseases*, *35*(7), 1115–1120. https://doi.org/10.1007/s10096-016-2642-8

Garlet, T. B., Ribeiro, J. L. D., de Souza Savian, F., & Mairesse Siluk, J. C. (2019). Paths and barriers to the diffusion of distributed generation of photovoltaic energy in southern Brazil. *Renewable and Sustainable Energy Reviews*, *111*, 157–169. https://doi.org/10.1016/j.rser.2019.05.013

Gerwien, F., Dunker, C., Brandt, P., Garbe, E., Jacobsen, I. D., & Vylkova, S. (2020). Clinical Candida albicans Vaginal Isolates and a Laboratory Strain Show Divergent Behaviors during Macrophage Interactions. *MSphere*, *5*(4). https://doi.org/10.1128/mSphere.00393-20

Ghaddar, N., Anastasiadis, E., Halimeh, R., Ghaddar, A., Dhar, R., AlFouzan, W., Yusef, H., & El Chaar, M. (2020). Prevalence and antifungal susceptibility of Candida albicans causing vaginal discharge among pregnant women in Lebanon. *BMC Infectious Diseases*, *20*(1), Article 32. https://doi.org/10.1186/s12879-019-4736-2

Giraldo, P. (2000). Vaginal colonization by Candida in asymptomatic women with and without a history of recurrent vulvovaginal candidiasis. *Obstetrics & Gynecology*, *95*(3), 413–416. https://doi.org/10.1016/S0029-7844(99)00577-3

Gonçalves, B., Azevedo, N. M., Henriques, M., & Silva, S. (2020). Hormones modulate Candida vaginal isolates biofilm formation and decrease their susceptibility to azoles and hydrogen peroxide. *Medical Mycology*, *58*(3), 341–350. https://doi.org/10.1093/mmy/myz070

Gonçalves, B., Ferreira, C., Alves, C. T., Henriques, M., Azeredo, J., & Silva, S. (2016). Vulvovaginal candidiasis: Epidemiology, microbiology and risk factors. *Critical Reviews in Microbiology*, *42*(6), 905–927. https://doi.org/10.3109/1040841X.2015.1091805

Gondo, D. C. A. F., Duarte, M. T. C., Silva, M. G. da, & Parada, C. M. G. de L. (2010). Abnormal Vaginal Flora in Low-Risk Pregnant Women Cared for by a Public Health Service: prevalence and Association with Symptoms and Findings from Gynecological Exams. *Revista Latino-Americana de Enfermagem*, *18*(5), 919–927. https://doi.org/10.1590/S0104-11692010000500012

Gondo, F., da Silva, M. G., Polettini, J., Tristao, A. da R., Peracoli, J. C., Witkin, S. S., & Rudge, M. V. C. (2011). Vaginal Flora Alterations and Clinical Symptoms in Low-Risk Pregnant Women. *Gynecologic and Obstetric Investigation*, *71*(3), 158–162. https://doi.org/10.1159/000316051

Guédou, F. A., Van Damme, L., Deese, J., Crucitti, T., Becker, M., Mirembe, F., Solomon, S., & Alary, M. (2013). Behavioural and medical predictors of bacterial vaginosis recurrence among female sex workers: longitudinal analysis from a randomized controlled trial. *BMC Infectious Diseases*, *13*(1), Article 208. https://doi.org/10.1186/1471-2334-13-208

Higgins, J. P. T., Thomas, J., Chandler, J., Cumpston, M., Li, T., Page, M. J., & Welch, V. A. (2019). *Cochrane handbook for systematic reviews of interventions*. John Wiley & Sons. http://www. cochrane-handbook. org

IBGE. (2020). *Conheça cidades e estados do Brasil*. Gov.br. https://cidades.ibge.gov.br/

IBGE, I. B. (2015). Síntese de indicadores sociais: uma análise das condições de vida da população brasileira - 2015. Instituto Brasileiro de Geografia e

Estatística.

Jackson, B. R., Chow, N., Forsberg, K., Litvintseva, A. P., Lockhart, S. R., Welsh, R., Vallabhaneni, S., & Chiller, T. (2019). On the Origins of a Species: What Might Explain the Rise of Candida auris? *Journal of Fungi*, *5*(3), Article 58. https://doi.org/10.3390/jof5030058

Júnior, E. G. M., Paiva, R. M. S. de, Ferreira, A. C., Pacopahyba, L. D., Tavares, A. S., Ferreira, F. A., & Pott, A. (2015). Updated checklist of aquatic macrophytes from Northern Brazil. *Acta Amazonica*, *45*(2), 111–132. https://doi.org/10.1590/1809-4392201402662

Konadu, D. G., Owusu-Ofori, A., Yidana, Z., Boadu, F., Iddrisu, L. F., Adu-Gyasi, D., Dosoo, D., Awuley, R. L., Owusu-Agyei, S., & Asante, K. P. (2019). Prevalence of vulvovaginal candidiasis, bacterial vaginosis and trichomoniasis in pregnant women attending antenatal clinic in the middle belt of Ghana. *BMC Pregnancy and Childbirth*, *19*(1), 341. https://doi.org/10.1186/s12884-019-2488-z

Krishnasamy, L., Rubini, D., Senthilganesh, J., Saikumar, C., Kumaramanickavel, G., Aruni, A. W., & Nithyanand, P. (2020). Phylogenetic characterization of biofilm forming multidrug resistant Candida albicans and Non albicans Candida causing vulvovaginal candidiasis. *Gene Reports*, *19*, Article 100644. https://doi.org/10.1016/j.genrep.2020.100644

Lacerda, F. F., Nobre, P., Sobral, M. C., Lopes, G. M. B., Chou, S. C., Assad, E. D., & Brito, E (2015). Long-term Temperature and Rainfall Trends over Northeast Brazil and Cape Verde. *Journal of Earth Science & Climatic Change*, *6*(8), Article 296. https://doi.org/10.4172/2157-7617.1000296

Lago, R. F., Simões, J. A., Bahamondes, L., Camargo, R. P. ., Perrotti, M., & Monteiro, I. (2003). Follow-up of users of intrauterine device with and without bacterial vaginosis and other cervicovaginal infections. *Contraception*, *68*(2), 105–109. https://doi.org/10.1016/S0010-7824(03)00109-4

Latitude and Longitude Finder. (2020). LatLong. https://www.latlong.net/

Luan, T., Liu, X., Mao, P., Wang, X., Rui, C., Yan, L., Wang, Y., Fan, C., Li, P., & Zeng, X. (2020). The Role of 17β-Estrogen in Candida albicans Adhesion on Human Vaginal Epithelial Cells via FAK Phosphorylation. *Mycopathologia*, *185(3),* 25-38. https://doi.org/10.1007/s11046-020-00440-1

Maraki, S., Mavromanolaki, V. E., Stafylaki, D., Nioti, E., Hamilos, G., & Kasimati, A. (2019). Epidemiology and antifungal susceptibility patterns of Candida isolates from Greek women with vulvovaginal candidiasis. *Mycoses*, *62*(8), 692–697. https://doi.org/10.1111/myc.12946

Marconi, C., Duarte, M. T. C., Silva, D. C., & Silva, M. G. (2015). Prevalence of and risk factors for bacterial vaginosis among women of reproductive age attending cervical screening in southeastern Brazil. *International Journal of Gynecology & Obstetrics*, *131*(2), 137–141. https://doi.org/10.1016/j.ijgo.2015.05.016

Miranda, A. E., Merçon-de-Vargas, P. R., Corbett, C. E. P., Corbett, J. F., & Dietze, R. (2009). Perspectives on sexual and reproductive health among women in an ancient mining area in Brazil. *Revista Panamericana de Salud Publica*, *25*, 157–161.

Mitchell, H. (2004). Vaginal discharge—causes, diagnosis, and treatment. *BMJ*, *328*(7451), 1306–1308. https://doi.org/10.1136/bmj.328.7451.1306

Moralejo, D., El Dib, R., Prata, R. A., Barretti, P., & Corrêa, I. (2018). Improving adherence to Standard Precautions for the control of health care-associated infections. *Cochrane Database of Systematic Reviews*, (2), Article CD010768 https://doi.org/10.1002/14651858.CD010768.pub2

Moreira, D., & Paula, C. R. (2006). Vulvovaginal candidiasis. *International Journal of Gynecology & Obstetrics*, *92*(3), 266–267. https://doi.org/10.1016/j.ijgo.2005.12.007

Mascarenhas, R. E. M., Machado, M. S. C., Silva, B. F. B. C., Pimentel, R. F. W., Ferreira, T. T., Leoni, F. M. S., & Grassi, M. F. R. (2012). Prevalence and Risk Factors for Bacterial Vaginosis and Other Vulvovaginitis in a Population of Sexually Active Adolescents from Salvador, Bahia, Brazil. *Infectious Diseases in Obstetrics and Gynecology*, *2012*, Article 378640. https://doi.org/10.1155/2012/378640

Mucci, M. J., Cuestas, M. L., Landanburu, M. F., & Mujica, M. T. (2017). Prevalence of Candida albicans , Candida dubliniensis and Candida africana in pregnant women suffering from vulvovaginal candidiasis in Argentina. *Revista Iberoamericana de Micología*, *34*(2), 72–76. https://doi.org/10.1016/j.riam.2016.09.001

Muniz, S. D. B. (2018). Prevalência de Candidiase Vulvovaginal recorrente em mulheres com idade entre 18 a 30 anos em uma unidade básica de saúde no municipio de cajazeiras-PB. *Journal of Biology & Pharmacy and Agricultural Management*, *15*(1).

Munn, Z., Moola, S., Lisy, K., Riitano, D., & Tufanaru, C. (2015). Methodological guidance for systematic reviews of observational epidemiological studies reporting prevalence and cumulative incidence data. *International Journal of Evidence-Based Healthcare*, *13*(3), 147–153. http://doi.org/10.1097/XEB.0000000000000054

Munn, Z., Moola, S., Riitano, D., & Lisy, K. (2014). The development of a critical appraisal tool for use in systematic reviews addressing questions of prevalence. *International Journal of Health Policy and Management*, *3*(3), 123-128. http://doi.org/10.15171/IJHPM.2014.71

Nayak, B. K., Maniar, R., Moreker, S., & others. (2005). The agony and the ecstasy of the peer-review process. *Indian Journal of Ophthalmology*, *53*(3), 153-155. http://doi.org/10.4103/0301-4738.16672

Neto, J. L. S. (2005). Decálogo da climatologia do sudeste brasileiro. *Revista Brasileira de Climatologia*, *1*(1), 43–60. http://dx.doi.org/10.5380/abclima.v1i1.25232

Okungbowa, F. I., Isikhuemhen, O. S., & Dede, A. P. O. (2003). The distribution frequency of Candida species in the genitourinary tract among symptomatic individuals in Nigerian cities. *Rev Iberoam Micol*, *20*, 60–63.

Oliveira, F. A., Pfleger, V., Lang, K., Heukelbach, J., Miralles, I., Fraga, F., Sousa, A. Q., Stoffler-Meilicke, M., Ignatius, R., Kerr, L. F. S., & Feldmeier, H. (2007). Sexually transmitted infections, bacterial vaginosis, and candidiasis in women of reproductive age in rural Northeast Brazil: a population-based study. *Memórias Do Instituto Oswaldo Cruz*, *102*(6), 751–756. https://doi.org/10.1590/S0074-02762007000600015

Ouzzani, M., Hammady, H., Fedorowicz, Z., & Elmagarmid, A. (2016). Rayyan—a web and mobile app for systematic reviews. *Systematic Reviews*,

5(1), Article 210. https://doi.org/10.1186/s13643-016-0384-4

Penna, A. C., Torres, R. R., Garcia, S. R., & Marengo, J. A. (2020). Moisture flows on Southeast Brazil: Present and future climate. *International Journal of Climatology*, *41*(S1), E935-E951. https://doi.org/10.1002/joc.6738

Pramanick, R., Mayadeo, N., Warke, H., Begum, S., Aich, P., & Aranha, C. (2019). Vaginal microbiota of asymptomatic bacterial vaginosis and vulvovaginal candidiasis: Are they different from normal microbiota? *Microbial Pathogenesis*, *134*, Article 103599. https://doi.org/10.1016/j.micpath.2019.103599

Ramos, M. S., de Toledo, L., Calixto, G., Bonifácio, B., de Freitas Araújo, M., dos Santos, L., de Almeida, M., Chorilli, M., & Bauab, T. (2016). Syngonanthus nitens Bong. (Rhul.)-Loaded Nanostructured System for Vulvovaginal Candidiasis Treatment. *International Journal of Molecular Sciences*, *17*(8), Article 1368. https://doi.org/10.3390/ijms17081368

Rani, E., Sahai, S., & Kumar, A. (2020). Importance of Socio-demographic Status of Symptomatic Vaginal Discharge in Females, North India. *IOSR Journal of Dental and Medical Sciences*, *19*(5), 11–16.

Ribeiro, M. A., Dietze, R., Paula, C. R., Da Matta, D. A., & Colombo, A. L. (2001). Susceptibility profile of vaginal yeast isolates from Brazil. *Mycopathologia*, *151*(1), 5–10. http://doi.org/10.1023/a:1010909504071

Rodríguez-Cerdeira, C., Gregorio, M. C., Molares-Vila, A., López-Barcenas, A., Fabbrocini, G., Bardhi, B., Sinani, A., Sánchez-Blanco, E., Arenas-Guzmán, R., & Hernandez-Castro, R. (2019). Biofilms and vulvovaginal candidiasis. *Colloids and Surfaces B: Biointerfaces*, *174*, 110–125. https://doi.org/10.1016/j.colsurfb.2018.11.011

Sanches, J. M., Giraldo, P. C., Bardin, M. G., Amaral, R., Discacciati, M. G., & Rossato, L. (2020). Laboratorial Aspects of Cytolytic Vaginosis and Vulvovaginal Candidiasis as a Key for Accurate Diagnosis: A Pilot Study. *Revista Brasileira de Ginecologia e Obstetrícia / RBGO Gynecology and Obstetrics*, *42*(10), 634–641. https://doi.org/10.1055/s-0040-1715139

Sangamithra, V., Verma, R., Sengottuvelu, S., & Sumathi, R. (2013). Candida infections of the genitourinary tract. *Research Journal of Pharmacy and Technology*, *6*(10), 1111–1115.

Sangaré, I., Sirima, C., Bamba, S., Zida, A., Cissé, M., Bazié, W. W., Sanou, S., Dao, B., Menan, H., & Guiguemdé, R. T. (2018). Prevalence of vulvovaginal candidiasis in pregnancy at three health centers in Burkina Faso. *Journal de Mycologie Médicale*, *28*(1), 186–192. https://doi.org/10.1016/j.mycmed.2017.08.006

Santos, C. M. da C., Pimenta, C. A. de M., & Nobre, M. R. C. (2007). The PICO strategy for the research question construction and evidence search. *Revista Latino-Americana de Enfermagem*, *15*(3), 508–511. https://doi.org/10.1590/S0104-11692007000300023

Silva, S., Negri, M., Henriques, M., Oliveira, R., Williams, D. W., & Azeredo, J. (2012). Candida glabrata, Candida parapsilosis and Candida tropicalis : biology, epidemiology, pathogenicity and antifungal resistance. *FEMS Microbiology Reviews*, *36*(2), 288–305. https://doi.org/10.1111/j.1574-6976.2011.00278.x

Soares, V. L., de Mesquita, A. M. T. S., Cavalcante, F. G. T., Silva, Z. P., Hora, V., Diedrich, T., de Carvalho Silva, P., de Melo, P. G., Dacal, A. R. C., de Carvalho, E. M. F., & Feldmeier, H. (2003). Sexually transmitted infections in a female population in rural north-east Brazil: prevalence, morbidity and risk factors. *Tropical Medicine and International Health*, *8*(7), 595–603. https://doi.org/10.1046/j.1365-3156.2003.01078.x

Sobel, J. D. (2007). Vulvovaginal candidosis. *The Lancet, 369*(9577), 1961-1971. https://doi.org/10.1016/S0140-6736(07)60917-9

Sobel, J. D. (2016). Recurrent vulvovaginal candidiasis. *American Journal of Obstetrics and Gynecology*, *214*(1), 15–21. https://doi.org/10.1016/j.ajog.2015.06.067

Tacconelli, E. (2010). Systematic reviews: CRD's guidance for undertaking reviews in health care. *The Lancet Infectious Diseases*, *10*(4), 226. https://doi.org/10.1016/S1473-3099(10)70065-7

Tufa, & Denning. (2019). The Burden of Fungal Infections in Ethiopia. *Journal of Fungi*, *5*(4), 109. https://doi.org/10.3390/jof5040109

Venugopal, D., Husain, K., Mustafa, S. A., & Sabeen, S. (2020). Epidemiology, risk factors and antimicrobial profile of Vulvovaginal Candidiasis (VVC): A study among women in the central region of Saudi Arabia. *Journal de Mycologie Médicale*, *31*(2), Article 101049. https://doi.org/10.1016/j.mycmed.2020.101049

Waikhom, S. D., Afeke, I., Kwawu, G. S., Mbroh, H. K., Osei, G. Y., Louis, B., Deku, J. G., Kasu, E. S., Mensah, P., Agede, C. Y., & others. (2020). Prevalence of vulvovaginal candidiasis among pregnant women in the Ho municipality, Ghana: species identification and antifungal susceptibility of Candida isolates. *BMC Pregnancy and Childbirth*, *20*(1), Article 266. https://doi.org/10.1186/s12884-020-02963-3

Watson, C. J., Fairley, C. K., Grando, D., Garland, S. M., Myers, S. P., & Pirotta, M. (2013). Associations with asymptomatic colonization with candida in women reporting past vaginal candidiasis: an observational study. *European Journal of Obstetrics & Gynecology and Reproductive Biology*, *169*(2), 376–379. https://doi.org/10.1016/j.ejogrb.2013.03.030

Yano, J., Sobel, J. D., Nyirjesy, P., Sobel, R., Williams, V. L., Yu, Q., Noverr, M. C., & Fidel, P. L. (2019). Current patient perspectives of vulvovaginal candidiasis: incidence, symptoms, management and post-treatment outcomes. *BMC Women's Health*, *19*(1), Article 48. https://doi.org/10.1186/s12905-019-0748-8

CHAPTER 3

Infection caused by *Candida auris*: state of the art

Gabriel Davi Marena[#], **Gabriela Corrêa Carvalho**[#], Luis Gustavo Silva Monazzi, Taiza Maschio-Lima, Margarete Teresa Gottardo de Almeida, Juliana Leal Monteiro dos Silva, Giovanna Capaldi Fortunato, Victor Hugo de Souza Araújo, Daniele Cristina Vitorelli Venancio, Marilene Rodrigues Chang, Marlus Chorilli[*]

[#]These authors contributed equally to this work

Mycosphere, v. 13, n. 1, pp. 820-861, 2022.

Reprinted under the Creative Commons Copyright License

Abstract

Candida auris, a new emerging yeast that was isolated for the first time in 2009 in the ear canal of a Japanese patient, has increasingly been associated with outbreaks, threatening the whole world. As a highly lethal and contagious microorganism, *C. auris* can be considered a threat to public health, mainly due to the high death rate in hospital environments and ability to resist to the main first-line antifungal agents (echinocandins, azoles and polyenes), what limits its treatment and infection control. As it is a microorganism with few scientific and clinical knowledge, controlling its infection is still a great challenge. Faced with the worrying situation, this review article presents important information about morphology and biology of *C. auris*, as well as resistance mechanism, updated epidemiology, virulence, immune response escape mechanism, pathogenesis and processor involved in the pathogenesis mechanism, clinical manifestations, laboratory diagnosis and sample collection methods, molecular diagnostics, infection treatment (main drugs used and future therapies) and prophylactic methods, with the objective of not only clarifying doubts of the scientific and medical population but also helping to control new outbreaks of *C. auris* worldwide.

1. Introduction

Fungal infections are becoming more and more frequent in the world. The main factors that influence fungus infections increase are population rise, displacement between regions/travels, growth of human habitats and the uncontrolled use of medicines (Guarner & Brandt, 2011). In short, these infections have gone from diseases caused by obscure agents rarely studied, to highly lethal and complex infections that affect the entire vulnerable population (Ostrosky-Zeichner & Sobel, 2016).

Among the most prevalent fungal infections, the ones caused by *Candida* species stand out. Single-celled yeasts of this genus are commonly found in the human microbiota (30 to 50% of individuals), as in the skin, lower gastro tract and genitourinary system. However, physiological disorders cause an imbalance in the body and promotes infections by these microorganisms such as superficial diseases, dermatitis, vulvovaginal candidiasis and candidemia (Evans, 2010). Therefore, *Candida* spp is an opportunistic microorganism, mainly affecting people with compromised immune system, chronic diseases (like diabetes, cirrhosis, pneumonia, kidney failure) and transplanted. Since under these conditions the organism is limited in defending itself from attacks, *Candida* ssp finds a favorable environment for its development and dissemination, changing from a commensal to a pathogenic condition (highly lethal) (Mba & Nweze, 2020).

Another factor that has caused the increase in *Candida* ssp. infections is the Coronavirus disease 2019 (COVID 19), a pandemic of global concern that has affected billions of people worldwide. Immune imbalance, increased length of stay in intensive care units, use of central venous catheters for extended times and broad-spectrum antimicrobial therapy may be the main factors of COVID 19 related to the increase in *Candida* ssp infection (Arastehfar et al., 2020; Pemán et al., 2020).

Infections in mucous membranes can affect the skin, being more common in the mouth, genitourinary system, ear, nails and skin. However, these infections can vary from superficial to deeper and systemic infections, reaching deep tissues and organs, such as kidneys, liver and brain, presenting mortality rates that can reach 60% (Das et al., 2011; Du et al., 2020; Smeekens et al., 2013; Sobel, 2007).

Among the most frequently isolated species, *C. albicans* is the most prevalent among fungal infections, affecting about 75% of women at least once in their lives. However, other non-*albicans* species are increasingly frequent, such as *C. glabrata, C. kruseis, C. tropicalis* and *C. parapsilosis*. Furthermore, the uncontrolled use of antifungal agents and climatic changes may favor new species emergence, that are even more resistant, such as *C. auris* (Poulain, 2015).

C. auris is an emerging pathogen first reported in the ear canal of a Japanese patient in 2009. The Centers for Disease Control and Prevention (CDC) (CDC, 2021) reports that clones of *C. auris* exist in different regions of the world, but they are different lineages. This new *Candida* specie may

have emerged due to changes in the environment and appeared simultaneously in different regions, with different characteristics, followed by subsequent transmission in hospital environments. When isolated and identified, resistance profiles after exposure to the antifungal were observed. However, its identification is hampered by the lack of scientific knowledge. Furthermore, the unknown prevalence of the population, uncertain environmental niches and unclear mechanisms of dissemination have made its control difficult (de Oliveira et al., 2019; Jeffery-Smith et al., 2018; Vallabhaneni et al., 2016). In addition to changes in the environment, the uncontrolled use of drugs such as echinocandins, amphotericin B and fluconazole may have contributed to the emergence of these new species of pathogenic fungus (Lockhart et al., 2017; Marena, Ramos, Carvalho, et al., 2022). Studies report that this uncontrolled use is related to the widespread use of these drugs, resulting in the isolation of other, even more resistant, *Candida* species. In addition, other circumstances such as prolonged treatment, repeated therapy in episodes of candidiasis or candidemia, use of single doses of oral and topical azoles are related to uncontrolled use of drugs, isolation of new resistant species and increased deaths around the world (Azoulay et al., 2012; Sujana et al., 2016).

Studies report the involvement of *C. auris* infection in the blood with high morbidity mortality in the world. This gets worse every year, mainly due to its ease dissemination, survival in the environment, ability to colonize very quickly on the patient's skin and greater transmissibility within the hospital environment, leading to severe and prolonged outbreaks. In addition, an alarming feature is its ability to persist on dry and wet surfaces, floors, sinks, air conditioning, skin, beds, nasal cavities and internal tissues of infected patients, being persistent on average for 7 days in these locations. It is estimated that approximately 4 hours is the minimum contact period for the acquisition of *C. auris* contamination. Furthermore, it can colonize and be expelled from the skin at a rate of approximately 10^6 cells/hours (Abastabar et al., 2019; Sekyere, 2018; Piedrahita et al., 2017; Schelenz et al., 2016).

Owning to the increased infections caused by *C. auris* and the difficulty of diagnosis and resistance, this review presents information that can contribute to the clinical scope with updated information about this new microorganism and what measures should be taken for a better diagnosis and therapy in order to address this major public health concern.

2. Epidemiology

With the first case of *C. auris* infection in 2009, researchers conducted a retrospective case study and found that *C. auris* had already been isolated and misidentified as *C. haemulonii*, where the first case was in 1996. These two yeasts have similarities and even today they can be confused if not correctly diagnosed (Cortegiani et al., 2018; Du et al., 2020). Since then, this species has spread throughout the world. Patients with *C. auris* have risks similar to those with other *Candida* species

with mortality associated with 30-70% of cases with prolonged illness, facilitating its spread in the hospital environment. Over time, many types of research have been carried out on this species, since it presents multi-resistance to the main classes of antifungal drugs, being therefore called today "Super fungus" (Chowdhary et al., 2016; Cortegiani et al., 2018).

Clade of South Asia (clade I), clade of East Asian (clade II), clade of South African (clade III), clade of South American (clade IV), and clade of Iranian (clade V) (Chow et al., 2019; Vila et al., 2020). The fifth Iranian clade was recently detected and has approximately 200,000 nucleotide polymorphisms distinct from the other clades. Its emergence in different geographic locations is still debatable, but the hypotheses include animals as a reservoir and climate change that leads to these microorganisms modifying themselves to adapt and maintain their species (Ahmad & Alfouzan, 2021; Chow et al., 2019; Forsberg et al., 2019).

Each clade of *C. auris* has variable characteristics, such as aggregative forms, virulence, resistance, growth time in culture medium and yeast size (Naicker et al., 2021). South American and South Asian clades are responsible for the greatest cause of bloodstream infections (between 47 and 76%). The South African clade can affect urinary tract infections/colonization (about 38%) (Tian et al., 2021). Clade II has isolates with a slower growth rate than the other clades. Clade I and Clade III present aggregated yeasts while Clade II species present a non-aggregative form (Ruiz-Gaitán et al., 2018). One study reported variability between clades I, II and IV exposed to UV radiation, and the results showed that non-aggregative species were more susceptible to UV radiation when compared to aggregative species (Chatterjee et al., 2020). The virulence factor was more evident for the South American side (Clade IV), according to infection results in mice (Forgács et al., 2020). Another study points out that Clade II is more susceptible to environmental stress and treatment with azoles and other antifungals. However, almost all Clade I, III isolates and approximately half of the Clade IV isolates are resistant to azoles (Muñoz et al., 2018). Furthermore, the isolates of Clades I and IV present genomic modifications that give them the characteristic of fluconazole resistance in the transcriptional factor TAC1b that regulates the Candida drug resistance 1 (CDR1) efflux pump. Finally, approximately 7% of the isolates of Clades I, III and IV show resistance to the echinocandin group (Muñoz et al., 2018). In view of this, *C. auris* has been reported in 44 countries (Vila et al., 2020) (**Figure 1**).

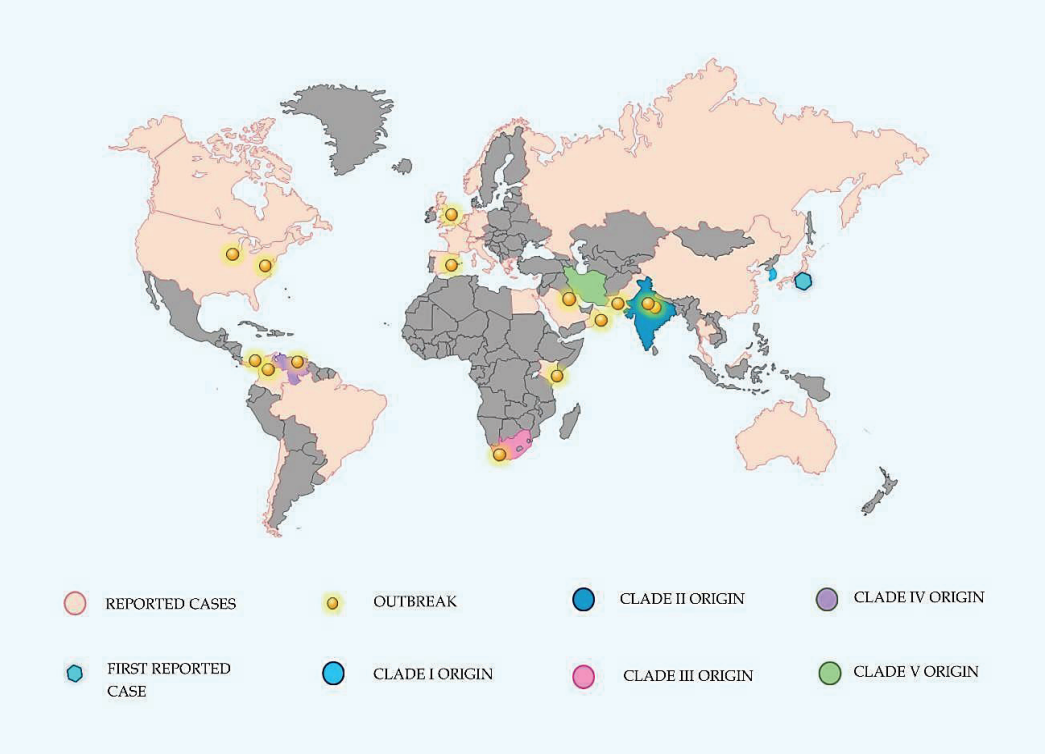

Figure 1: Reported cases of *Candida auris* around the world. Outbreaks of *C. auris* occurred in India, South Africa, Pakistan, Japan, Spain.

Cases of *C. auris* in the United States have increased dramatically in recent months. According to the CDC, this increase is related to local spread within health facilities. Among the states with the most cases of infection, New York, California, Illinois and Florida stand out with 285, 245, 242 and 135 cases, respectively. In 2017, New York, California, IIIinois, and Florida had 99, 1, 11, and 2 cases of *C. auris* infection, respectively, so a large increase in the number of cases in a short period of time is observed. Also in North America, between 2012 and 2019, Canada reported 24 cases of colonization due to infection caused by *C. auris* (CDC, 2021).

According to data from the European Center for Disease Prevention and Control (ECDC), 29 out of 30 European Union/ European Economic Area countries diagnosed cases of *C. auris* in May 2019. A total of 349 cases were reported and the countries with the most cases were: Spain (n = 291), England (n = 48), Germany (n = 3) and Holland (n = 2). Bloodstream infection was the most prevalent, 24% of reported cases. Among the cases, 92.8% were acquired in the local region and 5.4% were considered imported because they had a history of hospitalizations in countries with reported cases. In

another 1.7% of cases, the location of the possible acquisition of the infection was unknown (Plachouras et al., 2020).

On the Asian continent, the first case of *C. auris* in China was reported in 2018 in bronchoalveolar lavage (Wang et al., 2018). In 2021, another 38 cases were reported in China (Tian et al., 2021). Singapore (Tan & Tan, 2018) and Malaysia (Tap et al., 2018) also reported the first cases. In India, the first case was reported in 2013 (Chowdhary et al., 2013), however the numbers of reported cases increased in 2020 (15 cases in New Delhi), mainly due to the pandemic caused by COVID 19 (Chowdhary et al., 2020). In Japan, more than 300 strains were isolated from bloodstream between 2002 to 2013 (Ishikane et al., 2016). Kuwait, South Korea, Israel, Qatar Oman, Saudi Arabia, United Arab Emirates also reported cases of *C. auris* (Alfouzan et al., 2019; Kim et al., 2009).

The African continent had the first reported case of *C. auris* in 2009. However, this notification was only confirmed in 2014 as the infection was initially misidentified as *C. haemulonii* (a closely related yeast). South Africa has a clade separate from other clades around the world, with thousands of distinct nucleotide polymorphisms. This feature suggests that *C. auris* African arose independently of other clades and simultaneously on other continents (Ahmad & Alfouzan, 2021; Lockhart et al., 2017). By the year 2016, more than 1600 cases of *C. auris* were reported in South Africa (Ahmad & Alfouzan, 2021). It is worth highlighting that between the years 2016–2017, candidemia was the third most common cause in South Africa (Naicker et al., 2021).

In Oceania, the first case of *C. auris* reported in Australia was in 2018 (Lane et al., 2020), four cases were identified in Victoria and three in Sydney (Biswas et al., 2020). However, another study reports a case reported in 2015 in a 65-year-old visiting patient from Kenya with sternal osteomyelitis (Heath et al., 2019).

The first cases caused by *C. auris* in South America occurred between 2012 and 2016, and the first outbreak reached about 18 people in Venezuela, of which 13 were pediatric patients and all had previously uninvasive medical procedures, antibiotic therapy and was in the Intensive Care Unit (ICU). The yeast was found in clinical specimens of peritoneal fluid, cerebrospinal fluid, bone, urine, in addition to being responsible for causing fungemia in a percentage of infected patients (Santos et al., 2017).

In Colombia, cases were misdiagnosed at baseline and correctly diagnosed 28 days later. There were 17 isolates from 17 patients in 6 different hospitals, most samples were obtained from blood, and the rest from peritoneal fluid, cerebrospinal fluid, bone, or urine. Patients had a catheter and risk factors for candidemia. All had been treated before the diagnosis of *C. auris* with antibiotic and antifungal therapy, but the 30-day mortality rate was 35.2% (Morales-López et al., 2017).

Brazil presented three of the most recent reported cases of *C. auris* infection, both patients were hospitalized in the same intensive care unit due to complications of COVID-19, and curiously both isolated species were related to clade I (South Asia) (de Almeida et al., 2021).

3. Resistance and virulence

Resistance

The emergence of new highly pathogenic and multidrug-resistant microorganisms represents a global threat, causing disorder in the fight against infectious diseases (Fisher et al., 2018). Worrying consequences are observed in the area of health and economy, causing several world organizations such as the European Commission, CDC, World Health Organization (WHO), among others, recognize the alarming situation of the emergence of a new resistant fungus and the need for new studies and development of surveillance and control. The European Commission, for example, created the European Antimicrobial Resistance Surveillance System, a national surveillance organization with the aim of collecting comparable information and reliable tools with the aim of collecting variations in antimicrobial resistance over time, locating and providing the basis for evaluating the effectiveness of prevention programs and policy decisions (Bronzwaer et al., 2002).

The diagnosis of *C. auris* has increased over the years. New outbreaks of this new species have been reported in several regions and this is of extreme concern. This increase in outbreaks is related to the high resistance of this microorganism to antifungal therapy. Studies report the resistance of clinical isolates tested against all available antifungals (Spivak & Hanson, 2018).

The resistance presented by *C. auris* is very worrying, mainly due to the small number of isolated clinical strains that present sensitivity to conventional therapy. Studies indicate that *C. auris* has greater antimicrobial resistance when compared to other strains of the same species. Furthermore, clinical isolates from different regions have already shown low sensitivity to first-line antifungal agents. Among the factors related to resistance, there are genetic modifications, enzymatic activity and drug inhibition, biofilm and efflux pump (Kean & Ramage, 2019).

Many clinical samples of *C. auris* were isolated throughout the world and these clinical isolates showed multi-resistance to azoles, amphotericin B and echinocandins (Bidaud et al., 2018). Some genes found in *C. auris* genome are targeted by antifungal agents, such as the lanosterol 14 α-demethylase gene (ERG11) which is targeted by azoles, the 1.3-beta-glucan synthase gene (FKS1) target of the echinocandins group and the uracil phosphoribosyl-transferase gene that is a target of flucytosine. Genes, such as ERG11, mutate randomly and resistant genotypes (Y132F and K143R) are selected and maintained by other generations (Healey et al., 2018). These mutations were enough to modify the antifungal target site. 54 clinical isolates of *C. auris* and treated with antifungal agents were

evaluated. The results showed that *C auris* showed a resistance of 93, 54, 35, 7 and 6% to fluconazole, voriconazole, amphotericin B, echinocandins group and flucytosine, respectively (Chow et al., 2018; Muñoz et al., 2018).

Important mutations were evidenced in ERG11 in *C. auris* resistant to the azoles groups. Amino acid substitutions at position Y132 and K143 were detected in the ERG11 sequence. Studies have shown high resistance to fluconazole and voriconazole after heterologous overexpression of *C. auris* ERG11 -Y132 and ERG11 -K143 alleles (variant strains) in *Saccharomyces cerevisiae* (Lockhart et al., 2017).

Ergosterol is an abundant component present in the fungal membrane and is important in cell development. The enzyme lanosterol 14-alpha-demethylase (encoded by the ERG11 gene) is responsible for its synthesis by converting lanosterol into ergosterol (Chaabane et al., 2019). Some antifungals, like polyenes, act by inactivating this enzyme, preventing ergosterol biosynthesis and avoiding the development of fungal cells. However, some mutations located in the ERG11 gene (between amino acids 105-165, 266-287 and 405-488) promote less sensitivity to polyenes with activity against the ergosterol-forming enzyme, making the strains resistant to therapy. Genetic modifications in the ERG11 gene were detected in clinical isolates of Indian (Chowdhary et al., 2018) and Colombian (Healey et al., 2018) *C. auris*. Both isolates showed greater resistance to antifungal agents with enzymatic action of ergosterol inhibition (Chaabane et al., 2019; Vandeputte et al., 2012).

Modifications in the FKS1 gene are related to resistance to the echinocandin group, since the mutations promote changes in the drug's binding site. Thus, the inhibition of the 1-3-β-glucan synthase enzyme does not occur (Schelenz et al., 2016). Four isolates showed resistance to panechinocandin by amino acid substitution, S639F at position S645 of the FKS1 gene, which is associated with echinocandin resistance by *C. albicans* (Bidaud et al., 2018).

One of the main resistance mechanisms acquired by fungi is the efflux pump, since this resistance feature allows the microorganism to transport drugs from the interior of the cell to the outside, reducing the concentration of the drug inside the cell and the antimicrobial action, increasing fungal survival. Two types of efflux pumps can be highlighted: ATP Binding Cassette (ABC) and Major Facilitator Superfamily (MFS) transporters (Chaabane et al., 2019). Furthermore, about 2.4% of *C. auris* genes encode ABC and MFS along with other resistance factors such as iron transporters and oligopeptide transporters (Chatterjee et al., 2015).

The MFS are proteins embedded in the plasma membrane that act as H^+ anti-carriers (Vu & Moye-Rowley, 2018). Among the MFS superfamily there are two subfamilies of transporters, the transmembrane spans (TMS), within the transmembrane domain: DHA (drug: H^+ antiporter)1; (12 TMS), and the DHA2 (14 TMS) (Cannon et al., 2009). ABC are proteins found in prokaryotic and

eukaryotic cells, being important exporters of multiple drugs from inside the cells to the outside, thus, an important mechanism of microbial resistance. They are indiscriminate exporters and have the potential to structure a wide variety of substrates, metals, drugs, lipids and xenobiotics. A study indicated that the *C. auris* clinical isolated (CBS 10913T) recovered in 2009 from a Japanese patient presented 28 putative ABC proteins and that the presence of drugs promoted an overexpression of a wide variety of modified ABC transporters, suggesting a potential resistance mechanism of this strain (Wasi et al., 2019).

Molecular study show that the presence of proteins anchored by glycophosphatidylinositol (GPI), such as PLB3, IFF4, PGA52, PGA26, CSA1, HYR3, and PGA7 were observed in *C. auris* (which are also conserved in *C. haemulonii, C. duobushaemulonii* and *C. pseudohaemulonii*). These proteins were regulated by clinical strains of *C. auris* in biofilm formation and may be associated with the resistance mechanism (Muñoz et al., 2018), Zinc cluster transcription (TAC1) and protein kinases have also been identified in clinical strains of *C. auris*. These protein kinases are found in microbial stress, increasing the fungi tolerance against antifungal agents (Sharma et al., 2016).

In view of this, the speed that *C. auris* has in acquiring drug resistance are worrying. The low availability of antifungals and few therapeutic discoveries in recent years is even more alarming. All these factors contribute to the increase in outbreaks and new cases of infection caused by *C. auris*.

Virulence

Several clinical isolates from bloodstream showed high percentage of virulence and mortality in *in vivo* models (60 to 70% mortality) (Xin et al., 2019). The continuous increase in outbreaks related to systemic infection of *C. auris* is directly related to virulence factors, since these characteristics are responsible for the dissemination, persistence, resistance and maintenance of the species in several different geographic locations at the same time. The filamentation factors, enzymatic hydrolysis, biofilms, tolerance to temperature changes, osmo-tolerance and phenotypic exchange stand out as the main virulence mechanisms present in *C. auris* (Billamboz et al., 2021).

At first, it was believed that *C. auris* did not have the ability to form filaments. However, further studies discard this information, showing that this specie has a filamentous character. Initial studies also demonstrated that this potential is present in systemic infections in mammalian host, indicating that *C. auris* did not have filaments. In addition, three different types of *C. auris* were identified: typical cells, filament-competent cells and filamentous cells (Billamboz et al., 2021; Garcia-bustos et al., 2021; Yue et al., 2018).

Another important virulence factor in *C. auris* is its ability to survive in environments with high concentration of salt, allowing this specie to grow in places such as swimming pools, sea water

and even in human skin. Studies indicate the ability of *C. auris* to resist disinfectants (Jackson et al., 2019; Satoh et al., 2009). The literature informs that the high concentration of salt can promote morphological alteration in this fungus as an adaptation method to stress (Wang et al., 2018).

Most microorganisms that live on planet Earth are unable to survive at temperatures similar to those of the human organism. However, a virulence factor to be highlighted is *C. auris* survival at temperatures above 40 ºC. In fact, high temperatures caused by global warming may have contributed to the emergence and evolution of *this fungus* as a microorganism capable to survive at similar temperatures to the human body, especially in stress, causing infections (Casadevall & Kontoyiannis, 2019).

The enzymes produced by *C. auris* are capable of causing degradation of infected tissues to capture nutrients, favoring its spread. Furthermore, hydrolytic enzymes act by inhibiting the action of antimicrobials and the immune response, activating inflammatory mediators and provoking cell lysis. Among the main enzymes, proteinases, hemolysins, lipases and phospholipases can be emphasized (Billamboz et al., 2021; Chaffin, 2008).

Morphological plasticity is a very common strategic factor used by microorganisms to quickly adapt to climate change. These transitions are part of the virulence mechanism of *Candida* sp as well as *C. auris*. These microorganisms can spontaneously undergo morphological changes in response to weather signals, being important in the maintenance of the species (Du et al., 2020). Study indicates that *C. auris* can be in the form of single cells or in aggregated cells of the pseudo-hyphae type. In most cases, aggregated yeasts are more resistant to antifungal agents when compared to isolated cells. However, isolated cells have a significantly higher level of virulence (Singh et al., 2019).

Another important virulence factor is the evasion of the host's immune system, being observed that neutrophils are not as efficient for phagocytosis of *C. auris* compared to other *Candida* sp. It is not yet known what factors influence this condition (Bruno et al., 2020).

4. Biofilm

Biofilms are structures formed by a community of microorganisms, which may be composed of more than one species of microorganism (bacteria and fungus in a symbiotic association) aggregated on a biotic or abiotic surface and protected by an extracellular polymeric matrix (EPS). This matrix has the ability to protect microorganisms from the external environment, against immune response or drug attacks (Burmølle et al. 2014, Ramos et al. 2018).

Figure 2 shows the yeast biofilm formation scheme. In general, biofilm formation begins with the adhesion of planktonic yeast cells to surface and recognition of the location for the formation of a basal layer (A). After adhesion, cells begin to proliferate over the entire surface in a reversible manner

(B). The cells continue to proliferate and the production of EPS begins in an irreversible way (C). The amount of EPS increases with the development of mature biofilm (D). Finally, the amount of nutrients and toxins lead part of this biofilm to disintegrate, forming small groups of cell clusters or individual cells that deposit on another surface and originate a new cycle of biofilm formation (Burmølle et al. 2014, Tsui et al. 2016).

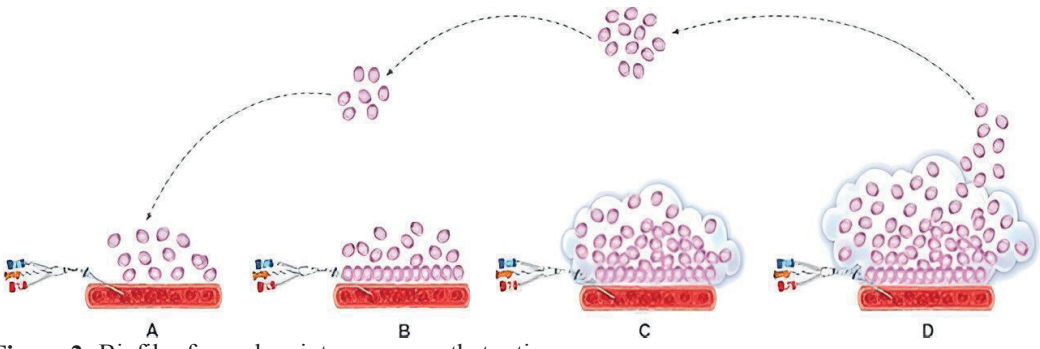

Figure 2: Biofilm formed on intravenous catheter tip.

Initially, there was not enough evidence that *C. auris* was able to form biofilms. However, years later, this fungus was recovered in several clinical materials, such as line ends catheters, neurological shunts, as well as in fomite materials in nosocomial environment and probes, suggesting that *C. auris* can form biofilms in both, hosts and surfaces. Furthermore, more sophisticated multi-omics techniques prove the formation of biofilms with high antifungal tolerance (Eyre et al. 2018, Kean & Ramage 2019).

Other study shows the alarming capacity of *C. auris* to form biofilms on hospital surfaces, favoring transmission between patients or environments (bedroom and intensive care unit), being considered an important factor in its installation and persistence in the environment of healthcare facilities (Uppuluri 2020).

C. auris biofilm has a large amount of blastoconidia and, occasionally, pseudo-hyphae composing a limited EPS. They are characterized by low susceptibility to antifungal agents, including azoles, polyenes and echinocandins (Billamboz et al. 2021). This fungus biofilm has the ability to resist antifungal agents that have effective activity against their planktonic counterparts (Sherry et al. 2017). Studies indicate that antifungals have activities in planktonic cells, however, the results are not satisfactory compared to biofilms treatment, requiring higher concentrations. Voriconazole had a Minimum Inhibitory Concentration (MIC) ranging from 8 to 32 µg/mL in planktonic cells, however, in biofilm it did not show effective activity up to 32 µg/mL. Micafungin MICs ranged from 0.5 to

0.0062 μg/mL, however, most tested strains showed resistance up to 32 μg/mL in biofilms (Pierce et al. 2006, Sherry et al. 2017).

Finally, biofilm is an extremely important defense mechanism for *Candida* sp, especially *C. auris*, which can defend itself from drug attack during treatment. Considered an intelligent adaptation and protection mechanism. Biofilms have become a threat in hospital environments, especially in the ICU. Associated with the biofilm, the mechanisms of virulence make this microorganism a global threat and a serious public health problem.

5. Pathogenesis and pathology

The clinical features of infection can be nonspecific and difficult to interpret in most cases since other systemic infections can present similar clinical presentations (Sekyere, 2018). However, what can facilitate the correct identification of a disease caused by *C. auris* are the signs and symptoms at the site of *C. auris* isolation, differentiating colonization from infection. Reports of patients with positive culture results in the skin, oropharynx, ear canal, respiratory and urinary tract (non-sterile areas of the body) without clinical signs, are probable more associated with colonization than infections (Chowdhary et al., 2016; Cortegiani et al., 2018; Jung et al., 2020).

Colonization by *C. auris* was detected, for example, in the nostrils, groin, armpit and rectum, and isolated for 3 months or longer after first detection, despite treatment in the intermediate period. In health services, these findings suggest the need for continuous patient isolation after treatment and on readmission, as they act as sources of contamination for other patients and for the environment (Jeffery-Smith et al., 2018; Vallabhaneni et al., 2016).

Invasive infections have increased, especially candidemia associated with invasive procedures (Kean et al., 2020; Sekyere, 2018). In fact, patients undergoing invasive procedures and devices are at greater risk of acquiring bloodstream infection, as catheters, for example, once they provide to the fungus easy access to the hematogenous route (Cortegiani et al., 2018; Rudramurthy et al., 2017). Other infections associated with urinary tract, respiratory tract, pericarditis, myocarditis, meningitis, skin abscesses, bone and wound infections have been related to *C. auris,* but is still poorly elucidated (Chowdhary et al., 2016; Jeffery-Smith et al., 2018; Rudramurthy et al., 2017).

The ability of *C. auris* to cause infection is attributed to several factors related to adhesion in host cells, biofilm formation, secretion of extracellular enzymes as phospholipases and proteinases. Pathogenicity processes have been elucidated *in vivo* in invertebrate, fish and murine models (Kean et al., 2020). Study performed by Fakhim et al. (2018) in murine observed that *C. auris* was able to produce lethal infections in immunocompetent mice, revealing in the histopathological examination a high fungal load in kidneys followed by spleen, liver and lungs, thus causing a disseminated infection,

in which only yeast cells without pseudo-hyphae formation were observed. However, Ben-Ami et al. (2018) observed cell aggregates in mouse kidneys, suggesting that aggregation may be a mode of immune evasion and tissue persistence.

According to Forgács et al. (2020), who also carried out a study in murine model, the heart and kidneys were the most affected organs and the fungal load results showed a correlation with lethality, that is, *C. auris* isolates with higher lethality produced high fungal loads, with the increase observed between the second and sixth day of infection. The presence of pseudo-hyphae in the tissues was not evidenced, however all the isolates produced large cell aggregates in the organs, except the spleen. In the histopathological findings, there were multiple foci of yeasts between the myofibers of the sub-endocardial myocardium and in the pericardium in the late stages of the infection, with the presence of coagulative necrosis of myocytes and loss of cross-striations of myocardial fibers. In the kidneys, there was multifocal infiltration in the parenchyma with destruction of the tubules and frequent areas of necrosis. In the liver large multifocal lesions were observed with central necrosis of the lobes and the presence of the fungi spread radially in the liver parenchyma. Unlike such organs, only yeast cells were seen in the spleen (Forgács et al., 2020).

The kidney, heart and brain were the organs with the highest fungal loads of *C. auris* in neutropenic and immunocompetent mice, according to a study carried out by Torres et al. (2020). In other organs such as bladder, uterus, spleen, intestines, stomach and lungs, the fungal load was modest. Histology revealed abscesses with necrotic cores in the kidneys expanding to the renal capsule and inflammatory foci with numerous neutrophils infiltrating the interstitium between renal tubules. Large abscesses also occurred in the heart with extensive inflammation spreading to the pericardium, with numerous intact yeasts in such abscesses and an inflammatory infiltrate rich in macrophages. In the brain, microabscesses with isolated and agglomerated yeasts were observed. The results also revealed viable *C. auris* cells shed in mice urine and feces.

6. Clinical manifestations

Candidemia

Around the world, *C. auris* infection is associated with severe invasive infection and candidemia. However, although few, non-invasive clinical isolates were detected in other locations, such as urinary tract, respiratory tract, skin, etc (Eyre et al., 2018).

The concern of *C. auris* to spread within the hospital environment exists all over the world. As well as other infections, *C. auris* can be acquired in the hospital, and the infection manifests itself within several weeks of patient admission. As a suggestion, there is an exogenous source, lack of control in the norms for fighting infection and inappropriate use of personal protective equipment.

There is already a strong hypothesis that central venous catheter (CVC), urinary catheter and surgical procedure act as entry points that result in introduction or reinfection, in which removal of catheters resolved several candidemia (Chowdhary et al., 2013; Lee et al., 2011; Lockhart et al., 2017).

Among the factors that may favor infection by *C. auris*, we can highlight the presence of catheters (central, venous and urinary), parenteral nutrition, surgical procedures, invasive medical devices, prolonged hospitalizations or hospitalizations in the intensive care unit, mechanical ventilation, previous or ongoing exposure to broad-spectrum antimicrobial therapy, immunosuppressive therapies. In addition to comorbidities such as diabetes mellitus, human immunodeficiency virus/ acquired immunodeficiency syndrome (HIV/AIDS), cancer and transplants (Sekyere, 2018).

The first three *C. auris* isolates from the bloodstream are from South Korea. One of the isolates was recovered from a blood culture on the 51st day of hospitalization of a pediatric patient who underwent surgery, as well as central catheterization and mechanical ventilation due to aspiration pneumonia and encephalopathy hypoxic, in which the patient was previously under treatment for candidemia caused by *C. albicans.* In another case, *C. auris* fungemia was diagnosed on the 53rd day of admission of a patient undergoing total laryngectomy who developed complications of aspiration pneumonia and lower gastrointestinal requiring antibiotics, central catheterization and angiographic embolization. In this patient, fungemia persisted until his death due to septic shock and multiple organ failure after seventy-one days of hospitalization. The third isolate came from a pediatric patient on her 12th day of hospitalization, who was undergoing chemotherapy with a recent history of colectomy after colitis perforation, the patient had a clinical picture of disseminated intravascular coagulation and the cause of death was reported as septic shock due to persistent fungemia (Lee et al., 2011).

Cases of candidemia by *C. auris* in a hospital in India were associated with some risk factors such as the use of indwelling urinary catheter, CVC, parenteral nutrition, admission to the intensive care unit and use of broad-spectrum antimicrobials. In addition to conditions more closely related to immunosuppression such as diabetes mellitus, chronic kidney disease, chronic obstructive pulmonary disease, cancer chemotherapy, HIV infection, neutropenia, and hematologic malignancies. The main source in these infections was attributed to urogenital colonization by yeast, as most patients used an indwelling urinary catheter, although no urine sample had been cultured. Most of these patients had persistent candidemia and in some of them sepsis and septic shock was present (Chowdhary et al., 2013).

Sepsis and septic shock were also present in cases of fungemia caused by *C. auris* in Venezuela. The affected patients had been admitted to intensive care units prior to *C. auris* isolation in blood culture, so they were already seriously ill and had been previously exposed to antibiotics and various

invasive medical procedures such as CVC and surgery (Calvo et al., 2016). In some cases of fungemia, in addition to blood culture, *C. auris* was isolated from other sites such as peritoneal fluid, catheter tip, urine, pharyngeal and rectal surveillance cultures (Ruiz-Gaitán et al., 2017). There is even a report of persistence of fungemia up to 3 weeks after starting antifungal treatment (Chowdhary et al., 2013).

Urinary tract infection

There are several reports that describe patients with proven or suspected candiduria of *C. auris* associated with candidemia (Ruiz-Gaitán et al., 2019; Vallabhaneni et al., 2017). Furthermore, episodes of recurrent candidiasis are likely features of persistent colonization (Al-Siyabi et al., 2017; Ruiz-Gaitán et al., 2019; Vallabhaneni et al., 2017).

Clinical conditions such as diarrhea and gastrointestinal decompression were associated with increased susceptibility to infection or colonization by *C. auris* in the urinary tract, acting as risk factors. In these cases, it is inferred that the source of *C. auris* could be the intestine, a region colonized by some *Candida* sp. Thus, it is believed that *C. auris* could migrate from the intestinal region to the urinary tract, resulting in infection or colonization; however, this hypothesis needs further investigation (Tian et al., 2018). Another study in mice showed that *C. auris* can easily aggregate in the kidneys, indicating that the possible cause of the invasive infection is due to the aggregation (Schelenz et al., 2016).

Patient with a history of ICU admission and diagnosed with obstructive ureteral stones, perirenal inflammatory changes, and moderate hydronephrosis, underwent ureteral stent and central venous catheter placement, obtained positive blood cultures and urine cultures for *C. auris*. It is also worth mentioning that the presence of *C. auris* was observed in cultures from the skin, armpit and groin one week after the end of antifungal treatment, confirming colonization. After discharge, the patient was advised to continue with hygiene care and hand washing in order to avoid recurrence (Anwar et al., 2020).

Incomplete identification and interpretation of *C. auris* presence in urine results in treatment difficulties as reported by Biagi et al. (2019). In this case, the patient was a nursing home resident, with comorbidities, such as quadriplegia, multiple chronic wounds, hip osteomyelitis with abscess formation and deep vein thrombosis in the upper limb. In addition to having chronic tracheostomy, chronic indwelling urinary catheter, enteral feeding tube and colostomy. Initially, this patient was admitted to the hospital, with positive blood cultures for bacteria (coagulase-negative *Staphylococcus* sp. and carbapenem-resistant *Klebsiella pneumoniae*) and positive urine cultures for *Candida* sp. which was considered by the medical staff as colonization, although imaging tests revealed a thickening of the bladder wall suggestive of cystitis. After treatment with antibiotics, blood cultures

became negative, but urine cultures remained positive for yeast, then, on the 27th day yeast was also isolated in the blood. However, the yeast was only identified as *C. auris* a few days later.

Respiratory tract infection

Patients with cystic fibrosis can acquire pulmonary infections, causing greater limitations to the lung and worsening of the clinical prognosis. These patients often have *Pseudomonas aeruginosa* infections that progress to a chronic phase. In a report, *C. auris* was isolated from the upper airways of a patient with cystic fibrosis associated with chronic *P. aeruginosa* infection without exacerbation for two years. In the case of this patient, due to the presence of excessive coughing with sputum production, a diagnosis of pulmonary exacerbation with subsequent deterioration of 30% in pulmonary function was made. At first, sputum cultures were positive for *Aspergillus fumigatus*, *Aspergillus terreus* and for *Candida* non-*albicans*, which was not identified at the specie level. After four months, a new culture repetition, using a throat smear, revealed the presence of *C. auris*, but it was not possible to determine whether the previously isolated *Candida* non-*albicans* was already *C. auris*. This was the first report of *C. auris* isolated in a patient with cystic fibrosis, highlighting the importance of correctly identifying the isolated yeasts at the species level. In addition, these patients undergo periods of hospitalization and are monitored in outpatient clinics, where colonization by *C. auris* can contribute to the spread of the fungus not only in the healthcare environment but also to other patients (Stathi et al., 2021).

C. auris was also isolated from bronchoalveolar lavage (BAL) from a patient hospitalized for nephritic syndrome, which is the first report of the identification of this *Candida* species in China. In complementary tests, it was observed that this isolate was susceptible to all antifungals tested, including amphotericin B, fluconazole and caspofungin (Wang et al., 2018). In another report, *C. auris* was isolated in BAL from a newly transplanted lung. In the pre-implantation culture *P. aeruginosa* and *Candida haemulonii* growth was observed, additionally Gram coloring reveled abundant yeast. Five days after the transplant, the patient developed pneumothorax due to complications from ventricular tachycardia, hypotension and respiratory arrest, requiring tubular thoracotomy and endotracheal intubation. Chest X-ray imaging revealed retrocardiac opacification and laboratory tests showed peripheral leukocyte counts of 28.000 cells/μL. The isolated yeast was submitted to the CDC for definitive identification and three days later the patient died. The CDC confirmed the identification of *C. auris*. This is another example of incorrect initial identification of *C. auris* (Azar et al., 2017).

Otitis

In a case of bilateral acute otomastoiditis caused by *C. auris*, sanguinolent secretions were observed in the ear canal on physical examination. The samples were sent for laboratory tests where the total white blood cell count (total of 54.600/μL) and C-reactive protein of 4.16 mg/dL were performed. Tomographic findings of the temporal bone showed fluid in both mastoid air cells, this fact was reversed after treatment with antifungal in which the tomography revealed good aeration of the temporal bone and tympanic cavities without any finding related to inflammation. However, before the patient improves, a ventilation tube was inserted, as well as surgical debridement for infection control. In this case, *C. auris* was isolated from a culture of ear secretion and a surgical specimen from the site of infection (Choi et al., 2017).

In another case, *C. auris* was isolated from a patient with recurrent complaints of otalgia and a history of treatment for clinically diagnosed otomycosis nine months before. This patient underwent oral surgery which resulted in an odontogenic brain abscess requiring hospitalization. During hospitalization, a computed tomography scan of the temporal bone showed chronic otitis media with mastoiditis and mastoid osteomyelitis, being treated with antibiotics. On a new admission for treatment of a left frontal brain abscess, the patient underwent tympanostomy with drainage of clear fluid and an ear drainage swab of *C. auris* was isolated. The fungus also grew in four repeated smears of secretion from the same ear, over a period of six weeks, also showing evidence of meningitis and external otitis with the presence of moist white debris and clear secretion (Schwartz & Hammond, 2017).

Study conducted by Jung et al. (2020) in a medical center in South Korea, observed that most patients, 87%, with positive culture for *C. auris* presented a clinical condition of chronic otitis media and had previously attended the otolaryngology clinic for complaints of otorrhea, ear fullness, dizziness, earache, hearing difficulty or itchy feeling. Few patients had suspected invasive infection when they had skull base osteomyelitis and surgical site infection after kidney transplantation.

Ear pain, intense itching, hearing loss and creamy white secretion in the ear canal were also clinical manifestations associated with *C. auris* infection. In the study performed by Abastabar et al. (2019), physical examination showed signs of inflammation, tympanic membrane perforation even without known trauma, and redness, the patient only reported that he used to swim in a public pool three times a week before the signs and symptoms appeared. The patient had repeated positive cultures for *C. auris* from the ear secretion, but in other areas such as the groin, armpits, oropharynx, rectum, respiratory and urinary tract the cultures were negative. Furthermore, environmental samples from patient contact areas at home negative cultures were also obtained.

Ophthalmitis

In rare report, *C. auris* was isolated from a case of pan-ophthalmitis, in which it was observed that this fungus is able to contribute to fulminant infection in an immunocompromised patient without a history of trauma, which resulted in loss of vision and structural eye integrity. In this case, the patient had HIV infection and syphilis, and initially presented fatigue, irritation and central blind spot in the visual field of the right eye. It then progressed to total vision loss in the right eye and difficulty in opening both eyes. Physical examination revealed periorbital edema, proptosis, chemosis and purulent discharge with the right pupil fixed and non-reactive to light. Magnetic resonance imaging revealed thrombosis of the cavernous sinus and orbit computed tomography suggested the occurrence of endogenous pan-ophthalmitis with orbital cellulitis, as there was no history of trauma, surgery or corneal ulceration. In vitreous cultures, *Pseudomonas aeruginosa* and yeast were isolated, which the support laboratory confirmed to be *C. auris* (Shenoy et al., 2019).

Pericarditis

C. auris was associated with a rare case of fungal pericarditis, the patient had several comorbidities such as chronic alcoholism, chronic liver disease, ascites and grade II hepatic encephalopathy. Initially the patient hospitalization, blood, sputum and ascitic fluid cultures were negative, but two weeks later she started with dyspnea, cough and sputum. Imaging examinations revealed gross bilateral crackles in the lower lung fields, interstitial edema and gross cardiomegaly, and pericardial effusion with tamponade. The patient was placed on ventilatory support and pericardiocentesis was performed with drainage of hemorrhagic fluid. Initially, fungus was observed in the culture, which were identified as *Candida haemulonii*. Later, urine, blood and bronchoalveolar lavage were collected. The isolates were sent for molecular identification that showed 99% similarity with a Korean isolate of *C. auris*. So, the yeast was mistakenly identified as *Candida haemulonii* by the commercial identification system VITEK®2 and later confirmed as *C. auris* by molecular methods (Khillan et al., 2014). In conclusion, this study shows the importance of correctly identifying the agent causing the infection for an effective and safe treatment.

Finally, the knowledge of the clinical manifestations as well as the pathology caused by the infection of *C. auris* is of crucial importance to the clinical environment, since it allows greater security in the decision making about the clinical condition of the patient. Furthermore, knowing the clinical features of an infection avoids possible misdiagnosis.

7. Immune response to *C. auris* infection

One of the reasons for the increase in the incidence of disease caused by fungi is the increase in the number of immunosuppressed patients. Among the main related factors are biological immunomodulatory agents for the treatment of autoimmune diseases, HIV transmission, viral hepatitis, chemotherapies, immunosuppressive therapies, internal medical devices such as intravenous catheters, prolonged hospitalization and especially in the use of broad-spectrum antibiotics (Oliveira et al., 2021).

Microorganisms, including fungi, have co-evolved with their mammalian hosts over the course of millions of years of existence. This fact is related to the emergence complex immune surveillance mechanisms in the host with the sophisticated strategies of fungi to antagonize the immune response (Romani, 2011).

Considered a fast and conserved mechanism, the innate immune response of hosts has the function of protecting the organism from the attack of pathogens and preventing the spread and infection. The defense mechanism established by the skin barrier, mucosal cells of the superficial epithelium, as well as defensins, collectins and microbial antagonism, recognize and control the entry of pathogenic fungi and possible infections. In addition, other cells contribute to the attack and control of infection, as well as phagocytic cells (monocytes, macrophages and neutrophils) and even non-phagocytic cells (endothelial and epithelial cells), which act by helping the innate response to fungi through the process of phagocytosis and direct killing of microorganisms (Johnson et al., 2018).

For optimal activation of the antigen-specific adaptive immune defense system to occur, activation of the innate immune system's pathogen detection mechanism must first occur. In the event of a fungal infection in a host, several pattern recognition receptors (PRRs) can be stimulated by pathogen-associated molecular patterns (PAMPs) by different combinations. This combination will depend on the type of fungal species and the types of cells involved. For example, the contribution of individual Toll-like receptors may vary depending on the fungal species, route of infection, fungal morphotypes, and receptor cooperativity (Romani, 2011).

The adaptive immune response mechanism of dendritic cells (DC) against a fungus will depend on the cooperation and specialization between DC subsets. It is known that the immune response mechanism of dominant T helper 1 (TH1) cells is correlated with the protective response against fungi. The important function of TH1 cells is to activate phagocytic cells (phagocytes) at the infection site. Therefore, any failure of phagocytes activation by T cells can cause serious damage to the body, causing overwhelming infections, limiting antifungal therapy, and favoring the persistence of fungal infection. This infectious persistence can cause the death of the patient. In addition, another important defense mechanism is the interleukin (IL) IL-4 and IL-13. These cytokines have the potent action of

providing proximal signals for the commitment of naive T cells to the T helper 2 cell lineage, for dampen the protective responses of TH1 cells and promote the alternative pathway of macrophage activation, causing allergic responses related to fungi and inhibition of the infection (Romani, 2011).

To ensure their survival inside the host the fungi have mechanisms that can “dribble” or “cheat” the host’s immune system, known as regulatory factors of the inflammatory response. By masking the detection signals performed by the host's immune system, the fungi can prevent the inflammatory response, favoring its spread, growth and opportunism at the site. The fungal structure is also a very important factor in this stage of infection and inflammatory inactivation. The fungal cell wall is an important dynamic structure that is constantly changing over time and during morphological changes. External stresses, cell growth and hyphae also affect the cell wall. These factors contribute to the decrease in the recognition of the host's defense cells, inactivating the inflammatory response and favoring the infection (Oliveira et al., 2021).

In general, the interaction between the fungus and the host's immune system can determine whether this microorganism will be considered commensal or threat to the organism, classifying it as a pathogen, however this factor can continually change (Romani, 2011).

Among the fungi, *Candida* spp. stands out because a small part of these species can commonly colonize the human microbiota, however, any physiological imbalance caused by immunosuppression or another underlying disease can make this microorganism pathogenic and cause infection. Among the most common species in invasive human infections are *C. albicans* and non-*albicans* species (Oliveira et al., 2021).

The immune defense mechanism against *Candida* spp. depends directly on an adjusted interaction between the innate immune response and the adaptive immune response. The first defense response against *Candida* spp. is the skin and mucosa, which act as a physical barrier. Fungi may not be recognized by innate immune defense cells, however, these cells can be recognized through PAMPs in the fungal wall by various PRRs located on the surface of immune defense cells, for example: C-type lectin receptors such as dectin-1, dectin-2, macrophage mannose receptor, non-integrin dendritic cell-specific intercellular adhesion, TLR2 and TLR4, which can activate mechanisms of microbial elimination such as phagocytosis, production of pro- and anti-inflammatory cytokines, and release of reactive oxygen species (ROS) (Bruno et al., 2020).

Despite the emergence of *C. auris* is well discussed earlier in this article, reporting its worrying transmission and severe invasive infection its pathogenicity mechanism is still debatable and new information emerges over time. *C. auris* has some similarities with other species of *Candida* sp., however, neutropenia has not been diagnosed for *C. auris*. In this case, the absence of neutropenia in

infections suggests that the neutrophil response may not be adequate to control the invasive infection of *C. auris* in the host (Nett, 2019).

Neutrophils are leukocytes of the innate immune system with a fundamental role in the control of systemic candidiasis, fighting the fungus by phagocytosis or by trapping extracellular neutrophils (NETs), which are structures of genetic material, proteins and histone. The phagocytosis mechanism practiced by neutrophils has more action against single yeasts, while NET has action against hyphae. However, one study reports that *C. auris* can elude the neutrophil response, causing neutrophils to be unable to phagocytose or release NETs effectively (Dominguez et al., 2019; Horton & Nett, 2020; Johnson et al., 2018). Research study using an alternative *in vivo* model of infected Zebrafish showed that neutrophil recruitment in *C. auris* infected groups was approximately 50% lower when compared to *C. albicans*. This result reinforces the worrying situation of *C. auris* eluding the immune response (Johnson et al., 2018). Furthermore, this information suggests that the innate defense cell cannot be activated in the face of a *C. auris* infection, justifying the high mortality rates (Rossato & Colombo, 2018).

The opposite is observed in mouse models, where the immune response of these rodents acts more effectively. One study reported that the response against *C. auris* was better when compared to *C. albicans*, with *C. auris* being less virulent. It is not clearly explained why the rodent immune system responds more effectively when compared to human neutrophils. What can be justified is the difference in neutrophil receptors between species. Furthermore, the virulence and resistance of *C. auris* can vary between species (Johnson et al., 2018). An *in vivo* study reported that several clinical isolates, as well as clades of *C. auris*, with the exception of clade V, show greater intensity of immune response when compared to *C. albicans*. Using a mouse model of systemic infection, the authors reported that phagocytes acted more effectively against *C. auris* infection when compared to *C. albicans*. In this study, was observed that the level of macrophage lysis and virulence of *C. auris* was lower (Bruno et al., 2020).

The way in which *C. auris* can activate/stimulate host defense cells is associated with the sequential involvement of the different components present in the fungal wall. The early (4 h) immune response is induced by β-glucans. This component, as well as mannans, were crucial in the recognition by defense cells (Bruno et al., 2020).

Neutrophils coordinate their recruitment against pathogens, cooperating in increasing antimicrobial activity. Swarming is a very important process in the containment of *C. albicans* and this process involves leukotriene B4, myeloperoxidase (MPO), ROS and NETs. Although the clusters were identical in size, the swarms formed by *C. auris* and *C. glabrata* were smaller when compared to the swarms formed by *C. albicans*, (Alex et al., 2020).

Among the most important mechanisms in swarming and restriction of fungal growth are ROS, MPO and NETs. In addition, the cytokines granulocyte macrophage colony stimulating factor and granulocyte colony-stimulating factor have the function of acting as mediators in swarming and increasing antifungal function (Alex et al., 2020).

One study reported a distinct stimulation of cytokine production in peripheral blood mononuclear cells (PBMCs) between *Candida* species compared *C. auris*. The results showed that *C. auris* induces robust transcriptional modifications in PBMCs in the human organism. This leads to include not only common pathways induced by *C. albicans*, but also by more robust specific interferons (IFN)-dependent transcription programs and explicit cytokine responses. A study reported the strong link between *C. auris* mannans with serum Immunoglobulin G (IgG) and the mannose binding lectin, this opsonization in human serum is necessary for the production of cytokines induced by *C. auris* mannan. This amount of cytokines is correlated with the specific properties of each clade of *C. auris*. Furthermore, this difference can influence colonization and persistence in the infected organism (Bruno et al., 2020).

One study used mice infected with *C. auris* and *C. albicans* to evaluate the immunological profile against these pathogens. According to the data, innate and adaptive immune system cytokine production against *C. auris* is fully functional in an immunocompetent host. *C. auris* has genes that provide mechanisms of virulence and resistance, as well as genes for the development of biofilms, aspartyl proteinases, phospholipases, lipases and secreted transporters (Rossato & Colombo, 2018). All these factors justify virulence, antifungal resistance and survival in natural niches and hosts (Du et al., 2020).

As previously discussed, yeast aggregation is associated with the mechanism of tissue invasion and the persistence of infection in the host. The aggregation mechanism practiced by *C. auris* hinders the immune response, developing a barrier preventing the action of defense cells. This barrier protects the pathogen from immune attack and contributes to its persistence in the body. Furthermore, this characteristic allows greater resistance of *C. auris* against the main antifungal agents (Du et al., 2020; Rossato & Colombo, 2018).

It is known that biofilms act as a protective mechanism for *C. auris* against the antifungal agent, making it resistant. However, the mechanism of immune response influenced by biofilms is still unknown (Nett, 2019). A study reported that *C. auris* clade III, related to invasive infection, induces a higher proportion of cytokines when compared to other clades and this higher production of cytokines is related to the ability to form aggregates (Bruno et al., 2020).

According to the information obtained, it is concluded that the body's immune response against *C. auris* can be considered as a classic antifungal mechanism. However, some specific responses are triggered by structures present in *C. auris* cells. It is important to emphasize that more information about the immunological profile and defense mechanisms needs to be further investigated.

8. Diagnosis

Once the infection confirmation and the etiological agent identification are essential to ensure a correct and effective treatment *C. auris* diagnosis is of fundamental importance, being generally carried out by combining the clinical condition with laboratorial exams (Hani et al., 2015).

The clinical samples collected are processed firstly for direct assay where it is possible to observe the feasible etiological agent. Next, the culture is carried out, by placing the isolate in substances favorable for the yeast growth, making it able to visualize its macroscopic characteristics and proceed with the diagnosis for the specie identification, where each one develops specific structures, different biochemical characteristics, enabling identify them and deal with most appropriate way. Therefore, it is worth mentioning that the correct diagnosis of the species involved in fungal infections is not only of epidemiological but also clinical interest. The great difficulty in diagnosis is related to the lack of sensitivity or specificity in laboratory techniques. These limiting factors make treatment difficult and worsen the patient's prognosis, where many end up dying due to incorrect diagnoses and ineffective treatment (Anane & Khalfallah, 2007; Zhang & Izadjoo, 2015).

Laboratory Diagnosis of C. auris

It is extremely important that infections caused by fungi or bacteria are detected as soon as possible, being a crucial step in effective antimicrobial treatment. Unfortunately, most mycology laboratories which use conventional phenotypic tests are not prepared to identify with the necessary speed and accuracy this important pathogen. In developing countries there is a lack of technology where *C. auris* is still unknown and even the most common *Candida* species are not identified at the species level (Saris et al., 2018).

In the past, the diagnosis of infection caused by species of the *Candida* sp. was performed using the classic laboratory approaches: microbiological, immunological and histopathological. However, the identification of *C. auris* requires specialized laboratory methods, since the conventional biochemical methods (manual and some automated systems) and those with based on morphological analysis (direct mycological examinations and microculture on slide) cannot identify it (McCarty & Pappas, 2016).

Classic microbiological methods (direct mycological examinations and culture) generally allow the identification of *Candida* sp. but do not identify *C. auris* (Pappas et al., 2018). Routine laboratory tests, especially in developing countries, can lead to delays in diagnosis of diseases caused by this yeast (Arastehfar et al., 2018).

Candida auris isolates were identified in different biological samples, including urine, blood, organs, eschar, bronchoalveolar lavage, abdominal pus, purulent exudate and central venous catheter tips (Almaghrabi et al., 2020; Ruiz-Gaitán et al., 2018). The emergence of *C. auris* has brought great concern to the development of new diagnostic protocols (Keighley et al., 2021).

The collection of clinical samples for the isolation and detection of *C. auris* depends on the anatomical site involved and is done in the same way for the diagnosis of candidiasis caused by other *Candida* sp. The collection can be made using rayon tip swabs, nylon flocked swabs or by using sponge sticks and placed in a zip-top bag containing 45 mL of phosphate-buffered saline (PBS) with 0.02% Tween 80 (Centers for Disease Control and Prevention, 2022; Welsh et al., 2017). It is worth mentioning that the semi-solid transport medium is the most advisable for dry swabs, as they preserve the microorganism viability (Chowdhary et al., 2017; Keighley et al., 2021; Bayona et al., 2020).

C. auris has been isolated from surveillance samples, including patient swabs from nose, skin, oropharyngeal, nasopharynx, rectum, axilla, groin, vulva, tracheostomy, and wounds (Chowdhary et al., 2017; Eyre et al., 2018; Leach et al., 2018; Welsh et al., 2017). It has also been isolated from environmental samples as reusable equipment, including axillary temperature probes and pulse oximeters (Eyre et al., 2018; Leach et al., 2018). The effective method and gold standard in the diagnosis of candidemia remain blood culture (21-75% in bloodstream infection, ~5-20% in abdominal candidiasis). Furthermore, the blood culture time in an incubator can last up to 7 days (Clancy & Nguyen, 2017; Pappas et al., 2018; Pitarch et al., 2018). **Table 1** presents information on the type of infection, biological samples usually collected and sample collection methods in patients infected with *C. auris*.

Table 1: Characteristics and method of collecting samples infected by *C. auris*.

Disease	Biological samples (n)	Collection method	Reference
Otitis	Purulent exudate	Ear exudate collection	(Pekard-Amenitsch et al., 2018; Satoh et al., 2009)
Candidemia	Blood	Aseptic venipuncture or catheter tip (central venous catheter)	(Castro et al., 2019; S. Das et al., 2018; Emara et al., 2015; Lee et al., 2011; Noginskiy et al., 2018; Parra-Giraldo et al., 2018)
Vulvovaginitis	Exudate	Aseptic collection of two high vaginal swabs	(Kumar et al., 2015)
Otomastoiditis	Bloody exudate	Ear exudate collection	(Choi et al., 2017; Schwartz & Hammond, 2017)
Preseptal cellulitis	Purulent exudate	Swab exudate collection	(Parra-Giraldo et al., 2018)
Urinary tract infection	Urine or Bedsore ulcer and urine	Urinary catheter or biopsy	(Almaghrabi et al., 2020; Tian et al., 2018)
Intra-abdominal infection	Abdominal washout surgical cultures	aspirate	(Almaghrabi et al., 2020)
Postoperative wound	purulent exudate	swab exudate collection	Almaghrabi et al., 2020)
Lung	Bronchoalveolar fluid	Bronchoalveolar lavage	(Almaghrabi et al., 2020; Wang et al., 2018)
Osteomielitis	Borne tissue	Biopsy	(Fernández-Chagüendo et al., 2020)
Spondylodiscitis	Tissue	Tissue collected during discectomy and curettage of the lumbar spine	(Supreeth et al., 2020)

Routine laboratory test

Direct mycological examination and staining techniques used in mycology laboratory routine do not differentiate *C. auris* from another *Candida* sp. However, they can be the laboratory's first step toward identifying species in the clinical sample (Mahmoudi et al., 2019). Although still widely used, conventional methods of diagnosis, such as microscopy and culture are essential in many investigations but lack sensitivity and can delay diagnosis (Avni et al., 2011). On microscopy, *C. auris* present spherical morphology, with many oval-elongated buds (single or aggregated), smooth surface and a size of approximately 2.0–3.0 x 2.5 –5.0 μm (**Figure 3**) (Kathuria et al., 2015; Satoh et al., 2009).

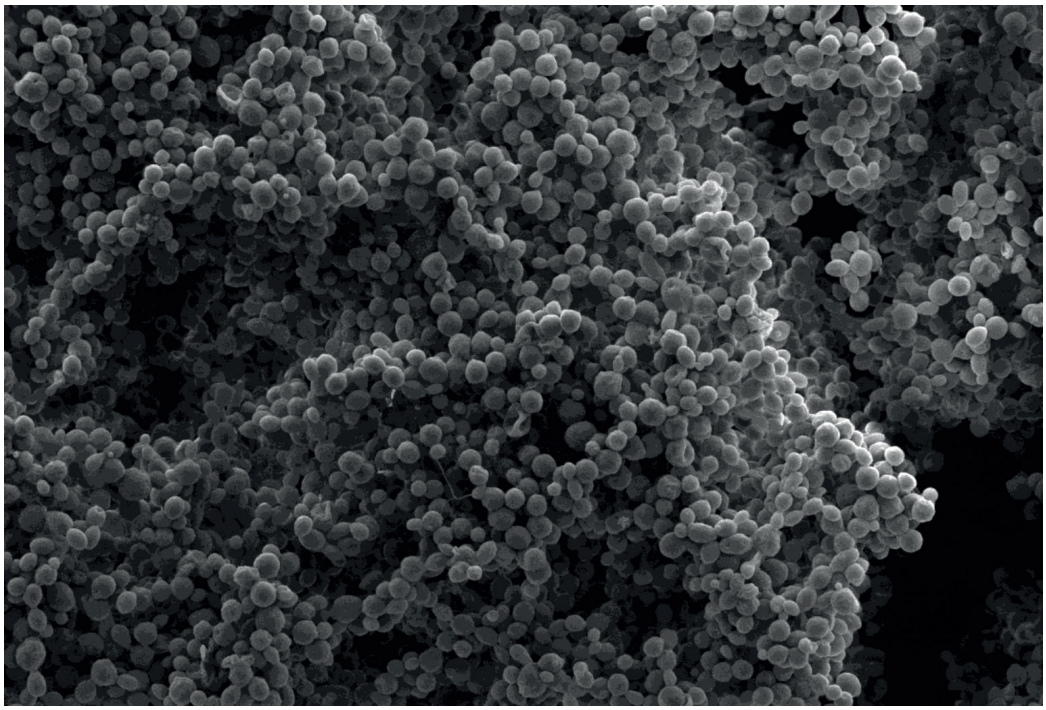

Figure 3: Biofilms were analyzed in scanning electron microscopy (SEM) using a Jeol JSM-6610LV scanning electron microscope at 5000X magnification on *C. auris* morphology.

C. auris grows at temperature range of 25 to 42 °C (Almaghrabi et al., 2020; Arastehfar et al., 2018) and has an ideal growth temperature of 37-40 °C (Ahmad et al., 2019; Prakash et al., 2016; Welsh et al., 2017). *C. auris* grows well in culture media used in routine laboratories such as Sabouraud Dextrose Agar (SDA), Glucose Yeast Extract Peptone Agar, and chromogenic agar (like CHROMagar®) after 2 to 5 days of incubation. In fact, 48 h of incubation after enrichment may be enough for its growth (Ruiz-Gaitán et al., 2018). It should be mentioned that this fungus does not grow on medium containing 0.1-0.01% cycloheximide (Khillan et al., 2014; Satoh et al., 2009).

The performance of culture and identification tests varies according to each laboratory's protocols. The use of selective enrichment broth optimized *C. auris* growth providing a faster result (lower time) in clinical specimens, with greater sensitivity and specificity (Adams et al., 2018). Welsh et al. (2017) observed that different to other *Candida* sp, *C. auris* grows well in salinity (10%wt/vol) in Sabouraud (with 10% Dulcitol with chloramphenicol and gentamicin), salt Sabouraud dulcitol enrichment broth and Yeast Nitrogen Base broths with dulcitol or mannitol as carbon sources.

As for the visual aspects, *C. auris* colonies on SDA are smooth, from white to cream (Chew et al., 2018; Kathuria et al., 2015; Satoh et al., 2009) as also observed in other *Candida* species of medical

interest (Keighley et al., 2021).Clinical specimens can be processed for isolation of *C. auris* by direct plating on CHROMagar® or using the salt Sabouraud Dextrose enrichment method (Welsh et al., 2017). Chromogenic methods such as CHROMagar® *Candida* despite being useful, as they allow a relatively rapid presumptive identification (incubation time of 24–48 h and 40–42ºC), does not specifically differentiate *C. auris* (Bayona et al., 2021). According to the CDC, confirmation must be made by other more specific methods, that will be mentioned during this review (CDC 2021).

It is worth mentioning that on chromogenic agar plates, *C. auris* colonies' texture is smooth and glossy. On the Brilliance™ Candida Agar (Oxoid, UK) presents beige to pink colonies (Chew et al., 2018; Keighley et al., 2021; Satoh et al., 2009), pale pink colonies on *Candida* CHROMagarTM (Becton Dickinson, Heidelberg, Germany) (Chew et al., 2018), and on CHROMIDR *Candida* (BioMerieux, France) *C. auris* can be seen as pale pink colonies (Bentz et al., 2019; Borman et al., 2021; Chew et al., 2018; Kathuria et al., 2015; Keighley et al., 2021; Bayona et al., 2021; Satoh et al., 2009). The color variation problem appears to have been solved on the new chromogenic agar, CHROMagar Candida Plus (CHROMagar, France) which presents a new specific color for this species: light blue with a blue halo at 36 h of incubation (with a sensitivity and specificity of 100%). This medium can be a good alternative for clinical laboratories when rapid identification and presumptive differentiation of *C. auris* from other *Candida* species are desired (Borman et al., 2021; Keighley et al., 2021; Bayona et al., 2021).

Since it is desirable to identify microorganisms in less time and easily, automation has been used (Carvalho et al., 2020), such as phenotypic methods such as:

Since it is desirable to identify microorganisms in less time by easy execution, automation has been used (Carvalho et al., 2020). In this regard, phenotypic methods such as VITEK 2 YST, API 20C, API ID 32C, MicroScan, RapID Yeast Plus, GenMark ePlex BCID-FP Panel, BD Phoenix, bioMérieux VITEK MS MALDITOF and Bruker Biotyper MALDI-TOF can be cited (Keighley et al., 2021). However, the disadvantage of these methods is that they may misidentify *C. auris* or require other more specific methods (CDC, 2019). A reason why *C. auris* cannot be reliably identified by standard biochemical identification platforms/kits is because there is a lack of this organism in their databases (Mizusawa et al., 2017). Therefore, other more efficient methods are extremely important for a correct and timely identification of this pathogen, such as spectrophotometric, molecular and serological method (Cendejas-Bueno et al., 2012; Keighley et al., 2021). In **Figure 4** it is possible to observe biochemical-based methods commonly used to identify *Candida* species and *C. auris* possible misidentification.

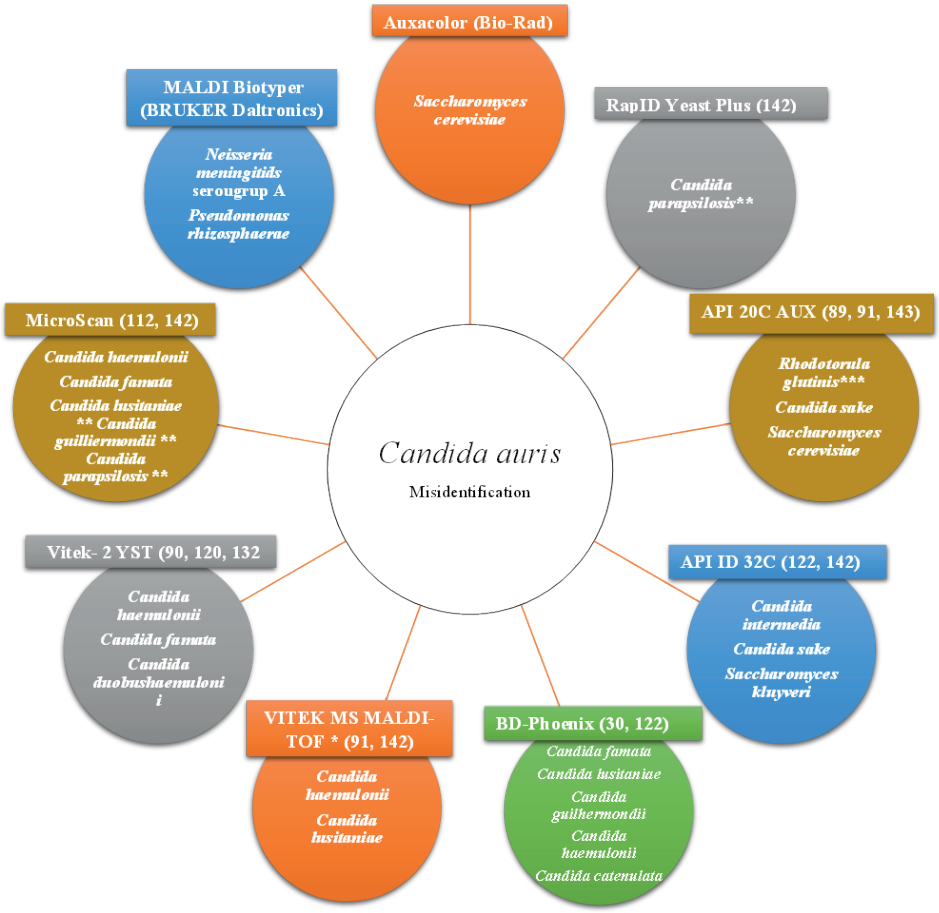

Figure 4: Biochemical-based methods commonly used to identify *Candida* species and associated with *C. auris* misidentification. * Misidentification of *C. auris* with *C. lusitaniae* and *C. famata*. More specific tests need to be performed. ** *C. lusitaniae, C. guilliermondii* and *C. parapsilosis* can form pseudo-hyphae on cornmeal agar. In the absence of pseudo-hyphae, *C. auris* may be suspected since it does not produce pseudo-hyphae. However, some species of *C. auris* can form hyphae. It is important to consider the growth of *C. lusitaniae, C. guilliermondii* and *C. parapsilosis* identified by the MicroScan test or any *C. parapsilosis* isolates identified in RapID Yeast Plus as possible *C. auris*. Finally, this isolate must be sent for identification tests. *** Characteristic red color not present.

Serological assay

Conventional tests based on fungal culture have limitations in identifying the microorganism, mainly because they do not contain markers or biomarkers for detection and require a longer time for diagnosis. Moreover, culture-based tests can prevent the growth of microorganism species. Non-

culture-based tests were developed with the aim of overcoming the limitations of culture tests. Although they are efficient, their low specificity and sensitivity are limitations. As an example, the biomarker, 1, 3-Beta-D-glucan can be mentioned. This biomarker has a sensitivity ranging from 75 to 80% for candidemia, which highlights the need to develop a more sensitive test (Chibabhai et al., 2019; Farooqi et al., 2021).

Matrix-assisted laser desorption/ionization time-of-flight mass spectrometry (MALDI-TOF)

After obtaining the correct isolate, identification of *C. auris* can be performed using the matrix-assisted laser desorption/ionization time-of-flight (MALDI-TOF) method (Caceres et al., 2019).

MALDI-TOF is a promising technique for microbial identification, such as *C. auris,* using a MALDI Biotyper (Bruker Daltonik; Bremen, Germany and Bruker MALDI Biotyper CA and Research Use Only [RUO] databases) or a MALDI-TOF MS BioMerieux 3.2 systems, two important methods available (Huang et al., 2021; Schwartz & Hammond, 2017). MALDI-TOF is a proteomic method, based on the spectral comparison generated for each sample type with the reference database (Mahmoudi et al., 2019). This equipment is capable of properly identify several *C. auris* isolates in biological samples (Chow et al., 2019; Chowdhary et al., 2017; Schelenz et al., 2016). It should be emphasized that this method allows faster and more accurate diagnosis of pathogens when compared to conventional tests. However, as disadvantages include the need for a greater investment, which generates low availability of equipment in routine laboratories (Ong et al., 2019).

Molecular assays

As reported, the biggest challenge for the diagnosis of *C. auris* is to avoid identification errors caused by the limitations of conventional and commercial tests available in the routine laboratory. Even assays such as MALDI-TOF have limitations in detecting *C. auris*. In view of this, new methods based on deoxyribonucleic acid (DNA) and proteins are being developed and evaluated against the detection of *C. auris* (Mahmoudi et al., 2019; Ong et al., 2019).

Due to the high cost of genomic sequencing, several methods based on independent DNA sequencing have been developed, mainly for the differentiation of *C. auris* from other closely related *Candida* spp that can be easily mis-identified by other tests (Mahmoudi et al., 2019).

A very important technique in microbiological diagnostics is the polymerase chain reaction (PCR) method, such conventional PCR and real-time PCR. The difference between them is that real-time PCR has greater speed, reproducibility, quantitative capacity, sensitivity and reproducibility, and can be substituted for conventional PCR in routine laboratories (Paiva-Cavalcanti et al., 2010).

The sequencing of the internal transcribed spacer (ITS) regions and/or the D1/D2 regions of 28S ribosomal DNA presents the ability to confirm species and phylogenetic information. Studies report the importance of conventional and real-time PCR targeting the ITS2 region as it has the ability to quickly and accurately identify clinical isolates of *C. auris* in a short period of time (approximately 2 hours). However, test sensitivity was not confirmed for all isolates (Hou et al., 2019; Ong et al., 2019). TaqMan real-time PCR test targeting the ITS2 region were able to detect *C. auris* within a period of 4 hours. It is worth mentioning that this test was able to detect *C. auris* DNA even in samples (armpit, groin, nostril, ear, rectal and wound swabs, besides environmental sponges from different hospital sites) with negative results for other assays (Leach et al., 2018). Kordalewska et al. (2017) evaluated 140 fungal isolates and human genomic DNA in conventional and real-time PCR. According to the results, the detection accuracy for *C. auris* was 100% for both tests.

Multiplex Probe Amplification (MPA) technology is another type of PCR that stands out for being an effective method for the simultaneous detection of *C. krusei*, *C. auris* and *C. glabrata*. Containing probes from the variable domains D1/D2 of the LSU rDNA locus, MPA has high specificity and selectivity, and can be used in hospital environment for the control of *C. auris* outbreaks (Jainlabdin et al., 2019).

In order to identify new outbreaks of *C. auris* and avoid the increase of positive cases, genomic sequencing of this microorganism was performed and the amplified fragment length polymorphism (AFLP) was used for molecular typing. Since AFLP is complex and expensive a simpler and less expensive technique was developed based on short tandem repetitions in the *C. auris* genome. The results proved to be accurate for a faster, more reliable and economical technique for genome sequencing analysis, aiding in the investigation of new outbreaks (de Groot et al., 2020).

Other commercially available and high-efficiency methods include PCR-RFLP, T2 magnetic resonance system, loop-mediated isothermal amplification (LAMP) and GPSTM MONODOSE CanAur dtecqPCR (dried single-dose PCR tubes). The latter presents speed in the analysis because it has dehydrated tubes available for use, requiring only the addition of a DNA template. The disadvantages of these experiments are that they are considered high-cost trials with low availability, especially in developing countries (Mahmoudi et al., 2019). Results show that GPSTM MONODOSE CanAur dtecqPCR has the ability to detect *C. auris* within 1 h (Martínez-Murcia et al., 2018).

Other commercial assays can be highlighted, such as the AurisID and the Fungiplex, a test used in surveillance detection or directly for blood samples. Additionally, the T2 magnetic resonance imaging assay can be used to detect bloodstream infection or to *C. auris* colonization screening. It is also worth noting that for positive blood cultures, the Food and Drug Administration (FDA), approved the use of BioFire Blood Culture Identification (BCID) 2 and GenMark Dx Panel ePlex BCID- fungal

pathogen (FP) methods (Lockhart et al. 2022). **Figure 5** represents a summary of laboratory tests for the diagnosis of *C. auris*, as described by Lockhart et al. (2022).

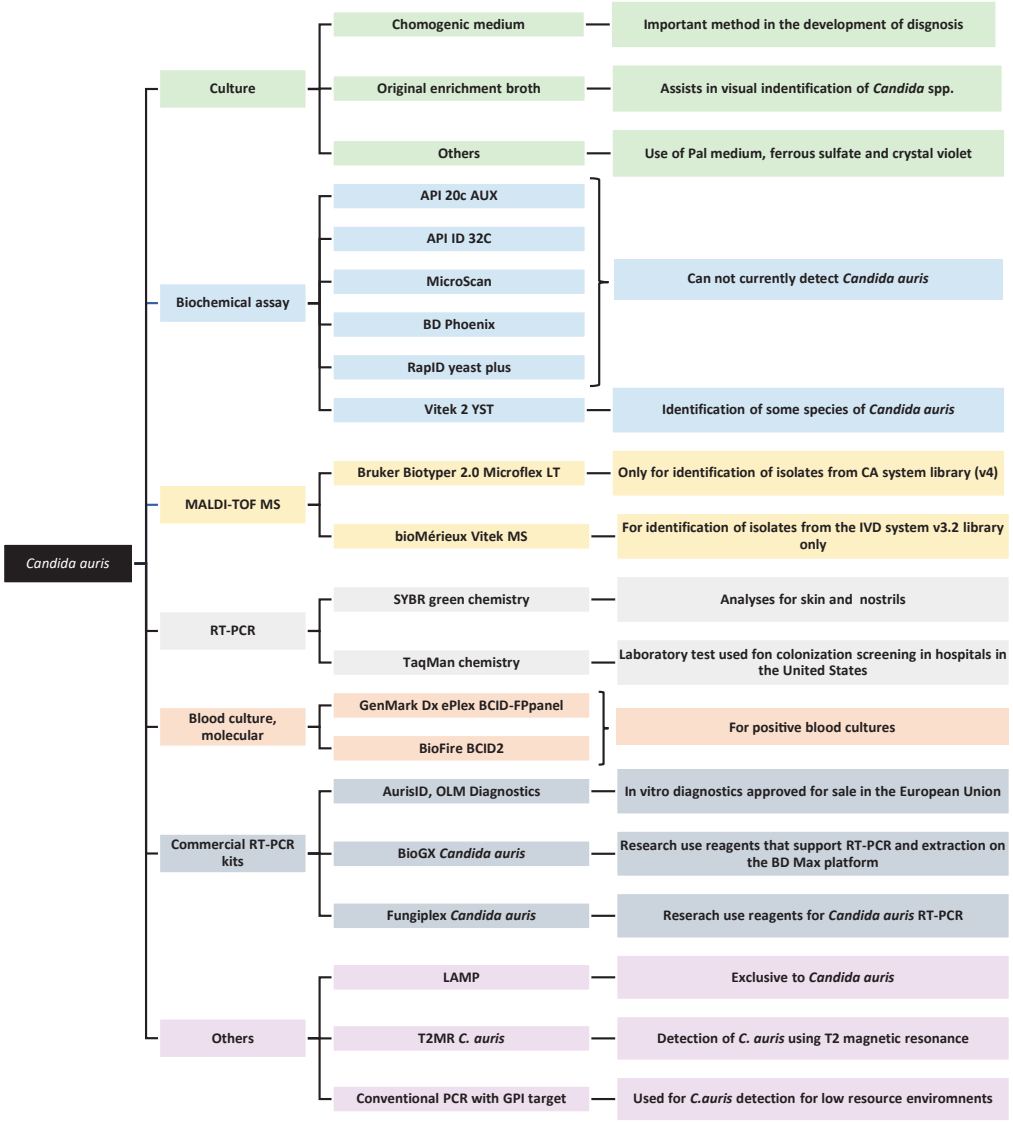

Figure 5: Methods that may contribute to the diagnosis of *C. auris.*

In conclusion, the correct identification of *C. auris* becomes a serious issue, since a large number of routine laboratories have just biochemical methods for the identification of *Candida* spp., mainly due to the high cost of more sophisticated tests (molecular and MALD TOF tests for example),

increasing the chance of misdiagnosis and inappropriate treatment. **Table 2** presents the main molecular tests based on *C. auris* detection primers.

Table 2: Primers used to identify *C. auris* using molecular techniques.

Molecular Method	Target	Region	Primer name	Base Sequences (5'-3')	Reference
Sequence analysis	*C. auris*	ITS1-4	ITS-1 ITS-4	TCCGTAGGTGAACCTTGCGG TCCTCCGCTTATTGATATGC	(Kathuria et al., 2015)
AFLP	*C. auris*	ITS	V9G LS266 V9G and ITS1 LS266 and ITS4	TTACGTCCCTGCCCTTTGTA GCATTCCCAAACAACTCGACTC TCCGTAGGTGAACCTGCGG TCCTCCGCTTATTGATATGC	(Calvo et al., 2016)
Multiplex PCR	*C. auris* and *C. haemulonii*	ITS2	*C. auris* *C. haemulonii*	CCACCGCGAAGATTGGTG CCGTTGGTGGATTTGTTTCT	(Theill et al., 2018)
Real-time PCR	*C. auris*	ITS2	CauF CauR	CGCACATTGCGCCTTGGGGTA GTAGTCCTACCTGATTTGAGGCGAC	(Kordalewska et al., 2017)
	C. auris and related species (*C. duobushaemulonii, C. haemulonii*, and *C. lusitaniae*)		CauRelF CauRelR	GCGATACGTAGTATGACTTGCAGACG CAGCGGGTAGTCCTACCTGA	
PCR	*C. auris*	GPI-protein genes	03410_F 03410_R	GCCGCTAGATTGATCACCGT TAGGTGTGGGTACCCTTGGT	(Ruiz-Gaitán et al., 2018)
			05701_F 05701_R	GCAGCACTCGTGAGAGAACT GGCTGGTTCTCCTGCTCATT	
			05701_F2 05701_R2	TGCAACCACAGTGACCAC CTTGCTACAGTCTGAGAG	
		5.8S rDNA	RDN58_F RDN58_R	GGATCTCTTGGTTCTCGC CGCTCAAACAGGCATGC	
Real-time PCR	*C. auris*	ITS2	CAURF CAURR	CAGACGTGAATCATCGAATCT TTTCGTGCAAGCTGTAATTT	
PCR and Sequence analysis	*C. auris*	ITS1-4	ITS1 ITS4	TCCGTAGGTGAACCTGCGG TCCTCCGCTTATTGATATGC	(Kaur et al., 2020)
		D1/D2	NL1 NL4GG	GCATATCAATAAGCGGAGGAAAAG TCCGTGTTTCAAGACGG	

Sequence analysis	*C. auris*	ITS D1/D2	pITS-F pITS-R NL1 NL4	GTCGTAACAAGGTTAACCTGCGG TCCTCCGCTTATTGATATGC GCATATCAATAAGCGGAGGAAAAG GGTCCGTGTTTCAAGACGG	(Lee et al., 2011)
Real-time PCR	*C. auris*	ITS2	V2424 V2426	CAGACGTGAATCATCGAATCT TTTCGTGCAAGCTGTAATTT	(Leach et al., 2018)
Loop-Mediated Isothermal Amplification (LAMP)	*C. auris*		AurisFIP AurisBIP AurisLoop-F AurisLoop-B AurisF3 AurisB3	AGGCTACTGAGCTTGCTGGTGTAACCAAA CCAACAGGAGAGG ACGGTTTCAGGGTTAGCATGGCTCAACAA AGTCGCTGGTACA CATCTCGAAGGCCTCGGT CACATACTCGAACGGAGTC GGGAAAGGAACCCTGACCT GGACACAGCATTCGAAGTGT	(Yamamoto et al., 2018)
Real-time PCR	*C. auris*	ITS1 ITS2	*C. auris*	CGTGATGTCTTCTCACCAATCT TACCTGATTTGAGGCGACAAC	(Lima et al., 2019)
Real-time PCR	*C. auris*	ITS2	CA1 4605 CA2 4605	TCAGGTAGGACTACCCGCTG CTGCATTCCCAAACAACTCGACTC	(Walchak et al., 2020)
Real-time PCR	*C. auris*	ITS1 ITS2		TCC TCCGCTTATTGATATGC GGAAGTAAAAGTCGTAACAAGG	(Teke et al., 2021)
RT-qPCR	*C. auris*	ITS2	V2424F (CAURF) V2426 (CAURR)	CAGACGTGAATCATCGAATCT TTTCGTGCAAGCTGTAATTT	(Freitas et al., 2022)

9. Treatment and prophylaxis of *C. auris* infections

The treatment of infections caused by *C. auris* is a great challenge to be overcome, since many strains are resistant to antifungal agents commonly used in clinical practice, such as azoles, polyenes and echinocandins (Giacobbe et al., 2021; Lockhart et al., 2017). In 2017 the first report of multidrug-resistant *C. auris* occurred in Canada, isolated from a 64-year-old patient with chronic external otitis. In the susceptibility tests, the strain presented Minimum Inhibitory Concentration (MIC) values of 128.0, 2.0 and 0.5 µg/mL for fluconazole (class of azoles), amphotericin B (class of polyenes) and micafungin (class of echinocandins) respectively. According to the authors, these values were compared with the tentative MIC breakpoints of the CDC, which are ≥ 32, ≥ 2 and ≥ 4µg/mL respectively. Thus, it could be said that the isolated strain was resistant to fluconazole and amphotericin B but susceptible to micafungin (Schwartz & Hammond, 2017).

In a study, susceptibility tests were performed on clinical isolates from 54 patients (from South Africa, Pakistan, India and Venezuela) with *C. auris* infection and in the type specimen from Japan. The most common resistance was observed against fluconazole, 93% of the isolates, followed by resistance to amphotericin B and echinocandins, 35% and 7% respectively. It was also observed that 41% of the isolates were resistant to 2 antifungals classes and 4% to 3 classes. It is noteworthy that 63% of the patients were using urinary catheter, 73% using a CVC and 61% had bloodstream infection. For the site of infection, blood, urine and respiratory tract were more prevalent, 61, 7 and 5% respectively. The authors concluded that the treatment of this pathogen is limited due to resistance problems. Additionally, the authors suggested that risk factors and transmission mechanisms need to be better studied to enable efficient control measures (Lockhart et al., 2017).

The CDC recommends three drugs from echinocandin class for *C. auris* infections as initial therapy, are they: anidulafungin, caspofungin and micafungin (**Table 3**). With tentative MIC breakpoints of ≥ 4 ≥ 2 and ≥ 4 µg/mL respectively. However, if treatment is not sufficient and the infection persists for > 5 days, the CDC recommends switching treatment to liposomal amphotericin B (5 mg/kg per day). It is noteworthy that CDC does not recommends treatment when this fungus is isolated in a non-sterile and noninvasive site (such as urine, external ear, respiratory tract and skin colonization) when the clinical disease is not present (CDC, 2021). According to the European Center for Disease Prevention and Control (ECDC) publication, the treatment of this fungus is still a limitation, as it is resistant to both, fluconazole (class of azoles) and echinocandins. However, the resistance to the latter is more variable since almost all *C. auris* isolates are resistant to fluconazole. It is worth noting that these two are the most prescribed options for candidemia treatment once they are less toxic than amphotericin B (ECDC, 2018). The Pan American Health Organization, the National Health Surveillance Agency (ANVISA) - Brazil, and the Public Health England - United Kingdom,

also brings the class of echinocandins as the first-line treatment (ANVISA, 2020; Pan American Health Organization, 2021; Public Health England, 2017).

Echinocandin class is an essential fungicide against most *Candida* spp. They act by inhibiting a cell-wall enzyme complex, causing cell wall damage. Their applications are desirable once they have lower toxicity, less drug interaction (as they are not or poor substrate for tissue or intestinal P-glycoprotein and cytochrome P450 enzymes respectively) and mild adverse effects (like headache, fever, liver toxic effects, local phlebitis (caspofungin), histamine release, hemolysis and rash). The great difficulty in using this class is linked to malabsorption by oral administration, which can lead to low bioavailability, what makes the injectable route a better option (Denning, 2003). Despite being considered a first-line treatment, the problem of *C. auris* resistance to this class has been growing more and more. Thus, the study of new drug candidates is increasingly necessary (Mahmoudi et al., 2019; Pan American Health Organization, 2021).

Among the new therapeutic candidates, ibrexafungerp can be mentioned. Ibrexafungerp is the first antifungal of the enfumafungin-derived triterpenoid class and has a fungicidal action by inhibiting a cell wall component. Its advantage over echinocandin is its good oral bioavailability, which favors administration by this route (Ghannoum et al., 2020). As can be seen in **Table 4** several studies have been carried out in order to evaluate the use of this drug in the treatment of *C. auris* strains. In *in vitro* studies, despite the MIC_{90} commonly observed be 1 µg/mL, it was also possible to observe MIC_{90} in the range of 0.06 - 2 mg/L. However, when compared to controls, especially those with a known resistance problem, like fluconazole and amphotericin B, ibrexafungerp proves to be an excellent therapeutic alternative once its MIC values are lower (Arendrup et al., 2020; Berkow et al., 2017; Larkin et al., 2017; Wiederhold et al., 2021).

Table 3: Types of infection and clinical samples of *C. auris* isolation worldwide.

Drug	Adult dosing	Pediatric dosing	Neonatal dosing (2 months of age)	Antifungal class	Mechanism of action	Reference
Anidulafungin	loading dose of 200 mg IV, followed by 100 mg IV daily	not approved	-	Echinocandin	Inhibits beta-(1,3)-glucan, damaging fungi cell wall	(CDC, 2021; Denning, 2003)
Caspofungin	loading dose of 70 mg IV, followed by 50 mg IV daily	loading dose of 70mg/m^2/day IV*, followed by 50mg/m^2/day IV	25 mg/m^2/day IV*	Echinocandin		
Micafungin	100 mg IV daily	2mg/kg/day IV, being possible to increase to 4mg/kg/day IV in 40 kg children	10mg/kg/day IV	Echinocandin		

Legend: * based on body surface area

Table 4: Main results of articles involving drugs that are already in clinical evaluation stages.

Drug	Mechanism of action	Study type	Strain/	Main test result	Comparative control	Reference
Ibrexafungerp	(1→3)-β-D-glucan synthase (component of the cell wall) inhibition, weakening fungal cell wall	*In vitro*	Clinical isolates (Germany, Japan, India, and South Korea)	MIC_{90}: 1 µg/mL	fluconazole: >64 µg/mL amphotericin B: 4 µg/mL anidulafungin:0.25 µg/mL caspofungin:1 µg/mL micafungin: 1 µg/mL	(Larkin et al., 2017)
			Clinical isolates (From countries all over the world)	MIC_{90}: 1 µg/mL	anidulafungin: 0.125 to >16 µg/mL caspofungin: 0.03 to >16 µg/mL micafungin: 0.03 to >8 µg/mL	(Berkow et al., 2017)
			122 clinical isolates collected from individual patients in six tertiary care hospitals in India	MIC_{90}: 0.06–2 mg/L	amphotericin B: 0.5 - 1 mg/L fluconazole: 0.5 – ≥64 mg/L anidulafungin: 0.016 - >32 mg/L micafungin: 0.03 - >32 mg/L isavuconazole: ≤0.004 - 2 mg/L voriconazole: ≤0.004 - 4 mg/L	(Arendrup et al., 2020)

		Reference strains (CBS12372; CBS12373; CBS10913)	MIC_{90}: CBS12372: 0.125 mg/L CBS12373: 0.5 mg/L CBS10913: 0.06 mg/L	-	
		54 isolates	MICs:0.25 – 2 µg/mL MIC_{50} and MIC_{90}: 1 µg/mL	caspofungin and micafungin: 0.06 to >8 µg/mL (mainly 1 to 2 dilutions lower than for ibrexafungerp)	(Wiederhold et al., 2021)
	In vivo in Guinea pig model	MRL 35368	Log CFU after the best concentration tested (10 mg / kg) in 7 days of treatment: 2,8 ± 0,7	non-treated group Log CFU: approximately 4,25 micafungin Log CFU: 3,6 ± 1,2	(Ghannoum, Isham, et al., 2020)
	In vivo in neutropenic mice	Clinical isolate	Log_{10} after the treatment for 7 days: 1.83 - 3.85 Log_{10} CFU/g (>1.5 Log_{10} CFU/g for 30 mg/kg groups and > 2.5 Log_{10} CFU/g for 40 mg/kg groups)	vehicle control group: 5.36 Log_{10} CFU/g fluconazole group: 5.79 Log_{10} CFU/g caspofungin group: 4.50 Log_{10} CFU/g	(Wiederhold et al., 2021)
	Phase 3	30 patients (estimated value) with candidiasis, including candidemia, caused by *Candida Auris*	Recruiting	non-comparator, single arm	(National Institutes of Health, 2021b)

Fosmanogepix (Manogepix pro-drug)	Enzyme Gwt1 inhibition, compromising cell wall mannoproteins proper localization compromising cell wall integrity, biofilm formation and germ tube formation (defected fungal growth)	*In vitro*	200 isolates (clinical and Surveillance) during an outbreak	MIC_{90}: 0.03 mg/L	anidulafungin: 1.0 mg/L caspofungin: 0.25 mg/L micafungin: 0.25 mg/L fluconazole: 256 mg/L isavuconazole: 1.0 mg/L itraconazole:1.0 mg/L posaconazole:0.5 mg/L voriconazole: 2 mg/L amphotericin B: 2 mg/L flucytosine: 32 mg/L	(Zhou et al., 2020)
			11clinical isolates	MIC_{90}: 0.03 mg/L	anidulafungin: 0.25 mg/L micafungin: 0.25 mg/L fluconazole: >128 mg/L posaconazole: 0.5 mg/L voriconazole: 2 mg/L amphotericin B: 1 mg/L	(Pfaller et al., 2021)
			10 isolates from CDC FDA Antibiotic Resistance Bank And 3 clinical isolates	MIC_{50}: 0.03 µg/mL MIC_{90}: 0.125 µg/mL	fluconazole: MIC_{50} and MIC_{90} at 64 µg/mL caspofungin: MIC_{50} at 0.25 µg/mL and MIC_{90} values and 0.5 µg/mL.	(Wiederhold et al., 2019)

	In vivo in neutropenic mice	UTHSCSA DI17-46	After 8 days of treatment: -kidney fungal burden: Log_{10} CFU/g after the best concentration tested (260 mg/kg): 3.86 -brain fungal burden: Log_{10} CFU/g after the best concentration tested (260 mg/kg): 2.99 After 21 days of treatment: -kidney fungal burden: Log_{10} CFU/g (range of all doses tested): 4.47 to 4.55 -brain fungal burden: Log_{10} CFU/g (range of all doses tested): 3.10 to 3.27	After 8 days of treatment: -kidney fungal burden: vehicle control: 5.61 log_{10} CFU/g caspofungin:3.41 log_{10} CFU/g; fluconazole: no fungal reduction (5.88 log_{10} CFU/g) -brain fungal burden: vehicle control: 4.40 log_{10} CFU/g caspofungin: 4.36 log_{10} CFU/g fluconazole: 4,91 log_{10} CFU/g After 21 days of treatment: -kidney fungal burden: vehicle control: 7.90 log_{10} CFU/g caspofungin: - fluconazole: no fungal reduction -brain fungal burden: - vehicle control: - caspofungin: 2.70 log_{10} CFU/g fluconazole: no fungal reduction	(Wiederhold et al., 2019)
	Phase 2	9 participants with candidemia and/or Invasive candidiasis caused by *Candida Auris*	Not Provided (The trial was closed early due the impact of COVID-19 on trial-related activities - the study was successfully met)	single Group Assignment	(National Institutes of Health, 2021a)

The potential of ibrexafungerp in the treatment of *C. auris* was also observed in *in vivo* studies (**Table 4**), as groups treated with this drug showed a greater reduction in Log_{10} CFU/g than the other groups tested, such as vehicle group, untreated group, micafungin group, fluconazole group and caspofungin group (Ghannoum et al., 2020; Wiederhold et al., 2021). Those promising *in vitro* and *in vivo* results led ibrexafungerp to be considered an excellent therapeutic alternative, so currently this drug is undergoing a phase 3 multicentric study, in recruitment phase. It is an open-label, single-arm and non-comparator study whose objective is to evaluate safety, efficacy, tolerability and pharmacokinetics of ibrexafungerp administered orally, for up to 90 days, in people of both sex, age over 18 with documented *C. auris* infection (National Institutes of Health, 2021b).

Another therapeutic option is fosmanogepix, a N-phosphonooxymethylene pro-drug that after systemic phosphatases action gives rise to manogepix, its active moiety (Shaw & Ibrahim, 2020). Manogepix is a first-in-class, small-molecule, that targets the fungal enzyme inositol acylase (Gwt1), which catalyzes the initial step in the glycosylphosphatidylinositol (GPI) anchor biosynthesis pathway. The inhibition of this enzyme compromises the proper localization of cell wall mannoproteins, compromising not only the cell wall integrity, but also the germ tube formation (which causes defects in fungal growth) and biofilm (Covel et al., 2019; Watanabe et al., 2012; Zhu et al., 2020). The great advantage about the use of this antifungal in the therapy is because its mechanism of action is new, without resistance problems, making it highly effective against strains resistant to echinocandins and azoles, for example (Shaw & Ibrahim, 2020).

In vitro and *in vivo* studies have also been carried out in order to assess the potential of this drug in the therapy of *C. auris* infections (**Table 4**). In *in vitro* assays, more than one study showed MIC_{90} of 0.03 mg/L, a value much lower than the controls used in those articles, such as, anidulafungin, micafungin, fluconazole, posaconazole, voriconazole and amphotericin B. What confirms that fosmanogepix could be an interesting option for the treatment of infections caused by strains resistant to several of those drugs (Pfaller et al., 2021; Zhu et al., 2020). This fact is in agreement with a study carried out in neutropenic rats, where it was observed that the fungal burden in the kidney, in the 8-day treatment, was lower than the one observed in the vehicle and fluconazole groups, and similar to the caspofungin group. As for the fungal burden in the brain, the fosmanogepix group presented fungal burden much lower than the other groups (2.99 Log_{10} CFU/g compared to 4.36 - 4.91 Log_{10} CFU/g in controls). In the 21-day treatment both, fosmanogepix and caspofungin groups, showed significant reductions in fungal burden, both in the kidney and in the brain. Those reductions were not observed in the vehicle and fluconazole groups of both organs. Reinforcing the potential use of this new drug in the therapy of systemic infections caused by *C. auris*, mainly in replacement of drugs with resistance problems, such as fluconazole (Wiederhold et al., 2019). Finally, it is noteworthy that a clinical trial,

in phase 2, was conducted. In this trial, the drug was tested in 9 participants with candidemia and/or invasive candidiasis caused by this fungus. Despite not having detailed results available, the clinical trial was successfully met (National Institutes of Health, 2021a).

Although only two drugs are in clinical evaluation stages, according to the Clinical Trials website, several other molecules and new strategies have been tested *in vitro* against this pathogen (Billamboz et al., 2021; National Institutes of Health, 2021b, 2021a; Wall et al., 2018). Ebselen, for example, has antioxidant, anti-inflammatory, and cytoprotective activity and showed excellent MIC_{50} results (approximately 2.5 μM) against *C. auris* 0390, a strain resistant to azoles and amphotericin B and with decreased susceptibility against echinocandins. Therefore, ebselen is considered a repositionable agent for the treatment of *C. auris* infections refractory to conventional treatments (Wall et al., 2018). Another example that can be cited is miltefosine, a drug currently used to treat leishmaniasis and breast cancer, that has shown activity against several fungal strains, including *C. auris* (Barreto et al., 2020; Spadari et al., 2019; Widmer et al., 2006).

In one study, miltefosine showed MIC values ranging from 1–4 μg/mL, against clinical strains, with a fungicidal effect. When tested against biofilms, this drug showed activity in both situations, during their formation (0.25–4 μg/mL) and on pre-formed biofilms (16–32 μg/mL). The authors also studied this drug antifungal activity in *Galleria mellonella* larval infection model, but at this time they tried both, the free drug and encapsulated in alginate nanoparticles. This association strategy with alginate nanoparticles was motivated by the inherent toxicity of miltefosine. The possibility of a sustained release that could reduce its toxicity without impairing its anti-*Candida* activity turns out to be extremely desirable. The free drug, in both doses tested (20 or 40 mg/kg), reduced 2 logs of the fungal load of the *C. auris* CBS 10913 strain, and 0.5-1.0 log of *C. auris* CBS 12766 strain (resistant strain considered more virulent and with a faster fungal growth when compared to the other strain tested). The nanosystem (100 mg/kg) was also able to significantly reduce the fungal load of the *C. auris* CBS 10913 strain, but the same was not observed with the *C. auris* CBS 12766 strain. The histopathological analyzes performed corroborated with the fungal load results. Taking into account the results obtained *in vitro* and *in vivo* and considering the few therapeutic options for *C. auris* infections, the authors consider the free and encapsulated miltefosine as promising alternatives (Barreto et al., 2020).

It is noteworthy that the use of nanotechnology is an excellent alternative when it is desirable to overcome weaknesses in therapies considered first-line, such as problems related to toxicity and resistance (Barreto et al., 2020; Carvalho et al., 2020; Marena et al., 2022). In a recent study, amphotericin B nanoemulsions were developed and evaluated for their potential activity against *C. auris*. This study was motivated not only by the resistance problems that this drug has been showing

to *C. auris* strains, but also by its toxicity. In the *in vitro* test (MIC) it was observed that both, the nanoemulsion with amphotericin B and the free drug, had the same MIC value against the *C. auris* strain (CDC B11903), 0.062 μg/mL. However, based on *in vivo* study, also performed in *G. mellonella* larval infection model, it can be said that the nanoemulsion increased the drug's activity. Although amphotericin B initially presented a greater logarithmic reduction of CFU/larva over the days, this reduction was overcome by the nanoemulsion containing the drug, and on days 4 and 5 it was possible to observe more than 1 log difference between them. Finally, in the acute toxicity assay, also carried out in *G. mellonella*, it was observed that free amphotericin B presents greater toxicity than the nanosystems, which did not cause deaths in all concentrations tested. Thereby, in addition to increasing the drug's activity, the nanosystem was also capable to reduce the drug side effects (Marena et al., 2022).

Although just some of the most recent strategies are mentioned here, it is possible to observed that the concern with the treatment of this emerging fungus is a consensus. Strategies such as the development of new drugs, combinations of drugs already used in therapy with nanotechnology and even drug combinations, such as the association of colistin (an antibacterial drug without antifungal activity) with echinocandins (in order to obtain a synergistic effect), are very current alternatives (Barreto et al., 2020; Bidaud et al., 2020; Marena et al., 2022; Wall et al., 2018). Despite the need for effective treatments, which is a real necessity, the demand for prevention cannot be forgotten.

In this sense, it is important to highlight the necessity of using infection prevention measures, such as following hand hygiene practices, allocating colonized patients in individual rooms, following precautions based on transmission, cleaning and disinfection (with appropriate products) of the environment in which the patient is being cared. In addition, it is of fundamental importance to screen contacts of newly diagnosed patient cases and communication between units (in the case of transfer) about the infection status. Moreover, an efficient laboratory surveillance of clinical samples is essential for the detection of new cases (CDC, 2021; Centers for Desease Control and Prevention, 2022; Ong et al., 2019; Snyder & Wright, 2019).

10. Acknowledgments

We thank São Paulo Research Foundation – FAPESP (grant#2019/09831-9, and grand#2019/26821-7). We would like to thank the Central Scanning Electron Microscopy Laboratory of the Faculty of Dentistry of the Araraquara Campus for the availability of using the Scanning Electron Microscope and we thank the Brazilian.

11. Disclosure statement

No potential conflict of interest was reported by the author(s).

12. References

Abastabar, M., Haghani, I., Ahangarkani, F., Rezai, M. S., Taghizadeh Armaki, M., Roodgari, S., Kiakojuri, K., Al-Hatmi, A. M. S., Meis, J. F., & Badali, H. (2019). Candida auris otomycosis in Iran and review of recent literature. *Mycoses, 62*(2), 101–105. https://doi.org/10.1111/myc.12886

Adams, E., Quinn, M., Tsay, S., Poirot, E., Chaturvedi, S., Southwick, K., Greenko, J., Fernandez, R., Kallen, A., Vallabhaneni, S., & others. (2018). Candida auris in healthcare facilities, New York, USA, 2013–2017. *Emerging Infectious Diseases, 24*(10), 1816–1824. https://doi.org/10.3201/eid2410.180649

Ahmad, A., Spencer, J. E., Lockhart, S. R., Singleton, S., Petway, D. J., Bagarozzi, D. A., & Herzegh, O. T. (2019). A high-throughput and rapid method for accurate identification of emerging multidrug-resistant Candida auris. *Mycoses, 62*(6), 513–518. https://doi.org/10.1111/myc.12907

Ahmad, S., & Alfouzan, W. (2021). Candida auris: Epidemiology, diagnosis, pathogenesis, antifungal susceptibility, and infection control measures to combat the spread of infections in healthcare facilities. *Microorganisms, 9*(4), Article 807. https://doi.org/10.3390/microorganisms9040807

Alex, H., Scherer, A., Kreuzburg, S., Abers, M. S., Zerbe, C. S., Dinauer, M. C., Mansour, M. K., & Irimia, D. (2020). Neutrophil swarming delays the growth of clusters of pathogenic fungi. *Nature Communications, 11*(1), 1–15. https://doi.org/10.1038/s41467-020-15834-4

Alfouzan, W., Dhar, R., Albarrag, A., & Al-Abdely, H. (2019). The emerging pathogen Candida auris: A focus on the Middle-Eastern countries. *Journal of Infection and Public Health, 12*(4), 451–459. https://doi.org/10.1016/j.jiph.2019.03.009

Almaghrabi, R. S., Albalawi, R., Mutabagani, M., Atienza, E., Aljumaah, S., Gade, L., Forsberg, K., Litvintseva, A., & Althawadi, S. (2020). Molecular characterisation and clinical outcomes of Candida auris infection: Single-centre experience in Saudi Arabia. *Mycoses, 63*(5), 452–460. https://doi.org/10.1111/myc.13065

Al-Siyabi, T., Al Busaidi, I., Balkhair, A., Al-Muharrmi, Z., Al-Salti, M., & Al'Adawi, B. (2017). First report of Candida auris in Oman: Clinical and microbiological description of five candidemia cases. *Journal of Infection, 75*(4), 373–376. https://doi.org/10.1016/j.jinf.2017.05.016

Anane, S., & Khalfallah, F. (2007). Diagnostic biologique des candidoses systémiques: difficultés et perspectives. *Pathologie Biologie, 55*(5), 262–272. https://doi.org/10.1016/j.patbio.2006.03.003

ANVISA. *Nota técnica GVIMS/GGTES/ANVISA nº 11/2020*. (2020) Orientações para identificação, prevenção e controle de infecções por Candida auris em serviços de saúde. Agência Nacional de Vigilância Sanitária. https://www.gov.br/anvisa/pt-br/centraisdeconteudo/publicacoes/servicosdesaude/notas-tecnicas/2020/nota-tecnica-gvims_n-11_2020_orientacoes_candida-auris_21-12-2020.pdf/view

Anwar, S., Glaser, A., Acharya, S., & Yousaf, F. (2020). Candida auris-an impending threat: A case report from home. *American Journal of Infection Control, 48*(11), 1407–1408. https://doi.org/10.1016/j.ajic.2020.01.020

Arastehfar, A., Carvalho, A., Hong Nguyen, M., Hedayati, M. T., Netea, M. G., Perlin, D. S., & Hoenigl, M. (2020). Covid-19-associated candidiasis (Cac): An underestimated complication in the absence of immunological predispositions? *Journal of Fungi, 6*(4), 1–13. https://doi.org/10.3390/jof6040211

Arastehfar, A., Fang, W., Badali, H., Vaezi, A., Jiang, W., Liao, W., Pan, W., Hagen, F., & Boekhout, T. (2018). Low-cost tetraplex PCR for the global spreading multi-drug resistant fungus, Candida auris and its phylogenetic relatives. Frontiers in *Microbiology, 9*, Article 1119. https://doi.org/10.3389/fmicb.2018.01119

Arendrup, M. C., Jørgensen, K. M., Hare, R. K., & Chowdhary, A. (2020). In Vitro Activity of Ibrexafungerp (SCY-078) against *Candida auris* Isolates as Determined by EUCAST Methodology and Comparison with Activity against C. albicans and C. glabrata and with the Activities of Six Comparator Agents. *Antimicrobial Agents and Chemotherapy, 64*(3). https://doi.org/10.1128/AAC.02136-19

Avni, T., Leibovici, L., & Paul, M. (2011). PCR diagnosis of invasive candidiasis: Systematic review and meta-analysis. *Journal of Clinical Microbiology, 49*(2), 665–670. https://doi.org/10.1128/JCM.01602-10

Azar, M. M., Turbett, S. E., Fishman, J. A., & Pierce, V. M. (2017). Donor-derived transmission of *Candida auris* during lung transplantation. *Clinical Infectious Diseases, 65*(6), 1040–1042. https://doi.org/10.1093/cid/cix460

Azoulay, E., Dupont, H., Tabah, A., Lortholary, O., Stahl, J. P., Francais, A., Martin, C., Guidet, B., & Timsit, J. F. (2012). Systemic antifungal therapy in critically ill patients without invasive fungal infection. *Critical Care Medicine, 40*(3), 813–822. https://doi.org/10.1097/CCM.0b013e318236f297

Barreto, T. L., Rossato, L., de Freitas, A. L. D., Meis, J. F., Lopes, L. B., Colombo, A. L., & Ishida, K. (2020). Miltefosine as an alternative strategy in the treatment of the emerging fungus *Candida auris*. *International Journal of Antimicrobial Agents, 56*(2). https://doi.org/10.1016/j.ijantimicag.2020.106049

Bayona, J. V. M., Salvador García, C., Tormo Palop, N., & Gimeno Cardona, C. (2020). Evaluation of a novel chromogenic medium for Candida spp. identification and comparison with CHROMagarTM Candida for the detection of *Candida auris* in surveillance samples. *Diagnostic Microbiology and Infectious Disease, 98*(4), Article 115168. https://doi.org/10.1016/j.diagmicrobio.2020.115168

Bayona, J. V. M., Salvador García, C., Tormo Palop, N., & Gimeno Cardona, C. (2021). Validation and implementation of a commercial real-time PCR assay for direct detection of *Candida auris* from surveillance samples. *Mycoses, 64*(6), 612–615. https://doi.org/10.1111/myc.13250

Ben-ami, R., Berman, J., Novikov, A., Bash, E., Shachor-meyouhas, Y., Zakin, S., Maor, Y., Tarabia, J., Schechner, V., Adler, A., & Finn, T. (2018). Multidrug-Resistant *Candida haemulonii* and *C. auris*, Tel Aviv, Israel. *Emerging Infectious Diseases, 23*(2), 195-203. http://doi.org/10.3201/eid2302.161486

Bentz, M. L., Joseph Sexton, D., Welsh, R. M., & Litvintseva, A. P. (2019). Phenotypic switching in newly emerged multidrug-resistant pathogen *Candida auris*. *Medical Mycology, 57*(5), 636–638. https://doi.org/10.1093/mmy/myy100

Berkow, E. L., Angulo, D., & Lockhart, S. R. (2017). In Vitro Activity of a Novel Glucan Synthase Inhibitor, SCY-078, against Clinical Isolates of *Candida auris*. *Antimicrobial Agents and Chemotherapy, 61*(7). https://doi.org/10.1128/AAC.00435-17

Biagi, M. J., Wiederhold, N. P., Gibas, C., Wickes, B. L., Lozano, V., Bleasdale, S. C., & Danziger, L. (2019). Development of high-level echinocandin resistance in a patient with recurrent candida auris candidemia secondary to chronic candiduria. *Open Forum Infectious Diseases, 6*(7), 1–5. https://doi.org/10.1093/ofid/ofz262

Bidaud, A. L., Chowdhary, A., & Dannaoui, E. (2018). *Candida auris*: An emerging drug resistant yeast – A mini-review. *Journal de Mycologie Medicale, 28*(3), 568–573. https://doi.org/10.1016/j.mycmed.2018.06.007

Bidaud, A. L., Djenontin, E., Botterel, F., Chowdhary, A., & Dannaoui, E. (2020). Colistin interacts synergistically with echinocandins against *Candida auris*. *International Journal of Antimicrobial Agents, 55*(3), Article 105901. https://doi.org/10.1016/j.ijantimicag.2020.105901

Billamboz, M., Fatima, Z., Hameed, S., & Jawhara, S. (2021). Promising drug candidates and new strategies for fighting against the emerging superbug *Candida auris*. *Microorganisms, 9*(3), 1–39. https://doi.org/10.3390/microorganisms9030634

Biswas, C., Wang, Q., Van Hal, S. J., Eyre, D. W., Hudson, B., Halliday, C. L., Mazsewska, K., Kizny Gordon, A., Lee, A., Irinyi, L., & others. (2020). Genetic heterogeneity of australian candida auris isolates: Insights from a nonoutbreak setting using whole-genome sequencing. *Open Forum Infectious Diseases, 7*(5), 1–5. https://doi.org/10.1093/OFID/OFAA158

Borman, A. M., Fraser, M., & Johnson, E. M. (2021). Chromagartmcandida plus: A novel chromogenic agar that permits the rapid identification of *Candida auris*. *Medical Mycology, 59*(3), 253–258. https://doi.org/10.1093/mmy/myaa049

Bronzwaer, S. L. A. M., Cars, O., Udo Buchholz, S. M., Goettsch, W., Veldhuijzen Jacob L Kool, I. K., Sprenger, M. J. W., & Degener, J. E. (2002). A European study on the relationship between antimicrobial use and antimicrobial resistance. *Emerging Infectious Diseases, 8*(3), 278–282. https://doi.org/10.3201/eid0803.010192

Bruno, M., Kersten, S., Bain, J. M., Jaeger, M., Rosati, D., Kruppa, M. D., Lowman, D. W., Rice, P. J., Graves, B., Ma, Z., & others (2020). Transcriptional and functional insights into the host immune response against the emerging fungal pathogen *Candida auris*. *Nature Microbiology, 5*(12), 1516–1531. https://doi.org/10.1038/s41564-020-0780-3

Caceres, D. H., Forsberg, K., Welsh, R. M., Sexton, D. J., Lockhart, S. R., Jackson, B. R., & Chiller, T. (2019). *Candida auris*: A review of recommendations for detection and control in healthcare settings. *Journal of Fungi, 5*(4), 1–11. https://doi.org/10.3390/jof5040111

Calvo, B., Melo, A. S. A., Perozo-Mena, A., Hernandez, M., Francisco, E. C., Hagen, F., Meis, J. F., & Colombo, A. L. (2016). First report of Candida auris in America: Clinical and microbiological aspects of 18 episodes of candidemia. *Journal of Infection, 73*(4), 369–374. https://doi.org/10.1016/j.jinf.2016.07.008

Cannon, R. D., Lamping, E., Holmes, A. R., Niimi, K., Baret, P. V., Keniya, M. V., Tanabe, K., Niimi, M., Goffeau, A., & Monk, B. C. (2009). Efflux-mediated antifungal drug resistance. *Clinical Microbiology Reviews, 22*(2), 291–321. https://doi.org/10.1128/CMR.00051-08

Carvalho, G. C., Bugno, A., Buzzo, A. A., Silva, F. P. de L. e, & Pinto, T. de J. A. (2020). Validation and applicability of an alternative method for dialysis. *Brazilian Journal of Nephrology, 42*, 163–174. https://doi.org/10.1590/2175-8239-JBN-2019-0203

Carvalho, G. C., Sábio, R. M., de Cássia Ribeiro, T., Monteiro, A. S., Pereira, D. V., Ribeiro, S. J. L., & Chorilli, M. (2020). Highlights in Mesoporous Silica Nanoparticles as a Multifunctional Controlled Drug Delivery Nanoplatform for Infectious Diseases Treatment. *Pharmaceutical Research, 37*(10), 1–30. https://doi.org/10.1007/s11095-020-02917-6

Casadevall, A., & Dimitrios P. Kontoyiannis, V. R. (2019). On the Emergence of *Candida auris*: Climate Change, Azoles, Swamps, and Birds. mBio, 10(8), 1397–1419. https://doi.org/10.1128/mBio.01397-19

Castro, L. Á., Álvarez, M. I., Rojas, F., Giusiano, G., & Martínez, E. (2019). Candida auris infection in the central catheter of a patient without sepsis symptoms. *Colombia Medica, 50*(4), 293–298. https://doi.org/10.25100/cm.v50i4.4248

CDC. (2021). *Tracking Candida auris: Candida auris Fungal Diseases* CDC. Centers for Disease Control and Prevention. https://www.cdc.gov/fungal/Candida-auris/index.html%0Ahttps://www.cdc.gov/fungal/candida-auris/

Cendejas-Bueno, E., Kolecka, A., Alastruey-Izquierdo, A., Theelen, B., Groenewald, M., Kostrzewa, M., Cuenca-Estrella, M., Gómez-López, A., & Boekhout, T. (2012). Reclassification of the *Candida haemulonii* complex as *Candida haemulonii* (*C. haemulonii* group I), *C. duobushaemulonii* sp. nov. (*C. haemulonii* group II), and *C. haemulonii* var. vulnera var. nov.: Three multiresistant human pathogenic yeasts. *Journal of Clinical Microbiology, 50*(11), 3641–3651. https://doi.org/10.1128/JCM.02248-12

Center of Disease Control and Prevention (CDC). (2019). *Antibiotic Resistance Threats in The United States 2019*. 10(1). http://dx.doi.org/10.15620/cdc:82532.

Center of Disease Control and Prevention (CDC). (2021). *Infection Prevention and Control for Candida auris*. Centers for Disease Control and Prevention. https://www.cdc.gov/fungal/candida-auris/c-auris-infection-control.html

Centers for Disease Control and Prevention. (2022, december 14). *Treatment and Management of C. auris Infections and Colonizations*. Centers for Disease Control and Prevention. https://www.cdc.gov/fungal/candida-auris/c-auris-treatment.html

Chaabane, F., Graf, A., Jequier, L., & Coste, A. T. (2019). Review on Antifungal Resistance Mechanisms in the Emerging Pathogen *Candida auris*. *Frontiers in Microbiology*, 10, Article 2788. https://doi.org/10.3389/fmicb.2019.02788

Chaffin, W. L. (2008). Candida albicans Cell Wall Proteins. *Microbiology and Molecular Biology Reviews, 72*(3), 495–544. https://doi.org/10.1128/mmbr.00032-07

Chatterjee, P., Choi, H., Ochoa, B., Garmon, G., Coppin, J. D., Allton, Y., Lukey, J., Williams, M. D., Navarathna, D., & Jinadatha, C. (2020). Clade-specific variation in susceptibility of Candida auris to broad-spectrum ultraviolet C light (UV-C). Infection Control and Hospital Epidemiology, 41(12), 1384–1387. https://doi.org/10.1017/ice.2020.410

Chatterjee, S., Alampalli, S. V., Nageshan, R. K., Chettiar, S. T., Joshi, S., & Tatu, U. S. (2015). Draft genome of a commonly misdiagnosed multidrug resistant pathogen *Candida auris*. *BMC Genomics, 16*, Article 686. https://doi.org/10.1186/s12864-015-1863-z

Chew, Y. L., Mahadi, A. M., Wong, K. M., & Goh, J. K. (2018). Anti-methicillin-resistance Staphylococcus aureus (MRSA) compounds from Bauhinia kockiana Korth. And their mechanism of antibacterial activity. *Complementary and Alternative Medicine, 18*, 1–9. https://doi.org/10.1186/s12906-018-2137-5

Chibabhai, V., Fadana, V., Bosman, N., & Nana, T. (2019). Comparative sensitivity of 1,3 beta-D-glucan for common causes of candidaemia in South Africa. *Mycoses, 62*(11), 1023–1028. https://doi.org/10.1111/myc.12982

Choi, H. Il, An, J., Hwang, J. J., Moon, S. Y., & Son, J. S. (2017). Otomastoiditis caused by Candida auris: Case report and literature review. *Mycoses, 60*(8), 488–492. https://doi.org/10.1111/myc.12617

Chow, N. A., De Groot, T., Badali, H., Abastabar, M., Chiller, T. M., & Meis, J. F. (2019). Potential fifth clade of *Candida auris*, Iran, 2018. *Emerging Infectious Diseases, 25*(9), 1780–1781. https://doi.org/10.3201/eid2509.190686

Chow, N. A., Gade, L., Tsay, S. V., Forsberg, K., Greenko, J. A., Southwick, K. L., Barrett, P. M., Kerins, J. L., Lockhart, S. R., Chiller, T. M., & others. (2018). Multiple introductions and subsequent transmission of multidrug-resistant Candida auris in the USA: a molecular epidemiological survey. *The Lancet Infectious Diseases, 18*(12). https://doi.org/10.1016/S1473-3099(18)30597-8

Chowdhary, A., Prakash, A., Sharma, C., Kordalewska, M., Kumar, A., Sarma, S., Tarai, B., Singh, A., Upadhyaya, G., Upadhyay, S., & others. (2018). A multicentre study of antifungal susceptibility patterns among 350 Candida auris isolates (2009-17) in India: Role of the ERG11 and FKS1 genes in azole and echinocandin resistance. *Journal of Antimicrobial Chemotherapy, 73*(4), 891–899. https://doi.org/10.1093/jac/dkx480

Chowdhary, A., Sharma, C., Duggal, S., Agarwal, K., Prakash, A., Singh, P. K., Jain, S., Kathuria, S., Randhawa, H. S., Hagen, F., & Meis, J. F. (2013). New clonal strain of Candida auris, Delhi, India. *Emerging Infectious Diseases, 19*(10), 1670–1673. https://doi.org/10.3201/eid1910.130393

Chowdhary, A., Sharma, C., & Meis, J. F. (2017). Candida auris: A rapidly emerging cause of hospital-acquired multidrug-resistant fungal infections globally. *PLoS Pathogens, 13*(5), 1–10. https://doi.org/10.1371/journal.ppat.1006290

Chowdhary, A., Tarai, B., Singh, A. S. (2020). Infections in Critically Ill Coronavirus Disease Patients, India, April-July 2020. *Emerging Infectious Diseases, 26*(11), 2694–2696.

Chowdhary, A., Voss, A., & Meis, J. F. (2016). *Candida auris* multi-resistente há infecciones nosocomiales. *J Hosp Infect, 94*(2), 209–212.

Clancy, C. J., & Nguyen, M. H. (2017). Emergence of candida auris: An international call to arms. *Clinical Infectious Diseases, 64*(2), 141–143. https://doi.org/10.1093/cid/ciw696

Cortegiani, A., Misseri, G., Fasciana, T., Giammanco, A., Giarratano, A., & Chowdhary, A. (2018). Epidemiology, clinical characteristics, resistance, and treatment of infections by *Candida auris*. *Journal of Intensive Care, 6*(1). https://doi.org/10.1186/s40560-018-0342-4

Covel, J. A., Soltow, Q. A., Kapoor, M., Moloney, M. K., Webb, P. J., Trzoss, M., Sharp, M., & Shaw, K. J. (2019). The Discovery of Manogepix/Fosmanogepix and Other Gwt1 Inhibitors for the Treatment of Invasive Fungal Infections. *In Bronson, J. J. (Ed.), 2019 Medicinal chemistry reviews: From the medicinal chemistry division of the ACS* (pp. 221–237). Division of Medicinal Chemistry. https://doi.org/10.29200/acsmedchemrev-v54.ch10

Das, I., Nightingale, P., Patel, M., & Jumaa, P. (2011). Epidemiology, clinical characteristics, and outcome of candidemia: Experience in a tertiary referral center in the UK. *International Journal of Infectious Diseases, 15*(11), e759–e763. https://doi.org/10.1016/j.ijid.2011.06.006

Das, S., Rai, G., Tigga, R. A., Srivastava, S., Singh, P. K., Sharma, R., Datt, S., Singh, N. P., & Dar, S. A. (2018). *Candida auris* in critically ill patients: Emerging threat in intensive care unit of hospitals. *Journal de Mycologie Medicale, 28*(3), 514–518. https://doi.org/10.1016/j.mycmed.2018.06.005

de Almeida, J. N., Francisco, E. C., Hagen, F., Brandão, I. B., Pereira, F. M., Dias, P. H. P., Costa, M. M.M., Jordão, R. T. S., de Groot, T., & Colombo, A. L. (2021). Emergence of candida auris in brazil in a covid-19 intensive care unit. *Journal of Fungi, 7*(3). https://doi.org/10.3390/jof7030220

de Groot, T., Puts, Y., Berrio, I., Chowdhary, A., & Meis, J. F. (2020). Development of Candida auris short tandem repeat typing and its application to a global collection of isolates. *mBio, 11*(1), 1–9. https://doi.org/10.1128/mBio.02971-19

de Oliveira, H. C., Monteiro, M. C., Rossi, S. A., Pemán, J., Ruiz-Gaitán, A., Mendes-Giannini, M. J. S., Mellado, E., & Zaragoza, O. (2019). Identification of Off-Patent Compounds That Present Antifungal Activity against the Emerging Fungal Pathogen *Candida auris*. *Frontiers in Cellular and Infection Microbiology, 9*, 1–10. https://doi.org/10.3389/fcimb.2019.00083

Denning, D. W. (2003). Echinocandin antifungal drugs. *Lancet, 362*(9390), 1142–1151. https://doi.org/10.1016/S0140-6736(03)14472-8

Dominguez, E. G., Zarnowski, R., Choy, H. L., Zhao, M., Sanchez, H., Nett, J. E., & Andes, D. R. (2019). Conserved Role for Biofilm Matrix Polysaccharides in *Candida auris* Drug Resistance. *mSphere, 4*(1), 2–8. https://doi.org/10.1128/mspheredirect.00680-18

Du, H., Bing, J., Hu, T., Ennis, C. L., Nobile, C. J., & Huang, G. (2020). *Candida auris*: Epidemiology, biology, antifungal resistance, and virulence. *PLoS Pathogens, 16*(10). https://doi.org/10.1371/journal.ppat.1008921

Emara, M., Ahmad, S., Khan, Z., Joseph, L., Al-Obaid, I., Purohit, P., & Bafna, R. (2015). *Candida auris* Candidemia in Kuwait, 2014. *Emerging Infectious Diseases, 21*, 1091–1092. http://dx.doi.org/10.3201/eid2106.150270

Evans, S. E. (2010). Coping with Candida infections. *Proceedings of the American Thoracic Society, 7*(3), 197–203. https://doi.org/10.1513/pats.200907-075AL

Eyre, D. W., Sheppard, A. E., Madder, H., Moir, I., Moroney, R., Quan, T. P., Griffiths, D., George, S., Butcher, L., Morgan, M., & others. (2018). A *Candida auris* Outbreak and Its Control in an Intensive Care Setting. *New England Journal of Medicine, 379*(14), 1322–1331. https://doi.org/10.1056/nejmoa1714373

Fakhim, H., Vaezi, A., Dannaoui, E., Chowdhary, A., Nasiry, D., Faeli, L., Meis, J. F., & Badali, H. (2018). Comparative virulence of Candida auris with Candida haemulonii, Candida glabrata and Candida albicans in a murine model. *Mycoses, 61*(6), 377–382. https://doi.org/10.1111/myc.12754

Farooqi, J., Niamatullah, H., Irfan, S., Zafar, A., Malik, F., & Jabeen, K. (2021). Comparison of β-D-Glucan levels between *Candida auris* and other Candida species at the time of candidaemia: a retrospective study. *Clinical Microbiology and Infection, 27*(10), 1519.e1-1519.e5. https://doi.org/10.1016/j.cmi.2021.05.031

Fernández-Chagüendo, C. M., Girón-Mera, I. J., Muñoz-Mora, D. F., & González-Cuellar, F. E. (2020). Osteomielitis por *Candida auris*: reporte de caso. *Revista de la Facultad de Medicina, 68*(3), 2018–2021. https://doi.org/10.15446/revfacmed.v68n3.75599

Fisher, M. C., Hawkins, N. J., Sanglard, D., & Gurr, S. J. (2018). *Worldwide emergence of resistance to antifungal drugs challenges human health and food security*. Science. https://www.science.org/doi/10.1126/science.aap7999

Forgács, L., Borman, A. M., Prépost, E., Tóth, Z., Kardos, G., Kovács, R., Szekely, A., Nagy, F., Kovacs, I., & Majoros, L. (2020). Comparison of in vivo pathogenicity of four *Candida auris* clades in a neutropenic bloodstream infection murine model. *Emerging Microbes and Infections, 9*(1), 1160–1169. https://doi.org/10.1080/22221751.2020.1771218

Forsberg, K., Woodworth, K., Walters, M., Berkow, E. L., Jackson, B., Chiller, T., & Vallabhaneni, S. (2019). *Candida auris*: The recent emergence of a multidrug-resistant fungal pathogen. *Medical mycology, 57*(1). https://doi.org/10.1093/mmy/myy054

Freitas, B. L., Leach, L., Chaturvedi, V., & Chaturvedi, S. (2022). Reverse Transcription-Quantitative Real-Time PCR (RT-qPCR) Assay for the Rapid Enumeration of Live Candida auris Cells from the Health Care Environment Bryanna. *Journal of clinical microbiology, 60*(2), Article e0077921. https://doi.org/10.1128/jcm.00779-21

Garcia-bustos, V., Pemán, J., Ruiz-gaitán, A., & Cabañero-navalon, M. D. (2021). Host – pathogen interactions upon *Candida auris* infection: fungal behaviour and immune response in Galleria mellonella. *Emerging Microbes & Infections, 11*, (1), 136-146. https://doi.org/10.1080/22221751.2021.2017756

Ghannoum, M., Arendrup, M. C., Chaturvedi, V. P., Lockhart, S. R., McCormick, T. S., Chaturvedi, S., Berkow, E. L., Juneja, D., Tarai, B., Azie, N., & others. (2020). Ibrexafungerp: A Novel Oral Triterpenoid Antifungal in Development for the Treatment of *Candida auris* Infections. *Antibiotics, 9*(9), 539. https://doi.org/10.3390/antibiotics9090539

Ghannoum, M., Isham, N., Angulo, D., Borroto-Esoda, K., Barat, S., & Long, L. (2020). Efficacy of Ibrexafungerp (SCY-078) against Candida auris in an In Vivo Guinea Pig Cutaneous Infection Model. *Antimicrobial Agents and Chemotherapy, 64*(10). https://doi.org/10.1128/AAC.00854-20

Giacobbe, D. R., Magnasco, L., Sepulcri, C., Mikulska, M., Koehler, P., Cornely, O. A., & Bassetti, M. (2021). Recent advances and future perspectives in the pharmacological treatment of Candida auris infections. *Expert Review of Clinical Pharmacology, 14*(10), 1205-1220. https://doi.org/10.1080/17512433.2021.1949285

Guarner, J., & Brandt, M. E. (2011). Histopathologic diagnosis of fungal infections in the 21st century. *Clinical Microbiology Reviews, 24*(2), 247–280. https://doi.org/10.1128/CMR.00053-10

Hani, U., Shivakumar, H., Vaghela, R., M. Osmani, R., & Shrivastava, A. (2015). Candidiasis: A Fungal Infection- Current Challenges and Progress in Prevention and Treatment. Infectious *Disorders - Drug Targets, 15*(1), 42–52. https://doi.org/10.2174/1871526515666150320162036

Healey, K. R., Kordalewska, M., Ortigosa, C. J., Singh, A., Berrío, I., Chowdhary, A., & Perlin, D. S. (2018). Limited ERG11 mutations identified in isolates of *Candida auris* directly contribute to reduced azole susceptibility. *Antimicrobial Agents and Chemotherapy, 62*(10). https://doi.org/10.1128/AAC.01427-18

Heath, C. H., Dyer, J. R., Pang, S., Coombs, G. W., & Gardam, D. J. (2019). *Candida auris* Sternal Osteomyelitis in a Man from Kenya Visiting Australia, 2015 Christopher. *Emerging Infectious Diseases, 191*(31), Article E865. https://doi.org/10.1503/cmaj.190433

Horton, M. V, & Nett, J. E. (2020). *Candida auris* Infection and Biofilm Formation: Going Beyond the Surface What Is the Clinical Presentation of *C. auris*. *Current clinical microbiology reports, 7*, 51–56. https://doi.org/10.1007/s40588-020-00143-7

Hou, X., Lee, A., Jiménez-Ortigosa, C., Kordalewska, M., Perlin, D. S., & Zhao, Y. (2019). Rapid Detection of ERG11-Associated Azole Resistance and FKS-Associated Echinocandin Resistance in *Candida auris*. *Antimicrobial agents and chemotherapy, 63*(1). https://doi.org/10.1128/AAC.01811-18

Huang, X., Welsh, R. M., Deming, C., Proctor, D. M., Thomas, P. J., Gussin, G. M., Huang, S. S., Kong, H. H., Bentz, M. L., Vallabhaneni, S., & others. (2021). Skin Metagenomic Sequence Analysis of Early *Candida auris* Outbreaks in U.S. Nursing Homes. *mSphere, 6*(4). https://doi.org/10.1128/msphere.00287-21

Ishikane, M., Hayakawa, K., Kutsuna, S., Takeshita, N., & Ohmagari, N. (2016). Epidemiology of blood stream infection due to candida species in a tertiary care hospital in Japan over 12 years: Importance of peripheral line-associated candidemia. *PLoS ONE, 11*(10), 1–14. https://doi.org/10.1371/journal.pone.0165346

Jackson, B. R., Chow, N., Forsberg, K., Litvintseva, A. P., Lockhart, S. R., Welsh, R., Vallabhaneni, S., & Chiller, T. (2019). On the origins of a species: What might explain the rise of *Candida auris*? *Journal of Fungi, 5*(3), 1–17. https://doi.org/10.3390/jof5030058

Jainlabdin, M. H., Batra, A., Sánchez Paredes, E., Hernández Hernández, F., Fu, G., & Tovar-Torres, J. (2019). Single-tube, dual channel pentaplexing for the identification of Candida strains associated with human infection. *Scientific Reports, 9*(1), 1–14. https://doi.org/10.1038/s41598-019-51198-6

Jeffery-Smith, A., Taori, S. K., Schelenz, S., Jeffery, K., Johnson, E. M., Borman, A., Manuel, R., & Browna, C. S. (2018). *Candida auris*: A review of the literature. *Clinical Microbiology Reviews, 31*(1). https://doi.org/10.1128/CMR.00029-17

Johnson, C. J., Davis, J. M., Huttenlocher, A., Kernien, J. F., & Netta, J. E. (2018). Emerging Fungal Pathogen Candida auris Evades Neutrophil Attack. *mBio, 9*, 1–9. -18. https://doi.org/10.1128/mBio.01403-18

Jung, J., Kim, M. J., Kim, J. Y., Lee, J. Y., Kwak, S. H., Hong, M. J., Chong, Y. P., Lee, S. O., Choi, S. H., Kim, Y. S., & others. (2020). Candida auris colonization or infection of the ear: A single-center study in South Korea from 2016 to 2018. *Medical Mycology, 58*(1), 124–127. https://doi.org/10.1093/mmy/myz020

Kathuria, S., Singh, P. K., Sharma, C., Prakash, A., Masih, A., Kumar, A., Meis, J. F., & Chowdhary, A. (2015). Multidrug-resistant Candida auris misidentified as Candida haemulonii: Characterization by matrix-assisted laser desorption ionization-time of flight mass spectrometry and DNA sequencing and its antifungal susceptibility profile variability by vitek 2, CLSI broth microdilution, and etest method. *Journal of Clinical Microbiology, 53*(6). https://doi.org/10.1128/JCM.00367-15

Kaur, H., Singh, S., Rudramurthy, S., Ghosh, A., Jayashree, M., Narayana, Y., Ray, P., & Chakrabarti, A. (2020). Candidaemia in a tertiary care centre of developing country: Monitoring possible change in spectrum of agents and antifungal susceptibility. *Indian Journal of Medical Microbiology, 38*(1), 109–115. https://doi.org/10.4103/ijmm.IJMM_20_112

Kean, R., Brown, J., Gulmez, D., Ware, A., & Ramage, G. (2020). *Candida auris*: A Decade of Understanding of an Enigmatic Pathogenic Yeast. *Journal of Fungi, 6*(1), Article 30. https://doi.org/10.3390/jof6010030

Kean, R., & Ramage, G. (2019). Combined Antifungal Resistance and Biofilm Tolerance: the Global Threat of Candida auris. *mSphere, 4*(4), 1–10. https://doi.org/10.1128/msphere.00458-19

Keighley, C., Garnham, K., Harch, S. A. J., Robertson, M., Chaw, K., Teng, J. C., & Chen, S. C. A. (2021). Candida auris: Diagnostic Challenges and Emerging Opportunities for the Clinical Microbiology Laboratory. *Current Fungal Infection Reports, 15*(3), 116–126. https://doi.org/10.1007/s12281-021-00420-y

Khan, M. A., Khan, A., Khan, S. H., Azam, M., Khan, M. M. U., Khalilullah, H., & Younus, H. (2020). Coadministration of liposomal methylglyoxal increases the activity of amphotericin B against Candida albicans in leukopoenic mice. *Journal of Drug Targeting, 29*(1), 78-87. https://doi.org/10.1080/1061186X.2020.1803333

Khillan, V., Rathore, N., Kathuria, S., & Chowdhary, A. (2014). A rare case of breakthrough fungal pericarditis due to fluconazole-resistant *Candida auris* in a patient with chronic liver disease. *JMM Case Reports, 1*(3). https://doi.org/10.1099/jmmcr.0.t00018

Kim, M. N., Shin, J. H., Sung, H., Lee, K., Kim, E. C., Ryoo, N., Lee, J. S., Jung, S. L., Park, K. H., Kee, S. J., & others. (2009). *Candida haemulonii* and closely related species at 5 university hospitals in Korea: Identification, antifungal susceptibility, and clinical features. *Clinical Infectious Diseases, 48*(6), 57–61. https://doi.org/10.1086/597108

Kordalewska, M., Zhao, Y., Lockhart, S. R., Chowdhary, A., Berrio, I., & Perlina, D. S. (2017). Rapid and Accurate Molecular Identification of the Emerging. *Journal of clinical microbiology, 55*(8), 2445–2452.

Kumar, D., Banerjee, T., Pratap, C. B., & Tilak, R. (2015). Itraconazole-resistant Candida auris with phospholipase, proteinase and hemolysin activity from a case of vulvovaginitis. *Journal of Infection in Developing Countries, 9*(4), 435–437. https://doi.org/10.3855/jidc.4582

Lane, C. R., Seemann, T., Worth, L. J., Easton, M., Pitchers, W., Wong, J., Cameron, D., Azzato, F., Bartolo, R., Mateevici, C., & others. (2020). Incursions of *Candida auris* into Australia, 2018. *Emerging Infectious Diseases, 26*(6), 2019–2021.https://doi.org/10.3201/eid2606.190936

Larkin, E., Hager, C., Chandra, J., & Mukherjee, P. K. (2017). The Emerging Pathogen *Candida auris*: Growth Phenotype, Virulence Factors, Activity of Antifungals, and Effect of SCY-078, a Novel Glucan Synthesis Inhibitor, on Growth Morphology and Biofilm Formation. *Antimicrobial Agents and Chemotherapy, 61*, Article e02396-16. https://doi.org/10.1128/AAC.02396-16

Leach, L., Zhu, Y., & Chaturvedi, S. (2018). Development and validation of a real-time pcr assay for rapid detection of *Candida auris* from surveillance samples. *Journal of Clinical Microbiology, 56*(2), 1–7. https://doi.org/10.1128/JCM.01223-17

Lee, W. G., Shin, J. H., Uh, Y., Kang, M. G., Kim, S. H., Park, K. H., & Jang, H. C. (2011). First three reported cases of nosocomial fungemia caused by Candida auris. *Journal of Clinical Microbiology, 49*(9), 3139–3142. https://doi.org/10.1128/JCM.00319-11

Lima, A., Widen, R., Vestal, G., Uy, D., & Silbert, S. (2019). A TaqMan probe-based real-time PCR assay for the rapid identification of the emerging multidrug-resistant pathogen *Candida auris* on the BD max system. *Journal of Clinical Microbiology, 57*(7), 1–8. https://doi.org/10.1128/JCM.01604-18

Lockhart, S. R., Etienne, K. A., Vallabhaneni, S., Farooqi, J., Chowdhary, A., Govender, N. P., Colombo, A. L., Calvo, B., Cuomo, C. A., Desjardins, C. A., & others. (2017). Simultaneous emergence of multidrug-resistant candida auris on 3 continents confirmed by whole-genome sequencing and epidemiological analyses. *Clinical Infectious Diseases, 64*, 134–140. https://doi.org/10.1093/cid/ciw691

Lockhart, S. R., Lyman, M. M., & Joseph Sexton, D. (2022). Tools for Detecting a "Superbug": Updates on Candida auris Testing. *Journal of Clinical Microbiology, 60*(5), Article e00808-21. https://doi.org/10.1128/jcm.00808-21

Mahmoudi, S., Agha Kuchak Afshari, S., Aghaei Gharehbolagh, S., Mirhendi, H., & Makimura, K. (2019). Methods for identification of *Candida auris*, the yeast of global public health concern: A review. *Journal de Mycologie Medicale, 29*(2), 174–179. https://doi.org/10.1016/j.mycmed.2019.04.004

Marena, G. D., Ramos, M. A. D. S., Lima, L. C., Chorilli, M., & Bauab, T. M. (2022). *Galleria mellonella* for systemic assessment of anti-*Candida auris* using amphotericin B loaded in nanoemulsion. *Science of The Total Environment, 807*, Article 151023. https://doi.org/10.1016/j.scitotenv.2021.151023

Marena, G. D., Ramos, M. A. dos S., Carvalho, G. C., de Lima, L. C., Nascimento, A. L. C. S. do, Sábio, R. M., Rodero, C. F., Spósito, L., Bauab, T. M., & Chorilli, M. (2022). Development and characterization of an amphotericin B - loaded nanoemulsion applied to *Candida auris* biofilms control. *Journal of Drug Delivery Science and* Technology, *74*, Article 103566. https://doi.org/10.1016/j.jddst.2022.103566

Martínez-Murcia, A., Navarro, A., Bru, G., Chowdhary, A., Hagen, F., & Meis, J. F. (2018). Internal validation of GPSTM MONODOSE CanAur dtec-qPCR kit following the UNE/EN ISO/IEC 17025:2005 for detection of the emerging yeast *Candida auris*. *Mycoses, 61*(11), 877–884. https://doi.org/10.1111/myc.12834

Mba, I. E., & Nweze, E. I. (2020). The use of nanoparticles as alternative therapeutic agents against Candida infections: an up-to-date overview and future perspectives. World *Journal of Microbiology and Biotechnology, 36*(11), 163–183. https://doi.org/10.1007/s11274-020-02940-0

McCarty, T. P., & Pappas, P. G. (2016). Invasive Candidiasis. *Infectious Disease Clinics of North America, 30*(1), 103–124. https://doi.org/10.1016/j.idc.2015.10.013

Mizusawa, M., Miller, H., Green, R., Lee, R., Durante, M., Perkins, R., Hewitt, C., Simner, P. J., Carroll, K. C., Hayden, R. T., & Zhang, S. X. (2017). Can multidrug-resistant *Candida auris* be reliably identified in clinical microbiology laboratories? *Journal of Clinical Microbiology, 55*(2), 638–640. https://doi.org/10.1128/JCM.02202-16

Morales-López, S. E., Parra-Giraldo, C. M., Ceballos-Garzón, A., Martínez, H. P., Rodríguez, G. J., Álvarez-Moreno, C. A., & Rodríguez, J. Y. (2017). Invasive infections with multidrug-resistant yeast *Candida auris*, Colombia. *Emerging Infectious Diseases, 23*(1), 162–164. https://doi.org/10.3201/eid2301.161497

Muñoz, J. F., Gade, L., Chow, N. A., Loparev, V. N., Juieng, P., Berkow, E. L., Farrer, R. A., Litvintseva, A. P., & Cuomo, C. A. (2018). Genomic insights into multidrug-resistance, mating and virulence in *Candida auris* and related emerging species. *Nature Communications, 9*(1), 1–13. https://doi.org/10.1038/s41467-018-07779-6

Naicker, S. D., Maphanga, T. G., Chow, N. A., Allam, M., Kwenda, S., Ismail, A., & Govender, N. P. (2021). Clade distribution of *Candida auris* in South Africa using whole genome sequencing of clinical and environmental isolates. Emerging *Microbes and Infections, 10*(1), 1300–1308. https://doi.org/10.1080/22221751.2021.1944323

National Institutes of Health. (2021a). *An Open-label Study of APX001 for Treatment of Patients With Candidemia/Invasive Candidiasis Caused by Candida Auris (APEX)*. ClinicalTrials.gov. https://clinicaltrials. gov/ct2/show/NCT04148287

National Institutes of Health. (2021b). *Open-Label Study to Evaluate the Efficacy and Safety of Oral Ibrexafungerp (SCY-078) in Patients With Candidiasis Caused by Candida Auris* (CARES) (CARES). ClinicalTrials.gov. https://classic.clinicaltrials.gov/ct2/show/NCT03363841

Nett, J. E. (2019). *Candida auris*: An emerging pathogen "incognito"? *PLoS Pathogens, 15*(4), 6–11. https://doi.org/10.1371/journal.ppat.1007638

Noginskiy, I., Samra, A., Nielsen, K., & Kalavar, M. R. (2018). A Case of Multiple Myeloma Presenting as *Streptococcus pneumoniae* Meningitis with *Candida auris* Fungemia. *Case Reports in Oncology, 11*(3), 705–710. https://doi.org/10.1159/000493852

Oliveira, L. V. N., Wang, R., Specht, C. A., & Levitz, S. M. (2021). Vaccines for human fungal diseases: close but still a long way to go. npj *Vaccines, 6*(1), 1–8. https://doi.org/10.1038/s41541-021-00294-8

Ong, C. W., Chen, S. C. -A., Clark, J. E., Halliday, C. L., Kidd, S. E., Marriott, D. J., Marshall, C. L., Morris, A. J., Morrissey, C. O., Roy, R., & others. (2019). Diagnosis, management and prevention of *Candida auris* in hospitals: position statement of the Australasian Society for Infectious Diseases. *Internal Medicine Journal, 49*(10), 1229–1243. https://doi.org/10.1111/imj.14612

Ostrosky-Zeichner, L., & Sobel, J. D. (2016). Fungal Infections. *Infectious Disease Clinics of North America, 30*(1), xiii–xiv. https://doi.org/10.1016/j.idc.2015.12.001

Paiva-Cavalcanti, M., Regis-da-Silva, C. G., & Gomes, Y. M. (2010). Comparison of real-time PCR and conventional PCR for detection of *leishmania (leishmania) infantum* infection: A mini-review. *Journal of Venomous Animals and Toxins Including Tropical Diseases, 16*(4), 537–542. https://doi.org/10.1590/S1678-91992010000400004

Pan American Health Organization (2021). *Epidemiological Alert: Candida auris outbreaks in health care services in the context of the COVID-19 pandemic. Regional Office for the Americas of the World Health Organization*. PAHO/WHO. https://www.paho.org/en/documents/epidemiological-alert-candida-auris-outbreaks-health-care-services-context-covid-19

Pappas, G. P., Lionakis, M. S., Arendrup, M. C., Zeichner, L. O., & Kullberg, B. J. (2018). Invasive Candidiasis. *Infectious Disease Clinics of North America, 30*(1), 103–124. https://doi.org/10.1016/j.idc.2015.10.013

Parra-Giraldo, C. M., Valderrama, S. L., Cortes-Fraile, G., Garzón, J. R., Ariza, B. E., Morio, F., Linares-Linares, M. Y., Ceballos-Garzón, A., de la Hoz, A., Hernandez, C., & others. (2018). First report of sporadic cases of *Candida auris* in Colombia. *International Journal of Infectious Diseases, 69*, 63–67. https://doi.org/10.1016/j.ijid.2018.01.034

Pekard-Amenitsch, S., Agnes Schriebl, W. P., Willinger, B., Kölli, B., & Buzina, W. (2018). Isolation of *Candida auris* from Ear of Otherwise Healthy Patient, Austria, 2018. *Emerging Infectious Diseases, 24*(8), 2017–2018.

Pemán, J., Ruiz-Gaitán, A., García-Vidal, C., Salavert, M., Ramírez, P., Puchades, F., García-Hita, M., Alastruey-Izquierdo, A., & Quindós, G. (2020). Fungal co-infection in COVID-19 patients: Should we be concerned? *Revista Iberoamericana de Micologia, 37*(2), 41–46. https://doi.org/10.1016/j.riam.2020.07.001

Pfaller, M. A., Huband, M. D., Flamm, R. K., Bien, P. A., & Castanheira, M. (2021). Antimicrobial activity of manogepix, a first-in-class antifungal, and comparator agents tested against contemporary invasive fungal isolates from an international surveillance programme (2018–2019). *Journal of Global Antimicrobial Resistance, 26*, 117–127. https://doi.org/10.1016/j.jgar.2021.04.012

Piedrahita, C. T., Cadnum, J. L., Jencson, A. L., Shaikh, A. A., Ghannoum, M. A., & Donskey, C. J. (2017). Environmental Surfaces in Healthcare Facilities are a Potential Source for Transmission of *Candida auris* and Other Candida Species. *Infection Control and Hospital Epidemiology, 38*(9), 1107–1109. https://doi.org/10.1017/ice.2017.127

Pitarch, A., Nombela, C., & Gil, C. (2018). Diagnosis of Invasive Candidiasis: From Gold Standard Methods to Promising Leading-edge Technologies. *Current Topics in Medicinal Chemistry, 18*(16), 1375–1392. https://doi.org/10.2174/1568026618666181025093146

Plachouras, D., Lötsch, F., Kohlenberg, A., Monnet, D. L., Lass-Flörl, C., Muchl, R., Willinger, B., Lagrou, K., Philipova, I., Budimir, A., & others. (2020). *Candida auris*: Epidemiological situation, laboratory capacity and preparedness in the European Union and European Economic Area, January 2018 to May 2019. Eurosurveillance, 25(12). https://doi.org/10.2807/1560-7917.ES.2020.25.12.2000240

Poulain, D. (2015). *Candida albicans*, plasticity and pathogenesis. *Critical Reviews in Microbiology, 41*(2), 208–217. https://doi.org/10.3109/1040841X.2013.813904

Prakash, A., Sharma, C., Singh, A., Kumar Singh, P., Kumar, A., Hagen, F., Govender, N. P., Colombo, A. L., Meis, J. F., & Chowdhary, A. (2016). Evidence of genotypic diversity among *Candida auris* isolates by multilocus sequence typing, matrix-assisted laser desorption ionization time-of-flight mass spectrometry and amplified fragment length polymorphism. *Clinical Microbiology and Infection, 22*(3), 277.e1-277.e9. https://doi.org/10.1016/j.cmi.2015.10.022

Public Health England (2017). *Guidance for the laboratory investigation, management and infection prevention and control for cases of Candida auris*. Public Health England London, United Kingdom.

Romani, L. (2011). Immunity to fungal infections. *Nature Reviews Immunology, 11*(4), 275–288. https://doi.org/10.1038/nri2939

Rossato, L., & Colombo, A. L. (2018). *Candida auris*: What have we learned about its mechanisms of pathogenicity? Frontiers in Microbiology, 9, 1–6. https://doi.org/10.3389/fmicb.2018.03081

Rudramurthy, S. M., Chakrabarti, A., Paul, R. A., Sood, P., Kaur, H., Capoor, M. R., Kindo, A. J., Marak, R. S. K., Arora, A., Sardana, R., & others. (2017). *Candida auris* candidaemia in Indian ICUs: Analysis of risk factors. *Journal of Antimicrobial Chemotherapy, 72*(6), 1794–1801. https://doi.org/10.1093/jac/dkx034

Ruiz-Gaitán, A. C., Moret, A., Hontangas, J. L. L., Molina, J. M., López, A. I. A., Cabezas, A. H., Maseres, J. M., Arcas, R. C., Ruiz, M. D. G., Chiveli, & others. (2017). Fungemia nosocomial por *Candida auris*: primeros cuatro casos en Europa continental. *Revista Iberoamericana de Micologia, 34*(1), 23–27. https://doi.org/10.1016/j.riam.2016.11.002

Ruiz-Gaitán, A. C., Cantón, E., Fernández-Rivero, M. E., Ramírez, P., & Pemán, J. (2019). Outbreak of Candida auris in Spain: A comparison of antifungal activity by three methods with published data. *International Journal of Antimicrobial Agents, 53*(5), 541–546. https://doi.org/10.1016/j.ijantimicag.2019.02.005

Ruiz-Gaitán, A. C., Fernández-Pereira, J., Valentin, E., Tormo-Mas, M. A., Eraso, E., Pemán, J., & de Groot, P. W. J. (2018). Molecular identification of *Candida auris* by PCR amplification of species-specific GPI protein-encoding genes. *International Journal of Medical Microbiology, 308*(7), 812–818. https://doi.org/10.1016/j.ijmm.2018.06.014

Santos, P. S., Dalla Lana, D. F., & Mezzari, A. (2017). *Candida Auris*: Emergence and Epidemiology of a Highly Pathogenic Yeast. *Clinical & Biomedical Research, 37*(3), 247–254. https://doi.org/10.4322/2357-9730.73982

Saris, K., Meis, J. F., & Voss, A. (2018). *Candida auris*. *Current Opinion in Infectious Diseases*, *31*(4), 334-340. https://doi.org/10.1097/QCO.0000000000000469

Satoh, K., Makimura, K., Hasumi, Y., Nishiyama, Y., Uchida, K., & Yamaguchi, H. (2009). Candida auris sp. nov., a novel ascomycetous yeast isolated from the external ear canal of an inpatient in a Japanese hospital. *Microbiology and Immunology, 53*(1), 41–44. https://doi.org/10.1111/j.1348-0421.2008.00083.x

Schelenz, S., Hagen, F., Rhodes, J. L., Abdolrasouli, A., Chowdhary, A., Hall, A., Ryan, L., Shackleton, J., Trimlett, R., Meis, J. F., & others. (2016). First hospital outbreak of the globally emerging *Candida auris* in a European hospital. *Antimicrobial Resistance and Infection Control, 5*, Article 35. https://doi.org/10.1186/s13756-016-0132-5

Schwartz, I., & Hammond, G. (2017). First reported case of multidrug-resistant *Candida auris* in Canada. *Canada Communicable Disease Report, 43*(7–8), 150–153. https://doi.org/10.14745/ccdr.v43i78a02

Sekizuka, T., Iguchi, S., Umeyama, T., Inamine, Y., Makimura, K., Kuroda, M., Miyazaki, Y., & Kikuchi, K. (2019). Clade II *Candida auris* possess genomic structural variations related to an ancestral strain. *PLoS ONE, 14*(10), 1–22. https://doi.org/10.1371/journal.pone.0223433

Sekyere, J. O. (2018). *Candida auris*: A systematic review and meta-analysis of current updates on an emerging multidrug-resistant pathogen. *MicrobiologyOpen, 7*(4), 1–29. https://doi.org/10.1002/mbo3.578

Sharma, C., Kumar, N., Pandey, R., Meis, J. F., & Chowdhary, A. (2016). Whole genome sequencing of emerging multidrug resistant *Candida auris* isolates in India demonstrates low genetic variation. *New Microbes and New Infections, 13*, 77–82. https://doi.org/10.1016/j.nmni.2016.07.003

Shaw, K. J., & Ibrahim, A. S. (2020). Fosmanogepix: A Review of the First-in-Class Broad Spectrum Agent for the Treatment of Invasive Fungal Infections. *Journal of Fungi, 6*(4), Article 239. https://doi.org/10.3390/jof6040239

Shenoy, V., Ballenberger, M., Prince, A., & Maslak, S. (2019). Panophthalmitis from Candida auris. *Annals of Internal Medicine, 171*(12), 941–943. https://doi.org/10.7326/L19-0323

Singh, R., Kaur, M., Chakrabarti, A., Shankarnarayan, S. A., & Rudramurthy, S. M. (2019). Biofilm formation by *Candida auris* isolated from colonising sites and candidemia cases. *Mycoses, 62*(8), 706–709. https://doi.org/10.1111/myc.12947

Smeekens, S. P., van de Veerdonk, F. L., Kullberg, B. J., & Netea, M. G. (2013). Genetic susceptibility to Candida infections. *EMBO Molecular Medicine, 5*(6), 805–813. https://doi.org/10.1002/emmm.201201678

Snyder, G. M., & Wright, S. B. (2019). The Epidemiology and Prevention of *Candida auris*. *Current Infectious Disease Reports, 21*(6), 19. https://doi.org/10.1007/s11908-019-0675-8

Sobel, J. D. (2007). Vulvovaginal candidosis. *Lancet, 369*(9577), 1961–1971. https://doi.org/10.1016/S0140-6736(07)60917-9

Spadari, C. de C., de Bastiani, F. W. M. da S., Lopes, L. B., & Ishida, K. (2019). Alginate nanoparticles as non-toxic delivery system for miltefosine in the treatment of candidiasis and cryptococcosis. *International Journal of Nanomedicine*, *14*, 5187–5199. https://doi.org/10.2147/IJN.S205350

Spivak, E. S., & Hanson, K. E. (2018). *Candida auris*: an Emerging Fungal Pathogen. *Journal of clinical microbiology, 56*(2), 1–10. https://doi.org/10.1128/JCM.01588-17

Stathi, A., Loukou, I., Kirikou, H., Petrocheilou, A., Moustaki, M., Velegraki, A., & Zachariadou, L. (2021). Isolation of *Candida auris* from cystic fibrosis patient, Case report Identification of Candida auris Antifungal susceptibility. *Eurosurveillance |, 24*, 1–8.

Sujana, B. M., Chintamaneni, R., Chennupati, A., Nahar, P., Chaluvadi, R. S., Vemugunta, R., & Prabhat, M. V. P. (2016). Evaluation of antifungal efficacy of ethanolic crude lawsone and listerine mouthwash in uncontrolled diabetics and denture wearers - A randomized clinical trial. *Journal of Clinical and Diagnostic Research, 10*(6), ZC90–ZC95. https://doi.org/10.7860/JCDR/2016/19463.8036

Supreeth, S., Al Ghafri, K. A., Jayachandra, R. K., & Al Balushi, Z. Y. (2020). First Report of Candida auris Spondylodiscitis in Oman: A Rare Presentation. *World Neurosurgery, 135*, 335-338. https://doi.org/10.1016/j.wneu.2019.09.021

Tan, Y. E., & Tan, A. L. (2018). Arrival of *Candida auris* Fungus in Singapore: Report of the First 3 Cases. *Annals of the Academy of Medicine, Singapore, 47*(7), 260–262.

Tap, R. M., Lim, T. C., Kamarudin, N. A., Ginsapu, S. J., Abd Razak, M. F., Ahmad, N., & Amran, F. (2018). A Fatal Case of *Candida auris* and Candida tropicalis Candidemia in Neutropenic Patient. *Mycopathologia, 183*(3), 559–564. https://doi.org/10.1007/s11046-018-0244-y

Teke, L., Sargin Altunok, E., & Genç Moralar, D. (2021). The Second Case of *Candida auris* Candidemia from Turkey: An Impending Threat to the Global Health. Mediterranean *Journal of Infection, Microbes and Antimicrobials, 10*, 8–11. https://doi.org/10.4274/mjima.galenos.2021.2021.48

Theill, L., Dudiuk, C., Morales-Lopez, S., Berrio, I., Rodríguez, J. Y., Marin, A., Gamarra, S., & Garcia-Effron, G. (2018). Single-tube classical PCR for *Candida auris* and *Candida haemulonii* identification. *Revista Iberoamericana de Micologia, 35*(2), 110–112. https://doi.org/10.1016/j.riam.2018.01.003

Tian, S., Bing, J., Chu, Y., Chen, J., Cheng, S., Wang, Q., Zhang, J., Ma, X., Zhou, B., Liu, L., & others. (2021). Genomic epidemiology of *Candida auris* in a general hospital in Shenyang, China: a three-year surveillance study. *Emerging Microbes and Infections, 10*(1), 1088–1096. https://doi.org/10.1080/22221751.2021.1934557

Tian, S., Rong, C., Nian, H., Li, F., Chu, Y., Cheng, S., & Shang, H. (2018). First cases and risk factors of super yeast *Candida auris* infection or colonization from Shenyang, China article. *Emerging Microbes and Infections, 7*(1), 128–138. https://doi.org/10.1038/s41426-018-0131-0

Torres, S. R., Pichowicz, A., Torres-Velez, F., Song, R., Singh, N., Lasek-Nesselquist, E., & De Jesus, M. (2020). Impact of *Candida auris* infection in a neutropenic murine model. *Antimicrobial Agents and Chemotherapy, 64*(3), 1–7. https://doi.org/10.1128/AAC.01625-19

Vallabhaneni, S., Kallen, A., Tsay, S., Chow, N., Welsh, R., Kerins, J., Kemble, S. K., Pacilli, M., Black, S. R., Landon, E., & others (2017). Investigation of the First Seven Reported Cases of *Candida auris*, a Globally Emerging Invasive, Multidrug-Resistant Fungus—United States, May 2013–August 2016. *American Journal of Transplantation, 17*(1), 296–299. https://doi.org/10.1111/ajt.14121

Vallabhaneni, S., Mody, R. K., Walker, T., & Chiller, T. (2016). The Global Burden of Fungal Diseases. *Infectious Disease Clinics of North America, 30*(1), 1–11. https://doi.org/10.1016/j.idc.2015.10.004

Vandeputte, P., Ferrari, S., & Coste, A. T. (2012). Antifungal resistance and new strategies to control fungal infections. *International Journal of Microbiology*, 2012, Article 713687. https://doi.org/10.1155/2012/713687

Vila, T., Sultan, A. S., Montelongo-Jauregui, D., & Jabra-Rizk, M. A. (2020). *Candida auris*: A fungus with identity crisis. *Pathogens and Disease, 78*(4), 1–8. https://doi.org/10.1093/femspd/ftaa034

Villa, S., Hamideh, M., Weinstock, A., Qasim, M. N., Hazbun, T. R., Sellam, A., Hernday, A. D., & Thangamani, S. (2020). Transcriptional control of hyphal morphogenesis in *Candida albicans*. *FEMS Yeast Research, 20*(1), 1–17. https://doi.org/10.1093/femsyr/foaa005

Vu, B. G., & Moye-Rowley, W. S. (2018). Construction and Use of a Recyclable Marker to Examine the Role of Major Facilitator Superfamily Protein Members in *Candida glabrata* Drug Resistance Phenotypes. *mSphere, 3*(2), 1–12. https://doi.org/10.1128/msphere.00099-18

Walchak, R. C., Buckwalter, S. P., Zinsmaster, N. M., Henn, K. M., Johnson, K. M., Koelsch, J. M., Herring, S. A., Steinmetz, L. K., Reed, K. A., Barth, J. E., & others. (2020). *Candida auris* direct detection from surveillance swabs, blood, and urine using a laboratory-developed pcr method. *Journal of Fungi, 6*(4), 1–16. https://doi.org/10.3390/jof6040224

Wall, G., Chaturvedi, A. K., Wormley, F. L., Wiederhold, N. P., Patterson, H. P., Patterson, T. F., & Lopez-Ribot, J. L. (2018). Screening a Repurposing Library for Inhibitors of Multidrug-Resistant *Candida auris* Identifies Ebselen as a Repositionable Candidate for Antifungal Drug Development. *Antimicrobial Agents and Chemotherapy, 62*(10). https://doi.org/10.1128/AAC.01084-18

Wang, X., Bing, J., Zheng, Q., Zhang, F., Liu, J., Yue, H., Tao, L., Du, H., Wang, Y., Wang, H., & Huang, G. (2018). The first isolate of Candida auris in China: Clinical and biological aspects article. *Emerging Microbes and Infections, 7*(1), 93–102. https://doi.org/10.1038/s41426-018-0095-0

Wasi, M., Khandelwal, N. K., Moorhouse, A. J., Nair, R., Vishwakarma, P., Ruiz, G. B., Ross, Z. K., Lorenz, A., Rudramurthy, S. M., Chakrabarti, A., & others. (2019). ABC transporter genes show upregulated expression in drug-resistant clinical isolates of *Candida auris*: A genome-wide characterization of atp-binding cassette (abc) transporter genes. *Frontiers in Microbiology, 10*, 1–16. https://doi.org/10.3389/fmicb.2019.01445

Watanabe, N., Miyazaki, M., Horii, T., Sagane, K., Tsukahara, K., & Hata, K. (2012). E1210, a New Broad-Spectrum Antifungal, Suppresses *Candida albicans* Hyphal Growth through Inhibition of Glycosylphosphatidylinositol Biosynthesis. *Antimicrobial Agents and Chemotherapy, 56*(2), 960–971. https://doi.org/10.1128/AAC.00731-11

Welsh, R. M., Bentz, M. L., Shams, A., Houston, H., Lyons, A., Rose, L. J., & Litvintseva, A. P. (2017). Survival, Persistence, and Isolation of the Emerging Multidrug-Resistant Pathogenic Yeast *Candida auris* on a Plastic Healthcare Surface. *Journal of Clinical Microbiology, 55*(10). https://doi.org/10.1128/JCM.00921-17

Widmer, F., Wright, L. C., Obando, D., Handke, R., Ganendren, R., Ellis, D. H., & Sorrell, T. C. (2006). Hexadecylphosphocholine (Miltefosine) Has Broad-Spectrum Fungicidal Activity and Is Efficacious in a Mouse Model of Cryptococcosis. *Antimicrobial Agents and Chemotherapy, 50*(2), 414–421. https://doi.org/10.1128/AAC.50.2.414-421.2006

Wiederhold, N. P., Najvar, L. K., Olivo, M., Morris, K. N., Patterson, H. P., Catano, G., & Patterson, T. F. (2021). Ibrexafungerp Demonstrates In Vitro Activity against Fluconazole-Resistant *Candida auris* and In Vivo Efficacy with Delayed Initiation of Therapy in an Experimental Model of Invasive Candidiasis. *Antimicrobial Agents and Chemotherapy, 65*(6). https://doi.org/10.1128/AAC.02694-20

Wiederhold, N. P., Najvar, L. K., Shaw, K. J., Jaramillo, R., Patterson, H., Olivo, M., Catano, G., & Patterson, T. F. (2019). Efficacy of Delayed Therapy with Fosmanogepix (APX001) in a Murine Model of *Candida auris* Invasive Candidiasis. *Antimicrobial Agents and Chemotherapy, 63*(11). https://doi.org/10.1128/AAC.01120-19

Xin, H., Mohiuddin, F., Tran, J., Adams, A., & Eberle, K. (2019). Experimental Mouse Models of Disseminated *Candida auris* Infection. *mSphere, 4*(5), 1–9. https://doi.org/10.1128/msphere.00339-19

Yamamoto, M., Alshahni, M. M., Tamura, T., Satoh, K., Iguchi, S., Kikuchi, K., Mimaki, M., & Makimurab, K. (2018). Rapid detection of *Candida auris* based on loop-mediated isothermal amplification (LAMP). *Journal of Clinical Microbiology, 56*(9), 1–5. https://doi.org/10.1128/JCM.00591-18

Yue, H., Bing, J., Zheng, Q., Zhang, Y., Hu, T., Du, H., Wang, H., & Huang, G. (2018). Filamentation in *Candida auris*, an emerging fungal pathogen of humans: passage through the mammalian body induces a heritable phenotypic switch. *Emerging Microbes and Infections, 7*(1). https://doi.org/10.1038/s41426-018-0187-x

Zhang, B., & Izadjoo, M. (2015). Differential diagnosis of candida species with real-time polymerase chain reaction and melting temperature analyses (RTPCR-MTA). *Military Medicine, 180*(6), 652–659. https://doi.org/10.7205/MILMED-D-14-00294

Zhou, X., Su, Q., Zhao, H., Cao, X., Yang, Y., & Xue, W. (2020). Metal-Phenolic Network-Encapsulated Nanovaccine with pH and Reduction Dual Responsiveness for Enhanced Cancer Immunotherapy. *Molecular Pharmaceutics, 17*(12), 4603–4615. https://doi.org/10.1021/acs.molpharmaceut.0c00802

Zhu, Y., Kilburn, S., Kapoor, M., Chaturvedi, S., Shaw, K. J., & Chaturvedi, V. (2020). In Vitro Activity of Manogepix against Multidrug-Resistant and Panresistant *Candida auris* from the New York Outbreak. *Antimicrobial Agents and Chemotherapy, 64*(11). https://doi.org/10.1128/AAC.01124-20

CHAPTER 4

Lycopene: From tomato to its nutraceutical use and its association with nanotechnology

Gabriela Corrêa Carvalho*, Bruna Almeida Furquim de Camargo, Jennifer Thayanne Cavalcante de Araújo, Marlus Chorilli*

Trends in Food Science & Technology, v. 118, pp. 447-458, 2021.

Reprinted with permission in accordance with the journal's author's rights policy - Elsevier.

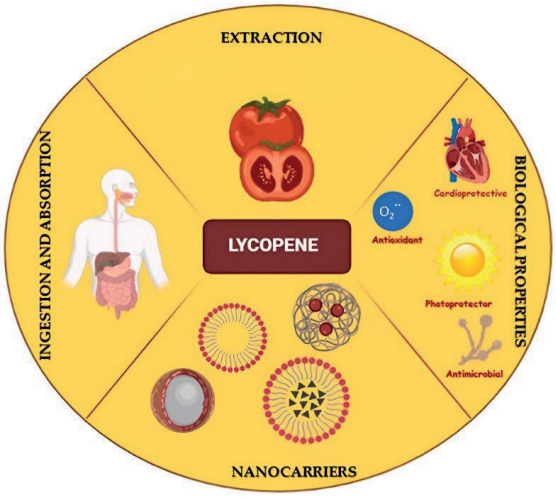

Abstract

Lycopene, a red-colored carotenoid, has several biological properties, such as antioxidant, cardioprotective, antihypercholesterolemic, antidiabetic, antimicrobial, photoprotector and anticancer, making desirable its use as nutraceutical. Despite the fact that it can be found in several foods, tomato deserves great prominence because it is the major extraction source and the cheapest raw material, being therefore the human most ingested source. Tomato also stands out for being the source where lycopene was first discovered. This review article seeks to highlight the entire route that lycopene passes until its use as a nutraceutical, highlighting the main methods of extraction, concentration and quantification. Solvent extraction and super-critical fluid extraction, centrifugation and evaporation and HPLC and UV-vis spectrophotometer were the researchers most chosen methods of extraction, concentration and quantification, respectively. It also was noted that its association with nanotechnology is desirable to circumvent limitations related to its physicochemical characteristics that limit, not only its extraction process but also its nutraceutical use.

1. Introduction

Lycopene, a carotenoid with a molecular structure of $C_{40}H_{56}$ (**Figure 1**), is responsible for the red coloring of various foods like tomatoes, watermelon, papaya, pink grapefruit and guava (Carvalho et al., 2020). Tomato represents the most important lycopene source, as it is the cheapest raw material, supplying a large part of this carotenoid on the market. It is also the most ingested source, either in the form of tomatoes or as a processed products. Comment need to be made that it was also the source where it was discovered, as a red pigment, by Millardet, in 1876 (Ghadage et al., 2019; Vogele, 1937).

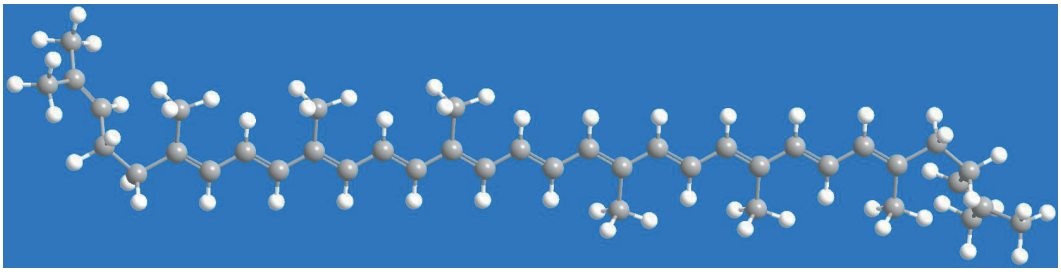

Figure 1: Chemical structure of the lycopene.

The name lycopene is derivative from tomatoes scientific name, *Solanum lycopersicum*. Today is known that this reddish color is related to the 11 conjugated double bonds present in its structure (from a total of 13 double bonds), since the phytoene, its precursor, does not have double bonds and is colorless (Hussain & Khan, 2020; Sasaki, & Ohmiya, 2008). It is worth mentioning that, due to these double bonds there are two possible lycopene configurations (cis and trans) and 1056 possible isomers (Colle et al., 2010).

The function of this pigment in food is to absorb light in the photosynthesis process, photoprotect the plant against visible and ultraviolet light and attract animals for pollination and seed dispersal (Shi & Maguer, 2000; Tanaka et al., 2008). Many factors interfere with tomatoes lycopene content, the water supply, for example, is shown to interfere inversely proportional. 50% and 75% of the ideal water supply leads to a higher lycopene content when compared to a water supply of 100% (Brandt et al., 2003; Takács et al., 2020). On the other hand, tomatoes grown in greenhouse have a higher lycopene content than those grown in the field, probably because in the field it is difficult to control climatic factors such as rainfall and temperature. It is worth mentioning that temperatures above 30 °C, during tomatoes cultivation, inhibit lycopene synthesis. In addition, the more exposure to solar radiation the higher temperature to which the fruits are exposed, and the lower the fruit color shade, which is directly related to lycopene content (Brandt et al., 2003; Brandt et al., 2006; Daood et al., 2021; Pék et al., 2011). Genetic factors and tomato varieties are also shown to interfere with these

carotenoid content, cherry tomatoes have a higher content than Daniela F1 and Delfine F1, for example (Brandt et al., 2003; Daood et al., 2014). Transgenic modifications and genetic manipulation are areas that have been increasingly studied in order to increase tomato pigmentation and consequently increasing lycopene content (Ilahy et al., 2017, 2019).

When ingested by a human, this red pigment brings several health benefits (Ghadage et al., 2019). Although lycopene is found predominantly as all-trans isomer, 5-cis, 9-cis, 13-cis, and 15-cis can also be identified (Rao et al., 2006). Lycopene cis isomer is better absorbed by the human body, when compared to all trans-lycopene due to its greater solubility in the bile acid micelles, making it more bioavailable. This cis-trans isomerization occurs due to factors such as acid, oxygen, heat and light (Boileau et al., 1999; Shi & Maguer, 2000). As for activity difference between cis-trans isomers, there are few, and not totally clear, studies in the literature (Honest et al., 2011; Soares et al., 2019). It is worth mentioning that due to their structural differences, cis-lycopene has a different bioactivity potency when compared to trans-lycopene, and there are reports that cis-lycopene participates more in biological reactions, providing more health benefits than all-trans (Böhm et al., 2002; Shi & Maguer, 2000).

However, this pigment was isolated for the firth time only in 1910 by Willstxtter and Escher, having its hydrocarbon nature attributed (Vogele, 1937). Due to its chemical structure, lycopene has a molecular weight of 536.85 Da and present solubility in chloroform, benzene, hexane, carbon disulfide, acetone and petroleum ether, being insoluble in water, ethanol and methanol (Shi & Maguer, 2000). These physicochemical characteristics are important when the production of a nutraceutical is aimed. Nutraceuticals are formed by a group of active substances extracted from food, that has both, pharmacological and nutritional value (Santini et al., 2017). A trend that has been observed, is the association of nutraceuticals insoluble in aqueous solvents with low chemical stability, like lycopene, with nanocarriers, in order to circumvent these limitations, increasing not only their solubility and stability, but also its bioaccessibility and bioavailability (Carvalho et al., 2020; Jafari & McClements, 2017; Jones et al., 2019; Singh et al., 2021). In this context, this review article seeks to highlight the entire route that lycopene passes from its extraction and purification from tomatoes to its nutraceutical use and its association with nanotechnology.

2. Obtaining lycopene from food

The desirable biological effect of lycopene attracts its use as nutraceuticals, supplements and functional foods, being, therefore, observed an exponential increase in both, market space and price. In addition to the usual extraction and purification techniques, new technologies have been developed in order to improve its recovery, mainly from tomato peel, its main extraction source (Santini et al.,

2017; Zuorro, 2020). Lycopene extraction process from the food matrix is of fundamental importance because increases its bioavailability in the human body. Thermal processing also stands out for this same purpose (Shi & Maguer, 2000). However, it is important to highlight that thermic process must be done with caution because it leads not only to all trans-lycopene isomerization but also to degradation, which needs to be avoided as it affects the final products sensorial quality and health benefits (Murakami et al., 2018; Shi & Maguer, 2000).

Mayeaux and collaborators (2006) evaluated lycopene thermal stability and observed that some exposure to heat conditions led to a degradation of 50% in lycopene pattern, are they: 100 °C for 60 minutes, 125 °C for 20 min and 150 °C for less than 10 min. In another study, where lycopene thermal degradation kinetics was evaluated, in tomato juice, several heating conditions were evaluated in a water bath (70, 80, 90 and 100 °C for 20, 40, 60 and 80 min). Among them, significant degradation increase was observed, following first-order kinetics. Additionally, it was noted that lycopene content decreased at temperatures of 80, 90 and 100 °C when compared to a temperature of 70 °C (rate constant of 0.0014, 0.002, 0.0025 and 0.001 km^{-1}, respectively) (Aliyu et al., 2020).

On the other hand, Colle et al., (2010) tested various temperatures and realized that the heat treatment of 130 and 140 °C for 30 min preserved 74% to 75% of the lycopene content present in tomato pulp. It is worth mentioning that the amount of all trans-lycopene remaining in the sample processed at 140 °C for 30 min was 84%. It should also be noted that lycopene bioaccessibility *in vitro* was improved in the two treatment conditions mentioned above. However, the authors point out that this type of intense processing affects not only other tomatoes nutrients, such as vitamin C, but also its quality (due to variations in color, flavor and viscosity), causing product rejection by the consumer.

Lycopene extraction methods can be divided into two categories, organic solvent extraction (conventional) and green technique (alternative). This second category started to be used because organic solvents are toxic to the environment, furthermore, toxic traces in the final product makes it unsuitable for use. In the first category we can mention, as the commonly used methods, solvent extraction (liquid-liquid extraction), Soxhlet extraction, enzyme-assisted extraction, microwave-assisted extraction, ultrasound-assisted extraction and high hydrostatic pressure-assisted extraction. As a green technique, supercritical fluid extraction can be mentioned (Ashraf et al., 2020; Choksi & Joshi, 2007; Domínguez et al., 2020). **Table 1** summarizes the principle of each technique mentioned above, and its advantages and disadvantages.

Table 1: Main characteristics of some lycopene extraction methods.

Extraction method	Principle	Advantage	Disadvantage	References
Solvent extraction	The extraction occurs due to the affinity of the solute for the solvent, since the sample is divided into two immiscible phases, the organic and the aqueous.	Simple; considered a classic method with various solvent options.	Risk of analyte loss; use of large amounts of organic solvents (toxic); residual impurities (from solvent) which give toxicity to the sample; lengthy method; risk of analyte adsorption in glassware.	(Queiroz et al., 2001)
Soxhlet extraction	Subject the sample to organic solvents at its boiling temperature in a specific apparatus.	Traditional technique; simple; provide efficient extractions.	Time-consuming; use of large amount of solvent; lead to oxidation and isomerization.	(Barriada-Pereira et al., 2003; Cardenas-Toro et al., 2015; Castro & Priego-Capote, 2010; Shi & Maguer, 2000)
Enzyme-assisted extraction	Enzymes are used to disintegrate cell structures, like the cell wall, exposing the intracellular material. It is followed by solvent extraction process.	Higher extraction yield; use lower temperature in a shorter extraction time, avoiding lycopene degradation.	Despite lesser quantities, it still uses organic solvent; requires specific knowledge of food matrix composition.	(Gomez et al., 2020; Xianquan et al., 2005; Zuorro et al., 2011)
Microwave assisted extraction	It is based on a rapid heating of the polar cellular components, transferring lycopene to the extractor solvent	Quick; easy; shorter extraction time; great performance	Inhomogeneous heating; possibility of isomerization; still uses organic solvent (lower amounts).	(Barriada-Pereira et al., 2003; Honda et al., 2018; Lianfu & Zelong, 2008)
Ultrasound assisted extraction	A mechanical action is carried out on the sample, increasing cell walls rupture, improving the extracting solvent penetration	Shorter extraction time; higher yield; higher extract purity; reduced temperature; decreased energy consumed and CO_2 emissions.	Low reproducibility; low ultrasound power delivered directly to the sample; still uses organic solvent (lower amounts).	(Amiri-Rigi et al., 2016; Chemat et al., 2017; Chemat et al., 2011)
High hydrostatic pressure-assisted extraction	The samples are subjected to a high hydrostatic pressure, which is able to cause cellular structural changes,	Shorter extraction time; do not accelerate chemical reactions; minimizes damages providing a safe and high quality extract (as it	High initial cost; still uses organic solvent (less quantities).	(Briones-Labarca et al., 2019; Strati et al., 2015; Yamamoto, 2017)

	that allows better extracting solvent permeability	inactivates microorganisms and enzymes responsible for loss of quality); good extraction yields; improves antioxidant capacity extractability.		
Super-critical fluid extraction	Pressure and critical temperature of the solvent can be overcome, increasing its extraction power due to its solubilization power increase.	Quick and effective extraction; carbon dioxide (CO_2) is the solvent used so it is non-toxic, non-explosive and easy to eliminate; save energy and use of lower temperatures.	High equipment cost.	(Maul et al., 1996; Yousefi et al., 2019)

To obtain a more stable extract, in terms of its physical-chemical and microbiological characteristics, after the extraction, a concentration process (partial or total) is carried out. This process removes the solvent from the sample, decreasing its humidity, what results in greater shelf life and reduces transportation costs (Kubola et al., 2013; Rodrigues et al., 2016). As concentration most common methods hot-air, rotating evaporator, spray-dryer, far-infrared radiation and lyophilization can be cited (Rodrigues et al. 2016; Kumar et al. 2005). It is worth mentioning that the temperature used in this stage is the main disadvantage of some methods, such as hot-air and spray-dryer, as it leads to degradation, such as color darkening, nutritive value, flavor changes and lycopene isomerization. For this reason rotating evaporator, far-infrared radiation and lyophilization are the most recommended (Ba et al., 2020; Cox et al., 2003; Goula & Adamopoulos, 2005; Kumar et al., 2005).

Another purpose of the concentration methods is to prepare the sample for identification analysis (Queiroz et al., 2001). Identification analysis is an essential step because it assesses if the obtained extract is within the quality standard through lycopene quantification and purity evaluation, before making the product available in the market (Alves et al., 2019; Yadav et al., 2020). Carvalho et al., (2020) determined various analytical methods use percentage for lycopene quantification through a database survey. It was pointed out that high-performance liquid chromatography (HPLC) was the most used, present in 76% of the recovered articles. Nuclear magnetic resonance was the second, 9%, followed by Ultraviolet-Visible (UV-Vis) spectroscopy and Infrared spectroscopy, both with 7%. The remaining 1% was identified by the authors as others spectrophotometric techniques. It is worth mentioning that in order to ensure analyzes quality and reliability the use of any of these identification methods must be preceded by a validation according to official compendiums and current legislation (International conference on harmonization, 2005; Queiroz et al., 2001). **Table 2** describes in detail characteristics of lycopene extraction processes in samples from tomatoes in articles published in the last 5 years.

Table 2: Main characteristics of studies that addressed lycopene extraction in tomatoes samples in the last 5 years.

Extraction method	Concentration method	Analytical method	Lycopene content in the extract	References
SE	Evaporation under reduced pressure	HPLC	Optimized condition: 93.4 ± 1.6%	(Honda et al., 2021)
SE	Evaporation under reduced pressure	HPLC	Optimized condition: 82.0 ± 0.8%	
SCFE	Vacuum rotary evaporator	Spectrophotometric method	Optimized condition: 8.11 ± 0.65 mg/g DW	(Mihalcea et al., 2021)
		HPLC	Optimized condition: 92.23%	
SCFE	Vacuum rotary evaporator	Spectrophotometric method	Optimized condition: 39.11 ± 0.59 mg/g DW	
		HPLC	Optimized condition: 76%	
Pulsed electric fields-assisted extraction followed by SE	Centrifugation	UV-Vis	Optimized condition: 8861 mg/kg DW	(Pataro et al., 2020)
		HPLC	Optimized condition: 6311 ± 254 mg/kg DW	
SE	-	UV-Vis	Optimized condition: 98.55%	(Zuorro, 2020)
SE	-	UV-Vis	Optimized condition: 79.55%	
EAE followed by SE	Rotary evaporator	UV-Vis	Optimized condition: 4.30 ± 0.08 ($mg_{lycopene}/Kg_{tomato}$)	(Lombardelli et al., 2020)
SCFE	-	HPLC	Optimized condition: 1.78 ± 0.11 mg kg^{-1} dry matter	(Scaglia et al., 2020)
SCFE	-	UV-Vis	Optimized condition: 0.86 ± 0.06 mg/100 g DW	(Pellicanò et al., 2020)
UAE	Centrifugation	UV-Vis	Optimized condition: 1334.8 ± 83.9 µg/g	(Silva et al., 2019)
UAE	-	UV-Vis	Optimized condition: 1446.6 lg/g,	(Silva et al., 2019)
SE	Centrifugation	UV-Vis	Optimized condition: 88% of extraction efficiency.	(Amiri-Rigi & Abbasi, 2019)
UAE followed by EAE	Filtration followed by decantation	UV-Vis	Optimized condition: 94.3 g/100 g DM	(Rahimpour & Dinani, 2018)
SE	Rotary vacuum evaporator	HPLC	Optimized condition: 0.19 g lycopene/kg feed	

SCFE	-	HPLC	Optimized condition: 0.17 g lycopene/kg feed	(Vallecilla-Yepez & Ciftci, 2018)
SCFE	-	HPLC	Optimized condition:728.98 ± 31.17 mg/kg	(Kehili et al., 2017)
SE	Rotary vacuum evaporator	HPLC	Optimized condition: 608,94 ± 10.05 mg/kg	
SE	Centrifugation	HPLC	Optimized condition: 57.19 mg/kg	(Yilmaz et al., 2017)
UAE	Centrifugation	HPLC	Optimized condition: 76.87 ± 0.33 mg/kg	

Legend: Solvent extraction: SE; Supercritical CO_2 Extraction: SCFE; Enzyme-assisted extraction: EAE; Ultrasound-assisted extraction: UAE; dry weight: DW;

Although extraction from foods, such as tomatoes, is well established in the literature, other methods of obtaining this carotenoid have been increasingly studied in order to increase the extraction yield. The first one that can be mentioned is the chemical synthesis, despite having high yield it also has the advantage of low raw material cost. On the other hand, it presents some limitations, such as execution complexity, difficulty in controlling double bonds stereo-selectivity and chemical residues presence in the final extract, which can affect its safety and quality (Li et al., 2020; T. Sun et al., 2014; Xu et al., 2020). With the growing interest in the nutraceutical properties of this promising carotenoid, both, the extraction from food and chemical synthesis, have been showing signs that they are not following such increase. In this sense, more researches have been carried out in order to seek alternative routes, such as metabolic engineering (Jing et al., 2021; Li et al., 2020).

The metabolic engineering for lycopene biosynthesis have been extensively researched nowadays, mainly in order to optimize microorganisms (such as *Escherichia coli, Saccharomyces cerevisiae* and cyanobacterium) culture conditions (Farmer & Liao, 2001; Li et al., 2020; Taylor & Heap, 2020; Xie et al., 2015). The metabolic engineering seems to be the future perspective for this area once it has low-cost non-food lignocellulosic feedstocks, high-yield and is environment-friendly, been considered an ideal method (Deng et al., 2021; Wang, Sun, Yang, & Yang, 2020; Yuan & Alper, 2019).

3. Ingestion and absorption

Classified as a non-essential food, there is no established daily recommended lycopene amount, however, studies indicate a daily intake of 0.7 to 35 mg/day (Petyaev et al., 2018; Rao & Shen, 2002; Riedl et al., 1999; Ziegler et al., 1996).

Due to the fact that lycopene cis isomer has greater solubility in bile acid, it has greater absorption, making it more bioavailable in the human body (Boileau et al., 1999; Shi & Maguer, 2000). However, in the nature, above 80% of lycopene content is found as trans isomer, reducing its absorption and bioavailability. Therefore, its ingestion in combination with lipid sources or after some thermal or mechanical processing cause isomerization (trans to cis), allowing better lycopene absorption (Farinetti et al., 2017; Viuda-Martos et al., 2014). Some studies have shown an increase in lycopene bioavailability due to its isomerization from trans to cis when using fish oil and olive oil. Also, there may be a synergism between the ingredients used together with lycopene food sources like onion, garlic, leek, shiitake mushroom, and edible algae, for example, as they promote isomerization through sulfur compounds, increasing its bioavailability (Saini et al., 2020).

Lycopene isomerization mechanism after absorption, is not known, once there is no lycopene isomerase enzyme in the mammalian organism. However, it can be suggested that cis isomer

formation can be caused by the heat inside the body tissues, due to absorption, transportation, and tissues absorption process (Arballo et al., 2021).

Thus, from the diet, around 10 % to 30 % of this carotenoid is absorbed in the gastrointestinal system (Zhu et al., 2020). The absorption process starts with the tomato chewing, fundamental step for the first break of the food matrix to release lycopene. In the stomach, its release from the food matrix occurs partially, through the action of enzymes and acidic pH, sequentially lycopene must be loaded into the micellar fraction before being absorbed. The ingestion of foods with a high lipid content favors lycopene bioavailability in the gastrointestinal tract, as lipids release free fatty acids and monoacylglycerols, which provide an increase in the solubilization of mixed micelles, consequently, increasing lycopene solubilization (Cervantes-Paz et al., 2017). Being able to be loaded in the lipid droplets present in the stomach, lycopene is then transported to the small intestine, where the process of breaking down the food matrix, through the action of bile acids and enzymes, is completed. Therefore, lycopene is captured by enterocytes and then absorbed by chylomicrons, which released it into the lymphatic system. In the blood, it is transported to the liver, prostate, adipose tissue, among others, this process occurs mainly through LDL (Agarwal et al., 2001; Cervantes-Paz et al., 2017; Moritz & Tramonte, 2006; Rao et al., 2006).

4. Biological properties of lycopene

Lycopene has two possible mechanisms that can act together to trigger its biological activities (**Figure 2**). The oxidative mechanism, that acts by reducing oxidative stress and increasing antioxidant enzymes levels, and the non-oxidative mechanism, that acts on other pathways such as Gap junction communication, cell cycle regulation, modulation of gene expression, and improvement of the immune response (Mirahmadi et al., 2020).

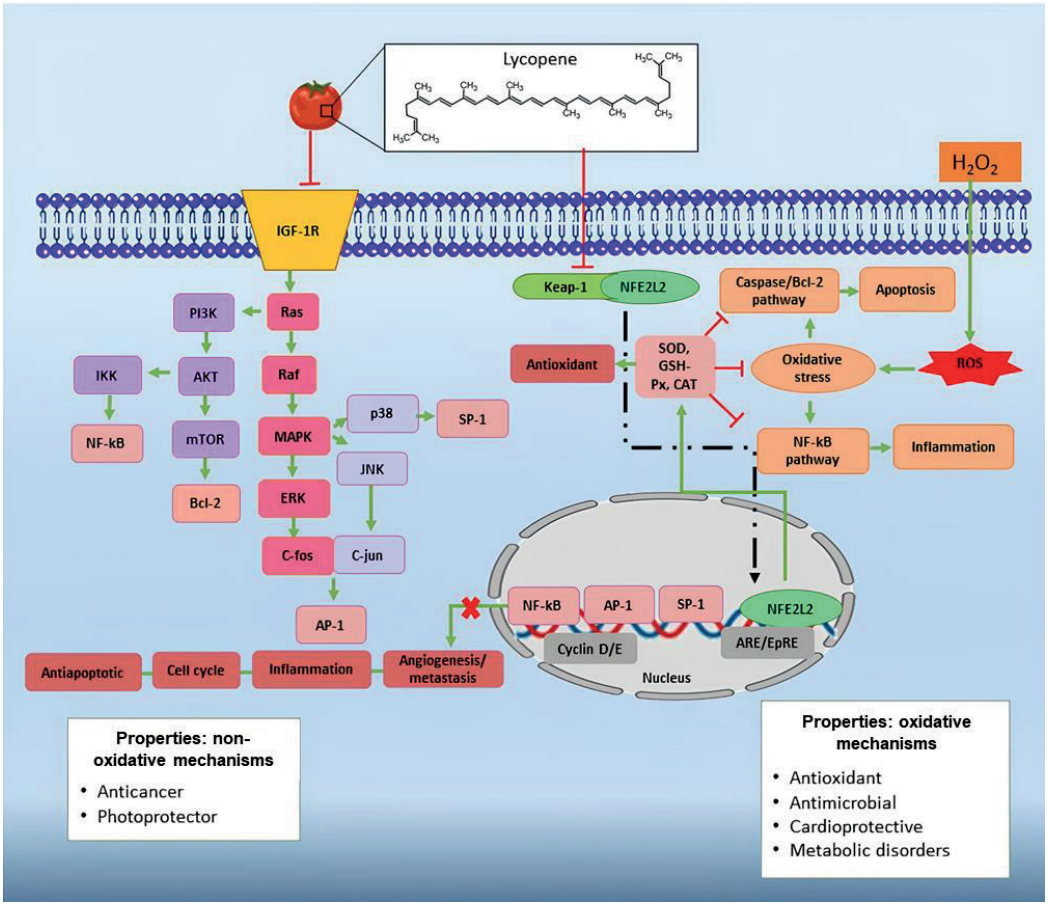

Figure 2: Schematic illustration of the oxidative and non-oxidative mechanisms of lycopene.

Legend: Lycopene promotes the inhibition of IGF-1R and dependent signaling pathways (Ras/Raf/MAPK, p38/JNK and PI3K/AKT/mTOR) that are associated with the process of carcinogenesis, invasion and metastasis. Furthermore, it breaks the complex with Keap-1/NFE2L2 and promotes the translocation of NFE2L2 to the nucleus binding to the ARE, in order to regulate the production of antioxidant enzymes that block oxidative stress, apoptotic and inflammatory pathways.

Antioxidant

Lycopene is an excellent antioxidant compound due to the high reactivity between its long polyene chain and free radicals, allowing singlet oxygen elimination and reducing reactive oxygen species (ROS) (Caseiro et al., 2020). Among its antioxidant mechanism of action can be cited the reduction of ROS accumulation and oxidative stress, inhibition of inflammatory pathways (TNF-α, IL-6, and IL-1β), Nuclear factor kappa B (NF-kB) and apoptotic (caspase and B-cell lymphoma 2 (Bbl-2)), and activation of the nuclear factor E2-related factor 2 (NFE2L2)-antioxidant response element (ARE), increasing antioxidant enzymes levels like superoxide dismutase (SOD), catalase

(CAT) and glutathione peroxidase (GSH-Px) in H_2O_2-induced oxidative lesion in bovine mammary epithelial cells (bMECs) (Sun et al., 2019). In cardiac myofibroblast cells (H9c2), also with the oxidative damage induction, there was an increase in heme oxidase (HO-1) messenger ribonucleic acid (mRNA) expression (Zheng et al., 2020).

In THP-1 cells exposed to H_2O_2, lycopene reduced levels of kinases overexpress in oxidative stress (p-ERK1/2, p-JNK, and p-p38), of stress proteins (heat shock protein (hsp)70 and hsp90), and an indicator of ROS-induced DNA damage (8-hydroxy-2′-deoxyguanosine). Also inhibited activation/phosphorylation of kappa-B kinase subunit alpha, nuclear factor of kappa light polypeptide gene enhancer in B-cells inhibitor, alpha involved in NF-kB inactivation and nicotinamide adenine dinucleotide phosphate hydrogen (NADPH) oxidase-4 expression associated with ROS production (Catalano et al., 2013). Other antioxidant mechanisms dependent on NFE2L2 pathway were a reduction in the levels of interferon-gamma and IL-10, observed in C57BL/6 mice lungs after cigarette smoke exposure (Campos et al., 2017), and in Sprague-Dawley rats with thermal trauma (oxidative injury), which demonstrated a reduction in malondialdehyde (MDA), myeloperoxidase (MPO), caspase-3 in lungs and kidneys tissues (Çevik et al., 2012).

Cardioprotective

Lycopene has been explored to prevent cardiovascular diseases. For isoproterenol-induced myocardial infarction in Wistar rats, lycopene improved heart pressure, avoided reducing levels of antioxidant enzymes (SOD, CAT, GSH-Px, and GSH) and cardiac markers (creatine kinase-MB) and lactate dehydrogenase (LDH)), inhibited lipid peroxidase, reduced the formation of MDA and edema, and prevented myocardial necrosis (Ojha et al., 2013). The same effect was observed in Swiss mice, in which lycopene was used to attenuate the cardiotoxicity induced by tulathromycin and sodium diclofenac. It also showed a reduction of cardiac-specific troponin-T, NO, CK, inhibited caspase-3, and Bax expression (Abdel-Daim et al., 2018).

This carotenoid could also reduce the size of infarction, cardiomyocytes apoptosis, cardiac markers release, stress marker of the endoplasmic reticulum (glucose-regulated protein 78), the caspase-9, and caspase-3, and cytochrome c expression. Besides, it increased levels of protein kinase B (AKT or PKB), extracellular signal-regulated kinases (ERK) 1/2, and glycogen synthase kinase 3 beta phosphorylation in hypercholesterolemic Wistar rats (Duan et al., 2019).

Other mechanisms involved in lycopene cardioprotective action are reduction expression of apoptotic protease activating factor 1, AST, total cholesterol, triglycerides, low-density lipoprotein (LDL), TNF- α, and MPO. Also, to the increased expression of Bcl-2, high-density lipoprotein (HDL), lipid peroxides, lysosomal enzymes, vitamin c, inhibition of the mitochondrial permeability

transition pore, negative regulation of NF-kB-dependent adhesion molecule expression, and protection of the redox balance (di Tomo et al., 2012; Li et al., 2019; Mohamadin et al., 2012).

Antihypercholesterolemic

Hypercholesteremia is considered a risk factor for cardiovascular diseases, and lycopene has shown potential against it. It was verified in THP-1 cells that lycopene inhibits the expression of 3-hydroxy-3-methylglutaryl coenzyme A reductase (HMG-CoA reductase) and Rho, activating the expression of peroxisome proliferator-activated receptor gamma (PPARγ) and liver X receptor α (LXRα), increase levels of adenosine triphosphate (ATP)-binding cassette 1 (ABCA1) and caveolin-1 (Palozza et al., 2011). In intestinal cells (CaCo-2), lycopene inhibited the absorption of cholesterol and also the expression of Niemann-Pick-C1-like 1 (Zou & Feng, 2015).

In *in vivo* studies, there was a reduction in proprotein convertase subtilisin/kexin type 9 expression and inhibition of HMG-CoA reductase, confirmed also by *in silico* tests (Navarro-González et al., 2014; Alvi et al., 2017), and inflammatory markers (IL-1β, IL-6, TNF-α, and C-reactive protein), MDA, lipid levels in plasma (triglycerides, total cholesterol, LDL) and increased paraoxonase-1 and HDL (Navarro-González et al., 2014; Periago et al., 2016; Alvi et al., 2017).

Antidiabetic

The high level of free radicals present in diabetics can trigger complications, but the use of antioxidant agents, like lycopene, can mitigate complications and act as an antidiabetic (Soleymaninejad et al., 2017). In type 2 diabetes-induced in Sprague Dawley rats, lycopene activated antioxidant enzymes (SOD and GSH-Px), reducing pancreatic tissue MDA, reducing triglycerides, total cholesterol (blood and liver), LDL and increasing HDL, improving resistance to insulin, and blood glucose reduction (Yin et al., 2019). In another study, the same beneficial effect was observed, reducing also aspartate transaminase (AST), alanine aminotransferase (ALT) (Bayramoglu et al., 2013), TNF-α, C-reactive protein, glycosylated hemoglobin (Zheng et al., 2019) and reaching normal blood glucose levels within 21 days of treatment (Haribabu et al., 2013).

In diabetic Wistar rats hippocampus, lycopene prevented apoptosis by increasing the expression of Bcl-2 and B-cell lymphoma-extra-large (Bcl-xL) and reducing the expression of Bax (Soleymaninejad et al., 2017). Lycopene could also prevent brain damage in insulin-resistant by increasing CAT, GSH and reducing insulin receptors, insulin-like growth factor 1 (IGF-1R), phosphoinositide 3-kinase (PI3K), PPAR γ, NF-kBp65, IL-1β, lipid peroxidation in homeostasis model assessment-estimated insulin resistance and mammalian acetylcholinesterase (Yin et al., 2014).

In diabetic nephropathy, lycopene prevented kidney damage by reducing urine protein levels, NF-kB, attenuating oxidative stress, positively regulating HO-1 mRNA intracellular levels (Guo et al., 2015), regulating p-AKT and connective tissue growth factor (Li et al., 2014). In *in vitro* assay, lycopene protected endothelial progenitor cells from oxidative autophagy and apoptosis, which are important in any vascular complications resulting from diabetes (Zeng et al., 2017).

Antimicrobial

Against *Candida albicans* lycopene showed antifungal effect by inducing apoptosis by caspase activation and increased intracellular ROS production. Intracellular Ca^{2+} contributed to depolarization and cytochrome c release from mitochondria to the cytoplasm, causing mitochondrial dysfunction (Choi & Lee, 2015). Its antibacterial activity, observed against *Escherichia coli,* is also related to intracellular ROS production increase, causing DNA damage and interrupting cell division, (Lee & Lee, 2014).

Photoprotector

In the literature, there are studies about lycopene photoprotective capacity. In a trial with volunteers using foods rich in lycopene a reduction was demonstrated in UV-induced erythema, protecting the basal thermal defense against irradiation (Stahl et al., 2006; Stahl & Sies, 2012), reducing matrix metalloproteinase (MMP)-1 and mitochondrial DNA damage (Rizwan et al., 2011), also with a mixture of carotenoids upregulation of IL-6 and TNF- α was observed. The pre-treatment of HaCaT cells with lycopene and UVB exposure also demonstrated an increase in Bax and caspase-3, in addition to an effect on the cell division cycle, reducing the G0/G1 phase (Kim et al., 2016). Despite showing encouraging mechanisms of systemic photoprotection, this information is still not enough to replace topical sunscreens (Stahl & Sies, 2012).

Anticancer

Lycopene has demonstrated anticarcinogenic activity against different cancer types, such as prostate (Jiang et al., 2019), breast (dos Santos et al., 2018), esophageal (Cui et al., 2020), gastric (Kim et al., 2019), tongue (El-Rouby, 2011), cervical (Aktepe et al., 2021), renal (Sahin et al., 2015), liver (Yang et al., 2012), skin (Ascenso et al., 2014), oral (Wang et al., 2020), head and neck (Ye et al., 2016).

Its main anticarcinogenic mechanisms are for suppressing inflammatory response, reducing levels of interleukins (IL-1, IL-6 e IL-8), TNF-α, inducing apoptosis (Jiang et al., 2019), inhibiting cell proliferation via the PPARγ-LXRα-ABCA1 pathway (Yang, Lu, et al., 2012) and the upregulation of microRNA-let-7f-1 expression and down-regulation of AKT2 expression (Li et al., 2016). Also by

cell cycle arrest in G0/G1 phase or G2/M (Gloria et al., 2014; Teodoro et al., 2012), DNA fragmentation and mitochondrial dysfunction (dos Santos et al., 2018), anti-angiogenic, upregulation of IL-12 and IFN-γ (Huang et al., 2013), inhibition MMP-9 and MMP-2, reduction of IGF-1R, inhibition of ERK, p38, and c-Jun NH2-terminal kinase (JNK) signaling pathway (Huang, Fan, Lin, & Hu, 2007; Yang, Hu, & Hu, 2012), increasing expression levels of PPARγ and antioxidants enzymes, reducing expression of NF-kB, ciclo-oxigenase-2, MDA (Cui et al., 2020), deactivating the PI3K/AKT/ mammalian target of rapamycin (mTOR) signaling (Wang et al., 2020), inhibition of PI3K/AKT and mitogen-activated protein kinase (MAPK) signaling pathway (Ye et al., 2016), and reducing glycogen synthase kinase-3 beta phosphorylation (Kim et al., 2019).

5. Use of nanocarriers to improve lycopene solubility, stability and bioavailability

Although lycopene has various biological properties, the use of this nutraceutical presents some difficulties due to characteristics like high lipophilicity, insolubility in aqueous solvents, problems with stability and degradation (Carvalho et al., 2020). Solutions, like its association with nanotechnology, are sought to circumvent these difficulties. Nanotechnology has been widely studied as a support to increase lycopene accessibility, bioavailability and absorption, as it can protect the molecule, improve characteristics such as solubility and bioavailability and circumvented problems related to toxicity (Carvalho et al., 2020; Yao & Martins, 2020). **Table 3** summarizes how some articles analyzed the use of nanotechnology to improve lycopene action.

Table 3: Abstracts of studies using nanotechnology to improve lycopene action.

Systems	Action	Experiment	Form of analysis	References
Emulsion	Bioaccessibility	*In vitro* digestion	Form specific mesophases	Bezelgues et al., 2009
Emulsion and Nanoemulsion	Bioaccessibility	*In vitro* digestion	Micelle fraction	Salvia-Trujillo & McClements, 2016
Nanoemulsion	Bioaccessibility	*In vitro* absorption	Lycopene content inside and outside micelles	Ha et al., 2015
Nanoemulsion	Degradation	Accelerated shelf-life tests	Lycopene concentration in the beverage	Kim et al., 2014
Nanoemulsion	Bioaccessibility	*In vitro* digestion	Micelle fraction (solubilized and available for absorption)	Sotomayor-Gerding et al., 2016
Nanoemulsion	Stability and Bioaccessibility	Storage stability and *in vitro* digestion	The stability was determined by nanoemulsions particle size and zeta potential. The bioaccessibility was determined according to the lycopene concentration in the micelle fraction (dissolved and available for absorption)	Zhao et al., 2020
Microemulsion	Solubilization	Solubilization Measurements and Self-Diffusion Measurements	Amount (ppm) of lycopene solubilized in the microemulsion	Spernath et al., 2002
Solid lipid nanoparticles	Stability	Physical stability studies	Analysis of the diameter, dispersity index and Encapsulation efficiency were measured after two months	Nazemiyeh et al., 2016
Nanostructured lipid carriers	Stability	Physical stability studies	Analysis of the particle size, size distribution, and zeta potential of lycopene-loaded NLC for 120 days	Okonogi & Riangjanapatee, 2015
Nanostructured lipid carriers	Stability	Stability test	Analysis of the particle size, size distribution, and zeta potential of lycopene-loaded NLC for 30 days	Riangjanapatee & Okonogi, 2012

Polymeric nanoparticles	Pharmacokinetic	*In vivo* pharmacokinetic study	Release, concentration of lycopene in plasma, absorption and elimination	Li et al., 2017
Polymeric Microparticles	Bioavailability, stability and antioxidant activity.	Stability study, *in vivo* plasma quantification of lycopene and pharmacokinetic study	Plasma sample from the retro-orbital plexus	Jain et al., 2016
Micelles and chylomicrons	Bioavailability	Bioavailability of lycopene	Blood collection after oral administration (gavage) and intravenous injection	Chen et al., 2014
Nanofibers	Solubility	Carotenoid extract solubility in water	Absorbance quantitation in the UV-Vis spectrophotometer	İnanç Horuz & Belibağlı, 2018
Solid dispersion	Bioavailability and Pharmacokinetics study	Bioavailability and Pharmacokinetics study	Blood collection after oral administration (gavage)	Faisal et al., 2013
Vesicles	Stabilization	DPPH	DPPH evaluation after storage under different conditions	Luxsuwong et al., 2014

Legend: ppm: parts per million; NLC: Nanostructured lipid carriers; DPPH: 2,2-Diphenyl-1-picrylhydrazyl

Lipid-based systems, like emulsion, microemulsion, and nanoemulsion, are of great interest for increase lipophilic bioactive solubility, as they are composed by oil, water, and surfactant (Bernegossi et al., 2020). Bezelgues and collaborators (2009) evaluated two different oil-in-water (O/W) emulsions prepared with milk protein and a fraction of bovine milk fat globule membrane, once lycopene has the ability to accumulate in micelles in their digestion process. It was found that low-fat system can be used to increase the bioavailability of fat-soluble compounds for better absorption. The use of nanoemulsion is also studied, as in the work of Salvia-Trujillo and McClements (2016), which was compared with an emulsion. In this work, lycopene bioaccessibility in tomato juice was evaluated in association with the ingestion of an emulsion and a nanoemulsion to simulate food products that can be consumed or mixed with tomato juices. Additionally, the presence or not of thermal treatment was also evaluated. It was possible to observe that the greatest bioaccessibility was observed when juice and nanoemulsion were mixed before performing the heat treatment, which facilitates lycopene transference to mixed micelles for absorption, suggesting that the use of lipid sources with the intake of lycopene source products is desirable. Also assessing lycopene bioaccessibility Ha and collaborators (2015) found that nanoemulsion showed high lycopene values in both, inside the micelles and in released content.

Through encapsulation in nanoemulsion Kim and collaborators (2014) evaluated lycopene as an additive in beverages and quantified its stability in the face of degradation at different temperatures. It was found that the nanoemulsion allowed lycopene stabilization at temperatures of 4 and 20°C, which provides interesting results in the beverage production area. Nanoemulsion can be also used to protect lycopene, like other carotenoids, from processing and storage conditions, as it was shown in the study performed by Sotomayor-Gerding and collaborators (2016).

Recently, the effect of three different oils on the stability and digestion of nanoemulsion containing lycopene was evaluated. With lower viscosity, higher density, and less unsaturation, sesame oil proved to be the best candidate for the composition of the system oil phase, allowing greater lycopene bioaccessibility and greater stability of the nanoemulsion. The study demonstrated the importance of choosing the better nanosystem composition (Zhao et al., 2020). Microemulsion was also studied for assessing lycopene solubilization (Spernath et al., 2002).

Solid lipid nanoparticles (SLN) and nanostructured lipid carriers (NLC), other types of nanocarriers also considered promising, are colloidal systems composed of a lipid nucleus stabilized by surfactants present in an aqueous medium, differing between them in the lipid phase composition. SLN are composed only by solid lipids, while NLC have a combination of solid and liquid lipids. This change allows the formation of a matrix with less ordered structures, allowing greater bioactive encapsulating capacity. These systems are widely used for lipophilic substances, as they are capable of providing

greater resistance to physiological obstacles and good storage, release, and protection capacity (Araujo et al., 2021).

Lycopene stability, in terms of physical and chemical characteristics, was studied when loaded into solid lipid nanoparticles, Nazemiyeh & collaborators (2016) obtained positive results. Regarding the use of NLC, Okonogi & Riangjanapatee (2015) also evaluated lycopene chemical stabilization and found a lower degradation of this carotenoid at low temperatures, being considered an excellent system to guarantee its stability. The same result was found in the work performed by Riangjanapatee & Okonogi, (2012), where NLC allowed a lower lycopene degradation profile when comparing it free in solution.

Systems composed by polymers, like polymeric nanoparticles (PN), have also been studied. PN can be classified into nanocapsules and nanospheres, both are composed by polymers, surfactants, and aqueous phase, being nanospheres constituted by a polymeric matrix, while nanocapsules by a nucleus, which can be oily or not, depending on the presence of lipid constituents or not (Camargo et al., 2020).

Li and collaborators (2017) studied the use of PN as a lycopene protector against the stomach acidic environment. It prevented not only lycopene degradation but also potentiated its pharmacokinetic parameters. The use of polymer is also well studied in the development of microparticles, an area that has also been well explored, like in the work performed by Jain and collaborators (2016) which presented satisfactory results of increased bioavailability, stability and antioxidant activity.

In addition to the drug delivery systems mentioned above, others, also of great importance, present fewer studies involving their use with lycopene. Chen and collaborators (2014) compared the bioavailability of lycopene micelles and chylomicrons. *In vivo* results showed that lycopene chylomicrons presented greater oral bioavailability, being promising for clinical applications. Nanofibers are another choice that can be explored, as it has been shown that the water solubility of a carotenoid extract has been increased when compared without the use of nanofibers (Horuz & Belibağli, 2018). One approach that should be further studied is the use of solid dispersion. A study involving this technology compared lycopene incorporation in this system with commercial lycopene (Lycovit®) *in vivo*. Lycopene bioavailability increased in the developed system, in addition to its solubilization and absorption (Faisal et al., 2013). Vesicles are also a system that must be invested, which also can stabilize this carotenoid (Luxsuwong et al., 2014). **Figure 3** illustrate the most cited delivery systems presented in this session.

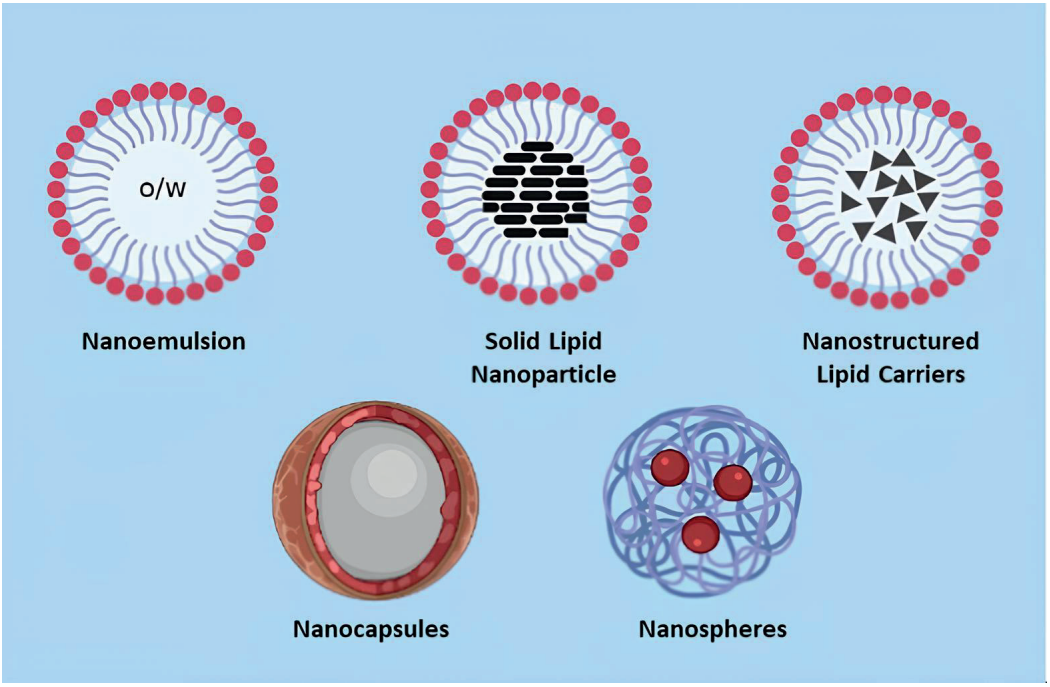

Figure 3: Representative scheme of the structure of Nanoemulsion, Solid Lipid Nanoparticle, Nanostructured Lipid Carriers, Nanocapsules and Nanospheres

6. Conclusions

Due to its chemical structure, lycopene has several isomers, although the difference in activity between the cis and trans isomers is not clear in the literature. The isomer cis is more soluble in the gastrointestinal tract, which facilitates its absorption. On the other hand, this is not the isomer abundantly found in nature, it is usually the result of an isomerization. The isomerization processes are caused by external factors, mainly high temperatures, which can cause a degradation in the final product, affecting not only its sensory quality but also its health benefits.

For the extraction techniques, it was observed that solvent extraction and supercritical fluid extraction were the most used in recent years. The most used concentration method was centrifugation and evaporation, mainly by vacuum rotary evaporator. HPLC and UV-vis spectrophotometer were the analytical methods most chosen by researchers. Another point that is worth noting is that factors such as insolubility in aqueous solvents, stability and degradation hinder the use of lycopene as a nutraceutical. In this context, nanotechnology has been increasingly used in order to circumvent these limitations, especially nanoemulsions, NLC, PN, nanofibers and solid dispersion. It is, therefore, necessary to encourage studies exploring other types of nanocarriers, such as inorganic nanoparticles.

7. Acknowledgments

This work was supported by São Paulo Research Foundation (FAPESP, Brazil) grant number nº 2019/26821-7 and 2020/06212-3, and the Coordenação de Aperfeiçoamento de Pessoal de Nível Superior (CAPES) [Finance Code 001].

8. References

Abdel-Daim, M., Eltaysh, R., Hassan, A., & Mousa, S. (2018). Lycopene Attenuates Tulathromycin and Diclofenac Sodium-Induced Cardiotoxicity in Mice. *International Journal of Molecular Sciences*, *19*(2), Article 344. https://doi.org/10.3390/ijms19020344

Agarwal, A., Shen, H., Agarwal, S., & Rao, A. V. (2001). Lycopene Content of Tomato Products: Its Stability, Bioavailability and In Vivo Antioxidant Properties. *Journal of Medicinal Food*, *4*(1), 9–15. https://doi.org/10.1089/10966200152053668

Aktepe, O. H., Şahin, T. K., Güner, G., Arik, Z., & Yalçin, Ş. (2021). Lycopene sensitizes the cervical cancer cells to cisplatin via targeting nuclear factor- kappa B (NF-κB) pathway. *Turkish Journal of Medical Sciences*, *51*(1), 368–374. https://doi.org/10.3906/sag-2005-413

Aliyu, A., Kabiruyunusa, A., & Abdullahi, N. (2020). Kinetics of the thermal degradation of lycopene in tomatoes. *Croatian Journal of Food Science and Technology*, *12*(1), 84–89. https://doi.org/10.17508/CJFST.2020.12.1.11

Alves, R. C., Fernandes, R. P., Fonseca-Santos, B., Victorelli, F. D., & Chorilli, M. (2019). A critical review of the properties and analytical methods for the determination of curcumin in biological and pharmaceutical matrices. *Critical Reviews in Analytical Chemistry*, *49*(2), 138–149.

Amiri-Rigi, A., & Abbasi, S. (2019). Extraction of lycopene using a lecithin-based olive oil microemulsion. *Food Chemistry*, *272*, 568–573. https://doi.org/10.1016/j.foodchem.2018.08.080

Amiri-Rigi, A., Abbasi, S., & Scanlon, M. G. (2016). Enhanced lycopene extraction from tomato industrial waste using microemulsion technique: Optimization of enzymatic and ultrasound pre-treatments. *Innovative Food Science & Emerging Technologies*, *35*, 160–167. https://doi.org/10.1016/j.ifset.2016.05.004

Amjad, M., Hussain, S., & Rehman Khan, A. (2020). Development and Validation of HPLC assay of Lycopene in Different Matrices. *World Journal of Applied Chemistry*, *5*(2), 26-33. https://doi.org/10.11648/j.wjac.20200502.13

Araujo, V. H. S., Delello Di Filippo, L., Duarte, J. L., Spósito, L., Camargo, B. A. F. de, da Silva, P. B., & Chorilli, M. (2021). Exploiting solid lipid nanoparticles and nanostructured lipid carriers for drug delivery against cutaneous fungal infections. *Critical Reviews in Microbiology*, *47*(1), 79–90. https://doi.org/10.1080/1040841X.2020.1843399

Arballo, J., Amengual, J., & Erdman, J. W. (2021). Lycopene: A Critical Review of Digestion, Absorption, Metabolism, and Excretion. *Antioxidants*, *10*(3), Article 342. https://doi.org/10.3390/antiox10030342

Ascenso, A., Ribeiro, H., Marques, H. C., Oliveira, H., Santos, C., & Simões, S. (2014). Chemoprevention of photocarcinogenesis by lycopene. *Experimental Dermatology*, *23*(12), 874–878. https://doi.org/10.1111/exd.12491

Ashraf, W., Latif, A., Lianfu, Z., Jian, Z., Chenqiang, W., Rehman, A., Karim, A. (2020). Technological Advancement in the Processing of Lycopene: A Review. *Food Reviews International*, 38(5), 857-883. https://doi.org/10.1080/87559129.2020.1749653

Ba, C., Fu, Y., Niu, F., Wang, M., Jin, B., Li, Z., Chen, G., Zhan, H., Li, X. (2020). Effects of environmental stresses on physiochemical stability of β-carotene in zein-carboxymethyl chitosan-tea polyphenols ternary delivery system. *Food Chemistry*, *311*, Article 125878. https://doi.org/10.1016/j.foodchem.2019.125878

Barriada-Pereira, M., Concha-Graña, E., González-Castro, M., Muniategui-Lorenzo, S., López-Mahía, P., Prada-Rodríguez, D., & Fernández-Fernández, E. (2003). Microwave-assisted extraction versus Soxhlet extraction in the analysis of 21 organochlorine pesticides in plants. *Journal of Chromatography A*, *1008*(1), 115–122. https://doi.org/10.1016/S0021-9673(03)01061-6

Bayramoglu, A., Bayramoglu, G., & Senturk, H. (2013). Lycopene Partially Reverses Symptoms of Diabetes in Rats with Streptozotocin-Induced Diabetes. *Journal of Medicinal Food*, *16*(2), 128–132. https://doi.org/10.1089/jmf.2012.2277

Bernegossi, J., Fontana, C. R., Caiaffa, K. S., Duque, C., & Chorilli, M. (2020). Inhibitory Effect of a KSL-W Peptide-Loaded Poloxamer 407-Based Microemulsions for Buccal Delivery on Fusobacterium nucleatum Biofilm. *Journal of Biomedical Nanotechnology*, *16*(3), 390–397. https://doi.org/10.1166/jbn.2020.2896

Bezelgues, J.-B., Morgan, F., Palomo, G., Crosset-Perrotin, L., & Ducret, P. (2009). Short communication: Milk fat globule membrane as a potential delivery system for liposoluble nutrients. *Journal of Dairy Science*, *92*(6), 2524–2528. https://doi.org/10.3168/jds.2008-1725

Böhm, V., Puspitasari-Nienaber, N. L., Ferruzzi, M. G., & Schwartz, S. J. (2002). Trolox Equivalent Antioxidant Capacity of Different Geometrical Isomers of α-Carotene, β-Carotene, Lycopene, and Zeaxanthin. *Journal of Agricultural and Food Chemistry*, *50*(1), 221–226. https://doi.org/10.1021/jf010888q

Boileau, A. C., Merchen, N. R., Wasson, K., Atkinson, C. A., & Erdman Jr, J. W. (1999). Cis-lycopene is more bioavailable than trans-lycopene in vitro and in vivo in lymph-cannulated ferrets. *The Journal of Nutrition*, *129*(6), 1176–1181. https://doi.org/10.1093/jn/129.6.1176

Brandt, S., Lugasi, A., Barna, É., Hóvári, J., Pék, Z., & Helyes, L. (2003). Effects of the growing methods and conditions on the lycopene content of tomato fruits. *Acta Alimentaria-academiae Scientiarum Hungaricae*, *32*(3), 269–278. https://doi.org/10.1556/aalim.32.2003.3.6

Brandt, S., Pék, Z., Barna, É., Lugasi, A., & Helyes, L. (2006). Lycopene content and colour of ripening tomatoes as affected by environmental conditions. *Journal of the Science of Food and Agriculture*, *86*(4), 568–572. https://doi.org/10.1002/jsfa.2390

Briones-Labarca, V., Giovagnoli-Vicuña, C., & Cañas-Sarazúa, R. (2019). Optimization of extraction yield, flavonoids and lycopene from tomato pulp by high hydrostatic pressure-assisted extraction. *Food Chemistry*, *278*, 751–759. https://doi.org/10.1016/j.foodchem.2018.11.106

Camargo, B. A. F., Silva, D. E. S., Silva, A. N., Campos, D. L., Ribeiro, T. R. M., Mieli, M. J., Zanatta, M. B., Silva, P. B., Pavan, R.F., & others (2020). New Silver(I) Coordination Compound Loaded into Polymeric Nanoparticles as a Strategy to Improve In Vitro Anti- Helicobacter pylori Activity . *Molecular Pharmaceutics, 17*(7), 2287-2298. https://doi.org/10.1021/acs.molpharmaceut.9b01264

Campos, K. K. D., Araújo, G. R., Martins, T. L., Bandeira, A. C. B., Costa, G. de P., Talvani, A., Garcia, C. C. M., Oliveira, L. A. M., Costa, D.C., Bezerra, F. S. (2017). The antioxidant and anti-inflammatory properties of lycopene in mice lungs exposed to cigarette smoke. *The Journal of Nutritional Biochemistry*, *48*, 9–20. https://doi.org/10.1016/j.jnutbio.2017.06.004

Cardenas-Toro, F. P., Alcázar-Alay, S. C., Coutinho, J. P., Godoy, H. T., Forster-Carneiro, T., & Meireles, M. A. A. (2015). Pressurized liquid extraction and low-pressure solvent extraction of carotenoids from pressed palm fiber: Experimental and economical evaluation. *Food and Bioproducts Processing*, *94*, 90–100. https://doi.org/10.1016/j.fbp.2015.01.006

Carvalho, G. C., Sábio, R. M., & Chorilli, M. (2020). An Overview of Properties and Analytical Methods for Lycopene in Organic Nanocarriers. *Critical Reviews in Analytical Chemistry*, 1–13. https://doi.org/10.1080/10408347.2020.1763774

Carvalho, S. G., Araujo, V. H. S., dos Santos, A. M., Duarte, J. L., Silvestre, A. L. P., Fonseca-Santos, B., Villanova, J. C. O., Gremião, M. P. D., Chorilli, M. (2020). Advances and challenges in nanocarriers and nanomedicines for veterinary application. *International Journal of Pharmaceutics*, *580*, Article 119214. https://doi.org/10.1016/j.ijpharm.2020.119214

Carvalho, V. F. M., Salata, G. C., de Matos, J. K. R., Costa-Fernandez, S., Chorilli, M., Steiner, A. A., Araujo, G. L. B., Silveira, E. R., Costa-Lotufo, L. V., Lopes, L. B. (2019). Optimization of composition and obtainment parameters of biocompatible nanoemulsions intended for intraductal administration of piplartine (piperlongumine) and mammary tissue targeting. *International Journal of Pharmaceutics*, *567*, Article 118460. https://doi.org/10.1016/j.ijpharm.2019.118460

Caseiro, M., Ascenso, A., Costa, A., Creagh-Flynn, J., Johnson, M., & Simões, S. (2020). Lycopene in human health. *LWT*, *127*, Article 109323. https://doi.org/10.1016/j.lwt.2020.109323

Catalano, A., Simone, R. E., Cittadini, A., Reynaud, E., Caris-Veyrat, C., & Palozza, P. (2013). Comparative antioxidant effects of lycopene, apo-10′-lycopenoic acid and apo-14′-lycopenoic acid in human macrophages exposed to H_2O_2 and cigarette smoke extract. *Food and Chemical Toxicology*, *51*, 71–79. https://doi.org/10.1016/j.fct.2012.08.050

Cervantes-Paz, B., Ornelas-Paz, J. de J., Ruiz-Cruz, S., Rios-Velasco, C., Ibarra-Junquera, V., Yahia, E. M., & Gardea-Béjar, A. A. (2017). Effects of pectin on lipid digestion and possible implications for carotenoid bioavailability during pre-absorptive stages: A review. *Food Research International*, *99*, 917–927. https://doi.org/10.1016/j.foodres.2017.02.012

Çevik, Ö., Oba, R., Macit, Ç., Çetinel, Ş., Çilingir Kaya, Ö. T., Şener, E., & Şener, G. (2012). Lycopene inhibits caspase-3 activity and reduces oxidative organ damage in a rat model of thermal injury. *Burns*, *38*(6), 861–871. https://doi.org/10.1016/j.burns.2012.01.006

Chemat, F., Rombaut, N., Sicaire, A.-G., Meullemiestre, A., Fabiano-Tixier, A.-S., & Abert-Vian, M. (2017). Ultrasound assisted extraction of food and natural products. Mechanisms, techniques, combinations, protocols and applications. A review. *Ultrasonics Sonochemistry*, *34*, 540–560. https://doi.org/10.1016/j.ultsonch.2016.06.035

Chemat, F., Zill-e-Huma, & Khan, M. K. (2011). Applications of ultrasound in food technology: Processing, preservation and extraction. *Ultrasonics Sonochemistry*, *18*(4), 813–835. https://doi.org/10.1016/j.ultsonch.2010.11.023

Chen, Y. J., Inbaraj, B. S., Pu, Y. S., & Chen, B. H. (2014). Development of lycopene micelle and lycopene chylomicron and a comparison of bioavailability. *Nanotechnology*, *25*(15), Article 155102. https://doi.org/10.1088/0957-4484/25/15/155102

Choi, H., & Lee, D. G. (2015). Lycopene induces apoptosis in *Candida albicans* through reactive oxygen species production and mitochondrial dysfunction. *Biochimie*, *115*, 108–115. https://doi.org/10.1016/j.biochi.2015.05.009

Choksi, P. M., & Joshi, V. Y. (2007). A Review on Lycopene—Extraction, Purification, Stability and Applications. *International Journal of Food Properties*, *10*(2), 289–298. https://doi.org/10.1080/10942910601052699

Colle, I., Lemmens, L., Van Buggenhout, S., Van Loey, A., & Hendrickx, M. (2010). Effect of thermal processing on the degradation, isomerization, and bioaccessibility of lycopene in tomato pulp. *Journal of Food Science*, *75*(9), C753-C759. https://doi.org/10.1111/j.1750-3841.2010.01862.x

Cox, S. E., Stushnoff, C., & Sampson, D. A. (2003). Relationship of fruit color and light exposure to lycopene content and antioxidant properties of tomato. *Canadian Journal of Plant Science*, *83*(4), 913–919. https://doi.org/10.4141/P03-041

Cui, L., Xu, F., Wu, K., Li, L., Qiao, T., Li, Z., Chen, T., Sun, C. (2020). Anticancer effects and possible mechanisms of lycopene intervention on N-methylbenzylnitrosamine induced esophageal cancer in F344 rats based on PPARγ1. *European Journal of Pharmacology*, *881*, Article 173230. https://doi.org/10.1016/j.ejphar.2020.173230

Daood, H. G., Bencze, G., Palotas, G., Pek, Z., Sidikov, A., & Helyes, L. (2014). HPLC Analysis of Carotenoids from Tomatoes Using Cross-Linked C18 Column and MS Detection. *Journal of Chromatographic Science*, *52*(9), 985–991. https://doi.org/10.1093/chromsci/bmt139

Daood, H. G, Ráth, S., Palotás, G., Halász, G., Hamow, K., & Helyes, L. (2021). Efficient HPLC Separation on a Core-C30 Column with MS2 Characterization of Isomers, Derivatives and Unusual Carotenoids from Tomato Products. *Journal of Chromatographic Science, 60*(4), 336-347.

https://doi.org/10.1093/chromsci/bmab085

Deng, Y., Zhao, S., Yang, X., Hou, F., Fan, L., Wang, W., Xu, E., Cheng, H., Guo, M., Liu, D. (2021). Evaluation of extraction technologies of lycopene: Hindrance of extraction, effects on isomerization and comparative analysis - A review. *Trends in Food Science & Technology*, *115*, 285–296. https://doi.org/10.1016/j.tifs.2021.06.051

di Tomo, P., Canali, R., Ciavardelli, D., Di Silvestre, S., De Marco, A., Giardinelli, A., Pipino, C., Pietro, N., Virgili, F., Pandolfi, A. (2012). β-Carotene and lycopene affect endothelial response to TNF-α reducing nitro-oxidative stress and interaction with monocytes. *Molecular Nutrition & Food Research*, *56*(2), 217–227. https://doi.org/10.1002/mnfr.201100500

Domínguez, R., Gullón, P., Pateiro, M., Munekata, P. E. S., Zhang, W., & Lorenzo, J. M. (2020). Tomato as Potential Source of Natural Additives for Meat Industry. A Review. *Antioxidants*, *9*(1), 73. https://doi.org/10.3390/antiox9010073

dos Santos, R. C., Ombredane, A. S., Souza, J. M. T., Vasconcelos, A. G., Plácido, A., Amorim, A. das G. N., Barbosa, E. A., Lima, F. C. D. A., Rolke, C. D., Alves, M. M. M., & others (2018). Lycopene-rich extract from red guava (*Psidium guajava L.*) displays cytotoxic effect against human breast adenocarcinoma cell line MCF-7 via an apoptotic-like pathway. *Food Research International*, *105*, 184–196. https://doi.org/10.1016/j.foodres.2017.10.045

Duan, L., Liang, C., Li, X., Huang, Z., Liu, S., Wu, N., & Jia, D. (2019). Lycopene restores the effect of ischemic postconditioning on myocardial ischemia-reperfusion injury in hypercholesterolemic rats. *International Journal of Molecular Medicine*. https://doi.org/10.3892/ijmm.2019.4166

El-Rouby, D. H. (2011). Histological and immunohistochemical evaluation of the chemopreventive role of lycopene in tongue carcinogenesis induced by 4-nitroquinoline-1-oxide. *Archives of Oral Biology*, *56*(7), 664–671. https://doi.org/10.1016/j.archoralbio.2010.12.007

Faisal, W., Ruane-O'Hora, T., O'Driscoll, C. M., & Griffin, B. T. (2013). A novel lipid-based solid dispersion for enhancing oral bioavailability of Lycopene – *In vivo* evaluation using a pig model. *International Journal of Pharmaceutics*, *453*(2), 307–314. https://doi.org/10.1016/j.ijpharm.2013.06.027

Farinetti, A., Zurlo, V., Manenti, A., Coppi, F., & Mattioli, A. V. (2017). Mediterranean diet and colorectal cancer: A systematic review. *Nutrition*, *43–44*, 83–88. https://doi.org/10.1016/j.nut.2017.06.008

Farmer, W. R., & Liao, J. C. (2001). Precursor Balancing for Metabolic Engineering of Lycopene Production in *Escherichia coli*. *Biotechnology Progress*, *17*(1), 57–61. https://doi.org/10.1021/bp000137t

Ghadage, S. R., Mane, K. A., Agrawal, R. S., & Pawar, V. N. (2019). Tomato lycopene: potential health benefits. *The Pharma Innovation Journal*, *8*(6), 1245–1248.

Gloria, N. F., Soares, N., Brand, C., Oliveira, F. L., Borojevic, R., & Teodoro, A. J. (2014). Lycopene and beta-carotene induce cell-cycle arrest and apoptosis in human breast cancer cell lines. *Anticancer Research*, *34*(3), 1377–1386.

Gomez, L. P., Alvarez, C., Zhao, M., Tiwari, U., Curtin, J., Garcia-Vaquero, M., & Tiwari, B. K. (2020). Innovative processing strategies and technologies to obtain hydrocolloids from macroalgae for food applications. *Carbohydrate Polymers*, *248*, Article 116784. https://doi.org/10.1016/j.carbpol.2020.116784

Goula, A. M., & Adamopoulos, K. G. (2005). Stability of lycopene during spray drying of tomato pulp. *LWT - Food Science and Technology*, *38*(5), 479–487. https://doi.org/10.1016/j.lwt.2004.07.020

Guo, Y., Liu, Y., & Wang, Y. (2015). Beneficial effect of lycopene on anti-diabetic nephropathy through diminishing inflammatory response and oxidative stress. *Food & Function*, *6*(4), 1150–1156. https://doi.org/10.1039/C5FO00004A

Ha, T. V. A., Kim, S., Choi, Y., Kwak, H.-S., Lee, S. J., Wen, J., Oey, I., Ko, S. (2015). Antioxidant activity and bioaccessibility of size-different nanoemulsions for lycopene-enriched tomato extract. *Food Chemistry*, *178*, 115–121. https://doi.org/10.1016/j.foodchem.2015.01.048

Haribabu, T., Divakar, K., & Goli, D. (2013). Evaluation of anti-diabetic activity of Lycopene and its synergistic effect with Metformin hydrochloride and Glipizide in Alloxan induced diabetes in rats. *Sch. Acad. J. Pharm*, *2*(2), 119–124.

Honda, M., Murakami, K., Ichihashi, K., Takada, W., & Goto, M. (2021). Enriched (Z)-lycopene in Tomato Extract via Co-Extraction of Tomatoes and Foodstuffs Containing Z-isomerization-accelerating Compounds. *Catalysts*, *11*(4), Article 462. https://doi.org/10.3390/catal11040462

Honda, M., Sato, H., Takehara, M., Inoue, Y., Kitamura, C., Takemura, R., Fukaya, T., Wahyudiono, Kanda, H,. Goto, M. (2018). Microwave-Accelerated Z -Isomerization of (all- E)-Lycopene in Tomato Oleoresin and Enhancement of the Conversion by Vegetable Oils Containing Disulfide Compounds. *European Journal of Lipid Science and Technology*, *120*(7), Article 1800060. https://doi.org/10.1002/ejlt.201800060

Honest, K. N., Zhang, H. W., & Zhang, L. (2011). Lycopene: Isomerization Effects on Bioavailability and Bioactivity Properties. *Food Reviews International*, *27*(3), 248–258. https://doi.org/10.1080/87559129.2011.563392

Horuz, T. İ., & Belibağli, K. B. (2018). Nanoencapsulation by electrospinning to improve stability and water solubility of carotenoids extracted from tomato peels. *Food Chemistry*, *268*, 86–93. https://doi.org/10.1016/j.foodchem.2018.06.017

Huang, C.-S., Chuang, C.-H., Lo, T.-F., & Hu, M.-L. (2013). Anti-angiogenic effects of lycopene through immunomodualtion of cytokine secretion in human peripheral blood mononuclear cells. *The Journal of Nutritional Biochemistry*, *24*(2), 428–434. https://doi.org/10.1016/j.jnutbio.2012.01.003

Huang, C.-S., Fan, Y.-E., Lin, C.-Y., & Hu, M.-L. (2007). Lycopene inhibits matrix metalloproteinase-9 expression and down-regulates the binding activity of nuclear factor-kappa B and stimulatory protein-1. *The Journal of Nutritional Biochemistry*, *18*(7), 449–456. https://doi.org/10.1016/j.jnutbio.2006.08.007

Ilahy, R., Siddiqui, M. W., Piro, G., Lenucci, M. S., Hdider, C., & Helyes, L. (2017). A focus on high-lycopene tomato cultivars: horticultural performance

and functional quality. *Acta Horticulturae*, (1159), 57–64. https://doi.org/10.17660/ActaHortic.2017.1159.9

Ilahy, R., Tlili, I., Helyes, L., Siddiqui, M. W., Lenucci, M. S., Pék, Z., & Hdider, C. (2019). Organically grown high-lycopene tomatoes: a novel adventure within functional quality. *Acta Horticulturae*, (1233), 67–72. https://doi.org/10.17660/ActaHortic.2019.1233.11

International Conference on Harmonization. (2005). Validation of analytical procedures: text and methodology Q2 (R1). *International Conference on Harmonization, Geneva, Switzerland*.

Jafari, S. M., & McClements, D. J. (2017). *Nanotechnology Approaches for Increasing Nutrient Bioavailability, 81,* 1-30. https://doi.org/10.1016/bs.afnr.2016.12.008

Jain, A., Thakur, D., Ghoshal, G., Katare, O. P., Singh, B., & Shivhare, U. S. (2016). Formation and functional attributes of electrostatic complexes involving casein and anionic polysaccharides: An approach to enhance oral absorption of lycopene in rats in vivo. *International Journal of Biological Macromolecules*, *93*, 746–756. https://doi.org/10.1016/j.ijbiomac.2016.08.071

Jiang, L.-N., Liu, Y.-B., & Li, B.-H. (2019). Lycopene exerts anti-inflammatory effect to inhibit prostate cancer progression. *Asian Journal of Andrology*, *21*(1), 80-85. https://doi.org/10.4103/aja.aja_70_18

Jing, Y., Guo, F., Zhang, S., Dong, W., Zhou, J., Xin, F., Zhang, W., Jiang, M. (2021). Recent Advances on Biological Synthesis of Lycopene by Using Industrial Yeast. *Industrial & Engineering Chemistry Research*, *60*(9), 3485–3494. https://doi.org/10.1021/acs.iecr.0c05228

Jones, D., Caballero, S., & Davidov-Pardo, G. (2019). *Bioavailability of nanotechnology-based bioactives and nutraceuticals, 88,* 235-273. https://doi.org/10.1016/bs.afnr.2019.02.014

Kehili, M., Kammlott, M., Choura, S., Zammel, A., Zetzl, C., Smirnova, I., Allouche, N., Sayadi, S. (2017). Supercritical CO_2 extraction and antioxidant activity of lycopene and β-carotene-enriched oleoresin from tomato (*Lycopersicum esculentum L.*) peels by-product of a Tunisian industry. *Food and Bioproducts Processing*, *102*, 340–349. https://doi.org/10.1016/j.fbp.2017.02.002

Kim, B.-S., Gaul, C., Paul, N. E., Dewor, M., Stromps, J.-P., Hwang, S. S., Nourbakhsh, M., Bernhagen, J., Rennekampff, H. O., Pallua, N. (2016). The Effect of Lipoaspirates on Human Keratinocytes. *Aesthetic Surgery Journal*, *36*(8), 941–951. https://doi.org/10.1093/asj/sjw049

Kim, M., Kim, S. H., Lim, J. W., & Kim, H. (2019). Lycopene induces apoptosis by inhibiting nuclear translocation of β-catenin in gastric cancer cells. *J. Physiol. Pharmacol*, *70*(4), 605–611. https://doi.org/10.26402/jpp.2019.4.11

Kim, S. O., Ha, T. V. A., Choi, Y. J., & Ko, S. (2014). Optimization of Homogenization-Evaporation Process for Lycopene Nanoemulsion Production and Its Beverage Applications. *Journal of Food Science*, *79*(8), N1604–N1610. https://doi.org/10.1111/1750-3841.12472

Knockaert, G., Pulissery, S. K., Colle, I., Van Buggenhout, S., Hendrickx, M., & Loey, A. Van. (2012). Lycopene degradation, isomerization and in vitro bioaccessibility in high pressure homogenized tomato puree containing oil: Effect of additional thermal and high pressure processing. *Food Chemistry*, *135*(3), 1290–1297. https://doi.org/10.1016/j.foodchem.2012.05.065

Kubola, J., Meeso, N., & Siriamornpun, S. (2013). Lycopene and beta carotene concentration in aril oil of gac (Momordica cochinchinensis Spreng) as influenced by aril-drying process and solvents extraction. *Food Research International*, *50*(2), 664–669. https://doi.org/10.1016/j.foodres.2011.07.004

Kumar, D. G. P., Hebbar, H. U., Sukumar, D., & Ramesh, M. N. (2005). Infrared and hot-air drying of onions. *Journal of Food Processing and Preservation*, *29*(2), 132–150. https://doi.org/10.1111/j.1745-4549.2005.00019.x

Lee, W., & Lee, D. G. (2014). Lycopene-induced hydroxyl radical causes oxidative DNA damage in Escherichia coli. *Journal of Microbiology and Biotechnology*, *24*(9), 1232–1237. https://doi.org/10.4014/jmb.1406.06009

Li, D., Chen, L., Zhao, W., Hao, J., & An, R. (2016). MicroRNA-let-7f-1 is induced by lycopene and inhibits cell proliferation and triggers apoptosis in prostate cancer. *Molecular Medicine Reports*, *13*(3), 2708–2714. https://doi.org/10.3892/mmr.2016.4841

Li, L., Liu, Z., Jiang, H., & Mao, X. (2020). Biotechnological production of lycopene by microorganisms. *Applied Microbiology and Biotechnology*, *104*(24), 10307–10324. https://doi.org/10.1007/s00253-020-10967-4

Li, M., Xia, Q., Zhang, H., Zhang, R., & Yang, J. (2020). Metabolic Engineering of Different Microbial Hosts for Lycopene Production. *Journal of Agricultural and Food Chemistry*, *68*(48), 14104–14122. https://doi.org/10.1021/acs.jafc.0c06020

Li, W., Wang, G., Lu, X., Jiang, Y., Xu, L., & Zhao, X. (2014). Lycopene ameliorates renal function in rats with streptozotocin-induced diabetes. *International Journal of Clinical and Experimental Pathology*, *7*(8), Article 5008.

Li, Weikun, Yalcin, M., Lin, Q., Ardawi, M.-S. M., & Mousa, S. A. (2017). Self-assembly of green tea catechin derivatives in nanoparticles for oral lycopene delivery. *Journal of Controlled Release*, *248*, 117–124. https://doi.org/10.1016/j.jconrel.2017.01.009

Li, X., Jia, P., Huang, Z., Liu, S., Miao, J., Guo, Y., Wu, N., Jia, D. (2019). Lycopene protects against myocardial ischemia-reperfusion injury by inhibiting mitochondrial permeability transition pore opening. *Drug Design, Development and Therapy*, *13*, 2331–2342. https://doi.org/10.2147/DDDT.S194753

Lianfu, Z., & Zelong, L. (2008). Optimization and comparison of ultrasound/microwave assisted extraction (UMAE) and ultrasonic assisted extraction (UAE) of lycopene from tomatoes. *Ultrasonics Sonochemistry*, *15*(5), 731–737. https://doi.org/10.1016/j.ultsonch.2007.12.001

Lombardelli, C., Liburdi, K., Benucci, I., & Esti, M. (2020). Tailored and synergistic enzyme-assisted extraction of carotenoid-containing chromoplasts from tomatoes. *Food and Bioproducts Processing*, *121*, 43–53. https://doi.org/10.1016/j.fbp.2020.01.014

Luque de Castro, M. D., & Priego-Capote, F. (2010). Soxhlet extraction: Past and present panacea. *Journal of Chromatography A*, *1217*(16), 2383–2389. https://doi.org/10.1016/j.chroma.2009.11.027

Luxsuwong, D., Indranupakorn, R., & Wongtrakul, P. (2014). Preparation of Vesicles Entrapped Lycopene Extract. *Journal of Oleo Science*, *63*(6), 645–652. https://doi.org/10.5650/jos.ess13216

Marena, G. D., Fonseca-Santos, B., Santos, R. M. A., dos Santos, K. C., Bauab, T. M., & Chorilli, M. (2020). Incorporation of Ursolic Acid in Liquid Crystalline Systems Improves the Antifungal Activity Against Candida Sp. *Journal of Pharmaceutical Innovation, 16,* 576-586. https://doi.org/10.1007/s12247-020-09470-0

Maul, A. A., Wasicky, R., & Bacchi, E. M. (1996). Extração por fluido supercrítico. *Revista Brasileira de Farmacognosia*, *5*(2). https://doi.org/10.1590/S0102-695X1996000200006

Mayeaux, M., Xu, Z., King, J. M., & Prinyawiwatkul, W. (2006). Effects of Cooking Conditions on the Lycopene Content in Tomatoes. *Journal of Food Science*, *71*(8), C461–C464. https://doi.org/10.1111/j.1750-3841.2006.00163.x

Mihalcea, L., Crăciunescu, O., Gheonea (Dima), I., Prelipcean, A.-M., Enachi, E., Barbu, V., Bahrim, G. E., Râpeanu, G., Oancea, A., Stănciuc, N. (2021). Supercritical CO_2 Extraction and Microencapsulation of Lycopene-Enriched Oleoresins from Tomato Peels: Evidence on Antiproliferative and Cytocompatibility Activities. *Antioxidants*, *10*(2), Article 222. https://doi.org/10.3390/antiox10020222

Mirahmadi, M., Azimi-Hashemi, S., Saburi, E., Kamali, H., Pishbin, M., & Hadizadeh, F. (2020). Potential inhibitory effect of lycopene on prostate cancer. *Biomedicine and Pharmacotherapy*, *129*, Article 110459. https://doi.org/10.1016/j.biopha.2020.110459

Mohamadin, A. M., Elberry, A. A., Mariee, A. D., Morsy, G. M., & Al-Abbasi, F. A. (2012). Lycopene attenuates oxidative stress and heart lysosomal damage in isoproterenol induced cardiotoxicity in rats: A biochemical study. *Pathophysiology*, *19*(2), 121–130. https://doi.org/10.1016/j.pathophys.2012.04.005

Moritz, B., & Tramonte, V. L. C. (2006). Biodisponibilidade do licopeno. *Revista de Nutrição*, *19*(2), 265–273. https://doi.org/10.1590/S1415-52732006000200013

Murakami, K., Honda, M., Takemura, R., Fukaya, T., Kanda, H., Goto, M., & others. (2018). Effect of thermal treatment and light irradiation on the stability of lycopene with high Z-isomers content. *Food Chemistry*, *250*, 253–258. https://doi.org/10.1016/j.foodchem.2018.01.062

Navarro-González, I., Pérez-Sánchez, H., Martín-Pozuelo, G., García-Alonso, J., & Periago, M. J. (2014). The Inhibitory Effects of Bioactive Compounds of Tomato Juice Binding to Hepatic HMGCR: In Vivo Study and Molecular Modelling. *PLoS One*, *9*(1), Article e83968. https://doi.org/10.1371/journal.pone.0083968

Nazemiyeh, E., Eskandani, M., Sheikhloie, H., & Nazemiyeh, H. (2016). Formulation and Physicochemical Characterization of Lycopene-Loaded Solid Lipid Nanoparticles. *Advanced Pharmaceutical Bulletin*, *6*(2), 235–241. https://doi.org/10.15171/apb.2016.032

Ojha, S., Goyal, S., Sharma, C., Arora, S., Kumari, S., & Arya, D. (2013). Cardioprotective effect of lycopene against isoproterenol-induced myocardial infarction in rats. *Human & Experimental Toxicology*, *32*(5), 492–503. https://doi.org/10.1177/0960327112454890

Okonogi, S., & Riangjanapatee, P. (2015). Physicochemical characterization of lycopene-loaded nanostructured lipid carrier formulations for topical administration. *International Journal of Pharmaceutics*, *478*(2), 726–735. https://doi.org/10.1016/j.ijpharm.2014.12.002

Palozza, P., Simone, R., Catalano, A., Parrone, N., Monego, G., & Ranelletti, F. O. (2011). Lycopene regulation of cholesterol synthesis and efflux in human macrophages. *The Journal of Nutritional Biochemistry*, *22*(10), 971–978. https://doi.org/10.1016/j.jnutbio.2010.08.010

Pataro, G., Carullo, D., Falcone, M., & Ferrari, G. (2020). Recovery of lycopene from industrially derived tomato processing by-products by pulsed electric fields-assisted extraction. *Innovative Food Science & Emerging Technologies*, *63*, Article 102369. https://doi.org/10.1016/j.ifset.2020.102369

Pék, Z., Szuvandzsiev, P., Nemenyi, A., Helyes, L., & Lugasi, A. (2011). The Effect of Natural Light on Changes in Antioxidant Content and Color Parameters of Vine-ripened Tomato (Solanum lycopersicum L.) Fruits. *HortScience*, *46*(4), 583–585. https://doi.org/10.21273/HORTSCI.46.4.583

Pellicanò, T. M., Sicari, V., Loizzo, M. R., Leporini, M., Falco, T., & Poiana, M. (2020). Optimizing the supercritical fluid extraction process of bioactive compounds from processed tomato skin by-products. *Food Science and Technology*, *40*(3), 692–697. https://doi.org/10.1590/fst.16619

Periago, M. J., Martín-Pozuelo, G., González-Barrio, R., Santaella, M., Gómez, V., Vázquez, N., Navarro-González, I., García-Alonso, J. (2016). Effect of tomato juice consumption on the plasmatic lipid profile, hepatic HMGCR activity, and fecal short chain fatty acid content of rats. *Food & Function*, *7*(10), 4460–4467. https://doi.org/10.1039/C6FO00344C

Petyaev, I. M., Dovgalevsky, P. Y., Klochkov, V. A., Chalyk, N. E., Pristensky, D. V., Chernyshova, M. P., Udumyan, R., Kochryan, T., Kyle, N. H & others. (2018). Effect of lycopene supplementation on cardiovascular parameters and markers of inflammation and oxidation in patients with coronary vascular disease. *Food Science & Nutrition*, *6*(6), 1770–1777. https://doi.org/10.1002/fsn3.734

Queiroz, S. C. N., Collins, C. H., & Jardim, I. C. S. F. (2001). Métodos de extração e/ou concentração de compostos encontrados em fluidos biológicos para posterior determinação cromatográfica. *Química Nova*, *24*(1), 68-76. https://doi.org/10.1590/S0100-40422001000100013

Rahimpour, S., & Taghian Dinani, S. (2018). Lycopene extraction from tomato processing waste using ultrasound and cell-wall degrading enzymes. *Journal of Food Measurement and Characterization*, *12*(4), 2394–2403. https://doi.org/10.1007/s11694-018-9856-7

Rao, A. V., Ray, M. R., & Rao, L. G. (2006). Lycopene. *Advances in Food and Nutrition Research*, 51, 99-164 https://doi.org/10.1016/S1043-4526(06)51002-2

Rao, A. V., & Shen, H. (2002). Effect of low dose lycopene intake on lycopene bioavailability and oxidative stress. *Nutrition Research*, *22*(10), 1125–1131. https://doi.org/10.1016/S0271-5317(02)00430-X

Riangjanapatee, P.; Okonogi, S. (2012). Effect of surfactant on lycopene-loaded nanostructured lipid carriers. *Drug Discoveries & Therapeutics, 6*(3),

163-168. https://doi.org/10.5582/ddt.2012.v6.3.163

Riedl, J., Linseisen, J., Hoffmann, J., & Wolfram, G. (1999). Some Dietary Fibers Reduce the Absorption of Carotenoids in Women. *The Journal of Nutrition*, *129*(12), 2170–2176. https://doi.org/10.1093/jn/129.12.2170

Rizwan, M., Rodriguez-Blanco, I., Harbottle, A., Birch-Machin, M. A., Watson, R. E. B., & Rhodes, L. E. (2011). Tomato paste rich in lycopene protects against cutaneous photodamage in humans in vivo: a randomized controlled trial. *British Journal of Dermatology*, *164*(1), 154–162. https://doi.org/10.1111/j.1365-2133.2010.10057.x

Rodrigues, F. A., Pimenta, V. de S. C., Braga, K. M. da S., & de Araújo, E. G. (2016). Obtenção de extratos de plantas do cerrado. *Enciclopédia Biosfera*, *13*(23), 870–887. https://doi.org/10.18677/Enciclopedia_Biosfera_2016_075

Sahin, K., Cross, B., Sahin, N., Ciccone, K., Suleiman, S., Osunkoya, A. O., Master, V., Harris, W., Carthon, B., Mohammad, R., & others (2015). Lycopene in the prevention of renal cell cancer in the TSC2 mutant Eker rat model. *Archives of Biochemistry and Biophysics*, *572*, 36–39. https://doi.org/10.1016/j.abb.2015.01.006

Saini, R. K., A. Bekhit, A. E.-D., Roohinejad, S., Rengasamy, K. R. R., & Keum, Y.-S. (2020). Chemical Stability of Lycopene in Processed Products: A Review of the Effects of Processing Methods and Modern Preservation Strategies. *Journal of Agricultural and Food Chemistry*, *68*(3), 712–726. https://doi.org/10.1021/acs.jafc.9b06669

Salvia-Trujillo, L., & McClements, D. J. (2016). Enhancement of lycopene bioaccessibility from tomato juice using excipient emulsions: Influence of lipid droplet size. *Food Chemistry*, *210*, 295–304. https://doi.org/10.1016/j.foodchem.2016.04.125

Santini, A., Tenore, G. C., & Novellino, E. (2017). Nutraceuticals: A paradigm of proactive medicine. *European Journal of Pharmaceutical Sciences*, *96*, 53–61. https://doi.org/10.1016/j.ejps.2016.09.003

Scaglia, B., D'Incecco, P., Squillace, P., Dell'Orto, M., De Nisi, P., Pellegrino, L., Botto, A., Cavicchi, C., Adani, F. (2020). Development of a tomato pomace biorefinery based on a CO_2-supercritical extraction process for the production of a high value lycopene product, bioenergy and digestate. *Journal of Cleaner Production*, *243*, 118650. https://doi.org/10.1016/j.jclepro.2019.118650

Shi, J., & Maguer, M. Le. (2000). Lycopene in tomatoes: chemical and physical properties affected by food processing. *Critical Reviews in Food Science and Nutrition*, *40*(1), 1–42. https://doi.org/10.1080/10408690091189275

Silva, Y. P. A., Ferreira, T. A. P. C., Celli, G. B., & Brooks, M. S. (2019). Optimization of Lycopene Extraction from Tomato Processing Waste Using an Eco-Friendly Ethyl Lactate–Ethyl Acetate Solvent: A Green Valorization Approach. *Waste and Biomass Valorization*, *10*(10), 2851–2861. https://doi.org/10.1007/s12649-018-0317-7

Silva, Y. P. A., Ferreira, T. A. P. C., Jiao, G., & Brooks, M. S. (2019). Sustainable approach for lycopene extraction from tomato processing by-product using hydrophobic eutectic solvents. *Journal of Food Science and Technology*, *56*(3), 1649–1654. https://doi.org/10.1007/s13197-019-03618-8

Singh, A. R., Desu, P. K., Nakkala, R. K., Kondi, V., Devi, S., Alam, M. S., Hamid, H., Athawale, R. B., Kesharwani, P. (2021). Nanotechnology-based approaches applied to nutraceuticals. *Drug Delivery and Translational Research, 12,* 485-499. https://doi.org/10.1007/s13346-021-00960-3

Soares, N. da C. P., Elias, M. de B., Machado, C. L., Trindade, B. B., Borojevic, R., & Teodoro, A. J. (2019). Comparative Analysis of Lycopene Content from Different Tomato-Based Food Products on the Cellular Activity of Prostate Cancer Cell Lines. *Foods*, *8*(6), Article 201. https://doi.org/10.3390/foods8060201

Soleymaninejad, M., Joursaraei, S. G., Feizi, F., & Jafari Anarkooli, I. (2017). The Effects of Lycopene and Insulin on Histological Changes and the Expression Level of Bcl-2 Family Genes in the Hippocampus of Streptozotocin-Induced Diabetic Rats. *Journal of Diabetes Research*, *2017*, 1–9. https://doi.org/10.1155/2017/4650939

Sotomayor-Gerding, D., Oomah, B. D., Acevedo, F., Morales, E., Bustamante, M., Shene, C., & Rubilar, M. (2016). High carotenoid bioaccessibility through linseed oil nanoemulsions with enhanced physical and oxidative stability. *Food Chemistry*, *199*, 463–470. https://doi.org/10.1016/j.foodchem.2015.12.004

Spernath, A., Yaghmur, A., Aserin, A., Hoffman, R. E., & Garti, N. (2002). Food-Grade Microemulsions Based on Nonionic Emulsifiers: Media To Enhance Lycopene Solubilization. *Journal of Agricultural and Food Chemistry*, *50*(23), 6917–6922. https://doi.org/10.1021/jf025762n

Stahl, W., Heinrich, U., Aust, O., Tronnier, H., & Sies, H. (2006). Lycopene-rich products and dietary photoprotection. *Photochem. Photobiol. Sci.*, *5*(2), 238–242. https://doi.org/10.1039/B505312A

Stahl, W., & Sies, H. (2012). β-Carotene and other carotenoids in protection from sunlight. *The American Journal of Clinical Nutrition*, *96*(5), 1179S-1184S. https://doi.org/10.3945/ajcn.112.034819

Strati, I. F., Gogou, E., & Oreopoulou, V. (2015). Enzyme and high pressure assisted extraction of carotenoids from tomato waste. *Food and Bioproducts Processing*, *94*, 668–674. https://doi.org/10.1016/j.fbp.2014.09.012

Sultan Alvi, S., Ansari, I. A., Khan, I., Iqbal, J., & Khan, M. S. (2017). Potential role of lycopene in targeting proprotein convertase subtilisin/kexin type-9 to combat hypercholesterolemia. *Free Radical Biology and Medicine*, *108*, 394–403. https://doi.org/10.1016/j.freeradbiomed.2017.04.012

Sun, T., Miao, L., Li, Q., Dai, G., Lu, F., Liu, T., Zhang, X., Ma, Y. (2014). Production of lycopene by metabolically-engineered *Escherichia coli*. *Biotechnology Letters*, *36*(7), 1515–1522. https://doi.org/10.1007/s10529-014-1543-0

Sun, X., Jia, H., Xu, Q., Zhao, C., & Xu, C. (2019). Lycopene alleviates H_2O_2 -induced oxidative stress, inflammation and apoptosis in bovine mammary epithelial cells via the NFE2L2 signaling pathway. *Food & Function*, *10*(10), 6276–6285. https://doi.org/10.1039/C9FO01922G

Takács, S., Pék, Z., Csányi, D., Daood, H. G., Szuvandzsiev, P., Palotás, G., & Helyes, L. (2020). Influence of Water Stress Levels on the Yield and Lycopene Content of Tomato. *Water*, *12*(8), 2165. https://doi.org/10.3390/w12082165

Tanaka, Y., Sasaki, N., & Ohmiya, A. (2008). Biosynthesis of plant pigments: anthocyanins, betalains and carotenoids. *The Plant Journal*, *54*(4), 733–749. https://doi.org/10.1111/j.1365-313X.2008.03447.x

Tang, C.-H. (2021). Assembly of food proteins for nano- encapsulation and delivery of nutraceuticals (a mini-review). *Food Hydrocolloids*, *117*, Article 106710. https://doi.org/10.1016/j.foodhyd.2021.106710

Taylor, G. M., & Heap, J. T. (2020). Combinatorial metabolic engineering platform enabling stable overproduction of lycopene from carbon dioxide by cyanobacteria. *BioRxiv*. https://doi.org/10.1101/2020.03.11.983833

Teodoro, A., Oliveira, F., Martins, N., Maia, G. de, Martucci, R., & Borojevic, R. (2012). Effect of lycopene on cell viability and cell cycle progression in human cancer cell lines. *Cancer Cell International*, *12*(1), 36. https://doi.org/10.1186/1475-2867-12-36

Vallecilla-Yepez, L., & Ciftci, O. N. (2018). Increasing cis-lycopene content of the oleoresin from tomato processing byproducts using supercritical carbon dioxide. *LWT*, *95*, 354–360. https://doi.org/10.1016/j.lwt.2018.04.065

Viuda-Martos, M., Sanchez-Zapata, E., Sayas-Barberá, E., Sendra, E., Pérez-Álvarez, J. A., & Fernández-López, J. (2014). Tomato and Tomato Byproducts. Human Health Benefits of Lycopene and Its Application to Meat Products: A Review. *Critical Reviews in Food Science and Nutrition*, *54*(8), 1032–1049. https://doi.org/10.1080/10408398.2011.623799

Vogele, A. C. (1937). Effect of environmental factors upon the color of the tomato and the watermelon. *Plant Physiology*, *12*(4), 929 -955. http://doi.org/10.1104/pp.12.4.929

Wang, R., Lu, X., & Yu, R. (2020). Lycopene Inhibits Epithelial–Mesenchymal Transition and Promotes Apoptosis in Oral Cancer via PI3K/AKT/m-TOR Signal Pathway. *Drug Design, Development and Therapy*, *14*, 2461–2471. https://doi.org/10.2147/DDDT.S251614

Wang, Z., Sun, J., Yang, Q., & Yang, J. (2020). Metabolic Engineering Escherichia coli for the Production of Lycopene. *Molecules*, *25*(14), Article 3136. https://doi.org/10.3390/molecules25143136

Xianquan, S., Shi, J., Kakuda, Y., & Yueming, J. (2005). Stability of Lycopene During Food Processing and Storage. *Journal of Medicinal Food*, *8*(4), 413–422. https://doi.org/10.1089/jmf.2005.8.413

Xie, W., Lv, X., Ye, L., Zhou, P., & Yu, H. (2015). Construction of lycopene-overproducing Saccharomyces cerevisiae by combining directed evolution and metabolic engineering. *Metabolic Engineering*, *30*, 69–78. https://doi.org/10.1016/j.ymben.2015.04.009

Xu, X., Tian, L., Tang, S., Xie, C., Xu, J., & Jiang, L. (2020). Design and tailoring of an artificial DNA scaffolding system for efficient lycopene synthesis using zinc-finger-guided assembly. *Journal of Industrial Microbiology and Biotechnology*, *47*(2), 209–222. https://doi.org/10.1007/s10295-019-02255-6

Yadav, R. B., Kumar, B., Vats, A., Singh, S. N., Pathak, D. P., & Arora, R. (2020). Development, Standardization and Validation of Analytical Method for Quality Assurance and Quality Control of Aloe-Based Pharmaceuticals and Nutraceuticals. *Trakia Journal of Sciences*, *18*(4), 294–309. https://doi.org/10.15547/tjs.2020.04.003

Yamamoto, K. (2017). Food processing by high hydrostatic pressure. *Bioscience, Biotechnology, and Biochemistry*, *81*(4), 672–679. https://doi.org/10.1080/09168451.2017.1281723

Yang, C.-M., Hu, T.-Y., & Hu, M.-L. (2012). Antimetastatic Effects and Mechanisms of Apo-8′-Lycopenal, an Enzymatic Metabolite of Lycopene, Against Human Hepatocarcinoma SK-Hep-1 Cells. *Nutrition and Cancer*, *64*(2), 274–285. https://doi.org/10.1080/01635581.2012.643273

Yang, C.-M., Lu, Y.-L., Chen, H.-Y., & Hu, M.-L. (2012). Lycopene and the LXRα agonist T0901317 synergistically inhibit the proliferation of androgen-independent prostate cancer cells via the PPARγ-LXRα-ABCA1 pathway. *The Journal of Nutritional Biochemistry*, *23*(9), 1155–1162. https://doi.org/10.1016/j.jnutbio.2011.06.009

Yao, C. G., & Martins, P. N. (2020). Nanotechnology Applications in Transplantation Medicine. *Transplantation*, *104*(4), 682–693. https://doi.org/10.1097/TP.0000000000003032

Ye, M., Wu, Q., Zhang, M., & Huang, J. (2016). Lycopene inhibits the cell proliferation and invasion of human head and neck squamous cell carcinoma. *Molecular Medicine Reports*, *14*(4), 2953–2958. https://doi.org/10.3892/mmr.2016.5597

Yilmaz, T., Kumcuoglu, S., & Tavman, S. (2017). Ultrasound-assisted extraction of lycopene and [beta]-carotene from tomato-processing wastes. *Italian Journal of Food Science*, *29*(1), 186-194.

Yin, Q., Ma, Y., Hong, Y., Hou, X., Chen, J., Shen, C., Sun, M., Shang, Y., Dong, S., Zeng, Z., & others (2014). Lycopene attenuates insulin signaling deficits, oxidative stress, neuroinflammation, and cognitive impairment in fructose-drinking insulin resistant rats. *Neuropharmacology*, *86*, 389–396. https://doi.org/10.1016/j.neuropharm.2014.07.020

Yin, Y., Zheng, Z., & Jiang, Z. (2019). Effects of lycopene on metabolism of glycolipid in type 2 diabetic rats. *Biomedicine & Pharmacotherapy*, *109*, 2070–2077. https://doi.org/10.1016/j.biopha.2018.07.100

Yousefi, M., Rahimi-Nasrabadi, M., Pourmortazavi, S. M., Wysokowski, M., Jesionowski, T., Ehrlich, H., & Mirsadeghi, S. (2019). Supercritical fluid extraction of essential oils. *TrAC Trends in Analytical Chemistry*, *118*, 182–193. https://doi.org/10.1016/j.trac.2019.05.038

Yuan, S.-F., & Alper, H. S. (2019). Metabolic engineering of microbial cell factories for production of nutraceuticals. *Microbial Cell Factories*, *18*(1), 46. https://doi.org/10.1186/s12934-019-1096-y

Zeng, Y.-C., Peng, L.-S., Zou, L., Huang, S.-F., Xie, Y., Mu, G.-P., Zeng, X.-H., Zhou, X.-L., Zeng, Y.-C. (2017). Protective effect and mechanism of lycopene on endothelial progenitor cells (EPCs) from type 2 diabetes mellitus rats. *Biomedicine & Pharmacotherapy*, *92*, 86–94. https://doi.org/10.1016/j.biopha.2017.05.018

Zhao, C., Wei, L., Yin, B., Liu, F., Li, J., Liu, X., Wang, J., Wang, Y. (2020). Encapsulation of lycopene within oil-in-water nanoemulsions using lactoferrin: Impact of carrier oils on physicochemical stability and bioaccessibility. *International Journal of Biological Macromolecules*, *153*, 912–920. https://doi.org/10.1016/j.ijbiomac.2020.03.063

Zheng, S., Deng, Z., Chen, F., Zheng, L., Pan, Y., Xing, Q., Xing, Q., Tsao, R., Li, H. (2020). Synergistic antioxidant effects of petunidin and lycopene in H9c2 cells submitted to hydrogen peroxide: Role of Akt/Nrf2 pathway. *Journal of Food Science*, *85*(6), 1752–1763. https://doi.org/10.1111/1750-3841.15153

Zheng, Z., Yin, Y., Lu, R., & Jiang, Z. (2019). Lycopene Ameliorated Oxidative Stress and Inflammation in Type 2 Diabetic Rats. *Journal of Food Science*, *84*(5), 1194–1200. https://doi.org/10.1111/1750-3841.14505

Zhu, R., Chen, B., Bai, Y., Miao, T., Rui, L., Zhang, H., Xia, B., Li, Y., Gao, S., & others. (2020). Lycopene in protection against obesity and diabetes: A mechanistic review. *Pharmacological Research*, *159*, Article 104966. https://doi.org/10.1016/j.phrs.2020.104966

Ziegler, R. G., Colavito, E. A., Hartge, P., McAdams, M. J., Schoenberg, J. B., Mason, T. J., & Fraumeni Jr, J. F. (1996). Importance of α-carotene, β-carotene, and other phytochemicals in the etiology of lung cancer. *JNCI: Journal of the National Cancer Institute*, *88*(9), 612–615.

Zou, J., & Feng, D. (2015). Lycopene reduces cholesterol absorption through the downregulation of Niemann-Pick C1-like 1 in Caco-2 cells. *Molecular Nutrition & Food Research*, *59*(11), 2225–2230. https://doi.org/10.1002/mnfr.201500221

Zuorro, A. (2020). Enhanced Lycopene Extraction from Tomato Peels by Optimized Mixed-Polarity Solvent Mixtures. *Molecules*, *25*(9), Article 2038. https://doi.org/10.3390/molecules25092038

Zuorro, A., Fidaleo, M., & Lavecchia, R. (2011). Enzyme-assisted extraction of lycopene from tomato processing waste. *Enzyme and Microbial Technology*, *49*(6–7), 567–573. https://doi.org/10.1016/j.enzmictec.2011.04.020

CHAPTER 5

An overview of properties and analytical methods for lycopene in organic nanocarriers

Gabriela Corrêa Carvalho, Rafael Miguel Sábio*, Marlus Chorilli

Critical Reviews in Analytical Chemistry, v. 51, n. 7, pp. 674-686, 2021.

©copyright [2021], reprinted by permission of Informa UK Limited, trading as Taylor & Taylor & Francis Group.

Abstract

Lycopene (LYC), a natural compound responsible for the red color of some fruits like pink grapefruit, red guava, watermelon, papaya and, mainly, present in tomatoes (*Solanum lycopersicum*). LYC has been extensively studied because of its various pharmacological properties such as antioxidant, cardioprotective, hypocholesterolemic, antineophasic, photoprotection, antidiabetic and antimicrobial activity. However, LYC uses in therapy is limited due to its insolubility in aqueous solvents, resulting in low bioavailability and stability. In order to overcome these drawbacks, it is essential to use of organic nanocarriers for LYC controlled release. Up to now, the description of LYC-loaded organic nanocarriers is scarce, mainly related to organic nanosystems based on lipid nanostructures such as nanoemulsions (NE), liposomes (LP), niosomes (NI), nanostructured lipid carriers (NLC) and solid lipid nanoparticles (SLN). Taking into account the development of new formulations, is indispensable the use of sensitive and suitable analytical methods previously validated. Among the analytical methods described here, high performance liquid chromatography (HPLC) stands out due to its good accuracy, precision and desirable detection limit. In this review, we highlight the main biological and physicochemical properties of LYC, as well as LYC-based organic nanocarriers for controlled drug delivery and the analytical methods described in literature to determine LYC in any kind of matrix.

1. Introduction

Lycopene (LYC) is a carotenoid synthesized by plants and microorganisms. In nature its function is not only to attract animals to pollinate and disperse seeds, but also to absorb light during photosynthesis, providing protection to the plant from photosensitization caused by visible and ultraviolet (UV) light (Shi & Maguer, 2000; Tanaka et al., 2008). Due to its chemical structure, LYC is responsible for giving a reddish coloration to many foods such as tomatoes, pink grapefruit, red guava, watermelon and papaya been tomatoes (*Solanum lycopersicum*) ingestion the main source of LYC in the human diet (Andreassi et al., 2004; Shi & Maguer, 2000; Story et al., 2010).

Although LYC from tomatoes can be widely used as a food colorant, searches shows that LYC could suffer degradation during processing, affecting the product final quality (Andreassi et al., 2004; Shi et al., 1999; Shi & Maguer, 2000). LYC degradation occurs mainly by isomerization and oxidation processes. LYC from tomatoes and tomato-based foods appear essentially in *trans*-configuration. Isomerization from trans- to *cis*- LYC can be increased by thermal processes and long processing time whereas oxidation can be catalyzed by the presence of metal ions such as Cu^{2+} and Fe^{2+} under heating.(Shi et al., 1999; Shi & Maguer, 2000) Beyond that, *cis*-LYC form shows better bioavailability and absorption by organism regarding trans-LYC form (Boileau et al., 1999; Willcox et al., 2003).

LYC has several pharmacological properties, such as antioxidant, cardioprotective, hypocholesterolemic, antineophasic, photoprotective, antidiabetic and antimicrobial activity (Andreassi et al., 2004; di Mascio et al., 1989; Sharma et al., 2017; Tao et al., 2010; Zhang et al., 1991). LYC uses in therapy is limited due to its insolubility in aqueous solvents, resulting in low bioavailability, however this fact can be circumvented by the drug incorporation in delivery nanosystems (da Silva et al., 2014; Huang et al., 2010; Rahman et al., 2019; Shi & Maguer, 2000). In this way, the design of new nanocarriers for controlled LYC delivery comprises a few exploited and very interesting way to overcome drawbacks such as unspecific and uncontrolled delivery, low bioavailability, low stability in aqueous media, decrease of LYC bioactivity and changes in its pharmacology properties. Specifically, few reports in literature concerning LYC-loaded nanosystems are based on lipid nanostructures such as nanoemulsions (NE), liposomes (LP), niosomes (NI), nanostructured lipid carriers (NLC) and solid lipid nanoparticles (SLN) (Butnariu & Giuchici, 2011; Jain et al., 2017; Jhan & Pethe, 2019; Najafi et al., 2018; Okonogi & Riangjanapatee, 2015; Sharma et al., 2016, 2017; Singh et al., 2017; Stojiljkovic et al., 2018; Zhao et al., 2018).

However, taking into account the development of new formulations based on LYC@nanocarriers, is essential the use of sensitive and suitable analytical methods previously validated that allow quantifying active specimens and possible impurities present in the evaluated

formulations (Alves et al., 2010; International conference on harmonization, 2005; Sutton & Singer, 2011).

Among several analytical methods, the high-performance liquid chromatography (HPLC) stands out due to its good accuracy, precision and desirable detection limit. In the area of controlled drug release, HPLC is widely used in order to identify and quantify LYC in extracts and also determine encapsulation efficiency (% EE) and loading capacity (% LC) (Alves et al., 2010; Hofer et al., 2007; Jain et al., 2018; Ladole et al., 2018; Wang et al., 2005; Xu et al., 2006). In this context, this review aims to evaluate articles addressing the use of LYC-loaded organic nanocarriers applied in therapeutics, as well as the main analytical methods described in the literature for LYC analysis in distinct matrices.

2. Physicochemical properties of the LYC

LYC consists of a long chemical structure ($C_{40}H_{56}$, **Figure 1A and B**) highly hydrophobic with molecular weight of 536.85 Da, soluble in benzene, carbon disulfide, chloroform, hexane, petroleum ether and acetone, but insoluble in water, methanol and ethanol. LYC has a melting point of 172 – 175 ºC been sensitive to light, heat, oxygen and acid media (Shi & Maguer, 2000).

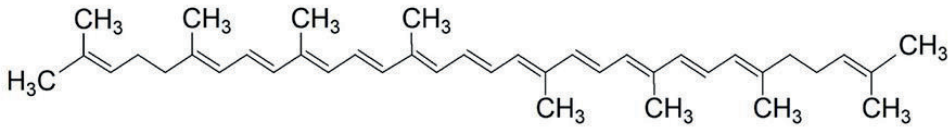

A

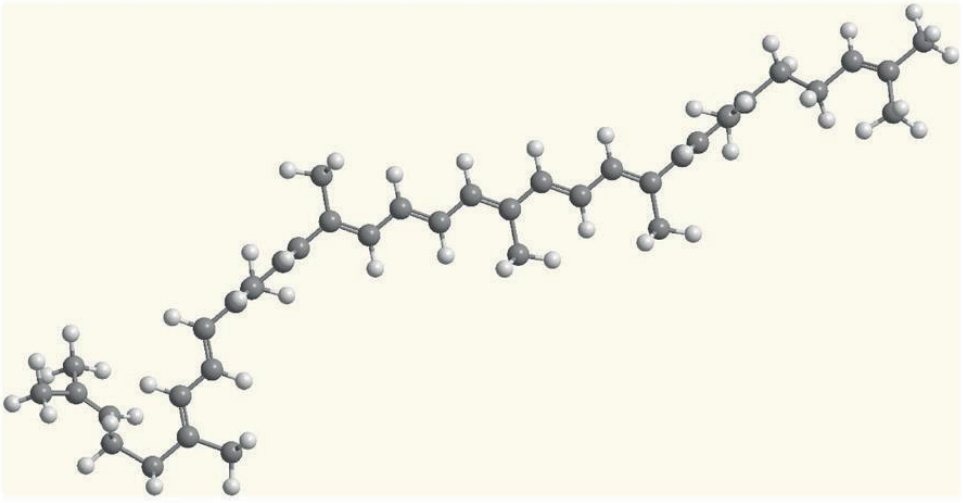

B

Figure 1: Chemical structure of LYC (A) and optimized 3D all-trans LYC structure (B).

As a carotenoid, LYC is a 40-carbon double-bonded isoprenoid formed by the 2C-methyl-D-erythritol-4-phosphate pathway (Hirschberg, 2001). Phytoene, precursor of LYC, is a colorless compound, but when double bonds are added to it, it becomes reddish, giving rise to LYC (Tanaka et al., 2008). Due to the presence of its double bonds, LYC exhibits absorption spectrum with three characteristic peaks: 450, 470 and 505 nm, with 470 nm corresponding to the maximum absorption peak (Andreassi et al., 2004; Wang et al., 2005; Xu et al., 2006). From these absorption bands, analytical methods can be employed to quantify LYC in any kind of matrix.

3. Pharmacological properties

Although many carotenoids are sources of vitamin A in animals, LYC has no pro-vitamin A activity due to the beta-ionone ring lack (Krinsky, 1989; Shi & Maguer, 2000). On the other hand, the conjugate double bonds in its chemical structure leads to antioxidant effects, been considered the most efficient carotenoid that inhibits singlet oxygen ($^1O_2$) generation promoting the reduction of DNA and lipid membrane oxidation and, consequently, the risk of cancer (di Mascio et al., 1989). Giovannuci et al.(1995) and Gann et al.(1999) evidenced that LYC is directly related to the prostate cancer risk reduction.

Authors reported additional mechanisms for LYC action against cancer cells (Astorg et al., 1997; Levy et al., 1995; Zhang et al., 1991). Zhang et al. (1991) demonstrated the chemopreventive ability of several carotenoids, including LYC, by inhibiting neoplastic transformation in 10T1/2 cells. The authors concluded that LYC is capable to enhance junctional communication, showing an important role in cell growth control and carcinogenesis. Other authors exhibited LYC as a protective compound against pre-neoplastic lesions induced in rat liver by modulating cytochrome P-450 2E1 (Astorg et al., 1997). In addition to its inhibitory properties on pulmonary and mammary endometrial cancer cell lines, LYC acts also on the growth suppression induced by insulin-like growth factor 1, which are growth regulators of mammary and endometrial cells (Levy et al., 1995).

Due to its antioxidant properties, LYC shows protection against UV light. This kind of light can generate oxygen radicals that react with skin lipids inducing lipid peroxidation leading to premature aging, psoriasis or atopic dermatitis (Andreassi et al., 2004; Halliday et al., 1998; Pecorelli et al., 2019). Additionally, LYC exhibits cardioprotective activity by not only preventing vascular cells and lipoprotein oxidation, but also by inhibiting the synthesis of 3-hydroxy-3-methyl-glutaryl-CoA reductase (HMG-CoA), a hypocholesterolemic agent, because this enzyme belongs to the mevalonate pathway, which is responsible for cholesterol production in animals. Beyond that, LYC can increase macrophage low-density lipoprotein (LDL) receptor activity, leading to a significant reduction in plasma LDL cholesterol concentrations (Fuhrman et al., 1997; Willcox et al., 2003).

LYC have demonstrated interesting antimicrobial properties, as stated by Tao et al.(2010) These authors described the minimal inhibitory concentration of LYC that shows effective antimicrobial activity against *E. coli*, *S. aureus*, *B. subtilis*, *S. cerevisiae* and *R. oryzae* by using diffusion method.

In order to elucidate mechanism of action as an antifungal, authors analyzed its action on *Candida albicans*, and concluded that it not only caused cell membrane damage but also inhibited the budding process by destroying membrane integrity (Sung et al., 2007). LYC can induces the accumulation of reactive oxygen species (ROS) as hydroxyls groups, causing DNA damage and consequently, cellular apoptosis in *C. albicans* (Choi & Lee, 2015). LYC also reduces the amount of intracellular ROS, inhibiting apoptosis of neuronal cells. Researchers have demonstrated that oxidative stress is largely responsible for neurodegenerative diseases such as Alzheimer, Parkinson and Huntington. The authors show LYC as a promising drug applied in therapies to treat these kind of diseases (Chen et al., 2019; Manoharan et al., 2016).

According to Najafi et al.(2018) and Swami et al.(2017), cryopreservation process generates ROS compromising animal sperm viability. In addition, Najafi et al.(2018) reported the use of LYC-loaded nanosystems as an effective antioxidant that improve the quality and fertility of rooster sperm.

LYC has been reported as a promising anti-diabetic drug. Sharma et al.(2017) evaluated the anti-diabetic activity of LYC-loaded nisome nanocarriers. From *in vivo* assays, significant reduction of glucose level in blood was detected relating to diabetic control up to 14 days of treatment. Biochemical parameters as cholesterol, triglyceride, LDL and very-low-density lipoprotein also decrease by using LYC-based nano-niosomes, confirming the potential and successful LYC action against induced diabetes.

4. Bioavailability

The LYC content in fresh tomatoes varies according to the season and region of cultivation (Moritz & Tramonte, 2006). In a study conducted by Alda et al.(2009), LYC content of approximately 12 mg/100 g was observed in fresh tomatoes whereas in tomato paste a content of 16 mg/100 g was detected. Regarding the LYC bioavailability, some authors described higher values of LYC content when tomatoes are submitted to thermal processing regarding fresh tomatoes (Gärtner et al., 1997). As stated by Shi and Maguer (2000), tomatoes processing can increase LYC bioavailability by reducing the bonding forces between LYC and the matrix.

In fresh tomatoes, the prevalent isomerization is *trans*-LYC (**Figure 1B**) whereas after thermal treatment is *cis*-LYC isomer. While *trans*-LYC isomer shows poor absorption, *cis*-LYC isomer is better absorbed by the human body (Willcox et al., 2003). Authors comparing both isomer's

bioavailability *in vitro* and *in vivo* reporting higher concentration of *cis*-–LYC isomers in tissues explained by the *cis*-LYC solubility in bile acid micelles, favoring its absorption by chylomicrons (Boileau et al., 1999).

5. LYC-related drawbacks

LYC is commonly found in fresh tomatoes as a *trans* isomer, but suffers isomerization whether exposed to light, heat and acid media. On the other hand, *cis* isomers are more soluble in nonpolar solvents but exhibits low bioactivity, stability and more susceptible to oxidation (Shi et al., 1999; Shi & Maguer, 2000). LYC can also suffer oxidation when exposed to air and in catalyzed reaction by metals such as Cu^{2+} and Fe^{2+}. Although both degradation factors are very common during LYC extraction from natural sources, this drawback can be easily overlaid by the addition of antioxidant and neutralizing agents. Additionally, its oxidation during storage could be avoided when performed in inert atmosphere or vacuum (Shi & Maguer, 2000).

The mainly problem to use LYC in the clinical area comprises its lipophilicity character, non-solubility in aqueous solvents which results in low bioavailability.(Rahman et al., 2019; Shi & Maguer, 2000) Drawbacks as low bioavailability, degradation and low stability can be circumvented by the incorporation of LYC in alternative systems based on nanotechnology (da Silva et al., 2014; Huang et al., 2010).

6. Nanotechnology-based drug delivery systems for LYC

Nanotechnology, “nano” from Greek meaning billionth of something, is the application of nanometric structures in various areas of science. Regarding biological and pharmaceutical applications, nanosystems can be used as nanocarriers for controlled drug delivery (Lyra et al., 2007; Tonet & Leonel, 2019).

The use of nanocarriers can promotes controlled drug delivery on the specific target site without modify drug bioactivity and pharmacology properties but improving the stability and solubility of lipophilic and hydrophilic drugs in the most type of media, expanding the possibilities of drugs applied in therapies (Nazemiyeh et al., 2016; Sahoo et al., 2008; Sahoo & Labhasetwar, 2003).

Nanocarriers can be fabricated from a wide variety of materials such as biodegradable polymers, inorganic particles, lipids and amphiphilic structures (Sahoo & Labhasetwar, 2003). However, the most of searches reported in the literature using nanocarriers containing LYC consist on lipid-based nanostructures such as NE, LP, NI, NLC and SLN, as exhibited in Figure 2 (Butnariu & Giuchici, 2011; Jain et al., 2017; Jhan & Pethe, 2019; Najafi et al., 2018; Okonogi & Riangjanapatee, 2015; Sharma et al., 2016, 2017; Stojiljkovic et al., 2018; Swami et al., 2017; Zhao et al., 2018).

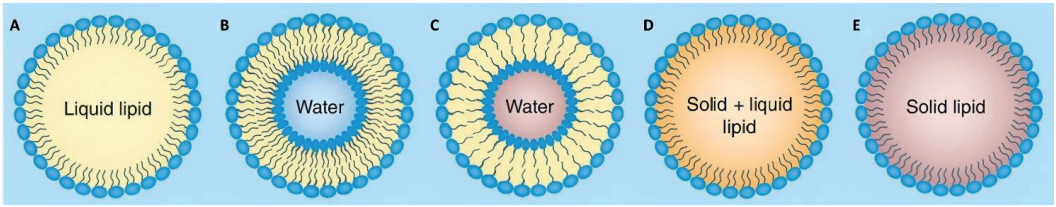

Figure 2: Schematic representation of nanoemulsion (A), liposome (B), niosome (C), nanostructured lipid carriers (D), solid lipid nanoparticles (E).(Poonia et al., 2016)

Lipid-based nanocarriers

Lipid-based nanosystems such as NE, LP, NI, NLC and SLN appear as effective tools to overcome non-aqueous solubility of lipophilic drugs like LYC (Singh et al., 2017).

NE are emulsion that contain small droplets with average size from 10 to 100 nm as shown in **Figure 2A**. The nanosized droplets are stabilized by a layer composed by surfactant and co-surfactant. NE can be optically transparent or opaque systems, formed by two immiscible liquids through mechanical shear, allowing drug dispersion in nanoscale droplets (Mason et al., 2006; Shakeel et al., 2012; Tamjidi et al., 2013). NE have been applied as carriers for lipophilic drugs in topical formulations due to its interesting characteristics such as fluidity, small droplet size and good permeability. These properties allow NE rapidly interact with skin cells (Rai et al., 2018; Shakeel et al., 2012).

LP appear as another lipid-based structure, corresponding to small spherical vesicles formed when natural cholesterol and phospholipids are dispersed in aqueous medium. These systems can incorporate hydrophilic and hydrophobic drugs, the first one, in the phospholipid bilayer, and the later, incorporated into their aqueous interior as exhibited in **Figure 2B** (Allen, 1997; Sahoo & Labhasetwar, 2003; Singh et al., 2011). LP present low toxicity, good biocompatibility and size flexibility (from nano to micrometers). LP can modify drug pharmacokinetics, changing their biodistribution in therapeutic targets, making them versatile and desirable systems for clinical applications (Allen, 1997).

Similar to LP, niosomes (NI, **Figure 2C**) are small nanovesicles formed by non-ionic surfactants despites phospholipidic bilayer. These nanosystems show advantages relating to LP such as less toxicity, better permeability, high stability and good biodegradability. Beyond that, nonionic surfactants are cheaper than phospholipids making NI economically viable (Bartelds et al., 2018; Caritá et al., 2018; Kazi et al., 2010).

Other type of lipid-based structures, NLC are derived from water-in-oil (k) nanoemulsions. These nanosystems comprise a stabilizing agent (surfactant), lipids and water. The lipidic phase contain solid and liquid (oil) lipids at room or body temperature, as depicted in **Figure 2D** (Müller et

al., 2002b; Tamjidi et al., 2013). NLC have high bioavailability, are biodegradable, biocompatible, have good stability over time, desirable shelf life and can avoid drug's degradation.(Okonogi & Riangjanapatee, 2015; Wissing et al., 2004) The NLC are very interesting systems as carotenoid delivery systems acting as protective nanostructures against oxidation and decomposition processes (Nazemiyeh et al., 2016).

SLN are nanosystems also derived from nanoemulsions but different of NLC; the SLN are composed by surfactant that stabilizes one solid lipid or a blend of solid lipids at room or body temperature, as displayed in **Figure 2E** (Müller et al., 2002a; Tamjidi et al., 2013; Wissing et al., 2004). Additionally, the hydrophobic solid matrix core with a phospholipid monolayer of SLN favor the efficient entrapment of hydrophobic drugs regarding to liposomes (Mehnert & Mäder, 2001).

However, NLC systems shows some advantages regarding to the SLN such as higher drug encapsulation efficiency, greater size stability, good polydisperse index and better release rates even with low drugs volume incorporated (Das et al., 2012). **Table 1** shows an overview about lipid-based nanocarriers containing LYC, the incorporation processes and their applications.

Table 1: Types of nanocarriers containing LYC, the incorporation procedure and their respective applications.

Nanocarrier	Incorporation	Application	Reference
Liposome (LP)	LYC methanolic solution was added to a lipid solution, then through a rotary evaporator the organic solvents were removed, leaving only a lipid film, in which phosphate buffer was added under vigorous stirring to form vesicles. The suspension was placed in a sonicator in order to decrease vesicles size.	Cardio protective activity	(Jhan & Pethe, 2019)
Liposome (LP)	Firstly, LYC and soy lecithin mixture was dissolved in ethanol. This solution was taken to an evaporator and a dry lipid film was obtained, which was then hydrated with PBS and stirred to give an emulsion and then to form the liposomes. Their size was reduced through a homogenizer. Liposomes containing LYC were stored at 4 °C.	Sperm Cryopreservation	(Najafi et al., 2018)
Liposome (LP)	LYC was encapsulated in a 10% phospholipid nanoparticles solution (acquired as nanospheres). Then, by centrifugation the encapsulated nanoparticles were isolated	Kidney Injury	(Stojiljkovic et al., 2018)
Liposome (LP)	LYC was added in a solution of cholesterol and lecithin dissolved in dichloromethane. Then through an evaporator the organic solvent was removed until a lipid film was obtained. The flask was filled with N_2 and then PBS with glycerin and glass beads. The mixture was rotated to hydrate the lipid film, and then sonicated in a water bath. Subsequently through a probe-ultrasonic disruptor it was disintegrated and subsequently cooled in an ice water bath. The suspension was centrifuged and stored in a bottle containing N_2.	Ischemic brain damage	(Zhao et al., 2018)
Solid lipid nanoparticles (SLN)	LYC was incorporated into SLN by adding 10 mg of LYC with lipid in organic dispersion phase Non-incorporated LYC was removed through cellulose dialysis bag. The suspension was filtered (0.45 µm membrane filter) to remove excess lipid.	Breast cancer	(Jain et al., 2017)
Niosomes (NI)	LYC was dispersed in a solvent mixture (n-hexane: acetone: ethanol in 2:1:1 v/v). Then, span 60 and cholesterol (1:1 mol) was adsorbed over an inert medium under constant stirring at 60 °C. The aqueous phase containing mannitol was slowly added to the LYC-loaded inert media under constant stirring at 60 °C. After that, the solution was sonicated by an ultrasonic cell crusher for 3 cycles of 60 s, and then held for 2-3 h to stabilize the niosomes. The suspension was filtered to remove inert material and passed by column chromatography to remove non-incorporated LYC. Finally, LYC-loaded niosomes vesicles were collected and lyophilized.	Anti-Diabetic Activity	(Sharma et al., 2017)
Nanostructured lipid carrier (NLC)	Solid lipid (Precirol ATO 5 (9-15% w/v) and liquid lipid vitamin E were heated and under stirring LYC extract (oil phase) was added. At the same time tween 80 and	Breast cancer	(Singh et al., 2017)

	poloxamer solution (1: 2) was heated at the same temperature as the oil phase. This hot surfactant solution was dispersed in the oil phase dropwise under constant stirring. Then the pre-dispersion was obtained by ultrasound. After reaching room temperature the dispersion was stored at 4 °C.		
Niosomes (NI)	LYC was dispersed in a solvent mixture (n-hexane: acetone: ethanol in 2:1:1 v/v). Then, span 60 and cholesterol (1:1 mol) was adsorbed over an inert medium under constant stirring at 60 °C. The aqueous phase containing mannitol was slowly added to the LYC-loaded inert media under constant stirring at 60 °C. After that, the solution was sonicated by an ultrasonic cell crusher for 3 cycles of 60 s, and then held for 2-3 h to stabilize the niosomes. The suspension was filtered to remove inert material and passed by column chromatography to remove non-incorporated LYC. Finally, LYC-loaded niosomes vesicles were collected and lyophilized.	Anticancer Activity	(Sharma et al., 2016)
Nanostructured lipid carrier (NLC)	LYC was dissolved in a lipid mixture, orange wax and rice oil, resulting in the oil phase. For the aqueous phase, Eumulgin® was dissolved in water. After heating, the phases were mixed and stirred. Subsequently, with the aid of a homogenizer a preemulsion was obtained. This hot pre-emulsion was subjected to an HPH (Micron LAB40, Homogenizer Systems, Germany) and was abruptly cooled.	Formulations for topical administration	(Okonogi & Riangjanapatee, 2015)
Nanoemulsion (NE)	Under stirring, LYC was added to an aqueous propolis solution, the mixture was placed in an ultrasonic bath at 20 kHz for 20 min to form LYC-propolis loaded nanoparticles. Subsequently, the mixture was kept at 22 °C. Excess of organic solvent was evaporated on a rotary evaporator and the samples were stored at 25 °C.	UVA skin protection	(Butnariu & Giuchici, 2011)

Other types of LYC-associated carriers

Jain et al.(2018) incorporated LYC ethanolic solution into whey-isolated protein particles to evaluate this system in breast cancer therapy. Authors fabricated spherical nanoformulations with average size from 100-350 nm. From in *vitro* and *in vivo* assays, the proposed formulation comprises a new controlled LYC delivery system that increases bioavailability, therapeutic efficacy and safety profiling compared to plain LYC.

Authors have explored the ability of some bacteria such as *Salmonella sp*., *Clostridium sp*. and *Bifidobacterium sp*. to colonize solid tumors. The researches have described the use of these bacteria as genes carriers that encode prodrug enzymes, toxins, cytosines, angiogenesis inhibitors, therapeutic nucleotides and antibodies for cancer therapy (C.-H. Chang et al., 2016; Liu et al., 2014; Pawelek et al., 2003). Chang et al.(2016) conducted studies using *Escherichia coli* as carrier for insoluble drugs. Specifically, authors reported LYC synthesized by *Escherichia coli* via pathway engineering aiming to apply these bacteria as a novel LYC carrier. *In vitro* studies displayed *E. coli* as an efficient carrier inhibiting the growth of HER2/neu-positive breast cancer cells, been a promising strategy to targeted cancer therapies.

LYC has been incorporated in polymeric matrices as gelatin and used as drug delivery systems. Authors described the incorporation of LYC in gelatin fibers via electrospinning technique. After encapsulation, an increasing of thermal stability, water solubility and, mainly, an enhancement of antioxidant activity by ten times were detected. These results corroborate the evaluated carriers as interesting systems for drug delivery applications (Horuz & Belibağli, 2018).

7. Analytical methods for the determination of LYC

The development of efficient formulations is directly related to the application of potential drugs in innovative pharmaceutical products (Leroux, 2017). LYC have been extensively studied according to its potential applications in several area as food, cosmetics, pharmaceutical, among others (Andreassi et al., 2004; Butnariu & Giuchici, 2011; Jain et al., 2017; Jhan & Pethe, 2019; Najafi et al., 2018; Okonogi & Riangjanapatee, 2015; Sharma et al., 2016, 2017; Shi et al., 1999; Singh et al., 2017; Stojiljkovic et al., 2018; Zhao et al., 2018). Notwithstanding, research towards the association of "lycopene and controlled drug delivery" and "lycopene and analytical methods" remain scarce up to now, as depicted in **Figure 3**.

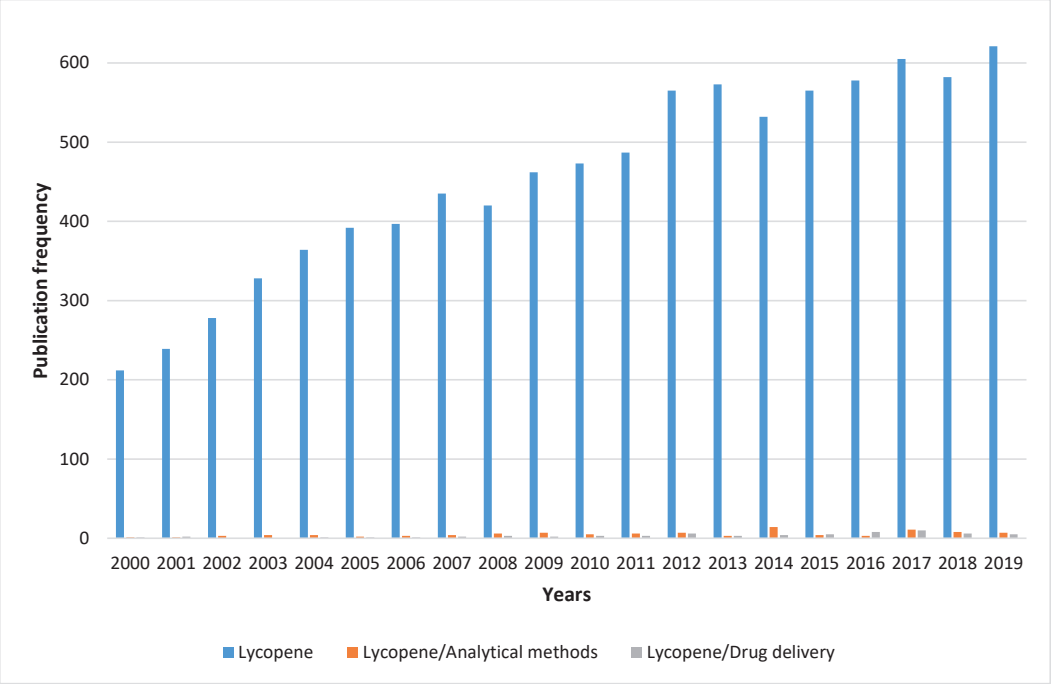

Figure 3: Publication frequency per year in the last nineteen years in the SCOPUS® database (all types of publications, *e.g.*, letters, notes, short survey, conference papers, book chapter, book, reviews and articles), all areas of knowledge, with the main keywords "lycopene", "lycopene and controlled drug delivery" and "lycopene and analytical methods" in the article title, abstract, or keyword list (Data accessed December 15, 2019).

Considering **Figure 3**, the development of new carriers as LYC delivery systems and analytical methods to quantify LYC comprise a promising research field few explored nowadays. Although some nanocarriers containing LYC have been previously described, exists a lack of efficient nanocarriers and a wide universe to be explored to fabricate effective controlled LYC delivery systems for clinical applications.

On the other hand, employing reliable analytical methods is primordial to determine the quality of developed products because it enables the quantification of active specimens besides detected and quantified the impurities present in the samples (Alves et al., 2019). Therefore, sensitive and suitable analytical methods are indispensable to obtain real information about the samples, that means, the method should be previously validated before any analyzes (International conference on harmonization, 2005; Sutton & Singer, 2011).

The validation purpose comprises to confirm and provide evidence that the new method is

suitable for the intended analysis. A satisfactory validation must follow steps such as design qualification, installation qualification, operational qualification and performance qualification. The latter includes the proof that the new method is suitable for recurrent use in agreement with the criteria described by the compendia (INMETRO, 2016; International conference on harmonization, 2005).

High-performance liquid chromatography

Among several methods used to quantify LYC, HPLC comprises a very interesting and useful method. This can be confirmed by the **Figure 4**, in which the keywords association "lycopene and high-performance liquid chromatography" exhibits the largest number of manuscripts published in the last 19 years corresponding to 76% of the total analytical methods searched. Despite the drawback concerning the inherent cost of the column, the instrumental system and the solvents, most of researches choose this technique due to its good accuracy, precision and desirable detection limit (Alves et al., 2019; Hofer et al., 2007).

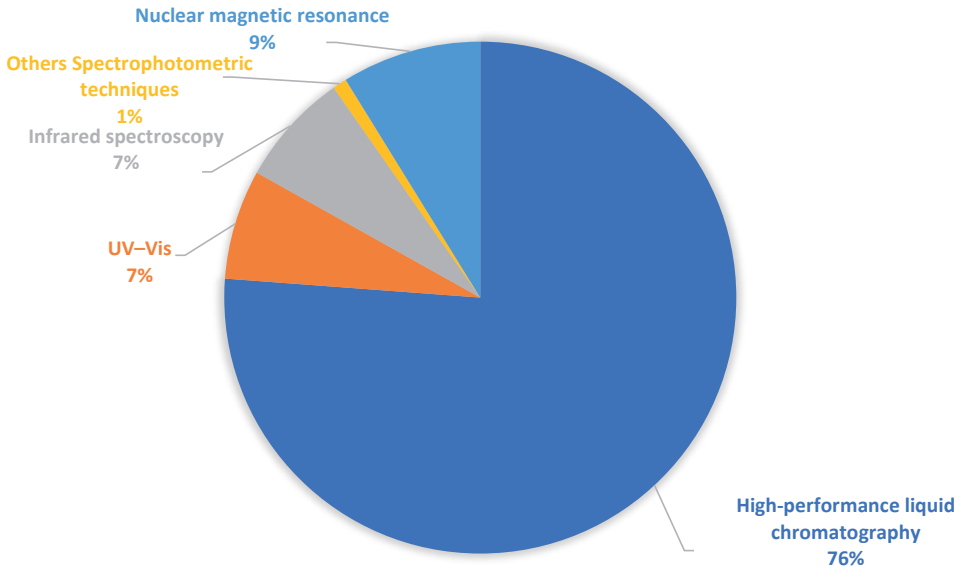

Figure 4: Percentage of several analytical methods used for LYC quantification. The numbers of manuscripts were retrieved from SCOPUS® database by searching "lycopene/High-performance liquid chromatography", "lycopene/UV–Vis", "lycopene/Infrared spectroscopy", "lycopene/Spectrophotometric techniques" and "lycopene/Nuclear magnetic resonance" (Data accessed December 15, 2019).

HPLC consists on a technique based on the separation of chemical compounds from a solution by using two phases, mobile and stationary phase through stereochemical interactions, size exclusion, partition, adsorption or ion exchange (Brasil, 2019).

Usually, HPLC can be applied to identify and quantify LYC in extracts and also evaluate the % EE and % LC. However, due to the susceptibility of LYC to oxidation, the analysis should be carried out quickly allowing to achieve accurate results. Aiming the LYC detection, its absorption spectrum starting from 360 to 550 nm with three characteristic peaks at 450, 470 and 505 nm. The maximum absorption peak appears at 470 nm with retention time of 4.2 min (Andreassi et al., 2004; Jain et al., 2018; Ladole et al., 2018; Wang et al., 2005; Xu et al., 2006).

Taking into account the use of nanocarriers in controlled drug release, the evaluation of drug % EE and % LC are essentials. % EE comprises the amount that is incorporated into nanocarriers whereas % LC refers to the maximum load capacity as a function of the nanosystems mass, according to the equations 1 and 2 (Alves et al., 2019; Horuz & Belibağli, 2019).

$$\mathrm{EE}(\%) = \frac{\text{drug added} - \text{free unentrapped drug}}{\text{drug added}} \text{ x } 100 \qquad (1)$$

$$\mathrm{LC}(\%) = \frac{\text{entrapped drug}}{\text{nanoparticles weight}} \text{ x } 100 \qquad (2)$$

Horuz & Belibağli (2019) reported LYC EE in zein fibers with values above to 90% by using HPLC technique, showing that LYC-loaded zein fibers promote better LYC retention and increase its antioxidant activity in 11-fold regarding free LYC. In another work, authors described similar results, quantifying LYC incorporated in gelatin nanofibers with EE values also above 90% (Horuz & Belibağli, 2018). Jain et al.(2018) evaluated EE of the LYC in isolated whey protein nanoparticles with distinct sizes in intestinal fluid, showing values from 50 to 65%, concluding that the system proved to be adequate when administered orally. From *in vitro* and *in vivo* assays, authors demonstrated the potential of this system in cancer therapeutic and intervention.

Carvalho et al. (2017) applied HPLC technique to determine LYC EE in microemulsions and quantified LYC release from *in vitro* studies in Franz diffusion cells. Results exhibited LYC detection in stratum corneum and skin layers but not in receptor phase. This observation suggests no LYC skin permeation since no LYC was detected by HPLC in the receptor phase at the first 6 h of analysis.

Jain et al. (2017) also used HPLC in order to evaluate EE and the release of LYC incorporated in SLN. From *in vitro* assays, authors reported a rapid initial release followed by a slow and sustained

LYC release been possible to predict the pharmacokinetic of this system. Additionally, Jain et al. (2016) formulated LYC-loaded microparticles by using biopolymers. EE and LC of around 67 and 70% were detected from these systems, respectively. *In vitro* release was evaluated by HPLC technique showing around 86% of LYC release up to 24 h. From *in vivo* assays, the LYC bioavailability and the pharmacokinetic study were determined by quantification of LYC plasma level via HPLC analysis. Authors concluded that LYC-loaded microparticles enhanced the oral LYC bioavailability improving stability and prolonged antioxidant activity regarding to free LYC.

Authors reported HPLC technique to evaluate the purity of LYC extracted from tomatoes (Singh et al., 2017). In addition, authors evaluated LYC EE in NLC, *in vitro* LYC release besides the nanosystems permeation from *in vivo* assays, which confirm the HPLC versatility for several kind of samples, especially in researches about the efficacy of new pharmaceutical formulations (Singh et al., 2017). **Table 2** exhibited distinct HPLC methods to quantify LYC in several matrices.

Table 2: HPLC methods described in the literature for analysis of LYC in distinct matrices.

Samples	Method	Detector	Column	Mobile phase	λ (nm)	R_T (min)	Reference
Composite zein nanofibers containing LYC extracted from tomato peel	HPLC	UV-Vis	C30 column (250×4.6 mm I.D)	A: methanol/MTBE/water (81:15:4), and B: methanol/MTBE/water (7:90:3)	450	-	(Horuz & Belibağli, 2019)
LYC extracted from tomato, red sweet pepper and emulsions	reversed phase Ultra-high HPLC	UV	C18 column (1.7 µm, 2.1 × 100 mm)	Eluent A: acetonitrile:methanol:aqueous Tris-HCl buffer (0.1 M pH 8.0) (72:8:3,v/v/v) Eluent B: methanol:ethyl acetate (68:32, v/v)	503	-	(Kirkhus et al., 2019)
Whey protein nanoparticles	reversed phase HPLC	UV-Vis	C18 column (10 µm, 4.6 mm x 250 mm	(70:15:15 v/v/v) methanol:ethyl acetate:acetonitrile	472	-	(Jain et al., 2018)
LYC extracted from raw materials and gelatin nanofibers	HPLC	UV-Vis	C30 column (250 × 4.6 mm I.D.)	A: methanol/MTBE/water (81:15:4) B: methanol/MTBE/water (7:90:3)	450	-	(Horuz & Belibağli, 2018)
LYC non-aqueous microemulsion	HPLC	UV	C18 column (150 × 4.6 mm)	acetonitrile/methanol (52:48 v/v)	470	-	(Carvalho et al., 2017)
LYC loaded in lipidic nanostructured particles	HPLC	PDA (photodio de arrays)	C-18 column (150 mm×4.6 mm i.d., particle size 5 µm)	methanol/acetonitrile/ethylacetate (70:15:15, v/v)	472	-	(Jain et al., 2017)
Nanostructured lipid carrier of LYC	reversed phase HPLC	UV	C-18 column (150 x 4.6 mm)	acetonitrile, methanol and tetrahydrofuran (70:25:5 % v/v)	475	3.0 min	(Singh et al., 2017)

Tomato extract-loaded dripping pills	reversed phase HPLC	PDA	C18 column (250 × 4.0 mm, i.d., 5 µm)	methanol and tetrahydrofurane (75:25, v/v)	475	-	(Chang et al., 2016)
LYC microparticles	HPLC	PDA	C-18 column (150 mm×4.6 mm i.d., particle size 5 µm)	methanol/acetonitrile/ethylacetate (70:15:15, v/v)	472	-	(Jain et al., 2016)

Nuclear magnetic resonance

Regarding other analytical methods to determine LYC, Nuclear Magnetic Resonance (NMR) spectroscopy consists of the application of a magnetic field that can interact with molecules promoting transition of nuclear spin between ground state to excited state energy levels. This technique allows to analyze the structure, composition and kind of chemistry bound that organic and inorganic compounds can perfomed (Dieguez et al., 2018; Lovchinsky et al., 2016). Despites the requires of macroscopic samples amount, liquid and solid samples can be evaluated by this technique. In light of this, NMR spectroscopy comprises 9% of all techniques used to determine pure LYC or LYC-based extracts, as depicted in **Figure 4.**

Takehara et al. (2014) carried out extraction and purification of (all-E)-LYC from tomato paste besides evaluated its physicochemical properties, performing also NMR analysis. Authors proposed to evaluate (all-E)-LYC and its isomers by using one and two-dimensional NMR techniques including ^{1}H and ^{13}C NMR, homonuclear correlation spectroscopy, heteronuclear multiple-quantum coherence and heteronuclear multiple bond connectivity. NMR results helped to identify the Z isomers present in natural sources, the generated (Z) isomers obtained by (all-E)-LYC thermal process and determine (all-E)-LYC extracted with high purity.

Naviglio et al. (2008) described a method for the extraction of high purity LYC from tomato wastes. The method is based on pressured extraction of LYC in the 0.7-0.9 MPa range using as starting material tomato skin residues from tomatoes processing in a water dispersion. The LYC extraction without lost its biological activity by converting all *trans* to *cis* configuration was evaluated by ^{1}H and ^{13}C NMR. Authors concluded that no *trans* to *cis*-LYC conversion was detected, as confirmed by the typical *trans*-LYC configuration signs identified in NMR spectra. Besides that, the proposed extraction method is ideal to obtain interesting LYC percentage from tomato byproducts.

Gupta et al., (2013) proposed to extract LYC from tomato aiming to evaluate its chemotherapeutic properties. From ^{1}H NMR analysis, LYC structure was successfully identified been able to start the chemopreventive *in vivo* tests. Authors confirmed the chemopreventive efficacy of LYC in hepatocarcinogenesis by reduction in tumour incidence (42.05%), tumour burden (1.39) and tumour multiplicity (3.42).

Authors described the use of solid-state (SS) NMR and suspended-state NMR in order to evaluate crystalline LYC and three samples of dried LYC powders formulated with gelatin. From NMR results, information about LYC stereochemistry within the protective colloid gelatin were achieved besides the characterization of LYC@gelatin nanoparticles. The rigid LYC structure can't be detected with suspended-state HR/MAS NMR technique due to strong dipole-dipole interactions whereas LYC micronizates can be clearly observed via SS cross-polarization/magic-angle-spinning

(CP/MAS) NMR. Beyond that, CP/MAS ^{13}C NMR provided spectra with characteristic pattern that made possible to classify LYC particles aggregation. Authors concluded that NMR techniques comprise a versatile characterization method for similar class of organic compounds (Wegmann et al., 2002).

In another study, LYC was extracted from tomato paste by using ursodeoxycholic acid (UDCA) as inclusion complex. ^{1}H NMR was performed in order to identify LYC molecular structure. Authors reported that NMR spectrum displayed good LYC purity corroborating HPLC and ultraviolet–visible (UV-Vis) analysis. UDCA as host matrix to extract LYC consist on an efficient method to obtain LYC with interesting purity (Seifi et al., 2013).

Ultraviolet-Visible spectroscopy

UV-Vis is a sensitive analytical method in molecular spectroscopy based on the absorption, scattering, diffraction, refraction, and reflection properties of the analyzed sample. The absorption of UV-Vis light is restricted to molecules with functional groups or that present many electrons capable to absorb light, known as chromophores (Roberts et al., 2018). The Beer–Lambert law describes the correlation among molecule light absorption, light path length of the sample and the concentration of absorbing molecules in liquid medium (Roberts et al., 2018; Upstone, 2013). This spectroscopy technique is widely used in pharmaceutical and industrial area due to advantages such as easy handling, low cost and speed of analysis. Despites these advantages, **Figure 4** displays that only UV-Vis spectroscopy corresponds to 7% of all techniques applied to quantify and determine pure LYC or LYC-based extracts. This observation can be ascribed to the high demand for more sensitive techniques as HPLC and HPLC combined with other techniques (Soares et al., 2008).

Abdullah et al.(2019) reported UV-Vis analysis to identify and characterize LYC extracted from vine tomato wastes. Authors calculated % III/II, with III being the longest-wavelength absorption peak, and II being the middle absorption peak aiming to evaluate LYC purification process. The % III/II found for the purified LYC was 50%, whereas purified LYC submitted to the incubation for a month in the dark at room temperature exhibited stability reduction achieving % III/II of 40%. The authors concluded that with UV-Vis measurements was possible to assign % III/II reduction to all-*trans* to *cis*-LYC isomerization.

Poojary et al. (2015) demonstrated the optimization of all-*trans*-LYC extraction from tomato pulp waste by employing full factorial design including four independent variables (extraction temperature, time, percentage of acetone in n-hexane and solvent volume). UV-Vis technique was used in order to calculate % LYC recovery. Authors reported 94.7% of LYC recovery, concluding that the

proposed extraction method minimizes isomerization and degradation processes, been very attractive from an industrial point of view.

Ladole et al. (2018) evaluated the effects of sonication and enzyme co-immobilized amino-functionalized magnetic nanoparticles aiming to enhance LYC extraction from waste tomatoes. Authors described HPLC, UV-Vis and Fourier-transform infrared spectroscopy (FTIR) techniques to determine and quantify LYC from the extract. The effect of sonication and enzymes co-immobilized amino-functionalized magnetic nanoparticles was synergistic resulting in LYC extraction yield up to 1.3 folds regarding other extraction process. This efficient method evaluated by HPLC, UV-Vis and FTIR can be potentially applied for industrial purposes.

Infrared spectroscopy

Infrared (IR) or Fourier transform infrared (FTIR) consists on a spectroscopy technique based on molecular vibrations detection generated by absorption of radiation in the infrared region, which provides characteristic absorption bands of each functional group (Berthomieu & Hienerwadel, 2009; Cozzolino, 2014). IR is an interesting tool to identify and quantify several compounds due to advantages such as easy execution, speed analysis and sample nondestructive.

Bansal et al. (2019) proposed to design a gel containing LYC-loaded colloidal microparticles. Colloidal microparticles (containing cellulose derivatives and tween as surfactant) were successfully prepared. FTIR analysis confirm the LYC presence into microparticles but no chemical interaction between pristine LYC and the excipients was detected. This result confirm that LYC properties were preserved and successfully incorporation into colloidal microparticles was achieved. The designed formulation showed sustained LYC release been a promising tool to prevent human skin against UVR-induced effects.

In another study, Li et al. (2018) evaluated the LYC influence on the formation and physical properties of oil-in-water (O/W) nanoemulsions stabilized by octenyl succinate anhydride modified starch. FTIR-attenuated total reflectance (FTIR-attenuated total reflectance (ATR)) technique was applied to determine LYC structure into O/W nanoemulsion. Authors stated that bands detected in FTIR-ATR spectra suggested amorphous LYC satisfactorily encapsulated into nanoemulsion without promotes any changes in nanoemulsion stability.

Tamburini et al. (2017) developed near-infrared spectroscopy on-line method to determine LYC and β-carotene content in post-harvesting watermelons as a direct and non-destructive application. In order to improve product quality, enhance nutritional values and increase consumer awareness, each fruit was marketed with a QR code label, which makes possible to quantify LYC content and other nutritional information in fruits. Authors concluded that the implementation of this

system as routine analysis could provide quality for the fruits and improve their values as a functional food.

8. Conclusions

Lycopene (LYC), a carotenoid extracted mainly from tomatoes, has been described as a potential drug for disease's treatment due to its unique properties such as antioxidant and antimicrobial activities, cardio, neuro and photoprotective effects besides antitumor action. However, its application in therapies is restricted due to its lipophilic character, which can be circumvented using the nanotechnology to develop new pharmaceutical formulations.

Although several nanocarriers have been shown in this review, only few studies concerning organic-based carriers was found, and, more specifically, the most of literature concern LYC incorporated into lipid-based nanocarriers. In this sense, this review encourages new researches towards the incorporation of LYC in other organic and inorganic-based nanocarriers.

Among the analytical methods described in the literature, HPLC was the most used, corresponding to the 76 % of the total researches regarding searched analytical methods. Although HPLC comprises a high-cost technique, it has been shown to be the most used by researchers during the development of formulations. This technique is versatile and can be used for drugs quantification in natural extracts even though used for the EE% evaluation and the *in vitro* and *in vivo* release assays.

9. Acknowledgments

We thank São Paulo Research Foundation – FAPESP. This study was financed in part by the Coordenação de Aperfeiçoamento de Pessoal de Ensino Superior – Brasil (CAPES) – Finance code – 001.

10. Disclosure statement

The authors declare no potential conflict of interest.

11. References

Abdullah, M. A. I. A., Al Dajah, S., Murad, A. A. B. U., El-Salem, A. M., & Khafajah, A. L. I. M. (2019). Extraction, Purification, and Characterization of Lycopene from Jordanian Vine Tomato Cultivar, and Study of its Potential Natural Antioxidant Effect on Samen Baladi *Current Research in Nutrition and Food Science*, 7(2), 532-546. http://dx.doi.org/10.12944/CRNFSJ.7.2.22

Alda, L. M., Gogoasa, I., Bordean, D.-M., Gergen, I., Alda, S., Moldovan, C., & Nita, L. (2009). Lycopene content of tomatoes and tomato products. *Journal of Agroalimentary Processes and Technologies*, *15*(4), 540–542.

Allen, T. M. (1997). Liposomes. *Drugs*, *54*(4), 8–14. https://doi.org/10.2165/00003495-199700544-00004

Alves, L. D. S., Rolim, L. A., Fontes, D. A. F., Rolim-Neto, P. J., Soares, M. F. de L. R., & Soares Sobrinho, J. L. (2010). Desenvolvimento de método analítico para quantificação do efavirenz por espectrofotometria no UV-Vis. *Química Nova*, *33*(9), 1967–1972. https://doi.org/10.1590/S0100-40422010000900026

Alves, R. C., Fernandes, R. P., Fonseca-Santos, B., Victorelli, F. D., & Chorilli, M. (2019). A critical review of the properties and analytical methods for the determination of curcumin in biological and pharmaceutical matrices. *Critical Reviews in Analytical Chemistry*, *49*(2), 138–149. https://doi.org/10.1080/10408347.2018.1489216

Andreassi, M., Stanghellini, E., Ettorre, A., Di Stefano, A., & Andreassi, L. (2004). Antioxidant activity of topically applied lycopene. *Journal of the European Academy of Dermatology and Venereology*, *18*(1), 52–55. https://doi.org/10.1111/j.1468-3083.2004.00850.x

Astorg, P., Gradelet, S., Bergès, R., & Suschetet, M. (1997). Dietary lycopene decreases the initiation of liver preneoplastic foci by diethylnitrosamine in the rat. *Nutrition and Cancer,* 29(1), 60-68. https://doi.org/10.1080/01635589709514603

Bansal, M., Walia, M. K., Singh, G., & Harikumar, S. L. (2019). Formulation And evaluation of lycopene loaded colloidal microparticles gel. *International Journal of Applied Pharmaceutics*, 165–170. http://dx.doi.org/10.22159/ijap.2019v11i6.35130

Bartelds, R., Nematollahi, M. H., Pols, T., Stuart, M. C. A., Pardakhty, A., Asadikaram, G., & Poolman, B. (2018). Niosomes, an alternative for liposomal delivery. *PloS One*, *13*(4). Article e0194179. https://doi.org/10.1371/journal.pone.0194179

Berthomieu, C., & Hienerwadel, R. (2009). Fourier transform infrared (FTIR) spectroscopy. *Photosynthesis Research*, *101*(2–3), 157–170. https://doi.org/10.1007/s11120-009-9439-x

Boileau, A. C., Merchen, N. R., Wasson, K., Atkinson, C. A., & Erdman Jr, J. W. (1999). Cis-lycopene is more bioavailable than trans-lycopene in vitro and in vivo in lymph-cannulated ferrets. *The Journal of Nutrition*, *129*(6), 1176–1181. https://doi.org/10.1093/jn/129.6.1176

Brasil. (2019). *Farmacopéia brasileira* (6th ed.). Brasil. Agência Nacional de Vigilância Sanitária (ANVISA).

Butnariu, M. V, & Giuchici, C. V. (2011). The use of some nanoemulsions based on aqueous propolis and lycopene extract in the skin's protective mechanisms against UVA radiation. *Journal of Nanobiotechnology*, *9*(1), Article 3. https://doi.org/10.1186/1477-3155-9-3

Caritá, A. C., Eloy, J. O., Chorilli, M., Lee, R. J., & Leonardi, G. R. (2018). Recent advances and perspectives in liposomes for cutaneous drug delivery. *Current Medicinal Chemistry*, *25*(5), 606–635. https://doi.org/10.2174/0929867324666171009120154

Carvalho, V. F., de Lemos, D. P., Vieira, C. S., Migotto, A., & Lopes, L. B. (2017). Potential of non-aqueous microemulsions to improve the delivery of lipophilic drugs to the skin. *AAPS PharmSciTech*, *18*(5), 1739–1749. https://doi.org/10.1208/s12249-016-0643-7

Chang, C.-H., Tsai, C.-K., Lee, T.-T., Chiang, C.-J., & Chao, Y.-P. (2016). Targeted delivery of bio-synthetic lycopene by the bacterial carrier. *Journal of the Taiwan Institute of Chemical Engineers*, *59*, 91–97. https://doi.org/10.1016/j.jtice.2015.08.003

Chang, C.-W., Wang, C.-Y., Wu, Y.-T., & Hsu, M.-C. (2016). Enhanced solubility, dissolution, and absorption of lycopene by a solid dispersion technique: The dripping pill delivery system. *Powder Technology*, *301*, 641–648. https://doi.org/10.1016/j.powtec.2016.07.013

Chen, D., Huang, C., & Chen, Z. (2019). A review for the pharmacological effect of lycopene in central nervous system disorders. *Biomedicine & Pharmacotherapy*, *111*, 791–801. https://doi.org/10.1016/j.biopha.2018.12.151

Choi, H., & Lee, D. G. (2015). Lycopene induces apoptosis in *Candida albicans* through reactive oxygen species production and mitochondrial dysfunction. *Biochimie*, *115*, 108–115. https://doi.org/10.1016/j.biochi.2015.05.009

Cozzolino, D. (2014). Use of infrared spectroscopy for in-field measurement and phenotyping of plant properties: instrumentation, data analysis, and examples. *Applied Spectroscopy Reviews*, *49*(7), 564–584. https://doi.org/10.1080/05704928.2013.878720

da Silva, P. B., dos Santos, R., Aparecido, M., Bonifácio, B. V., Negri, K. M. S., Sato, M. R., Bauab, T. M., & Chorilli, M. (2014). Nanotechnological strategies for vaginal administration of drugs—A review. *Journal of Biomedical Nanotechnology*, *10*(9), 2218–2243. https://doi.org/10.1166/jbn.2014.1890

Das, S., Ng, W. K., & Tan, R. B. H. (2012). Are nanostructured lipid carriers (NLCs) better than solid lipid nanoparticles (SLNs): development, characterizations and comparative evaluations of clotrimazole-loaded SLNs and NLCs? *European Journal of Pharmaceutical Sciences*, *47*(1), 139–151. https://doi.org/10.1016/j.ejps.2012.05.010

di Mascio, P., Kaiser, S., & Sies, H. (1989). Lycopene as the most efficient biological carotenoid singlet oxygen quencher. *Archives of Biochemistry and Biophysics*, *274*(2), 532–538. https://doi.org/10.1016/0003-9861(89)90467-0

Dieguez, C. M. T., Montanheiro, L. V, Cleto, L. B., Bonfim, M. J. C., & Dartora, C. A. (2018). Os fundamentos quânticos da Ressonância Magnética Nuclear. *Revista Brasileira de Ensino de Física*, *40*(1). https://doi.org/10.1590/1806-9126-RBEF-2017-0093

Fuhrman, B., Elis, A., & Aviram, M. (1997). Hypocholesterolemic effect of lycopene and β-carotene is related to suppression of cholesterol synthesis and augmentation of LDL receptor activity in macrophages. *Biochemical and Biophysical Research Communications*, *233*(3), 658–662. https://doi.org/10.1006/bbrc.1997.6520

Gann, P. H., Ma, J., Giovannucci, E., Willett, W., Sacks, F. M., Hennekens, C. H., & Stampfer, M. J. (1999). Lower prostate cancer risk in men with elevated plasma lycopene levels: results of a prospective analysis. *Cancer Research*, *59*(6), 1225–1230.

Gärtner, C., Stahl, W., & Sies, H. (1997). Lycopene is more bioavailable from tomato paste than from fresh tomatoes. *The American Journal of Clinical Nutrition*, *66*(1), 116–122. https://doi.org/10.1093/ajcn/66.1.116

Giovannucci, E., Ascherio, A., Rimm, E. B., Stampfer, M. J., Colditz, G. A., & Willett, W. C. (1995). Intake of carotenoids and retino in relation to risk of prostate cancer. *JNCI Journal of the National Cancer Institute*, *87*(23), 1767–1776. https://doi.org/10.1093/jnci/87.23.1767

Gupta, P., Bansal, M. P., & Koul, A. (2013). Spectroscopic characterization of lycopene extract from *Lycopersicum esculentum* (Tomato) and its evaluation as a chemopreventive agent against experimental hepatocarcinogenesis in mice. *Phytotherapy Research*, *27*(3), 448–456.

https://doi.org/10.1002/ptr.4741

Halliday, G. M., Bestak, R., Yuen, K. S., Cavanagh, L. L., & Barnetson, R. S. C. (1998). UVA-induced immunosuppression. *Mutation Research/Fundamental and Molecular Mechanisms of Mutagenesis*, *422*(1), 139–145. https://doi.org/10.1016/S0027-5107(98)00185-7

Hirschberg, J. (2001). Carotenoid biosynthesis in flowering plants. *Current Opinion in Plant Biology*, *4*(3), 210–218. https://doi.org/10.1016/S1369-5266(00)00163-1

Hofer, J. D., Olsen, B. A., & Rickard, E. C. (2007). Is HPLC assay for drug substance a useful quality control attribute? *Journal of Pharmaceutical and Biomedical Analysis*, *44*(4), 906–913. https://doi.org/10.1016/j.jpba.2007.04.023

Horuz, T. İ., & Belibağli, K. B. (2018). Nanoencapsulation by electrospinning to improve stability and water solubility of carotenoids extracted from tomato peels. *Food Chemistry*, *268*, 86–93. https://doi.org/10.1016/j.foodchem.2018.06.017

Horuz, T. İ., & Belibağli, K. B. (2019). Nanoencapsulation of carotenoids extracted from tomato peels into zein fibers by electrospinning. *Journal of the Science of Food and Agriculture*, *99*(2), 759–766. https://doi.org/10.1002/jsfa.9244

Huang, Q., Yu, H., & Ru, Q. (2010). Bioavailability and delivery of nutraceuticals using nanotechnology. *Journal of Food Science*, *75*(1), R50-R57. https://doi.org/10.1111/j.1750-3841.2009.01457.x

Instituto Nacional de Metrologia, Qualidade e Tecnologia (INMETRO), C. G. de A. (2016). Orientação sobre validação de métodos analíticos. *Coordenação Geral de Acreditação*: Rio de Janeiro, Brasil, 1-31.

International Conference on Harmonization. (2005). Validation of analytical procedures: text and methodology Q2 (R1). *International Conference on Harmonization, Geneva, Switzerland*.

Jain, A., Sharma, G., Ghoshal, G., Kesharwani, P., Singh, B., Shivhare, U. S., & Katare, O. P. (2018). Lycopene loaded whey protein isolate nanoparticles: An innovative endeavor for enhanced bioavailability of lycopene and anti-cancer activity. *International Journal of Pharmaceutics*, *546*(1–2), 97–105. https://doi.org/10.1016/j.ijpharm.2018.04.061

Jain, A., Sharma, G., Kushwah, V., Thakur, K., Ghoshal, G., Singh, B., Jain, S., Shivhare, U. S., & Katare, O. P. (2017). Fabrication and functional attributes of lipidic nanoconstructs of lycopene: An innovative endeavour for enhanced cytotoxicity in MCF-7 breast cancer cells. *Colloids and Surfaces B: Biointerfaces*, *152*, 482–491. https://doi.org/10.1016/j.colsurfb.2017.01.050

Jain, A., Thakur, D., Ghoshal, G., Katare, O. P., Singh, B., & Shivhare, U. S. (2016). Formation and functional attributes of electrostatic complexes involving casein and anionic polysaccharides: An approach to enhance oral absorption of lycopene in rats in vivo. *International Journal of Biological Macromolecules*, *93*, 746–756. https://doi.org/10.1016/j.ijbiomac.2016.08.071

Jhan, S., & Pethe, A. M. (2019). Double-loaded liposomes encapsulating lycopene β-cyclodextrin complexes: preparation, optimization, and evaluation. *Journal of Liposome Research*, *30*(1), 80-92. https://doi.org/10.1080/08982104.2019.1593450

Kazi, K. M., Mandal, A. S., Biswas, N., Guha, A., Chatterjee, S., Behera, M., & Kuotsu, K. (2010). Niosome: a future of targeted drug delivery systems. *Journal of Advanced Pharmaceutical Technology & Research*, *1*(4), Article 374. https://doi.org/10.4103/0110-5558.76435

Kirkhus, B., Afseth, N. K., Borge, G. I. A., Grimsby, S., Steppeler, C., Krona, A., & Langton, M. (2019). Increased release of carotenoids and delayed in vitro lipid digestion of high pressure homogenized tomato and pepper emulsions. *Food Chemistry*, *285*, 282–289. https://doi.org/10.1016/j.foodchem.2019.01.124

Krinsky, N. I. (1989). Carotenoids and cancer in animal models. *The Journal of Nutrition*, *119*(1), 123–126. https://doi.org/10.1093/jn/119.1.123

Ladole, M. R., Nair, R. R., Bhutada, Y. D., Amritkar, V. D., & Pandit, A. B. (2018). Synergistic effect of ultrasonication and co-immobilized enzymes on tomato peels for lycopene extraction. *Ultrasonics Sonochemistry*, *48*, 453–462. https://doi.org/10.1016/j.ultsonch.2018.06.013

Leroux, J.-C. (2017). Drug delivery: too much complexity, not enough reproducibility? *Angewandte Chemie International Edition*, *56*(48), 15170–15171. https://doi.org/10.1002/anie.201709002

Levy, J., Bosin, E., Feldman, B., Giat, Y., Miinster, A., Danilenko, M., & Sharoni, Y. (1995). Lycopene is a more potent inhibitor of human cancer cell proliferation than either α-carotene or β-carotene. *Nutrition and Cancer,* 24(3), 257-266.

Li, D., Li, L., Xiao, N., Li, M., & Xie, X. (2018). Physical properties of oil-in-water nanoemulsions stabilized by OSA-modified starch for the encapsulation of lycopene. *Colloids and Surfaces A: Physicochemical and Engineering Aspects*, *552*, 59–66. https://doi.org/10.1016/j.colsurfa.2018.04.055

Liu, S., Xu, X., Zeng, X., Li, L., Chen, Q., & Li, J. (2014). Tumor-targeting bacterial therapy: A potential treatment for oral cancer. *Oncology Letters*, *8*(6), 2359–2366. https://doi.org/10.3892/ol.2014.2525

Lovchinsky, I., Sushkov, A. O., Urbach, E., de Leon, N. P., Choi, S., De Greve, K., Evans, R., Gertner, R., Bersin, E., Müller, C., & others. (2016). Nuclear magnetic resonance detection and spectroscopy of single proteins using quantum logic. *Science*, *351*(6275), 836–841. https://doi.org/10.1126/science.aad8022

Lyra, M.A.M.; Soares-Sobrinho, J.L.; 1, T. Brasileiro, M.T.; Roca, M.F.; Barraza, J.A; Viana, O.S.; Rolim-Neto, P. (2007). Sistemas matriciais hidrofílicos e mucoadesivos para liberação controlada de fármacos. *Latin American Journal of Pharmacy*, *26*(5), 784–793.

Manoharan, S., Guillemin, G. J., Abiramasundari, R. S., Essa, M. M., Akbar, M., & Akbar, M. D. (2016). The role of reactive oxygen species in the pathogenesis of Alzheimer's disease, Parkinson's disease, and Huntington's disease: a mini review. *Oxidative Medicine and Cellular Longevity*, *2016*, Article 8590578. https://doi.org/10.1155/2016/8590578

Mason, T. G., Wilking, J. N., Meleson, K., Chang, C. B., & Graves, S. M. (2006). Nanoemulsions: formation, structure, and physical properties. *Journal*

of Physics: Condensed Matter, *18*(41), Article R635.https://doi.org/ 10.1088/0953-8984/18/41/R01

Mehnert, W., & Mäder, K. (2001). Solid lipid nanoparticles: production, characterization and applications. *Advanced Drug Delivery Reviews*, *47*(2–3), 165–196. https://doi.org/10.1016/j.addr.2012.09.021

Moritz, B., & Tramonte, V. L. C. (2006). Biodisponibilidade do licopeno. *Revista de Nutrição*, *19*(2), 265–273. https://doi.org/10.1590/S1415-52732006000200013

Müller, R. H., Radtke, M., & Wissing, S. A. (2002a). Nanostructured lipid matrices for improved microencapsulation of drugs. *International Journal of Pharmaceutics*, *242*(1–2), 121–128. https://doi.org/10.1016/S0378-5173(02)00180-1

Müller, R. H., Radtke, M., & Wissing, S. A. (2002b). Solid lipid nanoparticles (SLN) and nanostructured lipid carriers (NLC) in cosmetic and dermatological preparations. *Advanced Drug Delivery Reviews*, *54*, S131-S155. https://doi.org/10.1016/S0169-409X(02)00118-7

Najafi, A., Taheri, R. A., Mehdipour, M., Farnoosh, G., & Martínez-Pastor, F. (2018). Lycopene-loaded nanoliposomes improve the performance of a modified Beltsville extender broiler breeder roosters. *Animal Reproduction Science*, *195*, 168–175. https://doi.org/10.1016/j.anireprosci.2018.05.021

Naviglio, D., Caruso, T., Iannece, P., Aragòn, A., & Santini, A. (2008). Characterization of high purity lycopene from tomato wastes using a new pressurized extraction approach. *Journal of Agricultural and Food Chemistry*, *56*(15), 6227–6231. https://doi.org/10.1021/jf703788c

Nazemiyeh, E., Eskandani, M., Sheikhloie, H., & Nazemiyeh, H. (2016). Formulation and Physicochemical Characterization of Lycopene-Loaded Solid Lipid Nanoparticles. *Advanced Pharmaceutical Bulletin*, *6*(2), 235–241. https://doi.org/10.15171/apb.2016.032

Okonogi, S., & Riangjanapatee, P. (2015). Physicochemical characterization of lycopene-loaded nanostructured lipid carrier formulations for topical administration. *International Journal of Pharmaceutics*, *478*(2), 726–735.

Pawelek, J. M., Low, K. B., & Bermudes, D. (2003). Bacteria as tumour-targeting vectors. *The Lancet Oncology*, *4*(9), 548–556. https://doi.org/10.1016/S1470-2045(03)01194-X

Pecorelli, A., Woodby, B., Prieux, R., & Valacchi, G. (2019). Involvement of 4-hydroxy-2-nonenal in pollution-induced skin damage. *BioFactors*. *45*(4), 536–547. https://doi.org/10.1002/biof.1513

Poojary, M. M., & Passamonti, P. (2015). Optimization of extraction of high purity all-trans-lycopene from tomato pulp waste. *Food Chemistry*, *188*, 84–91. https://doi.org/10.1016/j.foodchem.2015.04.133

Poonia, N., Kharb, R., Lather, V., & Pandita, D. (2016). Nanostructured lipid carriers: versatile oral delivery vehicle. *Future Science OA*, *2*(3), Article FSO135. https://doi.org/10.4155/fsoa-2016-0030

Rahman, Y., Amin, S., Mir, S. R., & Kohli, K. (2019). Pre-Formulation Study for Palatable Microbeads of Lycopene. *Journal of Drug Delivery and Therapeutics*, *9*(4-A), 320–327. https://doi.org/10.22270/jddt.v9i4-A.3484

Rai, V. K., Mishra, N., Yadav, K. S., & Yadav, N. P. (2018). Nanoemulsion as pharmaceutical carrier for dermal and transdermal drug delivery: Formulation development, stability issues, basic considerations and applications. *Journal of Controlled Release*, *270*, 203–225. https://doi.org/10.1016/j.jconrel.2017.11.049

Roberts, J., Power, A., Chapman, J., Chandra, S., & Cozzolino, D. (2018). The use of UV-Vis spectroscopy in bioprocess and fermentation monitoring. *Fermentation*, *4*(1), Article 18. https://doi.org/10.3390/fermentation4010018

Sahoo, S. K., Dilnawaz, F., & Krishnakumar, S. (2008). Nanotechnology in ocular drug delivery. *Drug Discovery Today*, *13*(3–4), 144–151. https://doi.org/10.1016/j.drudis.2007.10.021

Sahoo, S. K., & Labhasetwar, V. (2003). Nanotech approaches to drug delivery and imaging. *Drug Discovery Today*, *8*(24), 1112–1120. https://doi.org/10.1016/S1359-6446(03)02903-9

Seifi, M., Seifi, P., Hadizadeh, F., & Mohajeri, S. A. (2013). Extraction of lycopene from tomato paste by ursodeoxycholic acid using the selective inclusion complex method. *Journal of Food Science*, *78*(11), C1680-C1685. https://doi.org/10.1111/1750-3841.12264

Shakeel, F., Shafiq, S., Haq, N., Alanazi, F. K., & Alsarra, I. A. (2012). Nanoemulsions as potential vehicles for transdermal and dermal delivery of hydrophobic compounds: an overview. *Expert Opinion on Drug Delivery*, *9*(8), 953–974. https://doi.org/10.1517/17425247.2012.696605

Sharma, P. K., Saxena, P., Jaswanth, A., Chalamaiah, M., & Balasubramaniam, A. (2017). Anti-Diabetic Activity of Lycopene Niosomes: Experimental Observation. *J Pharm Drug Devel*, *4*(1), Article 103.

Sharma, P. K., Saxena, P., Jaswanth, A., Chalamaiah, M., Tekade, K. R., & Balasubramaniam, A. (2016). Novel encapsulation of lycopene in niosomes and assessment of its anticancer activity. *Journal of Bioequivalence & Bioavailability*, *8*(5), 224–232. https://doi.org/10.4172/jbb.1000300

Shi, J., Le Maguer, M., Kakuda, Y., Liptay, A., & Niekamp, F. (1999). Lycopene degradation and isomerization in tomato dehydration. *Food Research International*, *32*(1), 15–21. https://doi.org/10.1016/S0963-9969(99)00059-9

Shi, J., & Maguer, M. Le. (2000). Lycopene in tomatoes: chemical and physical properties affected by food processing. *Critical Reviews in Food Science and Nutrition*, *40*(1), 1–42. https://doi.org/10.1080/10408690091189275

Singh, A., Neupane, Y. R., Panda, B. P., & Kohli, K. (2017). Lipid Based nanoformulation of lycopene improves oral delivery: formulation optimization, ex vivo assessment and its efficacy against breast cancer. *Journal of Microencapsulation*, *34*(4), 416–429.

Singh, S., Pandey, V. K., Tewari, R. P., & Agarwal, V. (2011). Nanoparticle based drug delivery system: advantages and applications. *Indian Journal of Science and Technology*, *4*(3), 177–180. https://doi.org/10.17485/ijst/2011/v4i3/29960

Soares, M., Soares-Sobrinho, J. L., Grangeiro-Júnior, S., Silva, K. E. R., Rolim-Neto, P. J., & SP-Brasil, A. F. S. A. (2008). Métodos de determinação do ornidazol em comprimidos revestidos: desenvolvimento, validação e comparação estatística. *Lat Am J Pharm*, *27*(5), 688–694.

Stojiljkovic, N., Ilic, S., Jakovljevic, V., Stojanovic, N., Stojnev, S., Kocic, H., Stojanovic, M., & Kocic, G. (2018). The encapsulation of lycopene in nanoliposomes enhances its protective potential in methotrexate-induced kidney injury model. *Oxidative Medicine and Cellular Longevity*, *2018*, Article 2627917. https://doi.org/10.1155/2018/2627917

Story, E. N., Kopec, R. E., Schwartz, S. J., & Harris, G. K. (2010). An update on the health effects of tomato lycopene. *Annual Review of Food Science and Technology*, *1*, 189–210. https://doi.org/10.1146/annurev.food.102308.124120

Sung, W. S., Lee, I.-S., & Lee, D. G. (2007). Damage to the cytoplasmic membrane and cell death caused by lycopene in *Candida albicans*. *Journal of Microbiology and Biotechnology*, *17*(11), 1797–1804.

Sutton, S., & Singer, D. (2011). Microbiological best laboratory practices, USP< 1117> value and recent changes to a Guidance of Quality Laboratory Practices. *Amer Pharm Rev*, *14*(4), 1–6.

Swami, D. S., Kumar, P., Malik, R. K., Saini, M., Kumar, D., & Jan, M. H. (2017). Cysteamine supplementation revealed detrimental effect on cryosurvival of buffalo sperm based on computer-assisted semen analysis and oxidative parameters. *Animal Reproduction Science*, *177*, 56–64. https://doi.org/10.1016/j.anireprosci.2016.12.006

Takehara, M., Nishimura, M., Kuwa, T., Inoue, Y., Kitamura, C., Kumagai, T., & Honda, M. (2014). Characterization and thermal isomerization of (all-E)-lycopene. *Journal of Agricultural and Food Chemistry*, *62*(1), 264–269. https://doi.org/10.1021/jf404497k

Tamburini, E., Costa, S., Rugiero, I., Pedrini, P., & Marchetti, M. G. (2017). Quantification of lycopene, β-carotene, and Total soluble solids in intact red-flesh watermelon (Citrullus lanatus) using on-line Near-Infrared Spectroscopy. *Sensors*, *17*(4), Article 746. https://doi.org/10.3390/s17040746

Tamjidi, F., Shahedi, M., Varshosaz, J., & Nasirpour, A. (2013). Nanostructured lipid carriers (NLC): A potential delivery system for bioactive food molecules. *Innovative Food Science & Emerging Technologies*, *19*, 29–43. https://doi.org/10.1016/j.ifset.2013.03.002

Tanaka, Y., Sasaki, N., & Ohmiya, A. (2008). Biosynthesis of plant pigments: anthocyanins, betalains and carotenoids. *The Plant Journal*, *54*(4), 733–749. https://doi.org/10.1111/j.1365-313X.2008.03447.x

Tao, N., Gao, Y., Liu, Y., Ge, F., & others. (2010). Carotenoids from the peel of Shatian pummelo (Citrus grandis Osbeck) and its antimicrobial activity. *American-Eurasian Journal of Agricultural and Environmental Science*, *7*(1), 110–115.

Tonet, M. D., & Leonel, A. A. (2019). Nanociência e Nanotecnologia: uma revisão bibliográfica acerca das contribuições e desafios para o ensino de Física. *Caderno Brasileiro de Ensino de Física*, *36*(2), 431–456. http://dx.doi.org/10.5007/2175-7941.2019v36n2p431

Upstone, S. L. (2013). Ultraviolet/visible light absorption spectrophotometry in clinical chemistry. In Meyers, R. A. (Ed.), *Encyclopedia of Analytical Chemistry: Applications, Theory and Instrumentation*. John Wiley & Sons. https://doi.org/10.1002/9780470027318.a0547.pub2

Wang, L., Du, Z., Li, R., & Wu, D. (2005). Supramolecular aggregates of lycopene. *Dyes and Pigments*, *65*(1), 15–19. https://doi.org/10.1016/j.dyepig.2004.05.012

Wegmann, J., Krucker, M., Bachmann, S., Fischer, G., Zeeb, D., Lienau, A., Glaser, T., Runge, F., Lüddecke, E., & Albert, K. (2002). Characterization of lycopene nanoparticles combining solid-state and suspended-state NMR spectroscopy. *Journal of Agricultural and Food Chemistry*, *50*(26), 7510–7514. https://doi.org/10.1021/jf020715g

Willcox, J. K., Catignani, G. L., & Lazarus, S. (2003). *Tomatoes and cardiovascular health*. *Critical Reviews in Food Science and Nutrition, 43*(1), 1–18. https://doi.org/10.1080/10408690390826437

Wissing, S. A., Kayser, O., & Müller, R. H. (2004). Solid lipid nanoparticles for parenteral drug delivery. *Advanced Drug Delivery Reviews*, *56*(9), 1257–1272. https://doi.org/10.1016/j.addr.2003.12.002

Xu, F., Yuan, Q. P., & Dong, H. R. (2006). Determination of lycopene and β-carotene by high-performance liquid chromatography using sudan I as internal standard. *Journal of Chromatography B*, *838*(1), 44–49. https://doi.org/10.1016/j.jchromb.2006.04.004

Zhang, L.-X., Cooney, R. V, & Bertram, J. S. (1991). Carotenoids enhance gap junctional communication and inhibit lipid peroxidation in C3H/10T1/2 cells: relationship to their cancer chemopreventive action. *Carcinogenesis*, *12*(11), 2109–2114. https://doi.org/10.1093/carcin/12.11.2109

Zhao, Y., Xin, Z., Li, N., Chang, S., Chen, Y., Geng, L., Chang, H., Shi, H., & Chang, Y.-Z. (2018). Nano-liposomes of lycopene reduces ischemic brain damage in rodents by regulating iron metabolism. *Free Radical Biology and Medicine*, *124*, 1–11. https://doi.org/10.1016/j.freeradbiomed.2018.05.082

CHAPTER 6

Highlights in mesoporous silica nanoparticles as a multifunctional controlled drug delivery nanoplatform for infectious diseases treatment

Gabriela Corrêa Carvalho[#], Rafael Miguel Sábio[#*], Tais de Cássia Ribeiro, Andreia Sofia Monteiro, Daniela Vassalo Pereira, Sidney José Lima Ribeiro, Marlus Chorilli

[#]These authors contributed equally to this work

Pharmaceutical Research, v. 37, n. 10,191 pp. 1-30, 2020.

Reproduced with permission from Springer Nature

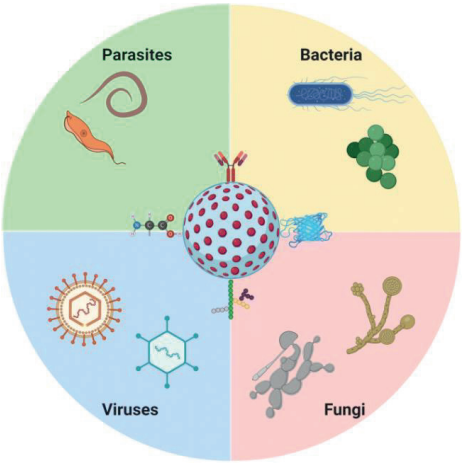

Abstract

Infectious diseases are a major global concern being responsible for high morbidity and mortality mainly due to the development and enhancement of multidrug-resistant microorganisms exposing the fragility of medicines and vaccines commonly used to these treatments. Taking into account the scarcity of effective formulation to treat infectious diseases, nanotechnology offers a vast possibility of ground-breaking platforms to design new treatment through smart nanostructures for drug delivery purposes. Among the available nanosystems, mesoporous silica nanoparticles (MSNs) stand out due their multifunctionality, biocompatibility and tunable properties make them emerging and actual nanocarriers for specific and controlled drug release. Considering the high demand for diseases prevention and treatment, this review exploits the MSNs fabrication and their behavior in biological media besides highlighting the most of strategies to explore the wide MSNs functionality as engineered, smart and effective controlled drug release nanovehicles for infectious diseases treatment.

1. Introduction

Infectious diseases are increasingly emerging as a cause of morbidity and mortality worldwide, mainly due to the fact that some diseases are caused by multi-resistant microorganisms to existing drugs (Ogunsona et al., 2020; Zaidi et al., 2017). Antimicrobial resistance occurs when microorganisms (such as bacteria, fungi, viruses and parasites) change when they are exposed to antimicrobial drugs (such as antibiotics, antifungals, antivirals, antimalarials, and anthelmintics). As a result, the medicines become ineffective and infections persist in the body, increasing the risk of spread to others. Without effective antimicrobials for prevention and treatment of infections, medical procedures such as organ transplantation, cancer chemotherapy, diabetes management and major surgery (for example, caesarean sections or hip replacements) become very high risk. Beyond that, antimicrobial resistance increases the cost of health care with lengthier stays in hospitals and more intensive care required, as stated by World Health Organization (WHO) (Ogunsona et al., 2020; WHO, 2020c).

Considering the health concern, nanotechnology offers potential opportunities to design effective medicines and vaccines for diseases treatment (Chen et al., 2020; Lee et al., 2019; Weiss et al., 2020). Nanotechnology is a multidisciplinary science field that studies the fabrication and application of structures with one of its dimensions less than 100 nm (Emerich & Thanos, 2003; Vallet-Regí et al., 2019). The use of nanostructures in health area are desirable due to the fact that their size are 100 to 10000 times smaller than eukaryotic cells and similar size to the most biological molecules and structures including DNA, proteins, cell membranes and pathogenic microorganisms (Singh et al., 2008; Smerkova et al., 2020). In addition, the nanometric size can potentialize nanomaterials action and efficacy comprising an emerging tools to develop therapeutic agents, diagnosis systems, medical devices and drug delivery platforms including medicines and vaccines for infectious diseases treatment (Drouet, 2020; Li et al., 2019; Pallotta et al., 2019; Sábio et al., 2019; Vallet-Regí et al., 2019).

The use of nanomaterials as carriers for controlled drug release has increasingly been explored due to their small size, high surface area and ability to pass through epithelial and endothelial barriers increasing drugs permeability without change its pharmacological properties (Bonifácio et al., 2013; Calixto et al., 2016; Nazemiyeh et al., 2016; S. Sahoo et al., 2008). These nanosystems can reach the action site with considerable drugs concentration increasing their specific retention time reducing side effects (Arriagada et al., 2019; Bonifácio et al., 2013; Calixto et al., 2016; Nazemiyeh et al., 2016; S. Sahoo et al., 2008; Vallet-Regí et al., 2019). Nanoparticles can be produced from various materials such as amphiphilic structures, lipids, biodegradable polymers and inorganic compounds (Calixto et al., 2016; Ogunsona et al., 2020; Sahoo & Labhasetwar, 2003; Zaidi et al., 2017). Specifically, inorganic platforms as mesoporous silica nanoparticles (MSNs) comprise a potential nanosystem for

healthcare applications due to interesting characteristics such as easy functionalization, large surface area, high chemical and physical stabilities and hydroxyl groups available in their surface/pores. In addition, MSNs tunable morphology, size, surface charges and pores make them carriers with good biocompatibility and biodegradability, low toxicity, good biodistribution and elimination (Chen et al., 2019; Madhusoodana et al., 2006; Manzano & Vallet-Regí, 2020; Mohammadpour et al., 2020; Sábio et al., 2019; Sábio et al., 2020a; Sábio, et al., 2020b; Yokoi et al., 2012). Drugs loaded into MSNs pores leading to pharmacological properties maintenance besides protection against degradation and immediate drug release (Baeza et al., 2017; Chen et al., 2019; Lu et al., 2010; Manzano & Vallet-Regí, 2020).

Taking into account that infectious diseases are a serious global public health concern and MSNs present several interesting properties that make them widely desirable to design controlled drug delivery systems, this review reports a brief overview of MSNs properties and their influence in biological behavior as well as highlights the advances in MSNs applications as multifunctional controlled drug release nanoplatforms for infectious diseases treatment.

2. Infectious diseases

Infectious diseases are those caused by pathogenic microorganisms such as bacteria, fungi, viruses and parasites, which invade host's cells in order to reproduce and thereby damage tissues causing disease. These diseases are transmitted directly or indirectly from person to person (Guido et al., 2010; National Institutes of Health, 2007; WHO, 2020b). Currently, infectious diseases are emerging at a global level and a rate never seen before, representing a challenge for the 21st century regarding to the discovery and development of new formulations (Guido et al., 2010; Rohr et al., 2019).

The WHO brings cholera, Ebola virus, influenza, meningitis, Coronavirus disease 2019 (COVID-19), poliomyelitis, yellow fever as public health emergencies. Five of them are caused by virus and two by bacteria (considering that the main meningitis causing agent is bacteria) (WHO, 2020a). This may explain the data obtained in **Figure 1**, where the association of the keywords “infectious diseases and virus and new formulations” recovered the largest number of manuscripts published in the period from 2000 to 2020, corresponding to 41%, followed by the association of the keywords “infectious diseases and bacteria and new formulations” which are assigned to 28%.

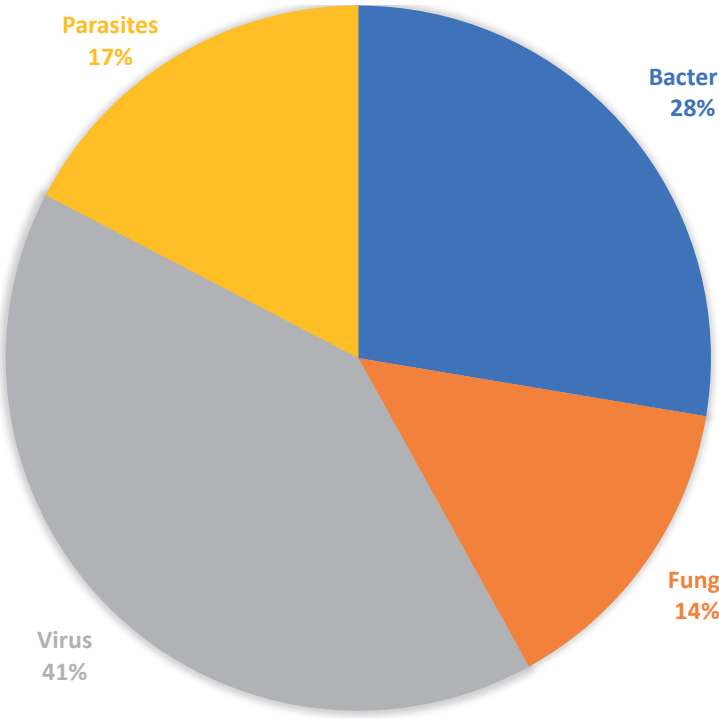

Figure 1: Percentage of new formulations research in the infectious diseases field. The numbers of manuscripts were retrieved from SCOPUS® database by searching "infectious diseases/virus/new formulations", "infectious diseases/bacteria/new formulations", "infectious diseases/parasites/new formulations" and "infectious diseases/fungi/new formulations" (Data accessed June 01, 2020).

Because virus cannot reproduce or shows metabolism outside a host cell, it is not considered an organism, but rather particles, which are coated with a protein or lipid capsid. As for the genetic material, they are divided into double or single stranded deoxyribonucleic acid (DNA) viruses, or ribonucleic acid (RNA), single or double stranded viruses (National Institutes of Health, 2007). Viruses listed as a public health emergency by the WHO, Ebola virus, influenza, COVID-19, poliomyelitis and yellow fever, are all single stranded RNA viruses (Arroyo et al., 2001; Barrett & Higgs, 2007; Fujii et al., 2003; Kitamura et al., 1981; G. Li et al., 2020; Poddar, 2002; Sissoko et al., 2017).

Coronavirus, which causes COVID-19, is the current major threat due to its ability to spread quickly (Li et al., 2020; Tatara, 2020). Until May 31, 2020 5,956,883 confirmed cases (being that the largest number of cases are concentrated in the Americas) and 366,409 deaths worldwide, which shows the seriousness of this pandemic started in December 2019. Generally, this virus causes infection in

the upper respiratory tract, or, in some patients in the lower respiratory tract, presenting fever, cough and headache as main symptoms (Li et al., 2020; Tatara, 2020; Weiss et al., 2020; WHO, 2020a; Zhu et al., 2020).

In the period of 2014-2016, worldwide efforts were focused on combating the outbreak caused by Ebola virus in West Africa, a severe hemorrhagic fever, fatal in many cases, the average mortality rate in this period was 50%. In addition to the great local concern, the world community feared for dissemination throughout the world and for its use as a biological weapon. Although the outbreak period has passed, there is currently a great concern related to the persistence of this virus in the reproductive tract of male people who survived this disease (Feldmann & Geisbert, 2011; Sissoko et al., 2017; WHO, 2020a).

The yellow fever virus, transmitted by mosquitoes of the genera *Haemagogus* and *Aedes*, was the cause of severe epidemics that occurred in the 17th, 18th and 19th centuries. In the 1930s, fundamental vaccines were developed to contain this disease, but it is not the same that is used nowadays due to the appearance of adverse reactions. Even with the vaccine, this disease is still epidemic in many regions such as Africa and South America. It is a severe acute disease that presents as symptoms fever, epigastric pain, nausea, vomiting, renal failure, hepatitis accompanied by jaundice, hemorrhage, shock and death in 20-60% of cases (Barrett & Higgs, 2007; Monath & Vasconcelos, 2015; Tuboi et al., 2007; WHO, 2020a).

In the years 1918 and 1919, the influenza virus was the cause of a pandemic that caused about 20 to 50 million fatal victims worldwide (Tumpey, 2005). This pandemic causing strain was the influenza virus type A, which has the subtypes H1N1, H3N2 and H5N1, although influenza virus type B and type C are also infectious in humans (Heikkinen et al., 2008; Poddar, 2002). Nowadays, the major concern consists on prevents and controls this seasonal disease in order to avoid new influenza pandemics from happening (WHO, 2020a).

Poliomyelitis is a disease that has been plaguing humanity for centuries, its first clinical description dates from 1789, being that only in 1955 the first vaccine was developed (Henry, 2019). Children are the most affected by this disease, which can affect the nervous system and cause paralysis. Nowadays, it is endemic in areas of Afghanistan and Pakistan, and in the period of 10 years, 200,000 new cases were observed, probably due to failures in strategic actions implementation, leading to a high transmission of this virus (WHO, 2020a).

Bacteria, another infectious disease causative agent, are prokaryotic single-cell microorganisms. They are classified according to their morphology and the Gram stain reaction (National Institutes of Health, 2007). An example of a bacterial infectious disease would be cholera, caused by *Vibrio cholerae*, a gram-negative bacterium. It is an old disease, which has been the cause

of seven pandemics throughout human history, the first being dated in 1817 (Deen et al., 2020; Lahiri et al., 2012).

Cholera is considered serious because it is the cause of acute watery diarrhea and severe dehydration. Currently, cholera still is considered a serious public health problem by the WHO, being contracted by the ingestion of contaminated water or food and considered a social inequality indicator. It is responsible for 21,000 to 143,000 deaths per year, in areas such as Asia, Africa and the Americas, where this disease only evolves (Deen et al., 2020; WHO, 2020a).

Meningitis is another bacterial disease considered by WHO as an emergency, although also caused by fungi and viruses, the most frequent cause is bacterial. *Neisseria meningitidis* and *Streptococcus pneumoniae* are the largely responsible for the threat to public health related to this disease. Meningitis has high morbidity due to the inflammatory response resulting from their passage through the blood-brain barrier causing inflammation in the meninges and brain edema, leading to neurological sequelae in this disease survivors (Epstein et al., 1992; Koelman et al., 2019; WHO, 2020a).

Although fungal and parasitic diseases are not placed as a public health emergency by WHO, it is worth noting that fungi, single or multi-celled eukaryotic microorganisms, cause infections ranging from superficial and mucous membranes to systemic infections, which can lead the patient to death. Fungal diseases epidemiology is difficult to measure, as they are often underdiagnosed (Emerich & Thanos, 2003; Silva et al., 2016; National Institutes of Health, 2007).

As for parasitic diseases, they are caused by protozoa (single-celled eukaryotic cells) and helminths (invertebrate animals) (Lyra et al., 2007; National Institutes of Health, 2007). Parasitic diseases are a public health concern that affects humans throughout history, leading to the millions death of people annually (Hobbs et al., 2019; Momčilović et al., 2019).

Faced with the human being fragility in relation to the severity of some infectious diseases that prove to be a worldwide public health problem, the current scenario in which the planet finds itself sparing no effort in order to face a pandemic or even in the fight against resistant microorganisms, considering the new formulations development essential. In light of this, the drugs association with promising nanocarriers such as MSNs is fundamental to achieve new smart nanotherapeutics systems for all aforementioned diseases (Edrissian et al., 2016; Figueiras et al., 2014; Sábio et al., 2019; Sahoo & Labhasetwar, 2003; Soares et al., 2020).

3. Mesoporous silica nanoparticles

3.1. Synthesis and types of Mesoporous Silica Nanoparticles

Need for materials with high thermal, chemical and mechanical properties have led to the development of MSNs. As per International Union of Pure and Applied Chemistry (IUPAC), mesoporous materials are define as the one having a pore size in the range of 2-50 nm and an ordered arrangement of pores giving an ordered structure to it (Narayan et al., 2018; Trewyn et al., 2007). Mobil Research and Development Corporation was the first to synthesize mesoporous solids from aluminosilicate gels using liquid crystal template mechanism in the year 1992. They designated it as (Mobil Crystalline Materials or Mobil Composition of Matter) MCM-41. The pore size of the mesoporous materials could be varied and tuned through the choice of surfactants used. MCM-41 is hexagonal with a pore diameter from 2.5 to 6 nm wherein cationic surfactants were used as templates. Various other materials of mesoporous nature have also been synthesized by varying the starting precursors and reaction conditions. These mesoporous materials may vary in their structural arrangement or the pore size. MCM-48 has a cubic arrangement whereas MCM-50 has a lamella-like arrangement (Narayan et al., 2018; Øye et al., 2001). Non-ionic triblock copolymers like alkyl poly (ethylene oxide) (PEO) oligomeric surfactants and poly(alkylene oxide) block copolymers have also been used by University of California, Santa Barbara for synthesized the named Santa Barbara Amorphous materials (SBA). The ratio of ethylene oxide to propylene oxide was varied to achieve the desired symmetry of mesoporous materials (SBA-11 (cubic), SBA-12 (3-d hexagonal), SBA-15 (hexagonal) and SBA-16 (cubic cage-structured) (Narayan et al., 2018). This is different from MCM in that they possess larger pores of 4.6-30 nm and thicker silica walls. FSM-16, that is, folded sheets of mesoporous materials are another type of mesoporous materials, which are synthesized using quaternary ammonium surfactant as a template and layered polysilicate kanemite (Tozuka et al., 2005). Various other MSNs have been synthesized which vary in their pore symmetry and shape, TUD-1 (Technical Delft University), HMM-33 (Hiroshima Mesoporous Material-33), COK-12 (Centrum Voor Oppervlaktechemie en Katalyse/Centre for Research Chemistry and Catalysis) (Nandiyanto et al., 2009). The schematic representation of several MSNs structures is shown in **Figure 2** as well as structural characteristics and applications of some mesoporous materials are listed in **Table 1**.

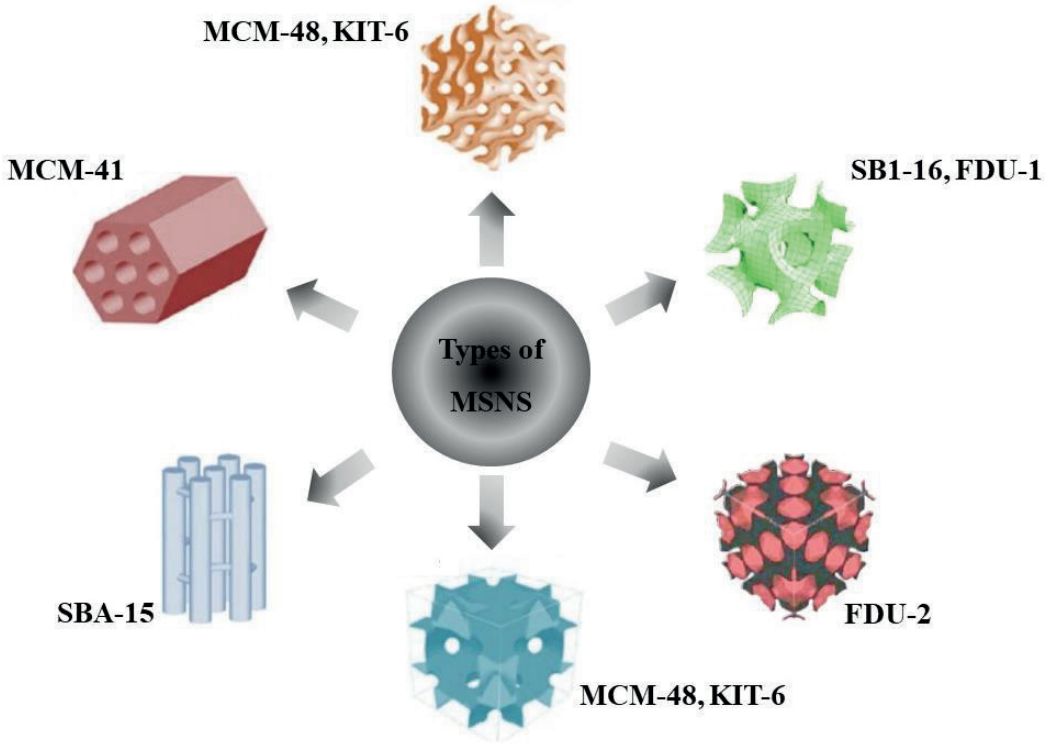

Figure 2: Schematic representation of distinct types of MSNs.

Table 1: Some of the types of MSNs and their structural characteristics and applications.

MSN Family	MSN type	Pore size (nm)	Pore symmetry	Applications	References
M41S	MCM-41	1.5–8	2D hexagonal P6mm	Drug delivery	(Kumar et al., 2001; Narayan et al., 2018)
	MCM-48	2–5	3D cubic Ia3d		
	MCM-50	2–5	Lamellar p2	Adsorbents; Catalysis	(Ukmar & Planinšek, 2010; Wang & Li, 2006)
SBA	SBA-11	2.1–3.6	3D cubic Pm3m		(Ukmar & Planinšek, 2010)
	SBA-12	3.1	3D hexagonal P63/mmc		(Narayan et al., 2018; Ukmar & Planinšek, 2010)
	SBA-15	6–0	2D hexagonal p6mm	Drug delivery	(Kleitz et al., 2003; Narayan et al., 2018)
	SBA-16	5–15	Cubic Im3m		(Jammaer et al., 2009; Narayan et al., 2018)

MSNs are characterized by high surface area and large pore volume, uniform and tunable pore size, facile surface functionalization and a stable and rigid framework (Gao et al., 2006).

MSNs are commonly prepared by sol-gel "chimie douce" process in aqueous solution. This process involves the synthesis of an inorganic polymeric network at low temperature, being the gel formed from a colloidal suspension or by hydrolysis and subsequent condensation of an silica precursor ($Si(OEt)_4$), generally the most used is a tetraethyl orthosilicate, TEOS, in solution. In hydrolysis reactions, the alkoxide group (OR) of the silica precursor is replaced by the silanol group (Si-OH), forming an alcohol in parallel, due to the nucleophilic attack of the oxygen atom of the water hydroxyl group (Grün et al., 1997; Stöber et al., 1968). In condensation reactions, dimers, linear trimers, cyclic and polymeric species with siloxane bonds (Si-O-Si) are formed (Stöber et al., 1968). In order to obtain mesoporous nanomaterials, surfactants have been used, such as cetyltrimethylammonium bromide (also known as CTAB) (Flodström et al., 2004). Usually, the surfactant will self-aggregate into micelles at a concentration higher than the critical micelle concentration (CMC). Then, the silica precursors can condense at the micelles surface forming MSNs. Finally, the template surfactant can be removed either by calcination or by solvent extraction to generate pores (Flodström et al., 2004; Hollamby et al., 2012), as depicted in **Figure 3**.

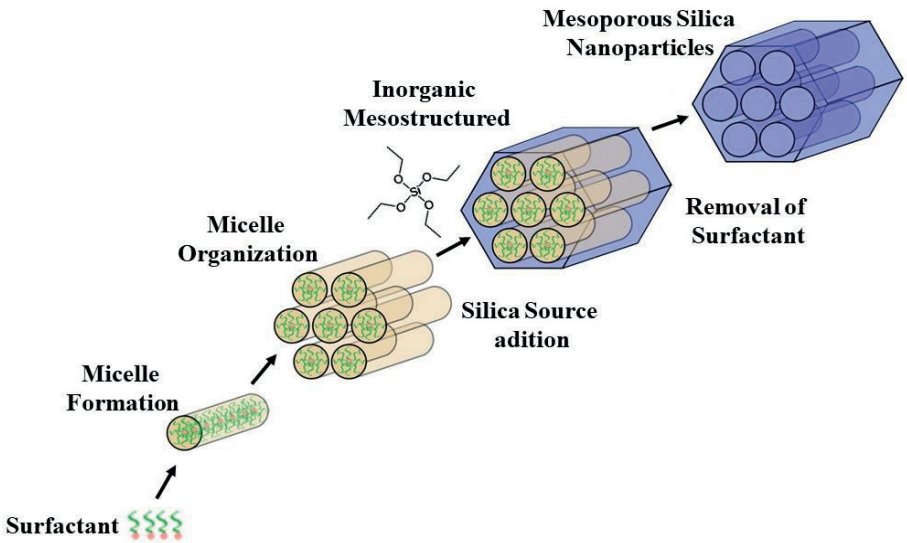

Figure 3: Schematic representation of MSNs fabrication.

Considering the abundant availability of various surfactants types and the deep understanding of sol–gel chemistry, MSNs with different structures have been developed. The size, morphology, pore

size, and pore structure of MSNs can be rationally designed and the synthesis process can be freely controlled.

The resulting silica-based mesoporous matrices may offer the following unique structural: 1) *ordered porous structure*. MSNs have along-range ordered porous structure without interconnection between individual porous channels, which allows fine control of the drug loading and release kinetics; 2) *large pore volume and surface area*. The pore volume and surface area of MSNs are usually above $1cm^3\ g^{-1}$ and 700 $m^2\ g^{-1}$, respectively, showing high potential for molecules loading and dissolution enhancement; 3) *tunable particle size*. The MSNs particle size can be controlled from 50 to 300 nm, which is suitable for facile endocytosis by living cells; 4) *two functional surfaces*, namely cylindrical pore surface and exterior particle surface. These silanol-contained surfaces can be selectively functionalized to achieve better control over drug loading and release. Moreover, the external surface can be conjugated with targeting ligands for efficient cell-specific drug delivery (Edler, 2005; Flodström et al., 2004; Hollamby et al., 2012; Narayan et al., 2018; Yang et al., 2012).

3.2. Properties effect of MSNs in drug delivery systems

Stable suspension formation in solution, tunable pore size and structure, controlled particle size and shape, high pore volume and surface area, make the MSNs ideal for applications as nanocarriers (Sábio et al., 2019; Yang et al., 2012).

The pores size control influences on loading and release rates of molecules. Increasing pores size, more molecules can be loaded inside the pores and consequently, an increase of release rates can be observed (Qu et al., 2006; Sábio et al., 2019; Yang et al., 2012). Pores volume is an important factor on drug loading properties. High pores volume can avoid strong drug-drug interactions consequently facilitating drug-pores wall intermolecular interactions leading to large filling of the mesopores channels (Sábio et al., 2019; Yang et al., 2012). The type of pores arrangement can also influence on cargo loading and release rates. Three distinct pore arrangement, TUD-1, MCM-41 and SBA-15 materials, were evaluated in processes on ibuprofen loading and release processes by Heikkilc et al. (2007a; 2007b). TUD-1 (disordered mesoporous) materials that present 3D pores arrangement showed faster drug release than 2D hexagonal mesopores materials (SBA-15 and MCM-41). Andersson et al. (2004) demonstrated that similar hexagonal mesostructured materials with interconnected (SBA-1) pores displayed faster release rate than unconnected (SBA-3) pores systems. For these systems, similar drug loading amounts were detected.

Large surface area is also a crucial characteristic regarding to cargo diffusion process from MSNs. Vallet-Regí group (Vallet-Regí, 2006; 2007a; 2007b) reported the 2-D hexagonal mesoporous

silica as carriers showing higher drugs adsorption values for MCM-41 (Specific surface area (S_{BET}) = 1157 $m^2 g^{-1}$) than for SBA-15 (S_{BET} = 719 $m^2 g^{-1}$) systems.

Particles size and shape can also influence their blood circulation, cellular uptake and tumor penetration, being determinant parameters to achieve therapeutic effects. Regarding particles size, a diameter range from 50 to 300 nm can favor an optimal cellular uptake, long circulation time, high drug loading and high accumulation in tumors (Sábio et al., 2019). Huang et al. (2010, 2011) described the importance of particle shape design towards therapeutic application showing faster and higher internalization of rod-shaped MSNs on tumor cells than spherical MSNs.

4. Biological behavior of MSN: biocompatibility, biodistribution, biodegradability and clearance

The biocompatibility, biodistribution, biodegradability and clearance of MSNs are subject to an ongoing discussion in research circles. In this section, conclusions are presented and few representative studies are highlighted.

4.1. Biocompatibility and biodistribution

Determining the safety and biocompatibility of MSNs is crucial owing to its variable characteristics. The data generated from literature suggest that careful control of particle size and shape is the determinant factor in the biodistribution and toxicity of MSNs. In addition, the safety and toxicity of MSNs also depend on the administered MSNs dosage. Surface MSNs properties also have a great impact on their biodistribution and biocompatibility (Croissant et al., 2018; Giret et al., 2015; Tang et al., 2012; Tozuka et al., 2005; Yang et al., 2019). The major toxicity pathway associated with silica is due to its surface chemistry (silanol groups) which can interact with the membrane components leading to the cells lysis and cellular components leaking (Nash et al., 1966; Slowing et al., 2009). Mesoporous silica exhibited lower hemolytic effect compared to non-porous silica (Mohammadpour et al., 2020). This could be attributed to the lower density of silanol groups on the surface of mesoporous structures (Lin & Haynes, 2010). Authors (Liu et al., 2011; Narayan et al., 2018) made an attempt to study the single and repeated dose MSNs toxicity following intravenous administration in mice. Lethal dose 50 (LD50) of MSNs was found to be higher than 1000 mg kg^{-1}. In single dose toxicity studies, mice were injected with MSNs at a low dose and high dose. At the higher dose of 1280 mg kg^{-1}, mice did not survive. In contrast, the groups treated with low MSNs dose did not show any behavioral changes nor any hematology or pathological changes. To carry out the detailed repeated dose toxicity studies, intravenous administration of hollow MSNs (HMSNs) was given to mice continuously for 14 days and observed for a month. During the one-month observation period, no mortality was observed. Moreover, no remarkable changes in pathology or blood parameters were observed. In order to assess the MSNs

fate after different administration routes, Fu et al. (2013) tested MSNs with a particle size of 110 nm in Institute of Cancer Research (ICR) mice. Following administration via hypodermic, intramuscular and intravenous injection as well as oral administration, the *in vivo* distribution of fluorescent-tagged MSNs was tracked. It was observed that of all the exposure routes, the oral route was found to be well tolerated even when the dose was increased to 5000 mg kg^{-1} and intravenous route seemed to have the least threshold. MSNs administered via intravenous route were found to preferentially accumulate in the liver and spleen at the end of 24 h and 7 days whereas those administered by other routes did not show any fluorescence in these organs. It was observed that a portion of the MSNs administered via intramuscular and hypodermic routes could cross different biological barriers with a slow absorption rate. The major excretion routes of MSNs were found to be via urine and feces with the highest values after oral administration as compared to other routes. No histopathological changes were observed in liver, spleen, kidney and lung at the end of 24 h and 7 days by different exposure routes. The results suggested that MSNs were found to be safe and well tolerated when administered by oral and intravenous routes (Fu et al., 2013; Tang et al., 2012).

4.2. Biodegradability

The silica particles do degrade into silicic acid ($Si(OH)_4$, pKa 9.6) in biological media by dissolution. Silicic acid is soluble in water and consists on the dominant silicon species at low concentration (< 2 x 10^{-3} M) (Croissant et al., 2017). It is also excreted through the urine and its good bioavailability even contributes to maintaining bone health (Croissant et al., 2017, 2018).

The dissolution process of amorphous silica in aqueous media includes three steps: i) hydration, in which water is adsorbed into the siloxane framework, ii) hydrolysis, in which siloxane are hydrolyzed into silanols, and ii) ion exchange processes, which consist of nucleophilic attack of OH^- leading to the silicic acid leaching. At the molecular level, silica hydrolyzes in aqueous media to form the same products as those of silica nanoparticles which are nontoxic and diffuse through the blood stream or the lymphatic system to be eventually cleared in the urine. Similar to silica nanoparticles, the solubility of silicic acid degradation products is key for the effective hydrolytic degradation of silica nanomaterials (Croissant et al., 2017; Finnie et al., 2009).

Investigations have been carried out to assess the direct influence of the size, morphology and degradation medium parameters on the silica nanoparticles degradation. The physicochemical engineering of MSNs thus allows one to tune the dissolution silica rate in biorelevant media for specific biomedical applications (Croissant et al., 2017). Some physicochemical parameters such as morphology, particles and pores size, surface charge and encapsulation efficiency (EE%) of the engineered MSNs-based nanocarriers for infectious diseases treatment are depicted in **Table 2.**

Table 2: Physicochemical parameters as morphology, particles and pores size, surface charge and encapsulation efficiency (EE%) of the engineered MSNs-based nanocarriers for infectious diseases treatment.

Carrier/ morphology	Encapsulation efficiency (%)	Particle size (nm)	Pores size (nm)	Zeta potential (mV)	References
Spherical MSNs	26.8 and 22.5, respectively	40 and 100, respectively	8 to 9	-20 and -16.9, respectively	(Subramaniam et al., 2019)
Spherical MCM-41-like MSNs	---	150	---	-25	(Martínez-Carmona et al., 2019)
Spherical MSNs-MCM-41, modified (vinyl groups) MSNs-MCM-41 and spherical MSNs-MCM-48	20	Modified and non-modified MSNs-MCM-41: ~60 and MSNs-MCM-48: ~46	MCM-41 types: 2.5-3.1 and MCM-48 type: 2.5-9	---	(Deaconu et al., 2019)
Spherical MSNs	---	80	---	-26.7	(Yang et al., 2018)
Spherical MSNs	---	210	2.4	---	(Zhou et al., 2018)
Rod shaped HMSNs with large cone-shaped pores and small cone-shaped pores	35 and 5, respectively	Length and width of 400 and 200, respectively, for both nanosystems	40 and 3, respectively	---	(Xu et al., 2018)
Spherical MSNs-MCM-41	---	200-400	1.75 to 2.98	---	(Deaconu et al., 2018)
MSNs-SBA-16 and MSMs-SBA-16/hydroxyapatite (HA)	28 to 31, respectively	---	3.4 and 3.8, respectively	-56 and 2.9, respectively	(Andrade et al., 2018)
Spherical MSNs	5.9 to 26.8	100	2.8	-21.2	(Chen et al., 2018)
Spherical and spherical modified MSNs	7.8	~150	2.4	-36.4 for non-modified MSNs and +31.8 to +37.4 for modified MSNs	(González et al., 2018)
Spherical MSNs-supported Ag-Bi nanoparticles	---	200-240	3.4-4.8	---	(Cao et al., 2020)

Spherical MSNs with large cone-shaped pores	Ag: 2 and Deoxyribonuclease (DNase) I: 32	200	42-43	---	(Tasia et al., 2020)
Spherical modified magnetic MSNs	10.7	240	3	-5.32	(Xu et al., 2019)
Spherical MSNs-MCM-41	---	150-300	2	MSNs: -45 and MSNs-Ag: +48	(Ding et al., 2020)
Spherical MSNs-MCM-41 and spherical modified MSNs-MCM-41	---	122-220	1.9-2.4	MSNs: -30 and modified MSNs: +5 to +25	(Encinas et al., 2019)
Spherical MSNs-MCM-41 and spherical modified MSNs-MCM-41	36	182	---	-30	(Clemens et al., 2019)
Spherical MSNs and spherical modified MSNs	11to 40	~72	3.3-4	MSNs: −22.9 and modified MSNs: Aminated MSNs: +19 Carboxyl functionalized MSNs: -53	(Gounani et al., 2018)
SBA-15 and modified SBA-15	93-98	100-300	SBA-15: 7 And modified SBA-15: 6-6.2	---	(Abdelbar et al., 2020)
Spherical MSNs-MCM-48 and spherical modified MSNs-MCM-48	27-31.5	150-600	3.2	MSNs-MCM-48: -28 to -34 and modified MSNs-MCM-48: +30 to +63	(Michailidis et al., 2017)
carboxylic acid functionalized thermally hydrocarbonized porous silicon nanoparticles (UnTHCPSi NPs)	---	176-184	---	-25.5	(Vale et al., 2017)

Spherical MSNs-MCM-41 and spherical modified MSNs-MCM-41	---	90	---	---	(Lee et al., 2016)
Hollow oblate MSNs and modified hollow oblate MSNs	56-64	Average long-axis length of~200 and a short-axis width of ~100	3.3-3.7	---	(Hao et al., 2015)
Spherical MSNs-MCM-41 and spherical modified MSNs-MCM-41	---	~50 and ~100	~2	MSNs-MCM-41: -26 to -29 and modified MSNs-MCM-41: +38 to +42.5	(Hwang et al., 2015)
Spherical MSNs and spherical modified MSNs	---	100-130	2.5	MSNs: -7 to -10.5 and modified MSNs: +30 to +39	(Clemens et al., 2012)
Spherical MSNs-MCM-41 and spherical modified MSNs-MCM-41	Up to ~70	100	~2	Phosphonate silane-modified MCM-41: -46.3 and amine-silane modified MCM-41: 38.8	(Li et al., 2015)
Spherical modified MSNs	---	117	3.8	+36	(Ruehle et al., 2017)
Spherical MSNs	Up to ~35	38.8	~7	-33	(Oliveira et al., 2016)
Spherical MSNs-MCM-41 and spherical modified MSNs-MCM-41	---	110	3.3	MSNs-MCM-41: -21 and modified MSNs-MCM-41: +45.5	(Nhavene et al., 2018)
Spherical MSNs	83	100 to 105	---	+32 to +30	(Tawfeek et al., 2019)
Mesoporous silica whiskers-SBA-15 and modified mesoporous silica whiskers-SBA-15	62.6 to 71.4	50	6	---	(Lehi et al., 2019)

Spherical MSNs-MCM-41 and spherical modified MSNs-MCM-41	Up to 42 and 63%	39-91	2.5	MSNs-MCM-41: -12 and modified MSNs-MCM-41: +32.5 to +33.6	(Montazeri et al., 2020)
Spherical MSNs and spherical modified MSNs	58.5	500	2	---	(Paramanantham et al., 2018)
Spherical MSNs-MCM-41	---	100	3-3.5	---	(Mas et al., 2014)
Spherical MSNs	10.7	20-40	2.5 to 3.1	---	(Mitra et al., 2015)
Spherical MSNs	---	400	~7.6	---	(Qasim et al., 2015)
Spherical MSNs and spherical modified MSNs	2	75-88	2.6-3.5	MSNs: -25 and modified MSNs: -0.26	(LaBauve et al., 2018)
Spherical MSNs and spherical modified MSNs	---	150-200	2	MSNs: -39.6 and modified MSNs: -29.5	(Lee et al., 2016)
Spherical MSNs and spherical modified MSNs	30-34	100-150	2	MSNs: -28.8 to -44.1 and modified MSNs: -32 to -40	(Lee et al., 2018)
Spherical MSNs and spherical modified MSNs	---	354-571	---	-11.2 to -20.5 (in PBS)	(Silva et al., 2016)
Spherical HMSNs	15	200	---	---	(Guo et al., 2012)

4.2.1. Effect of size

Chen et al. (2015) demonstrated that the degradation of MSNs is independent of their diameter with 390, 310, 200, and 150 nm nanoparticles in simulated body fluid (SBF) at 37 °C. During the first two days, the degradation rate was nearly 45% per day, which then slowed down to about 1% per day, and the degradation was completed in a week (Chen et al., 2015; Croissant et al., 2018; Huang et al., 2011). He et al. (2010) investigated the role of the surface area on the degradation of mesoporous silica, comparing three samples of surface areas of 958, 829, and 282 $m^2 g^{-1}$ at fixed concentration of 0.1 mg mL^{-1} in SBF, which were sealed in polyethylene bottles at 37 °C and shaken at 150 rpm with a mechanical shaker. This study indicated, on the one hand, that there was a burst degradation in the first 2 to 4 h, leading to 30, 70, and 90% of silica hydrolytic degradation as the surface increased, and, on the other hand, a complete degradation was obtained in 15 days.

4.2.2. Effect of morphology and degradation medium

A remarkable study was reported by Li et al. (2015) regarding the degradation of MSNs with spherical and rod-shaped morphologies with aspect ratios (ARs) of 1.75 and 5. Authors investigated these nanoparticles by TEM and sample weight measurements after degradation for 7 days by soaking in three different degradation media: simulated gastric fluid (pH 1.2), simulated intestinal fluid (SIF, pH 6.5), and SBF (pH 7). After a week in acidic gastric fluid, none of the three MSNs displayed significant alteration, and their degradation was only about 10 wt% for all nanoparticles. On the contrary, the degradation was much more pronounced and AR dependent in both simulated intestinal and body fluids. In general, the SIF generated more degradation than the SBF. The same group also showed that spherical MSNs were more rapidly degraded than rod-like MSNs with ARs of 2 and 4, and the presence of fetal bovine serum (FBS) in the Dulbecco's modified Eagle medium (DMEM) accelerated the degradation process (Croissant et al., 2018; Hao et al., 2012).

4.3. Clearance

When ingested by human beings through food sources, silicon species circulate through the blood plasma and are absorbed in the form of silicic acid being 41% excreted in the urine (Ehrlich et al., 2010). In the case of silica-based nanoparticles, the particle dissolution into silicic acid and its subsequent excretion was demonstrated *in vivo* on mice models as well as in human clinical trials (Croissant et al., 2018; Ehrlich et al., 2010). It is challenging to confidently draw trends between separated studies describing the clearance of silica nanoparticles because of the plethora of varying parameters, not least of which are the nanoparticle characteristics. Nevertheless, on animal models,

several trends have been observed between MSNs characteristics and their clearance: i) the effect of size, ii) the effect of surface functions, iii) the effect of surface charge, and iv) the effect of morphology.

4.3.1. Effect of size

He et al. (2011) reported an in-depth study of bare MSNs of various diameters (80, 120, 200, and 360 nm) and observed a significant nanoparticles excretion from 15 to 45% after the first 30 min with consistently higher excretion percentages for larger nanoparticles. Burns et al. (2009) have shown that nonporous silica quantum dots (3-6 nm) can be effectively (≈ 70%) cleared out of an animal body by renal excretion in 2 days, while Kumar et al. (2010) showed that larger silica nanoparticles (20-25 nm) preferred hepatobiliary excretion, with a complete clearance over a period of 15 days. Cho et al. (2009) studied dye-labeled nonporous silica nanoparticles of 50, 100 and 200 nm and demonstrated their clearance in the urine and bile. The 50 nm nanoparticles cleared faster than 100 and 200 nm ones, and 200 nm nanoparticles were less excreted.

4.3.2. Effect of surface functions

Some authors (Croissant et al., 2017; He et al., 2011; Sarparanta et al., 2012) showed that polyethylene glycol (PEG)-modified 45 nm nonporous silica nanoparticles exhibit a much longer blood circulation time ($t½$ = 180 ± 40 min) than unmodified silica nanoparticles ($t½$ = 80 ± 30 min) and carboxylated silica nanoparticles ($t½$ = 35 ± 10 min), being partly excreted via renal clearance. A stealth behavior is acquired by PEGylation, which reduces the RES uptake and increases the circulation half-life. As a result, PEGylated MSNs of various sizes (80, 120, 200, and 360 nm) were excreted slower than unfunctionalized ones due to the much slower particle capture by the liver and spleen.

4.3.3. Effect of charge

The particle charge-clearance dependence studies indicated that MSNs with a positive charge (+34 mV) at neutral pH are rapidly excreted from the liver into the gastrointestinal tract and then eliminated through the feces, while negatively charged (−18 mV) MSNs remained trapped in the liver (He et al., 2011; Souris et al., 2010).

4.3.4. Effect of morphology

The morphology influence on the clearance displayed that mesoporous silica nanorods of aspect ratio ≈1.5 (185 ± 22 nm long) are more rapidly cleared than longer nanorods of aspect ratio around 5 (720 ± 65 nm long). Comparing spherical-shaped and rod-shaped MSNs, nanospheres were mostly excreted during the first few hours, while nanorods had slower clearance rates (Croissant et al.,

2018; Huang et al., 2011). Several research groups consistently found nearly intact MSNs in the mice urine. Rod-shaped MSNs of various aspect ratios were also found in the urine and feces of mice (Croissant et al., 2017).

5. MSNs for infectious diseases treatment

The direct drugs application in preclinical trials can generate undesirable changes in their physicochemical, pharmacokinetic and biological properties, minimizing their action in infectious diseases treatment associated with the risk of resistance by pathogens. In this context, the development of smart and specific MSNs-based nanocarriers comprise a promising and effective approach for efficient drug delivery and consequently infectious diseases treatment (Rodrigues et al., 2019; Walvekar et al., 2019). **Table 3** depicted several examples of MSNs for infectious diseases treatment including bacterial, parasitic, fungal and viral infections as well as drugs type, MSNs-based carriers, microorganisms and drugs absorption and release mechanisms.

Table 3: MSNs as drug delivery platforms for infectious diseases treatment including bacterial, parasitic, fungal and viral infections besides drugs type, MSNs-based carriers, microorganisms and drugs absorption and release mechanisms.

Drug	Carrier	Assay	Microorganism	Adsorption mechanism	Release mechanism	References
Rifampicin (RIF)	MSNs with 40 and 100 nm	*In vitro*	*Staphylococcus aureus*	Passive diffusion method	Diffusion	(Subramaniam et al., 2019)
Levofloxacin (LEVO)	MSNs decorated with lectin concanavalin A (ConA) (MSN_{ConA})	*In vitro*	*Escherichia coli*	Impregnation method	Diffusion	(Martínez-Carmona et al., 2019)
Norfloxacin (NFX)	MSNs-MCM-41, modified (vinyl groups) MSNs-MCM-41 and MSNs-MCM-48	*In vitro*	*E. coli*	Impregnation method	Dissociation/diffusion	(Deaconu et al., 2019)
Gentamicin (GEN)	MSNs modified with a lipid bilayer surface shell and a bacterial-targeting peptide Ubiquicidin (UBI_{29-41}) (MSNs-LU)	*In vitro* and i*n vivo* (*S. aureus*-infected mice)	*S. aureus*	Impregnation method	Bacteria-responsive controlled release	(Yang et al., 2018)
Vancomycin (VAN)	MSNs dispersed onto gelatin matrix	*In vitro* and i*n vivo* (induced bone infection)	*S. aureus*	Impregnation method	Diffusion/sustained release	(Zhou et al., 2018)
Lysozyme (LYZ)	Hollow MSNs (HMSNs) with large and small cone shaped pores (HMSN-LP and HMSN-SP, respectively)	*In vitro*	*E. coli*	Ultrasonication method	Diffusion/sustained release	(Xu et al., 2018)
Doxycycline (DOXY)	MCM-41 modified with phenyl, mercaptopropyl, propylsulfonic and magnesium (MCM-C_6H_5, MCM-SH, MCM-SO_3H	*In vitro*	*Klebsiella pneumoniae*	Impregnation method	Dissociation/diffusion	(Deaconu et al., 2018)

	and MCM-Mg, respectively)					
Ciprofloxacin (CIP)	MSNs-SBA-16/hydroxyapatite (HA) modified with 3-aminopropyltriethoxysilane (APTES), anchored with diethylenetriaminepentaacetic acid (DTPA) for chelating technetium-99m (^{99}mTc-DTPA-SBA-16-APTES)	*In vitro*	*S. aureus*, *P. aeruginosa*, *E. coli* and *Bacillus cereus*	Impregnation method	Diffusion/sustained release	(Andrade et al., 2018)
Clofazimine (CFZ)	MSNs loaded with CFZ + acetophenone (AP)	*In vitro*	*Mycobacterium tuberculosis*	Impregnation method	Diffusion/AP-assisted release	(Chen et al., 2018)
Levofloxacin (LEVO)	MSN modified with [3-(2-aminoethylamino) propyl]trimethoxysilane (DAMO) (MSNs-DAMO)	*In vitro*	*E. coli*	Impregnation method	Diffusion/sustained release	(González et al., 2018)
Silver and bismuth nanoparticles (Ag and Bi, respectively)	Ag-Bi@MSNs	*In vitro* and *in vivo*	methicillin-resistant *S. Aureus* (MRSA)	*In situ* growth of Ag and Bi nanoparticles	Near-infrared (NIR)-responsive controlled release	(Cao et al., 2020)
DNase I(Deoxyribose nuclease I)	MSN-Ag	*In vitro*	*E. coli* and *Streptococcus mutans* biofilms	Impregnation method	Diffusion/sustained release	(Tasia et al., 2020)
VAN	Sufonated-hyaluronic acid (S-HA) terminated magnetic MSNs modified with *S. aureus* antibody (Ab) (Ab@S-HA@MMSNs)	*In vitro*	*S. aureus*	Impregnation method	Hyaluronidase (Hyal)-responsive controlled release	(Xu et al., 2019)

Silver nanoparticles (Ag)	Poly-L-glutamic acid and polyallylamine hydrochloride assembled by the layer-by-layer (LBL) technique onto MSN-Ag (LBL@MSN-Ag)	*In vitro* and *in vivo*	*S. aureus*-associated osteomyelitis infections	*In situ* growth of Ag nanoparticles	V8 enzyme-responsive controlled release	(Ding et al., 2020)
LEVO	Mixed-charge pseudo-zwitterionic MSNs and PEGylated (PEG)-MSN	*In vitro*	*E. coli* and *S. aureus*	Impregnation method	Diffusion/sustained release	(Encinas et al., 2019)
Moxifloxacin (MXF)	Disulfide snap-top redox-operated MSNs (MSN-SS)	*In vivo*	*Francisella tularensis*	Impregnation method	Redox-responsive controlled release	(Clemens et al., 2019)
Polymyxin B	MSNs, aminated MSNs and carboxyl modified MSNs	*In vitro*	*P. aeruginosa*, *E. coli* and *Acinetobacter baumannii*	Impregnation method	Diffusion/sustained release	(Gounani et al., 2018)
LEVO	MSNs-like SBA15, SBA15@NH_2 and SBA15@NH_2/polylactic acid	*In vitro*	*S. aureus, E. coli, C. albicans and Aspergillus niger*	Impregnation method	Acid pH-controlled release	(Abdelbar et al., 2020)
Biocide Parmetol S15	MSNs-like MCM-48 modified with quaternary ammonium salts	*In vitro*	*S. aureus* and *E. coli*	Impregnation method	Diffusion/sustained release	(Michailidis et al., 2017)
Ethionamide (ETH)	UnTHCPSi NPs	*In vitro*	multidrug-resistant *M. tuberculosis*	Covalent conjugation of ETH	---	(Vale et al., 2017)
MXF	Disulfide snap-top redox-operated MSNs modified with β-cyclodextrin (β-CD) (MSN-SS- β-CD)	*In vitro* and *in vivo*	*Francisella tularensis*	Impregnation method	Redox-responsive controlled release	(Lee et al., 2016)
Isoniazid (INH)	Hollow oblate MSNs (HOMSNs), trehalose-	*In vitro*	*M. smegmatis* (INH-resistant),	Impregnation method	Slow/sustained release	(Hao et al., 2015)

	conjugated HOMSNs and mannose-conjugated HOMSNs (HOMSNs-Man)		*Staphylococcus epidermidis* and *E. coli*			
INH	MSNs-CHO (aldehyde modified)-INH and MSNs-CHO-INH-poly(ethylene imine)-poly(ethylene glycol) (PEI-PEG)	*In vitro* and *in vivo*	*M. tuberculosis*	Impregnation method	pH-responsive controlled release	(Hwang et al., 2015)
INH and RIF	MSNs, PEI-MSNs and MSNs-MBI (1-methyl-1H-benzimidazole)-□CD (beta-cyclodextrin)	*In vitro* and *in vivo*	*M. tuberculosis*	Impregnation method	pH-responsive controlled release	(Clemens et al., 2012)
Moxifloxacin (MFX)	MSNs-anilinoalkane-*α*-CD (alpha-cyclodextrin) and MSNs-MBI (1-methyl-1H-benzimidazole)-*β*-CD (beta-cyclodextrin)	*In vitro* and *in vivo*	*F. tularensis*	Impregnation method	pH-responsive controlled release	(Li et al., 2015)
Model drugs (Fluorescein and Hoechst 33342)	MSNs- Ft-LVS-LPS-FB11	*In vitro*	*F. tularensis*	Impregnation method	Pathogen (Ft-LVS-LPS)-responsive controlled release	(Ruehle et al., 2017)
Soluble adult worm antigen preparation (SWAP)	MSNs	*In vivo*	*S. mansoni*	Impregnation and sonication methods	---	(Oliveira et al., 2016)
Benznidazole (BZ)	MSNs-MCM-41 functionalized with (3-glycidoxypropy) trimethoxysilane (GPTMS) and chitosan succinate (CS)	*In vitro*	*T. cruzi*	Simple impregnation Method	---	(Nhavene et al., 2018)

Praziquantel (PZQ)	MSNs	*In vivo*	*S. mansoni*	Simple impregnation method	Sustained release	(Tawfeek et al., 2019)
Metronidazole (MNZ)	Mesoporous silica whiskers-SBA-15 modified with tannic acid (TA)	*In vitro*	*Trichomonas gallinae*	Simple Impregnation method	pH-responsive controlled release	(Lehi et al., 2019)
Econazole (ECO)	MSNs functionalized with aminopropyl groups (MCM-41-NH_2)	*In vitro* and *In vivo*	*C. albicans*	Simple impregnation method	Slow/sustained release	(Montazeri et al., 2020)
Rose Bengal (RB)	Amino-modified MSNs conjugated with RB (MSNs-RB)	*In vitro*	*C. albicans*	Simple RB conjugation	Slow/controlled release	(Paramanantham et al., 2018)
Tebuconazole (TEB)	MSNs-N3 (3-[2-(2-aminoethylamino)ethylamino]propyltrimethoxysilane)	*In vitro*	*C. albicans* and *Saccharomyces cerevisiae*	Simple impregnation method	pH-responsive controlled release	(Mas et al., 2014)
Zinc ions (Zn^{2+})	ZnO@MSNs	*In vitro* and *In vivo*	*Aspergillus niger* (MTCC 10180 and MTCC 2196) and two strains of *Fusarium oxysporum* (NCIM 1043 and NCIM 1072)	*In situ* growth of Zn nanoparticles under heating	Slow/sustained release	(Mitra et al., 2015)
Silver ions (Ag^{+})	MSNs-AgNPs (silver nanoparticles)	*In vitro*	*C. albicans*	*In situ* AgNPs impregnation	Slow/sustained release	(Qasim et al., 2015)
VEEV inhibitor (ML336)	Lipid (1,2-distearoyl-sn-glycero-3-phosphocholine (DSPC):Cholestrol:1,2-distearoyl-sn-glycero-3-phosphoethanolamine-N-[methoxy(polyethylene	*In vitro* (TC-83 VEEV) and *in vivo* (TC-83 VEEV infected mice)	Venezuelan equine encephalitis virus (VEEV)	Impregnation/sonication methods	pH-responsive controlled release	(LaBauve et al., 2018)

	glycol)-2000] (DSPE-PEG(2000))-coated MSNs (LC-MSNs)					
---	GAGs (glycosaminoglycans, sodium benzene sulfonate) mimetic-functionalized MSNs (MSNs-SO_3)	*In vitro*	Herpes simplex type 1 and type 2 viruses (HSV1 and HSV2, respectively)	---	---	(Lee et al., 2016)
Acyclovir (ACV)	Benzene sulfonate-modified MSNs, propyl thiol-modified MSNs, propyl sulfonate-modified MSNs, zwitterionic sulfonate-modified MSNs and phenyl-modified MSNs (MSNs-Phenyl-SO_3, MSNs-Propyl-Thiol, MSNs-Propyl-SO_3, MSNs-Zw-SO_3 and MSNs-Phenyl, respectively)	*In vitro*	Herpes simplex type 1 and type 2 viruses (HSV1 and HSV2, respectively)	Sonication method	Slow/sustained release	(Lee et al., 2018)
---	APTES, GPTMS and trimethoxy-(2-phenylethyl)silane (TMPES) groups were used to modified MSNs surface and noted as MSNs-APTES, MSNs-GPTMS and MSNs-TMPES	*In vitro*	recombinant lentivirus with VSV-G and HIV-gp120 envelopes	---	---	(Silva et al., 2016)
PCV2 GST-ORF2-E protein	HMSNs	*In vitro* and *in vivo*	Porcine circovirus type 2 (PCV2)	Sonication method	Slow/sustained release	(Guo et al., 2012)

5.1. Bacterial infections

The great challenge concerning bacterial infections treatment comprises the development of antibiotic resistance in several bacteria species, leading to ineffective treatment. One way to overcome this drawback consists of the use of nanoparticles that can interact efficiently to the bacterial surface disrupting their cell wall leading to cell death. Interestingly, multifunctional nanoparticles can also interact with cellular organelles and biomolecules present in the bacteria, making difficult the resistance development against them (Ogunsona et al., 2020; Singh et al., 2020).

Considering the abovementioned advantages, authors have reported the use of MSNs containing peptides with antibacterial properties, aiming to prevent their enzymatic degradation potentiating their antimicrobial activity (Subramaniam et al., 2019). It can also guarantee the same effect for loading antimicrobial proteins (Xu et al., 2018). Other studies reported the use of hydrophobic antimicrobials drugs-loaded MSNs to enhance their effect in biological media (Chen et al., 2018; Deaconu et al., 2019; Yang et al., 2018). On the other hand, for hydrophilic antimicrobial drugs which are very soluble in an aqueous/biological environments, MSNs can also promote a controlled drug release (Deaconu et al., 2018).

The association of multifunctional MSNs with antimicrobial drugs allows, besides controlled drug release, efficient internalization in the bacterial environment (Abdullah et al., 2019; Martínez-Carmona et al., 2019). Drug-loaded mesoporous silica carriers were reported to access bone infections since fluids circulation in this region is very low which reduce drugs bioavailability via conventional administration (Andrade et al., 2018; Zhou et al., 2018). In addition, the MSNs specificity can be achieved by easily functionalization improving nanoplatforms action in target sites and controlled drugs release minimizing side effects. **Table 3** summarized examples of MSNs for bacterial infections treatment as well as drugs type, MSNs-based carriers, microorganisms and drugs absorption and release mechanisms.

Bacterial conventional treatment possesses challenges mainly due to the poor antimicrobial compound's permeation into the infected cells. In this regard, Subramaniam et al. (2019) proposed to evaluate distinct size of MSNs containing rifampicin (RIF) aiming to improve the intracellular bacterial infection treatment. Spherical MSNs were fabricated with average size of 40 and 100 nm (labeled MSNs-40 and MSNs-100, respectively), zeta potential values of -20 and -16.9 mV, respectively and pores size ranging from 8 to 9 nm. RIF was successfully encapsulated into MSNs-40 and MSNs-100 via passive diffusion method, showing encapsulation efficiency (EE) values of 26.8 and 22.5%, respectively. Cellular uptake assays performed in RAW 264.7 cells exhibited interesting MSNs-100 macrophage internalization achieving up to 80%, whereas MSNs-40 showed lower uptake values (up to 40%), assigned to the exocytosis process more pronounced for smaller nanoparticles.

From *in vitro* release assays, both RIF-loaded MSNs displayed low release rates up to 10% (in PBS buffer solution at pH 7.4). In contrast, at pH 5.0, no changes were detected in release profile for both nanosystems within 12 h, attributed to the low RIF solubility. Intracellular infection model was established using small colony variants of *Staphylococcus aureus* in macrophages. Results exhibited high MSNs-RIF internalization and an antibacterial activity enhancement regarding free RIF solution. Authors concluded that despites low release rates achieved, high internalization and bacterial activity enable these nanoplatforms to treat bacterial biofilms.

Regarding bacterial biofilms infections and resistance, Vallet-Regí group (Martínez-Carmona et al., 2019; Vallet-Regí et al., 2019) developed a smart nanocarrier based on antibiotic levofloxacin (LEVO)-loaded MSNs decorated with the lectin concanavalin A (ConA), as displayed in **Figure 4**. ConA was used to aggregate specificity to the nanosystem promoting better internalization into biofilm and then antimicrobial activity. MCM-41-like MSNs with spherical shape of 150 nm in size and hexagonal pores channel's structure were fabricated. *In vitro* release tests displayed that bare MSNs retained drug release achieving up to 30% after 48 h. This can be attributed to the hydrogen bonding interaction between MSNs Si-OH groups and LEVO zwitterionic form. On the other hand, MSN_{ConA} promoted total LEVO release up to 5 days, assigned to the interaction of ConA protein on MSNs surface with LEVO that leads to its fast release from the mesopores. The nanoantibiotic (labeled MSN_{ConA}@LEVO) targeting effect was successfully evaluated in *Escherichia coli* biofilm exhibiting a dose dependent internalization, that means the greater the MSN_{ConA}@LEVO concentration, the higher the nanosystem penetration. The nanoplatform with negatively charged surface (potential zeta of -25 mV) promoted high electrostatic affinity toward the biofilm polysaccharide. Antimicrobial *in vitro* assays were performed in three distinct MSN_{ConA}@LEVO concentrations (5, 10 and 20 μg mL^{-1}). Results confirm high internalization process displaying high antimicrobial efficacy values from 97 to 100%. Beyond that, cytotoxicity assays showed MSN_{ConA}@LEVO were nontoxic up to 50 μg mL^{-1} enabling these smart nanocarriers for further clinical translations.

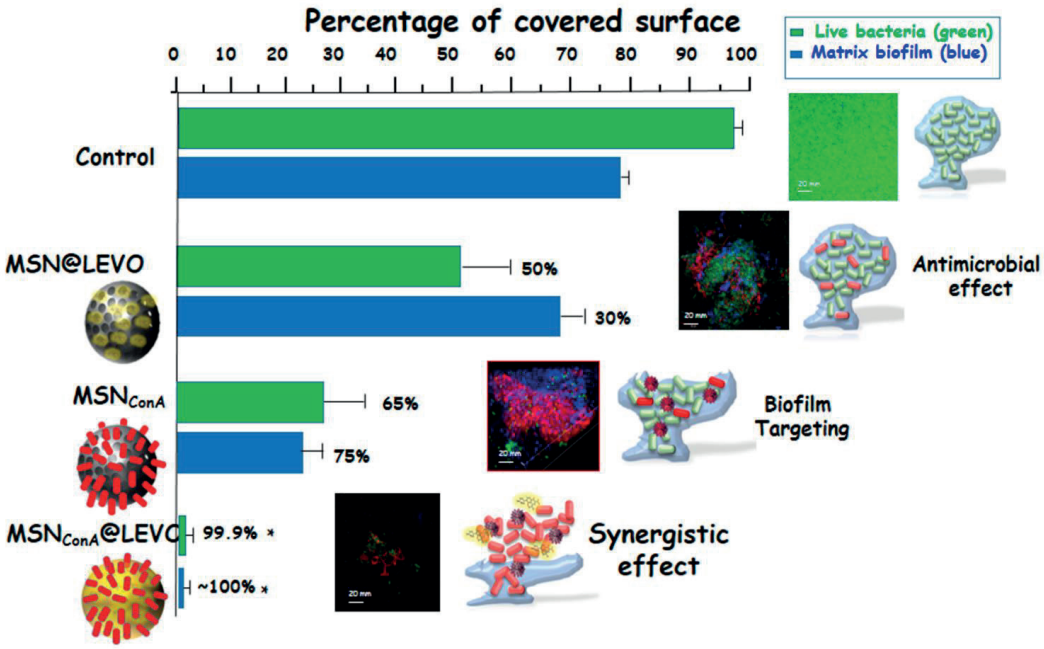

Figure 4: MSNs as nanocarrier of antimicrobial agent (levofloxacin, LEVO) and functionalized with a biofilm targeting agent (ConA). In this case, the functionalization of MSNs with ConA favors its internalization in *E. coli* biofilms affording a synergistic combination with LEVO-loaded MSNs, which triggers an efficient antimicrobial effect on *E. coli* biofilm. The image represents the percentage of covered surface by live bacteria (green) and mucopolysaccharide layer (blue) and the representative confocal images show a complete reduction after incubation with the nanosystems functionalized with ConA and loaded with LEVO (MSNConA@LEVO) (Vallet-Regí et al., 2019).

Deaconu et al. (2019) reported the fabrication of norfloxacin (NFX)-loaded modified and unmodified MCM-type MSNs to evaluate their action against *E. coli*. Authors synthesized five types of MSNs: MCM-41 with long mesopores channels, pristine MSNs without surfactant (MSN), surfactant non-extracted (MSN-E), modified with vinyl groups (MSN-vinyl) and MCM-48 nanosystems. All MCM-type carriers showed spherical nanosized morphologies up to 60 nm. High surface area (up to 1222 m^2 g^{-1}) and pores size ranging from 2.5 to 9 nm were detected for these nanocarriers. MCM-41 types exhibited hexagonal mesopores arrays with average size of 2.5-3.1 nm whereas MCM-48 showed interconnected pores forming cubic arrays with sizes of 2.5-9 nm. The successfully nanoconfinement into mesopores by impregnation method confirmed NFX amorphization. *In vitro* release studies demonstrated NFX-loaded MSNs carriers enhanced dissolution rates regarding free NFX in same conditions. In addition, the association and dissociation NFX-

nanocarriers processes were considered reversible with a first-order kinetics. In addition, high initial release of the antibiotic, which is suitable for applications in severe infections. Authors concluded that NFX-loaded MCM-based nanocarriers displayed good and similar antibacterial activity compared to free NFX. These nanosystems could be applied to avoid the use of high free NFX concentration, maximizing antibacterial effect in any biological media.

Conventional antibiotic treatments are less effective to *S. aureus* because this microorganism can invade host cells like osteoblasts and macrophages and use them as reservoir to reduce antibiotic action leading to infection recurrence. In this sense, Yang et al. (2018) proposed to design a gentamicin (GEN)-loaded MSNs modified with a lipid bilayer surface shell and an bacterial-targeting peptide ubiquicidin (UBI_{29-41}) onto lipid bilayer (labeled LU). Spherical MSNs with highly ordered mesoporous channels and average size of 80 nm were synthesized. GEN EE of 25.6% was achieved. MSNs surface modification was firstly performed with liposome layer aiming to prevent nonspecific nanoparticles uptake under physiological conditions whereas the conjugated UBI_{29-41} allows the nanosystems targeting to bacteria in infected tissues. In addition, the liposomal bilayer can act as a blocker avoiding GEN leakage. When the nanocarrier reaches the infected cells, the liposome can be degraded by bacterial enzymes and toxins. *In vitro* and *in vivo* assays were performed on planktonic and intracellular infection of *S. aureus* bacteria. *In vitro* tests revealed that the *S. aureus* growth on agar plates showed higher microbial inhibition for GEN@MSNs-LU than the unmodified nanosystem (GEN@MSNs) and free drug besides a responsive-bacterial toxin release. From *in vivo* assays, high specificity, bacterial reduction and no infection recurrence were detected by using GEN@MSNs-LU. In addition, physiopathology studies were performed and no histological changes were detected in major organs indicating no organ toxicity when submitted to GEN@MSNs-LU treatment. All these results enable this bacterial-responsive nanosytem as a promising and adaptable tool to delivery other drugs targeting distinct bacteria and, consequently, treat diverse kind of infections.

Infected bone defects often cause limited blood circulation in the infected sites resulting in poor ability to self-heal for restoring the structure and function of bone tissue. Take this into account, the development of bone implants based on specific and antibiotic controlled delivery systems is essential for an effective bone infection treatment. Zhou et al. (2018) designed scaffolds based on MSNs containing vancomycin (VAN) into mesopores channels dispersed in gelatinous matrix. In addition to control drug release, MSNs incorporated into polymer scaffolds can increase their mechanical properties, enhancing cell adhesion, proliferation and osteogenic osteoblasts differentiation. In this context, spherical MSNs were successfully prepared with average size and pores diameter of 210 and 2.4 nm, respectively. *In vitro* VAN release was investigated for VAN@gelatin and VAN@MSNs/gelatin. While VAN@gelatin displayed an initial burst release (up to 45% in the first

day), VAN@MSNs/gelatin presented an initial release of 19% (first day) and about 78% over 28 days, suggesting a sustained VAN release. From *in vitro* antibacterial (*S. aureus*) assays, both composite systems showed antibacterial activity dose-dependent with 95% of growth inhibition at 60 μg mL^{-1}. Additionally, cytocompatibility tests were carried out presenting good spreadability and proliferation of bone mesenchymal stem cells (BMSCs) in the evaluated scaffolds. Osteogenic differentiation tests suggested that the incorporation of MSNs facilitated the osteogenic differentiation of BMSCs and VAN-loaded into mesopores had no negative effects on its bioactivity. *In vivo* tests were established by bone infection induced in rabbits and the implantation of gelatin and MSNs/gelation were evaluated. High leukocytes levels were detected after 8 weeks of treatment for both samples. On the other hand, the implantation of VAN@MSNs/gelatin depicted the leukocyte concentration decreased significantly and reached a normal level after 4 weeks of treatment. The excellent result indicates that MSNs promoted a controlled VAN release at the specific site. Authors concluded that the composite scaffolds based on MSNs as nanocarriers leaded to slow and prolonged VAN release inhibiting local infection *in vivo* and, consequently, bone regeneration, constituting a promising tool for infected bone defects therapy.

The antibiotic ciprofloxacin (CIP) possesses wide antibacterial spectra and good permeation for bone tissues, however, low blood circulation in bone site, high drug concentration and several side effects makes its direct application inviable. In this context, Andrade et al. (2018) fabricated ciprofloxacin (CIP)-loaded SBA-16-type MSNs and SBA-16/hydroxyapatite (HA) composites for bone infection treatment. Both nanoplatforms were modified with 3-aminopropyltriethoxysilane (APTES), anchored with diethylenetriaminepentaacetic acid (DTPA) for chelating technetium-99m. The SBA-16 and SBA-16/HA exhibited ordered cubic mesoporous structures with average pores size of 3.4 and 3.8 nm, respectively. CIP loading ranging from 28 to 31% were detected for modified and unmodified SBA-16 carriers. *In vitro* CIP release studies (SBF pH 7.3) displayed that SBA-16-APTES and SBA-16/HA-APTES were similar with initial burst release of 42-43% in the first 9 h, achieving the maximum release (51-53%) in 76 h. These results suggested that at SBF solution with pH 7.3, the nitrogen of piperazinyl ring is protonated and classified as a zwitterionic species, which can lead to great CIP interaction with the amine groups modified onto SBA-16 surface. *In vitro* antimicrobial assays by using *S. aureus*, *Pseudomonas aeruginosa*, *E. coli* and *Bacillus cereus* were performed for CIP@SBA-16-APTES and CIP@SBA-16/HA-APTES. Both aminated platforms presented high antibacterial activity against all microorganisms especially relating to free CIP. It is worth emphasizing that the tested free CIP amount was approximately three times greater than CIP-loaded SBA-16 carriers. ^{99}mTc-DTPA-SBA-16-APTES and ^{99}mTc-DTPA-SBA-16/HA-APTES were prepared as radiotracer platforms aiming to evaluate their *in vivo* biodistribution. Both nanosystems were mostly

uptaken by liver and spleen, reaching the highest radioactivity level at 4 h post-injection. Considering bone uptake, a higher uptake for ^{99}mTc-DTPA-SBA-16/HA-APTES was detected relating to ^{99}mTc-DTPA-SBA-16-APTES, at 1 and 4 h post-injection. These results suggested ^{99}mTc-DTPA-SBA-16/HA-APTES was more specific for bone tissue than ^{99}mTc-DTPA-SBA-16-APTES, which can be attributed to the presence of hydroxyapatite in the nanosystem that possesses high affinity for bone matrix. Authors pointed out that the fabrication of these nanocarriers are relevant showing low cost and easy preparation and effective CIP release, which make them promising nanoplatforms to treat bone infections.

Bacterial biofilm comprises up to 70% of infection and inflammation in clinic being usually resistant to the most conventional antibiotic treatment. In light of this, Xu et al. (2018) prepared rod shaped hollow MSNs (HMSNs) with large and small cone shaped pores (HMSN-LP and HMSN-SP, respectively) via oil-water system containing lysozyme (LYZ) to treat *E. coli* biofilms. The synthetized nanosystems presented averages particle length and width of 400 and 200 nm, respectively. Average pores size of 40 and 3 nm were found for HMSN-LP and HMSN-SP, respectively. HMSN-LP exhibited loading capacity 7 times higher than HMSN-SP, ascribed to the pores size difference. *In vitro* release tests (PBS pH 7.4) revealed that slower drug release was achieved by HMSN-LP than HMSN-SP, with up to 80% of LYZ release over 48 h. Corroborating with the aforementioned results, antimicrobial assays using *E. coli* biofilms model confirmed the highest antimicrobial action of HMSN-LP-LYZ compared to HMSN-SP-LYZ and free LYZ. Additionally, the HMSN-LP was marked with fluorescent dye and its penetration ability into biofilms after 24 and 48 h of incubation was confirmed by confocal laser scanning microscope analysis. All results demonstrated the high therapeutic activity of HMSN-LP towards *E. coli* biofilms, which enable the design of novel and multi-responsive nanosystems against infectious pathogens.

Doxycycline (DOXY) is an antibiotic very hydrophilic and soluble in biological fluid showing a high bioavailability at short time being the most part quickly eliminated by the kidneys. Aiming to overcome the aforementioned drawback and considering the development of bacterial resistance, Deaconu et al. (2018) proposed to ally antibiotic properties and MSNs matrix by preparing DOXY-loaded MCM-41-type MSNs and modified MSNs to treat *Klebsiella pneumoniae* strains. MCM-41 (using hexadecyltrimethylammonium bromide (C_{16}TAB) and TMOS as surfactant and inorganic precursor, respectively) platforms were prepared and then modified with phenyl, mercaptopropyl, propylsulfonic and magnesium labeled (MCM-C_6H_5, MCM-SH, MCM-SO_3H and MCM-Mg, respectively). MCM-C_{14} was also synthetized by using reduced chain surfactant (C_{14}TAB) and TEOS as inorganic precursor. All MCM-41 nanoplatforms exhibited spherical shape ranging from 200-400 nm with ordered hexagonal mesopores channels arrays with mean pores size from 1.75 to 2.98 nm.

DOXY incorporation was performed for all nanocarriers by wetness impregnation method. From drug release studies (PBS pH 5.2) was detected that DOXY delivery profiles depend on the modification and distinct type of mesoporous silica matrix. The MCM-Mg showed lower DOXY release kinetic, which can be assigned to the enhanced basicity of the magnesium oxide particles formed on the silica surface. Despite distinct DOXY release kinetics obtained, effective and similar antibacterial activity was detected for all nanoplatforms. In addition, these results were similar to free DOXY expected that controlled and prolonged release can be achieved only by using the nanocarriers.

The use of MSNs to transport and deliver poorly soluble drugs to the target diseases sites comprises an attractive and useful method to improve drug's efficacy. Notwithstanding, high loading and also total release drugs amount is a great challenge due to the nanoconfinement and possible interaction with the matrix. In light of this, Chen et al. (2018) demonstrated the use of acetophenone (AP), an Food and Drug Administration (FDA)-approved food additive as co-solvent (known as chaperone) to promotes efficient clofazimine (CFZ) entrapment and release from MSNs channels to aqueous environment. CFZ is a water-insoluble antibiotic used to treat leprosy and multidrug-resistant tuberculosis. Spherical and monodisperse MSNs with highly ordered hexagonal mesopores arrays and average size of 100 nm were obtained as well as high surface area (1060 m^2 g^{-1}), negatively charged (zeta potential of -21.2 mV) with average pore size of 2.8 nm. All these results favor MSNs loading with CFZ and AP. CFZ loading and release assays were carried out in dimethylsulfoxide (DMSO) and AP solvents. The loading CFZ capacity by using AP increased as a function of CFZ concentration, showing 26.8% at 50 mM whereas by using DMSO the loading capacity was 5.9% at the same concentration. By using AP strategy, the CFZ release efficiency was 47.2% whereas by using DMSO was only 0.02%. The novel strategy showed release efficiency 2300 times higher than the conventional method with DMSO (0.02%). The high increase in CFZ release can be assigned to the release of AP from the MSNs pores carrying CFZ molecules together into the aqueous solution. The chaperon-based MSNs were evaluated in a macrophage model of *Mycobacterium tuberculosis* infection. The optimized CFZ-AP (10mM CFZ in AP)@MSNs exhibited high antimicrobial efficacy (dose-dependent) reducing the bacteria number by 1 log CFU (90% of bacteria were killed). In addition, no changes on the macrophages morphological appearance were detected for the applied nanosystems. This loading/delivery "chaperone-assisted" strategy can be used for other hydrophobic drugs with their suitable solvents (chaperone), opening opportunities to design novel drug delivery MSNs-based nanosystems for biomedical applications.

Despites the challenges cause by microbial biofilms formation and antibiotic resistance generation, Gram-negative bacteria possess outer membranes as a highly impermeable barrier as well as additional defense mechanisms no detect in Gram-positive bacteria (Lee et al., 2007). Considering

these drawbacks, González et al. (2018) developed nanoantibiotics based on levofloxacin (LEVO)-loaded MSNs covalently modified with third-generation poly(propyleneimine) dendrimer (G3), which has high affinity to negatively charged bacteria cell walls. Beyond that, LEVO-loaded [3-(2-aminoethylamino) propyl]trimethoxysilane (labeled DAMO)-modified MSNs (noted LEVO@MSNs-DAMO) were also fabricated to evaluate antimicrobial action against Gram-negative bacteria. Spherical-shaped MSNs with 2D hexagonal mesoporous arrangement were prepared, showing average diameter and pores size of 150 and 2.4 nm, respectively. In addition, negatively charged bare MSNs (-36.4 mV) after modification become positively charged achieving zeta potential around +31.8-37.4 mV, which make them enable to interact with negatively charged bacteria walls. LEVO loading amount up to 7.8% were detected for the nanovehicles. LEVO release performance (PBS pH 7.4) were evaluated exhibiting a first-order kinetics for all nanosystems (LEVO@MSNs, LEVO@MSNs-DAMO and LEVO@MSNs-G3), with 100% of LEVO release over 72 h for LEVO@MSNs-G3. LEVO@MSNs showed lower release values indicating strong interaction via hydrogen bonding between LEVO zwitterionic form (at pH 7.4) and Si-OH groups from MSNs. *E. coli* internalization assays confirmed good MSNs-DAMO and MSNs-G3 internalization due to their positive charge density making electrostatic interactions with *E. coli* cells walls possible. Additionally, MSNs-G3 displayed higher internalization than MSNs-DAMO, ascribed to the MSNs-G3 high surface flexibility and high interaction points with negatively charged *E. coli* phospholipid membranes regarding MSNs-DAMO. These results corroborated antimicrobial assays against *E. coli* biofilms showing the MSNs-G3 with higher and remarkable antimicrobial efficacy relating to the other nanosystems. These findings demonstrated that the synergistic combination of bacterial internalization and antimicrobial agents into MSNs-based nanovehicles lead to interesting and efficient antibiotics for infections treatment.

Regarding the high mortality and morbidity caused by bacterial resistance, Cao et al. (2020) proposed to ally the amazing properties of MSNs with metallic nanoparticles such as silver (Ag) and bismuth (Bi). Authors designed a multifunctional MSNs-supported Ag-Bi nanoparticles (NPs) associating hyperthermia generated by Bi nanoparticles with Ag release for synergistic antibacterial therapy as shown in **Figure 5** Ag-Bi nanoparticles were fabricated via *in situ* growth onto MSNs pore's structure aiming to avoid their aggregation and oxidation under physiological environment. Under the NIR laser irradiation (808 nm laser irradiation, 1 W cm^{-2}, 15 min), hyperthermia can be generated by Bi NPs destroying bacterial cell membrane and biofilm promoting and increasing Ag^{+} release from the nanocarrier, resulting in photothermal-enhanced antibacterial activity. Spherical nanosystems with average size and pores of 200-240 nm and 3.4-4.8 nm, respectively were successfully fabricated. In addition, Ag NPs showed average size of ~15 nm. Photothermal therapy (PTT) ability of Ag-

Bi@MSNs was evaluated exhibiting high stability and laser power irradiation and concentration dependence. As higher is laser power density and Ag-Bi@MSNs concentration, higher is the achieved temperature confirming great PTT performance. *In vitro* antibacterial activity was evaluated against MRSA cells by adding Ag-Bi@MSNs with or without laser irradiation. At same concentration (128 μg mL^{-1}), 22 and 76% of cells death were achieved without and with laser irradiation, respectively. Additionally, release studies were performed for 75 min with and without laser irradiation (at the same concentration, 200 μg mL^{-1}). Results corroborate antibacterial assays displaying a NIR-responsive Ag^{+} release, with 11.3 and 37.3% of release without and with laser irradiation, respectively. Aiming to prove the synergic antibacterial effect, MRSA-infected mice were investigated with five groups: PBS, Bi@MSNs, Ag-Bi@MSNs, Bi@MSNs + NIR and Ag-Bi@MSNs + NIR groups. Regarding to the control group (PBS), the number of colonies were reduced to 90.3, 74.6, 35.1 and 5.9% for Bi@MSNs, Bi@MSNs + NIR, Ag-Bi@MSNs and Ag-Bi@MSNs + NIR, respectively, indicating that multimodal synergistic therapy based on Ag-Bi@MSNs could effectively treat MRSA skin infection. The therapeutic effect was confirmed by histological analysis. Beyond that, the animals evaluated showed no obvious changes in their body weight suggesting no biotoxicity. These findings made Ag-Bi@MSNs a promising multimodal nanoplatform against bacterial infections and for further clinical translations.

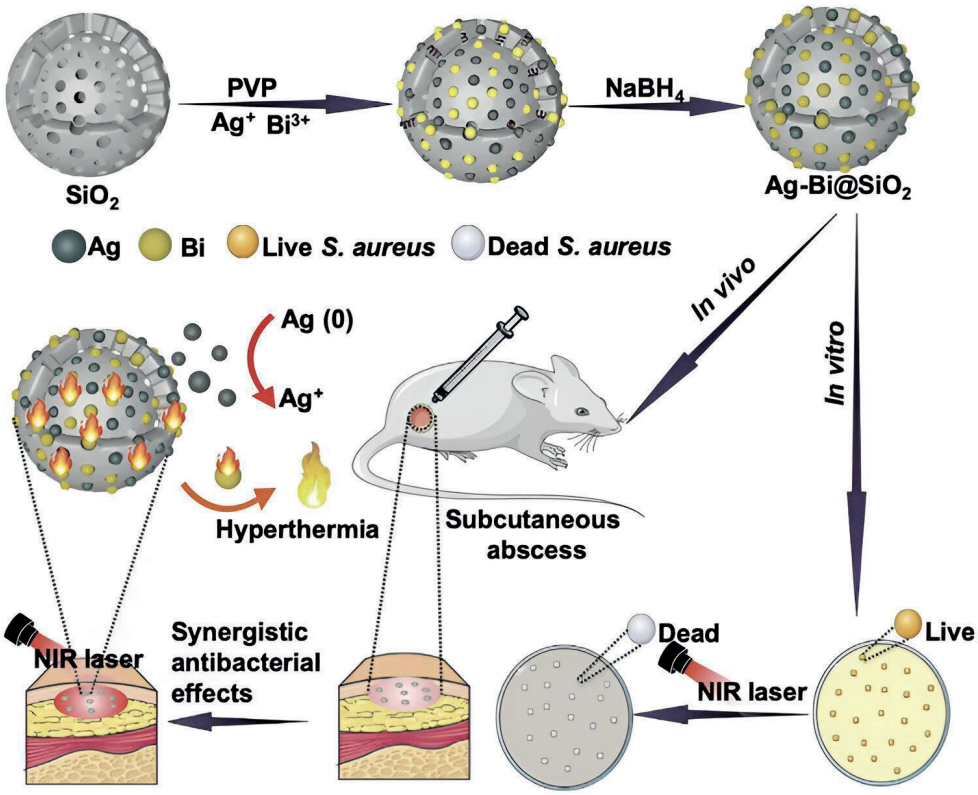

Figure 5: Schematic description for the preparation of Ag-Bi@MSNs and its synergistic antibacterial effects (Cao et al., 2020).

Fast and accurate bacteria detection and their effectively killing in the bloodstream in low doses are crucial and act as key roles in medicine and microbiology studies. Integrating diagnosis and treatment to achieve accurate diagnosis and efficient treatment of diseases has always been an important goal of modern medicine. In this context, Xu et al. (2019) developed a smart and theranostic nanoplatform based on vancomycin (VAN)-loaded magnetic (Fe_3O_4 NPs) MSNs (MMSNs) modified with sufonated-hyaluronic acid (S-HA) and *S. aureus* antibody (Ab) grafting via amidation reaction (labeled Ab@S-HA@MMSNs) for *S. aureus* detection and treatment in bloodstreams. S-HA was selected due to its capping and targeting function, biocompatibility, biodegradability besides promotes drug sustained release and anti-adhesion effects. Fe_3O_4 NPs displayed average size of 180 nm whereas spherical MMSNs achieved average size and pores diameter of 240 and 3 nm, respectively. In addition, Ab@S-HA@MMSNs exhibited 180 nm core uniformly wrapped with 30 nm shell, with zeta potential of -5.32 mV. Van loading efficacy of 10.7 wt% was achieved and antibacterial assays were carried out

since *S. aureus* can secrete hyaluronidase (Hyal), enzyme that degrades S-HA promoting controlled VAN release. Results exhibited 98% of bacterial reduction suggesting high antibacterial efficacy and Hyal-responsive controlled VAN release. *In vitro* release tests were conducted showing that no significant VAN was release without Hyal presence whereas after Hyal addition (up to 500 U mL^{-1}), up to 83% of VAN corroborating the Hyal role in the "on-demand" drug release. The Ab@S-HA@MMSNs magnetization behavior was evaluated and despites magnetization values reduction after all modification, the nanosystem presented good magnetic responsivity and can be utilized to modify the surface of magnetic glassy carbon electrode (MGCE) (noted Ab@S-HA@MMSNs/MGCE) by magnetic interaction. From electrochemical and analytical studies, the fabricated immunosensor exhibited an excellent electrochemical response towards *S. aureus* in the range of $1x10^{1}$–$1x10^{10}$ CFU mL^{-1} with high selectivity, stability and reproducibility. The detection limit with linear range was up to 3 CFU mL^{-1}, and this responsiveness was also well demonstrated in the blood environment. Beyond that S-HA-modified MMSNs possess anticoagulant property, the Ab@S-HA@MMSNs/MGCE displayed antiadhesion property, ensuring that it can be directly applied to detect *S. aureus* in whole blood. Additionally, increasing *S. aureus* amount of arriving at Ab@S-HA@MMSNs/MGCE, the capping Ab@S-HA@MMSNs were degraded by Hyal secreted by *S. aureus* and "on demand" VAN released was achieved. All results suggest this multifunctional theranostic nanoplatform for accurate diagnosis and efficient treatment of *S. aureus* bloodstream infection.

Zink group (Chen et al., 2018, 2019; Clemens et al., 2012, 2019; Hwang et al., 2015; Li et al., 2015; Ruehle et al., 2017) have designed stimuli-responsive controlled drug delivery MSNs-based nanoplatforms to treat infectious diseases such as caused by *Francisella tularensis* (Clemens et al., 2019; Lee et al., 2016; Li et al., 2015; Ruehle et al., 2017) and *M. tuberculosis* (Chen et al., 2018; Clemens et al., 2012; Hwang et al., 2015). From one of these works (Ruehle et al., 2017), authors developed a pathogen-specific detection and drug delivery nanoplatform based on MSNs modified with silane groups attached with lipopolysaccharide (LPS) chain of *F. tularensis* live vaccine strain (LVS) (Ft-LVS-LPS) as stalks (modified antigen) that interact with FB11 anti-O-antigen antibody (FB11) nanovalve as a capping agent to block the mesopores avoiding drug diffusion without specific stimulus. By manipulation of the non-covalently interaction MSNs modified antigen (Ft-LVS-LPS)-antibody (*Francisella tularensis* LPS antibody (FB11)), the antigen produced by the target bacteria can compete effectively for binding to the gatekeeper antibody, reducing stalk-nanovalve interaction, leading to displacement of the antibody, pore uncapping and finally cargo release. Model drugs such as fluorescein or Hoechst 33342 were used to evaluate the nanoplatform specificity and action. Spherical MSNs with high surface area (840 m^2 g^{-1}), surface charge of +36 mV and average diameter

and pores size of 117 and 3.8 nm, respectively, were prepared as nanoplatform. The specific antigen-antibody modification was successfully confirmed by immunostaining assay showing no nonspecific binding of the FB11 antibody to the unfunctionalized MSN surface and also no nonspecific binding of the fluorescent secondary goat anti-mouse immunostaining antibody to the unfunctionalized MSN surface or the Ft-LVS-LPS. Authors also evaluated whether a competitive FB11 antibodies displacement could be achieved in the presence of Ft-LVS-LPS. From immunostaining assays, by using both types of silane groups (APTES and triethoxy(3-isocyanatopropyl)silane) as stalks to interact with the modified antigen, successful displacement of FB11 antibodies from the MSN surface in the presence of Ft-LVS bacteria can be confirmed *in vitro* indicating that the operation of the nanovalve is feasible at high bacterial concentration. In addition, the reduction of the FB11 antibody affinity to the LPS-modified MSNs surface was achieved by acetylation of LPS-modified MSNs reducing the OH groups available for hydrogen-bonding with FB11, requiring lower Ft bacterial concentrations to displace FB11 antibody from the nanoplatform. From cargo release studies, authors reported that the use of LPS from a Ft O-antigen polymerase deletion mutant can promote better mesopores capping avoiding any cargo leakage before reach the target site. Beyond that, from this highly specific nature of the antibody-antigen interaction, a significant cargo release was detected only in Ft-LVS-LPS presence. These results suggested that the pathogen-sensitive controlled cargo release nanoplatforms can be also applied to other gram-negative bacteria as novel theranostic smart MSNs-based nanosystem for infectious diseases treatment.

5.2. Parasitic infections

MSNs have received great attention towards vaccines production due to the large amount of silanol groups on its surface that facilitates the functionalization and drugs incorporation. The surface functionalization with several molecules allows improving cells target and uptake besides favor drugs transport and release from the mesopores, leading to interesting immune and cellular responses, which makes MSNs attractive and potential nanoplatforms for vaccines fabrication against any infectious diseases (Yenkoidiok-Douti & Jewell, 2020).

Few studies have been reported in the literature applying MSNs for parasitic diseases treatment (as shown in **Table 3**). For instance, Oliveira et al. (2016) described that vaccine and prophylactic protection development against *Schistosoma mansoni* are essential to reduce the infection cases. In this way, authors reported the use of MSNs containing SWAP (soluble adult worm antigen preparation) as new strategy to treat *S. mansoni* infection. MSNs were characterized according to their size (38.8 nm), polydispersity index (0.24), zeta potential (-32.9 mV), surface area (871.19 m^2 g^{-1}) and porosity with pores volume and diameter of 0.243 cm^3 g^{-1} and 6.91 nm, respectively. SWAP was successfully

incorporated into MSNs showing EE up to 35.35%. Immunological tests indicated that MSNs were able to stimulate a high immune response compared to conventional adjuvants (SWAP-associated aluminum salt). Authors also reported that higher immunization performance observed for MSNs may be related to some unique characteristics presented by the nanosystem, such as high surface area, spherical morphology, high pores volume, stability, biocompatibility and non-toxicity which make SWAP-loaded MSNs a promising strategy to improve immune response against *S. mansoni* and enabling vaccines production.

In another study, Nhavene et al. (2018) designed multifunctional MSNs based on MCM-41 functionalized with (3-glycidoxypropy) trimethoxysilane (GPTMS) and chitosan succinate (CS) containing benznidazole (BZ) onto modified MSNs surface aiming to evaluate their action against the parasite *Trypanosoma cruzi* responsible for Chagas disease. The MSNs-like MCM-41 were successfully prepared with well-defined hexagonal arrays of uniform mesopores network, spherical shape and pores size of 3.3 nm. The MSNs functionalization with GPTMS and CS was confirmed by spectroscopic analysis. BZ anchored onto CS-modified MSNs surface via hydrogen bond interactions was confirmed by spectroscopic and density functional theory analysis. *In vitro* assays showed that the nanosystem can effectively performed BZ delivery being thirty times more active against epimastiogotes *T. cruzi* CL-Brener than free BZ, revealing its potential and effectiveness as nanocarrier for BZ delivery. Authors also concluded that all results demonstrated MSNs-GPTMS-CS as a potential and promising nanoplatform for drugs and genes delivery to treat neglected diseases such as Chagas disease or American trypanosomiasis.

Tawfeek et al. (2019) fabricated praziquantel (PZQ)-loaded MSNs in order to evaluate its therapeutic effect against murine S. *mansoni*. MSNs@PZQ showed spherical shape, average size ranging from 100 to 105 nm, zeta potential from +31.9 to +30 mV and EE of 83%. Mice were infected with *S. mansoni* and treated 6 weeks after infection with similar doses of MSNs@PQZ and free PZQ evaluating several concentrations, orally and intraperitoneally (IP). A maximum anti-schistosomal effect was achieved using MSNs@PZQ administered orally. The biomarkers related to liver oxidative stress status and immunomodulatory effect (serum TNF-α and IL-10) were significantly improved showing IP route was less effective for PQZ delivery. Authors also reported that the MSNs@PQZ administration allows the reduction of the effective therapeutic dose, indicating MSNs as a safe nanoplatform that enhances anti-schistosomal, antioxidant, immunomodulatory and anti-inflammatory PQZ actions in animal model infected by *S. mansoni*.

Lehi et al. (2019) synthesized whisker-formed SBA-15 nanoparticles as a pH-sensitive metronidazole (MNZ)-trapped nanocarrier. This nanosystem was modified with tannic acid (TA) aiming to block the mesopores and control drug release process. The SBA-15 nanowhiskers had small

fibrous structures 0.5-1.5 μm in length and up to 50 nm in diameter. Through characterization analysis, 2D ordered hexagonal mesostructures were detected, with surface area of 491.38 m^2 and pores volume and diameter of 0.593 cm^3 g^{-1} and 6.06 nm, respectively. In addition, the modification with TA increased MNZ EE from 62.6 to 71.4%. *In vitro* release assays exhibited fast MNZ release from unmodified SBA-15 nanowhiskers whereas TA-SBA-15 nanocarriers controlled MNZ release for an extended time. Interestingly, the modified nanosystems displayed a pH-sensitive behavior, showing MNZ release up to 85% at pH 5.8. The minimal lethal concentration (0.5 mg mL^{-1}) of TA-modified SBA-15@MNZ showed 100% protozoal growth inhibition for 180 min regarding to parasite control and free MNZ solution. These studies suggest this multifunctional nanoplatform as promising and efficient MNZ delivery system for parasitic diseases treatment.

5.3. Fungal infections

The development of new formulations against *Candida albicans* is essential to overcome drawbacks as multiple resistance mechanisms developed by biofilms formation, which makes this pathogen resistant to drugs such as fluconazole and amphotericin B, and, consequently, making difficult to treat effectively these infections, contributing to high morbidity and mortality rates in immunocompromised patients (Douglas, 2003; Paramanantham et al., 2018). In light of this, Paramanantham et al. (2018) reported a nanosystem based on MSNs modified with Rose Bengal (RB) as photodynamic therapy (PDT) as antimicrobial alternative to treat *C. albicans* biofilms. MSNs with average pores size and diameter of 2 and 500 nm, respectively, were amino functionalized aiming to increase the conjugation capacity of RB. RB is a photosensitizer, an organic compound that absorbs light of a suitable wavelength generating singlet oxygen and reactive oxygen species (ROS), which can kill microbial systems. High values of RB EE (58.54%) were achieved by amino-modified MSNs due to the good electrostatic interaction of the positively charged MSNs surface with anionic dye RB. Taking the aforementioned into account, *in vitro* release tests showed a slow and controlled RB release with a maximum of 66.38% after 3 h. Additionally, cellular uptake studies exhibited high MSNs-RB uptake (up to 47%) compared to the free RB (up to 10%) after 3 h. Through *in vitro* release results, amine groups modified onto MSNs enabled a slow and controlled release, by electrostatic attraction with the RB, which is desirable and allow a good PDT action after a single administration. When associated with PDT, high values of MSNs-RB antimicrobial action were achieved for both *C. albicans* planktonic cells (up to 88.7%) and biofilms (up to 79.7%) regarding pristine MSNs and free RB. Beyond that, after light irradiation, MSNs-RB exhibited high ROS production, proteins leakage (from cytoplasm *C. albicans* cells), DNA damage and lipid peroxidation. These results confirmed the MSNs-RB as an efficient nanosystem as antimicrobial PDT against infections caused by antifungal drug

resistant and biofilm forming strains, being its application extended to enhance *C. albicans* eradication on medical devices such as implants and catheters.

Econazole (ECO), an antifungal widely used for topical infections treatment has limited bioavailability due to its low aqueous solubility (Firooz et al., 2015). Aiming to overcome ECO solubility drawbacks, Montazeri et al. (2020) developed ECO-loaded MSNs modified with aminopropyl groups. Spherical shape and hexagonal mesopores arrays were detected for MSNs. Pristine MSNs, modified MSNs and ECO-loaded MSNs displayed average size ranging from 39 to 91 nm while the nanosystems presented average pores size up to 2.54 nm. In addition, MSNs was negatively charged (MSNs and MSNs-ECO showed -12.14 and -17.51 mV, respectively) whereas after amino modification the nanosystem showed positive surface charge (MSNs-NH_2 and MSNs-ECO-NH_2 exhibited +32.52 and +33.63 mV, respectively). MSNs and MSNs-NH_2 exhibited ECO EE of up to 42 and 63% and release rate of 29.57 and 38.65, respectively. Both MSNs and modified MSNs containing ECO were non-toxic to human dermal fibroblast strains cells. Distinct ECO/MSNs and modified MSNs ratios were evaluated being that the antifungal activity (*C. albicans*) for all nanosystems increased as drug amount loading increased. Greater antifungal activity was observed for modified nanosystems compared to the non-modified ones showing inhibition zone of up to 19.5 and 16.0 mm, respectively (at 1.2 mg mL^{-1} of ECO). ECO-loaded MSNs displayed greater antifungal activity regarding to the econazole cream, confirming the nanosystem efficiency for the infectious treatment caused by fungus such as *C. albicans*. Additionally, the developed nanosystem exhibited non induced skin irritation on rabbits, being cutaneous reaction negligible after 72 h. It is worth mentioning that the designed nanoplatform could reduce the treatment duration by increasing patient compliance, making this nanosystem desirable for fungal therapy purposes.

In another study, authors (Mas et al., 2014) fabricated pH-responsive gated MSNs-based nanosystem aiming to treat fungal infections such as vaginal candidiasis. The sensitive MSNs like MCM-41 nanoplatforms were loaded with tebuconazole (TEB) and modified with silane groups as 3-[2-(2-aminoethylamino)ethylamino]propyltrimethoxysilane (N3) used as gatekeepers that can avoid TEB leakage from the mesopores before the nanosystem reach the target site. Spherical-shaped silica nanoplatform with average size of 100 nm and hexagonal pores arrays with mean diameter of 2.45 nm were successfully prepared as well as the TEB loading (0.064 mmol g^{-1} of MSNs) into mesopores and subsequently capping with N3 groups (2.43 mmol g^{-1} of MSNs). For cellular uptake assays, fluorescein (FL, green dye) were loaded into MSNs and modified with the N3 gatekeeper. The simulated nanosystem exhibited good cellular internalization (*Saccharomyces cerevisiae* cells, incubated at pH 3.7) detected by fluorescence microscopy. In addition, *in vitro* release FL tests were performed at pHs 3.7 and 5.5. Results showed that more than 95% of FL was released after 12 h whereas almost no

release was detected at pH 3.7, confirming the design of pH-responsive nanosystem. At pH 3.7, the polyamines of N3 capping were more protonated than at pH 5.5, which allowed high rigid chain conformation and high interactions with anions (as SO_4^{2-}), that favor the mesopores blockage. At pH 5.5, the polyamine chains are more flexible allowing pores opening and FL release. After successful cellular uptake and FL release tests, *in vitro* antifungal assays (*C. albicans* cells) were performed with the MSNs-TEB-N3 and free TEB. Results exhibited high antifungal activity promoting 90% of cells death by using MSNs-TEB-N3 while free TB showed only 10% of action. In this way, the designed smart nanoplatform improved TEB efficacy comprising an interesting tool to overcome side effects associated with topical therapies for vulvovaginal infection and improve its cost-effectiveness. A schematic pH-responsive nanosystem action is displayed in **Figure 6**.

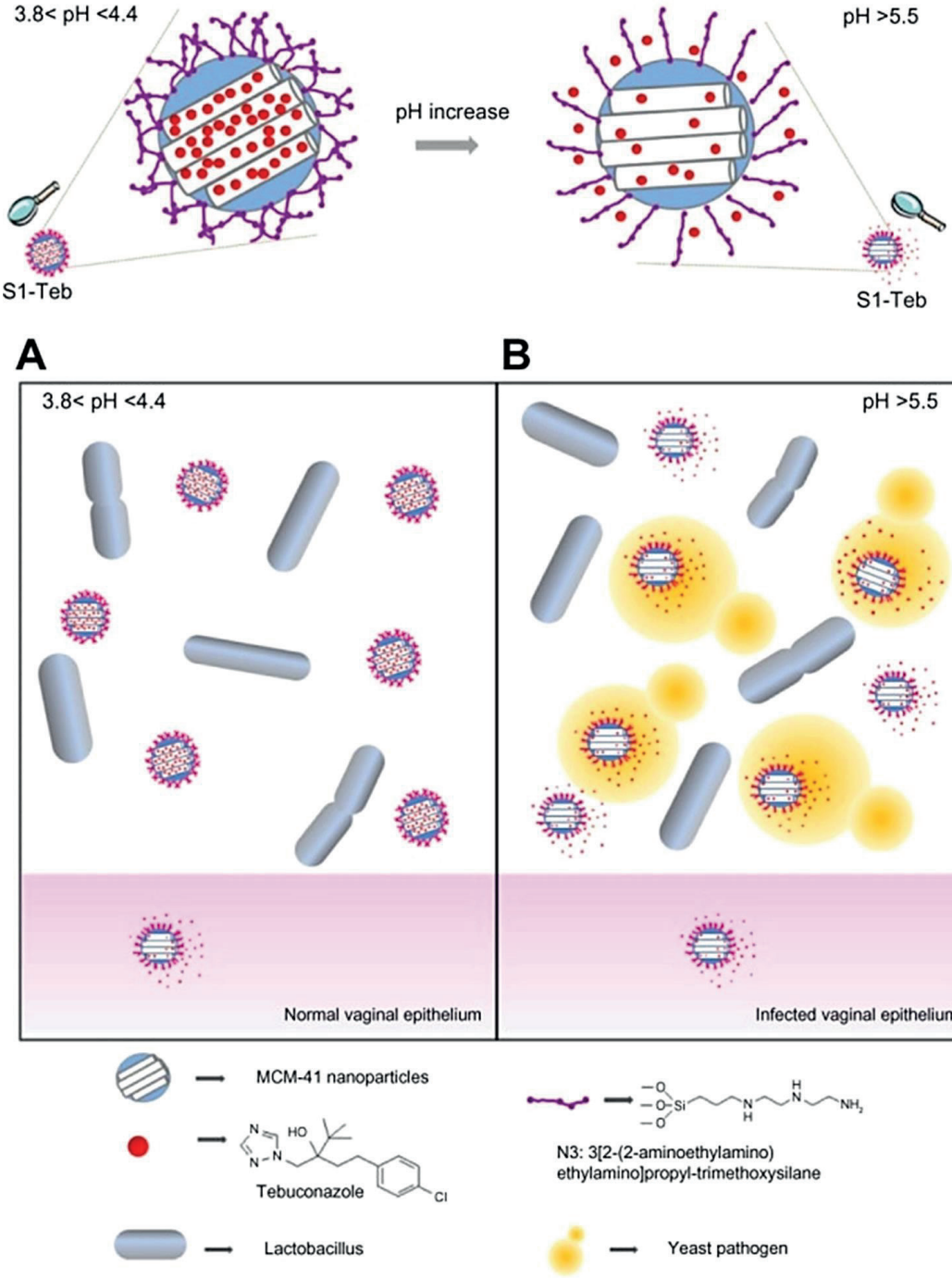

Figure 6: Schematic representation of the design and action mechanism of S1-Teb under usual vaginal conditions (A) and in the presence of *C. albicans* (B) (*S. cerevisiae* has been used in experimental

assays as a model organism). Legend: MCM-41, mobil composition of matter-41; S1-Teb, MCM-41 loaded with tebuconazole (Mas et al., 2014).

In order to facilitate metallic nanoparticles (MNPs) applications as multifunctional drug delivery systems, authors (Descalzo et al., 2006; Mitra et al., 2015; Qasim et al., 2015) have proposed their association with MSNs aiming to increase biocompatibility avoiding MNPs aggregation and action lost. Mitra et al. (2015) incorporated zinc oxide nanoparticles into MSNs (noted ZnO@MSNs) in order to evaluate the antifungal efficiency against two strains of *Aspergillus niger* (MTCC 10180 and MTCC 2196) and two strains of *Fusarium oxysporum* (NCIM 1043 and NCIM 1072). The MSNs and ZnO@MSNs nanosystems displayed spherical shape with a size ranging from 20 to 40 nm with average pore size ranging from 2.5 to 3.1 nm, respectively. The authors observed that ZnO@MSNs activity was dose dependent, requiring high doses to achieve antifungal response. The enzymatic tests showed that ZnO@MSNs activity occurred through the generation of oxidative stress through ROS generation. The generated oxidative stress caused morphological changes in the fungi. Both *in vitro* and *in vivo* tests indicated good biocompatibility of the developed nanosystem, with sustained release exerted by MSNs preventing the ZnO direct exposure reducing toxic effects, which makes the developed MSNs-based nanoplatform enable to desirable antimicrobial applications.

In another study, silver nanoparticles (AgNPs), synthesized by green synthesis using *Azadirachta indica* leaf extract as a reducing agent, were loaded into MSNs (noted MSNs-AgNPs) aiming to evaluate antifungal activity against *C. albicans* 077 strains. The fabricated MSNs presented spherical shape with size of around 400 nm and hexagonal pores structures with average size of ~7.6 nm. The impregnated AgNPs were detected onto MSNs pores/surface showing spherical shape with average size ranging from 5 to 50 nm. From antifungal activity assays, MSNs-AgNPs proved to be efficient in inhibiting the fungus growth in a dose-dependent manner, both in the disc diffusion and *in vitro* killing assays, being a promising alternative approach to infections treatment caused by *C. albicans*. However, more preclinical studies are already essential to better understand the real potential of the MSNs-AgNPs for future clinical translations (Qasim et al., 2015).

5.4. Viral infections

Viral infections and spreadability can be establish only by their interaction with host cells. The key and great challenge to develop viral infections treatment consist of understand and elucidate the interaction virus-host cells at molecular level. In addition, virus can evolve by genetic mutation and become drug resistant making urgent and essential the design of new drugs. In current medical scenario, the lack of antiviral broad-spectrum drugs, the fast and wide spreadability and the long time

demanded to elucidate virus mechanism action to design a safety and efficient vaccines or treatment making viral infections such as severe acute respiratory syndrome coronavirus 2 (SARS-CoV-2) a great threat to human global health (Lee et al., 2016, 2018; Nasrollahzadeh et al., 2020; Nikaeen et al., 2020; Weiss et al., 2020).

Taking the aforementioned into account, the design of new antiviral MSNs can be an effective approach to control viral infections inhibiting virus mechanism action by interaction with virus, targeted drug delivery, interaction with host cells receptors inducing cellular immune response (Lee et al., 2016, 2018; Nasrollahzadeh et al., 2020; Nikaeen et al., 2020; Weiss et al., 2020).

Venezuelan equine encephalitis virus (VEEV) comprises a great public health concern due to its possibility amenability for use as a bioterrorism agent and its severe health consequences in humans. In addition, natural VEEV outbreaks resulted in equine and human infections, provoking high death rates in equines (85%) and chronic neurological complications in humans. A chemical VEEV inhibitor known as ML336 was developed and its effectiveness in VEEV infection was confirmed in preclinical assays. However, the great limitation for ML336 clinical translation consists of its poor solubility and stability in biological media. Taking this into account, LaBauve et al. (2018) designed lipid-coated MSNs (LC-MSNs) as smart nanocarriers for ML336 delivery, as depicted in **Figure 7**. This nanovehicle was proposed to improve ML336 stability, promoting its controlled release for VEEV treatment. Narrow size distribution (~75 nm) and hexagonal pores structures (average pore size of 2.65 nm) were achieved for MSNs. The lipidic shell consists of a liposome structure composed by 1,2-distearoyl-sn-glycero-3-phosphocholine (DSPC): Cholestrol:1,2-distearoyl-sn-glycero-3-phosphoethanolamine-N-[methoxy(polyethylene glycol)-2000] (DSPE-PEG(2000)), which can enhance colloidal stability, circulation time besides reduce protein adsorption to the nanosystem surface. From electron microscopy analysis, LC-MSNs@ML336 showed a lipid bilayer thickness of 6 nm besides zeta potential of -1.76 mV. 20 μg ML336/mg LC-MSNs were loaded into the nanocarrier showing a ML336 release of 34% over 24 h. TC-83 VEEV infected HeLa cells were treated with LC-MSNs@ML336. Results displayed virus inhibition in a dose-dependent manner, with significantly decreased viral load by 4 orders of magnitude after 24 h and 6 orders of magnitude after 48 and 72 h. From *in vivo* assays, LC-MSNs were considered nontoxic at 0.11 g LC-MSNs/kg mouse dose administered per day for four days. In addition, LC-MSNs@ML336 exhibited significant reduction (about 10-fold) of brain viral titer in VEEV infected mice compared to PBS and other controls. These results highlighted the LC-MSNs@ML336 potential to treat VEEV infections and LC-MSNs as smart nanovehicles for antiviral applications.

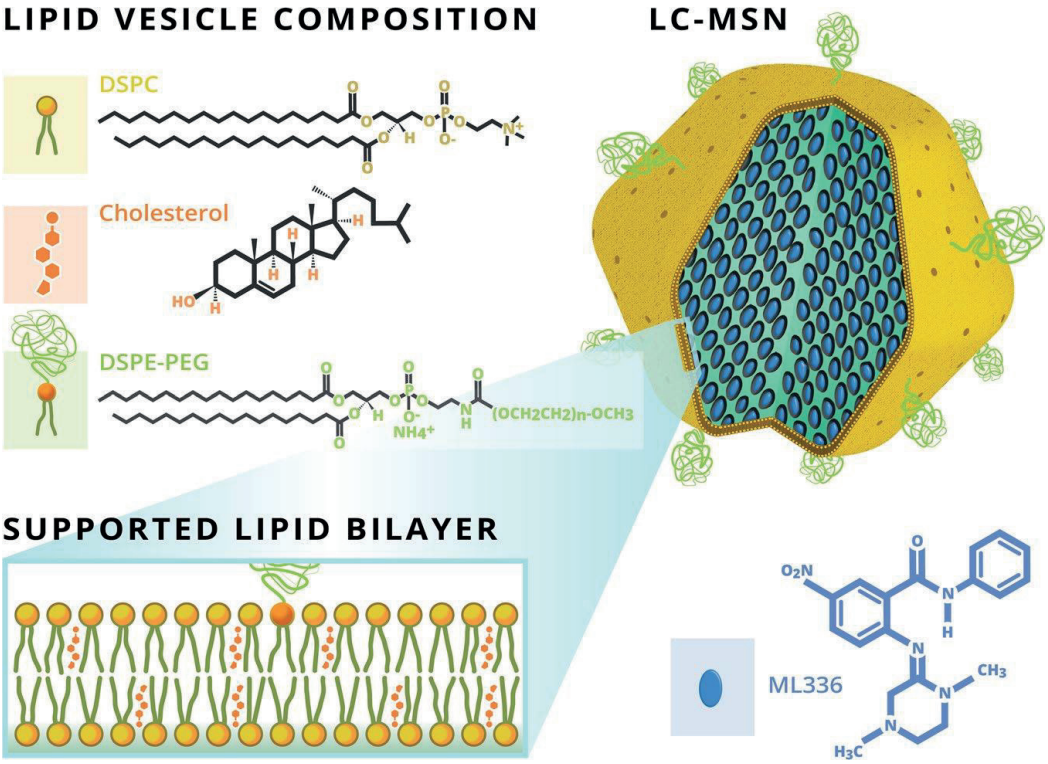

Figure 7: Schematic representation of LC-MSNs@ML336. The antiviral ML336 was incubated with MSNs prior to vesicle fusion with liposomes containing a composition of 77.5% DSPC:2.5% DSPE-PEG2000:20% cholesterol at mole ratios (LaBauve et al., 2018).

Herpes simplex virus (HSV) provokes several infectious diseases such as orolabial and genital herpes being currently treated by guanine analogues such as acyclovir, valaciclovir and others, which inhibit viral DNA replication. However, these compounds suffer from antiviral drug resistance especially in immunocompromised individuals besides show poor bioavailability being necessary several and high doses administration (Lee et al., 2016, 2018). The HSV cells infection can start by electrostatic and hydrophobic interactions between viral glycoprotein (gB or gC) and cell glycosaminoglycans (GAGs, heparan sulfate) composed of negatively charged sulfonate groups linked by hydrophobic moieties. Molecules that mimic GAGs can interact with virus avoiding their interaction and penetration into susceptible cells (E. C. Lee et al., 2016, 2018). In this context, Le et al. (2016, 2018) have designed GAG mimetic-functionalized MSNs to treat HSV-1 and HSV-2 infections. In a first work (Lee et al., 2016), aryl sulfonate GAG mimetic-modified MSNs exhibited low toxicity besides inhibited HSV-1 and HSV-2 penetration into health cells while controls were inactive. In this work, Lee et al. (2018) explored distinct functional groups related to GAG structure

attached to MSNs and investigated their activity against HSV-1 and HSV-2. In addition, authors evaluated GAG mimetic-functionalized MSNs as smart nanocarriers for acyclovir (ACV) delivery aiming simultaneously inhibition of viral penetration and DNA replication. Five modified MSNs were prepared: benzene sulfonate-modified MSNs, propyl thiol-modified MSNs, propyl sulfonate-modified MSNs, zwitterionic sulfonate-modified MSNs and phenyl-modified MSNs ((MSNs-Phenyl-SO_3, MSNs-Propyl-Thiol, MSNs-Propyl-SO_3, MSNs-Zw-SO_3 and MSNs-Phenyl, respectively). All nanoplatforms were characterized showing average size from 100-150 nm and negative surface charge (~ -40 mV), conferring good colloidal stability by interparticle repulsion. Antiviral *in vitro* assays toward HSV-1 and HSV-2 were carried out displaying that sulfonate group presence was as a prerequisite for antiviral activity, with the benzene group (from benzene sulfonate-modified MSNs) enhancing the antiviral response regarding to an alkyl group (propyl sulfonate-modified MSNs). Phenyl-modified MSNs showed a relatively weak antiviral activity, reinforcing the sulfonate group importance. From second study concerning ACV-loaded benzene sulfonate-modified MSNs (labeled ACV@MSNs-phenyl-SO_3), high drug loading (34% w/w) and controlled and prolonged ACV release (70% (w/w) up to 24 h) were detected. This release profile can be assigned to the mesopores functionalization with hydrophobic groups which can act as blockers controlling drug release. To evaluate post viral penetration into cells, Vero cells were infected with HSV-1 and then, treated with the nanoplatforms. Results exhibited higher antiviral activity for ACV@MSNs-phenyl-SO_3 than ACV@MSNs and free ACV. The targeting effect of GAG mimetic from ACV@MSNs-phenyl-SO_3 against HSV-1 was investigated achieving 100% antiviral activity whereas both no interaction with HSV-1 were detected for ACV@MSNs and free ACV. These results confirmed that the GAG mimetic-functionalized MSNs performed dual action mechanism against HSV-1 and HSV-2 opening new possibilities for virus infections treatment.

As aforementioned, viruses comprise a harmful pathogen to the humans responsible for millions of people death every year. Despites some therapies such as highly active anti-retroviral therapy available to treat human immunodeficiency virus (HIV), the demand for new therapies and vaccines are essential to fight against new viruses. To better understand the mechanism of antiviral MSNs action, Silva et al. (2016) developed modified MSNs to evaluate their biocompatibility and their ability to inhibit the virus transduction of target cells. (3-aminopropyl)triethoxysilane (APTES), (3-glycidyloxypropyl)trimethoxysilane (GPTMS) and trimethoxy-(2-phenylethyl)silane (TMPES) groups were used to modified MSNs surface and noted as MSNs-APTES, MSNs-GPTMS and MSNs-TMPES. Spherical-shaped modified MSNs with average size from 354-571 nm and negative surface charge (from -11.2 to -22.8 mV) were fabricated. Cytotoxicity assays were performed for the nanosystems exhibiting cells metabolic activity similar to the control at lower particle concentration

(10^{-5} g mL^{-1}) and cells nuclei morphology preserved after interaction. The inhibitory potential of the nanosystems to prevent virus transduction was evaluated by using a truncated version of the HIV-gp120 glycoprotein that can interact with cells containing CD4 receptor and vesicular stomatitis virus (VSV)-G envelope that can bind on different cell surfaces. When target cell was transduced by virus, green fluorescent protein (GFP) is expressed by the infected cell, that means, whether transduction occurs GFP can be detected. In this way, the pseudotyped preparation was treated with the nanosystems. At low concentration, all nanosystems reduced transduction for both recombinant lentivirus with VSV-G and HIV-gp120 envelopes. MSNs-APTES and MSNs-TMPES showed higher transduction reduction for VSV-G (~50%) and HIV-gp120 (~20%) envelopes, respectively. Theoretical studies suggested that higher hydrophobicity could favor interaction with HIV-gp120 whereas hydrophilicity could lead to better interaction with VSV-G, explain the distinct responses. These results provide new insights towards the design of specific MSNs-based nanocarriers as new strategies for viral control and anti-HIV therapy.

Porcine circovirus type 2 (PCV2) is a primary etiological agent of post-weaning multi-systemic wasting syndrome (PMWS). PMWS are severe in acute outbreaks, causing death of up to 80% of affected animals. To develop new therapies for PCV2 infections is essential for pig industries. For this reason, Guo et al. (2012) reported the preparation of PCV2 GST- open reading frames (ORF)2-E protein-loaded HMSNs as nanovaccines aiming to induce persistent immune responses of PCV2. The nanosystem was characterized exhibiting spherical shape with average size of 200 nm. Maximum protein loading amount of 15% (w/w) were achieved. Protein release profile (PBS at pH 7) was time-dependent showing rapid release (~50%) up to 12 h and slow release up to the sixth day. To evaluate the specificity of mice antibodies immunized by GST-ORF2-E, mouse sera were used in immunofluorescence experiments to determine the specificity of antibodies by PCV2-infected PK15 cells. Results displayed that no significant staining was detected suggesting specificity of the mouse antibody against PCV2. Indirect enzyme-linked immunosorbent assay assays displayed that the antibody titers of mice immunized with PCV2 GST-ORF2-E@HMSNs were higher than those of mice immunized with the GST-ORF2-E protein, especially at the third- and fourth-weeks post-vaccination. Furthermore, the T-lymphocyte proliferation response in mice induced by the PCV2 GST-ORF2-E@HMSNs remained at levels higher than those in mice immunized with the GST-ORF2-E protein, demonstrating that the proteins loaded into the HMSNs not only stimulate humoral and cellular immune responses but also induce persistent immune responses because of the release kinetics from HMSNs. Results confirmed HMSNs as an interesting efficient vaccine nanovehicle for PCV2 treatment and further studies regarding virus therapy.

6. Clinical translation, challenges, and future outlook

The challenges of any designed nanostructure for therapeutic purposes consists on achieve good biocompatibility, biodegradability, complete and short clearance time as already stated by US FDA. Considering the aforementioned, MSNs are very attractive as nanocarriers/nanotherapeutics because their interesting properties such as chemical and physical stabilities, size, morphology, surface and pores structures can be easily modulated to achieve good biological behavior and also effective drug loading and delivery at the desired site, comprising efficient nanoplatforms in most of pre-clinical assays. Internal, external or multi stimuli-responsive MSNs controlled drug delivery systems have been designed as smart nanoarchitectures that control pharmacokinetics parameters and emphasize the amazing properties of MSNs, stimulating researches towards their application in clinical trials (Farjadian et al., 2019; Kankala et al., 2020; Sábio et al., 2019).

Wiesner group (Benezra et al., 2011; Phillips et al., 2014) described the fabrication of "Cornell dots or C dots" (labeled ^{124}IcRGDY–PEG–C dots) as the first nanosilica approved by the FDA for clinical assays. A smart core-shell nanosilica containing cyanine5 dye and ^{124}I radiolabels for optical-positron emission tomography dual imaging was fabricated and modified with PEG and cyclic arginine-glycine-aspartic acid-tyrosine (cRGDY) peptides as target agent for molecular expression in human melanoma xenografts (Benezra et al., 2011; Phillips et al., 2014). Biological behavior was evaluated showing fast Cornell dots (C dots) excretion via the kidneys (~ 90%) and hepatobiliary route (~ 10%) with excretion times from 13 to 21 h (Phillips et al., 2014). These smart silica-based nanostructures were successfully applied as nanoprobes for tumors detection and monitoring in clinical assays (Bradbury et al., 2013, 2016; Phillips et al., 2014).

Chen et al. (2017) described the fabrication of C dots conjugated with the radiometal Zirconium-89 (^{89}Zr, t1/2 = 78.4 h) using two different strategies: chelator-free and chelator-based radiolabeling. The best nanosystem (labeled ^{89}Zr- desferrioxamine (DFO)-cRGDY-PEG-C′ dots) fabricated by chelator-based radiolabeling exhibited higher *in vivo* radiostability with good renal clearance, low reticuloendothelial system accumulation, high tumor uptake and target-to-background ratios relative to biological controls for human melanoma xenograft models. The first clinical trial using ^{89}Zr-DFO-cRGDY-PEG-C′ dots has been carried out for bioimaging of malignant brain tumors (NCT03465618).

Kharlamov et al. (2012) described the application of plasmonic photothermal therapy (PPTT) by using near-infrared (NIR) laser irradiation onto silica-gold nanoparticles (AuNPs) for Angioplasty and artery remodeling. Interesting safety level and significant treatment efficacy with plaque burden reduction (79.4 mm^3) was successfully achieved. In this regard, authors (Kharlamov et al., 2015) conducted a first-in-man trial (labeled NANOM-FIM, NCT01270139) by using multifunctional silica-

AuNPs-dispersed on-artery patch associated with PPTT for atherosclerosis treatment. Results exhibited significant regression of coronary atherosclerosis with good biocompatibility and no significant toxicity besides lower risk of cardiovascular death in humans. This bioengineered nanostructure offers great potential for further atherosclerosis theranostic purposes.

The clinical applications of aforementioned silica-based nanostructures encourage researchers focuses on MSNs clinical translation and further commercialization. Although several researches have been performed in the last two decades towards the biological behavior and preclinical evaluation of smart and engineered stimuli-responsive MSNs for monitoring and/or therapeutic purposes (Bobo et al., 2016; Croissant et al., 2017, 2018; Dogra et al., 2018; Kankala et al., 2020; Lei et al., 2020; Sábio et al., 2019; Yang et al., 2019), achieve their clinical translation is still a great challenge requiring long-term stability, scale-up of these nanostructures (from bench to industrial scale-up) and overcome obstacles in animal trials and regulating authorities evaluation (Farjadian et al., 2019; Kankala et al., 2020; Lei et al., 2020). Despites the numerously reports concerning multifunctional MSNs fabrication, their scale-up is rarely described. Some authors (Kim et al., 2019; Šoltys et al., 2018) reported large-scale synthesis of dense and hollow mesoporous silica micro/nanoparticles (Šoltys et al., 2018) and monodisperse small MSNs with a fine size distribution at room temperature (27 °C) (Kim et al., 2019), both methods using CTAB as template. The structural stability of nanoparticles is usually determined by interaction with the biological environment and between themselves. Poor colloidal and thermal stabilities can result in drawbacks with long-term storage and nanosystems administration. In this sense, MSNs present robust silica framework and exceptional electronic architecture easily optimized, making them amazing nanoarchitectures with interesting structural stability for biomedical applications (Kankala et al., 2019). Additionally, authors reported that the association of MSNs with metals such as iron, Pt, Al and others, can improve the nanoplatforms thermal and physical stabilities considering a critical ratio of metal to silica content (Kankala et al., 2019).

Up to now, preclinical assays related to MSNs were successfully performed whereas no MSNs have been described in clinical trials. Authors (Farjadian et al., 2019) suggested that the clinical translation has failed due to the large physiological distinction between small animals and humans, indicating that animal models are not the better indication for further nanostructures success in humans. In addition, authors suggest that rather than prolonged xenografting experiments (in cancer treatment), positive animal toxicological results could allow to start phase 1 of clinical trials.

Another concern related to MSNs or any nanostructures for clinical translation relies on regulatory agencies (as FDA) evaluation. Currently, nanostructured materials are evaluated as small-molecule drugs, being that some nanosystems can act only as nanoprobes or without loaded drugs. In this sense, the actual evaluation processes by agencies comprise a bottleneck that allow only a few

percentages of nanostructures can be approved for commercial purposes. Authors suggested that regulatory agencies could create specific evaluation category for nanomedicines aiming to streamline their translation (Farjadian et al., 2019; Kankala et al., 2020; Lei et al., 2020).

Finally, taking into account all abovementioned challenges, the tunable properties of MSNs and recent advances regarding smart and multi stimuli-responsive MSNs for diagnosis, therapy or theranostic applications, we can expect in the next years MSNs-based nanoplatforms and other silica-based nanosystems will become approved by FDA, impacting the treatment way and global human health.

7. Conclusions

Currently, there is a great global concern regarding infectious diseases, especially those without well-established therapy or, mostly, which exhibits multidrug resistant microorganisms. Recently, nanomedicine has emerged from the nanotechnology as a wide and great approach to overcome drawbacks in biomedical field imposed by several diseases. More precisely, MSNs have great potential for biomedical application due to their interesting properties including biocompatibility, biodegradability, easy clearance, tunable physicochemical properties as size, shape and pores size. MSNs multifunctionality opens up several possibilities to fabricate smart and targeted nanomedicines or nanovaccines for infectious diseases prevention and treatment. These nanoplatforms can promote specific and controlled drug release at target disease cells/tissues improving treatment efficacy minimizing side effects besides no patient compliance. Despites MSNs potential has received great attention in the last years towards the design of new formulations and therapies, MSNs applications to treat infectious diseases such as parasites, viruses and fungi have been already scarce up to now. As depicted in this review, only MSNs-based nanocarriers for bacterial infections and treatment have been widely exploited, which opens several opportunities to design multifunctional MSNs-based nanoplatforms for controlled drug delivery to threat the most of infectious diseases presented nowadays. Although very few reports are described regarding MSNs-based nanovehicles in clinical assays, the good biological behavior, unceasing preclinical tests performed and the last trends using these nanosystems, allow us to prospect a clinical translation in a near future.

8. Acknowledgments

This study was financed in part by the Coordenação de Aperfeiçoamento de Pessoal de Ensino Superior – Brasil (CAPES) – Finance code – 001. The authors also are grateful to the São Paulo Research Foundation (FAPESP, Brazil, Grant #2018/25377-3) for research fellowship and financial support. This study is part of the National Institute of Science and Technology in Pharmaceutical

Nanotechnology: a transdisciplinary approach INCT-NANOFARMA, which is supported by São Paulo Research Foundation (FAPESP, Brazil) Grant #2014/50928-2, and by "Conselho Nacional de Desenvolvimento Científico e Tecnológico" (CNPq, Brazil) Grant # 465687/2014-8.

9. Declaration of conflicts of interest

The authors report no conflicts of interest associated with this publication.

10. References

Abdelbar, M. F., Shams, R. S., Morsy, O. M., Hady, M. A., Shoueir, K., & Abdelmonem, R. (2020). Highly ordered functionalized mesoporous silicate nanoparticles reinforced poly (lactic acid) gatekeeper surface for infection treatment. *International Journal of Biological Macromolecules*, *156*, 858–868. https://doi.org/10.1016/j.ijbiomac.2020.04.119

Abdullah, M. A. I. A., Al Dajah, S., Murad, A. A. B. U., El-Salem, A. M., & Khafajah, A. L. I. M. (2019). Extraction, Purification, and Characterization of Lycopene from Jordanian Vine Tomato Cultivar, and Study of its Potential Natural Antioxidant Effect on Samen Baladi. *Current Research in Nutrition and Food Science*, 7(2), 532-546. http://dx.doi.org/10.12944/CRNFSJ.7.2.22

Andersson, J., Rosenholm, J., Areva, S., & Lindén, M. (2004). Influences of Material Characteristics on Ibuprofen Drug Loading and Release Profiles from Ordered Micro- and Mesoporous Silica Matrices. *Chemistry of Materials*, *16*(21), 4160–4167. https://doi.org/10.1021/cm0401490

Andrade, G. F., Faria, J. A. Q. A., Gomes, D. A., de Barros, A. L. B., Fernandes, R. S., Coelho, A. C. S., Takahashi, J. A., da Silva Cunha, A., & de Sousa, E. M. B. (2018). Mesoporous silica SBA-16/hydroxyapatite-based composite for ciprofloxacin delivery to bacterial bone infection. *Journal of Sol-Gel Science and Technology*, *85*(2), 369–381. https://doi.org/10.1007/s10971-017-4557-y

Arriagada, F., Nonell, S., & Morales, J. (2019). Silica-based nanosystems for therapeutic applications in the skin. *Nanomedicine*, *14*(16), 2243–2267. https://doi.org/10.2217/nnm-2019-0052

Arroyo, J., Miller, C. A., Catalan, J., & Monath, T. P. (2001). Yellow fever vector live-virus vaccines: West Nile virus vaccine development. *Trends in Molecular Medicine*, *7*(8), 350–354. https://doi.org/10.1016/S1471-4914(01)02048-2

Baeza, A., Ruiz-Molina, D., & Vallet-Regí, M. (2017). Recent advances in porous nanoparticles for drug delivery in antitumoral applications: inorganic nanoparticles and nanoscale metal-organic frameworks. *Expert Opinion on Drug Delivery*, *14*(6), 783–796. https://doi.org/10.1080/17425247.2016.1229298

Barrett, A. D. T., & Higgs, S. (2007). Yellow fever: a disease that has yet to be conquered. *Annu. Rev. Entomol.*, *52*, 209–229. https://doi.org/10.1146/annurev.ento.52.110405.091454

Benezra, M., Penate-Medina, O., Zanzonico, P. B., Schaer, D., Ow, H., Burns, A., DeStanchina, E., Longo, V., Herz, E., Iyer, S., Wolchok, J., Larson, S. M., & others. (2011). Multimodal silica nanoparticles are effective cancer-targeted probes in a model of human melanoma. *Journal of Clinical Investigation*, *121*(7), 2768–2780. https://doi.org/10.1172/JCI45600

Bobo, D., Robinson, K. J., Islam, J., Thurecht, K. J., & Corrie, S. R. (2016). Nanoparticle-Based Medicines: A Review of FDA-Approved Materials and Clinical Trials to Date. *Pharmaceutical Research*, *33*(10), 2373–2387. https://doi.org/10.1007/s11095-016-1958-5

Bonifácio, B., Silva, P., Ramos, M., Negri, K., Maria Bauab, T., & Chorilli, M. (2013). Nanotechnology-based drug delivery systems and herbal medicines: a review. *International Journal of Nanomedicine*, *9*(1), 1-15. https://doi.org/10.2147/IJN.S52634

Bradbury, M. S., Pauliah, M., Zanzonico, P., Wiesner, U., & Patel, S. (2016). Intraoperative mapping of sentinel lymph node metastases using a clinically translated ultrasmall silica nanoparticle. *Wiley Interdisciplinary Reviews: Nanomedicine and Nanobiotechnology*, *8*(4), 535–553. https://doi.org/10.1002/wnan.1380

Bradbury, M. S., Phillips, E., Montero, P. H., Cheal, S. M., Stambuk, H., Durack, J. C., Sofocleous, C. T., Meester, R. J. C., Wiesner, U., & Patel, S. (2013). Clinically-translated silica nanoparticles as dual-modality cancer-targeted probes for image-guided surgery and interventions. *Integrative Biology*, *5*(1), 74–86. https://doi.org/10.1039/c2ib20174g

Burns, A. A., Vider, J., Ow, H., Herz, E., Penate-Medina, O., Baumgart, M., Larson, S. M., Wiesner, U., & Bradbury, M. (2009). Fluorescent silica nanoparticles with efficient urinary excretion for nanomedicine. *Nano Letters*, *9*(1), 442–448. https://doi.org/10.1021/nl803405h

Calixto, G., Bernegossi, J., de Freitas, L., Fontana, C., & Chorilli, M. (2016). Nanotechnology-Based Drug Delivery Systems for Photodynamic Therapy of Cancer: A Review. *Molecules*, *21*(3), Article 342. https://doi.org/10.3390/molecules21030342

Cao, C., Ge, W., Yin, J., Yang, D., Wang, W., Song, X., Hu, Y., Yin, J., & Dong, X. (2020). Mesoporous Silica Supported Silver–Bismuth Nanoparticles as Photothermal Agents for Skin Infection Synergistic Antibacterial Therapy. *Small*, *16*(24), Article 2000436. https://doi.org/10.1002/smll.202000436

Chen, F., Ma, K., Zhang, L., Madajewski, B., Zanzonico, P., Sequeira, S., Gonen, M., Wiesner, U., & Bradbury, M. S. (2017). Target-or-Clear Zirconium-89 Labeled Silica Nanoparticles for Enhanced Cancer-Directed Uptake in Melanoma: A Comparison of Radiolabeling Strategies. *Chemistry of Materials*, *29*(19), 8269–8281. https://doi.org/10.1021/acs.chemmater.7b02567

Chen, G., Teng, Z., Su, X., Liu, Y., & Lu, G. (2015). Unique biological degradation behavior of Stöber mesoporous silica nanoparticles from their interiors to their exteriors. *Journal of Biomedical Nanotechnology*, *11*(4), 722–729. https://doi.org/10.1166/jbn.2015.2072

Chen, W., Cheng, C.-A., Lee, B.-Y., Clemens, D. L., Huang, W.-Y., Horwitz, M. A., & Zink, J. I. (2018). Facile strategy enabling both high loading and high release amounts of the water-insoluble drug Clofazimine using mesoporous silica nanoparticles. *ACS Applied Materials & Interfaces*, *10*(38), 31870–31881. https://doi.org/10.1021/acsami.8b09069

Chen, W., Glackin, C. A., Horwitz, M. A., & Zink, J. I. (2019). Nanomachines and Other Caps on Mesoporous Silica Nanoparticles for Drug Delivery. *Accounts of Chemical Research*, *52*(6), 1531–1542. https://doi.org/10.1021/acs.accounts.9b00116

Chen, Y.-C., Chen, S.-J., Cheng, H.-F., & Yeh, M.-K. (2020). Development of Yersinia pestis F1 antigen-loaded liposome vaccine against plague using microneedles as a delivery system. *Journal of Drug Delivery Science and Technology*, *55*, Article 101443. https://doi.org/10.1016/j.jddst.2019.101443

Cho, M., Cho, W.-S., Choi, M., Kim, S. J., Han, B. S., Kim, S. H., Kim, H. O., Sheen, Y. Y., & Jeong, J. (2009). The impact of size on tissue distribution and elimination by single intravenous injection of silica nanoparticles. *Toxicology Letters*, *189*(3), 177–183. https://doi.org/10.1016/j.toxlet.2009.04.017

Clemens, D. L., Lee, B.-Y., Plamthottam, S., Tullius, M. V., Wang, R., Yu, C.-J., Li, Z., Dillon, B. J., Zink, J. I., & Horwitz, M. A. (2019). Nanoparticle Formulation of Moxifloxacin and Intramuscular Route of Delivery Improve Antibiotic Pharmacokinetics and Treatment of Pneumonic Tularemia in a Mouse Model. *ACS Infectious Diseases*, *5*(2), 281–291. https://doi.org/10.1021/acsinfecdis.8b00268

Clemens, D. L., Lee, B.-Y., Xue, M., Thomas, C. R., Meng, H., Ferris, D., Nel, A. E., Zink, J. I., & Horwitz, M. A. (2012). Targeted Intracellular Delivery of Antituberculosis Drugs to Mycobacterium tuberculosis-Infected Macrophages via Functionalized Mesoporous Silica Nanoparticles. *Antimicrobial Agents and Chemotherapy*, *56*(5), 2535–2545. https://doi.org/10.1128/AAC.06049-11

Croissant, J. G., Fatieiev, Y., Almalik, A., & Khashab, N. M. (2018). Mesoporous silica and organosilica nanoparticles: physical chemistry, biosafety, delivery strategies, and biomedical applications. *Advanced Healthcare Materials*, *7*(4), Article 1700831. https://doi.org/10.1002/adhm.201700831

Croissant, J. G., Fatieiev, Y., & Khashab, N. M. (2017). Degradability and clearance of silicon, organosilica, silsesquioxane, silica mixed oxide, and mesoporous silica nanoparticles. *Advanced Materials*, *29*(9), Article 1604634. https://doi.org/10.1002/adma.201604634

Deaconu, M., Nicu, I., Tincu, R., Brezoiu, A.-M., Mitran, R.-A., Vasile, E., Matei, C., & Berger, D. (2018). Tailored doxycycline delivery from MCM-41-type silica carriers. *Chemical Papers*, *72*(8), 1869–1880. https://doi.org/10.1007/s11696-018-0457-z

Deaconu, M., Pintilie, L., Vasile, E., Mitran, R.-A., Pircalabioru, G. G., Matei, C., Chifiriuc, M. C., & Berger, D. (2019). Norfloxacin delivery systems based on MCM-type silica carriers designed for the treatment of severe infections. *Materials Chemistry and Physics*, *238*, Article 121886. https://doi.org/10.1016/j.matchemphys.2019.121886

Deen, J., Mengel, M. A., & Clemens, J. D. (2020). Epidemiology of cholera. *Vaccine*, *38*, A31-A40. https://doi.org/10.1016/j.vaccine.2019.07.078

Descalzo, A. B., Martínez-Máñez, R., Sancenón, F., Hoffmann, K., & Rurack, K. (2006). The Supramolecular Chemistry of Organic–Inorganic Hybrid Materials. *Angewandte Chemie International Edition*, *45*(36), 5924–5948. https://doi.org/10.1002/anie.200600734

Ding, Y., Hao, Y., Yuan, Z., Tao, B., Chen, M., Lin, C., Liu, P., & Cai, K. (2020). A dual-functional implant with an enzyme-responsive effect for bacterial infection therapy and tissue regeneration. *Biomaterials Science*, *8*(7), 1840–1854. https://doi.org/10.1039/C9BM01924C

Dogra, P., Adolphi, N. L., Wang, Z., Lin, Y.-S., Butler, K. S., Durfee, P. N., Croissant, J. G., Noureddine, A., Coker, E. N., Bearer, E. L., & others. (2018). Establishing the effects of mesoporous silica nanoparticle properties on in vivo disposition using imaging-based pharmacokinetics. *Nature Communications*, *9*(1), Article 4551. https://doi.org/10.1038/s41467-018-06730-z

Douglas, L. J. (2003). Candida biofilms and their role in infection. *Trends in Microbiology*, *11*(1), 30–36. https://doi.org/10.1016/S0966-842X(02)00002-1

Drouet, C. (2020). Nanotechnologies: A Key Role in Virus Fight. *Biomed. J. Sci. & Tech. Res.*, *27*(2), 20774–20782. https://doi.org/10.26717/BJSTR.2020.27.004500

Edler, K. J. (2005). Current understanding of formation mechanisms in surfactant-templated materials. *Australian Journal of Chemistry*, *58*(9), 627–643. https://doi.org/10.1071/CH05141

Edrissian, G., Rokni, M., & Mohebali, M. (2016). History of Medical Parasitology and Parasitic Infections in Iran. In *Archives of Iranian Medicine, 19*(8).

Ehrlich, H., Demadis, K. D., Pokrovsky, O. S., & Koutsoukos, P. G. (2010). Modern views on desilicification: biosilica and abiotic silica dissolution in natural and artificial environments. *Chemical Reviews*, *110*(8), 4656–4689. https://doi.org/10.1021/cr900334y

Emerich, D. F., & Thanos, C. G. (2003). Nanotechnology and medicine. *Expert Opinion on Biological Therapy*, *3*(4), 655–663. https://doi.org/10.1517/14712598.3.4.655

Encinas, N., Angulo, M., Astorga, C., Colilla, M., Izquierdo-Barba, I., & Vallet-Regí, M. (2019). Mixed-charge pseudo-zwitterionic mesoporous silica nanoparticles with low-fouling and reduced cell uptake properties. *Acta Biomaterialia*, *84*, 317–327. https://doi.org/10.1016/j.actbio.2018.12.012

Epstein, F. H., Quagliarello, V., & Scheld, W. M. (1992). Bacterial Meningitis: Pathogenesis, Pathophysiology, and Progress. *New England Journal of Medicine*, *327*(12), 864–872. https://doi.org/10.1056/NEJM199209173271208

Farjadian, F., Roointan, A., Mohammadi-Samani, S., & Hosseini, M. (2019). Mesoporous silica nanoparticles: Synthesis, pharmaceutical applications, biodistribution, and biosafety assessment. *Chemical Engineering Journal*, *359*, 684–705. https://doi.org/10.1016/j.cej.2018.11.156

Feldmann, H., & Geisbert, T. W. (2011). Ebola haemorrhagic fever. *The Lancet*, *377*(9768), 849–862. https://doi.org/10.1016/S0140-6736(10)60667-8

Figueiras, A. R. R., Coimbra, A. B., & Veiga, F. J. B. (2014). Nanotecnologia na saúde: aplicações e perspectivas. *Boletim Informativo Geum*, *5*(2), Article 14.

Finnie, K. S., Waller, D. J., Perret, F. L., Krause-Heuer, A. M., Lin, H. Q., Hanna, J. V., & Barbé, C. J. (2009). Biodegradability of sol–gel silica microparticles for drug delivery. *Journal of Sol-Gel Science and Technology*, *49*(1), 12–18. https://doi.org/10.1007/s10971-008-1847-4

Firooz, A., Nafisi, S., & Maibach, H. I. (2015). Novel drug delivery strategies for improving econazole antifungal action. *International Journal of Pharmaceutics*, *495*(1), 599–607. https://doi.org/10.1016/j.ijpharm.2015.09.015

Flodström, K., Wennerström, H., & Alfredsson, V. (2004). Mechanism of mesoporous silica formation. A time-resolved NMR and TEM study of silica-block copolymer aggregation. *Langmuir*, *20*(3), 680–688. https://doi.org/10.1021/la030173c

Fu, C., Liu, T., Li, L., Liu, H., Chen, D., & Tang, F. (2013). The absorption, distribution, excretion and toxicity of mesoporous silica nanoparticles in mice following different exposure routes. *Biomaterials*, *34*(10), 2565–2575. https://doi.org/10.1016/j.biomaterials.2012.12.043

Fujii, Y., Goto, H., Watanabe, T., Yoshida, T., & Kawaoka, Y. (2003). Selective incorporation of influenza virus RNA segments into virions. *Proceedings of the National Academy of Sciences*, *100*(4), 2002–2007. https://doi.org/10.1073/pnas.0437777210

Gao, C., Qiu, H., Zeng, W., Sakamoto, Y., Terasaki, O., Sakamoto, K., Chen, Q., & Che, S. (2006). Formation Mechanism of Anionic Surfactant-Templated Mesoporous Silica. *Chemistry of Materials*, *18*, 3904–3914. https://doi.org/10.1021/cm061107+

Giret, S., Wong Chi Man, M., & Carcel, C. (2015). Mesoporous-Silica-Functionalized Nanoparticles for Drug Delivery. *Chemistry – A European Journal*, *21*(40), 13850–13865. https://doi.org/10.1002/chem.201500578

González, B., Colilla, M., Díez, J., Pedraza, D., Guembe, M., Izquierdo-Barba, I., & Vallet-Regí, M. (2018). Mesoporous silica nanoparticles decorated with polycationic dendrimers for infection treatment. *Acta Biomaterialia*, *68*, 261–271. https://doi.org/10.1016/j.actbio.2017.12.041

Gounani, Z., Asadollahi, M. A., Meyer, R. L., & Arpanaei, A. (2018). Loading of polymyxin B onto anionic mesoporous silica nanoparticles retains antibacterial activity and enhances biocompatibility. *International Journal of Pharmaceutics*, *537*(1–2), 148–161. https://doi.org/10.1016/j.ijpharm.2017.12.039

Grün, M., Lauer, I., & Unger, K. K. (1997). The synthesis of micrometer- and submicrometer-size spheres of ordered mesoporous oxide MCM-41. *Advanced Materials*, *9*(3), 254–257. https://doi.org/10.1002/adma.19970090317

Guido, R. V. C., Andricopulo, A. D., & Oliva, G. (2010). Planejamento de fármacos, biotecnologia e química medicinal: aplicações em doenças infecciosas. *Estudos Avançados*, *24*(70), 81–98. https://doi.org/10.1590/S0103-40142010000300006

Guo, H.-C., Feng, X.-M., Sun, S.-Q., Wei, Y.-Q., Sun, D.-H., Liu, X.-T., Liu, Z.-X., Luo, J.-X., & Yin, H. (2012). Immunization of mice by Hollow Mesoporous Silica Nanoparticles as carriers of Porcine Circovirus Type 2 ORF2 Protein. *Virology Journal*, *9*(1), Article 108. https://doi.org/10.1186/1743-422X-9-108

Hao, N., Chen, X., Jeon, S., & Yan, M. (2015). Carbohydrate-Conjugated Hollow Oblate Mesoporous Silica Nanoparticles as Nanoantibiotics to Target Mycobacteria. *Advanced Healthcare Materials*, *4*(18), 2797–2801. https://doi.org/10.1002/adhm.201500491

Hao, N., Liu, H., Li, L., Chen, D., Li, L., & Tang, F. (2012). In vitro degradation behavior of silica nanoparticles under physiological conditions. *Journal of Nanoscience and Nanotechnology*, *12*(8), 6346–6354. https://doi.org/10.1166/jnn.2012.6199

He, Q., Shi, J., Zhu, M., Chen, Y., & Chen, F. (2010). The three-stage in vitro degradation behavior of mesoporous silica in simulated body fluid. *Microporous and Mesoporous Materials*, *131*(1–3), 314–320. https://doi.org/10.1016/j.micromeso.2010.01.009

He, Q., Zhang, Z., Gao, F., Li, Y., & Shi, J. (2011). In vivo biodistribution and urinary excretion of mesoporous silica nanoparticles: effects of particle size and PEGylation. *Small*, *7*(2), 271–280. https://doi.org/10.1002/smll.201001459

Heikkilä, T., Salonen, J., Tuura, J., Hamdy, M., Mul, G., Kumar, N., Salmi, T., Murzin, D., Laitinen, L., & Kaukonen, A. (2007). Mesoporous silica material TUD-1 as a drug delivery system. *International Journal of Pharmaceutics*, *331*(1), 133–138. https://doi.org/10.1016/j.ijpharm.2006.09.019-a

Heikkilä, T., Salonen, J., Tuura, J., Kumar, N., Salmi, T., Murzin, D. Y., Hamdy, M. S., Mul, G., Laitinen, L., Kaukonen, A. M., & others. (2007). Evaluation of Mesoporous TCPSi, MCM-41, SBA-15, and TUD-1 Materials as API Carriers for Oral Drug Delivery. *Drug Delivery*, *14*(6), 337–347. https://doi.org/10.1080/10717540601098823-b

Heikkinen, L. S., Kazlauskas, A., Melén, K., Wagner, R., Ziegler, T., Julkunen, I., & Saksela, K. (2008). Avian and 1918 Spanish influenza a virus NS1 proteins bind to Crk/CrkL Src homology 3 domains to activate host cell signaling. *Journal of Biological Chemistry*, *283*(9), 5719–5727. https://doi.org/10.1074/jbc.M707195200

Henry, R. (2019). Etymologia: Poliomyelitis. *Emerging Infectious Diseases*, *25*(8), Article 1611.https://doi.org/ 10.3201/eid2508.ET2508

Hobbs, E. C., Trevisan, C., Johansen, M. V., Dorny, P., & Gabriël, S. (2019). Value of electronic educational media in combatting parasitic diseases. *Trends in Parasitology*, *35*(3), 173–176. https://doi.org/10.1016/j.pt.2018.10.001

Hollamby, M. J., Borisova, D., Brown, P., Eastoe, J., Grillo, I., & Shchukin, D. (2012). Growth of mesoporous silica nanoparticles monitored by time-resolved small-angle neutron scattering. *Langmuir*, *28*(9), 4425–4433. https://doi.org/10.1021/la203097x

Huang, X., Li, L., Liu, T., Hao, N., Liu, H., Chen, D., & Tang, F. (2011). The shape effect of mesoporous silica nanoparticles on biodistribution, clearance, and biocompatibility in vivo. *ACS Nano*, *5*(7), 5390–5399. https://doi.org/10.1021/nn200365a

Huang, X., Teng, X., Chen, D., Tang, F., & He, J. (2010). The effect of the shape of mesoporous silica nanoparticles on cellular uptake and cell function. *Biomaterials*, *31*(3), 438–448. https://doi.org/10.1016/j.biomaterials.2009.09.060

Hwang, A. A., Lee, B.-Y., Clemens, D. L., Dillon, B. J., Zink, J. I., & Horwitz, M. A. (2015). pH-Responsive Isoniazid-Loaded Nanoparticles Markedly Improve Tuberculosis Treatment in Mice. *Small*, *11*(38), 5066–5078. https://doi.org/10.1002/smll.201500937

Jammaer, J., Aerts, A., D'Haen, J., Seo, J. W., & Martens, J. A. (2009). Convenient synthesis of ordered mesoporous silica at room temperature and quasi-neutral pH. *Journal of Materials Chemistry*, *19*(44), 8290–8293. https://doi.org/10.1039/B915273C

Kankala, R. K., Han, Y., Na, J., Lee, C., Sun, Z., Wang, S., Kimura, T., Ok, Y. S., Yamauchi, Y., Chen, A., & Wu, K. C. -W. (2020). Nanoarchitectured Structure and Surface Biofunctionality of Mesoporous Silica Nanoparticles. *Advanced Materials*, *32*(23), Article 1907035. https://doi.org/10.1002/adma.201907035

Kankala, R. K., Zhang, H., Liu, C., Kanubaddi, K. R., Lee, C., Wang, S., Cui, W., Santos, H. A., Lin, K., & Chen, A. (2019). Metal Species–Encapsulated Mesoporous Silica Nanoparticles: Current Advancements and Latest Breakthroughs. *Advanced Functional Materials*, *29*(43), Article 1902652. https://doi.org/10.1002/adfm.201902652

Kharlamov, A. N., & Gabinsky, J. L. (2012). Plasmonic Photothermic and Stem Cell Therapy of Atherosclerotic Plaque As a Novel Nanotool for Angioplasty and Artery Remodeling. *Rejuvenation Research*, *15*(2), 222–230. https://doi.org/10.1089/rej.2011.1305

Kharlamov, A. N., Tyurnina, A. E., Veselova, V. S., Kovtun, O. P., Shur, V. Y., & Gabinsky, J. L. (2015). Silica-gold nanoparticles for atheroprotective management of plaques: Results of the NANOM-FIM trial. *Nanoscale*, *7*(17), 8003–8015. https://doi.org/10.1039/c5nr01050k

Kim, C., Yoon, S., & Lee, J. H. (2019). Facile large-scale synthesis of mesoporous silica nanoparticles at room temperature in a monophasic system with fine size control. *Microporous and Mesoporous Materials*, *288*, Article 109595. https://doi.org/10.1016/j.micromeso.2019.109595

Kitamura, N., Semler, B. L., Rothberg, P. G., Larsen, G. R., Adler, C. J., Dorner, A. J., Emini, E. A., Hanecak, R., Lee, J. J., van der Werf, S., & others. (1981). Primary structure, gene organization and polypeptide expression of poliovirus RNA. *Nature*, *291*(5816), 547–553. https://doi.org/10.1038/291547a0

Kleitz, F., Liu, D., Anilkumar, G. M., Park, I.-S., Solovyov, L. A., Shmakov, A. N., & Ryoo, R. (2003). Large cage face-centered-cubic Fm 3 m mesoporous silica: synthesis and structure. *The Journal of Physical Chemistry B*, *107*(51), 14296–14300. https://doi.org/10.1021/jp036136b

Koelman, D. L. H., Brouwer, M. C., & van de Beek, D. (2019). *Targeting the complement system in bacterial meningitis*. Oxford University Press.

Kumar, D., Schumacher, K., von Hohenesche, C. du F., Grün, M., & Unger, K. K. (2001). MCM-41, MCM-48 and related mesoporous adsorbents: their synthesis and characterisation. *Colloids and Surfaces A: Physicochemical and Engineering Aspects*, *187*, 109–116. https://doi.org/10.1016/S0927-7757(01)00638-0

Kumar, R., Roy, I., Ohulchanskky, T. Y., Vathy, L. A., Bergey, E. J., Sajjad, M., & Prasad, P. N. (2010). In vivo biodistribution and clearance studies using multimodal organically modified silica nanoparticles. *ACS Nano*, *4*(2), 699–708. https://doi.org/10.1021/nn901146y LaBauve, A. E., Rinker, T. E., Noureddine, A., Serda, R. E., Howe, J. Y., Sherman, M. B., Rasley, A., Brinker, C. J., Sasaki, D. Y., & Negrete, O. A. (2018). Lipid-Coated Mesoporous Silica Nanoparticles for the Delivery of the ML336 Antiviral to Inhibit Encephalitic Alphavirus Infection. *Scientific Reports*, *8*(1), Article 13990. https://doi.org/10.1038/s41598-018-32033-w

Lahiri, B. B., Divya, M. P., Bagavathiappan, S., Thomas, S., & Philip, J. (2012). Detection of pathogenic gram negative bacteria using infrared thermography. *Infrared Physics & Technology*, *55*(6), 485–490. https://doi.org/10.1016/j.infrared.2012.07.011

Lee, B.-Y., Li, Z., Clemens, D. L., Dillon, B. J., Hwang, A. A., Zink, J. I., & Horwitz, M. A. (2016). Redox-Triggered Release of Moxifloxacin from Mesoporous Silica Nanoparticles Functionalized with Disulfide Snap-Tops Enhances Efficacy Against Pneumonic Tularemia in Mice. *Small*, *12*(27), 3690–3702. https://doi.org/10.1002/smll.201600892

Lee, E. C., Davis-Poynter, N., Nguyen, C. T. H., Peters, A. A., Monteith, G. R., Strounina, E., Popat, A., & Ross, B. P. (2016). GAG mimetic functionalised solid and mesoporous silica nanoparticles as viral entry inhibitors of herpes simplex type 1 and type 2 viruses. *Nanoscale*, *8*(36), 16192–16196. https://doi.org/10.1039/C6NR03878F

Lee, E. C., Nguyen, C. T. H., Strounina, E., Davis-Poynter, N., & Ross, B. P. (2018). Structure–Activity Relationships of GAG Mimetic-Functionalized Mesoporous Silica Nanoparticles and Evaluation of Acyclovir-Loaded Antiviral Nanoparticles with Dual Mechanisms of Action. *ACS Omega*, *3*(2), 1689–1699. https://doi.org/10.1021/acsomega.7b01662

Lee, J. H., Jeong, S. H., Cha, S.-S., & Lee, S. H. (2007). A lack of drugs for antibiotic-resistant Gram-negative bacteria. *Nature Reviews Drug Discovery*, *6*(11), 938–938. https://doi.org/10.1038/nrd2201-c1

Lee, N.-Y., Hsueh, P.-R., & Ko, W.-C. (2019). Nanoparticles in the Treatment of Infections Caused by Multidrug-Resistant Organisms. *Frontiers in Pharmacology*, *10*, Article 1153. https://doi.org/10.3389/fphar.2019.01153

Lehi, A. Y., Shagholani, H., Nikpay, A., Ghorbani, M., Soltani, M., & Others. (2019). Synthesis and modification of crystalline SBA-15 nanowhiskers as a pH-sensitive metronidazole nanocarrier system. *International Journal of Pharmaceutics*, *555*, 28–35. https://doi.org/10.1016/j.ijpharm.2018.11.034

Lei, Q., Guo, J., Noureddine, A., Wang, A., Wuttke, S., Brinker, C. J., & Zhu, W. (2020). Sol-Gel-Based Advanced Porous Silica Materials for Biomedical Applications. *Advanced Functional Materials*, *30*(41), Article 1909539. https://doi.org/10.1002/adfm.201909539

Li, A., Long, L., Liu, F., Liu, J., Wu, X., & Ji, Y. (2019). Antigen-labeled mesoporous silica-coated Au-core Pt-shell nanostructure: a novel nanoprobe for highly efficient virus diagnosis. *Journal of Biological Engineering*, *13*(1), 87. https://doi.org/10.1186/s13036-019-0220-1

Li, G., Fan, Y., Lai, Y., Han, T., Li, Z., Zhou, P., Pan, P., Wang, W., Hu, D., Liu, X., & others. (2020). Coronavirus infections and immune responses. *Journal of Medical Virology*, *92*(4), 424–432. https://doi.org/10.1002/jmv.25685

Li, L., Liu, T., Fu, C., Tan, L., Meng, X., & Liu, H. (2015). Biodistribution, excretion, and toxicity of mesoporous silica nanoparticles after oral administration depend on their shape. *Nanomedicine: Nanotechnology, Biology and Medicine*, *11*(8), 1915–1924.

https://doi.org/10.1016/j.nano.2015.07.004

Li, Z., Clemens, D. L., Lee, B.-Y., Dillon, B. J., Horwitz, M. A., & Zink, J. I. (2015). Mesoporous Silica Nanoparticles with pH-Sensitive Nanovalves for Delivery of Moxifloxacin Provide Improved Treatment of Lethal Pneumonic Tularemia. *ACS Nano*, *9*(11), 10778–10789. https://doi.org/10.1021/acsnano.5b04306

Lin, Y.-S., & Haynes, C. L. (2010). Impacts of mesoporous silica nanoparticle size, pore ordering, and pore integrity on hemolytic activity. *Journal of the American Chemical Society*, *132*(13), 4834–4842. https://doi.org/10.1021/ja910846q

Liu, T., Li, L., Teng, X., Huang, X., Liu, H., Chen, D., Ren, J., He, J., & Tang, F. (2011). Single and repeated dose toxicity of mesoporous hollow silica nanoparticles in intravenously exposed mice. *Biomaterials*, *32*(6), 1657–1668. https://doi.org/10.1016/j.biomaterials.2010.10.035

Lu, J., Liong, M., Li, Z., Zink, J. I., & Tamanoi, F. (2010). Biocompatibility, biodistribution, and drug-delivery efficiency of mesoporous silica nanoparticles for cancer therapy in animals. *Small*, *6*(16), 1794–1805. https://doi.org/10.1002/smll.201000538

Lyra, M. A. M. De, Soares-Sobrinho, J. L., Brasileiro, M. T., De, M. F., Roca, L., Barraza, J. A., Viana, O. D. S., & Rolim-Neto, P. J. (2007). Sistemas Matriciais Hidrofilicos e Mucoadesivos para Liberação Controlada de Fármacos. *Latin American Journal of Pharmacy*, *26*(5), 784–793.

Madhusoodana, C. D., Kameshima, Y., Nakajima, A., Okada, K., Kogure, T., & MacKenzie, K. J. D. (2006). Synthesis of high surface area Al-containing mesoporous silica from calcined and acid leached kaolinites as the precursors. *Journal of Colloid and Interface Science*, *297*(2), 724–731. https://doi.org/10.1016/j.jcis.2005.10.051

Manzano, M., & Vallet-Regí, M. (2020). Mesoporous silica nanoparticles for drug delivery. *Advanced Functional Materials*, *30*(2), 1902634. https://doi.org/10.1002/adfm.201902634

Martínez-Carmona, M., Izquierdo-Barba, I., Colilla, M., & Vallet-Regí, M. (2019). Concanavalin A-targeted mesoporous silica nanoparticles for infection treatment. *Acta Biomaterialia*, *96*, 547–556. https://doi.org/10.1016/j.actbio.2019.07.001

Mas, N., Galiana, I., Hurtado, S., Mondragón, L., Bernardos, A., Sancenón, F., Amorós, P., Abril-Utrillas, N., Marcos, D., Martinez-Máñez, R., & Murguía, J. R. (2014). Enhanced antifungal efficacy of tebuconazole using gated pH-driven mesoporous nanoparticles. *International Journal of Nanomedicine*, *9*(1), 2597–2606. https://doi.org/10.2147/IJN.S59654

Michailidis, M., Sorzabal-Bellido, I., Adamidou, E. A., Diaz-Fernandez, Y. A., Aveyard, J., Wengier, R., Grigoriev, D., Raval, R., Benayahu, Y., D'Sa, R. A., & Shchukin, D. (2017). Modified Mesoporous Silica Nanoparticles with a Dual Synergetic Antibacterial Effect. *ACS Applied Materials & Interfaces*, *9*(44), 38364–38372. https://doi.org/10.1021/acsami.7b14642

Mitra, S., Patra, P., Pradhan, S., Debnath, N., Dey, K. K., Sarkar, S., Chattopadhyay, D., & Goswami, A. (2015). Microwave synthesis of ZnO@mSiO2 for detailed antifungal mode of action study: Understanding the insights into oxidative stress. *Journal of Colloid and Interface Science*, *444*, 97–108. https://doi.org/10.1016/j.jcis.2014.12.041

Mohammadpour, R., Cheney, D. L., Grunberger, J. W., Yazdimamaghani, M., Jedrzkiewicz, J., Isaacson, K. J., Dobrovolskaia, M. A., & Ghandehari, H. (2020). One-year chronic toxicity evaluation of single dose intravenously administered silica nanoparticles in mice and their Ex vivo human hemocompatibility. *Journal of Controlled Release*, *324*, 471–481. https://doi.org/10.1016/j.jconrel.2020.05.027

Momčilović, S., Cantacessi, C., Arsić-Arsenijević, V., Otranto, D., & Tasić-Otašević, S. (2019). Rapid diagnosis of parasitic diseases: current scenario and future needs. *Clinical Microbiology and Infection*, *25*(3), 290–309. https://doi.org/10.1016/j.cmi.2018.04.028

Monath, T. P., & Vasconcelos, P. F. C. (2015). Yellow fever. *Journal of Clinical Virology*, *64*, 160–173. https://doi.org/10.1016/j.jcv.2014.08.030

Montazeri, M., Razzaghi-Abyaneh, M., Nasrollahi, S. A., Maibach, H., & Nafisi, S. (2020). Enhanced topical econazole antifungal efficacy by amine-functionalized silica nanoparticles. *Bulletin of Materials Science*, *43*(1), Article 13. https://doi.org/10.1007/s12034-019-1974-2

Nandiyanto, A. B. D., Kim, S.-G., Iskandar, F., & Okuyama, K. (2009). Synthesis of spherical mesoporous silica nanoparticles with nanometer-size controllable pores and outer diameters. *Microporous and Mesoporous Materials*, *120*(3), 447–453. https://doi.org/10.1016/j.micromeso.2008.12.019

Narayan, R., Nayak, U. Y., Raichur, A. M., & Garg, S. (2018). Mesoporous silica nanoparticles: A comprehensive review on synthesis and recent advances. *Pharmaceutics*, *10*(3), Article 118. https://doi.org/10.3390/pharmaceutics10030118

Nash, T., Allison, A. C., & Harington, J. S. (1966). Physico-chemical properties of silica in relation to its toxicity. *Nature*, *210*(5033), 259–261. https://doi.org/10.1038/210259a0

Nasrollahzadeh, M., Sajjadi, M., Soufi, G. J., Iravani, S., & Varma, R. S. (2020). Nanomaterials and Nanotechnology-Associated Innovations against Viral Infections with a Focus on Coronaviruses. *Nanomaterials*, *10*(6), Article 1072. https://doi.org/10.3390/nano10061072

National Institutes of Health. (2007). Understanding emerging and re-emerging infectious diseases. *Biological Sciences Curriculum Study. NIH Curriculum Supplement Series. National Institutes of Health, Bethesda, MD*.

Nazemiyeh, E., Eskandani, M., Sheikhloie, H., & Nazemiyeh, H. (2016). Formulation and physicochemical characterization of lycopene-loaded solid lipid nanoparticles. *Advanced Pharmaceutical Bulletin*, *6*(2), Article 235. https://doi.org/ 10.15171/apb.2016.032

Nhavene, E. P. F., da Silva, W. M., Junior, R. R. T., Gastelois, P. L., Venâncio, T., Nascimento, R., Batista, R. J. C., Machado, C. R., de Almeida Macedo, W. A., & de Sousa, E. M. B. (2018). Chitosan grafted into mesoporous silica nanoparticles as benznidazol carrier for Chagas diseases treatment. *Microporous and Mesoporous Materials*, *272*, 265–275. https://doi.org/10.1016/j.micromeso.2018.06.035

Nikaeen, G., Abbaszadeh, S., & Yousefinejad, S. (2020). Application of nanomaterials in treatment, anti-infection and detection of coronaviruses. *Nanomedicine*, *15*(15), 1501–1512. https://doi.org/10.2217/nnm-2020-0117

Ogunsona, E. O., Muthuraj, R., Ojogbo, E., Valerio, O., & Mekonnen, T. H. (2020). Engineered nanomaterials for antimicrobial applications: A review. *Applied Materials Today*, *18*, Article 100473. https://doi.org/10.1016/j.apmt.2019.100473

Oliveira, D. C. P., de Barros, A. L. B., Belardi, R. M., de Goes, A. M., de Oliveira Souza, B. K., & Soares, D. C. F. (2016). Mesoporous silica nanoparticles as a potential vaccine adjuvant against Schistosoma mansoni. *Journal of Drug Delivery Science and Technology*, *35*, 234–240. https://doi.org/10.1016/j.jddst.2016.07.002

Øye, G., Sjöblom, J., & Stöcker, M. (2001). Synthesis, characterization and potential applications of new materials in the mesoporous range. *Advances in Colloid and Interface Science*, *89*, 439–466. https://doi.org/10.1016/S0001-8686(00)00066-X

Pallotta, A., Clarot, I., Sobocinski, J., Fattal, E., & Boudier, A. (2019). Nanotechnologies for Medical Devices: Potentialities and Risks. *ACS Applied Bio Materials*, *2*(1), 1–13. https://doi.org/10.1021/acsabm.8b00612

Paramanantham, P., Antony, A. P., Lal, S. B. S., Sharan, A., Syed, A., Ahmed, M., Alarfaj, A. A., Busi, S., Maaza, M., & Kaviyarasu, K. (2018). Antimicrobial photodynamic inactivation of fungal biofilm using amino functionalized mesoporus silica-rose bengal nanoconjugate against *Candida albicans*. *Scientific African*, *1*, Article e00007. https://doi.org/10.1016/j.sciaf.2018.e00007

Phillips, E., Penate-Medina, O., Zanzonico, P. B., Carvajal, R. D., Mohan, P., Ye, Y., Humm, J., Gonen, M., Kalaigian, H., Schoder, H., & others. (2014). Clinical translation of an ultrasmall inorganic optical-PET imaging nanoparticle probe. *Science Translational Medicine*, *6*(260), Article 260ra149. https://doi.org/10.1126/scitranslmed.3009524

Poddar, S. K. (2002). Influenza virus types and subtypes detection by single step single tube multiplex reverse transcription-polymerase chain reaction (RT-PCR) and agarose gel electrophoresis. *Journal of Virological Methods*, *99*(1–2), 63–70. https://doi.org/10.1016/S0166-0934(01)00380-9

Qasim, M., Singh, B. R., Naqvi, A. H., Paik, P., & Das, D. (2015). *Silver nanoparticles embedded mesoporous SiO 2 nanosphere: an effective anticandidal agent against Candida albicans 077*. Nanotechnology, 26, Article 285102. https://doi.org/10.1088/0957-4484/26/28/285102

Qu, F., Zhu, G., Lin, H., Zhang, W., Sun, J., Li, S., & Qiu, S. (2006). A controlled release of ibuprofen by systematically tailoring the morphology of mesoporous silica materials. *Journal of Solid State Chemistry*, *179*(7), 2027–2035. https://doi.org/10.1016/j.jssc.2006.04.002

Rodrigues, G. R., López-Abarrategui, C., de la Serna Gómez, I., Dias, S. C., Otero-González, A. J., & Franco, O. L. (2019). Antimicrobial magnetic nanoparticles based-therapies for controlling infectious diseases. *International Journal of Pharmaceutics*, *555*, 356–367. https://doi.org/10.1016/j.ijpharm.2018.11.043

Rohr, J. R., Barrett, C. B., Civitello, D. J., Craft, M. E., Delius, B., DeLeo, G. A., Hudson, P. J., Jouanard, N., Nguyen, K. H., Ostfeld, R. S., & others. (2019). Emerging human infectious diseases and the links to global food production. *Nature Sustainability*, *2*(6), 445–456. https://doi.org/10.1038/s41893-019-0293-3

Ruehle, B., Clemens, D. L., Lee, B.-Y., Horwitz, M. A., & Zink, J. I. (2017). A Pathogen-Specific Cargo Delivery Platform Based on Mesoporous Silica Nanoparticles. *Journal of the American Chemical Society*, *139*(19), 6663–6668. https://doi.org/10.1021/jacs.7b01278

Sábio, R. M., Meneguin, A. B., Ribeiro, T. C., Silva, R. R., & Chorilli, M. (2019). New insights towards mesoporous silica nanoparticles as a technological platform for chemotherapeutic drugs delivery. *International Journal of Pharmaceutics*, *564*, 379–409. https://doi.org/10.1016/j.ijpharm.2019.04.067

Sábio, R. M., Santagneli, S. H., Gressier, M., Caiut, J. M. A., Pazin, W. M., Leite, I. S., Inada, N. M., Silva, R. R., Ribeiro, S. J. L., & Menu, M.-J. (2020a). Luminescent nanohybrids based on silica and silylated Ru(II)—Yb(III) heterobinuclear complex: new tools for biological media analysis. *Nanotechnology*, *31*(8), Article 085709. https://doi.org/10.1088/1361-6528/ab55c3

Sábio, R. M., Santagneli, S. H., Gressier, M., Caiut, J. M. A., Pazin, W. M., Ribeiro, S. J. L., & Menu, M.-J. (2020b). Near-infrared/visible-emitting nanosilica modified with silylated Ru(II) and Ln(III) complexes. *Nanotechnology*, *31*(3), Article 035602. https://doi.org/10.1088/1361-6528/ab494f

Sahoo, S., Dilnawaz, F., & Krishnakumar, S. (2008). Nanotechnology in ocular drug delivery. *Drug Discovery Today*, *13*(3–4), 144–151. https://doi.org/10.1016/j.drudis.2007.10.021

Sahoo, S. K., & Labhasetwar, V. (2003). Nanotech approaches to drug delivery and imaging. *Drug Discovery Today*, *8*(24), 1112–1120. https://doi.org/10.1016/S1359-6446(03)02903-9

Sarparanta, M., Bimbo, L. M., Rytkönen, J., Mäkilä, E., Laaksonen, T. J., Laaksonen, P., Nyman, M., Salonen, J., Linder, M. B., Hirvonen, J., & others. (2012). Intravenous delivery of hydrophobin-functionalized porous silicon nanoparticles: stability, plasma protein adsorption and biodistribution. *Molecular Pharmaceutics*, *9*(3), 654–663. https://doi.org/10.1021/mp200611d

Silva, J. M. S., Diniz, T., Hanchuk, M., Murilo, ‖, Santos, I., Rg Kobarg, J., Bajgelman, M. C., & Cardoso, M. B. (2016). *Viral Inhibition Mechanism Mediated by Surface-Modified Silica Nanoparticles*. 8(26), 16564–16572 https://doi.org/10.1021/acsami.6b03342

Singh, A., Gautam, P. K., Verma, A., Singh, V., Shivapriya, P. M., Shivalkar, S., Sahoo, A. K., & Samanta, S. K. (2020). Green synthesis of metallic nanoparticles as effective alternatives to treat antibiotics resistant bacterial infections: A review. *Biotechnology Reports*, *25*, Article e00427. https://doi.org/10.1016/j.btre.2020.e00427

Singh, M., Singh, S., Prasad, S., & Gambhir, I. S. (2008). Nanotechnology in medicine and antibacterial effect of silver nanoparticles. *Digest Journal of Nanomaterials and Biostructures*, *3*(3), 115–122.

Sissoko, D., Duraffour, S., Kerber, R., Kolie, J. S., Beavogui, A. H., Camara, A.-M., Colin, G., Rieger, T., Oestereich, L., Pályi, B., & others. (2017). Persistence and clearance of Ebola virus RNA from seminal fluid of Ebola virus disease survivors: a longitudinal analysis and modelling study. *The Lancet Global Health*, *5*(1), e80–e88. https://doi.org/10.1016/S2214-109X(16)30243-1

Slowing, I. I., Wu, C.-W., Vivero-Escoto, J. L., & Lin, V. S.-Y. (2009). Mesoporous silica nanoparticles for reducing hemolytic activity towards

mammalian red blood cells. *Small*, *5*(1), 57–62. https://doi.org/10.1002/smll.200800926

Smerkova, K., Dolezelikova, K., Bozdechova, L., Heger, Z., Zurek, L., & Adam, V. (2020). Nanomaterials with active targeting as advanced antimicrobials. *WIREs Nanomedicine and Nanobiotechnology*, *12*(5), Article e1636. https://doi.org/10.1002/wnan.1636

Soares, D. C. F., Soares, L. M., de Goes, A. M., Melo, E. M., de Barros, A. L. B., Bicalho, T. C. A. S., Leao, N. M., & Tebaldi, M. L. (2020). Mesoporous SBA-16 silica nanoparticles as a potential vaccine adjuvant against Paracoccidioides brasiliensis. *Microporous and Mesoporous Materials*, *291*, Article 109676. https://doi.org/10.1016/j.micromeso.2019.109676

Šoltys, M., Balouch, M., Kašpar, O., Lhotka, M., Ulbrich, P., Zadražil, A., Kovačík, P., & Štěpánek, F. (2018). Evaluation of scale-up strategies for the batch synthesis of dense and hollow mesoporous silica microspheres. *Chemical Engineering Journal*, *334*, 1135–1147. https://doi.org/10.1016/j.cej.2017.11.026

Souris, J. S., Lee, C.-H., Cheng, S.-H., Chen, C.-T., Yang, C.-S., Ja-an, A. H., Mou, C.-Y., & Lo, L.-W. (2010). Surface charge-mediated rapid hepatobiliary excretion of mesoporous silica nanoparticles. *Biomaterials*, *31*(21), 5564–5574. https://doi.org/10.1016/j.biomaterials.2010.03.048

Stöber, W., Fink, A., & Bohn, E. (1968). Controlled growth of monodisperse silica spheres in the micron size range. *Journal of Colloid and Interface Science*, *26*(1), 62–69. https://doi.org/10.1016/0021-9797(68)90272-5

Subramaniam, Thomas, Gustafsson, Jambhrunkar, Kidd, & Prestidge. (2019). Rifampicin-Loaded Mesoporous Silica Nanoparticles for the Treatment of Intracellular Infections. *Antibiotics*, *8*(2), Article 39. https://doi.org/10.3390/antibiotics8020039

Tang, F., Li, L., & Chen, D. (2012). Mesoporous silica nanoparticles: synthesis, biocompatibility and drug delivery. *Advanced Materials*, *24*(12), 1504–1534. https://doi.org/10.1002/adma.201104763

Tasia, W., Lei, C., Cao, Y., Ye, Q., He, Y., & Xu, C. (2020). Enhanced eradication of bacterial biofilms with DNase I-loaded silver-doped mesoporous silica nanoparticles. *Nanoscale*, *12*(4), 2328–2332. https://doi.org/10.1039/C9NR08467C

Tatara, A. M. (2020). Role of Tissue Engineering in COVID-19 and Future Viral Outbreaks. *Tissue Engineering Part A*, *26*(9–10), 468–474. https://doi.org/10.1089/ten.tea.2020.0094

Tawfeek, G. M., Baki, M. H. A., Ibrahim, A. N., Mostafa, M. A. H., Fathy, M. M., & Diab, M. S. E. D. M. (2019). Enhancement of the therapeutic efficacy of praziquantel in murine Schistosomiasis mansoni using silica nanocarrier. *Parasitology Research*, *118*(12), 3519–3533. https://doi.org/10.1007/s00436-019-06475-8

Tozuka, Y., Wongmekiat, A., Kimura, K., Moribe, K., Yamamura, S., & Yamamoto, K. (2005). Effect of pore size of FSM-16 on the entrapment of flurbiprofen in mesoporous structures. *Chemical and Pharmaceutical Bulletin*, *53*(8), 974–977. https://doi.org/10.1248/cpb.53.974

Trewyn, B. G., Slowing, I. I., Giri, S., Chen, H.-T., & Lin, V. S.-Y. (2007). Synthesis and functionalization of a mesoporous silica nanoparticle based on the sol--gel process and applications in controlled release. *Accounts of Chemical Research*, *40*(9), 846–853. https://doi.org/10.1021/ar600032u

Tuboi, S. H., Costa, Z. G. A., da Costa Vasconcelos, P. F., & Hatch, D. (2007). Clinical and epidemiological characteristics of yellow fever in Brazil: analysis of reported cases 1998--2002. *Transactions of the Royal Society of Tropical Medicine and Hygiene*, *101*(2), 169–175. https://doi.org/10.1016/j.trstmh.2006.04.001

Tumpey, T. M. (2005). Characterization of the Reconstructed 1918 Spanish Influenza Pandemic Virus. *Science*, *310*(5745), 77–80. https://doi.org/10.1126/science.1119392

Ukmar, T., & Planinšek, O. (2010). Ordered mesoporous silicates as matrices for controlled release of drugs. *Acta Pharmaceutica*, *60*(4), 373–385. https://doi.org/10.2478/v10007-010-0037-4

Vale, N., Correia, A., Silva, S., Figueiredo, P., Mäkilä, E., Salonen, J., Hirvonen, J., Pedrosa, J., Santos, H. A., & Fraga, A. (2017). Preparation and biological evaluation of ethionamide-mesoporous silicon nanoparticles against Mycobacterium tuberculosis. *Bioorganic & Medicinal Chemistry Letters*, *27*(3), 403–405. https://doi.org/10.1016/j.bmcl.2016.12.060

Vallet-Regí, M. (2006). Ordered Mesoporous Materials in the Context of Drug Delivery Systems and Bone Tissue Engineering. *Chemistry - A European Journal*, *12*(23), 5934–5943. https://doi.org/10.1002/chem.200600226

Vallet-Regí, M., Balas, F., & Arcos, D. (2007a). Mesoporous Materials for Drug Delivery. *Angewandte Chemie International Edition*, *46*(40), 7548–7558. https://doi.org/10.1002/anie.200604488

Vallet-Regi, M., Balas, F., Colilla, M., & Manzano, M. (2007b). Drug Confinement and Delivery in Ceramic Implants. *Drug Metabolism Letters*, *1*(1), 37–40. https://doi.org/10.2174/187231207779814382

Vallet-Regí, M., González, B., & Izquierdo-Barba, I. (2019). Nanomaterials as Promising Alternative in the Infection Treatment. *International Journal of Molecular Sciences*, *20*(15), Article 3806. https://doi.org/10.3390/ijms20153806

Walvekar, P., Gannimani, R., & Govender, T. (2019). Combination drug therapy via nanocarriers against infectious diseases. *European Journal of Pharmaceutical Sciences*, *127*, 121–141. https://doi.org/10.1016/j.ejps.2018.10.017

Wang, S., & Li, H. (2006). Structure directed reversible adsorption of organic dye on mesoporous silica in aqueous solution. *Microporous and Mesoporous Materials*, *97*(1–3), 21–26. https://doi.org/10.1016/j.micromeso.2006.08.005

Weiss, C., Carriere, M., Fusco, L., Fusco, L., Capua, I., Regla-Nava, J. A., Pasquali, M., Pasquali, M., Pasquali, M., Scott, J. A., & others (2020). Toward Nanotechnology-Enabled Approaches against the COVID-19 Pandemic. *ACS Nano*, *14*(6), 6383–6406. https://doi.org/10.1021/ACSNANO.0C03697/ASSET/IMAGES/LARGE/NN0C03697_0007.JPEG

WHO. (2020a) Disease outbreaks. *Emergencies*. World Health Organization. https://www.who.int/emergencies/diseases/en/

WHO. (2020b) *Infectious diseases*. World Health Organization. https://www.who.int/topics/infectious_diseases/en/

WHO. (2020c) *Antimicrobial resistance*. World Health Organization. https://www.who.int/news-room/fact-sheets/detail/antimicrobial-resistance

Xu, C., He, Y., Li, Z., Nor, Y. A., & Ye, Q. (2018). Nanoengineered hollow mesoporous silica nanoparticles for the delivery of antimicrobial proteins into biofilms. *Journal of Materials Chemistry B*, *6*(13), 1899–1902. https://doi.org/10.1039/C7TB03201C

Xu, T., Li, J., Zhang, S., Jin, Y., & Wang, R. (2019). Integration of diagnosis and treatment in the detection and kill of S.aureus in the whole blood. *Biosensors and Bioelectronics*, *142*, Article 111507. https://doi.org/10.1016/j.bios.2019.111507

Yang, B., Chen, Y., & Shi, J. (2019). Mesoporous silica/organosilica nanoparticles: Synthesis, biological effect and biomedical application. *Materials Science and Engineering: R: Reports*, *137*, 66–105. https://doi.org/10.1016/j.mser.2019.01.001

Yang, P., Gai, S., & Lin, J. (2012). Functionalized mesoporous silica materials for controlled drug delivery. *Chemical Society Reviews*, *41*(9), Article 3679. https://doi.org/10.1039/c2cs15308d

Yang, S., Han, X., Yang, Y., Qiao, H., Yu, Z., Liu, Y., Wang, J., & Tang, T. (2018). Bacteria-targeting nanoparticles with microenvironment-responsive antibiotic release to eliminate intracellular Staphylococcus aureus and associated infection. *ACS Applied Materials & Interfaces*, *10*(17), 14299–14311.

Yenkoidiok-Douti, L., & Jewell, C. M. (2020). Integrating Biomaterials and Immunology to Improve Vaccines Against Infectious Diseases. *ACS Biomaterials Science & Engineering*, *6*(2), 759–778. https://doi.org/10.1021/acsbiomaterials.9b01255

Yokoi, T., Kubota, Y., & Tatsumi, T. (2012). Amino-functionalized mesoporous silica as base catalyst and adsorbent. *Applied Catalysis A: General*, *421*, 14–37. https://doi.org/10.1016/j.apcata.2012.02.004

Zaidi, S., Misba, L., & Khan, A. U. (2017). Nano-therapeutics: A revolution in infection control in post antibiotic era. *Nanomedicine: Nanotechnology, Biology and Medicine*, *13*(7), 2281–2301. https://doi.org/10.1016/j.nano.2017.06.015

Zhou, X., Weng, W., Chen, B., Feng, W., Wang, W., Nie, W., Chen, L., Mo, X., Su, J., & He, C. (2018). Mesoporous silica nanoparticles/gelatin porous composite scaffolds with localized and sustained release of vancomycin for treatment of infected bone defects. *Journal of Materials Chemistry B*, *6*(5), 740–752. https://doi.org/10.1039/C7TB01246B

Zhu, N., Zhang, D., Wang, W., Li, X., Yang, B., Song, J., Zhao, X., Huang, B., Shi, W., Lu, R., Niu, P., Zhan, F., Ma, X., Wang, D., Xu, W., Wu, G., Gao, G. F., & Tan, W. (2020). A Novel Coronavirus from Patients with Pneumonia in China, 2019. *New England Journal of Medicine*, *382*(8), 727–733. https://doi.org/10.1056/NEJMoa2001017

CHAPTER 7

Physicochemical characterization of a lycopene-loaded mesoporous silica nanoparticle formulation

Gabriela Corrêa Carvalho, Gabriel Davi Marena, André Luiz Carneiro Soares do Nascimento, Bruna Almeida Furquim de Camargo, Rafael Miguel Sábio, Felipe Rebello Lourenço, Hélder A. Santos*, Marlus Chorilli*

Nano Select, v. 1, pp. 1-18, 2024

Reprinted under the Creative Commons Copyright License

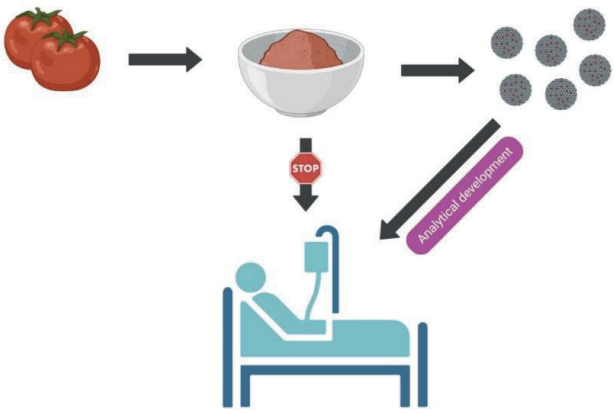

Abstract

Lycopene (LYC), a carotenoid extracted mainly from tomatoes, has several biological properties, making its use desirable as a nutraceutical and pharmaceutical active ingredient. Among its various applications vulvovaginal candidiasis stands out. However, the use of LYC in therapy has limitations related to its solubility and stability. In this study, mesoporous silica nanoparticles (MSNs) are used to load and protect LYC from degradation. The exact amount of drug incorporated was determined by analytical techniques, such as high-performance liquid chromatography (HPLC) and thermal analysis. For this we developed and validated an HPLC method for LYC quantification and evaluated LYC impregnation in MSNs, followed by thermogravimetry analysis (TGA). Differential scanning calorimetry (DSC) was also used in order to confirm drug incorporation. Additionally, an *in vitro* release study in simulated vaginal fluid was also carried out. The HPLC method was duly validated for the range of 26–125 μg/mL and proved to be suitable for LYC quantification. DSC measurements suggest an improvement in the stability of the impregnated drug, which was reinforced by the release assay. Overall, the developed method is suitable to quantify LYC-loaded porous materials enabling its use in vaginal applications.

1. Introduction

In view of lycopene (LYC) desirable biological properties, such as antimicrobial, antioxidant, antidiabetic, antihypercholesterolemic, anticancer, cardioprotective and photoprotection its use as nutraceutical and pharmaceutical active ingredient are increasingly being explored (Adetunji et al., 2021; Carvalho et al., 2021). Among these therapeutic activities, the antimicrobial one makes this drug an excellent option for the treatment of vulvovaginal candidiasis (VVC). VVC is an infection in the vulva region caused by the fungus *Candida sp.*, which is considered a public health problem since it is the second leading cause of vaginitis. In Brazil, for example, the estimated prevalence seems to be 18%, but as it is an underreported disease, this value may be even higher (Carvalho et al., 2021). Despite the wide range of drugs available, there are reports in the literature of ineffective treatments due to fungus susceptibility and resistance to several drugs currently used in therapy. Those ineffective treatments can lead to complications, including pelvic abscess, pelvic inflammatory disease, infertility and miscarriage, which makes the study of new therapeutic options of fundamental importance (Araujo et al., 2020; Barbedo et al., 2010; Jane et al., 2019; Marchaim et al., 2012). Because of this, plant-based alternatives, such as LYC have been gaining more and more attention (Carvalho et al., 2022; H. Choi & Lee, 2015; Natarajan et al., 2020; Sung et al., 2007).

However, this carotenoid, extracted mainly from tomato, has limitations related to its molecule, which is highly lipophilic, making it insoluble in aqueous solvents, hindering its use in therapy (Carvalho et al., 2020; Khan et al., 2021). Therefore, alternatives have been studied, such as the use of nanotechnology. Despite the various options for nanocarriers, it is only possible to find studies associating LYC with organic nanocarriers, except for a study recently published by our group, so its association with inorganic nanocarriers is, until then, a field to be better explored (Carvalho et al., 2021; Carvalho et al., 2022; Carvalho et al., 2020; Falsafi et al., 2021).

Among the various inorganics nanoparticles, mesoporous silica nanoparticles (MSNs) stand out as they present desirable properties, such as high thermal and chemical stabilities, large surface area, adjustable pore structure and particle diameter, free hydroxyls groups for functionalization, biocompatibility, biodegradability, low toxicity and easy elimination in living organisms, being widely applied in the biomedicine field (Carvalho et al., 2020; Croissant et al., 2020; Fussell et al., 2014; Kankala et al., 2022; Kankala et al., 2020; Rahikkala et al., 2018). In order to develop a nanoformulation, several types of molecules can be incorporated, both in MSNs pores and on their surfaces by different ways, such as adsorption on the silica matrix, interaction with silanol groups and even through different functionalization possibilities (Croissant et al., 2017; Hoffmann et al., 2006; Kankala et al., 2020; Rosenholm et al., 2011).

It should be noted that the possibility of incorporation into the mesopores provides protection to the drug against environmental factors, which, in the context of making possible the use of LYC in therapy, is extremely desirable since this drug can suffer degradation when in contact with light, heat, oxygen and acidic environment (Kankala et al., 2019; Manzano & Vallet-Regí, 2020; Shi & Maguer, 2000). In order to guarantee the quality of the nanoformulation under development, is important to know the amount of drug that the system is capable to load and its release profile (amount/time), since these factors are directly linked to the drug content that will be available to interact with the target site (Alves et al., 2019; Carvalho et al., 2020).

Although there are several analytical techniques for drug quantification, high performance liquid chromatography (HPLC) seems to be the most used (Carvalho et al., 2021; Carvalho et al., 2020). HPLC is considered to be an easy analytical method, which can be coupled to several types of detectors; however, the most explored one is the ultraviolet detector (UV-Vis) (Hussain et al., 2019; Lucini et al., 2012; Montesano et al., 2008). In addition to HPLC, another essential technique also widely used for drug quantification is thermal analysis. This technique enables to assess the melting/crystallization and purity of a given drug, in addition to also allow the assessment of its interaction with the nanocarrier after the incorporation process (Cheremisinoff, 1996; Giron, 2002; Limnell et al., 2011). It is worth mentioning that in the literature it is possible to observe works where the quantification results obtained from HPLC showed good correlation with those obtained by thermal analysis, making interesting the combination of these two techniques for the pharmaceutical development of new nanoformulations (Ceschel et al., 2003; Giron, 2002; Tsai et al., 2017). Thus, using these analytical techniques to determine the drug content in the incorporation and release tests, the present study seeks to develop a formulation based on mesoporous silica nanoparticles incorporated with LYC for future application in the treatment of VVC. **Figure 1** provides a schematic representation of the experimental steps carried out for the development of this study.

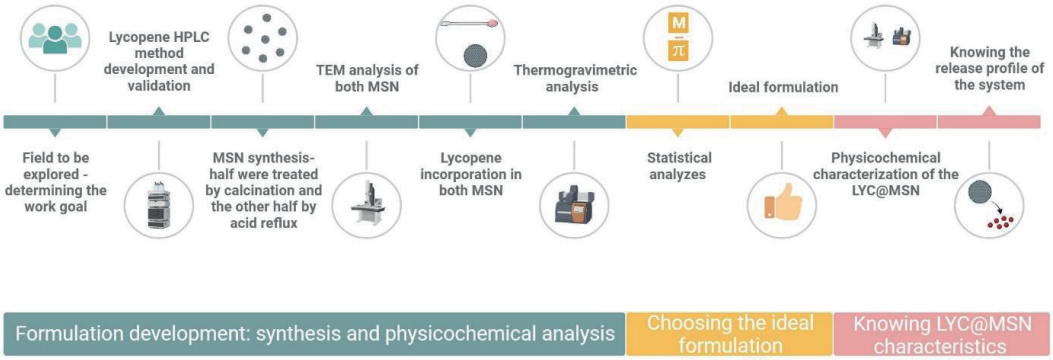

Figure 1: Timeline of the experimental stages of this study: from its conceptualization to *in vitro* studies

2. Methodology

2.1. Formulation development

2.1.1. Development and validation of an analytical method for LYC quantification

Firstly, tests with various mobile phase compositions, flow and injection volume were tested on a Waters e2695 HPLC instrument. The system consisted of a quaternary pump, a degasser, an autosampler, a column oven and a Waters 2998 model diode array detector (DAD). The best condition was achieved with a C18 column (250 mm × 4.6 mm, 5 µm - Agilent), maintained at 35 ºC with mobile phase of acetonitrile:chloroform (89:11) (both HPLC grade) at an isocratic flow of 2.0 mL/min, 20 µL injection volume and detection wavelength of 470 nm.

After defining the best method, the system suitability was evaluated according to the Food and Drug Administration (FDA) "Validation of chromatographic methods" guide. Then, in order to determine the efficiency and suitability of the method, a validation process was conducted in accordance with Q2 (R1) from International Conference on Harmonization, as described in **Table 1** (Carvalho et al., 2020; FDA, 1994; International conference on harmonization, 2005). It is worth mentioning that the LYC used for the validation stage was purchased from APIChem Technology Co. and the one used as reference chemical from Sigma-Aldrich®.

Table 1: Description of the criteria and forms of analysis used to validate the analytical method for LYC quantification. Source: (International conference on harmonization, 2005; Mayeaux et al., 2006; Perez, 2010; Shi & Maguer, 2000).

Criteria	Form of analysis	Acceptance Criteria
Accuracy	Solutions of three different concentration levels (25, 75 and 125 µg/mL) were prepared in triplicate	Agreement degree on LYC recovery percentage (from 80 to 120%)
Precision	Solutions were prepared, in triplicate, at three different concentration levels (25, 75 and 125 µg/mL), which were analyzed at different days. In order to assess the intermediate accuracy, two different analysts carried out the above process	Determination of the proximity between the results obtained by calculating the relative standard deviation (acceptable: less than or equal to 5)
Range	Linearity, precision and accuracy results interpretation	Compatibility with the intended purpose
Selectivity (specificity)	Assessment of non-interference of substances present or possibly present in the sample, they are: -mobile phase blank; -MSN-R and MSN-C blank dispersed in solvent equal to the mobile phase composition and centrifuged at 4000 RPM for 15 min; -Different pH: neutral and basic; -Degradation in 24 h by exposure in: visible light; UV light; oxygen; heat (100 ºC for 60 min); Additionally, the reference chemical LYC was compared with the one used in the applicability assay	Demonstration of the ability to identify and quantify LYC even in the presence of the mentioned factors and components by comparing the chromatograms
DL	Calculated through the residual's standard deviation, obtained in the linearity statistical analysis and through the intersection of the straight line of a linear regression (constructed by three linearity curves): $DL: \frac{3.3\ x\ residuals\ standard\ deviation}{calibration\ curve\ intersection}$	Analysis of the calculated result
QL	Calculated through the residual's standard deviation, obtained in the linearity statistical analysis and through the intersection of the straight line of a linear regression (constructed by three linearity curves): $QL: \frac{10\ x\ residuals\ standard\ deviation}{calibration\ curve\ intersection}$	Analysis of the calculated result
Linearity	Solutions at 5 concentration levels (25, 50, 75, 100 and 125 µg/mL) were prepared in triplicate	The square of the correlation coefficient (R^2), obtained through linear regression analysis, must be above 0.990. Additionally, data homoscedasticity proof was performed
Robustness	Small variations were analyzed in: - proportion of the mobile phase; - mobile phase flow; -injection volume; -column oven temperature These analyzes were performed at the average concentration (75 µg/mL)	Verification of the method's ability to resist small but deliberate variations using the accuracy criteria

Legend: MSN-R: refluxed mesoporous silica nanoparticle; MSN-C: Calcined mesoporous silica nanoparticle; LYC: Lycopene; DL: detection limit; QL: quantification limit

2.1.2. Analytical method applicability: LYC-incorporated MSNs

Firstly, refluxed and calcined MSM (MSNs-R and MSNs-C, respectively) were synthesized according to a previous study (Carvalho, Marena, Leonardi, et al., 2022). For this, 0.61 g of cetyltrimethylammonium bromide (CTAB) (Sigma-Aldrich®) and 180 mL of distilled water were added in a round bottom flask and kept under stirring at 60 °C. After 30 min, 55.8 mL of octane (Sigma-Aldrich®), 105 µL of styrene (NEON©) (previously washed three times with 2.5 M NaOH), 0.14 g of L-Lysine (Sigma-Aldrich®), 6.42 mL of tetraethyl orthosilicate (TEOS) (Sigma-Aldrich®) and 0.20 g of sodium dihydrochloride 2,2'-Azobis(2-methylproprylnamide) (AIBA) (Sigma-Aldrich®) were added. Then, maintaining the temperature and stirring, nitrogen atmosphere was added to this reaction mixture. After 3 h, the mixture was transferred to a separatory funnel for phase separation overnight at room temperature. The suspension phase was collected and centrifuged at 18,000 rpm for 15 min, then the precipitate obtained was washed 5 times with ethanol and distilled water, ultimately the precipitate was dried.

After the obtention of the dried material two procedures to remove organic residues from the pore were tested in parallel. For the first one, acid reflux, the dried material was resuspended with 60 mL of methanol, 15 mL of chloroform and 1.5 mL of hydrochloric acid. Then the mixture was kept stirring under reflux at 60 °C. After a period of 6 h the same centrifugation procedure mentioned above were applied to this reaction mixture. Finally, the precipitate was dried and stored in a desiccator. Meanwhile, for the second procedure the first step was the calcination (500 °C for 3 h) of an empty porcelain crucible in a muffle furnace, then it was stored in a desiccator until cool. Then the synthesis dried material obtained previously was transferred to it and calcinated at 550 °C for 6 h, the powder obtained was stored in a desiccator. After, MSNs-R and MSNs-C were analyzed by high-resolution transmission electron microscopy (HR-TEM) in a TEM-FEG equipment model JEM 2100F operating at a beam power of 200 kV.

Next, right before the impregnation process the nanoparticles were dried under vacuum for 1 h right. Then, 5 mg of each were added in glass vials with LYC solutions (in chloroform) at different concentrations (1.0; 1.5; 2.0; 2.5; 3.0; 3.5; 4.0 mg/mL). LYC solutions with MSNs were kept under stirring (100 rpm) for different periods of times (6; 12; 24; 36; 48 h) under cooling (15° C ± 5). After, LYC-loaded MSNs were centrifuged at 4000 rpm for 15 min and dried at room temperature under vacuum (Maturi et al., 2019; Sábio et al., 2019). The supernatant from the centrifugation was collected, filtered and analyzed by HPLC using the method under validation in order to determine the encapsulation efficiency percentage (EE%) and loading degree percentage (LD%), according to Equations 1 and 2 (Alves et al., 2019):

$$EE(\%) = \frac{\text{Total amount of drug added} - \text{Free amount in supernatant}}{\text{Total amount of drug added}} \times 100 \quad (1)$$

$$LD(\%) = \frac{\text{Encapsulated drug}}{\text{Nanoparticle weight}} \times 100 \quad (2)$$

In parallel, the precipitate was analyzed by Thermogravimetric analysis (TGA) in a TG-DSC 1 (Mettler Toledo) with purge gas of dry air atmosphere at a flow of 50 mL/min, heating rate of 10°C/min and temperature range of 30-800°C. The samples weighed about 3 mg and an open alumina crucibles were used for this experiment (Nascimento et al., 2019). Normalization of the samples was performed to provide a direct comparison of thermal curves. The LYC content on incorporated silica corresponds to a total mass variation (Δm_T) expressed as $\Delta m_T = \Delta m_S - \Delta m_{MSN}$, which is a product of subtracting the sample mass variation (ΔmS) by the empty silica (Δm_{MSN}), both measured after 170°C. In order to compare the HPLC LD% results with those of TGA, two-way analysis of variance (ANOVA) with multiple comparisons was performed in the software GraphPad Prism®8.

2.2. Choosing the ideal formulation

In order to evaluate the incorporation methods statistical analyzes were performed, namely: regression with stepwise term selection with the purpose of building a model to identify a useful subset of predictors. Then, this data was analyzed by t-test and ANOVA. Pareto graph, residual analysis, surface graph analyses and contour analyses were used to better visualize the results and better evaluate the interaction between variables. All of them performed by the Minitab® software.

2.3. Knowing LYC@MSN characteristics

To characterize the nanoformulation, that is, the incorporation condition considered as the best, named as LYC@MSN, it was analyzed by HR-TEM and differential scanning calorimetry (DSC) (in a TG-DSC 1 (Mettler Toledo). With the purpose of knowing the nanosystem release profile, a release study was carried out in a SteadyShake 757 Amerex® equipment, the samples (LYC@MSN and free LYC, in triplicate) remained throughout the test at a temperature of 37 ± 0.5 °C under constant agitation of 300 rpm (Rodero et al., 2018). In order to respect the sink condition, 1 mg of LYC@MSN and free LYC were added to 32.38 mL and 64.76 mL of acceptor medium, respectively (United States Pharmacopeia, 2020b). In order to mimic the vaginal environment, an acceptor medium composed of simulated vaginal fluid plus 2% of Span 60 and 5% of propanol was used. It is worth mentioning that the prepared simulated vaginal fluid was composed by (Falavigna et al., 2020): sodium chloride (3.510

g/L), potassium hydroxide (1.400 g/L), calcium hydroxide (0.222 g/L), bovine serum albumin (0.018 g/L), lactic acid (2.000 g/L), acetic acid (1.000 g/L), glycerol (0.160 g/L), urea (0.400 g/L) and glucose (5.000 g/L).

Although Span 60 and propanol were added in order to increase the solubility of the drug in the acceptor medium, it is worth mentioning that both, the maximum quantity of organic solvent permitted by the United States Pharmacopeia (USP) and the indication of using the lowest possible concentration of surfactant to reach the sink condition, was respected. It is worth noting that this acceptor medium had a pH of 4.5, compatible with the human vaginal pH (Marques et al., 2011; United States Pharmacopeia, 2020b). During the assay, 1 mL aliquots of samples were collected at predetermined times (0.25; 0.5; 1; 2; 4; 8; 12; 18; 24 and 32 h), in which 1 mL of acceptor medium was replaced. LYC content in the collected samples was centrifuged at 14000 rpm for 15 minutes and quantified in a BioTek Epoch 2 microplate spectrophotometer at a fixed wavelength of 470 nm, which was previously partial validated.

3. Results and discussion

3.1. Formulation development

3.1.1. Development and validation of an analytical method for LYC quantification

Initially, several methods already validated in the literature, with mobile phase composed of various combinations of water, acetonitrile and methanol were tested in a HPLC C18 column, which is shown to be the most used, together with C30, since, due to the fact that LYC is a nonpolar molecule interacts better with those types of columns (Carvalho et al., 2020). However, it was not possible to reproduce those methods once the highest intensity peak (probably related to trans-LYC) was not well separated from the other LYC isomers (Amjad et al., 2020; Carvalho et al., 2020; Hassan & Nam, 2021). As C18 columns have nonpolar stationary phase, ideally the mobile phase of choice would have to be composed of polar reagents, but in order to obtain a better spectrum (that best served the intended purpose), it was necessary to add an nonpolar solvent, like chloroform (Hassan & Nam, 2021; Vaudreuil et al., 2020).

As the developed method is meant to be used in the quantification of the total LYC incorporated in MSNs, it was opted for predominantly unite all isomers in a single peak, as shown in **Figure 2**. It is noteworthy that through the presence of the three characteristic peaks (approximately at 450, 470 and 505 nm) in the UV spectrum obtained, since the HPLC used is coupled to a DAD detector, it was possible to prove that such peak refers to LYC (Carvalho et al., 2020).

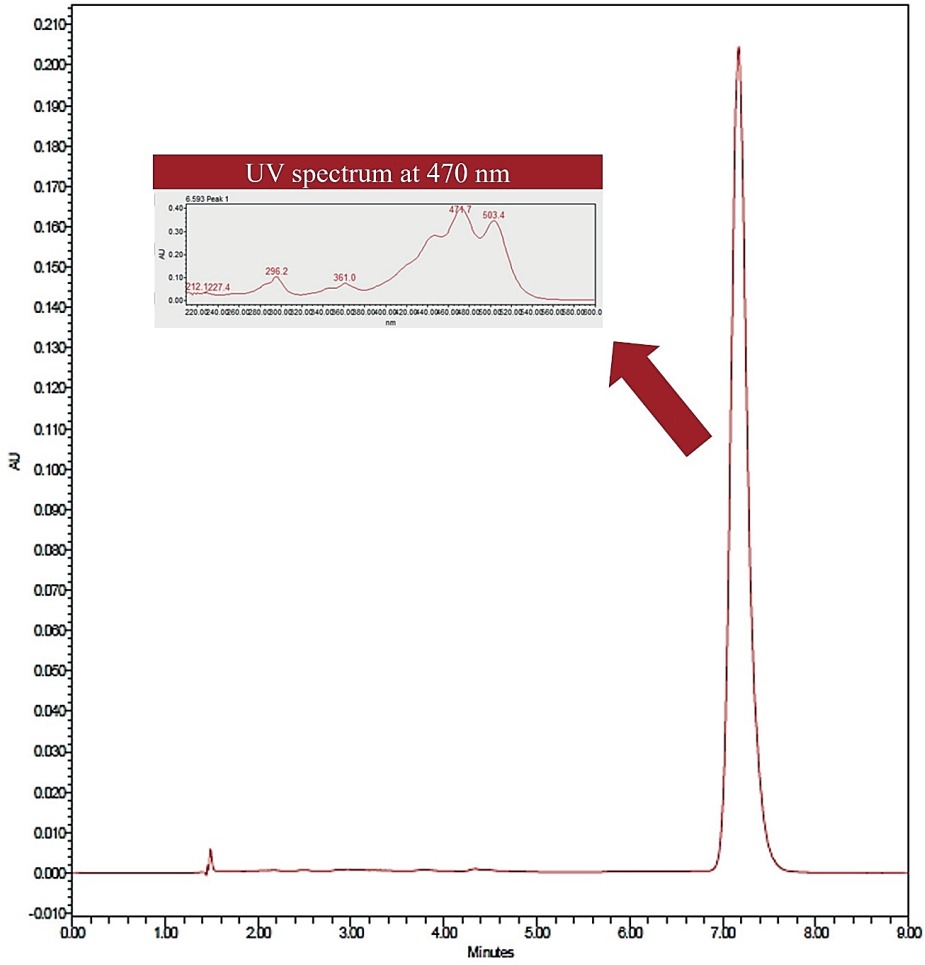

Figure 2: Chromatogram obtained for a 75 µg/mL LYC solution on a C18 column (250 mm × 4.6 mm, 5 µm), maintained at 35 ºC with mobile phase of acetonitrile:chloroform (89:11) in an isocratic flow of 2.0 mL min with an injection volume of 20 µL.

After the method development, the system suitability was evaluated. This step is of fundamental importance since prior the validation it is necessary to prove the method's performance quality and suitability for its intended use (FDA, 1994; United States Pharmacopeia, 2020a). According to USP 43, chapter 621, to assess system suitability, data from 5 injections of standard solutions should be compared if the relative standard deviation (RSD) for the parameter under evaluation is ≤ 2.0%. However, if the RSD is > 2.0, data from 6 injections must be evaluated. As can be seen in **Table 2**, data from 5 injections were evaluated since the RSD were < 2.0 (United States Pharmacopeia, 2020a). It is noteworthy that the criteria were manually calculated according to formulas described in USP 43 and FDA.

Table 2: Assessment of the developed method system suitability for LYC quantification.

Chromatograms	Criteria				
	Retention time	**Retention factor (K)**	**Theoretical plates**	**Symmetry factor**	**Tailing factor**
1	7.14	3.80	10,160.64	1.57	1.37
2	7.17	4.02	7,024.12	1.60	1.33
3	7.17	3.92	9,178.88	1.60	1.32
4	7.10	3.80	4,676.79	1.33	1.13
5	7.07	3.85	6,777.00	1.43	1.33
Average	7.13	3.88*	7,868.12	1.56	1.27
SD	0.04	-	-	-	-
RSD	0.56	-	-	-	-

Legend: *generally > 2; standard deviation (SD) and relative standard deviation (RSD) were calculated only when necessary for data interpretation.

In **Table 2** it can be seen that all mandatory criteria (injection precision - based on retention time RSD;, tailing factor and theoretical plates) are in accordance with the FDA recommendations (≤ 1%; ≤2; >2000, respectively), showing that the developed method is suitable and has excellent performance, being able to proceed to the validation step (FDA, 1994). Although the resolution criterion is mandatory, it is defined as the separation of two substances, as the purpose of this method is the quantification of a single substance, it could not be calculated. It is worth noting that although both, USP 43 and FDA, recommend the calculation of the asymmetry factor as it is not a mandatory item, they do not provide an acceptable limit for it (FDA, 1994; United States Pharmacopeia, 2020a).

3.1.2. Analytical methodology validation

Linearity

In the linear regression analysis (**Figure 3A**), it was possible to observe that there was a good correlation between the two variables, as the R^2 was greater than 0.990 and the slope was significantly different from zero, suggesting that the results have linearity. Additionally, ANOVA was performed for the statistical evaluation of the residuals, using a significance level of 5%, been possible to confirm their homoscedasticity, as they are randomly distributed (**Figure 3B**).

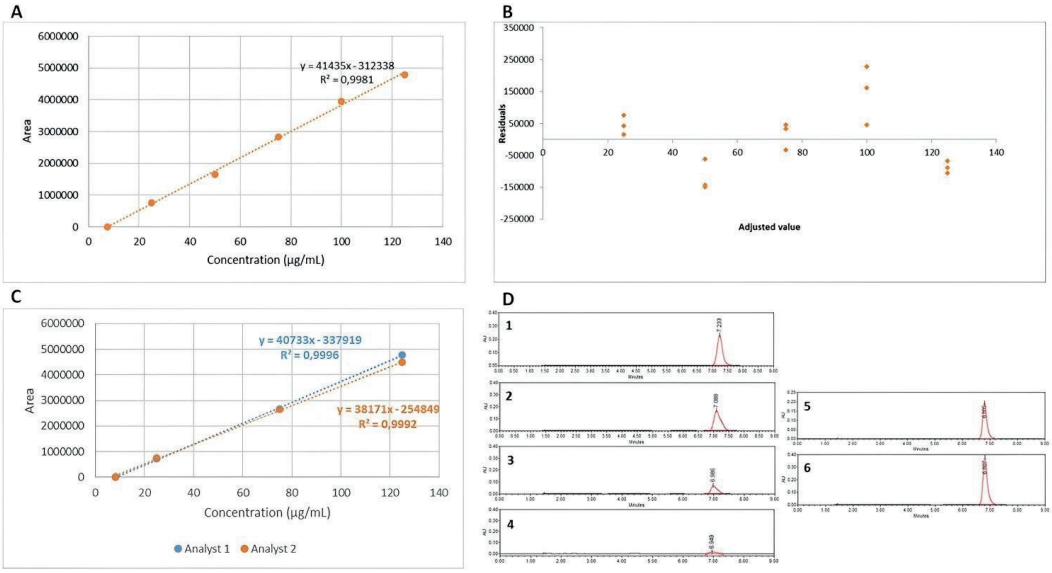

Figure 3: Analytical HPLC methodology for lycopene validation: (A) Linear representation of the results from the analysis of nine replicates of each concentration performed in three different days; (B) Residual graph of the linear representation; (C) Comparison of the results averages obtained for the intermediate precision of the two analysts performed in triplicate and on different days. (D) Degradation studies spectra carried out to assess the developed method specificity: 1: standard solution spectrum; 2: after temperature degradation; 3: after visible light degradation; 4: after UV light degradation; 5: after changing to pH close to neutral (7.6); 6: after changing to basic pH 8.5.

Accuracy

Table 3 shows that the data are accordingly with the recommended range to be accurate, as the percentage of recovery is within the range of 100 ± 20%, so it can be considered that the method is accurate for the evaluated range (25.0–125.0 µg/mL) (International conference on harmonization, 2005).

Table 3: Results obtained from the method validation and its respective recovery percentage.

Concentration (µg/mL)	Replicas (area value)			Average	SD	RSD	Experimental concentration	Accuracy (%)
	1	2	3					
125	4685072	4634211	4505611	4608298.0	92494.19	2.0	118.75	95.00
75	2448638	2537891	2484637	2490388.67	44903.63	1.80	67.64	90.19
25	696659	725397	681434	701163.33	22324.94	3.18	24.46	97.84

Legend: SD: standard deviation; RSD: relative standard deviation;

Precision

As it can be seen in **Table 4**, all the concentrations evaluated met the precision criterion, since all RSD were below 5 (International conference on harmonization, 2005; Perez, 2010).

Table 4: Precision data performed on different days by a single analyst.

Concentration (µg/mL)	Replicas			Average	SD	RSD
	Day 1	Day 2	Day 3			
125	4847745	4687509	4816669	4783974	84974.11	1.78
75	2739102	2642411	2587778	2656430	76629.92	2.88
25	723325	705900	702876	710700,3	11037.34	1.55

Legend: SD: standard deviation; RSD: relative standard deviation;

Additionally, in the intermediate precision analysis, the method was considered reproducible through the proximity of the standard deviation of the two analysts (below 5) (**Table 5**) and by both coefficient of variation being above 0.990 (**Figure 3C**) (International conference on harmonization, 2005).

Table 5: Average comparison of the precision data obtained by two analysts.

	Analyst 1					Analyst 2					Comparison between analysts	
Concentration (µg/mL)	**Day 1**	**Day 2**	**Day 3**	**Average**	**RSD**	**Day 1**	**Day 2**	**Day 3**	**Average**	**RSD**	**Average**	**RSD**
125	4847745	4687509	4816669	4783974.0	1.78	4628742	4392490	4421263	4480831.667	2.88	4632403.000	4.627
75	2739102	2642411	2587778	2656430.0	2.88	2765615	2688520	2522324	2658819.667	4.68	2657625.000	0.063
25	723325	705900	702876	710700.3	1.55	770031	709346	759136	746171.000	4.34	728435.666	3.443

Legend: SD: standard deviation; RSD: relative standard deviation;

Detection limit (DL) and quantification limit (QL)

The values obtained for DL and QL were 8.58 and 26.00 µg/mL, respectively, since the value obtained for the residual standard deviation of the linear regression was 107755.2877 and the value obtained for the slope of the linear regression line was 41435. So, based on these calculations it can be stated that the method under validation allows the detection of samples with a LYC content of at least 8.58 µg/mL, and its quantification from 26 µg/mL. On the other hand, experimentally, the lowest concentration evaluated during the validation process, 25 µg/mL, was determined with accuracy and precision, but when lower concentrations were tested, precise results were not detected (FDA, 1994; International conference on harmonization, 2005). It is worth noting that experimental determinations are less reliable than calculated ones, since there is the operator variability in several steps, such as weighing and pipetting (Carvalho et al., 2020; Vial & Jardy, 1999). In this sense, the formulas of the mentioned calculations in order to minimize operational errors in QL and DL experimental determination use correction values, 3.3 and 10 for QL and DL respectively. Those values are based on experimental standard deviation values of an ideal number of replicas (Vial & Jardy, 1999). Thus, it is possible to consider, with a higher level of reliability, that the QL for the method under validation is 26 µg/mL.

Range

Based on the results presented for the linearity, precision and accuracy criteria and taking into account the QL result the range of the method under validation is 26–125 µg/mL (International conference on harmonization, 2005).

Robustness

The data in **Table 6** shows the area obtained after small and deliberate variations of certain parameters, as well as its evaluation according to the accuracy criterion. In all tested variations, the recovery percentage complied with the acceptance criterion of 100 ± 20%, proving the method robustness (International conference on harmonization, 2005).

Table 6: Robustness results, at medium concentration, for the developed method.

Parameters	Variations	Replica			Average	RSD	Experimental concentration (µg/mL)	Accuracy (%)
		1	2	3				
Injection	22 µL	2879636	2852237	3052237	2928036.667	3.70	78.20	104.3
	18 µL	2411787	2412978	2375422	2400062.333	0.89	65.46	87.3
Column oven temperature	33 °C	2551764	2550736	2568953	2557151.000	0.40	69.25	92.3
	37 °C	2581679	2531772	2552768	2555406.333	0.98	69.21	92.3
Flow	1.8 mL/min	2535050	2537438	2567236	2546574.667	0.70	69.00	92.0
	2.2 mL/min	2523317	2511055	2501068	2511813.333	0.44	68.16	90.9
Mobile phase composition	Acetonitrile:chloroform 87:13	2657224	2721932	2749512	2709556.000	1.75	72.93	97.2
	Acetonitrile:chloroform 91:9	2562622	2584182	2574104	2573636.000	0.42	69.65	92.9

Legend: RSD: relative standard deviation;

Selectivity (specificity)

The method proved to be selective in quantifying LYC in the presence of both MSN-C and MSN-R, since only the baseline was observed. Additionally, the solvent (chloroform) non-interference was also proven for the same reason. In the degradation study, in order to verify the degradation products interference, exposure to oxygen and temperature did not significantly change the analyte recovery, since both were within the allowed percentage, 100 ± 20% (Table 7). In **Figure 3D** it is possible to observe that after temperature degradation there was a peak broadening, which can be explained by the cis-trans isomerization caused by this type of degradation, since during the development of the method it was chosen to unite the isomers. This justifies the non-appearance of additional peaks (Carvalho et al., 2020; Shi & Maguer, 2000).

Table 7: Degradation studies results carried out to assess the specificity of the developed method.

Degradation studies	Average area	Experimental concentration (µg/mL)	Recovery (%)
Oxygen	2388977.000	65.19	86.9
Temperature	2729366.667	73.41	97.9
Visible light	966014.666	30.85	41.1
UV light	175233.000	11.77	15.7
pH 7.6	2062346.000	57.31	76.4
pH 8.5	4240115.000	109.87	146.5

In the visible and UV light degradation spectra it was observed not only a lower analyte recovery percentage but also a lower peak intensity, which agrees with the literature data as light degradation causes a reduction in the total LYC content (both cis and trans) by oxidation. Moreover, in the case of temperature degradation, this reduction is caused by isomerization, which produce other degradation products that are probably not detected in the wavelength used (Shi et al., 2003; Tahmasebi & Emam-Djomeh, 2021). Finally, the change in the sample pH can be considered the limitation of this study, since, because chloroform is volatile, the measurement of the solution by a pH-meter was compromised by the non-stabilization of the value. In addition, the reading by a pH strip was also compromised as the sample has color, making the reading difficult. It is worth mentioning that the standard LYC solution (solubilized in the mobile phase) had a pH around 6 and is therefore considered acidic. Once LYC is degraded in acidic medium, the greater intensity observed in the sample peak at pH 8.5 is coherent, and, consequently, the greater recovery obtained (**Table 7** and **Figure 3D**). Finally, it is worth mentioning that the LYC chemical reference substance and the other LYC (used in the validation part) spectra did not display any significant difference.

3.1.3. Analytical method applicability: LYC@MSNs

In order to evaluate which would be the best treatment option for removal of the surfactant from the pores of the MSN, two procedures were compared, acid reflux and calcination. In **Figure 4 A2** and **B2** it is possible to observe that both MSN are spherical particles with the presence of randomly arranged pores, in accordance with works previously publish in the literature (Maturi et al., 2019; Sábio et al., 2019). It is also possible to observe variation in size for both synthesized nanoparticles (31–86 nm and 47–131 nm for MSN-C and MSN-R, respectively) (**Figure 4 A3** and **B3**), which is also common to observe in the literature (Choi & Kim, 2017; Sun et al., 2019; Vazquez et al., 2017).

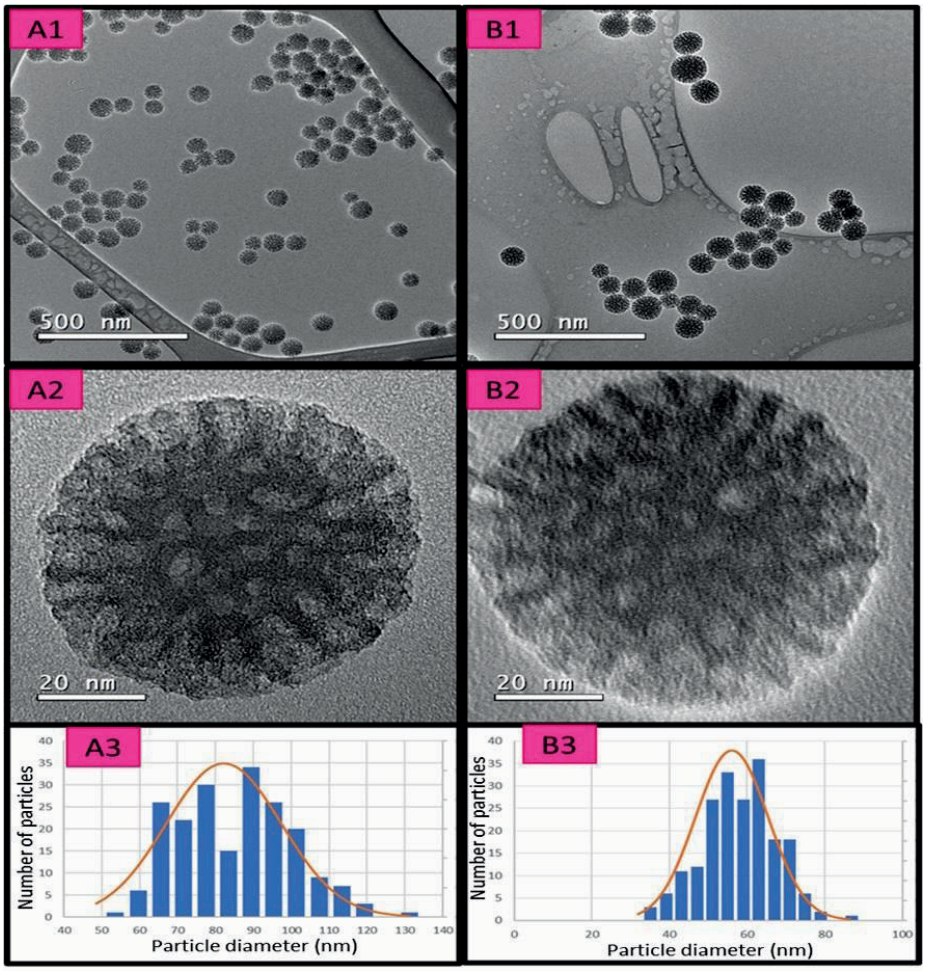

Figure 4: High-resolution transmission electron microscopy of MSN-C and MSN-R samples at different magnifications and their respective size distribution histograms obtained from counting 200 nanoparticles. A1: MSN-C at 500 nm magnification; A2: MSN-C at 200 nm magnification; A3: MSN-

C size distribution curve; B1: MSN-R at 500 nm magnification; B1: MSN-R at 200 nm magnification; B3: MSN-R size distribution curve.

Table 8 shows the average results obtained for all LYC-incorporated MSNs conditions. It is worth noting that the concentrations above the validated range were diluted and the analysis were repeated. As there are no previous studies in the literature regarding the incorporation of LYC in this type of nanoparticle making a parallel is complicated because the amount of drug that is incorporated depends on the interaction between the drug and the carrier, in addition to characteristics inherent to the silica matrix such as surface area and pore size and structure (Carvalho et al., 2020; Croissant et al., 2017; Deodhar et al., 2017; Falsafi et al., 2021; Hoffmann et al., 2006; Rosenholm et al., 2011). However, it can be observed that both MSNs had similar values of EE% and LD% under the same conditions, and that in some conditions the EE% value was close to 100%, which confirms that LYC was successfully incorporated into both MSNs.

Table 8: Average results obtained for all LYC-incorporated MSNs conditions evaluated.

MSN type/ Concentration (mg/mL)	Time														
	6h			12h			24 h			36 h			48h		
	Free LYC (mg/mL)	EE%	LD%	Free LYC (mg/mL)	EE%	LD%	Free LYC (mg/mL)	EE%	LD%	Free LYC (mg/mL)	EE%	LD%	Free LYC (mg/mL)	EE%	LD%
MSN-R/1.0	0.377	62.2	12.4	0.533	46.6	9.3	0.658	34.1	6.8	0.504	49.5	9.9	0.145	85.4	17.0
MSN-R/1.5	0.920	38.6	11.5	0.505	66.3	19.8	0.839	44.0	13.2	0.849	43.3	13.0	0.041	97.2	29.1
MSN-R/2.0	0.897	55.1	22.0	0.754	62.2	24.9	0.548	72.5	29.0	0.530	73.3	29.3	0.024	98.7	39.5
MSN-R/2.5	1.405	43.7	21.8	0.696	72.1	36.0	0.833	66.6	33.3	0.660	73.5	36.7	0.045	98.1	49.0
MSN-R/3.0	1.185	60.4	36.2	0.784	73.8	44.3	0.322	89.2	53.5	0.115	96.1	57.6	0.008	99.7	59.8
MSN-R/3.5	1.412	59.6	41.7	0.999	71.4	50.0	0.236	93.2	65.2	0.065	98.1	68.6	0.063	98.1	68.7
MSN-R/4.0	1.484	62.8	50.3	0.810	79.7	63.7	0.365	90.8	72.6	0.067	98.3	78.6	0.003	99.9	79.9
MSN-C/1.0	0.463	53.6	10.7	0.578	42.1	8.4	0.245	75.4	15.0	0.550	44.9	8.9	0.494	50.6	10.1
MSN-C/1.5	0.703	53.0	15.9	0.608	59.4	17.8	0.293	80.4	24.1	0.847	43.5	13.0	0.239	84.0	25.2
MSN-C/2.0	1.091	45.4	18.1	0.616	69.1	27.4	0.984	50.7	20.3	1.149	42.5	17.0	0.079	96.0	38.4
MSN-C/2.5	1.223	51.0	25.5	0.837	66.5	33.2	0.904	63.8	31.9	1.409	43.6	21.8	0.616	75.3	37.6
MSN-C/3.0	1.226	59.1	35.4	1.257	64.0	34.8	0.627	79.0	47.4	0.379	87.0	52.4	0.323	89.2	53.5
MSN-C/3.5	1.313	62.4	43.7	1.033	70.4	49.3	0.694	80.1	56.1	0.212	94.1	65.7	0.706	79.8	55.8
MSN-C/4.0	1.942	51.4	41.1	1.399	65.0	52.0	0.376	90.5	72.4	0.177	93.7	76.4	0.747	81.3	65.0

Legend: LYC: lycopene; EE: encapsulation efficiency; LD: loading degree; MSN-R: refluxed mesoporous silica nanoparticle; MSN-C Calcined mesoporous silica nanoparticle.

3.1.4. TGA analysis

Figure 5A shows the thermal behavior of LYC, MSN-C, and MSN-R up to 800 ºC. LYC thermal decomposition was observed starting at 170 °C, which presented 100% of mass loss in the TGA curve. Both MSN showed mass losses before LYC onset temperature of thermal decomposition, steps attributed to dehydration of the samples and discarded from calculations. Above this temperature, different total mass losses were also observed for calcinated (3.33%) and refluxed (4.67%) MSN, these values were attributed to the decomposition of organic matter.

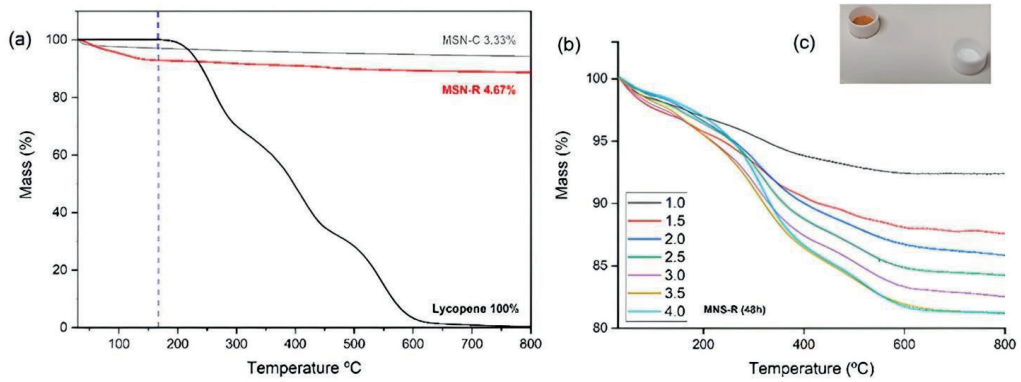

Figure 5: (A) Thermal behavior of LYC, MSN-C, and MSN-R up to 800ºC. (B) MSN-R at 48h incorporated with LYC in different concentrations total mass loss behavior in the TGA curve (condition representative of all samples studied in this work). (C) incorporated sample before and after the thermal analysis.

It can be observed that the total mass loss in the TGA curve increases with the increase of the LYC, looking like a pattern (**Figure 5B and Table 9**). The behavior of the MSN-R at 48h is representative of all samples studied in this work. The thermal profile of the samples is similar since the matrix is the same for all of them. Nevertheless, the sample with LYC concentration of 4.0 mg/mL presented a lower mass loss until 170ºC, causing the curve to overlap with its predecessor (LYC concentration of 3.5 mg/mL). Anyway, the total mass loss between 170–800 ºC still been higher for concentration 4.0 mg/mL. Additionally, **Figure 5C** shows the incorporated sample before and after the thermal analysis. As can be observed, it has a color change after 800ºC, which suggests that all organic matter correlated to LYC has been burned.

Table 9: Thermal data of incorporated silica in different times.

MSN type/ Concentration (mg/mL)	6h		12h		24h		36h		48h	
	Mass loss (%)	Δm_T %	Mass loss (%)	Δm_T %	Mass loss (%)	Δm_T %	Mass loss (%)	Δm_T %	Mass loss (%)	Δm_T %
MSN-R/1.0	5.94	1.27	12.13	7.46	9.38	4.71	10.83	6.16	11.75	7.08
MSN-R/1.5	10.53	5.86	12.73	8.06	11.41	6.74	12.15	7.48	13.84	9.17
MSN-R/2.0	14.24	9.57	13.60	8.93	13.21	8.54	16.11	11.44	15.74	11.07
MSN-R/2.5	17.06	12.39	12.80	8.13	13.52	8.85	16.87	12.20	15.62	10.95
MSN-R/3.0	17.22	12.55	14.48	9.81	15.68	11.01	17.98	13.31	16.49	11.82
MSN-R/3.5	17.92	13.25	15.78	11.11	16.33	11.66	18.68	14.01	20.23	15.56
MSN-R/4.0	19.59	14.92	18.54	13.87	19.47	14.80	19.85	15.18	20.59	15.92
MSN-C/1.0	5.70	2.37	7.49	4.16	5.58	2.25	5.78	2.45	5.02	1.69
MSN-C/1.5	6.83	3.50	9.64	6.31	9.02	5.69	7.18	3.85	8.85	5.52
MSN-C/2.0	7.50	4.17	11.31	7.98	9.17	5.84	8.64	5.31	12.04	8.71
MSN-C/2.5	7.73	4.40	12.03	8.70	12.15	8.82	11.77	8.44	12.82	9.49
MSN-C/3.0	10.37	7.04	13.82	10.49	14.59	11.26	13.88	10.55	14.88	11.55
MSN-C/3.5	10.47	7.14	14.27	10.94	14.91	11.58	14.14	10.81	15.25	11.92
MSN-C/4.0	13.73	10.4	14.70	11.37	15.24	11.91	16.57	13.24	16.48	13.15

Legend: MSN-R: refluxed mesoporous silica nanoparticle; MSN-C Calcined mesoporous silica nanoparticle; Δm_T: total mass variation

In **Figure 6** it is possible to observe that the TGA analysis was also able to quantify the LYC content in both MSN (represented by ΔmT), which, in the same way as observed in the HPLC results, was linear and followed the pattern: the higher the concentration of drug in the solution, the greater the amount of drug incorporated. Despite confirming the pattern observed by HPLC, the values obtained for LD% by TGA were significantly lower. Despite there are studies in the literature addressing the good results correlation between TGA and HPLC quantification, this fact was not observed in this study (Almaghrabi et al., 2023; Christoforidou et al., 2021; Tamasi et al., 2021; Zhang et al., 2010). A possible justification for this fact is that the technique used to determine the EE% and LD% by HPLC was the indirect technique, while for the TGA analysis was the direct one. It is possible to observe in the literature studies whose objective was to compare different drug incorporation methods, which observed that in the indirect method the quantification was greater than the one observed by the direct method, which is in agreement with the results obtained here (Amini et al., 2017; Bakonyi et al., 2017; Keawchaoon & Yoksan, 2011). Being the indirect method considered more reliable by some authors, mainly due to the smallest standard deviation and reproducibility (between different indirect methods) (Amini et al., 2017; Bakonyi et al., 2017; Khoshneviszadeh et al., 2016). However, those information does not seem to be a consensus in the literature (Daneshmand et al., 2018; de Câmara et al., 2016).

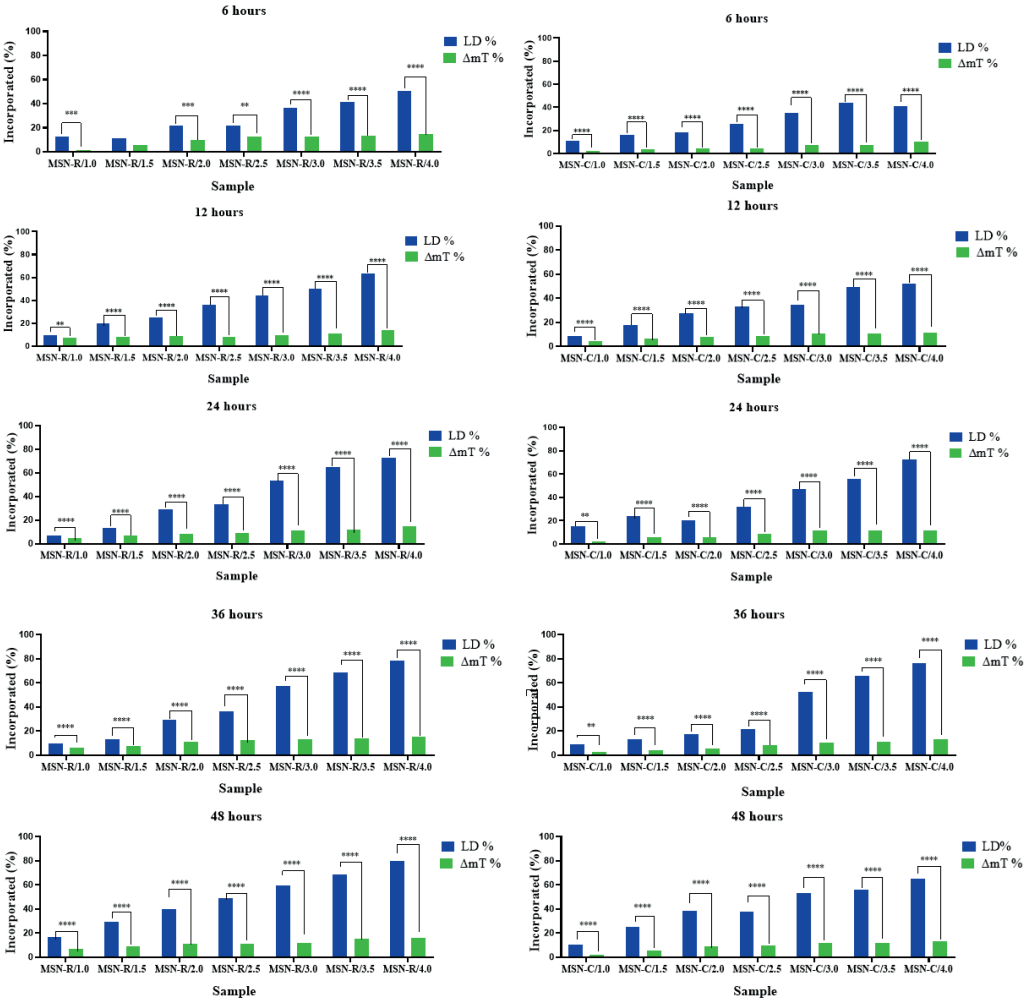

Figure 6: Comparison between Δm_T % and LD% for (A) refluxed mesoporous silica nanoparticle and (B) Calcined mesoporous silica nanoparticle. Legend: p-value; **< 0.005; ***< 0.001; ****<0.0001.

3.2. Choosing the ideal formulation

During the EE% statistical analysis, the p-value obtained was much lower than the Student's *t*-value (for both MSNs), been that the time and concentration variables interfere differently for the EE%. These results can be confirmed by the Pareto chart and by the surface graph (**Figure 7 A1, A2, A3** and **A4**). Additionally, the residuals ANOVA test confirmed that these data are homoscedastic, which increases the data reliability **(Figure 7 A5** and **A6)**.

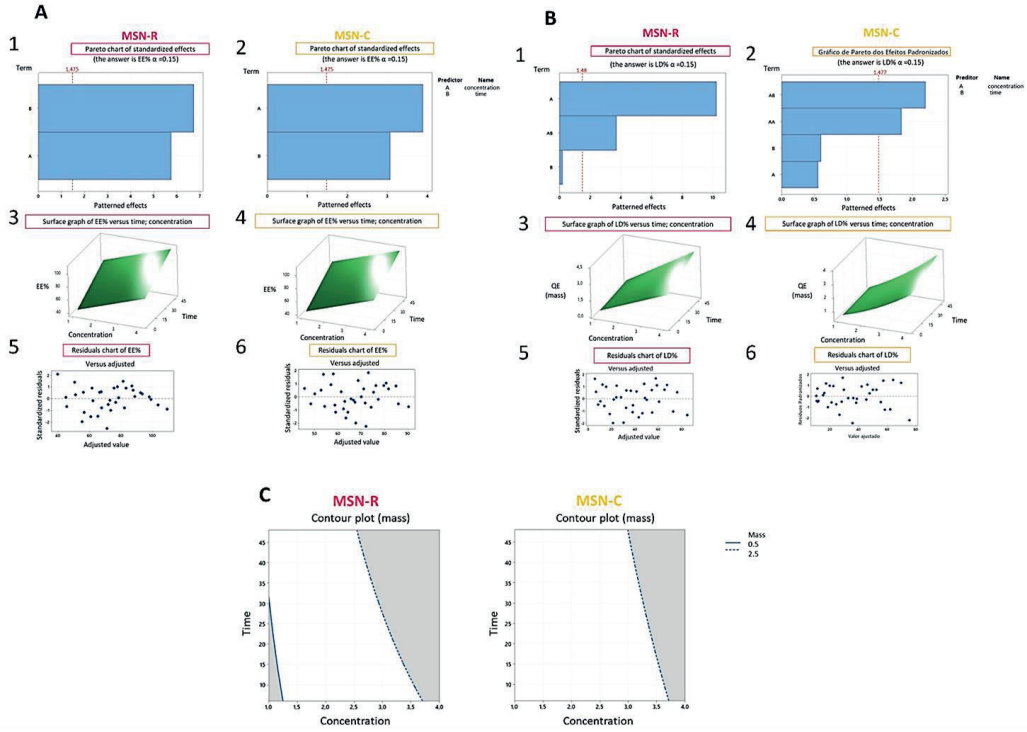

Figure 7: Statistical analysis graphical representation of the time and concentration interference in the (A) EE% data and (B) LD% data from both MSN.1: Pareto chart of the effect of concentration and time (MSN-R). 2: Pareto plot of the effect of concentration and time (MSN-C). 3: Surface graph of the effect of concentration and time (MSN-R). 4: Surface graph of the effect of concentration and time (MSN-C). 5: Residual chart (MSN-R). 6: Residual chart (MSN-C). (C) Contour graphic of the conditions tested to incorporate the drug. Legend: EE: encapsulation efficiency; LD: loading degree; MSN-R: refluxed mesoporous silica nanoparticle; MSN-C: Calcined mesoporous silica nanoparticle

In addition, the statistical analysis of the LD% data for the MSNs-R showed that the variables concentration and concentration with time interfere significantly for the LD% results. However, the isolated time variable does not significantly interfere because in addition to the Student's *t*-value be higher than the p-value (-0.20 and 0.839, respectively) the Pareto graph and the surface graph also reinforce this information (**Figure 7 B1, B3, B5)**. Additionally, the ANOVA test residuals confirmed that these data are homoscedastic, which increases the reliability of these findings.

In MSN-C LD% results, both variables showed to interfere significantly to the LD%, but this same pattern was not observed in their associations. The Pareto graph and the surface graph also

reinforce this information (**Figure 7 B2, B4, B6**). Additionally, the residuals ANOVA test confirmed that these data are homoscedastic, which increases their reliability. This difference in LD% between the two types of MSNs studied is not very clear in the literature, but a possible reason for a lower LD% value to MSN-C may be because during the calcination there is a repulsion between the silanol groups on its surface, which can cause aggregation, decreasing not only its dispersion in the solvent used for the incorporation step, but also the surface area available for drug loading (Ghasemi et al., 2017; Lin et al., 2012; Wu et al., 2013).

Additionally, contour graph (**Figure 7C**) was performed to assist in the decision making as it illustrates and predict the relationship between time and concentration. Emphasis was placed on the ideal incorporation of 2.5 mg/mL (this ideal incorporation value was defined based on previous study according to LYC minimum inhibitory concentration against *Candida albicans*) (Carvalho et al., 2022). Taking into account the conditions tested and the inherent cost of the drug, it can be said that the ideal incorporation condition for the MSN-R is 2.5 mg/mL and 3.0 mg/mL for MSN-C, both with the ideal time of 48 h. However, due to the fact that the MSN-R presents better LD% results and allows the ideal incorporation with a smaller amount of drug, the MSN-R incorporated with 2.5 mg/mL of drug for 48h was chosen for the following experiments, being called only LYC@MSN.

It is worth mentioning that all the statistical analyses of concentration/time performed with the conditions carried out in this study had the purpose to both help in choosing the best impregnation condition and also to reduce the time and cost of the formulation production, since conditions with higher drug concentration, in this study did not differ significantly from a formulation with lower drug concentration; however, the latter can have a lower cost. In addition, the difference in the treatment for removing organic residues from the pores of the two different MSN (calcination and reflux) could be an interference factor, since it is known in the literature that some techniques, such as acid reflux, can leave organic residues into the pores, which could lead to a lower incorporation of the drug due to the fact that the pore was “occupied”, however this fact was not confirmed in this study, since, on the contrary, the nanoparticle obtained by acid reflux presented better results (Carvalho et al., 2022).

3.3. Knowing LYC@MSN characteristics

3.3.1. TEM

According to the size distribution curve obtained from the HR-TEM images, and with the help of the Image J software for counting the nanoparticles (**Figure 8**), the LYC@MSN have a mean diameter of 66 nm (ranging from 34 at 118 nm). Although it is known in the literature that the

incorporation of drugs into this type of nanoparticle does not affect its size, the difference between the average diameter of pure MSN-R (82 nm, ranging from 48 to 131 nm) with LYC@MSN can be explained by the fact that the synthesis process carried out provided nanoparticles of different sizes and therefore this difference is due to the heterogeneity of the particles obtained and not to an increase in size after incorporation (Cao et al., 2018; Choi & Kim, 2017; Vazquez et al., 2017). In addition to the diameter, it is also possible to observe in **Figure 8** that after the drug incorporation process, the particles remained spherical with the presence of randomly arranged pores, as observed in previous works using this same type of nanoparticle (Cao et al., 2018; Choi & Kim, 2017; Lu et al., 2018).

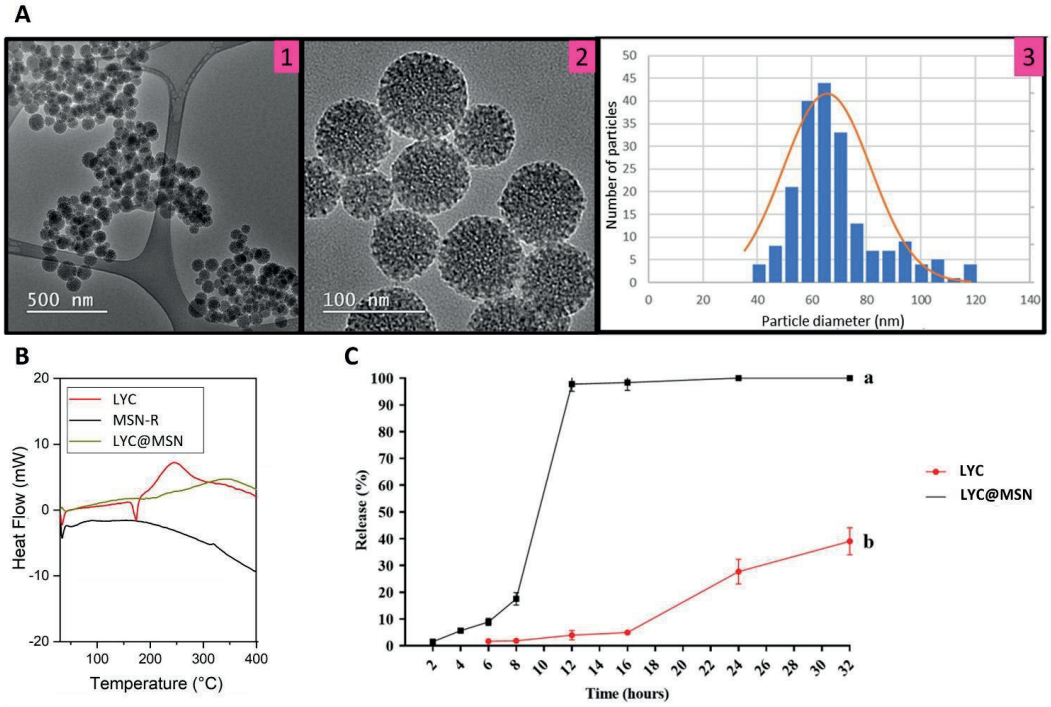

Figure 8. High-resolution transmission electron microscopy of LYC@MSN at different magnifications and their respective size distribution histograms obtained from counting 200 nanoparticles 1: in 500 magnification; 2 at 100 nm magnification; 3:particle size distribution curve obtained from HR-TEM images; (B) Lycopene, MSN-R and LYC@MSN DSC curves; (C) Release profile of LYC@LMSN and free lycopene in simulated vaginal medium at a temperature of 37ºC under constant agitation of 300 rpm. Legend: LYC@MSN: Mesoporous silica nanoparticle incorporated with lycopene; MSN-R: refluxed mesoporous silica nanoparticle;

3.3.2. Differential scattering calorimetry (DSC)

The incorporation condition considered as ideal was analyzed by DSC (**Figure 7B**), as well for the MSN-R and the free drug. It is possible to observe that the three DSC curves have a first endothermic event (up to 150 °C), attributed to loss of water or solvents adsorbed in the samples (Maturi et al., 2019). According to the literature, LYC may have two possible melting points, the first one in the region of 169.48 °C, referring to the cis isomer, and the second around 176.35 °C, referring to the trans isomer. According to LYC manufacturer (APIChem Technology Co.), the active pharmaceutical ingredient used here is composed only by the trans isomer (purity of 98.2% according to the report provided by the manufacturer), which therefore agrees with the endothermic peak observed around 180–190 °C in the DSC curves for free LYC and LYC@MSN (with almost imperceptible intensity in the latter) (Murakami et al., 2017; Takehara et al., 2014). This almost imperceptible intensity may suggest a change in LYC crystalline network, indicating that it is in the amorphous state within the mesopores of the MSN (Zardini et al., 2018; Pu & Tang, 2017).

In the DSC curve of free LYC, it is also possible to observe an exothermic event around 240 ºC, which, according to the literature, refers to the thermal decomposition of the drug (Pu & Tang, 2017). This event was not observed in the LYC@MSN curve, indicating the occurrence of interaction between the drug and the nanoparticle. It is also worth noting that this fact also indicates that the incorporation provided greater stability to the drug, which, after incorporation, began to be degraded at approximately 350 ºC. This profile mentioned here is an indication that LYC is inside the MSN mesopores (Pu & Tang, 2017).

3.3.3. In vitro release assay

As can be seen in **Figure 8C**, while the system was able to release 97.79% of the drug in 12 h and 100% in 24 h, the free drug released 39.03% in 32 h. A comparison with the literature is difficult since studies involving MSN with LYC are rare and the release profile is closely linked with the interactions between drug and nanoparticle. However, it is possible to suggest that the profile observed here differs slightly from those presented in the literature for this type of nanoparticle, such as in the work of Bolouki et al., (2015), who studied the release profile of MSN incorporated with curcumin, in different pH, through a methodology similar to the one used here, and observed that none of them reached a release of 100% (the maximum observed was 40-45%); however, around 8 to 10 h, a value close to the final release was reached.

However, in a similar study approaching the release profile of ibuprofen incorporated in different MSNs (the authors synthesized four types of MSNs varying the microwave power in the

range of 100-450 W) it was observed that all of them needed 50 h to reach a 100% of drug release. In around 20 h, all formulations showed a drug release of 70-90% (Kamarudin et al., 2014). Similarly, Peretti et al., (2018) evaluated the release profile of MSN incorporated with pentamidine and observed a release of 90% in 25 h. It is also worth mentioning that a rapid release (around 80% of the total drug) occurred in the first hours of the experiment (a little before 6 h).

Finally, it is worth mentioning that the use of the microplate reader was preferable for this assay, since the detection limit (determined experimentally during partial validation) was 4.6 µg/mL, well below to the one obtained with the HPLC method.

4. Conclusion

When it comes to the development of a new nanoformulation, the use of analytical techniques in order to both characterize the system and to predict its behavior in a future human application is of fundamental importance. The HPLC method developed here proved to be linear, accurate, precise and robust, in addition to being selective under the tested conditions, including its application for LYC quantification. So, it can be said that the developed method was duly validated for the range of 26–125 µg/mL. However, it proved to be suitable for the quantification of content for the incorporation conditions tested. The HPLC parallel with the TGA analysis was perhaps the limitation of this study. Additionally, by DSC it is possible to suggest that the drug could be incorporated in the mesopores, and that this fact protected the drug from degradation. This result is in agreement with the results of the release test, where the protection of the drug by the nanoparticle was also evident. These findings make MSN a promising nanocarrier for LYC incorporation in order to circumvent the limitations of using this drug in therapy. Finally, it is worth mentioning that despite the incorporation of this drug in the MSN mesopores can protect it against heat, light and oxygen, care must be taken during the impregnation process, such as absence of light, mild temperature and avoid exposure of the undiluted drug to oxygen for a long time.

5. Acknowledgements

This work was supported by São Paulo Research Foundation (FAPESP, Brazil) grant numbers nº 2019/26821-7; 2018/23357-5, 2019/09831-9 and 2018/25377-3, and the UMCG Research Funds. This publication is part of the Special Issue organized by COST Action NETPORE (CA20126), supported by COST (European Cooperation in Science and Technology).

6. References

Adetunji, C. O., Akram, M., Mtewa, A. G., Jeevanandam, J., Egbuna, C., Ogodo, A. C., Gautam, A. K., Gupta, A., Onyekere, P. F., Tupas, G. D., & others. (2021). Biochemical and pharmacotherapeutic potentials of lycopene in drug discovery. In *Preparation of Phytopharmaceuticals for the Management of Disorders* (pp. 307–360). Elsevier.

Almaghrabi, M., Alqurshi, A., Jadhav, S. A., Mazzacuva, F., Cilibrizzi, A., Raimi-Abraham, B., & Royall, P. G. (2023). Evaluating Thermogravimetric Analysis for the Measurement of Drug Loading in Mesoporous Silica Nanoparticles (MSNs). *Thermochimica Acta, 730,* Article 179616. https://doi.org/10.1016/j.tca.2023.179616

Alves, R. C., Perosa Fernandes, R., Fonseca-Santos, B., Damiani Victorelli, F., & Chorilli, M. (2019). A Critical Review of the Properties and Analytical Methods for the Determination of Curcumin in Biological and Pharmaceutical Matrices. *Critical Reviews in Analytical Chemistry*, *49*(2), 138–149. https://doi.org/10.1080/10408347.2018.1489216

Amini, Y., Amel Jamehdar, S., Sadri, K., Zare, S., Musavi, D., & Tafaghodi, M. (2017). Different methods to determine the encapsulation efficiency of protein in PLGA nanoparticles. *Bio-Medical Materials and Engineering*, *28*(6), 613–620. https://doi.org/10.3233/BME-171705

Amjad, M., Hussain, S., & Rehman Khan, A. (2020). Development and Validation of HPLC assay of Lycopene in Different Matrices. *World Journal of Applied Chemistry*, *5*(2), 26-33. https://doi.org/10.11648/j.wjac.20200502.13

Araujo, V. H. S., Duarte, J. L., Carvalho, G. C., Silvestre, A. L. P., Fonseca-Santos, B., Marena, G. D., Ribeiro, T. de C., dos Santos Ramos, M. A., Bauab, T. M., & Chorilli, M. (2020). Nanosystems against candidiasis: a review of studies performed over the last two decades. *Critical Reviews in Microbiology*, *46*(5), 508–547. https://doi.org/10.1080/1040841X.2020.1803208

Bakonyi, M., Berkó, S., Budai-Szűcs, M., Kovács, A., & Csányi, E. (2017). DSC for evaluating the encapsulation efficiency of lidocaine-loaded liposomes compared to the ultracentrifugation method. *Journal of Thermal Analysis and Calorimetry*, *130*(3), 1619–1625. https://doi.org/10.1007/s10973-017-6394-1

Barbedo, L. S., Sgarbi, D.B.G. (2010). Candidíase. *DST J Bras Doenças Sex Transm*, *22*, 22–38.

Bolouki, A., Rashidi, L., Vasheghani-Farahani, E., & Piravi-Vanak, Z. (2015). Study of mesoporous silica nanoparticles as nanocarriers for sustained release of curcumin. *International Journal of Nanoscience and Nanotechnology*, *11*(3), 139–146.

Cao, L., Zhou, Z., Niu, S., Cao, C., Li, X., Shan, Y., & Huang, Q. (2018). Positive-Charge Functionalized Mesoporous Silica Nanoparticles as Nanocarriers for Controlled 2,4-Dichlorophenoxy Acetic Acid Sodium Salt Release. *Journal of Agricultural and Food Chemistry*, *66*(26), 6594–6603. https://doi.org/10.1021/acs.jafc.7b01957

Carvalho, G. C., Bugno, A., Almodovar, A. A. B., Silva, F. P. de L. e, & Pinto, T. de J. A. (2020). Validation and applicability of an alternative method for dialysis water and dialysate quality analysis. *Brazilian Journal of Nephrology*, *42*(2), 163–174. https://doi.org/10.1590/2175-8239-jbn-2019-0203

Carvalho, G. C., de Camargo, B. A. F., de Araújo, J. T. C., & Chorilli, M. (2021). Lycopene: From tomato to its nutraceutical use and its association with nanotechnology. *Trends in Food Science & Technology*, *118*, 447–458. https://doi.org/10.1016/j.tifs.2021.10.015

Carvalho, G. C., de Oliveira, R. A. P., Araujo, V. H. S., Sábio, R. M., de Carvalho, L. R., Bauab, T. M., Corrêa, I., & Chorilli, M. (2021). Prevalence of vulvovaginal candidiasis in Brazil: A systematic review. *Medical Mycology, 59*(10), 946–957. https://doi.org/10.1093/mmy/myab034

Carvalho, G. C., Marena, G. D., Karnopp, J. C. F., Jorge, J., Sábio, R. M., Martines, M. A. U., Bauab, T. M., & Chorilli, M. (2022). Cetyltrimethylammonium bromide in the synthesis of mesoporous silica nanoparticles: General aspects and in vitro toxicity. *Advances in Colloid and Interface Science*, *307,* Article 102746. https://doi.org/10.1016/j.cis.2022.102746

Carvalho, G. C., Marena, G. D., Leonardi, G. R., Sábio, R. M., Corrêa, I., Chorilli, M., & Bauab, T. M. (2022). Lycopene, Mesoporous Silica Nanoparticles and Their Association: A Possible Alternative against Vulvovaginal Candidiasis? *Molecules*, *27*(23), Article 8558. https://doi.org/10.3390/molecules27238558

Carvalho, G. C., Sábio, R. M., & Chorilli, M. (2020). An Overview of Properties and Analytical Methods for Lycopene in Organic Nanocarriers. *Critical Reviews in Analytical Chemistry*, *51*(7), 67-86. https://doi.org/10.1080/10408347.2020.1763774

Carvalho, G. C., Sábio, R. M., de Cássia Ribeiro, T., Monteiro, A. S., Pereira, D. V., Ribeiro, S. J. L., & Chorilli, M. (2020). Highlights in Mesoporous Silica Nanoparticles as a Multifunctional Controlled Drug Delivery Nanoplatform for Infectious Diseases Treatment. *Pharmaceutical Research*, *37*(10), Article 191. https://doi.org/10.1007/s11095-020-02917-6

Ceschel, G., Badiello, R., Ronchi, C., & Maffei, P. (2003). Degradation of components in drug formulations: a comparison between HPLC and DSC methods. *Journal of Pharmaceutical and Biomedical Analysis*, *32*(4–5), 1067–1072. https://doi.org/10.1016/S0731-7085(03)00210-3

Cheremisinoff, N. P. (1996). *Polymer Characterization Laboratory Techniques and Analysis*. Noyes Publications. https://doi.org/10.1016/B978-0-8155-1403-9.50004-2

Choi, E., & Kim, S. (2017). How Can Doxorubicin Loading Orchestrate in Vitro Degradation Behaviors of Mesoporous Silica Nanoparticles under a Physiological Condition? *Langmuir*, *33*(20), 4974–4980. https://doi.org/10.1021/acs.langmuir.7b00332

Choi, H., & Lee, D. G. (2015). Lycopene induces apoptosis in Candida albicans through reactive oxygen species production and mitochondrial dysfunction. *Biochimie*, *115*, 108–115. https://doi.org/10.1016/j.biochi.2015.05.009

Christoforidou, T., Giasafaki, D., Andriotis, E. G., Bouropoulos, N., Theodoroula, N. F., Vizirianakis, I. S., Steriotis, T., Charalambopoulou, G., & Fatouros, D. G. (2021). Oral Drug Delivery Systems Based on Ordered Mesoporous Silica Nanoparticles for Modulating the Release of Aprepitant. *International Journal of Molecular Sciences*, *22*(4), Article 1896. https://doi.org/10.3390/ijms22041896

Croissant, J. G., Butler, K. S., Zink, J. I., & Brinker, C. J. (2020). Synthetic amorphous silica nanoparticles: toxicity, biomedical and environmental implications. *Nature Reviews Materials*, *5*(12), 886–909. https://doi.org/10.1038/s41578-020-0230-0

Croissant, J. G., Fatieiev, Y., & Khashab, N. M. (2017). Degradability and clearance of silicon, organosilica, silsesquioxane, silica mixed oxide, and mesoporous silica nanoparticles. *Advanced Materials*, *29*(9), Article 1604634. https://doi.org/10.1002/adma.201604634

Daneshmand, S., Golmohammadzadeh, S., Jaafari, M. R., Movaffagh, J., Rezaee, M., Sahebkar, A., & Malaekeh-Nikouei, B. (2018). Encapsulation challenges, the substantial issue in solid lipid nanoparticles characterization. *Journal of Cellular Biochemistry*, *119*(6), 4251–4264. https://doi.org/10.1002/jcb.26617

de Câmara, A. A., Dupont, S., Beney, L., Gervais, P., Rosenthal, A., Correia, R. T. P., & Pedrini, M. R. da S. (2016). Fisetin yeast-based bio-capsules via osmoporation: effects of process variables on the encapsulation efficiency and internalized fisetin content. *Applied Microbiology and Biotechnology*, *100*(12), 5547–5558. https://doi.org/10.1007/s00253-016-7425-8

Deodhar, G. V, Adams, M. L., & Trewyn, B. G. (2017). Controlled release and intracellular protein delivery from mesoporous silica nanoparticles. *Biotechnology Journal*, *12*(1), Article 1600408. https://doi.org/10.1002/biot.201600408

Falavigna, M., Pattacini, M., Wibel, R., Sonvico, F., Škalko-Basnet, N., & Flaten, G. E. (2020). The Vaginal-PVPA: A Vaginal Mucosa-Mimicking In Vitro Permeation Tool for Evaluation of Mucoadhesive Formulations. *Pharmaceutics*, *12*(6), Article 568. https://doi.org/10.3390/pharmaceutics12060568

Falsafi, S. R., Rostamabadi, H., Babazadeh, A., Tarhan, Ö., Rashidinejad, A., Boostani, S., Khoshnoudi-Nia, S., Akbari-Alavijeh, S., Shaddel, R., & Jafari, S. M. (2021). Lycopene nanodelivery systems; recent advances. *Trends in Food Science & Technology*, *119*, 378–399. https://doi.org/10.1016/j.tifs.2021.12.016

FDA, (1994). *Reviewer guidance: Validation of chromatographic methods.* Center for Drug Evaluation Research (CDER). https://www.fda.gov/regulatory-information/search-fda-guidance-documents/reviewer-guidance-validation-chromatographic-methods

Fussell, A. L., Mah, P. T., Offerhaus, H., Niemi, S.-M., Salonen, J., Santos, H. A., & Strachan, C. (2014). Coherent anti-Stokes Raman scattering microscopy driving the future of loaded mesoporous silica imaging. *Acta Biomaterialia*, *10*(11), 4870–4877. https://doi.org/10.1016/j.actbio.2014.07.021

Ghasemi, S., Farsangi, Z. J., Beitollahi, A., Mirkazemi, M., Rezayat, S. M., & Sarkar, S. (2017). Synthesis of hollow mesoporous silica (HMS) nanoparticles as a candidate for sulfasalazine drug loading. *Ceramics International*, *43*(14), 11225–11232. https://doi.org/10.1016/j.ceramint.2017.05.172

Giron, D. (2002). Applications of thermal analysis and coupled techniques in pharmaceutical industry. *Journal of Thermal Analysis and Calorimetry*, *68*(2), 335–357. https://doi.org/10.1023/a:1016015113795

Hassan, M. M., & Nam, S.-W. (2021). High-Performance Liquid Chromatography for Determining a Mixture of Nonsteroidal Anti-inflammatory Drugs. *Electronic Materials Letters*, *17*(5), 414–420. https://doi.org/10.1007/s13391-021-00306-8

Hoffmann, F., Cornelius, M., Morell, J., & Fröba, M. (2006). Cover Picture: Silica-Based Mesoporous Organic--Inorganic Hybrid Materials (Angew. Chem. Int. Ed. 20/2006). *Angewandte Chemie International Edition*, *45*(20), Article 3187. https://doi.org/10.1002/anie.200690070

Hussain, A., Pu, H., & Sun, D. W. (2019). Measurements of lycopene contents in fruit: A review of recent developments in conventional and novel techniques. *Critical Reviews in Food Science and Nutrition*, *59*(5), 758–769. https://doi.org/10.1080/10408398.2018.1518896

International Conference on Harmonization. (2005). Validation of analytical procedures: text and methodology Q2 (R1). *International Conference on Harmonization, Geneva, Switzerland*.

Jane, W. J., Iramiot, J. S., & Kalule, J. B. (2019). Prevalence and Antifungal Susceptibility patterns of Candida Isolated on CHROMagarTMCandida at a Tertiary Referral Hospital, Eastern Uganda. *Microbiology Research Journal International*, *28*(6), 1–6. https://doi.org/10.9734/mrji/2019/v28i630151

Kamarudin, N. H. N., Jalil, A. A., Triwahyono, S., Artika, V., Salleh, N. F. M., Karim, A. H., Jaafar, N. F., Sazegar, M. R., Mukti, R. R., Hameed, B. H., & Johari, A. (2014). Variation of the crystal growth of mesoporous silica nanoparticles and the evaluation to ibuprofen loading and release. *Journal of Colloid and Interface Science*, *421*, 6–13. https://doi.org/10.1016/j.jcis.2014.01.034

Kankala, R. K., Han, Y.-H., Xia, H.-Y., Wang, S.-B., & Chen, A.-Z. (2022). Nanoarchitectured prototypes of mesoporous silica nanoparticles for innovative biomedical applications. *Journal of Nanobiotechnology*, *20*(1), Article 126. https://doi.org/10.1186/s12951-022-01315-x

Kankala, R. K., Han, Y., Na, J., Lee, C., Sun, Z., Wang, S., Kimura, T., Ok, Y. S., Yamauchi, Y., Chen, A., & Wu, K. C. -W. (2020). Nanoarchitectured Structure and Surface Biofunctionality of Mesoporous Silica Nanoparticles. *Advanced Materials*, *32*(23), Article 1907035. https://doi.org/10.1002/adma.201907035

Kankala, R. K., Liu, C.-G., Yang, D.-Y., Wang, S.-B., & Chen, A.-Z. (2020). Ultrasmall platinum nanoparticles enable deep tumor penetration and synergistic therapeutic abilities through free radical species-assisted catalysis to combat cancer multidrug resistance. *Chemical Engineering Journal*, *383*, Article 123138. https://doi.org/10.1016/j.cej.2019.123138

Kankala, R. K., Zhang, H., Liu, C.-G., Kanubaddi, K. R., Lee, C.-H., Wang, S.-B., Cui, W., Santos, H. A., Lin, K., & Chen, A.-Z. (2019). Metal species-encapsulated mesoporous silica nanoparticles: current advancements and latest breakthroughs. *Advanced Functional Materials*, *29*(43), Article 1902652. https://doi.org/10.1002/adfm.201902652

Keawchaoon, L., & Yoksan, R. (2011). Preparation, characterization and in vitro release study of carvacrol-loaded chitosan nanoparticles. *Colloids and Surfaces B: Biointerfaces*, *84*(1), 163–171. https://doi.org/10.1016/j.colsurfb.2010.12.031

Khan, U. M., Sevindik, M., Zarrabi, A., Nami, M., Ozdemir, B., Kaplan, D. N., Selamoglu, Z., Hasan, M., Kumar, M., Alshehri, M. M., & Sharifi-rad, J.

(2021). Review Article Lycopene : Food Sources , Biological Activities , and Human Health Benefits. *Oxidative Medicine and Cellular Longevity*, *2021,* 1-10. https://doi.org/10.1155/2021/2713511

Khoshneviszadeh, R., Fazly, B. B. S., Housaindokht, M. R., Ebrahim, H. A., & Rajabi, O. (2016). A comparison of explanation methods of encapsulation efficacy of hydroquinone in a liposomal system. *Journal of Paramedical Sciences,* 7(2), 23-28.

Limnell, T., Heikkilä, T., Santos, H. A., Sistonen, S., Hellstén, S., Laaksonen, T., Peltonen, L., Kumar, N., Murzin, D. Y., Louhi-Kultanen, M., & others. (2011). Physicochemical stability of high indomethacin payload ordered mesoporous silica MCM-41 and SBA-15 microparticles. *International Journal of Pharmaceutics, 416*(1), 242–251. https://doi.org/10.1016/j.ijpharm.2011.06.050

Lin, Y.-S., Hurley, K. R., & Haynes, C. L. (2012). Critical Considerations in the Biomedical Use of Mesoporous Silica Nanoparticles. *The Journal of Physical Chemistry Letters*, *3*(3), 364–374. https://doi.org/10.1021/jz2013837

Lu, H., Wen, C., Gao, S., Dong, Y., Zhang, M., Li, B., Hu, W., & Dong, J. (2018). Incorporation of nanoscale zero-valent iron particles in monodisperse mesoporous silica nanospheres: Characterization, reactivity, transport in porous media. *Colloids and Surfaces A: Physicochemical and Engineering Aspects*, *553*, 28–34. https://doi.org/10.1016/j.colsurfa.2018.05.038

Lucini, L., Pellizzoni, M., Baffi, C., & Molinari, G. Pietro. (2012). Rapid determination of lycopene and β-carotene in tomato by liquid chromatography/electrospray tandem mass spectrometry. *Journal of the Science of Food and Agriculture*, *92*(6), 1297–1303. https://doi.org/10.1002/jsfa.4698

Manzano, M., & Vallet-Regí, M. (2020). Mesoporous silica nanoparticles for drug delivery. *Advanced Functional Materials*, *30*(2), Article 1902634. https://doi.org/10.1002/adfm.201902634

Marchaim, D., Lemanek, L., Bheemreddy, S., Kaye, K. S., & Sobel, J. D. (2012). Fluconazole-resistant *Candida albicans* vulvovaginitis. *Obstetrics & Gynecology*, *120*(6), 1407–1414. http://10.1097/AOG.0b013e31827307b2

Marques, M. R. C., Loebenberg, R., Almukainzi, M., & others. (2011). Simulated biological fluids with possible application in dissolution testing. *Dissolution Technol*, *18*(3), 15–28.

Maturi, F. E., Sábio, R. M., Silva, R. R., Lahoud, M. G., Meneguin, A. B., Valente, G. T., Caface, R. A., Leite, I. S., Inada, N. M., & Ribeiro, S. J. L. (2019). Luminescent Mesoporous Silica Nanohybrid Based on Drug Derivative Terbium Complex. *Materials*, *12*(6), Article 933. https://doi.org/10.3390/ma12060933

Mayeaux, M., Xu, Z., King, J. M., & Prinyawiwatkul, W. (2006). Effects of Cooking Conditions on the Lycopene Content in Tomatoes. *Journal of Food Science*, *71*(8), C461–C464. https://doi.org/10.1111/j.1750-3841.2006.00163.x

Montesano, D., Fallarino, F., Cossignani, L., Bosi, A., Simonetti, M. S., Puccetti, P., & Damiani, P. (2008). Innovative extraction procedure for obtaining high pure lycopene from tomato. *European Food Research and Technology*, *226*(3), 327–335. https://doi.org/10.1007/s00217-006-0541-4

Murakami, K., Honda, M., Takemura, R., Fukaya, T., Kubota, M., Wahyudiono, Kanda, H., & Goto, M. (2017). The thermal Z-isomerization-induced change in solubility and physical properties of (all-E)-lycopene. *Biochemical and Biophysical Research Communications*, *491*(2), 317–322. https://doi.org/10.1016/j.bbrc.2017.07.103

Nascimento, A. L. C. S., Ashton, G. P., Parkes, G. M. B., Ekawa, B., Fernandes, R. P., Carvalho, A. C. S., Ionashiro, M., & Caires, F. J. (2019). Novel solid-state compounds of heavy rare-earth (III) picolinates. A pyrolytic study using: TG-DSC-IR, HSM-MS and GC-MS. *Journal of Analytical and Applied Pyrolysis*, *144*, Article 104709. https://doi.org/10.1016/j.jaap.2019.104709

Natarajan, K., Gajendran, P. L., Arjunkumar, R., & Kumar, S. R. (2020). Anti-fungal activity of chitosan nanoparticle incorporated lycopene against *Candida albicans* using minimal inhibitory concentration assay. *Plant Cell Biotechnology and Molecular Biology*, 73–82.

Peretti, E., Miletto, I., Stella, B., Rocco, F., Berlier, G., & Arpicco, S. (2018). Strategies to Obtain Encapsulation and Controlled Release of Pentamidine in Mesoporous Silica Nanoparticles. *Pharmaceutics*, *10*(4), Article 195. https://doi.org/10.3390/pharmaceutics10040195

Perez, M. Â. F. (2010). Validação de métodos analíticos: Como fazer? Por que ela é importante. *Boletim de Tecnologia e Desenvolvimento de Embalagens*, *22*(3), 1–9.

Pu, C., & Tang, W. (2017). Encapsulation of lycopene in Chlorella pyrenoidosa : Loading properties and stability improvement. *Food Chemistry*, *235*, 283–289. https://doi.org/10.1016/j.foodchem.2017.05.069

Rahikkala, A., Pereira, S. A. P., Figueiredo, P., Passos, M. L. C., Araújo, A. R. T. S., Saraiva, M. L. M. F. S., & Santos, H. A. (2018). Mesoporous Silica Nanoparticles for Targeted and Stimuli-Responsive Delivery of Chemotherapeutics: A Review. *Advanced Biosystems*, *2*(7), 1–33. https://doi.org/10.1002/adbi.201800020

Rodero, C. F., Calixto, G. M. F., Santos, K., Sato, M. R., Ramos, M. S., Miró, M. S., Rodríguez, E., Vigezzi, C., Bauab, T. M., Sotomayor, C. E., & others. (2018). Curcumin-loaded liquid crystalline systems for controlled drug release and improved treatment of vulvovaginal candidiasis. *Molecular Pharmaceutics*, *15*(10), 4491–4504. https://doi.org/10.1021/acs.molpharmaceut.8b00507

Rosenholm, J. M., Sahlgren, C., & Lindén, M. (2011). Multifunctional mesoporous silica nanoparticles for combined therapeutic, diagnostic and targeted action in cancer treatment. *Current Drug Targets*, *12*(8), 1166–1186. https://doi.org/10.2174/138945011795906624

Sábio, R. M., Santagneli, S. H., Gressier, M., Caiut, J. M. A., Pazin, W. M., Ribeiro, S. J. L., & Menu, M.-J. (2019). Near-infrared/visible-emitting nanosilica modified with silylated Ru (II) and Ln (III) complexes. *Nanotechnology*, *31*(3), Article 35602. https://doi.org/ 10.1088/1361-6528/ab494f

Shi, J., & Maguer, M. Le. (2000). Lycopene in tomatoes: chemical and physical properties affected by food processing. *Critical Reviews in Food Science and Nutrition*, *40*(1), 1–42. https://doi.org/10.1080/10408690091189275

Shi, J., Maguer, M., Bryan, M., & Kakuda, Y. (2003). Kinetics of lycopene degradation in tomato puree by heat and light irradiation. *Journal of Food Process Engineering*, *25*(6), 485–498. https://doi.org/10.1111/j.1745-4530.2003.tb00647.x

Sun, J.-G., Jiang, Q., Zhang, X.-P., Shan, K., Liu, B.-H., Zhao, C., & Yan, B. (2019). Mesoporous silica nanoparticles as a delivery system for improving antiangiogenic therapy. *International Journal of Nanomedicine*, *14*, 1489–1501. https://doi.org/10.2147/IJN.S195504

Sung, W. S., Lee, I.-S., & Lee, D. G. (2007). Damage to the cytoplasmic membrane and cell death caused by lycopene in *Candida albicans*. *Journal of Microbiology and Biotechnology*, *17*(11), 1797–1804.

Tahmasebi, M., & Emam-Djomeh, Z. (2021). Lycopene degradation and color characteristics of fresh and processed tomatoes under the different drying methods: a comparative study. *Chemical Papers*, *75*(7), 3617–3623. https://doi.org/10.1007/s11696-021-01611-0

Takehara, M., Nishimura, M., Kuwa, T., Inoue, Y., Kitamura, C., Kumagai, T., & Honda, M. (2014). Characterization and thermal isomerization of (all-E)-lycopene. *Journal of Agricultural and Food Chemistry*, *62*(1), 264–269. https://doi.org/10.1021/jf404497k

Tamasi, G., Pardini, A., Croce, R., Consumi, M., Leone, G., Bonechi, C., Rossi, C., & Magnani, A. (2021). Combined Experimental and Multivariate Model Approaches for Glycoalkaloid Quantification in Tomatoes. *Molecules*, *26*(11), Article 3068. https://doi.org/10.3390/molecules26113068

Tsai, S.-Y., Lin, H.-Y., Hong, W.-P., & Lin, C.-P. (2017). Evaluation of preliminary causes for vitamin D series degradation via DSC and HPLC analyses. *Journal of Thermal Analysis and Calorimetry*, *130*(3), 1357–1369. https://doi.org/10.1007/s10973-017-6209-4

United States Pharmacopeia. (2020a). *<621> CHROMATOGRAPHY* .43. ed. Rockville: The United States Pharmacopeia Convention.

United States Pharmacopeia. (2020b). *<1092> The Dissolution Procedure: Development and Validation.* 43. ed. Rockville: The United States Pharmacopeia Convention.

Vaudreuil, M.-A., Vo Duy, S., Munoz, G., Furtos, A., & Sauvé, S. (2020). A framework for the analysis of polar anticancer drugs in wastewater: On-line extraction coupled to HILIC or reverse phase LC-MS/MS. *Talanta*, *220*, Article 121407. https://doi.org/10.1016/j.talanta.2020.121407

Vazquez, N. I., Gonzalez, Z., Ferrari, B., & Castro, Y. (2017). Synthesis of mesoporous silica nanoparticles by sol–gel as nanocontainer for future drug delivery applications. *Boletín de La Sociedad Española de Cerámica y Vidrio*, *56*(3), 139–145. https://doi.org/10.1016/j.bsecv.2017.03.002

Vial, J., & Jardy, A. (1999). Experimental Comparison of the Different Approaches To Estimate LOD and LOQ of an HPLC Method. *Analytical Chemistry*, *71*(14), 2672–2677. https://doi.org/10.1021/ac981179n

Wu, S.-H., Mou, C.-Y., & Lin, H.-P. (2013). Synthesis of mesoporous silica nanoparticles. *Chemical Society Reviews*, *42*(9), 3862- 3875. https://doi.org/10.1039/c3cs35405a

Zardini, A. A., Mohebbi, M., Farhoosh, R., & Bolurian, S. (2018). Production and characterization of nanostructured lipid carriers and solid lipid nanoparticles containing lycopene for food fortification. *Journal of Food Science and Technology*, *55*(1), 287–298. https://doi.org/10.1007/s13197-017-2937-5

Zhang, Y., Zhi, Z., Jiang, T., Zhang, J., Wang, Z., & Wang, S. (2010). Spherical mesoporous silica nanoparticles for loading and release of the poorly water-soluble drug telmisartan. *Journal of Controlled Release*, *145*(3), 257–263. https://doi.org/10.1016/j.jconrel.2010.04.029

CHAPTER 8

Lycopene, mesoporous silica nanoparticles and their association: A possible alternative against vulvovaginal candidiasis?

Gabriela Corrêa Carvalho, Gabriel Davi Marena, Gabriela Ricci Leonardi, Rafael Miguel Sábio, Ione Corrêa, Marlus Chorilli*, Tais Maria Bauab*

Molecules, v. 27, n. 23, 8558 pp. 1-13, 2022.

Reprinted under the Creative Commons Attribution License

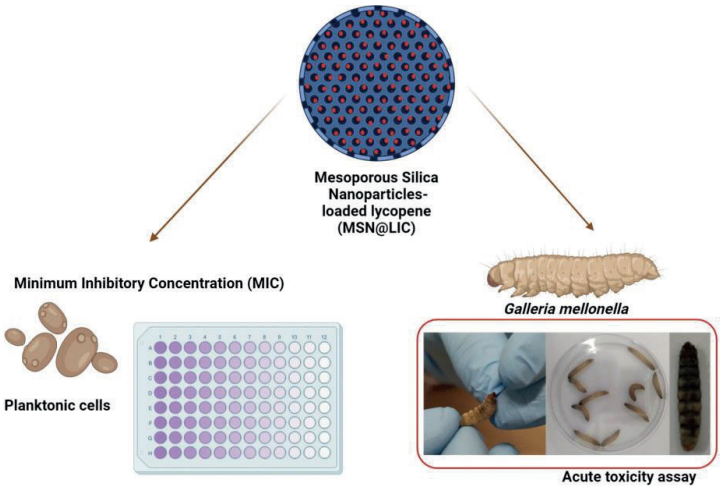

Abstract

Commonly found colonizing the human microbiota, *Candida albicans* is a microorganism known for its ability to cause infections, mainly in the vulvovaginal region known as vulvovaginal candidiasis (VVC). This pathology is, in fact, one of the main *C. albicans* clinical manifestations, changing from a colonizer to a pathogen. The increase in VVC cases and limited antifungal therapy make *C. albicans* an increasingly frequent risk in women's lives, especially in immunocompromised patients, pregnant women and the elderly. Therefore, it is necessary to develop new therapeutic options, especially those involving natural products associated with nanotechnology, like lycopene and mesoporous silica nanoparticles. From this perspective, this study sought to assess whether lycopene, mesoporous silica nanoparticles and their combination would be an attractive product for the treatment of this serious disease through microbiological *in vitro* tests and acute toxicity tests in an alternative *in vivo* model of *Galleria mellonella*. Although they did not show desirable antifungal activity for VVC therapy, the present study strongly encourages the use of mesoporous silica nanoparticles impregnated with lycopene for the treatment of other human pathologies, since the products evaluated here did not show toxicity in the *in vivo* test performed, being therefore, a topic to be further explored.

1. Introduction

Vulvovaginal candidiasis (VVC) is an opportunistic and endogenous fungal infection of the vulva and vagina, caused by *Candida spp.*. (Balakrishnan et al., 2022; Cruz et al., 2020; Czechowicz et al., 2022). This genus comprises approximately 200 different species, being *Candida albicans* the responsible for 70 to 90% of the cases (Firmiano et al., 2020; Salazar et al., 2022; Soares et al., 2018). According to the United States Centers for Disease Control and Prevention (CDC), in the USA, VVC is considered the second most common cause of genital infection in women of reproductive age, and about 75% of women worldwide will have at least one episode of these disease in their lifetime(CDC, 2022; Denning et al., 2018). Of these, 10 to 20% develop recurrent vaginal candidiasis, with four or more episodes per year (Soares et al., 2018; Sobel, 2002).

From this perspective, the infection may be associated with recurrent and common habits among women, such as the use of tight and/or synthetic underwear, which make the environment favorable for *C. albicans* multiplication, in addition to the use of systemic or topical antibiotics, which reduces the protection of the vaginal flora, allowing *C. albicans* to colonize (Firmiano et al., 2020; Mohamed et al., 2022). Furthermore, the etiologic agent infection can occur endogenously, once it is an opportunistic pathogen found in the healthy human microbiota, if the host presents an imbalance in its immune system, this fungus can spread and cause infections, or exogenously, through the contact with contaminated mucous membranes and secretions, or sexual contact, being more frequent in sexually active women, although it is not considered a sexually transmitted disease (Álvares et al., 2007; Davis, 2020; Mason et al., 2012; Ruiz-Sánchez et al., 2003).

Clinically, VVC is characterized by intense vulvar itching, mainly by the presence of whitish discharge, by signs of inflammation accompanied by burning sensations and by occasional white-yellow spots on the vaginal walls and cervix (Farr et al., 2021; Soares et al., 2018). Regarding treatment, despite the wide range of drugs available (such as azoles, polyenes, echinocandins and fluoropyrimidines), there are currently several reports in the literature of ineffective treatments due to susceptibility and resistance to various antifungals (mainly in the case of the most widely used class for the treatment of VVC, the azoles), making the study of new therapeutic options of fundamental importance, including substances of natural origin, such as lycopene (Barbedo et al., 2010; Carvalho et al., 2021; Gonçalves et al., 2016; Jane et al., 2019; Marchaim et al., 2012; Sanglard, 2016; Vikrant et al., 2015). A carotenoid responsible for the red color of fruits such as watermelon, pink grapefruit, papaya, red guava and especially tomatoes (main source of lycopene in the human diet) (Carvalho et al., 2021).

Among the various pharmacological properties of lycopene, the antifungal activity stands out, especially against *Candida* sp.. However, it is worth noting that its insolubility in aqueous solvents is

a limiting factor in therapy, as it results in low bioavailability. Therefore, lycopene impregnation in nanocarriers proves to be an interesting option for overcoming most of drawbacks concerning its application (Carvalho et al., 2021; Carvalho et al., 2021; Falsafi et al., 2021). Mesoporous silica nanoparticles (MSN) comprise an interesting nanoplatform for biomedical applications due to several properties including high thermal and chemical stability, adjustable pore structure and particle diameter as well as large surface area, free hydroxyls groups for functionalization, good biocompatibility, biodegradability, low toxicity and easy excretion by the body (Carvalho et al., 2020; Giret et al., 2015; Sahoo & Labhasetwar, 2003; Zhou et al., 2022). This type of nanoparticle, which was used for the first time for the purpose of controlled drug release in 2001, has been increasingly used in research addressing this purpose since it is capable of hosting different types of molecules through their interactions with the surface silanol groups of the silica matrix. It is worth mentioning that its porous characteristic is the primordial factor for the process of carrying and releasing molecules (Vallet-Regí, 2022; Vallet-Regi et al., 2001).

Although it is possible to find works in the literature addressing the use of both compounds for the treatment of *C. albicans* infections, their association gives to this work an innovative character, especially bearing in mind the incessant search for new, and promise, therapeutic options (Carvalho et al., 2020; Carvalho et al., 2021). It is also worth noting that for the development of an ideal formulation, it is necessary, in addition to presenting excellent activity, to be considered safe specially in terms of toxicity, in this sense, the tests on *Galleria mellonella* larvae, although still scarce for the compounds mentioned here, are increasingly gaining space (Patnaik et al., 2021; Piatek et al., 2021; Wright & Kavanagh, 2022). With this, the present work seeks to evaluate the suitability (in terms of in vitro antifungal activity and in vivo toxicity assessment) of using lycopene and MSN, isolated and in association, against VVC.

2. Material and methods

2.1. Mesoporous silica nanoparticle (MSN) synthesis:

The synthesis was performed according to Nandiyanto et. al., (2013) and Maturi et.al., (2019) with adaptations. In a round bottom flask, 0.61 g of cetyltrimethylammonium bromide (CTAB) and 180 mL of distilled water were added and kept under stirring at 60 °C for 30 min. Posteriorly, 55.8 mL of octane, 105 µL of styrene (previously washed three times in 2.5 M NaOH), 0.14 g of L-Lysine, 6.42 mL of TEOS, 0.20 g of sodium dihydrochloride 2,2'-Azobis(2-methylproprylnamide) (AIBA), were added. Then, the reaction mixture was maintained by stirring at 60 °C for 3 h in nitrogen atmosphere. After this period, the suspension was transferred to a separatory funnel and kept overnight at room temperature for phase separation to occur. The supernatant was discarded and the MSN suspension

phase was centrifuged at 18,000 rpm for 15 min, then the precipitate was washed with ethanol and distilled water 5 times. After, the dried material was treated via reflux or calcination in order to remove organic residues.

2.1.1. Reflux treatment

The reflux was performed according to the methodology of Lungare et al., (2016) with adaptations. All material obtained in the synthesis was firstly dispersed in 60 mL of methanol, 1.5 mL of hydrochloric acid and 15 mL of chloroform, and then kept at reflux under stirring at 60 °C for 6 h. After this period, the suspension was centrifuged at 18,000 rpm for 15 min, then the precipitate was washed with methanol and distilled water 5 times. Lastly, the precipitate was dried and kept in a desiccator.

2.1.2. Calcination treatment

First, the porcelain crucible was calcined in a muffle furnace at 500 °C for 3 h and cooled in a desiccator (Brasil, 2019). Then, the material obtained in the synthesis was transferred to the porcelain crucible and calcined at a temperature of 550 °C for 6 h. Lastly, the material was stored in a desiccator (Li et al., 2020; Zhang et al., 2016).

2.2. Lycopene impregnation in MSN

Firstly, the MSN were vacuumed for 1 h. Then, 5 mg of MSN were added in glass vials with lycopene solution in chloroform (2.5 mg/mL), which were kept under stirring at 100 rpm for 48 h under cooling (15 ± 5 ºC). Subsequently, both lycopene-impregnated MSN (LYC@MSN) were centrifuged at 4000 rpm for 15 min and dried at room temperature under vacuum. In order to determine the amount of drug impregnated, the MSN@LYC were centrifuged at 14000 rpm for 15 minutes and the supernatant (previously filtered) was quantified by HPLC in a previously validated method. Then, the impregnation efficiency (IE)% and load capacity (LC)% was calculated according to equations 1 and 2, respectively (Carvalho et al., 2021).

Equation 1:

$$IE(\%) = \frac{Total\ amount\ of\ drug\ added\ -\ Free\ amount\ in\ supernatant}{Total\ amount\ of\ drug\ added}\ x\ 100$$

Equation 2:

$$LC(\%) = \frac{Encapsulated\ drug}{Nanoparticle\ weight} \times 100$$

2.4. Characterization of drug-free MSNs and LYC@MSN

The characteristic vibrations of the connections corresponding to the structure of the materials (MSN-R, MSN-C and LYC@MSN), that is, the formation of the silica network as well as the confirmation of the presence of the drug, were evaluated by vibrational absorption spectroscopy in the infrared region (FTIR). The FTIR spectra of the NSMs were obtained using an FTIR spectrometer, ALPHA Platinum ATR - FTIR from Bruker. Data were analyzed in the range of 4000 to 400 cm^{-1} with a resolution of 1 cm^{-1}.

2.5. Evaluation of antifungal activity *in vitro* by determining the Minimum inhibitory concentration (MIC)

Sample preparation conditions: amphotericin B was solubilized in 20% DMSO and 80% PBS (32 µg/mL initial solution), fluconazole was solubilized in Roswell Park Memorial Institute (RPMI 1640) (256 ug/mL initial solution) and lycopene was solubilized in propanol, tween 80 and RPMI 1640 (10, 2 and 88%, respectively) at an initial concentration of 4000 µg /mL. MSN and LYC@MSN were solubilized in RPMI 1640. MSN was maintained at a concentration equal to the LYC@MSN solution. LYC@MSN was maintained in an initial solution containing 4000 µg /ml of impregnated lycopene.

For this test, two *C. albicans* strains were used, the standard strain ATCC 18804 and a clinical strain resistant to azoles provided by the Medical School of São Paulo State University (UNESP), Botucatu Campus (Certificate of Presentation of Ethical Assessment: 55758222.6.0000.5411), referred here as strain FMB-01. Prior to the test, the strains were kept in Sabouraud Dextrose Broth (SDB) with 20% glycerol at -20 ºC. For performing the test, the strains were subcultured in 2 mL of SDB and incubated at 37 ºC for 48 h. Subsequently, the cultures were transferred to SDB in order to prepare a suspension corresponding to 0.5 on the McFarland scale, which was confirmed by spectrophotometric reading at 530 nm (approximately 1 x 10^6 cells/mL). The suspension underwent two consecutive dilutions, the first at 1:100 and the other at 1:20, in order to obtain a fungal suspension of 5.0 x 10^3 cells/mL (CLSI, 2017).

The test was conducted based on the Clinical and Laboratory Standards Institute (CLSI) document M27-A3 (2017). In a 96-well microplate, 100 µL of RPMI 1640 medium (pH 7.0 - 7.2) was added to all wells. Then, 100 µL of the test solutions (Lycopene and both MSN) were added in the wells of the first row of the plate and serial dilutions were performed in the 8 subsequent wells (each sample was

applied to the first well of two columns to perform analysis in duplicate on each plate). Finally, 100 µL of the standardized suspensions of the microorganism were added to each well of the microplates. As a positive control, amphotericin B and fluconazole were used. Additionally, control of the culture medium, yeast growth, sterility of the test substances and solvents were carried out (it is worth noting that in these columns no microorganism was added).

As for concentrations, amphotericin B was tested in the range of 0.25 - 0.0018 µg/mL, fluconazole in the range of 64 - 1 µg/mL for ATCC and 1000 - 15.625 µg/mL for clinical strain and finally lycopene, calcined MSN (MSN-C) and refluxed MSN (MSN-R) in the range of 1000 - 7.81 µg/mL. The microplates were incubated at 37 °C for 48 h. The experiments were performed in triplicate. For plate reading, 20 µL of a freshly prepared 2% triphenyltetrazolium chloride solution was added to each well of the microplate and incubated at 37 °C for 2 h. Wells that lack microbial growth remain colorless and those that show growth turn pink.

2.6. Determination of the minimum fungicide concentration (MFC)

After incubation of the 96-well microplates used in the MIC assay, the MFC determination was performed. With the aid of sterile wooden sticks, the mixture from each well (which showed antifungal activity) was transferred to SDA plates, which were incubated at 37 ºC for 48 h. MFC was defined as the minimum concentration necessary for the absence of colony forming units formation (Marena et al., 2022).

2.7. Evaluation of toxicity in *Galleria mellonella* larvae

Sample preparation conditions: lycopene was solubilized in mineral oil (100%) at concentrations ranging from 2000 to 125 mg/Kg. While MSN and LYC@MSN were solubilized in PBS (2000 to 125 mg/Kg). *G. mellonella* larvae were kept in an environment with temperature (25ºC - regional average temperature) and controlled feeding (Cook & McArthur, 2013; Fuchs et al., 2010; Marena et al., 2021; Pereira et al., 2018; Tsai et al., 2016; Wojda, 2017). Butterfly's eggs were kept in a dark environment at 25°C in large Petri dishes (140 mm, Sterilin) and maintained with artificial feeding. The artificial food was composed of a mixture of wheat germ, wheat flour, brewer's yeast, powdered milk, honey and glycerol. The dry ingredients were mixed followed by addition of the wet ingredients. The diet was substituted twice a week and unused food was kept at 4°C. All larvae were weighed and evaluated in a weight range of 0.2 to 0.3g (Trevijano-Contador et al., 2015).

The *in vivo* toxicity determination test in *G. mellonella* larvae was carried out based on the study performed by Marena et al. (2021) and Allegra et al., (2018). Seven groups were evaluated, namely: orifice control (the larvae were only punctured); death (100% methanol); lycopene; lycopene solvent

(100% mineral oil); MSN-C; MSN-R; MSN solvent (phosphate buffer). In order to reach the proper weight for testing (0.2-0.3 g) the larvae were kept in containers with food in a biochemical oxygen demand incubator at room temperature. The sample dose applied to all groups, with a Hamilton Microliter™ syringe, was 10 µL/larva. The application was performed on the penultimate proleg, as shown in **Figure 1**. Six concentrations were tested for the lycopene, MSN-C and MSN-R groups (2000, 1500, 1000, 500, 250 and 125 mg/Kg). It is worth noting that for the orifice control, death (methanol 99.9%), lycopene solvent and MSN solvent groups, 10 larvae per group was used, while for the lycopene, MSN-C and MSN-R groups, an n of 60 larvae was used, 10 for each dilution.

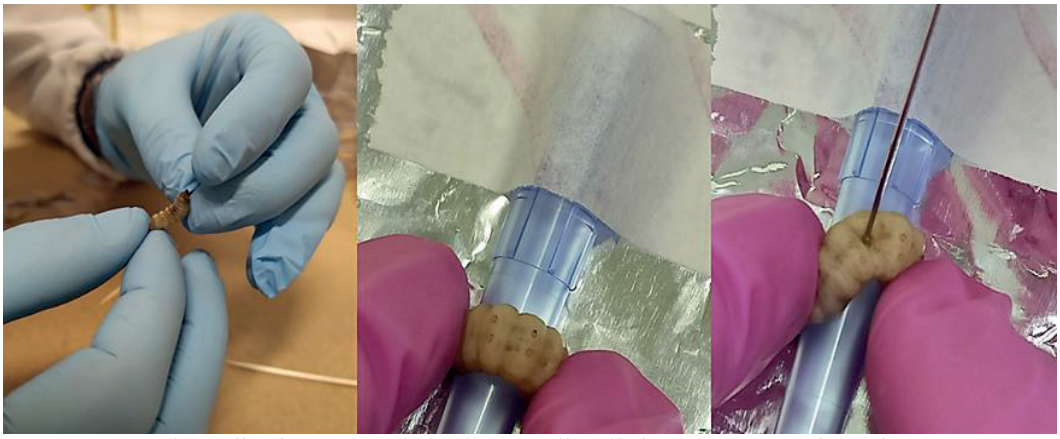

Figure 1: Sample application process in *Galleria mellonella* larvae. Source: The authors.

After samples application the larvae were transferred to Petri dishes and kept at 25 ºC protected from light. The analysis of the acute toxic potential was performed by visually monitoring the larvae at 24, 48 and 72 h. In this monitoring, death (absence of reaction after physical stimulation), loss of motility, cocoon formation and melanization were evaluated. Analyzes were performed in triplicate.

2.8. Statistical analyzes

Statistical analyzes were performed by bidirectional analysis of variance (ANOVA) one way followed by the Tukey post-test using the Graphpad Prism 7.0 software.

3. Results and discussion

3.1. Characterization of drug-free MSNs and LYC@MSN and Drug impregnation

By FTIR measurements, it was possible to observe in the spectra of both the MSN-R and MSN-C samples (**Figure 2A and 2B**, respectively) bands corresponding to symmetrical and asymmetrical axial

stretching of Si-O-Si at 800 and 1085 nm respectively, characteristic of the silica matrix. Additionally, in the spectrum of **Figure 2A**, a band attributed to an axial Si-OH stretching around 960 nm is observed, characteristic of the silanols available on the surface and in MSN-R pores. A broad band around 3400 cm^{-1} was detected and attributed to a stretching of the O-H bond of water molecules. Finally, a band corresponding to symmetric angular deformation in the plane of the O-H bond was observed at 1630 cm^{-1}, which was also attributed to the silanol groups available on the surface and pores of the MSN-R. Additionally, in the MSN-R spectrum it can also be observed that bands referring to the stretching of C-H (between 1400 and 1477cm^{-1}), indicative of organic matter residue (Nairi et al., 2018; Rocha, 2010; Sábio, 2012; Samadi-Maybodi & Vahid, 2011). In relation to **Figure 2B**, it is noteworthy that the MSN-C practically did not present OH groups while the MSN-R had this group preserved. The absence of the bands corresponding to the vibrations of the OH and Si-OH bonds for the MSN-C sample can be attributed to the thermal treatment of 550 ºC carried out in the calcination process. The hydroxylation level of the matrices is extremely important for future tests of lycopene incorporation and release, very likely, different levels of hydroxylation will directly influence the drug incorporation and release processes.

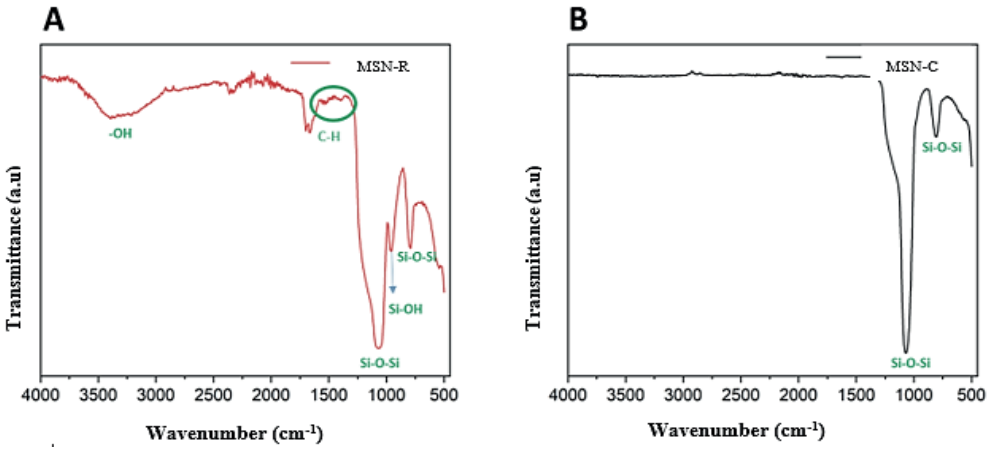

Figure 2: MSN-R and MSN-C infrared spectra. Legend: MSN-R: refluxed mesoporous silica nanoparticle; MSN-C: calcined mesoporous silica nanoparticle

Once characterized, we moved on to the impregnation stage, as can be seen in **Table 1**, the MSN-R presented slightly higher results than the MSN-C, therefore being the chosen one for the continuation of the work (called LYC@MSN).

Table 1: Values of impregnation efficiency, load capacity and amount of incorporated lycopene for both nanoparticles.

Sample	Impregnation efficiency (%)	Load capacity (%)	Amount of impregnated drug (g) in 5 mg of MSN
MSN-R	98.19±0,12	49.10±0,12	2.45
MSN-C	75.34±0,22	37.67±0,10	1.88

Legend: MSN: mesoporous silica nanoparticle; MSN-C: calcined mesoporous silica nanoparticle; MSN-R: refluxed mesoporous silica nanoparticle;

Figure 3 shows MSN-R, free lycopene and LYC@MSN spectra. In the LYC@MSN spectrum, in addition to the NSM characteristic bands, it is possible to observe additional bands, such as the band in the region of 2850-2960 cm $^{-1}$ corresponding to symmetric and asymmetric C-H stretching, a band that is also present in the LYC spectrum. It can also be observed that bands referring to the C-H stretching (between 1400 and 1477cm $^{-1}$) and the C=C stretching (1380 cm $^{-1}$) are also present in both spectra. These three bands suggest the presence of organic matter in the pores, that is, it indicates that lycopene was properly incorporated into the MSN (Aghel et al., 2011; Cancar et al., 2018).

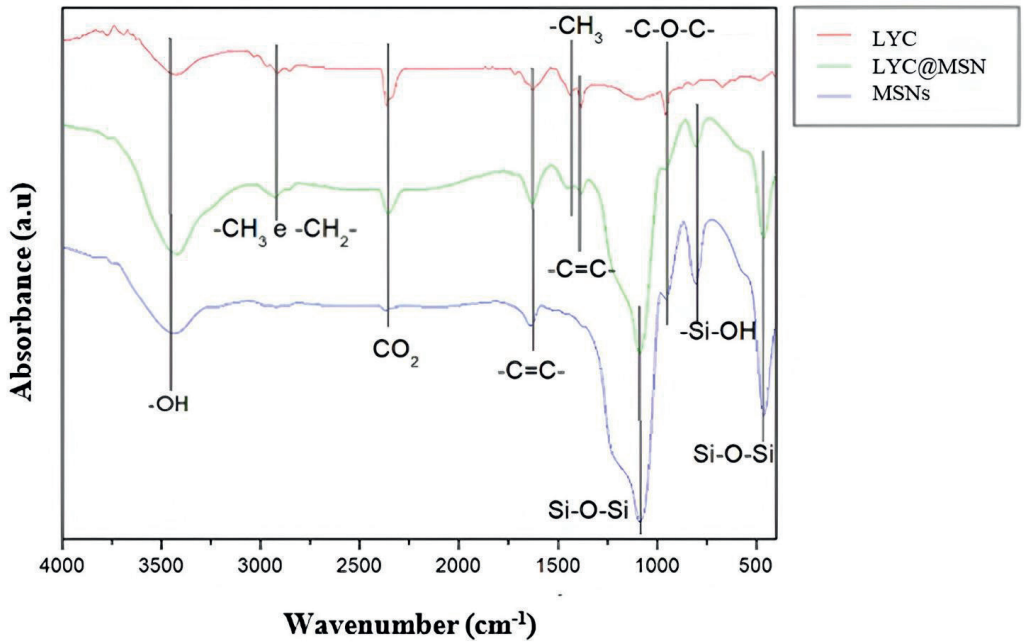

Figure 3: Infrared spectra of LYC, MSN and LYC@MSN diluted in KBr pellet. Legend: LYC: free lycopene; LYC@MSN: mesoporous silica nanoparticle incorporated with lycopene; MSN: pure mesoporous silica nanoparticle

3.2. Evaluation of antifungal activity *in vitro* by determining the Minimum inhibitory concentration (MIC)

Table 2 presents the results obtained in the determination of MIC for the groups tested. MIC was determined as the minimum concentration capable of inhibiting more than 90% of fungal growth.

Table 2: Minimum inhibitory concentration of the groups tested.

Strains	Minimum inhibitory concentration of the groups tested (µg/mL)					
	Amphotericin B	**Fluconazole**	**LYC**	**MSN-C**	**MSN-R**	**LYC@MSN**
Clinical -azole resistant (FMB-01)	1.0	125.0	500.0	500.0	NA	NA
ATCC 18804	0.06	1.0	500.0	500.0	1000.0	NA

Legend: NA: no activity in the tested range; LYC: lycopene; MSN-C: calcined mesoporous silica nanoparticle; MSN-R: refluxed mesoporous silica nanoparticle; LYC@MSN: mesoporous silica nanoparticle impregnated with lycopene

Although both strains are sensitive to amphotericin B (MIC ≤ 1.0 µg/mL), the ATCC 18804 strain presented a value below the lower limit recommended by NCCLS (2002) and by The European Committee on Antimicrobial Susceptibility Testing (EUCAST, 2020). However, the result obtained agrees with a previous study carried out with the same strain, where a value of 0.06 µg/mL was also observed (Bonifácio et al., 2015).

As recommended by CLSI (2020), the strain ATCC 18804 was sensitive to fluconazole since the value obtained was less than 2 µg/mL. The resistance profile of FMB-01 was confirmed since its MIC value was greater than ≥ 8 µg/mL (CLSI, 2020).

As reported in the literature, lycopene showed antifungal activity against the tested strains of *C. albicans* (Choi & Lee, 2015; Sung et al., 2007). However, the value obtained was higher than one of the few studies that reported lycopene MIC for a *C. albicans* strain, in this case TIMM 1768, where the authors obtained a value of 5 µg/mL (Sung et al., 2007). It is worth mentioning that the *C. albicans* strain TIMM 1768 originates in the feces of patients with oral and gastrointestinal candidiasis, unlike ATCC 18804, used in this research, which was isolated from a cutaneous lesion caused by interdigital erosion (ATCC, 2021; Panthee et al., 2018). On the other hand, Desai et al. (Desai et al., 2018) tested the activity of lycopene extracts, obtained from tomato and papaya, against *C. albicans* strain (ATCC 10231) and observed that they did not show activity at the concentrations tested, 5 - 100 µg/mL, which

is in agreement with the obtained results, showing that at lower concentrations lycopene did not exhibit anti-Candida activity (7.81 -250 µg/mL).

Despite being considered inert, both MSN showed activity against the ATCC 18804 strain, and the MSN-C showed activity against the FMB-01 strain, this can be attributed to the fact that amorphous MSNs generate low to moderate levels of reactive oxygen species (ROS) (Croissant et al., 2020). Despite the fact that this production of ROS by MSN is not a consensus, it is known that its accumulation causes DNA damage and may even lead to apoptosis of cells such as *C. albicans*, which may explain the observed antifungal activity (Choi & Lee, 2015; Garrido-Cano et al., 2021). Finally, it is worth noting that both (MSN and lycopene) when in association did not show activity. What was not expected since there are reports in the literature where when protected within the nanocarrier the drug showed greater antifungal activity when compared to the free drug (Abdellatif et al., 2019; Bonifácio et al., 2015; Natarajan et al., 2020). The issue of prolonged release may have been a limiting factor in this case, since small amounts of drug may be released gradually, which probably may not have followed the growth rate of the microorganism, in other words, the prolonged release here may have resulted in Insufficient amount of drug for the amount of fungus present on the microplate (Gambino et al., 2017; Salouti & Ahangari, 2014; Stamey, 1976). Another issue is the fact that the incorporated nanoparticles may have aggregated and sedimented at the bottom of the microplate well, which compromised its homogeneity in the well, thus limiting the drug release and action (Panáček et al., 2018).

3.3. MFC determination

Table 3 presents the results obtained in the determination of MFC for the groups tested.

Table 3: Minimum fungicidal concentration of the groups tested

Strains	Minimum fungicidal concentration (µg/mL)				
	Amphotericin B	Fluconazole	Lycopene	MSN-C	MSN-R
Clinical -azole resistant (FMB-01)	Fungicide at 1.0	Fungicide at 125.0	Fungistatic at 500.0	Fungistatic at 500.0	-
ATCC 18804	Fungicide at 0.06	Fungicide at 1.0	Fungistatic at 500.0	Fungistatic at 500.0	Fungistatic at 1000.0

Legend: -: not tested; MSN-C: calcined mesoporous silica nanoparticle; MSN-R: refluxed mesoporous silica nanoparticle;

As previously described in the literature, amphotericin B showed fungicidal activity (Guirao-Abad et al., 2017). Although fluconazole is considered fungistatic, in this study showed fungicidal

activity in all tested strains (Berkow & Lockhart, 2017; Rohr & Mikus, 2020). However, it is worth mentioning that in the literature there are reports of fluconazole acting as a fungicide, mainly dose-dependent and in the VVC treatment (Lee & Lee, 2018; Moosa et al., 2004; Narang & others, 2020).

The other groups tested, such as LYC, MSN-C and MSN-R, showed fungistatic activity. It is known in the literature that lycopene has its antifungal action based on mitochondrial dysfunction (depolarization and cytochrome release) and ROS production (which can lead to cellular apoptosis) (Choi & Lee, 2015). In addition, lycopene also acts destroying membrane integrity. It is worth mentioning that although lycopene interferes in budding division, it does not interfere in DNA replication (Sung et al., 2007). Despite several studies in the literature elucidating lycopene action mechanism against *C. albicans* strains, studies addressing whether this activity would be fungicidal or fungistatic are scarce. This scarcity can also be observed for MSN. As aforementioned, the toxicity of MSN is still a controversial issue, but as in this study both nanoparticles showed activity against ATCC 18804 strain and MSN-C against FMB-01, so it can be considered that, like LYC, they act in ROS production (Croissant et al., 2020; Garrido-Cano et al., 2021; Lehman & Larsen, 2014).

The big difference between fungicidal and fungistatic compounds lies in the fact that the first one is able to inhibit 99.9% of fungal growth, while the second has a lower inhibition (50%). Another definition also used is that fungicidal compounds are those that inhibit the regrowth (for many hours) of the pathogen after a limited exposure for a certain period of time, whereas fungistatic compounds would be those where, after its removal, a rapid new growth would be observed (Lewis & Graybill, 2008; López-Prieto et al., 2020). Thus, it can be said that this classification may be related to the amount/time of cell death permanence and not to the mechanism of the death cause.

3.4. Toxicity assessment in *Galleria mellonella* larvae

Despite the lack of studies evaluating the toxicity of lycopene and MSN through *Galleria mellonella* larvae, its use in predicting *in vivo* toxicity is of fundamental importance, since it fills the gap between *in vitro* and *in vivo* assays in mice, making a connection between them. It is also worth noting that this alternative *in vivo* model is increasingly gaining space due to advantages compared to those performed in mice, such as low cost (both operational and infrastructure), low biological risk and for being more ethically accepted (Champion et al., 2016; Moya-Andérico et al., 2021). Additionally, the immune system of these larvae is similar to mammals innate immune response, which makes their use even more desirable in predicting toxicity in humans (Browne et al., 2013). As can be seen in **Figure 4 A** and **B**, both MSN did not cause death or toxicity signs in the larvae, suggesting that their use can be considered safe at all doses tested.

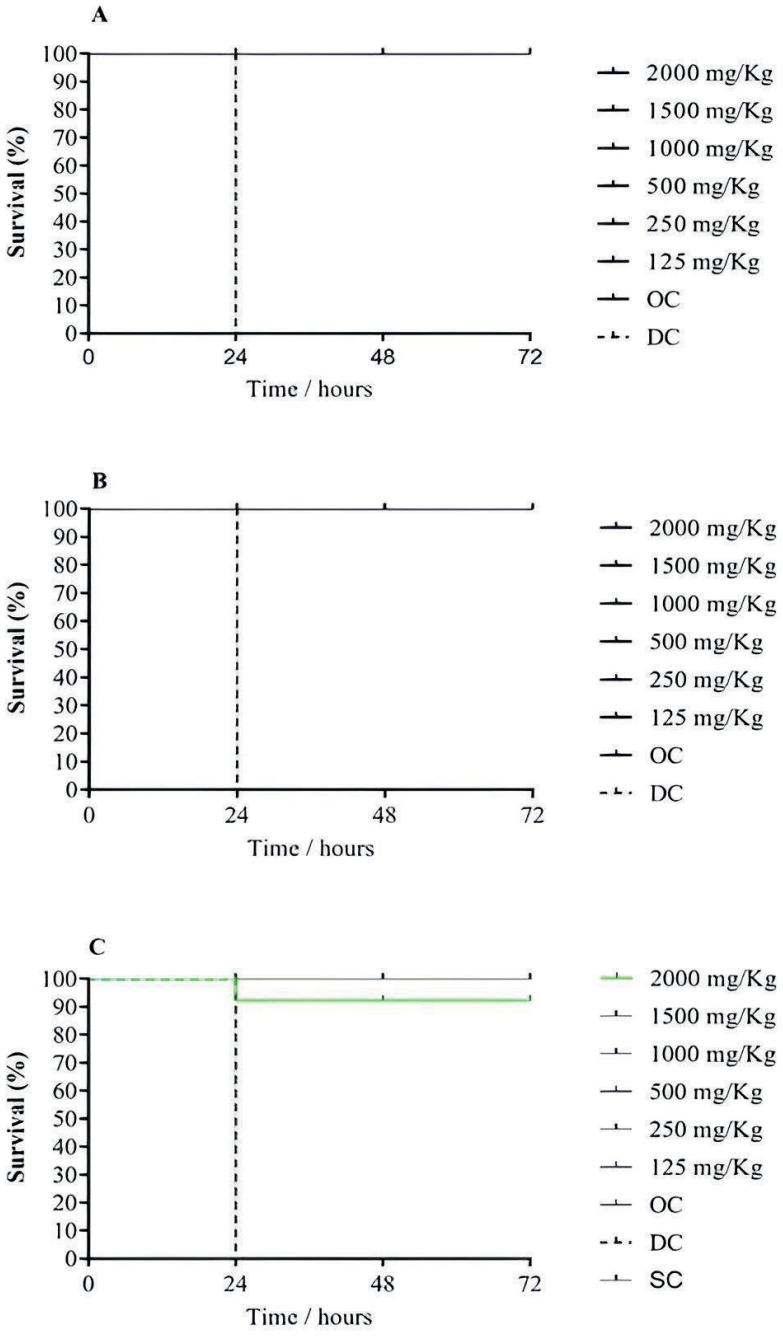

Figure 4: Kaplan-Meier survival curve of *G. mellonella* larvae for the analyzed groups at six different concentrations. Legend: A: MSN-C; B: MSN-R; C: lycopene; "*": melanization; "+": loss of motility and alteration in cocoon formation; OC: orifice control group; DC: death control group; SC: solvent control group

Finally, the lycopene group (**Figure 4 C**) showed 100% of viability at all evaluated concentrations, except for the highest one, 2000 mg/Kg, where the observed viability was 93.3% in 48 h. However, it is worth noting that because this value is above the mean lethal dose (LD50) (necessary concentration of a certain substance to kill 50% of the larvae in 48 h) it can be suggested that lycopene does not present toxicity, being therefore suitable for therapeutic applications (Moya-Andérico et al., 2021).

4. Conclusions

The results suggest that both nanoplatforms, MSN-R and MSN-C, and lycopene can be used for the most diverse therapeutic applications, since they did not show toxicity in *G. mellonella* larvae. However, both components (MSN and LYC) when isolated showed only a slight activity against the tested strains. Additionally, when in association (LYC@MSN) this slight activity was not even observed. Finally, it is strongly encouraged that other applications of this association are evaluated since both, the drug and the nanoparticle were non-toxic.

5. Acknowledgements

This work was supported by São Paulo Research Foundation (FAPESP, Brazil) grant number nº 2019/26821-7, 2019/09831-9 and 2018/25377-3.

6. Institutional review board statement

The study was conducted according to the guidelines of the Declaration of Helsinki and was approved by the Institutional Review Board (or Ethics Committee) of UNESP -Faculdade de Medicina de Botucatu (protocol code: 55758222.6.0000.5411; date of approval: 03/08/2022).

7.Conflicts of interest

The authors declare no conflict of interest.

8. References

Abdellatif, A. A. H., El-Telbany, D. F. A., Zayed, G., & Al-Sawahli, M. M. (2019). Hydrogel Containing PEG-Coated Fluconazole Nanoparticles with Enhanced Solubility and Antifungal Activity. *Journal of Pharmaceutical Innovation*, *14*(2), 112–122. https://doi.org/10.1007/s12247-018-9335-z

Aghel, N., Ramezani, Z., & Amirfakhrian, S. (2011). Isolation and quantification of lycopene from tomato cultivated in Dezfoul, Iran. *Jundishapur Journal of Natural Pharmaceutical Products,* 6(1), 9-15.

Allegra, E., Titball, R. W., Carter, J., & Champion, O. L. (2018). *Galleria mellonella* larvae allow the discrimination of toxic and non-toxic chemicals. *Chemosphere*, *198*, 469–472. https://doi.org/10.1016/j.chemosphere.2018.01.175

Álvares, C. A., Svidzinski, T. I. E., & Consolaro, M. E. L. (2007). Candidíase vulvovaginal: fatores predisponentes do hospedeiro e virulência das leveduras. *Jornal Brasileiro de Patologia e Medicina Laboratorial*, *43*(5). https://doi.org/10.1590/S1676-24442007000500004

ATCC. (2021). *Candida albicans* (Robin) Berkhout 18804™. https://www.atcc.org/products/18804

Balakrishnan, S. N., Yamang, H., Lorenz, M. C., Chew, S. Y., & Than, L. T. L. (2022). Role of Vaginal Mucosa, Host Immunity and Microbiota in Vulvovaginal Candidiasis. *Pathogens*, *11*(6), Article 618. https://doi.org/10.3390/pathogens11060618

Barbedo, L. S., Sgarbi, D.B.G. (2010). Candidíase. *DST J Bras Doenças Sex Transm*, *22*, 22–38.

Berkow, E., & Lockhart, S. (2017). Fluconazole resistance in Candida species: a current perspective. *Infection and Drug Resistance*, *Volume 10*, 237–245. https://doi.org/10.2147/IDR.S118892

Bonifácio, B. V., Ramos, M. A. S., da Silva, P. B., Negri, K. M. S., Lopes, É. O., de Souza, L. P., Vilegas, W., Pavan, F. R., Chorilli, M., & Bauab, T. M. (2015). Nanostructured lipid system as a strategy to improve the anti-*Candida albicans* activity of Astronium sp. *International Journal of Nanomedicine*, *10*, Article 5081. https://doi.org/10.2147/IJN.S79684

Brasil. (2019). *Farmacopéia brasileira* (6th ed.). Brasil. Agência Nacional de Vigilância Sanitária (ANVISA).

Browne, N., Heelan, M., & Kavanagh, K. (2013). An analysis of the structural and functional similarities of insect hemocytes and mammalian phagocytes. *Virulence*, *4*(7), 597–603. https://doi.org/10.4161/viru.25906

Cancar, H. D., Dedic, A., Alispahic, A., Muratovic, S., & Tahirovic, I. (2018). Chromatographic And Spectroscopic Characterisation Of Lycopen Extracted From Fresh And Thermally Processed Tomato Fruit. *Research Journal of Pharmaceutical Biological and Chemical Sciences*, *9*(6), 1094–1102.

Carvalho, G. C., de Camargo, B. A. F., de Araújo, J. T. C., & Chorilli, M. (2021). Lycopene: From tomato to its nutraceutical use and its association with nanotechnology. *Trends in Food Science & Technology*, *118*, 447–458. https://doi.org/10.1016/j.tifs.2021.10.015

Carvalho, G. C., Sábio, R. M., & Chorilli, M. (2021). An Overview of Properties and Analytical Methods for Lycopene in Organic Nanocarriers. *Critical Reviews in Analytical Chemistry*, *51*(7), 674–686. https://doi.org/10.1080/10408347.2020.1763774

Carvalho, G. C., Sábio, R. M., Ribeiro, T. C., Monteiro, A. S., Pereira, D. V., Ribeiro, S. J. L., & Chorilli, M. (2020). Highlights in Mesoporous Silica Nanoparticles as a Multifunctional Controlled Drug Delivery Nanoplatform for Infectious Diseases Treatment. *Pharmaceutical Research*, *37*(10), 191. https://doi.org/10.1007/s11095-020-02917-6

CDC. (2022). *Vaginal Candidiasis*. Centers for Disease Control and Prevention. https://www.cdc.gov/fungal/diseases/candidiasis/genital/index.html

Champion, O. L., Wagley, S., & Titball, R. W. (2016). Galleria mellonella as a model host for microbiological and toxin research. *Virulence*, *7*(7), 840–845. https://doi.org/10.1080/21505594.2016.1203486

Choi, H., & Lee, D. G. (2015). Lycopene induces apoptosis in Candida albicans through reactive oxygen species production and mitochondrial dysfunction. *Biochimie*, *115*, 108–115. https://doi.org/10.1016/j.biochi.2015.05.009

CLSI. (2017). *M27: reference method for broth dilution antifungal susceptibility testing of yeasts* (4th ed.) Clinical and Laboratory Standards Institute.

CLSI. (2020). *M60: Performance Standards for Antifungal Susceptibility Testing of Yeasts* (2nd ed.). Clinical and Laboratory Standards Institute.

Cook, S. M., & McArthur, J. D. (2013). Developing Galleria mellonella as a model host for human pathogens. *Virulence*, *4*(5), 350–353. https://doi.org/10.4161/viru.25240

Croissant, J. G., Butler, K. S., Zink, J. I., & Brinker, C. J. (2020). Synthetic amorphous silica nanoparticles: toxicity, biomedical and environmental implications. *Nature Reviews Materials*, *5*(12), 886–909. https://doi.org/10.1038/s41578-020-0230-0

Cruz, G. S., de Brito, E. H. S., Freitas, L. V., & Monteiro, F. P. M. (2020). Vulvovaginal candidiasis in primary health care: diagnosis and treatment. *Rev. Enferm. Atual In Derme. 94*(32), Article e-020074. https://doi.org/10.31011/reaid-2020-v.94-n.32-art.735

Czechowicz, P., Nowicka, J., & Gościniak, G. (2022). Virulence Factors of Candida spp. and Host Immune Response Important in the Pathogenesis of Vulvovaginal Candidiasis. *International Journal of Molecular Sciences*, *23*(11), Article 5895. https://doi.org/10.3390/ijms23115895

Davis, S. (2020). Bacterial vaginosis and Candida vulvovaginitis. *Professional Nursing Today*, *24*(3), 17–20.

Denning, D. W., Kneale, M., Sobel, J. D., & Rautemaa-Richardson, R. (2018). Global burden of recurrent vulvovaginal candidiasis: a systematic review. *The Lancet Infectious Diseases*, *18*(11), e339–e347. https://doi.org/10.1016/S1473-3099(18)30103-8

Desai, P. R., Holihosur, P. D., Marathe, S. V, Kulkarni, B. B., UK, V., Geetanjali, R. K., Rajeev, R. P., & Hiremath, S. V. (2018). Studies on Isolation and Quantification of Lycopene from Tomato and Papaya and its Antioxidant and Antifungal Properties. *International Journal of Agriculture Innovations and Research,* 6(5), 257-260.

EUCAST. (2020). The European Committee on Antimicrobial Susceptibility Testing. *Breakpoint tables for interpretation of MICs for antifungal agents,* version 10.0, 2020. The European Committee on Antimicrobial Susceptibility Testing. http://www.eucast.org/astoffungi/clinicalbreakpointsforantifungals/.

Falsafi, S. R., Rostamabadi, H., Babazadeh, A., Tarhan, Ö., Rashidinejad, A., Boostani, S., Khoshnoudi-Nia, S., Akbari-Alavijeh, S., Shaddel, R., & Jafari, S. M. (2021). Lycopene nanodelivery systems; recent advances. *Trends in Food Science & Technology, 119*, 378–399. https://doi.org/10.1016/j.tifs.2021.12.016

Farr, A., Effendy, I., Tirri, B. F., Hof, H., Mayser, P., Petricevic, L., Ruhnke, M., Schaller, M., Schaefer, A. P. A., Sustr, V., & others. (2021). Guideline: Vulvovaginal candidosis (AWMF 015/072, level S2k). *Mycoses*, *64*(6), 583–602. https://doi.org/10.1111/myc.13248

Firmiano, L., Dias, D. P., Santos, T. G., Terra, S. D. N., & Queiros, V. M. dos A. (2020). Beneficio dos Alimentos Usados como Terapia Complementar para Candidíase Vulvovaginal Recorrente / The Benefit of Food and its Usage as Complementary Therapy for Recurrent Vulvovaginal

Candidiasis. *ID on Line Revista de Psicologia*, *14*(53), 913–925. https://doi.org/10.14295/idonline.v14i53.2785

Fuchs, B. B., Eby, J., Nobile, C. J., El Khoury, J. B., Mitchell, A. P., & Mylonakis, E. (2010). Role of filamentation in Galleria mellonella killing by Candida albicans. *Microbes and Infection*, *12*(6), 488–496. https://doi.org/10.1016/j.micinf.2010.03.001

Gambino, M., Ahmed, M. A. A., Villa, F., & Cappitelli, F. (2017). Zinc oxide nanoparticles hinder fungal biofilm development in an ancient Egyptian tomb. *International Biodeterioration & Biodegradation*, *122*, 92–99. https://doi.org/10.1016/j.ibiod.2017.05.011

Garrido-Cano, I., Candela-Noguera, V., Herrera, G., Cejalvo, J. M., Lluch, A., Marcos, M. D., Sancenon, F., Eroles, P., & Martínez-Máñez, R. (2021). Biocompatibility and internalization assessment of bare and functionalised mesoporous silica nanoparticles. *Microporous and Mesoporous Materials*, *310*, Article 110593. https://doi.org/10.1016/j.micromeso.2020.110593

Giret, S., Wong Chi Man, M., & Carcel, C. (2015). Mesoporous-Silica-Functionalized Nanoparticles for Drug Delivery. *Chemistry-A European Journal*, *21*(40), 13850–13865. https://doi.org/10.1002/chem.201500578

Gonçalves, B., Ferreira, C., Alves, C. T., Henriques, M., Azeredo, J., & Silva, S. (2016). Vulvovaginal candidiasis: Epidemiology, microbiology and risk factors. *Critical Reviews in Microbiology*, *42*(6), 905–927. https://doi.org/10.3109/1040841X.2015.1091805

Guirao-Abad, J. P., Sánchez-Fresneda, R., Alburquerque, B., Hernández, J. A., & Argüelles, J.-C. (2017). ROS formation is a differential contributory factor to the fungicidal action of Amphotericin B and Micafungin in *Candida albicans*. *International Journal of Medical Microbiology*, *307*(4–5), 241–248. https://doi.org/10.1016/j.ijmm.2017.03.005

Jane, W. J., Iramiot, J. S., & Kalule, J. B. (2019). Prevalence and Antifungal Susceptibility patterns of Candida Isolated on CHROMagarTMCandida at a Tertiary Referral Hospital, Eastern Uganda. *Microbiology Research Journal International*, *28*(6)1–6. https://doi.org/10.9734/mrji/2019/v28i630151

Lee, W., & Lee, D. G. (2018). A novel mechanism of fluconazole: fungicidal activity through dose-dependent apoptotic responses in *Candida albicans*. *Microbiology*, *164*(2), 194–204. https://doi.org/10.1099/mic.0.000589

Lehman, S. E., & Larsen, S. C. (2014). Zeolite and mesoporous silica nanomaterials: greener syntheses, environmental applications and biological toxicity. *Environ. Sci.: Nano*, *1*(3), 200–213. https://doi.org/10.1039/C4EN00031E

Lewis, J. S., & Graybill, J. R. (2008). Fungicidal versus Fungistatic: what's in a word? *Expert Opinion on Pharmacotherapy*, *9*(6), 927–935. https://doi.org/10.1517/14656566.9.6.927

Li, C., Li, J., Zhang, W.-H., Wang, N., Ji, S., & An, Q.-F. (2020). Enhanced permeance for PDMS organic solvent nanofiltration membranes using modified mesoporous silica nanoparticles. *Journal of Membrane Science*, *612*, Article 118257. https://doi.org/10.1016/j.memsci.2020.118257

López-Prieto, A., Vecino, X., Rodríguez-López, L., Moldes, A., & Cruz, J. (2020). Fungistatic and Fungicidal Capacity of a Biosurfactant Extract Obtained from Corn Steep Water. *Foods*, *9*(5), Article 662. https://doi.org/10.3390/foods9050662

Lungare, S., Hallam, K., & Badhan, R. K. S. (2016). Phytochemical-loaded mesoporous silica nanoparticles for nose-to -brain olfactory drug delivery. *International Journal of Pharmaceutics, 513*, 280–293. https://doi.org/10.1016/j.ijpharm.2016.09.042

Marchaim, D., Lemanek, L., Bheemreddy, S., Kaye, K. S., & Sobel, J. D. (2012). Fluconazole-resistant *Candida albicans* vulvovaginitis. *Obstetrics & Gynecology*, *120*(6), 1407–1414. http://10.1097/AOG.0b013e31827307b2

Marena, G. D., Girotto, L., Saldanha, L. L., Ramos, M. A. dos S., De Grandis, R. A., da Silva, P. B., Dokkedal, A. L., Chorilli, M., Bauab, T. M., Pavan, F. R., & others. (2022). Hydroalcoholic Extract of Myrcia bella Loaded into a Microemulsion System: A Study of Antifungal and Mutagenic Potential. *Planta Medica*, *88*(05), 405–415. https://doi.org/10.1055/a-1323-3622

Marena, G. D., Ramos, M. A. D. S., Lima, L. C., Chorilli, M., & Bauab, T. M. (2021). *Galleria mellonella* for systemic assessment of anti-*Candida auris* using amphotericin B loaded in nanoemulsion. *Science of The Total Environment*, *807,* Article 151023. https://doi.org/10.1016/j.scitotenv.2021.151023

Mason, K. L., Downward, J. R. E., Mason, K. D., Falkowski, N. R., Eaton, K. A., Kao, J. Y., Young, V. B., & Huffnagle, G. B. (2012). *Candida albicans* and bacterial microbiota interactions in the cecum during recolonization following broad-spectrum antibiotic therapy. *Infection and Immunity*, *80*(10), 3371–3380. https://doi.org/10.1128/iai.00449-12

Maturi, F. E., Sábio, R. M., Silva, R. R., Lahoud, M. G., Meneguin, A. B., Valente, G. T., Caface, R. A., Leite, I. S., Inada, N. M., & Ribeiro, S. J. L. (2019). Luminescent Mesoporous Silica Nanohybrid Based on Drug Derivative Terbium Complex. *Materials*, *12*(6), Article 933. https://doi.org/10.3390/ma12060933

Moosa, M.-Y. S., Sobel, J. D., Elhalis, H., Du, W., & Akins, R. A. (2004). Fungicidal Activity of Fluconazole against Candida albicans in a Synthetic Vagina-Simulative Medium. *Antimicrobial Agents and Chemotherapy*, *48*(1), 161–167. https://doi.org/10.1128/AAC.48.1.161-167.2004

Mohamed, A. O., Mohamed, M. S., Mallhi, T. H., Hussain, M. A., Jalloh, M. A., Omar, K. A., Alhaj, M. O., & Ali, A. A. M. M. (2022). Prevalence of vulvovaginal candidiasis among pregnant women in Africa: A systematic review and meta-analysis. *The Journal of Infection in Developing Countries*, *16*(08), 1243–1251. https://doi.org/10.3855/jidc.15536

Moya-Andérico, L., Vukomanovic, M., Cendra, M. del M., Segura-Feliu, M., Gil, V., del Río, J. A., & Torrents, E. (2021). Utility of *Galleria mellonella* larvae for evaluating nanoparticle toxicology. *Chemosphere*, *266*, Article 129235. https://doi.org/10.1016/j.chemosphere.2020.129235

Nairi, V., Medda, S., Piludu, M., Casula, M. F., Vallet-Regì, M., Monduzzi, M., & Salis, A. (2018). Interactions between bovine serum albumin and mesoporous silica nanoparticles functionalized with biopolymers. *Chemical Engineering Journal*, *340*, 42–50. https://doi.org/10.1016/j.cej.2018.01.011

Nandiyanto, A. B. D., Arutanti, O., Ogi, T., Iskandar, F., Kim, T. O., & Okuyama, K. (2013). Synthesis of spherical macroporous WO_3 particles and their

high photocatalytic performance. *Chemical Engineering Science*, *101*, 523–532. https://doi.org/10.1016/j.ces.2013.06.049

Narang, R. S., & others. (2020). Formulation and in vitro evaluation of fluconazole loaded nanoemulgel against *Candida albicans*. *Journal of Natural Remedies*, *21*(5), 19–25.

Natarajan, K., Gajendran, P. L., Arjunkumar, R., & Kumar, S. R. (2020). Anti-fungal activity of chitosan nanoparticle incorporated lycopene against *Candida albicans* using minimal inhibitory concentration assay. *Plant Cell Biotechnology and Molecular Biology*, 73–82.

NCCLS. (2002). *Reference Method for Broth Dilution Antifungal Susceptibility Testing of Yeasts; Approved Standard—Second Edition* (2nd ed.). NCCLS.

Panáček, A., Kvítek, L., Smékalová, M., Večeřová, R., Kolář, M., Röderová, M., Dyčka, F., Šebela, M., Prucek, R., Tomanec, O., & Zbořil, R. (2018). Bacterial resistance to silver nanoparticles and how to overcome it. *Nature Nanotechnology*, *13*(1), 65–71. https://doi.org/10.1038/s41565-017-0013-y

Panthee, S., Hamamoto, H., Ishijima, S. A., Paudel, A., & Sekimizu, K. (2018). Utilization of Hybrid Assembly Approach to Determine the Genome of an Opportunistic Pathogenic Fungus, *Candida albicans* TIMM 1768. *Genome Biology and Evolution*, *10*(8), 2017–2022. https://doi.org/10.1093/gbe/evy166

Patnaik, S., Gorain, B., Padhi, S., Choudhury, H., Gabr, G. A., Md, S., Kumar Mishra, D., & Kesharwani, P. (2021). Recent update of toxicity aspects of nanoparticulate systems for drug delivery. *European Journal of Pharmaceutics and Biopharmaceutics*, *161*, 100–119. https://doi.org/10.1016/j.ejpb.2021.02.010

Pereira, T., de Barros, P., Fugisaki, L., Rossoni, R., Ribeiro, F., de Menezes, R., Junqueira, J., & Scorzoni, L. (2018). Recent Advances in the Use of Galleria mellonella Model to Study Immune Responses against Human Pathogens. *Journal of Fungi*, *4*(4), Article 128. https://doi.org/10.3390/jof4040128

Piatek, M., Sheehan, G., & Kavanagh, K. (2021). *Galleria mellonella*: The Versatile Host for Drug Discovery, In Vivo Toxicity Testing and Characterising Host-Pathogen Interactions. *Antibiotics*, *10*(12), Article 1545. https://doi.org/10.3390/antibiotics10121545

Rocha, L. A. (2010). *Materiais meso-estruturados luminescentes*. [Doctoral dissertation, São Paulo State University].,Unesp Institutional Repository. http://hdl.handle.net/11449/105768

Rohr, B. S., & Mikus, G. (2020). Proposal of a Safe and Effective Study Design for CYP3A-Mediated Drug-Drug Interactions. *The Journal of Clinical Pharmacology*, *60*(10), 1294–1303. https://doi.org/10.1002/jcph.1622

Ruiz-Sánchez, D., Calderón-Romero, L., Sánchez-Vega, J. T., & Tay, J. (2003). Intestinal candidiasis. A clinical report and comments about this opportunistic pathology. *Mycopathologia*, *156*(1), 9–11. https://doi.org/10.1023/A:1021326713470

Sábio, R. M. (2012). *Ancoragem de complexos de rutênio com ligantes siliados em sílica mesoporosa obtida via pirólise de spray*. [Master thesis, São Paulo State University]. Unesp Institutional Repository. http://hdl.handle.net/11449/97934

Sahoo, S. K., & Labhasetwar, V. (2003). Nanotech approaches to drug delivery and imaging. *Drug Discovery Today*, *8*(24), 1112–1120. https://doi.org/10.1016/S1359-6446(03)02903-9

Salazar, G. J. T., Carneiro, J. N. P., da Silva, A. C. A., Cruz, B. G., da Silva, R. O. M., da Costa, J. G. M., da Cruz, R. P., da Silva, J. C. P., Ferreira, M. H., dos Santos, A. T. L., & others. (2022). Antioxidant and Antifungal Activity of the *Cynophalla flexuosa* (L.) J. Presl (Capparaceae) against Opportunistic Fungal Pathogens. *Future Pharmacology*, *2*(1), 16–30. https://doi.org/10.3390/futurepharmacol2010002

Salouti, M., & Ahangari, A. (2014). Nanoparticle based Drug Delivery Systems for Treatment of Infectious Diseases. In Sezer, A. D. (Ed.), *Application of Nanotechnology in Drug Delivery*. InTech. https://doi.org/10.5772/58423

Samadi-Maybodi, A., & Vahid, A. (2011). High yield synthesis and characterization of well-ordered Mesoporous silica nanoparticles using Sodium Carboxy Methyl Cellulose. *Journal of Non-Crystalline Solids*, *357*(7), 1827–1830. https://doi.org/10.1016/j.jnoncrysol.2011.01.037

Sanglard, D. (2016). Emerging Threats in Antifungal-Resistant Fungal Pathogens. *Frontiers in Medicine*, *3*, Article 11 https://doi.org/10.3389/fmed.2016.00011

Soares, D. M., Lima, E. de O., Soares, D. M. M., Silva, N. F. da, Costa, N. G. M., Faria, F., & Rodriguez, A. F. R. (2018). Candidíase vulvovaginal: uma revisão de literatura com abordagem para *Candida albicans*. *Braz J. Surg and Clin Res--BJSCR*, *25*(1), 28–34.

Sobel, J. D. (2002). Pathogenesis of recurrent vulvovaginal candidiasis. *Current Infectious Disease Reports*, *4*(6), 514–519. https://doi.org/10.1007/s11908-002-0038-7

Stamey, T. A. (1976). Resistance to Nalidixic Acid. *JAMA*, *236*(16), 1857-1860. https://doi.org/10.1001/jama.1976.03270170023019

Sung, W. S., Lee, I.-S., & Lee, D. G. (2007). Damage to the cytoplasmic membrane and cell death caused by lycopene in *Candida albicans*. *Journal of Microbiology and Biotechnology*, *17*(11), 1797–1804.

Trevijano-Contador, N., Herrero-Fernández, I., García-Barbazán, I., Scorzoni, L., Rueda, C., Rossi, S. A., García-Rodas, R., & Zaragoza, O. (2015). Cryptococcus neoformans induces antimicrobial responses and behaves as a facultative intracellular pathogen in the non mammalian model *Galleria mellonella*. *Virulence*, *6*(1), 66–74. https://doi.org/10.4161/21505594.2014.986412

Tsai, C. J.-Y., Loh, J. M. S., & Proft, T. (2016). *Galleria mellonella* infection models for the study of bacterial diseases and for antimicrobial drug testing. *Virulence*, *7*(3), 214–229. https://doi.org/10.1080/21505594.2015.1135289

Vallet-Regí, M. (2022). Our contributions to applications of mesoporous silica nanoparticles. *Acta Biomaterialia*, *137*, 44–52. https://doi.org/10.1016/j.actbio.2021.10.011

Vallet-Regi, M., Rámila, A., del Real, R. P., & Pérez-Pariente, J. (2001). A New Property of MCM-41: Drug Delivery System. *Chemistry of Materials*,

13(2), 308–311. https://doi.org/10.1021/cm0011559

Vikrant, P., Priya, J., & Nirichan, K. B. (2015). Plants with anti-Candida activity and their mechanism of action: a review. *Journal of Environmental Research and Development*, *9*(4), Article 1189.

Wojda, I. (2017). Immunity of the greater wax moth *Galleria mellonella*. *Insect Science*, *24*(3), 342–357. https://doi.org/10.1111/1744-7917.12325

Wright, C. L., & Kavanagh, O. (2022). *Galleria mellonella* as a Novel In Vivo Model to Screen Natural Product-Derived Modulators of Innate Immunity. *Applied Sciences*, *12*(13), Article 6587. https://doi.org/10.3390/app12136587

Zhang, Z., Mayoral, A., & Melián-Cabrera, I. (2016). Protocol optimization for the mild detemplation of mesoporous silica nanoparticles resulting in enhanced texture and colloidal stability. *Microporous and Mesoporous Materials*, *220*, 110–119. https://doi.org/10.1016/j.micromeso.2015.08.026

Zhou, S., Zhong, Q., Wang, Y., Hu, P., Zhong, W., Huang, C.-B., Yu, Z.-Q., Ding, C.-D., Liu, H., & Fu, J. (2022). Chemically engineered mesoporous silica nanoparticles-based intelligent delivery systems for theranostic applications in multiple cancerous/non-cancerous diseases. *Coordination Chemistry Reviews*, *452*, Article 214309. https://doi.org/10.1016/j.ccr.2021.214309

CHAPTER 9

Cetyltrimethylammonium bromide in the synthesis of mesoporous silica nanoparticles: General aspects and *in vitro* toxicity

Gabriela Corrêa Carvalho[#], Gabriel Davi Marena[#], Juliana Camila Fischer Karnopp, Juliana Jorge, Rafael Miguel Sábio, Marco Antonio Utrera Martines, Taís Maria Bauab, Marlus Chorilli*

Advances in Colloid and Interface Science, v.307, 102746 pp. 1-14, 2022

[#]These authors contributed equally to this work

Reprinted with permission in accordance with the journal's author's rights policy - Elsevier.

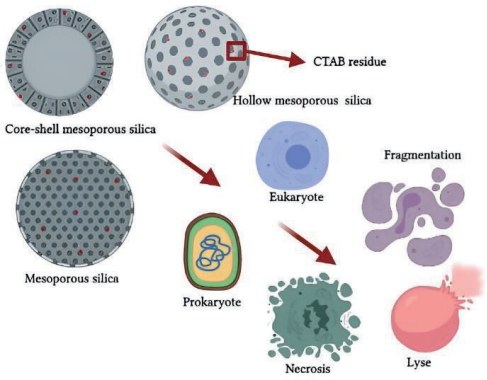

Abstract

Pharmaceutical nanotechnology has become a trend with incalculable advantages in the applicability of systems in the controlled, safe and effective release of drugs. Among the nanotechnological nanoparticles, the mesoporous silica nanoparticles stand out, a system with significant biocompatibility, good physical chemical stability, greater surface contact area with desirable and adjustable pore structure. Once developed and well defined, these pores can carry drugs and control their release. However, to create this type of nanoparticle is essential to use surfactants since they act as pore template. Among the most important surfactants, cetyltrimethylammonium bromide (CTAB) highlights, a quaternary ammonium compound widely used as a surfactant in the synthesis of mesoporous silica nanoparticles (MSNs), hollow mesoporous silica (HMSNs) and core-shell MSNs. However, for achieving good results of drug-loaded pores it is necessary to remove CTAB by extraction techniques, which provides pores formation throughout the silica and the incorporation of molecules. During and after the removal process, it is possible that CTAB residues remains inside the pores, despite several removal processes are described as efficient in the complete removal of surfactants. In turn, the presence of CTAB residues can be advantageous, especially when considering its antimicrobial activity. Meanwhile, it should be noted that the presence of CTAB may present high toxicity risks. This review seeks to explore not only general aspects of the use of CTAB in the synthesis of MSNs, but also to assess its toxicity in prokaryotic and eukaryotic cells, in order to determine whether CTAB residues are acceptable in MSNs that will be used as drug delivery systems for further *in vivo* and clinical assays.

1. Introduction

Nanoparticles have been extensively applied as carriers for controlled drug release once they provide greater drug concentration at the site of action, longer retention time, improved bioavailability and biodistribution, reducing side effects and drug aggregation (Arriagada et al., 2019; Bonifacio et al., 2014; Calixto et al., 2016; de Souza et al., 2021; Nazemiyeh et al., 2016; Sahoo et al., 2008; Vallet-Regí et al., 2019). The use of nanoparticles in drug delivery are desirable due to advantages such as large surface area, small size and ability to increase drugs permeability in biological barriers, while preserving their pharmacological properties (Bonifacio et al., 2014; Calixto et al., 2016; Nazemiyeh et al., 2016; Prabhakar & Banerjee, 2020; Pradhan et al., 2021; Sahoo et al., 2008).

Nanoparticles can be classified as organic, inorganic and hybrid systems (Li et al., 2019; Poon & Patel, 2020; Wang et al., 2020). Organics ones are considered non-toxic, biocompatible and biodegradable, while inorganics, despite the possibility of having a smaller size, may present higher levels of toxicity, non-biodegradability and non-biocompatibility (like some metallic nanoparticles that can accumulate in tissues). It is worth noting that the smaller the nanoparticle, greater the capacity of crossing cell membranes (even reaching the cell nucleus), and greater the possibility of causing toxicity (Fernández et al., 2019; Flora et al., 2008; Jergens & Winter, 2022; Poon & Patel, 2020). Otherwise, the hybrids systems are composed of organic and inorganic materials, showing advantages related to both contributions (Kibar et al., 2019; Wang et al., 2020). Among the various systems available, mesoporous silica particles stand out due not only to their good surface area, easy surface functionality, biocompatibility, well-defined and tunable physicochemical properties but also for having tunable pore size, volume and structure. The great advantage assigned to the pores present in this type of material is the capacity of hosting, releasing and protecting (from degradation processes) drugs, besides acting as an effective and smart carrier for controlled drug release and further treatment of several diseases (Carvalho et al., 2020; Manzano & Vallet-Regí, 2020; Sun et al., 2020; Vallet-Regí, 2022).

Pores formation and adjustability depend on the surfactant of choice, as they act as templates (Carvalho et al., 2020; Manzano & Vallet-Regí, 2020). Although there are several template possibilities, cetyltrimethylammonium bromide (CTAB), a quaternary ammonium surfactant, stand out due to be widely used fabricating mesostructured nanosilica. The widely use of CTAB can be justified due to its desirable characteristics like strong capacity for preventing particles aggregation (which will be better exposed hereafter) and for being considered a low cost surfactant (Abduraimova et al., 2021; Carvalho et al., 2020; He et al., 2010; Jang, 2021; Kaziem et al., 2022; Khoeini et al., 2019; Wu et al., 2013). Despite most of surfactants are eliminated after the end of the synthesis, depending on the methodology, residues can remain in the pore structure, conferring toxicity against

cells (Karnopp et al., 2020; Khoeini et al., 2019; Sun et al., 2020). Relying upon these premises, this review seeks to explore the main characteristics of CTAB use in the synthesis of mesoporous silica nanoparticles and their toxicity against eukaryotic and prokaryotic cells.

2. CTAB: general aspects around its surfactant use

Quaternary ammonium compounds have a positive charged quaternary amine group that may be bounded to one or two long alkyl chains. In the case of CTAB, a surfactant that belongs to this group, its cationic head, which is electrostatically bound to a counteranion (Br^-), is bounded to a 16-carbon hydrophobic alkyl chain (**Figure 1**) (Hartmann & Cressely, 1997; Pati & Arnold, 2020; Singh et al., 2011).

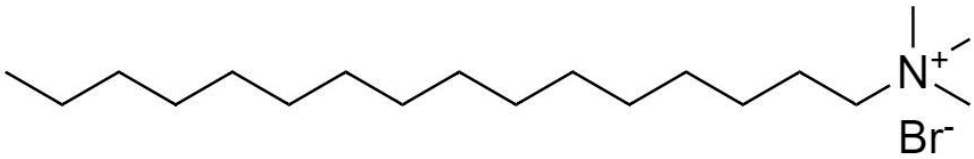

Figure 1: Cetyltrimethylammonium bromide chemical structure.

Surfactants, surface-active agents as they are also well-known, are amphiphilic molecules added to a formulation when the objective is to reduce the surface tension when an interface is formed (Ferri & Stebe, 2000; Kumar et al., 2021). During mesoporous materials synthesis, the use of this class of chemical components is important because there is a need for surfactant molecules aggregation for subsequent micelles formation, which will act as a template for pore and structure formation (Campos et al., 2016). Pore formation occurs at the micellar interface of the surfactant micelles, composed by anionic, nonionic or cationic species that interact with the silica source through electrostatic force or hydrogen bond. These interactions lead to mesoporous silica matrix formation (due to the silicate hydrolysis and condensation around the micelles) (Che et al., 2003; Lin & Mou, 2002; Singh et al., 2011).

Figure 2 illustrates different interactions between the surfactant head region and the silica matrix for mesopores formation. In general, the interactions can occur in several ways and are strongly influenced by the medium pH. Whether the reaction takes place in a basic medium, surfactants are used as structure-directing agents and the synthetic route is caused by the interaction of $S^+ I^-$ (S: surfactant; I: inorganic component). In this case, the silica species are in an anionic form and the surfactant needs to be a cationic option (**Figure 2 A**). However, when the silica matrix formation takes

place in an acidic medium (pH 2, approximately), and the surfactant is also a cationic option, it is necessary to add an X^- mediator ion (or counteranions – e.g. halide). In this process, the silica species are positively charged and the $S^+ X^- I^+$ interactions occur (**Figure 2 B**). When using negatively charged surfactant (anionic), it is possible to develop particles in acid medium and the synthetic route is caused by the interaction of S^-I^+ (**Figure 2 C**). It is also worth noting that the other interaction mechanism that can occur is the hydrogen bonding, where non-ionic surfactants and uncharged silica species ($S^0 I^0$) or ion pairs ($S^0 (XI)^0$ are used (**Figure 2 D and E** respectively) (Hoffmann et al., 2006; Sábio et al., 2019).

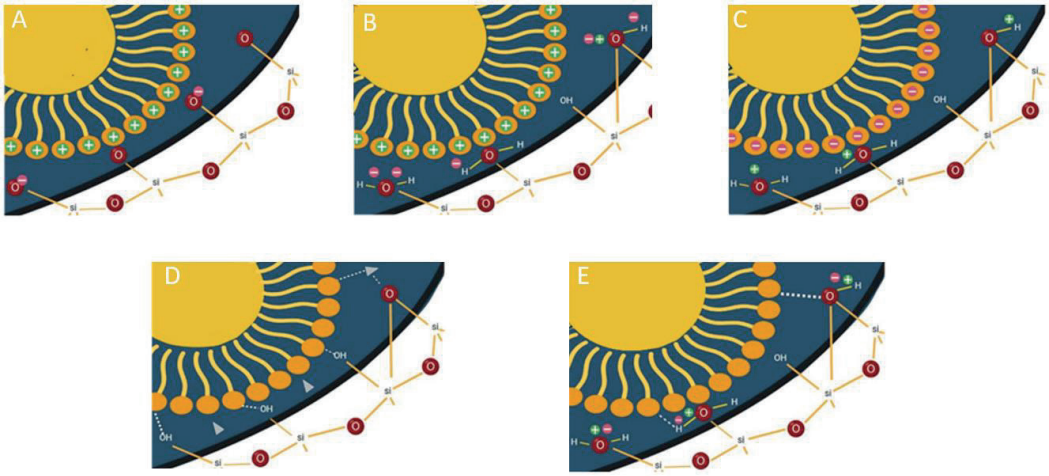

Figure 2: Interactions between the silica matrix and the surfactant micelles for mesopores formation. Legend: A: Cationic surfactant and anionic inorganic specie; B: Anionic surfactant and cationic inorganic specie; C: Cationic surfactant, its counterion and anionic inorganic specie; D: Nonionic surfactant, its counterion and nonionic inorganic specie; E: nonionic surfactant, or nonionic organic amines, and nonionic inorganic specie interaction by hydrogen bounds

Emphasis needs to be made on the formation mechanism with the cationic surfactant, (CTAB class). Cationic surfactants can self-assembly forming positively charged cylindrical-shaped micellar aggregates (liquid crystals). Subsequently, this positive charge interacts with the negatively charged silica source, replacing and releasing the surfactant's counteranions (Hoffmann et al., 2006; Lin & Mou, 2002; Sábio et al., 2019). Despite poorly understood, the presence of counteranions in the silicate-surfactant mesopores interface enables its structure manipulation, since different counteranions can decrease or increase its packing, leading to an increase or decrease in mesopores formation features since it interferes with the charge of the silica source-surfactant interface. This king

of charge is one of the factors that influence the packing of surfactants, influencing the architecture of the mesophase. Some works also reported that counteranions interfere in the formation of mesostructures by modulating the adsorption force of the surfactant heads. This adsorption capacity is directly linked to the pH of the solution, once $ClO_4^- < NO_3^- < Br^- < SO_4^{2-}$, $SO_3^{2-} < Cl^- < F^-$ and $NO_3^- > Br^- > Cl^- > SO_4^{2-} \approx F^-$ are the counteranions in increasing rate of formation order in basic and acidic media, respectively. It is described in the literature that in acidic media this last sequence of counterions (also known as binding strength Hofmeister series of anions for the cationic surfactant) is directly proportional to the surfactant packing parameter (g) (Che et al., 2005; Che et al., 2003; Lin & Mou, 2002).

The pH directly influences the formation, structure, hydrolysis and condensation of the silica. It is possible to form nanocomposites by the presence of cationic surfactants and silica since it increases the acidity of the silicate oligomers as they grow. The condensation step is catalyzed by acids (pH ~ 2 - isoelectric point) since negatively charged silicates favor nucleophilic attack (**Figure 3**), making the process faster once the bonding occurs by hydrogen bonds or strong electrostatic interactions. At pH > 2, the condensation process is greater but at pH up to 8 the condensation decreases again. At more acidic pH the particle size is generally larger compared to particles formed under alkaline pH conditions, this difference in size can be explained by the slower nucleation rate that occurs in acidic environment. The particle size can also be influenced by the amount of surfactant, having a smaller size as the surfactant length increases. Finally, the silica particles formed at acidic pH have a richer morphology, with a stickier characteristic (because of having more silanol on the surface) and softer (because of the weaker interaction between the surfactant and silicate). Otherwise, when in an environment with alkaline conditions, the silica nanoparticles tend to be smaller, with sub-micron size (Lin & Mou, 2002; Singh et al., 2011).

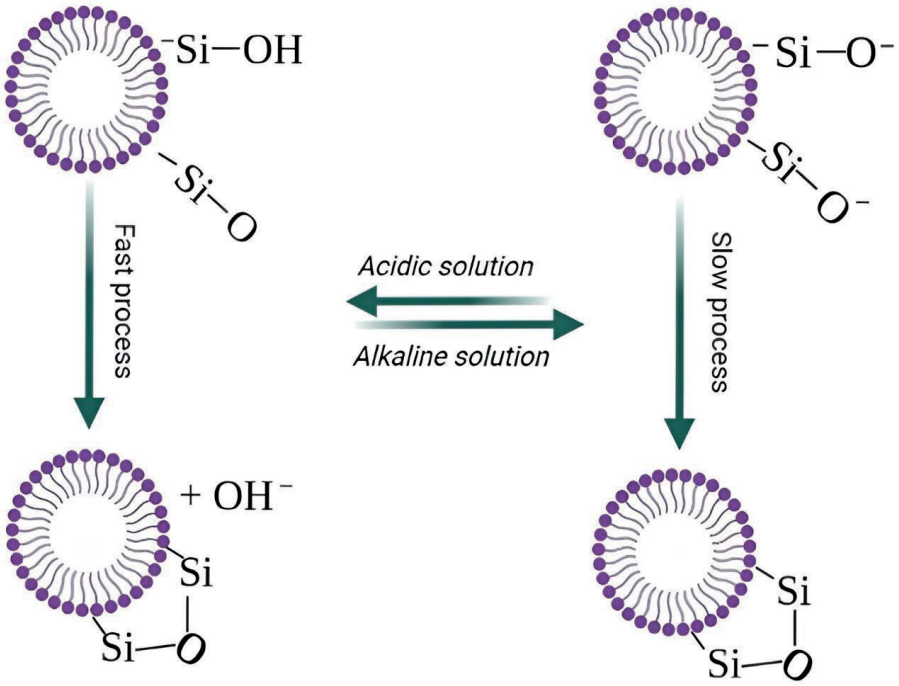

Figure 3: Influence of pH on interactions between the silica matrix and cationic surfactant micelles for mesopores formation.

In addition to controlling the particle size, three other important actions of CTAB can be mentioned, the porogenic, flocculant and dispersant functions. By using low surfactant:silica source ratio, the surfactant acts only as a porogenic agent. When a medium ratio is used it also acts as a particle diameter controller (the longer the surfactant chain, the smaller the particle size), porogenic and as a flocculant (favoring the grouping). Finally, when surfactant:silica ratio is high, the surfactants act as porogens and dispersants (assisting the solid to disperse in a liquid medium) (Singh et al., 2011; Yamada et al., 2014). In short, the understanding of media parameters as well as the CTAB characteristics and concentrations are essential for designing mesoporous silica nanoparticles with tunable physicochemical properties.

3. CTAB in the synthesis of mesoporous silica

Although the use of CTAB is already well established in the literature, this topic aims not only to exemplify its use in the synthesis of different types of mesoporous silica but also to discuss aspects, already known, but important. Since the type of surfactant and the mechanism of synthesis are directly associated to obtain mesoporous materials, three types of mesoporous silica particles were approached

in order to highlight this variability and point out inherent characteristics of the combination: CTAB verses type of mesoporous silica (Meynen et al., 2009; Soler-Illia et al., 2002).

3.1. Mesoporous silica nanoparticles

Mesoporous silica has been widely studied due to its properties and potential applications. Features such as high specific surface area (~1000 m^2 g^{-1}) and pore size around 2-50 nm allow its application in catalysis, High Performance Liquid Chromatography (HPLC) columns, biosensors, photonic devices, gas storage, heavy metal adsorption for environmental decontamination and in matrices for drug delivery and controlled release (Akinjokun et al., 2016; Li et al., 2019; Narayan et al., 2018; Shao et al., 2017). This type of material can be prepared by using tetraethyl orthosilicate (TEOS) as a silica source and surfactants as structure-directing agents/templates. In most syntheses, cationic surfactants, such as CTAB, are used due to their strong association with silica precursors. For example, for obtaining free mesopores, the surfactants must be removed through solvent extraction or heat treatment (Vazquez et al., 2017; Wu, Zhang, et al., 2016). **Figure 4** illustrates a general representation of MSNs synthesis.

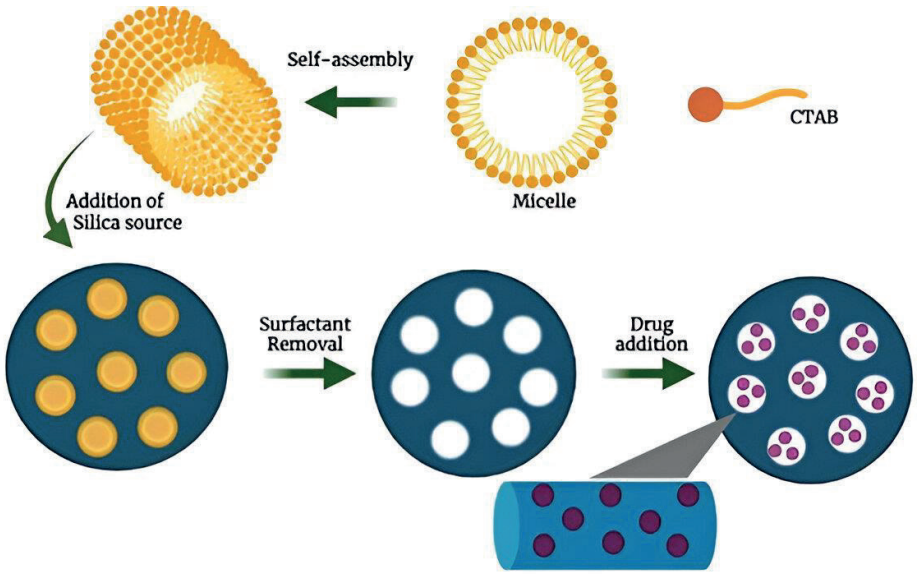

Figure 4: General representation of MSNs synthesis.

Morphology, surface area, particle and pore size are critical parameters for its application (Wu et al., 2016). Despite being well established in the literature, modifications of important parameters

such as temperature, pH, surfactants, silica precursor and solvent are still being studied by several researchers lately (Gu et al., 2012; Kim et al., 2021; Ma et al., 2011; Purnawira et al., 2019; Travaglini et al., 2019; Vazquez et al., 2017; Zhang et al., 2010).

Kim and collaborators (2021) optimized the synthesis of MSNs using an experimental statistical method called Box-design Behnken. The experiments were designed with three modification factors (quantities of CTAB, TEOS and NaOH) in order to maximize surface area, minimize particle size and obtain negative Zeta potential.

The authors reinforced CTAB role as a template for the micelle's formation. In addition, when a small amount of this surfactant was used (0.125g), small particles without complete mesoporous structure were observed (probably due to an increased ratio of alkoxide hydrolysis). On the other hand, when CTAB was used in excess (1.5 g), the fabricated mesoporous structure was not uniform. The authors also pointed out that among the factors statistically evaluated, CTAB influenced directly in the surface area values. Additionally, CTAB alters the hydrolysis of TEOS, also playing an important role in the formation of agglomerates. The increase in the amount of CTAB (0.5 to 1.5 g) leads to an increase in the Zeta potential, which indicates that through the formation of well-dispersed micelles, there is the formation and distribution of stable particles. Finally, the authors highlighted the importance of adjusting the proportions of TEOS and CTAB, since excesses of TEOS lead to reagent residues in the synthesis product (due to their incomplete hydrolysis), reducing the surface area and compromising the amount of loaded drug carried.

The proportion of surfactant interferes in the morphology of the synthesized particle, due to interactions between micelles and silicates. Particles synthesized with CTAB tend to have a more spherical morphology because this surfactant causes the formation of spherical micelles (Kim et al., 2021; Travaglini et al., 2019). In the study performed by Travaglini and collaborators (Travaglini et al., 2019) the correlation of CTAB with spherical morphology is very evident once they aimed to study the modifications in MSNs morphology based in changes of two surfactants concentration (CTAB and sodium deoxycholate (NaDC)). The study showed that particles with 2.5% of NaDC presented flattening of the spherical morphology, and this character was maintained increasing NaDC concentration, favoring more flattened and elongated morphology. On the other hand, it is important to note that despite the fact that CTAB interferes with the morphology of the particle, the type of synthesis is also a limiting factor for this, since in works involving the synthesis of MCM-41-type MSNs, with CTAB as the surfactant, the morphology obtained was honeycomb or hexagonal (Cai et al., 1999; Kim et al., 2021; Purnawira et al., 2019; Travaglini et al., 2019).

The amount of CTAB can also influence the morphology of the particles in another way, Vazquez and collaborators (2017) performed the synthesis of MSNs with TEOS:ethanol (1:20) and by

varying the proportions of H_2O:$NH_3 \cdot H_2O$:CTAB (proportions: 45.6 H_2O: 10.4 $NH_3 \cdot H_2O$: 0 CTAB or 45.6 H_2O: 10.4 $NH_3 \cdot H_2O$: 0.1 CTAB or 45.6 H_2O: 10.4 $NH_3 \cdot H_2O$: 0.1 CTAB or 600 H_2O: 10.4 $NH_3 \cdot H_2O$: 0.3 CTAB or 1200 H_2O: 10.4 $NH_3 \cdot H_2O$: 0.3 CTAB). It was noted that the increase in CTAB amount induced the growth of the silica mesoporous structure and the transformation of the spherical morphology into an ellipsoidal particle (elongated rod). The authors attributed this change in morphology to the "Ostwald Ripening" growth once different interactions between CTAB and alkoxysilane at the micelle/water interface can influence the ellipsoidal morphology of the particles (as mesopores begin to form along long axes). Moreover, the water content is the main factor that interferes in the length of these rods. As for the amounts of CTAB when using it in the proportions of 0.1 and 0.3 spherical particles with a specific surface area of 308 and 585 $m^2 g^{-1}$, respectively, were produced. On the other hand, increasing solvent content led to the formation of rod-like particles with a high specific surface area up to 1480 $m^2 g^{-1}$. However, as these particles have a high surface reactivity their dispersion in water is compromised.

Meanwhile, some authors report that the relationship between CTAB concentration and particle size is inversely proportional since the increase in the concentration of this surfactant causes the formation of the micellar structure, increasing the interaction with silica precursor. In the case of low concentrations of CTAB, the silica binds to the Si-O-Si group and not to the surfactant, which leads to an increased particle size (Purnawira et al., 2019; Zhao et al., 2012). Illustrating this correlation, in an alternative method for obtaining MCM-41-type MSNs (replacing TEOS with rice husk ash, due to its high silica content) proposed by Purnawira and collaborators (2019), different CTAB concentration was evaluated (1, 1.25 and 1.5%) in order to achieve the best mesoporous system. Emphasis was made in relation to the higher the concentration of CTAB, the smaller the particle size, since the synthesis with 1.5% of CTAB resulted in nanoparticles with an average size of 311 nm, whereas those with 1% exhibited particles with 482 nm.

A negative point related to the use of CTAB is when it is intended to use high temperatures during synthesis because it has thermal instability, which can cause instability in the micellar structure resulting in a product with a disordered mesoporous structure. This fact was mentioned in the study performed by Gu and collaborators (2012), who synthesized MSNs with controlled size, 50 nm, based on the suppressed growth strategy (performing particle size control with formaldehyde). In order to synthesize the nanoparticle, the authors tested conditions from 85 to 170 ºC with molar ratios of formaldehyde/TEOS 5.5, 11 and 33. The removal of organic matter was performed by calcination at 540 ºC for 6 h. All samples synthesized with formaldehyde showed spherical morphology with average diameter up to 50 nm. On the other hand, the particles synthesized by conventional route (MCM-41) were agglomerated with an average diameter of 100 nm. High temperatures used during the calcination

step can be the cause of this aggregation, and, since they had poorly ordered and narrow pores, this fact can cause mesopores to close. Still on the temperature variable, the authors also highlighted that the synthesis temperature range studied had little effect on particle size, whereas the temperature increase promoted random pores distribution reducing surface area values. Additionally, high temperatures lead to CTAB degradation (when exposed temperatures above 130 °C) and caused TEOS hydrolysis and polymerization (accelerating nanoparticles growth). These factors caused not only disorder to the mesoporous, which is not desirable, but also changed the color of the particles produced (after the treatments at 85 and 100 °C were white while those treated at 130 and 170 °C were brown-black).

3.2. Hollow mesoporous silica nanoparticles

Compared to the established porous silica nanoparticles, hollow mesoporous silica nanoparticles (HMSNs) exhibit unique physicochemical properties such as high surface area, chemical stability, tunable pore volume, non-toxicity, biocompatibility, easy surface modification and low density. These nanosystems have received great attention from researchers due to their wide range of applications in pharmacy, medicine, biochemistry, engineering, and technology areas (Deng et al., 2021; Jin et al., 2020; Sunwoo et al., 2021; Nguyen et al., 2019; Xie et al., 2021; Yasun et al., 2020).

It is important to highlight that HMSNs have advantages over MSNs in the controlled release of drugs once the large cavity inside them allows the incorporation of greater amount of drugs (Chen et al., 2015; Narayan et al., 2018; Nguyen et al., 2020; Shi et al., 2013). These characteristics led Nguyen and collaborators (Nguyen et al., 2020) to use this type of nanoparticle for the controlled release of doxorubicin. The authors synthesized these particles in three phases. First, by the modified Stöber method, a solid hard silica template was synthesized, then this hard template was coated with a layer of mesoporous silica (for this, 0.05 M of CTAB was used as template of the mesopores) which resulted in a core coated with mesoporous silica. Finally, these structures were mixed with an aqueous solution of Na_2CO_3 at 50 °C for 9 h (with free CTAB) in order to remove the templates. After that, the obtained material was lyophilized, and the synthesized HMSNs were immersed in acid acetic/ethanol solution over 24 h, and finally the HMSNs were washed exhaustively with deionized water to remove any remained CTAB.

When above critical micelle concentration (CMC), CTAB micelles are formed and if in an optimal ratio of CTAB:TEOS the latter, once negatively charged, interacts with the positive head groups of CTAB, accumulating around it. Since the hydrolysis process occurs before the condensation process, the hydroxyl groups also interacts with the hard core, through hydrogen bonds, thus linking the mesoporous silica matrix, that is being formed, with the hard core (Ghasemi et al., 2017). **Figure**

5 exemplifies a general representation of HMSNs synthesis, as illustrated, in order to obtain the central cavity, a selective chemical etching (usually by acids, but conjugate base of ammonium, for example, can also be used) is necessary to dissolve the hard templet. In this sense, free CTAB acts to redeposit the dissolved silica species in the outer shell (Abdollahi et al., 2022; Zhang et al., 2022). Although the etching step is fundamental for the synthesis of almost all HMSN, it is worth mentioning that in central nuclei composed of organic matter this additional step may not be necessary (Şen Karaman et al., 2015).

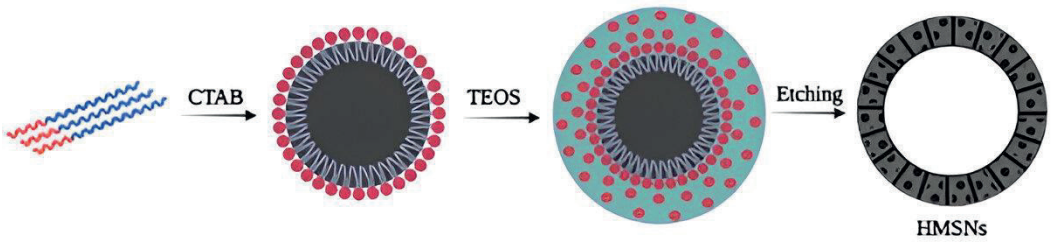

Figure 5: General representation of HMSNs synthesis.

Ghasemi and collaborators (2017) synthesized HMSNs using poly tert-butyl acrylate (PtBA) nanospheres, as hard template, and studied the effect of the molar ratio of CTAB/TEOS (0.073, 0.091, 0.11 and 0.12) in the nanosystems morphology (CTAB used here as the soft template). The lowest molar ratio studied was the only one that did not generate nanoparticles of spherical morphology, according to the authors, this is because the CTAB concentration is below its CMC, not being possible either the micellar formation or the arrangement on nanospherical polymers surface. Although the other molar ratio gave rise to spherical nanoparticles and adequately covered the polymeric nanosphere (through columbic interactions), aggregates were reported, which was attributed to a possible inadequate ratio and precursor excess. The sample with increased molar ratio, with more CTAB amount (spherical and without aggregates) was considered as having the ideal ratio of CTAB:TEOS (0.12:1). Additionally, the authors verified that the best process for removing CTAB from mesopores (generating particles defect-free) was achieved using NH_4NO_3 in ethanolic solution under reflux in comparison with calcination process. This finding can be explained by the fact that, during calcination silanol groups are eliminated, which can contribute to the aggregation of the particles, as, when present, they collaborate for the interparticle repulsion. It is also worth mentioning that in this study the hard core was removed by calcination (once the polymer used present exothermic nature).

In another work, Khoeini and collaborators (2019) fabricated monodisperse HMSNs, showing average size of 50 nm, using polystyrene and CTAB as template and surfactant, respectively. It is worth noting that in this study, the purpose of using the CTAB was to avoid aggregations and to control mesoporosity, size and morphology of the nanoparticles during the synthesis procedure. The control of agglomeration is important because it can increase the size of the suspended particles, leading to a thermodynamic instability of the system, which can conduct to their deposition within the system. As for the influence of CTAB on morphology, a correlation between CTAB and spherical morphology was also perceived for this type of mesoporous particle. The authors investigated the surfactant removal process by thermal treatment to prevent structural damages in the nanoparticles, and by thermogravimetry differential thermal analysis TG/DTA of the CTAB it was possible the state that the complete CTAB removal was achieved up at 350 °C, with a maximum between 200 to 300 °C with a heating rate of 10 °C/min. Suggesting that the surfactant removal process by thermal method should be designed for a minimum rate of organic material removal, so that the decomposed organic groups are not structurally destructed during removal and, thus structural defects are prevented.

Finally, it is worth noting that the ethanol:water ratio also influences the formation of the HMSNs mesoporous structure since it affects the micellar structure of the CTAB, as observed by Saputra and collaborators (2022). In their study, the authors observed that the increase in the proportion of ethanol reduced HMSN mesopores average size. This fact was attributed to the ionic interactions between the system and the surfactant head, since the greater the ionic interaction, the smaller the size of the CTAB micelle. This ionic interaction is influenced by the dielectric constant of the solvents used in the synthesis, and the higher their dielectric constant, the weaker the ionic interaction between the micelle and the system. Since ethanol has a lower dielectric constant than water, the greater the proportion of ethanol, the greater the ionic interaction and the smaller the size of the CTAB micelle, thus resulting in a smaller size of mesopores. The influence of pH on the diameter of CTAB micelles was also observed in this study, and as previously mentioned, the higher the pH (>2) the greater the micelles size.

3.3. Core-shell mesoporous silica nanoparticles

Core-shell nanoparticles are usually composed of a solid core coated with a thin shell (1–20 nm). Despite the wide range of materials of organic or inorganic origin used for the synthesis of this type of nanoparticle, mesoporous silica stands out due to advantages such as high stability (thermal, against coagulation and on storage for example) and being chemically inert, not affecting for example redox reactions on the core surface (when used as a shell base material). In addition, the mesopores give them high specific surface areas, which not only provides a high opportunity for surface modification

but also versatility for drug incorporation, desirable factors in drug delivery systems (Kalele et al., 2006; Kalyane et al., 2021; Mahdavi et al., 2020; Ung et al., 1998). Those particles prove to be very versatile in morphology, as it is possible to change it through the coating of the core. It is also noteworthy that these particles may have pores in the core, in the shell or in both, depending on their purpose, as can be seen in **Figure 6** (Su et al., 2020). In addition, the physicochemical characteristics of these systems differ from their source materials, being dependent on the core:shell ratio (Kalele et al., 2006).

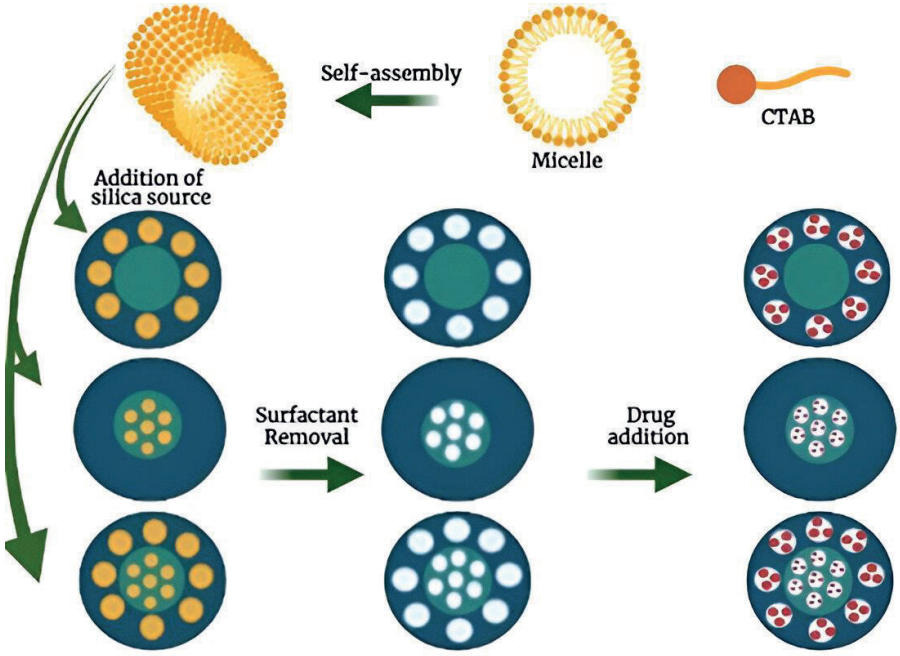

Figure 6: Representative scheme of mesoporous silica-based core-shell types.

When used to compose the core, a dielectric core is obtained, which, in order to achieve a greater surface area, is coated with nano-thick shells, usually composed by metal and other semi-conductive material. On the other hand, there is also the possibility of thicker shell synthesis, which is important when the objective is to provide thermal stability, for example (Kalele et al., 2006; Mahdavi et al., 2020). The use of mesoporous silica as the shell material has the advantage of adjustability in size, shape, porosity, pore size and volume and shell thickness. Furthermore, it increases the stability of the core particles and reduces the bulk conductivity (Girija & Balasubramanian, 2019; Kalyane et al., 2021). In general, as in other types of MSNs, to form the mesoporous silica matrix, the alkoxysilane undergoes hydrolysis (nucleation) and condensation (growth) processes. However, the interaction of

these two processes is fundamental for the efficient formation of a core-shell structure. When condensation is greater than the silica hydrolysis rate, is a favorable condition for core encapsulation. So, upon loss of the counteranion, the positively charged CTAB binds to the nucleus (ideally a negatively charged nanoparticle) and the silicon oligomers (that are produced by the silica source - TEOS for example), are then electrostatically attracted to the sphere micelles of CTAB (Chen et al., 2013; Hussain, 2021).

Asgari and collaborators (2019) synthesized, by inverse microemulsion method, nanosystems based on Fe_3O_4 nanoparticles core- mesoporous silica-based shell structures. For this, CTAB was used as surfactant, 1-butanol as co-surfactant, water as aqueous phase and cyclohexane as organic phase, which contained the silica precursor. The CTAB here was used to enable the transfer of the core to the aqueous phase once CTAB alkyl chains interact with oleic acid through Van der Waals interactions, providing self-assembly of the CTAB on the core surface, also favoring its use as soft removable template for the mesoporous silica-based shell. In order to obtain the core-shell structure, the CTAB was removed by a calcination process at 550 °C for 6 h. As mentioned in the previous study, Lee, Lee and Lee (Lee et al., 2022) highlighted that in addition to its role as a porogenic agent (for the synthesis of the shell in this case), CTAB also acts as a dispersing agent for nanoparticles (core) during the synthesis of a core-shell mesoporous silica nanoparticle, once the authors observed that the Mn_3O_4 nanoparticles were highly dispersed when in the presence of CTAB in the solution, while when absent the nanoparticles were severely aggregated.

In another study, authors proposed to develop core-shell mesoporous silica nanosystems by using metal oxide nanoparticles (MONPs) as core. Although CuO nanoparticles were used as a pilot, several other types of metal oxide can be used as core structure. MONPs, polyvinylpyrrolidone (PVP), ethanol, distilled water, aqueous ammonia solution, TEOS and CTAB were the reagents used for core-shell synthesis. CTAB micelles interacted with the PVP of the MONPs inducing silica shell crystallization. Additionally, the higher the CTAB concentration, the greater the shell thickness can be achieved. On the other hand, much higher CTAB concentration increases (like from 3.4 mM to 6.8 mM and 13.6 mM) irregular shape and core-less particles can be achieved. This reinforces the importance of studying the appropriate proportion of this surfactant, as the formation of core-less particles (accompanied by a reduction in the thickness of the shell) is due to the excess of CTAB micelles in relation to the amount of PVP molecules (Yang et al., 2020).

The importance of determining the ideal CTAB amount was also evaluated by Song and collaborators (2015). A discussion about CTAB role in a new method of core-shell synthesis using gold nanoparticles (AuNPs) as core and mesoporous silica as shell was performed. The fabricated AuNPs were transferred to an alkaline aqueous solution containing CTAB. During the synthesis, the

authors observed that low concentrations of CTAB (less than 4.5 mM) in alkaline solutions generated instability for the AuNPs, avoiding the coating process. Therefore, at concentrations higher than 6.4 mM (7 .8, 9.2, 10 and 12 mM), a large amount of hollow silica particles was detected. The authors highlighted that the concentration of CTAB is an important element for the mesoporous silica shell formation, since in addition to determining its formation on the core surface, it also determines the amount of pure hollow mesoporous silica that will be formed after synthesis. In a general way, for the formation of a core-shell nanoparticle, CTAB forms a micellar monolayer coating around the core. However, the authors discussed about another formation mechanism: the CTAB bilayer structure being responsible for the formation of the core-shell. This fact was justified for two reasons. The first one is because of the size of both, a single CTAB micelle (3-5 nm) is not able to coat a single AuNP (20 nm). The other reason is because CTAB has a hydrophobic tail, so it would not be possible to form a stable structure between the hydrophilic surface of the AuNPs and the aqueous solution. Therefore, when AuNPs are added to CTAB micelle solution, they adsorb the micelles on their surface and, at ideally high concentration, the CTAB bilayer begins to form. Subsequently, TEOS is hydrolyzed to form a mesoporous structure, thus forming the mesoporous silica shell. So, as well as in the previous study, it can be seen that determining the ideal core:CTAB ratio is essential for effective core-shell synthesis (Song et al., 2015; Yang et al., 2020).

In another study whose objective was to develop a general synthesis method for mesoporous silica shell to be applied in combination with any hydrophilic core, such as Au and small Ag (4 to 15 nm), CeO_2, Fe_3O_4, Gd_2O_3, $NaYF_4$, this CTAB bilayer issue was also highlighted. According to the authors, when using a single layer of CTAB (due to incorrect amount of surfactant), the hydrophobic tail of the same would be oriented away from the core, which is hydrophilic, resulting in phase separation and precipitation of the core. Furthermore, low amounts of CTAB may not be sufficient to interact with the negative charge of the core, leading to crosslinking and aggregation of the core prior to coating with the mesoporous matrix. Low amounts of CTAB can also generate an irregular shell coating (due to the lack of CTAB available to coat all cores). For these reasons the authors also emphasized the importance of determining the appropriate CTAB:core ratio. As discussed for HMSNs, ethanol:water ratio directly influences the formation of CTAB micelles, when in high amounts, this solvent changes the polarity of the medium, compromising the formation of the micelles, also altering the stability and morphology of the nanoparticles. On the other hand, the authors also observed that low amounts of ethanol resulted in irregular cores, which was controlled by the correct selection of this solvent amount (since this increased the shell thickness) (Zeng et al., 2021).

3. Methods for removing CTAB from the pore structures

In order to remove the surfactant from inside the pore, to make it free for drug incorporation, several types of methodologies are currently used (Ghaedi & Zhao, 2022). A first example, widely used and already well established in the literature, is calcination. This technique consists of applying high temperatures to remove the surfactant molecule by volatilization (Marzano et al., 2019). Several combinations of time and high temperatures can be observed in the literature, as 530 °C for 6 h (Travaglini et al., 2019), 540 ºC for 6 h (Gu et al., 2012; Zhang et al., 2010), 550 °C for 3 h (Vazquez et al., 2017), 550 °C for 4 h (Chen et al., 2013) and 550 °C for 6 h (Asgari et al., 2019; Yang et al., 2020). Although efficient, as mentioned earlier, this technique has the disadvantage of causing agglomeration between the particles (due to the narrowing that occurs during sintering). In addition, tests are important in order to determine the ideal combination of temperature and time of the process, since low temperatures may not be sufficient to adequately remove the surfactant, on the other hand, higher temperatures further favor agglomeration. Furthermore, because of the temperature, this technique can also decrease the size of the mesopores and the particle surface area due to particle growth (Marzano et al., 2019; Shamim et al., 2022).

However, in one study, CTAB (depending on the quantity used) showed to contribute to the prevention of hard agglomerates formation during the calcination process. Since it being cationic provides a less negative charge to the nanoparticles, thus increasing the repulsion between them. Another factor that also corroborates with it is the ability of this type of surfactant to provide steric stabilization, thus preventing thickening. Although the issue of CTAB residue permanence is better exemplified in the following topic, it is important to mention here that since after calcination, washing and drying, it is possible to observe CTAB residues, this surfactant permanence makes it possible to obtain particles less agglomerated. Therefore, it is worth reinforcing the importance of testing for the choice not only of the calcination temperature and time, but also for the concentration of this surfactant, since these aspects directly influence the permanence or not of residues (Graeve et al., 2013; Marzano et al., 2019; Napper, 1977). Regarding the biological application in a study whose objective was to compare three types of MSNs, two calcined and one by solvent extraction (acid reflux), it was observed that the calcined MSNs has a tendency to agglomerate in biological lipid membranes, which depending on the biological application can negatively impact during therapy since they can delay the uptake of the nanosystem by epithelial cells (Joyce et al., 2020).

Removal of CTAB by solvent extraction, mainly by reflux, is another widely used methodology. In this methodology, the CTAB is extracted from the pores through its affinity with the solvent (a mixture of solvents with different polarities is used) since it permeates and solubilizes the CTAB under a certain temperature (boiling point of the solvents) for several hours (so that the solvent is

continuously refluxed over the sample) (Alonso-Carrillo et al., 2017; Biesaga, 2011; Castro-Vargas et al., 2010; Khoddami et al., 2013; Queiroz et al., 2001). As examples of reflux conditions used to remove CTAB from the pores, the following can be cited: HCl/ethanol at 60 ºC for 3 h (Ezzati et al., 2019), HCL/ethanol solution at 60 ºC for 6 h (M. K. Kim et al., 2021), HCl/methanol at 50 °C for 6h (Ma et al., 2011), acetone at 60 °C for 6 h (Wu et al., 2016) and NH_4NO_3 in ethanolic solution at 70 °C for 5 h (Ghasemi et al., 2017). Although efficient, this methodology has limitations such as time (as well as calcination) and the use of large volumes of toxic solvents (Alonso-Carrillo et al., 2017). For this reason, studies involving green methods for CTAB removal are increasingly desirable. For example, to achieve a simple, fast, and low-cost method to synthesize HMSNs, Li and collaborators (2019) in order to remove CTAB from the pores dipped the nanosystems in boiling water at 90 °C for 24 h to induce the hollow core structure formation and finally remove the template. Basically, hot water, in addition to eroding the core of the nanoparticles, creating a hollow structure, can also dissolve CTAB, once dissolved, it is removed from the pores, leaving them free. The authors proved by FTIR analysis that the CTAB was completely removed.

Finally, it is worth mentioning another methodology, greener than reflux, also used to remove CTAB from pores: sonication. In this methodology the strong mold formed between the surfactant and the silica matrix can be removed by a shear force promoted by sonication, causing the disruption of micellar disintegration. This shear force is generated by the implosion of bubbles during sonication, that is, the rupture is promoted by thermal and solvodynamic shear effects that are associated with the process of acoustic cavitation in a solution (stage of formation, growth and collapse of micrometric bubbles). However, for complete removal of CTAB, it is necessary to use organic solvents, such as ethanol and methanol. This process allows the disintegrated surfactant to be released into the organic solvent, removing CTAB residues (Jabariyan & Zanjanchi, 2012; Xuan et al., 2011). Zanjanchi and collaborators (2014) used the sonication technique to remove CTAB from MSN mesopores. In this study, it was possible to observe that increasing the sonication time increases the concentration of CTAB in the solvent, that is, the sonication time interferes with the amount of CTAB removed. However, the authors pointed out that a shorter sonication time can preserve the structure of CTAB in ethanol. Finally, another point highlighted by the authors was that in addition to the advantage of using a smaller amount of organic solvent (when compared to the extraction method), sonication also has an advantage over the calcination method in relation to the process time, for sonication the authors mentioned the time of 15 min while for calcination it was 12.4 h.

5. Are CTAB residues acceptable in mesoporous silica nanoparticles for drug delivery?

Although there are several methods for removing CTAB from the pore structures, residues may remain in mesoporous silica samples (Javdani et al., 2020; Wang et al., 2009; Wu et al., 2021). In a study, whose objective was to evaluate the pH and the chirality impact on flurbiprofen release from chiral MSNs, CTAB was the surfactant of choice. Although CTAB was supposed to be removed by acid reflux (methanol solution of HCl 0.01M for 12 h), FTIR exhibited CTAB residue (about 3% w/w) in samples, assigned to peaks at 2855 and 2926 cm^{-1} (Wu et al., 2021). Joyce and collaborators (Joyce et al., 2020) synthesized MSNs using both, calcination (650°C for 8 h) and reflux (solution of methanol and HCl at 70°C overnight) methods to remove CTAB from mesopores. Although in the FTIR analysis, no CTAB residues were observed in both nanoparticles, in the thermogravimetric analysis (TGA) (10°C/min from 20 to 600°C, under nitrogen purging) a minor fraction (< 1 wt.%), attributed to the presence of CTAB residue, was observed in both.

In another study, CTAB or tannic acid were applied as template for the synthesis of four types of MSNs, two of them were prepared using both templates and the others two were similarly prepared but also modified *in situ* with amine groups. Among the various characterization techniques, emphasis was made to TGA (heating rate of 10 °C/min from 10 to 1000 °C under air atmosphere), where, according to the authors, the weight loss of the two non-functionalized MSNs may be related to residual template agents and volatilization of the adsorbed water in the pores (Javdani et al., 2020). Wang and collaborators (Wang et al., 2009) functionalized mesoporous silica with several organic groups (vinyl, 3-mercaptopropyl, 3-aminopropyl and secondary amine groups) in order to evaluate them for incorporation and release of molecules (rhodamine 6G and ibuprofen). Residues of CTAB were observed in the Solid-state Nuclear Magnetic Resonance (NMR) analysis (minor peaks at ~30 ppm) even after treatment to remove the surfactant template (stirring the functionalized mesostructured material with a solution of methanol and HCl for 5 h at 50 °C).

Based on the studies mentioned above, it is possible to observe that despite the different types of surfactant removal techniques available, residue permanence is possible (Javdani et al., 2020; Wang et al., 2009; Wu et al., 2021). Although there are advantages of residue permanence regarding the physicochemical stability of the particles, as mentioned in the previous topic (regarding the prevention of agglomerates formation during the calcination process) (Graeve et al., 2013), it is also worth reflecting on whether these residues are suitable in terms of biological application regarding its toxicity. Is the amount of CTAB residues remaining from synthesis processes capable of generating toxicity? Is this nanotechnological formulation safe for the patient and suitable for its intended purpose?

To try to answer these questions, it is necessary to study the toxicity of CTAB in different types of cells in order to determine acceptable residue limits, in other words, to determine a limit concentration below the one considered toxic. It is worth noting that this reflection on toxicity in different cell types is important to adapt this limit to the purpose for which the formulation is intended, although it is always necessary to respect the limit for toxicity of eukaryotic cells when it comes to a formulation for human application. However, when this application is intended for the treatment of an infectious disease (bacteria: prokaryotic cell; fungus: eukaryotic cell) toxic residues may be desirable as the killing or inactivation thereof is sought. **Table 1** summarizes the main points of studies (covered in topic 5.1) evaluating CTAB cytotoxicity in prokaryotic and eukaryotic cells.

Table 1: Cytotoxic evaluation of CTAB in prokaryotic and eukaryotic cells.

Cell type	Lineages/Species	Sample	Methods	Results	Reference
Eukaryotic	HT-29	CTAB and CTAB-capped gold nanorod	MTT assay	30 % of viability for CTAB 10 % of viability for CTAB- capped gold nanorod (1 nM)	(Alkilany et al., 2009)
Eukaryotic	Hep-2 and MDCK	CTAB and nanoparticles encapsulated CTAB.	MTT assay	Greater toxicity for CTAB (1 mM)-containing nanoparticles	(Zhang et al., 2012)
Eukaryotic	SAOS-2	CTAB only	Live/dead cell viability assay	Cytotoxic CTAB in all concentrations (in the range of 0.2 mM-2 mM, that is, including its critical micelle concentration)	(Kalbáčová et al., 2014)
Eukaryotic	NIH/3T3	CTAB only	MTT	Low percentage of survival, viability and cell proliferation	(Alexandrescu et al., 2013)
Eukaryotic	HaCaT and CRL-1490	CTAB only	MTT assay	HaCaT Cells: 64% viability in 2 h exposure time 0 % viability in 2 h exposure time CRL-1419 Cells: 0 % viability in 2 h exposure time 0 % viability in 2 h exposure time	(Zhang et al., 2015)
Eukaryotic	CCL-119 and CRL-1596	CTAB only	Flow cytometry	Uncontrolled cell death caused by electrostatic interaction	(Yasun et al., 2015)
Eukaryotic	Caco-2, HepG2, MCF-7 and SV-80	CTAB-SLNs	Alarm blue	IC50 (μg mL^{-1} of CTAB) Caco-2 traded in24h/48h: 8.91 μg mL^{-1} / 8.72 μg mL^{-1} HepG2 traded in24h/48h: 9.70 μg mL^{-1} / 9.04 μg mL^{-1} MCF-7 traded in24h/48h: 8.91 μg mL^{-1} / 9.11 μg mL^{-1} SV-80 traded in24h/48h: 9.31 μg mL^{-1} / 8.91 μg mL^{-1}	(Silva et al., 2019)
Eukaryotic	HeLa	CTAB and CTAB-capped gold nanorod	Live/dead cell viability assay	Almost 65% reduction at a concentration of 20 μM CTAB free	(Fernando et al., 2020)
Prokaryotic	*S. aureus, M. luteus, E. coli, S. marcescens, P. aeruginosa* and *P.vulgaris*	CTAB only	MIC in TSB	*S. aureus* and *E. coli* (16 mg L^{-1}), S. *marcescens* and *P. vulgaris* (128 mg L^{-1}), *P. aeruginosa* (> 1024 mg L^{-1})	(Nicoletti et al., 1993)
			MIC in MHB	*S. aureus* and *E. coli* (16 mg L^{-1}), S. *marcescens* and *P. vulgaris* (128 mg L^{-1}), *P. aeruginosa* (512 mg L^{-1})	

			MIC in SB	*S. aureus* (2 mg L^{-1}), *E. coli* (8 mg L^{-1}) *P. vulgaris* (32 mg L^{-1}) *S. marcescens* (64 mg L^{-1}) *and P. aeruginosa* (128 mg L^{-1})	
			MMC in TSB	*E. coli* (16 mg L^{-1}), *S. aureus* (32 mg L^{-1}), S. *marcescens* and *P. vulgaris* (256 mg L^{-1}) and *P. aeruginosa* (> 1024 mg L^{-1})	
			MMC in MHB	*E. coli* (16 mg L^{-1}), *S. aureus* (32 mg L^{-1}), *P. vulgaris* (128 mg/L^{-1}), S. *marcescens* (256 mg L^{-1}) and *P. aeruginosa* (512 mg L^{-1})	
			MMC in SB	*E. coli* (8 mg L^{-1}), *S. aureus* (16 mg/L^{-1}), S. *marcescens* and *P. vulgaris* (64 mg L^{-1}) *and P. aeruginosa* (128 mg L^{-1})	
Prokaryotic	*P. fluorescens*	CTAB only	Planktonic cells	Bacterial inactivation and ATP increase.	(Simões et al., 2005)
			Biofilm	Removal of 60% and 40% for laminar and turbulent biofilms, respectively.	
			Post-CTAB treatment	Increased cellular respiration for both biofilms	
Prokaryotic	*B. anthracis* spores	CTAB only	Detection in broth	Increased anti-sporocyst activity	(Banerjee et al., 2006)
Prokaryotic	*E. coli*	CTAB only	Growth time	Inhibition of E. coli growth in 10 µmol L^{-1}	(Ishikawa et al., 2009)
Prokaryotic	*E. coli* wild *E. coli* CTAB-resistant	CTAB only	BES fluorescent probes	ROS increase and inhibition of protein production	(Nakata et al., 2011)
Prokaryotic	*B. cereus, P. fluorescens* and *S. aureus*	CTAB only	Biofilm	*B. cereus* and *P. fluorescens* with death rates of 51.8% and 25.6%, respectively, and antibiofilm inhibition when combined with *S. aureus*	(Araújo et al., 2014)
Prokaryotic	*E. coli* and *S. aureus*	CTAB only	MIC	34 µg mL^{-1} and 1.8 µg mL^{-1} for *E. coli* and *S. aureus,* respectively	(Zhang et al., 2015)
Prokaryotic	*S. mutans, S. mitis*	CTAB only	Disk diffusion	5 mm for *S. aureus, S. mitis, S. mutans* and *P. aeruginosa,* 3 mm for *E. coli* and *P. gingivalis* and 2 mm for *S. salivarius*.	(Bucci et al., 2018)

	S. salivarius, Porphyromonas gingivalis, P. aeruginosa, S. aureus and *E. coli*		MIC	250 μg mL^{-1} for *S. mutans,* 31 μg mL^{-1} for *P. gingivalis* and *S. salivarius,* 16 μg mL^{-1} for *E. coli,* 4 μg mL^{-1} for *P. aeruginosa* and 2 μg mL^{-1} for *S. mitis*	
Prokaryotic	*B. subtilis, B. cereus* and *B. megaterium*	CTAB only	Spectrophotometric reading and agar culture	Increased dipicolinic acid in a 1:1 chelate with Ca2+ release and CFU inhibition	(Dong et al., 2019)
Prokaryotic	*Streptococcus sanguinis, E. faecalis, Fusobacterium nucleatum* and *Porphyromonas gingivalis*	CTAB only	Biofilm	Biofilm removal and bacterial death	(Bryce et al., 2020)
Eukaryotic	*C. albicans*	CTAB only	MIC TSB	32 mg L^{-1}	(Nicoletti et al., 1993)
			MIC MH	16 mg L^{-1}	
			MIC SB	2 mg L^{-1}	
			MMC TSB	64 mg L^{-1}	
			MMC MH	32 mg L^{-1}	
			MMC SB	8 mg L^{-1}	
Eukaryotic	*C. albicans*	CTAB only	Cell adhesion	CMC in 0.20 mM whit 99% binding to *C. albicans* cells.	(Ahlström et al., 1997)
Eukaryotic	*C. albicans*	CTAB only	fungal viability	50% inhibition of fungal viability and Haemolysis	(Simões et al., 2005)
Eukaryotic	*C. albicans*	CTAB only	MIC and Adhesion	MIC of 2 μg mL^{-1} and an anti-adhesion action of 16.05%	(Bucci et al., 2018)
Eukaryotic	*C. albicans*	CTAB only	MIC	8 μg mL^{-1}	(Maneedaeng et al., 2018)
			MFC	16 μg mL^{-1}	

Legend: HT-29: human colon carcinoma cells; MTT: Thiazolyl Blue Tetrazolium Bromide; HeLa: human cervical adenocarcinoma cells; HaCaT : human epidermal keratinocyte; CRL-1490: human lung fibroblast ; SAOS-2: Human osteoblast-like cell line; CCL-119:T cell, human acute lymphoblastic leukemia ; CRL-1596: B cell line, human Burkitt's lymphoma; NIH/3T3: mouse fibroblast cells; CTAB-SLNs: CTAB cationic solid lipid nanoparticles; Caco-2: epithelial colorectal adenocarcinoma; HepG2: human liver hepatocellular carcinoma; SV-80: human lung fibroblast; MCF-7: human breast adenocarcinoma; Hep-2: human larynx epithelioma cancer; MDCK: Madin-Darby Canine Kidney cells; IC50: Half-maximal inhibitory concentration TSB: Tryptic soy broth; MHB: Mueller Hinton Broth; SB: Synthetic Broth; ATP: adenosine triphosphate; CMC: critical micelle concentration; MMC: minimum microbicide concentration; MFC: Minimum Fungicidal Concentration; MIC: Minimum Inhibitory Concentration; BES: benzenesulfonyl

5.1. CTAB toxicity in eukaryotic and prokaryotic cells

CTAB has a strong electrostatic interaction with eukaryotic and prokaryotic cells, promoting disruption in the cell membrane, permeability modification and loss in intra- and extra-cellular constituents. This interaction is responsible for cell lysis and death (Nakata et al., 2011; Shao et al., 2017). Much has been discussed about cationic surfactants mechanism of action against microorganisms (Nakata et al., 2011). CTAB is highly absorbed by microorganism, making them available in cells cytoplasm. CTAB electropositive charge facilitates this absorption process once it interacts with electronegative charged microbial cells. This electrostatic interaction between them promotes cellular disorganization, making the microbial cells more negatively charged and hydrophobic. After absorption, CTAB can exert enzymatic inhibitory action, decrease metabolic activity and cause bacterial and fungi death (Bryce et al., 2020; Mcdonnell & Russell, 1999; Nakata et al., 2011; Pietsch et al., 2021; Zhang et al., 2015).

In mammalian cells CTAB monomers and double-layer structures exhibit a mechanism of action similar to that compared with microorganisms, which make them responsible for toxicity effects in those cells. As CTAB has electropositivity, it can bind to cells negative surface in a non-specific way by electrostatic interaction. This interaction can promote the formation of bubbles and defects (holes) in the cell membrane, leading to the death of cells (Yasun et al., 2015).

5.1.1. CTAB toxic in eukaryotic cells: mammalian and fungi

Mammal cells

The cytotoxic potential of different CTAB concentrations (in the range of 0.2 mM, including its CMC) was evaluated against human osteoblasts SAOS-2 derived from osteosarcoma. The results showed that all CTAB concentrations had significant cytotoxicity. However, it was inhibited in the presence of hyaluronan. The authors concluded that hyaluronan may have a protective role in inhibiting CTAB cytotoxicity at low concentrations (Kalbáčová et al., 2014). CTAB nanostructures based on nanofibers of fibers absorbed with CTAB (CTAB at 10% by weight) showed significant cytotoxic potential, mainly due to the presence of CTAB low percentage of survival, viability and cell proliferation was also observed in a study involving mouse fibroblast cells (3T3) (Alexandrescu et al., 2013).

Zhang and collaborators (2012) evaluated the cytotoxic potential of CTAB against human epidermal keratinocytes (HaCaT) and pulmonary fibroblast cells (CRL-1490). The results revealed that CTAB present higher percentage of cytotoxicity against CRL-1490 and the longer the exposure time, the higher the toxicity level. It was concluded that this surfactant has a high level of cytotoxicity and that the exposure time, in association with the cellular type, must be considered as a determinant

factor for cytotoxicity. High CTAB-induced cytotoxicity has also been reported for CCRF-CEM (CCL-119 T cells, human acute lymphoblastic leukemia), and Ramos (CRL-1596, B cell line, human Burkitt's lymphoma) (Yasun et al., 2015).

It is noteworthy that there is a gap in the literature on studies evaluating the toxicity of CTAB residues in mesoporous silica nanoparticles in mammalian cells. On the other hand, it would be possible to predict a possible toxicity, since studies evaluating another type of inorganic nanoparticle found that CTAB is responsible for conferring toxicity to them (Alkilany et al., 2009; Fernando et al., 2020; Jia et al., 2020; Silva et al., 2019; Zhang et al., 2012). Alkilany and collaborators (2009) evaluated CTAB cytotoxic against human colon carcinoma cells (HT-29). According to the results, CTAB cytotoxicity percentage was 70%. Furthermore, the authors also evaluated CTAB-loaded inorganic nanoparticles (AuNPs). This system presented more cytotoxic than compared with the same nanoparticles without CTAB. It can be concluded that this greater cytotoxicity is related to the CTAB, since it presented low levels of cell viability when evaluated separately. A similar study was carried out by Zhang and collaborators (Zhang et al., 2012), however, at this time the cell line used was human Hep-2 and canine MDCK cells. CTAB aqueous solution also showed high cytotoxicity capacity, being the toxicity related to the dose increase. Additionally, the AuNPs displayed greater cytotoxicity when compared with other nanoparticles (of the same type of material) synthesized without CTAB, reinforcing that the presence of CTAB conferred toxicity to the AuNPs.

Fernando and collaborators (2020) developed CTAB-containing gold nanotubes (AuNTs) to assess cell viability against human cervical adenocarcinoma cells (HeLa). The results showed that the AuNTs with the highest percentage of cytotoxicity were those that had CTAB in their composition. Furthermore, the CTAB-free solution showed a low percentage of cellular viability, justifying the higher cytotoxicity in CTAB-containing AuNTs. This toxicity can also be observed in organic nanoparticles, as in the study carried out by Silva and collaborators (2019) the authors noticed that CTAB is responsible for the toxic levels found in their developed system (solid cationic lipid nanoparticles). It is worth mentioning that this study was performed against Caco-2 (colorectal epithelial adenocarcinoma), HepG2 (liver hepatocellular carcinoma), SV-80 (lung fibroblast), MCF-7 (breast adenocarcinoma), and Y-79 (human retinoblastoma).

Fungi Cells

CTAB residues may be desirable when antifungal action is aimed, once this toxicity is widely explored as a mechanism of action against pathogenic fungi (Cheng et al., 2012; C. Dong et al., 2018; Xiang et al., 2019). Treatment with CTAB promoted *Candida albicans* cell hemolysis (CTAB > 0.001 mM) and 50% inhibition of its viability (CTAB at 0.3 mM) (Simões et al., 2005). Therefore, aiming

to explore CTAB potential Anti-*Candida albicans* at different concentrations, several studies has been performed, such as those described below. Nicoletti and collaborators (1993) evaluated CTAB Anti-*C. albicans* activity by minimum inhibitory concentration (MIC), performed in three different broths, Synthetic Broth (SB), Mueller-Hinton Broth (MH) and Tryptone Soya Broth (TSB) and by minimum microbicide concentration (MMC). The authors noted that CTAB MIC in SB, MH AND TSB were 2, 16 and 32 mg L^{-1}, respectively, and MMC were 4, 32 and 64 mg L^{-1}, respectively. In another study, CTAB showed high interaction with *C. albicans* cells, reaching 99% of binding (Ahlström et al., 1997).

Bucci and collaborators (2018) emphasized recent results about CTAB antifungal potential against *C. albicans*. The authors evaluated CTAB anti-adhesion activity and MIC. As results, an antifungal activity of 2 μg mL^{-1} and an anti-adhesion action of 16.05% were detected. Maneedaeng and collaborators (2018) determined the Anti-*C. albicans* action through MIC and Minimum Fungicidal Concentration (MFC). According to the results, CTAB exhibited a MIC and MFC of 8 and 16 μg mL^{-1}, respectively. Thus, it was possible to observe that CTAB toxicity in fungal cells is desirable when the purpose of the system is the antifungal application. It is noteworthy that although the mechanism of action is well established, few studies were found in the literature regarding to the pathogenicity against fungi, being essential to conduct more studies in this field.

5.1.2. CTAB toxic in prokaryotic cells: Bacteria

As well as for fungal cells, CTAB antibacterial mechanism of action is related to its rapid adsorption with microbial cells. The hydrophobic portion of the surfactant interacts with the phospholipid bilayer of the cell membrane, promoting cell disorganization and rupture, which eventually leads to cell death, conferring to this surfactant not only antifungal, but also antibacterial activity (Cheng et al., 2012; Dong et al., 2018; Xiang et al., 2019).

Bucci and collaborators (2018), evaluated the toxic activity of CTAB against strains of *Streptococcus mutans, Streptococcus mitis, Streptococcus salivarius, Porphyromonas gingivalis, Pseudomonas aeruginosa, Staphylococcus aureus* and *Escherichia coli.* Antimicrobial methods of choice were MIC and disk diffusion. The results in disk diffusion (inhibitory halo size in mm) showed inhibition of 5 mm against *S. aureus, S. mitis, S. mutans* and *P. aeruginosa,* 3 mm for *E. coli* and *P. gingivalis* and *2* mm for *S. salivarius.* According to the MIC data, the *S. mutans* strain showed greater resistance to CTAB treatment, with an activity of 250 μg mL^{-1}. *S. mitis* and *S. aureus* was the most sensitive strains to CTAB, with a MIC of 2 μg mL^{-1}. In conclusion, surfactants not only play a fundamental role in the solubilization and reduction of side effects of substances but also are an important alternative in antimicrobial potentiation.

Nicoletti and collaborators (1993) used *S. aureus, Micrococcus luteus, E. coli, Serratia marcescens, P. aeruginosa* and *Proteus vulgaris* in order to evidence CTAB activity against bacteria. The methodology addressed in this experiment was MIC and Minimum Bactericidal Concentration. In addition, the antimicrobial activity was evaluated in three different culture mediums: TSB, MHB, and SB. Among the three-culture medium, the most sensitive strains were *S. aureus* and *P. vulgaris,* both with a MIC value of 2 mg L^{-1} in SB (MMC of 16 mg L^{-1}). Moreover, the most resistant strain against CTAB was *P. aeruginosa* with MIC > 1024 mg L^{-1} in TSB (MMC > 1024 mg L^{-1}). Although *P. aeruginosa* seems to be resistant at the concentration tested, CTAB displayed promising results for the others bacterial strains in all broths evaluated.

CTAB antimicrobial potential was studied by Zhang and collaborators (2015) against *E. coli* and *S. aureus* strains. Antimicrobial activity was based on the MIC determination method. The *in vitro* assay showed CTAB with an inhibitory activity of 34 and 1.8 μg mL^{-1} for *E. coli* and *S. aureus*, respectively. It is worth highlighting that the results revealed a greater interaction for Gram-positive bacteria than for Gram-negative ones. This higher affinity and better antibacterial activity were justified by the lower permeability capacity in Gram-negative.

In another study, CTAB growth inhibition potential was tested against *E. coli,* and the growth time was significantly inhibited when in contact with CTAB at a concentration of 10 μM, which also promoted cell lysis. This inhibition may be related to CTAB deleterious effect on bacterial growth, viability, respiratory inhibition and autolysis induction (Ishikawa et al., 2002). *E. coli* was also the pathogen of choice in another study whose objective was evaluated the toxic potential of CTAB in stimulating the production of superoxide and hydrogen peroxide. The experiment was conducted in an *in situ* assay with benzenesulfonyl (BES) fluorescent probes. According to the results, CTAB significantly increased the percentage of superoxide and hydrogen peroxide in wild *E. coli* strains compared with CTAB-resistant *E. coli* strains. At appropriate concentrations, it was shown that CTAB induced short term cell lysis and bacterial suspension. The results exhibited that CTAB can inhibit the production of intracellular proteins essential for bacteria, justifying its antimicrobial action. This protein inhibition may be related to the role of CTAB in the protein translation process. In conclusion, the authors suggest that CTAB surfactant has good antimicrobial activity by increasing reactive oxygen species (Nakata et al., 2011).

It is important to point out that, when a microorganism finds itself in an unfavorable environment, with less source of nutrients (environmental stress), some microorganism species are able to transform into spores (Nicholson et al., 2000). These spores are bacterial structures that are highly resistant to environmental variations. These structures with dormant metabolic activity can withstand high temperatures and nutrient shortages. The spores form a highly resistant protective

barrier, containing the cytoplasm and all cell structures preserved until the environment to be suitable for growth (Banerjee et al., 2006; Moir et al., 2002).

Aiming at the worrying microbial resistance and its multiresistant forms, Banerjee and collaborators (2006) evaluated CTAB sporocyst capacity alone and in combination with tert-butyl hydroperoxide (TBHP) against *Bacillus anthracis* spores. The experiments were carried out in broth and the colony-forming units (CFU) were quantified in agar. The results showed that CTAB (0.03%) promoted spore inactivation. Furthermore, CTAB combined with TBHP exhibited a synergistic effect increasing anti-spore activity. The authors concluded that CTAB is a promising surfactant in combating resistant forms of microorganisms.

In another study, CTAB was evaluated against spores of *Bacillus subtilis, Bacillus cereus* and *Bacillus megaterium*. The study goal was to evaluate the ability of CTAB to release the deposit of chelate of dipicolinic acid present in spores and promote bacterial death. The methodology used different parameters such as pH and temperature in culture containing spores treated with 10 g L^{-1} of CTAB. The results displayed that CTAB promoted dipicolinic acid chelate release mainly at high temperatures. Approximately 100% of dipicolinic acid chelate was taken from *B. subtilis* spores at 60 °C, pH 8.4 within 60 min of incubation with CTAB. Additionally, *B. megaterium* spores were the most sensitive against CTAB. Finally, the assays to quantify colonies revealed the absence of microbial growth. It can be concluded that CTAB can be used against resistant forms of *Bacillus* ssp., mainly due to its action of breaking spores inner wall (Dong et al., 2019).

Acute infections are triggered by microorganisms that present planktonic forms, however, during the infection or the place where they adhere, these microbial cells develop strategies and adaptations to maintain their species. This strategy leads to the formation of a cohesive, strong community structure of microbial cells, known as a biofilm. Biofilm represents a heterogeneous microbial community, aggregated, organized and incorporated into a matrix of extracellular polymeric substances, allowing these microorganisms to irreversibly adhere to biotic and abiotic surfaces. Since these biofilms form a highly resistant structure, current therapy has several antibiofilm limitations. Therefore, it is extremely important to evaluate new substances with high antimicrobial potential against biofilms, such as cationic surfactants (Burmølle et al., 2014; Ramos et al., 2018; Fux et al., 2005).

In a study, the antimicrobial potential of CTAB against mature *Pseudomonas fluorescens* biofilms, formed on steel sheets, was evaluated by the aid of flow cell reactors. Furthermore, the antimicrobial activity was determined against planktonic cells by measuring cell respiration and ATP production. The results showed significant inactivation of planktonic bacteria in contact with CTAB. Complete inactivation was achieved with CTAB in the concentration of 0.5 mM. It was emphasized

that the amount of ATP was greater when the concentration of CTAB was increased. This increase was due to the bacteria lysis. CTAB exhibited high antibiofilm potential for both, biofilms formed in turbulent (inactivation of 40%) and for laminar biofilms (60%), being that biofilm removal was greater for laminar biofilms. It may be noted that after biofilms treatment with CTAB, the authors evaluated the possibility of post-CTAB microbial growth. According to the data, both biofilms displayed an increase in cellular respiration, indicating an increase in bacterial growth. However, this increase was smaller at high CTAB concentrations (Simões et al., 2005).

In another study, CTAB antimicrobial potential was evaluated against *S. aureus*, *B. cereus* and *P. fluorescens*. The assays followed the method of determination of antibiofilm in microtiter plates for *B. cereus* and *P. fluorescens.* Antibiofilm potential in microtiter plates against *S. aureus* in combination with *B. cereus* and *P. fluorescens* was also evaluated. Anti-biofilm activity was observed against *B. cereus* and *P. fluorescens*, with death rates of 51.8 and 25.6%, respectively. However, the antibiofilm activity of CTAB against *S. aureus* was inhibited in the presence of *B. cereus* and *P. fluorescens*. In conclusion, CTAB has potential antibiofilm activity against *B. cereus* and *P. fluorescens* strains. However, its antimicrobial potential was inhibited in the co-presence of *S. aureus* (Araújo et al., 2014).

Bryce and collaborators (2020) investigated the antibiofilm activity of CTAB against bacterial species isolated from root canals, being them *Streptococcus sanguinis, Enterococcus faecalis, Fusobacterium nucleatum* and *Porphyromonas gingivalis*. Biofilms were formed on nitrocellulose membranes for 72 h and immersed in CTAB. Although it did not reach 100% of biofilm removal, CTAB revealed good antibiofilm and cell death activity. It was pointed out that Gram-negatives were more sensitive compared with the Gram-positives. Additionally, the authors justified the antibiofilm activity of CTAB by the electrostatic interaction, weakening the extracellular matrix.

As for fungal cells, CTAB toxicity in bacterial cells is considered promising when an antibacterial action of the developing system is intended. It has to be pointed out that CTAB has its use desirable not only due its contribution in the inactivation and destruction of the bacterial cells, but also seems to be potential against spores and biofilms.

6. Conclusions

CTAB, a quaternary ammonium compound, is widely used as a surfactant in the synthesis of mesoporous silica nanoparticles, hollow mesoporous silica nanoparticles and core-shell mesoporous silica nanoparticles, for example, acting directly in the formation of the mesopores, as it acts as a template. However, the determination of CTAB optimal concentration for each nanosystem must be achieved through the study of an ideal molar ratio with the silica source, in order to fabricate more homogeneous nanoparticles. As for the methods of removing surfactants from the pores, calcination

and reflux are the most used, despite having several limitations such as time and the use of a large amounts of toxic solvents (in the case of reflux), but it is worth noting that greener and faster are increasingly a trend in the literature. Although this step is often efficient, it is worth emphasizing that there are reports of MSNs silica with CTAB residues being applied in controlled drug release. Since the science and technology of colloids and interfaces, among other issues, is dedicated to the study and development of new materials and synthesis processes, the proof of their safety is of fundamental importance.

Although there is a gap of studies analyzing the toxicity of CTAB-containing mesoporous silica in human cells, a possible toxicity can be predicted since CTAB was responsible for the toxicity of other types of particles, including inorganic ones. In addition, in the case of CTAB residues-containing mesoporous silica after any extraction treatment, the CTAB amount would be smaller, which further emphasizes the need for studies evaluating the toxicity of this type of sample since the literature consulted was not observed quantitative analysis of this remaining residue. Lastly, the presence of CTAB residues-containing mesoporous silica whether non-toxic to human conditions, could be a potential tool against infectious disease treatment, once this surfactant has known antimicrobial activity. However, as mentioned for human cells, a quantitative study of these residues would be necessary.

7. Acknowledgements

This work was supported by São Paulo Research Foundation (FAPESP, Brazil) grant number nº 2019/26821-7, 2019/09831-9 and 2018/25377-3.

8. References

Abdollahi, L., Dianat, M. J., Marcos, M. D., Martínez-Máñez, R., & Karimi, S. (2022). Hollow mesoporous silica nanoparticles: Effective silica etching using tri-di- and mono-valent cations. *Biomaterials Advances*, *133*, Article 112621. https://doi.org/10.1016/j.msec.2021.112621

Abduraimova, A., Molkenova, A., Duisembekova, A., Mulikova, T., Kanayeva, D., & Atabaev, T. S. (2021). Cetyltrimethylammonium Bromide (CTAB)-Loaded SiO_2–Ag Mesoporous Nanocomposite as an Efficient Antibacterial Agent. *Nanomaterials*, *11*(2), Article 477. https://doi.org/10.3390/nano11020477

Ahlström, B., Chelminska-Bertilsson, M., Thompson, R. A., & Edebo, L. (1997). Submicellar complexes may initiate the fungicidal effects of cationic amphiphilic compounds on Candida albicans. *Antimicrobial Agents and Chemotherapy*, *41*(3), 544–550. https://doi.org/10.1128/aac.41.3.544

Akinjokun, A. I., Ojumu, T. V., & Ogunfowokan, A. O. (2016). Biomass, Abundant Resources for Synthesis of Mesoporous Silica Material. *Microporous and Mesoporous Materials*, 105–117.

Alexandrescu, L., Syverud, K., Gatti, A., & Chinga-Carrasco, G. (2013). Cytotoxicity tests of cellulose nanofibril-based structures. *Cellulose*, *20*(4), 1765–1775. https://doi.org/10.1007/s10570-013-9948-9

Alkilany, A. M., Nagaria, P. K., Hexel, C. R., Shaw, T. J., Murphy, C. J., & Wyatt, M. D. (2009). Cellular uptake and cytotoxicity of gold nanorods: Molecular origin of cytotoxicity and surface effects. *Small*, *5*(6), 701–708. https://doi.org/10.1002/smll.200801546

Alonso-Carrillo, N., Aguilar-Santamaría, M. de los Á., Vernon-Carter, E. J., Jiménez-Alvarado, R., Cruz-Sosa, F., & Román-Guerrero, A. (2017). Extraction of phenolic compounds from Satureja macrostema using microwave-ultrasound assisted and reflux methods and evaluation of their antioxidant activity and cytotoxicity. *Industrial Crops and Products*, *103*, 213–221. https://doi.org/10.1016/j.indcrop.2017.04.002

Araújo, P. A., Mergulhão, F., Melo, L., & Simões, M. (2014). The ability of an antimicrobial agent to penetrate a biofilm is not correlated with its killing or removal efficiency. *Biofouling*, *30*(6), 675–683. https://doi.org/10.1080/08927014.2014.904294

Arriagada, F., Nonell, S., & Morales, J. (2019). Silica-based nanosystems for therapeutic applications in the skin. *Nanomedicine*, *14*(16), 2243–2267. https://doi.org/10.2217/nnm-2019-0052

Asgari, M., Soleymani, M., Miri, T., & Barati, A. (2019). A robust method for fabrication of monodisperse magnetic mesoporous silica nanoparticles with core-shell structure as anticancer drug carriers. *Journal of Molecular Liquids*, *292*, Article 111367. https://doi.org/10.1016/j.molliq.2019.111367

Banerjee, D., Markley, A. L., Yano, T., Ghosh, A., Berget, P. B., Minkley, E. G., Khetan, S. K., & Collins, T. J. (2006). "Green" oxidation catalysis for rapid deactivation of bacterial spores. *Angewandte Chemie - International Edition*, *45*(24), 3974–3977. https://doi.org/10.1002/anie.200504511

Biesaga, M. (2011). Influence of extraction methods on stability of flavonoids. *Journal of Chromatography A*, *1218*(18), 2505–2512. https://doi.org/10.1016/j.chroma.2011.02.059

Bonifacio, B. V., da Silva, P. B., dos Santos Ramos, M. A., Negri, K. M. S., Bauab, T. M., & Chorilli, M. (2014). Nanotechnology-based drug delivery systems and herbal medicines: a review. *International Journal of Nanomedicine*, *9*(1), 1-15. https://doi.org/10.2147/IJN.S52634

Bryce, G., Pratten, J., Ready, D., Ng, Y. L., & Gulabivala, K. (2020). Disruption and bactericidal indices depicted in polygonal graphs to show multiple outcome effects of root canal irrigant supplements on single- and dual-species biofilms. *Clinical Oral Investigations*, *24*(9), 3255–3264. https://doi.org/10.1007/s00784-020-03202-x

Bucci, A. R., Marcelino, L., Mendes, R. K., & Etchegaray, A. (2018). The antimicrobial and antiadhesion activities of micellar solutions of surfactin, CTAB and CPCl with terpinen-4-ol: applications to control oral pathogens. *World Journal of Microbiology and Biotechnology*, *34*(6), 1–9. https://doi.org/10.1007/s11274-018-2472-1

Burmølle, M., Ren, D., Bjarnsholt, T., & Sørensen, S. J. (2014). Interactions in multispecies biofilms: Do they actually matter? *Trends in Microbiology*, *22*(2), 84–91. https://doi.org/10.1016/j.tim.2013.12.004

Cai, Q., Lin, W.-Y., Xiao, F.-S., Pang, W.-Q., Chen, X.-H., & Zou, B.-S. (1999). The preparation of highly ordered MCM-41 with extremely low surfactant concentration. *Microporous and Mesoporous Materials*, *32*(1–2), 1–15. https://doi.org/10.1016/S1387-1811(99)00082-7

Calixto, G., Bernegossi, J., de Freitas, L., Fontana, C., & Chorilli, M. (2016). Nanotechnology-based drug delivery systems for photodynamic therapy of cancer: a review. *Molecules*, *21*(3), Article 342. https://doi.org/10.3390/molecules21030342

Campos, A. F. P. de, Ferreira, A. R. O., & Cardoso, D. (2016). Synthesis and properties of hybrid silicas containing cetyltrialkylammoniun surfactants. *Química Nova, 39*(3), 279-285. https://doi.org/10.5935/0100-4042.20160033

Carvalho, G. C., Sábio, R. M., de Cássia Ribeiro, T., Monteiro, A. S., Pereira, D. V., Ribeiro, S. J. L., & Chorilli, M. (2020). Highlights in Mesoporous Silica Nanoparticles as a Multifunctional Controlled Drug Delivery Nanoplatform for Infectious Diseases Treatment. *Pharmaceutical Research*, *37*(10), Article 191. https://doi.org/10.1007/s11095-020-02917-6

Castro-Vargas, H. I., Rodríguez-Varela, L. I., Ferreira, S. R. S., & Parada-Alfonso, F. (2010). Extraction of phenolic fraction from guava seeds (Psidium guajava L.) using supercritical carbon dioxide and co-solvents. *The Journal of Supercritical Fluids*, *51*(3), 319–324. https://doi.org/10.1016/j.supflu.2009.10.012

Che, S., Garcia-Bennett, A. E., Yokoi, T., Sakamoto, K., Kunieda, H., Terasaki, O., & Tatsumi, T. (2003). A novel anionic surfactant templating route for synthesizing mesoporous silica with unique structure. *Nature Materials*, *2*(12), 801–805. https://doi.org/10.1038/nmat1022

Che, S., Kaneda, M., Terasaki, O., & Tatsumi, T. (2003). Counteranion effect on the formation of mesoporous materials under acidic synthesis process. *Studies in Surface Science and Catalysis, 146,* 431–434. https://doi.org/10.1016/S0167-2991(03)80414-7

Che, S., Li, H., Lim, S., Sakamoto, Y., Terasaki, O., & Tatsumi, T. (2005). Synthesis Mechanism of Cationic Surfactant Templating Mesoporous Silica under an Acidic Synthesis Process. *Chemistry of Materials*, *17*(16), 4103–4113. https://doi.org/10.1021/cm050359s

Chen, F., Hong, H., Shi, S., Goel, S., Valdovinos, H. F., Hernandez, R., Theuer, C. P., Barnhart, T. E., & Cai, W. (2015). Engineering of Hollow Mesoporous Silica Nanoparticles for Remarkably Enhanced Tumor Active Targeting Efficacy. *Scientific Reports*, *4*(1), Article 5080. https://doi.org/10.1038/srep05080

Chen, W., Lu, F., Chen, C.-C. V., Mo, K.-C., Hung, Y., Guo, Z.-X., Lin, C.-H., Lin, M.-H., Lin, Y.-H., Chang, C., & Mou, C.-Y. (2013). Manganese-enhanced MRI of rat brain based on slow cerebral delivery of manganese(II) with silica-encapsulated Mn x Fe 1- x O nanoparticles. *NMR in Biomedicine*, *26*(9), 1176–1185. https://doi.org/10.1002/nbm.2932

Chen, Y., Wang, Q., & Wang, T. (2013). Fabrication of thermally stable and active bimetallic Au–Ag nanoparticles stabilized on inner wall of mesoporous silica shell. *Dalton Transactions*, *42*(38), Article 13940. https://doi.org/10.1039/c3dt51546j

Cheng, L., Weir, M. D., Zhang, K., Xu, S. M., Chen, Q., Zhou, X., & Xu, H. H. K. (2012). Antibacterial nanocomposite with calcium phosphate and quaternary ammonium. *Journal of Dental Research*, *91*(5), 460–466. https://doi.org/10.1177/0022034512440579

de Souza, M. P. C., de Camargo, B. A. F., Spósito, L., Fortunato, G. C., Carvalho, G. C., Marena, G. D., Meneguin, A. B., Bauab, T. M., & Chorilli, M. (2021). Highlighting the use of micro and nanoparticles based-drug delivery systems for the treatment of *Helicobacter pylori* infections. *Critical Reviews in Microbiology*, *47*(4), 1–26. https://doi.org/10.1080/1040841X.2021.1895721

Deng, S., Cui, C. X., Liu, L., Duan, L., Wang, J., Zhang, Y., & Qu, L. (2021). A facile and controllable one-pot synthesis approach to amino-functionalized hollow silica nanoparticles with accessible ordered mesoporous shells. *Chinese Chemical Letters*, *32*(3), 1177–1180. https://doi.org/10.1016/j.cclet.2020.09.002

Dong, C., You, W., Liuyang, R., Lei, Y., Zhang, A., & Lin, Y. (2018). Anti-Rhizoctonia solani activity by polymeric quaternary ammonium salt and its mechanism of action. *Reactive and Functional Polymers*, *125*, 1–10. https://doi.org/10.1016/j.reactfunctpolym.2018.01.020

Dong, W., Green, J., Korza, G., & Setlow, P. (2019). Killing of spores of Bacillus species by cetyltrimethylammonium bromide. *Journal of Applied Microbiology*, *126*(5), 1391–1401. https://doi.org/10.1111/jam.14242

Ezzati, N., Mahjoub, A. R., Abolhosseini Shahrnoy, A., & Syrgiannis, Z. (2019). Amino Acid-functionalized hollow mesoporous silica nanospheres as efficient biocompatible drug carriers for anticancer applications. *International Journal of Pharmaceutics*, *572*, Article 118709. https://doi.org/10.1016/j.ijpharm.2019.118709

Fernández, M. N., Muñoz-Olivas, R., & Luque-Garcia, J. L. (2019). SILAC-based quantitative proteomics identifies size-dependent molecular mechanisms involved in silver nanoparticles-induced toxicity. *Nanotoxicology*, *13*(6), 812–826. https://doi.org/10.1080/17435390.2019.1579374

Fernando, D., Sulthana, S., & Vasquez, Y. (2020). Cellular Uptake and Cytotoxicity of Varying Aspect Ratios of Gold Nanorods in HeLa Cells. *ACS Applied Bio Materials*, *3*(3), 1374–1384. https://doi.org/10.1021/acsabm.9b00986

Ferri, J. K., & Stebe, K. J. (2000). Which surfactants reduce surface tension faster? A scaling argument for diffusion-controlled adsorption. *Advances in Colloid and Interface Science*, *85*(1), 61–97. https://doi.org/10.1016/S0001-8686(99)00027-5

Flora, S. J. S., Mittal, M., Mehta, A., & others. (2008). Heavy metal induced oxidative stress & its possible reversal by chelation therapy. *Indian Journal of Medical Research*, *128*(4), Article 501.

Fux, C. A., Costerton, J. W., Stewart, P. S., & Stoodley, P. (2005). Survival strategies of infectious biofilms. *Trends in Microbiology*, *13*(1), 34–40. https://doi.org/10.1016/j.tim.2004.11.010

Ghaedi, H., & Zhao, M. (2022). Review on Template Removal Techniques for Synthesis of Mesoporous Silica Materials. *Energy & Fuels*, *36*(5), 2424–2446. https://doi.org/10.1021/acs.energyfuels.1c04435

Ghasemi, S., Farsangi, Z. J., Beitollahi, A., Mirkazemi, M., Rezayat, S. M., & Sarkar, S. (2017). Synthesis of hollow mesoporous silica (HMS) nanoparticles as a candidate for sulfasalazine drug loading. *Ceramics International*, *43*(14), 11225–11232. https://doi.org/10.1016/j.ceramint.2017.05.172

Girija, A. R., & Balasubramanian, S. (2019). Theragnostic potentials of core/shell mesoporous silica nanostructures. *Nanotheranostics*, *3*(1), 1–40. https://doi.org/10.7150/ntno.27877

Graeve, O. A., Fathi, H., Kelly, J. P., Saterlie, M. S., Sinha, K., Rojas-George, G., Kanakala, R., Brown, D. R., & Lopez, E. A. (2013). Reverse micelle synthesis of oxide nanopowders: Mechanisms of precipitate formation and agglomeration effects. *Journal of Colloid and Interface Science*, *407*, 302–309. https://doi.org/10.1016/j.jcis.2013.07.003

Gu, L., Zhang, A., Hou, K., Dai, C., Zhang, S., Liu, M., Song, C., & Guo, X. (2012). One-pot hydrothermal synthesis of mesoporous silica nanoparticles using formaldehyde as growth suppressant. *Microporous and Mesoporous Materials*, *152*, 9–15. https://doi.org/10.1016/j.micromeso.2011.11.047

Hartmann, V., & Cressely, R. (1997). Shear thickening of an aqueous micellar solution of cetyltrimethylammonium bromide and sodium tosylate. *Journal de Physique II*, *7*(8), 1087–1098. https://doi.org/10.1051/jp2:1997173

He, Q., Shi, J., Chen, F., Zhu, M., & Zhang, L. (2010). An anticancer drug delivery system based on surfactant-templated mesoporous silica nanoparticles. *Biomaterials*, *31*(12), 3335–3346. https://doi.org/10.1016/j.biomaterials.2010.01.015

Hoffmann, F., Cornelius, M., Morell, J., & Fröba, M. (2006). Silica-based mesoporous organic-inorganic hybrid materials. *Angewandte Chemie - International Edition*, *45*(20), 3216–3251. https://doi.org/10.1002/anie.200503075

Hussain, A. (2021). Hydrophobic Drug Release Studies from the Core/Shell Magnetic Mesoporous Silica Nanoparticles and their Anticancer Application. *Proceedings of the Pakistan Academy of Sciences: B. Life and Environmental Sciences*, *58*(1), 77–88. https://doi.org/10.53560/PPASB(58-1)646

Ishikawa, J., Maeda, T., Matsumura, I., Yasumi, M., Ujiie, H., Masaie, H., Nakazawa, T., Mochizuki, N., Kishino, S., & Kanakura, Y. (2009). Antifungal activity of micafungin in serum. *Antimicrobial Agents and Chemotherapy*, *53*(10), 4559–4562. https://doi.org/10.1128/AAC.01404-08

Ishikawa, S., Matsumura, Y., Katoh-Kubo, K., & Tsuchido, T. (2002). Antibacterial activity of surfactants against Escherichia coli cells is influenced by carbon source and anaerobiosis. *Journal of Applied Microbiology*, *93*(2), 302–309. https://doi.org/10.1046/j.1365-2672.2002.01690.x

Jabariyan, S., & Zanjanchi, M. A. (2012). A simple and fast sonication procedure to remove surfactant templates from mesoporous MCM-41. *Ultrasonics Sonochemistry*, *19*(5), 1087–1093. https://doi.org/10.1016/j.ultsonch.2012.01.012

Jang, E. (2021). Effect of Alcohol Chain Length on Formation of Cetyltrimethylammonium Bromide-templated Mesoporous Silica Layer on Gold Nanorods. *Bulletin of the Korean Chemical Society*, *42*(6), 828–831. https://doi.org/10.1002/bkcs.12283

Javdani, H., Khosravi, R., Etemad, L., Moshiri, M., Zarban, A., & Hanafi-Bojd, M. Y. (2020). Tannic acid-templated mesoporous silica nanoparticles as an effective treatment in acute ferrous sulfate poisoning. *Microporous and Mesoporous Materials*, *307*, Article 110486. https://doi.org/10.1016/j.micromeso.2020.110486

Jergens, E., & Winter, J. O. (2022). Nanoparticles caged with DNA nanostructures. *Current Opinion in Biotechnology*, *74*, 278–284. https://doi.org/10.1016/j.copbio.2021.12.010

Jia, Y. P., Shi, K., Liao, J. F., Peng, J. R., Hao, Y., Qu, Y., Chen, L. J., Liu, L., Yuan, X., Qian, Z. Y., & Wei, X. W. (2020). Effects of Cetyltrimethylammonium Bromide on the Toxicity of Gold Nanorods Both In Vitro and In Vivo: Molecular Origin of Cytotoxicity and Inflammation. *Small Methods*, *4*(3), 1–11. https://doi.org/10.1002/smtd.201900799

Jin, L., Liu, X., Bian, C., Sheng, J., Song, Y., & Zhu, Y. (2020). Fabrication linalool-functionalized hollow mesoporous silica spheres nanoparticles for efficiently enhance bactericidal activity. *Chinese Chemical Letters*, *31*(8), 2137–2141. https://doi.org/10.1016/j.cclet.2019.12.020

Joyce, P., Ulmefors, H., Maghrebi, S., Subramaniam, S., Wignall, A., Jõemetsa, S., Höök, F., & Prestidge, C. A. (2020). Enhancing the Cellular Uptake

and Antibacterial Activity of Rifampicin through Encapsulation in Mesoporous Silica Nanoparticles. *Nanomaterials*, *10*(4), Article 815. https://doi.org/10.3390/nano10040815

Kalbáčová, M., Verdánová, M., Mravec, F., Halasová, T., & Pekarˇ, M. (2014). Effect of CTAB and CTAB in the presence of hyaluronan on selected human cell types. *Colloids and Surfaces A: Physicochemical and Engineering Aspects*, *460*, 204–208. https://doi.org/10.1016/j.colsurfa.2013.12.048

Kalele, S., Gosavi, S. W., Urban, J., & Kulkarni, S. K. (2006). Nanoshell particles: synthesis, properties and applications. *Current Science*, *91*(8), 1038–1052.

Kalyane, D., Kumar, N., Anup, N., Rajpoot, K., Maheshwari, R., Sengupta, P., Kalia, K., & Tekade, R. K. (2021). Recent advancements and future submissions of silica core-shell nanoparticles. *International Journal of Pharmaceutics*, *609*, Article 121173. https://doi.org/10.1016/j.ijpharm.2021.121173

Karaman, D. S., Gulin-Sarfraz, T., Zhang, J., & Rosenholm, J. M. (2015). One-pot synthesis of pore-expanded hollow mesoporous silica particles. *Materials Letters*, *143*, 140–143. https://doi.org/10.1016/j.matlet.2014.12.067

Karnopp, J. C. F., Cardoso, T. F. M., Gonçalves, D. A., Carollo, A. R. H., Castro, G. R. de, Duarte, A. P., & Martines, M. A. U. (2020). Preparation of the Rutin-SBA-16 Drug Delivery System. *Journal of Biomaterials and Nanobiotechnology*, *11*(01), 1–13. https://doi.org/10.4236/jbnb.2020.111001

Kaziem, A. E., Yang, L., Lin, Y., Song, Z., Xu, H., & Zhang, Z. (2022). Efficiency of mesoporous silica/carboxymethyl β-glucan as a fungicide nano-delivery system for improving chlorothalonil bioactivity and reduce biotoxicity. *Chemosphere*, *287*, Article 131902. https://doi.org/10.1016/j.chemosphere.2021.131902

Khoddami, A., Wilkes, M., & Roberts, T. (2013). Techniques for Analysis of Plant Phenolic Compounds. *Molecules*, *18*(2), 2328–2375. https://doi.org/10.3390/molecules18022328

Khoeini, M., Najafi, A., Rastegar, H., & Amani, M. (2019). Improvement of hollow mesoporous silica nanoparticles synthesis by hard-templating method via CTAB surfactant. *Ceramics International*, *45*(10), 12700–12707. https://doi.org/10.1016/j.ceramint.2019.03.125

Kibar, G., Çalışkan, U., Erdem, E. Y., & Çetin, B. (2019). One-pot synthesis of organic–inorganic hybrid polyhedral oligomeric silsesquioxane microparticles in a double-zone temperature controlled microfluidic reactor. *Journal of Polymer Science Part A: Polymer Chemistry*, *57*(13), 1396–1403. https://doi.org/10.1002/pola.29399

Kim, M.-K., Ki, D.-H., Na, Y.-G., Lee, H.-S., Baek, J.-S., Lee, J.-Y., Lee, H.-K., & Cho, C.-W. (2021). Optimization of Mesoporous Silica Nanoparticles through Statistical Design of Experiment and the Application for the Anticancer Drug. *Pharmaceutics*, *13*(2), Article 184. https://doi.org/10.3390/pharmaceutics13020184

Kumar, M., Fu, Y., Wang, M., Swamy, B. E. K., Jayaprakash, G. K., & Zhao, W. (2021). Influence of cationic surfactant cetyltrimethylammonium bromide for electrochemical detection of guanine, uric acid and dopamine. *Journal of Molecular Liquids*, *321*, Article 114893. https://doi.org/10.1016/j.molliq.2020.114893

Lee, D. J., Lee, N., & Lee, J. E. (2022). One-pot Synthesis of Multifunctional Mn_3O_4/mesoporous Silica Core/shell Nanoparticles for Biomedical Applications. *Applied Chemistry for Engineering*, *33*(1), 113–118. https://doi.org/10.14478/ace.2021.1108

Li, A., Long, L., Liu, F., Liu, J., Wu, X., & Ji, Y. (2019). Antigen-labeled mesoporous silica-coated Au-core Pt-shell nanostructure: a novel nanoprobe for highly efficient virus diagnosis. *Journal of Biological Engineering*, *13*(1), Article 87. https://doi.org/10.1186/s13036-019-0220-1

Li, T., Geng, T., Md, A., Banerjee, P., & Wang, B. (2019). Novel scheme for rapid synthesis of hollow mesoporous silica nanoparticles (HMSNs) and their application as an efficient delivery carrier for oral bioavailability improvement of poorly water-soluble BCS type II drugs. *Colloids and Surfaces B: Biointerfaces*, *176*, 185–193. https://doi.org/10.1016/j.colsurfb.2019.01.004

Li, Z., Zhang, Y., & Feng, N. (2019). Mesoporous silica nanoparticles: synthesis, classification, drug loading, pharmacokinetics, biocompatibility, and application in drug delivery. *Expert Opinion on Drug Delivery*, *16*(3), 219–237. https://doi.org/10.1080/17425247.2019.1575806

Lin, H.-P., & Mou, C.-Y. (2002). Structural and Morphological Control of Cationic Surfactant-Templated Mesoporous Silica. *Accounts of Chemical Research*, *35*(11), 927–935. https://doi.org/10.1021/ar000074f

Ma, S., Wang, Y., & Zhu, Y. (2011). A simple room temperature synthesis of mesoporous silica nanoparticles for drug storage and pressure pulsed delivery. *Journal of Porous Materials*, *18*(2), 233–239. https://doi.org/10.1007/s10934-010-9375-3

Mahdavi, Z., Rezvani, H., & Keshavarz Moraveji, M. (2020). Core–shell nanoparticles used in drug delivery-microfluidics: a review. *RSC Advances*, *10*(31), 18280–18295. https://doi.org/10.1039/D0RA01032D

Maneedaeng, A., Phoemboon, S., Chanthasena, P., & Chudapongse, N. (2018). Synthesis, interfacial properties, and antimicrobial activity of a new cationic gemini surfactant. *Korean Journal of Chemical Engineering*, *35*(11), 2313–2320. https://doi.org/10.1007/s11814-018-0133-6

Manzano, M., & Vallet-Regí, M. (2020). Mesoporous silica nanoparticles for drug delivery. *Advanced Functional Materials*, *30*(2), Article 1902634. https://doi.org/10.1002/adfm.201902634

Marzano, M., Pontón, P. I., & Marinkovic, B. A. (2019). Co-precipitation of low-agglomerated Y2W3O12 nanoparticles: The effects of aging time, calcination temperature and surfactant addition. *Ceramics International*, *45*(16), 20189–20196. https://doi.org/10.1016/j.ceramint.2019.06.288

Mcdonnell, G., & Russell, A. D. (1999). Antiseptics and disinfectants: Activity, action, and resistance. *Clinical Microbiology Reviews*, *12*(1), 147–179. https://doi.org/10.1128/cmr.12.1.147

Meynen, V., Cool, P., & Vansant, E. F. (2009). Verified syntheses of mesoporous materials. *Microporous and Mesoporous Materials*, *125*(3), 170–223.

https://doi.org/10.1016/j.micromeso.2009.03.046

Moir, A., Corfe, B. M., & Behravan, J. (2002). Spore germination. *Cellular and Molecular Life Sciences*, *59*(3), 403–409. https://doi.org/10.1007/s00018-002-8432-8

Nakata, K., Tsuchido, T., & Matsumura, Y. (2011). Antimicrobial cationic surfactant, cetyltrimethylammonium bromide, induces superoxide stress in Escherichia coli cells. *Journal of Applied Microbiology*, *110*(2), 568–579. https://doi.org/10.1111/j.1365-2672.2010.04912.x

Napper, D. (1977). Steric stabilization. *Journal of Colloid and Interface Science*, *58*(2), 390–407. https://doi.org/10.1016/0021-9797(77)90150-3

Narayan, R., Nayak, U. Y., Raichur, A. M., & Garg, S. (2018). Mesoporous silica nanoparticles: A comprehensive review on synthesis and recent advances. *Pharmaceutics*, *10*(3), Article 118. https://doi.org/10.3390/pharmaceutics10030118

Nazemiyeh, E., Eskandani, M., Sheikhloie, H., & Nazemiyeh, H. (2016). Formulation and Physicochemical Characterization of Lycopene-Loaded Solid Lipid Nanoparticles. *Advanced Pharmaceutical Bulletin*, *6*(2), 235–241. https://doi.org/10.15171/apb.2016.032

Nguyen, T. N. T., Le, N. T. T., Nguyen, N. H., Ly, B. T. K., Nguyen, T. D., & Nguyen, D. H. (2020). Aminated hollow mesoporous silica nanoparticles as an enhanced loading and sustained releasing carrier for doxorubicin delivery. *Microporous and Mesoporous Materials*, *309*(April), 110543. https://doi.org/10.1016/j.micromeso.2020.110543

Nguyen, T. N. T., Nguyen-Tran, D. H., Bach, L. G., Du Truong, T. H., Trang Le, N. T., & Nguyen, D. H. (2019). Surface PEGylation of hollow mesoporous silica nanoparticles via aminated intermediate. *Progress in Natural Science: Materials International*, *29*(6), 612–616. https://doi.org/10.1016/j.pnsc.2019.10.002

Nicholson, W. L., Munakata, N., Horneck, G., Melosh, H. J., & Setlow, P. (2000). Resistance of Bacillus Endospores to Extreme Terrestrial and Extraterrestrial Environments . *Microbiology and Molecular Biology Reviews*, *64*(3), 548–572. https://doi.org/10.1128/mmbr.64.3.548-572.2000

Nicoletti, G., Boghossian, V., Gurevitch, F., Borland, R., & Morgenroth, P. (1993). The antimicrobial activity in vitro of chlorhexidine, a mixture of isothiazolinones ("Kathon" CG) and cetyl trimethyl ammonium bromide (CTAB). *Journal of Hospital Infection*, *23*(2), 87–111. https://doi.org/10.1016/0195-6701(93)90014-Q

Pati, S. G., & Arnold, W. A. (2020). Comprehensive screening of quaternary ammonium surfactants and ionic liquids in wastewater effluents and lake sediments. *Environmental Science: Processes & Impacts*, *22*(2), 430–441. https://doi.org/10.1039/C9EM00554D

Pietsch, F., Heidrich, G., Nordholt, N., & Schreiber, F. (2021). Prevalent Synergy and Antagonism Among Antibiotics and Biocides in Pseudomonas aeruginosa. *Frontiers in Microbiology*, *11*, 1–6. https://doi.org/10.3389/fmicb.2020.615618

Poon, C., & Patel, A. A. (2020). Organic and inorganic nanoparticle vaccines for prevention of infectious diseases. *Nano Express*, *1*(1), Article 12001. https://doi.org/10.1088/2632-959X/ab8075

Prabhakar, P., & Banerjee, M. (2020). Nanotechnology in Drug Delivery System: Challenges and Opportunities. *Journal of Pharmaceutical Sciences and Research*, *12*(4), 492–498.

Pradhan, D., Biswasroy, P., Goyal, A., Ghosh, G., & Rath, G. (2021). Recent Advancement in Nanotechnology-Based Drug Delivery System Against Viral Infections. *AAPS PharmSciTech*, *22*(1), Article 47. https://doi.org/10.1208/s12249-020-01908-5

Purnawira, B., Purwaningsih, H., Ervianto, Y., Pratiwi, V. M., Susanti, D., Rochiem, R., & Purniawan, A. (2019). Synthesis and characterization of mesoporous silica nanoparticles (MSNp) MCM 41 from natural waste rice husk. *IOP Conference Series: Materials Science and Engineering*, *541*(1), Article 012018. https://doi.org/10.1088/1757-899X/541/1/012018

Queiroz, S. C. N., Collins, C. H., & Jardim, I. C. S. F. (2001). Métodos de extração e/ou concentração de compostos encontrados em fluidos biológicos para posterior determinação cromatográfica. *Química Nova*, *24*(1). https://doi.org/10.1590/S0100-40422001000100013

Ramos, M. A. S., Da Silva, P., Spósito, L., De Toledo, L., Bonifácio, B., Rodero, C. F., Dos Santos, K., Chorilli, M., & Bauab, T. M. (2018). Nanotechnology-based drug delivery systems for control of microbial biofilms: a review. *International Journal of Nanomedicine*, *13*, 1179–1213. https://doi.org/10.2147/IJN.S146195

Sábio, R. M., Meneguin, A. B., Ribeiro, T. C., Silva, R. R., & Chorilli, M. (2019). New insights towards mesoporous silica nanoparticles as a technological platform for chemotherapeutic drugs delivery. *International Journal of Pharmaceutics, 564,* 379-409. https://doi.org/10.1016/j.ijpharm.2019.04.067

Sahoo, S. K., Dilnawaz, F., & Krishnakumar, S. (2008). Nanotechnology in ocular drug delivery. *Drug Discovery Today*, *13*(3–4), 144–151. https://doi.org/10.1016/j.drudis.2007.10.021

Saputra, O. A., Wibowo, F. R., & Lestari, W. W. (2022). High storage capacity of curcumin loaded onto hollow mesoporous silica nanoparticles prepared via improved hard-templating method optimized by Taguchi DoE. *Engineering Science and Technology, an International Journal*, *33*, Article 101070. https://doi.org/10.1016/j.jestch.2021.10.002

Shamim, S., Hornyak, G. L., Crespy, D., Kyaw, H., & Bora, T. (2022). Morphology and visible photoluminescence modulation in dye-free mesoporous silica nanoparticles using a simple calcination step. *Materials Research Bulletin*, *152*, Article 111842. https://doi.org/10.1016/j.materresbull.2022.111842

Shao, D., Lu, M-m, Zhao, Y-w., Zhang, F., Tan, Y.-f, Zheng, X., Pan, Y., Xiao, X.-a., Wang, Z., Dong, W.-f, & others. (2017). The shape effect of magnetic mesoporous silica nanoparticles on endocytosis, biocompatibility and biodistribution. *Acta Biomaterialia*, *49*, 531–540. https://doi.org/10.1016/j.actbio.2016.11.007

Shi, S., Chen, F., & Cai, W. (2013). Biomedical applications of functionalized hollow mesoporous silica nanoparticles: focusing on molecular imaging. *Nanomedicine*, *8*(12), 2027–2039. https://doi.org/10.2217/nnm.13.177

Silva, A. M., Martins-Gomes, C., Coutinho, T. E., Fangueiro, J. F., Sanchez-Lopez, E., Pashirova, T. N., Andreani, T., & Souto, E. B. (2019). Soft cationic nanoparticles for drug delivery: Production and cytotoxicity of solid lipid nanoparticles (SLNs). *Applied Sciences (Switzerland)*, *9*(20), Article 4438. https://doi.org/10.3390/app9204438

Simões, M., Pereira, M. O., & Vieira, M. J. (2005). Action of a cationic surfactant on the activity and removal of bacterial biofilms formed under different flow regimes. *Water Research*, *39*(2–3), 478–486. https://doi.org/10.1016/j.watres.2004.09.018

Singh, L. P., Bhattacharyya, S. K., Mishra, G., & Ahalawat, S. (2011). Functional role of cationic surfactant to control the nano size of silica powder. *Applied Nanoscience*, *1*(3), 117–122. https://doi.org/10.1007/s13204-011-0016-1

Soler-Illia, G. J. D. A. A., Sanchez, C., Lebeau, B., & Patarin, J. (2002). Chemical strategies to design textured materials: From microporous and mesoporous oxides to nanonetworks and hierarchical structures. *Chemical Reviews*, *102*(11), 4093–4138. https://doi.org/10.1021/cr0200062

Song, J.-T., Zhang, X.-S., Qin, M.-Y., & Zhao, Y.-D. (2015). One-pot two-step synthesis of core–shell mesoporous silica-coated gold nanoparticles. *Dalton Transactions*, *44*(17), 7752–7756. https://doi.org/10.1039/C5DT00912J

Su, H., Tian, Q., Hurd Price, C.-A., Xu, L., Qian, K., & Liu, J. (2020). Nanoporous core@shell particles: Design, preparation, applications in bioadsorption and biocatalysis. *Nano Today*, *31*, Article 100834. https://doi.org/10.1016/j.nantod.2019.100834

Sun, Y., Huffman, K., Freeman, W. R., Sailor, M. J., & Cheng, L. (2020). Intravitreal safety profiles of sol-gel mesoporous silica microparticles and the degradation product (Si(OH) 4). *Drug Delivery*, *27*(1), 703–711. https://doi.org/10.1080/10717544.2020.1760401

Sunwoo, Y., Karunakaran, G., & Cho, E. B. (2021). Hollow mesoporous silica nanospheres using pentablock copolymer micelle templates. *Ceramics International*, *47*(10), 13351–13362. https://doi.org/10.1016/j.ceramint.2021.01.192

Travaglini, L., Picchetti, P., Del Giudice, A., Galantini, L., & De Cola, L. (2019). Tuning and controlling the shape of mesoporous silica particles with CTAB/sodium deoxycholate catanionic mixtures. *Microporous and Mesoporous Materials*, *279*(August 2018), 423–431. https://doi.org/10.1016/j.micromeso.2019.01.030

Ung, T., Liz-Marzán, L. M., & Mulvaney, P. (1998). Controlled Method for Silica Coating of Silver Colloids. Influence of Coating on the Rate of Chemical Reactions. *Langmuir*, *14*(14), 3740–3748. https://doi.org/10.1021/la980047m

Vallet-Regí, M. (2022). Our contributions to applications of mesoporous silica nanoparticles. *Acta Biomaterialia*, *137*, 44–52. https://doi.org/10.1016/j.actbio.2021.10.011

Vallet-Regí, M., González, B., & Izquierdo-Barba, I. (2019). Nanomaterials as Promising Alternative in the Infection Treatment. *International Journal of Molecular Sciences*, *20*(15), Article 3806. https://doi.org/10.3390/ijms20153806

Vazquez, N. I., Gonzalez, Z., Ferrari, B., & Castro, Y. (2017). Synthesis of mesoporous silica nanoparticles by sol-gel as nanocontainer for future drug delivery applications. *Boletin de La Sociedad Espanola de Ceramica y Vidrio*, *56*(3), 139–145. https://doi.org/10.1016/j.bsecv.2017.03.002

Wang, C., Chen, S., Bao, L., Liu, X., Hu, F., & Yuan, H. (2020). Size-Controlled Preparation and Behavior Study of Phospholipid–Calcium Carbonate Hybrid Nanoparticles. *International Journal of Nanomedicine*, *15*, 4049–4062. https://doi.org/10.2147/IJN.S237156

Wang, G., Otuonye, A. N., Blair, E. A., Denton, K., Tao, Z., & Asefa, T. (2009). Functionalized mesoporous materials for adsorption and release of different drug molecules: A comparative study. *Journal of Solid State Chemistry*, *182*(7), 1649–1660. https://doi.org/10.1016/j.jssc.2009.03.034

Wu, L., Gou, K., Guo, X., Guo, Y., Chen, M., Hou, J., Li, S., & Li, H. (2021). Dual response to pH and chiral microenvironments for the release of a flurbiprofen-loaded chiral self-assembled mesoporous silica drug delivery system. *Colloids and Surfaces B: Biointerfaces*, *199*, Article 111501. https://doi.org/10.1016/j.colsurfb.2020.111501

Wu, L., Jiao, Z., Wu, M., Song, T., & Zhang, H. (2016). Formation of mesoporous silica nanoparticles with tunable pore structure as promising nanoreactor and drug delivery vehicle. *RSC Advances*, *6*(16), 13303–13311. https://doi.org/10.1039/c5ra27422b

Wu, L., Zhang, H., Wu, M., Zhong, Y., Liu, X., & Jiao, Z. (2016). Dual-templating synthesis of multi-shelled mesoporous silica nanoparticles as catalyst and drug carrier. *Microporous and Mesoporous Materials*, *228*, 318–328. https://doi.org/10.1016/j.micromeso.2016.03.040

Wu, S.-H., Mou, C.-Y., & Lin, H.-P. (2013). Synthesis of mesoporous silica nanoparticles. *Chemical Society Reviews*, *42*(9), 3862-3875. https://doi.org/10.1039/c3cs35405a

Xiang, S., Ma, X., Liao, S., Shi, H., Liu, C., Shen, Y., Lv, X., Yuan, M., Fan, G., Huang, J., & Sun, X. (2019). Cellulose nanocrystal surface cationization: A New Fungicide with High Activity against Phycomycetes capsici. *Molecules*, *24*(13), Article 2467. https://doi.org/10.3390/molecules24132467

Xie, Q., Lu, H., Wang, X., Zhang, Y., & Zhou, N. (2021). Functionalized hollow mesoporous silica for detection of Staphylococcus aureus and sterilization. *Journal of Environmental Chemical Engineering*, *9*(5), Article 105892. https://doi.org/10.1016/j.jece.2021.105892

Xuan, J., Pelletier, M., Xia, H., & Zhao, Y. (2011). Ultrasound-Induced Disruption of Amphiphilic Block Copolymer Micelles. *Macromolecular Chemistry and Physics*, *212*(5), 498–506. https://doi.org/10.1002/macp.201000624

Yamada, H., Urata, C., Higashitamori, S., Aoyama, Y., Yamauchi, Y., & Kuroda, K. (2014). Critical Roles of Cationic Surfactants in the Preparation of Colloidal Mesostructured Silica Nanoparticles: Control of Mesostructure, Particle Size, and Dispersion. *ACS Applied Materials & Interfaces*, *6*(5), 3491–3500. https://doi.org/10.1021/am405633r

Yang, H., Cui, X., Li, S., Cen, Y., Deng, T., Wang, J., Olsbye, U., & Fan, W. (2020). Developing a general method for encapsulation of metal oxide nanoparticles in mesoporous silica shell by unraveling its formation mechanism. *Microporous and Mesoporous Materials*, *305*, Article 110381. https://doi.org/10.1016/j.micromeso.2020.110381

Yasun, E., Gandhi, S., Choudhury, S., Mohammadinejad, R., Benyettou, F., Gozubenli, N., & Arami, H. (2020). Hollow micro and nanostructures for

therapeutic and imaging applications. *Journal of Drug Delivery Science and Technology*, *60*, Article 102094. https://doi.org/10.1016/j.jddst.2020.102094

Yasun, E., Li, C., Barut, I., Janvier, D., Qiu, L., Cu, C., & Tan, W. (2015). BSA Modification to Reduce CTAB Induced Nonspecificity and Cytotoxicity of Aptamer-Conjugated Gold Nanorods. *Nanoscale*, *22*(4), 10240–10248. https://doi.org/10.1039/c5nr01704a.BSA

Zanjanchi, M., & Jabariyan, S. (2014). Application of ultrasound and methanol for rapid removal of surfactant from MCM-41. *Journal of the Serbian Chemical Society*, *79*(1), 25–38. https://doi.org/10.2298/JSC130112056A

Zeng, M., Shu, Y., Parra-Robert, M., Desai, D., Zhou, H., Li, Q., Rong, Z., Karaman, D. Ş., Yang, H., Peng, J., & others. (2021). Scalable synthesis of multicomponent multifunctional inorganic core@mesoporous silica shell nanocomposites. *Materials Science and Engineering: C*, *128*, Article 112272. https://doi.org/10.1016/j.msec.2021.112272

Zhang, J., Liu, M., Zhang, A., Lin, K., Song, C., & Guo, X. (2010). Facile synthesis of mesoporous silica nanoparticles with controlled morphologies using water-acetone media. *Solid State Sciences*, *12*(2), 267–273. https://doi.org/10.1016/j.solidstatesciences.2009.11.005

Zhang, Q., Wu, M., Fang, Y., Deng, C., Shen, H.-H., Tang, Y., & Wang, Y. (2022). Dendritic Mesoporous Silica Hollow Spheres for Nano-Bioreactor Application. *Nanomaterials*, *12*(11), Article 1940. https://doi.org/10.3390/nano12111940

Zhang, S., Ding, S., Yu, J., Chen, X., Lei, Q., & Fang, W. (2015). Antibacterial activity, in vitro cytotoxicity, and cell cycle arrest of gemini quaternary ammonium surfactants. *Langmuir*, *31*(44), 12161–12169. https://doi.org/10.1021/acs.langmuir.5b01430

Zhang, Y., Xu, D., Li, W., Yu, J., & Chen, Y. (2012). Effect of size, shape, and surface modification on cytotoxicity of gold nanoparticles to human HEp-2 and Canine MDCK Cells. *Journal of Nanomaterials*, *2012,* Article 375496. https://doi.org/10.1155/2012/375496

Zhao, D., Wan, Y., & Zhou, W. (2012). *Ordered mesoporous materials*. John Wiley & Sons.

CHAPTER 10

Curcuma Longa: Nutraceutical Use and Association with Nanotechnology

Gabriela Corrêa Carvalho, Gabriel Davi Marena, Micaela Gaspar Gonçalves Fernandes, Gabriela Ricci Leonardi, Hélder A. Santos*, Marlus Chorilli*

Accepted for publication in Advanced Healthcare Materials

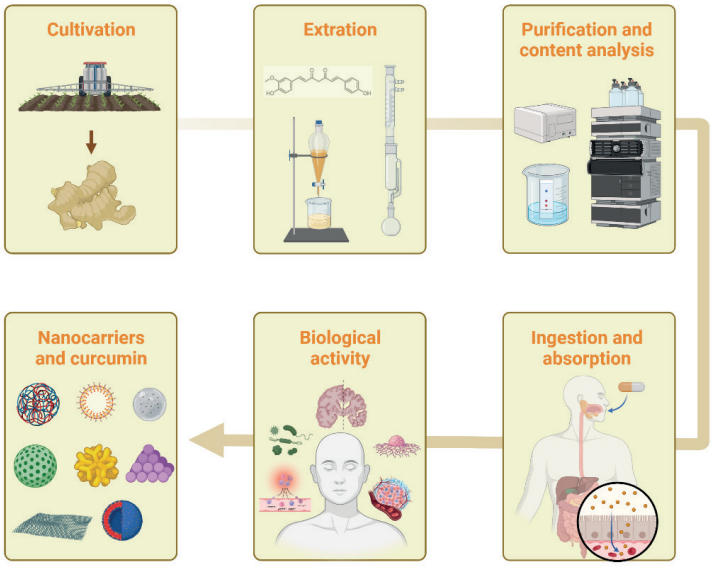

Abstract

Curcumin is a natural product found in the rhizome of Curcuma longa (L) and other Curcuma spp. As a lipophilic molecule, it has greater affinity for polar, non-polar, alkaline or extremely acidic organic solvents. Several studies indicate that curcumin has several benefits for human health, for example, against degenerative diseases, cancer and infectious diseases. To obtain a quality product with nutraceutical properties, it is necessary to know its physicochemical characteristics and preserve it from cultivation until ingestion by the human. However, its low solubility leads to low absorption, in this context, nanotechnological systems can contribute to increase curcumin bioavailability. This review aims to highlight important issues in all stages that curcumin goes through: from aspects related to its extraction, to its association with nanotechnology. Although curcumin extraction process is already well established, it is possible to observe that more and more research focused on increasing yield and being more environmentally friendly. Furthermore, curcumin's low absorption is notable due to its physicochemical characteristics, mainly due to its low aqueous solubility. However, its association with nanotechnology has shown to be promising and an increasingly growing trend, since the use of this "Indian solid gold" is the hope of many patients.

1. Introduction

Although research showing the potential of foods (such as curcumin) is old (in the 1949s the first research on curcumin benefits to human health was carried out), in the last decade there has been an increase in the population's knowledge and consumption of food to promote health. In this sense, a directly proportional relationship is observed between the reduction of synthetic additives and the increase in the consumption of functional foods, like nutraceuticals. (Nejatian et al., 2022; SCHRAUFSTÄTTER & BERNT, 1949; Tang, 2020) Nutraceuticals are a class of food-derived products that have beneficial properties to health and wellness to the body. Although its use is already a trend nowadays since the nutraceuticals market is a multimillion-dollar and high-impact branch, it is expected that this market will grow even more in the next decade.(Chopra et al., 2022; Nejatian et al., 2022)

Among the various nutraceuticals that have been the focus of research, emphasis must be placed on curcumin, as it has around 249,260 documents results in on Scopus, with 33,371 only in the year 2023 (search performed in November 12, 2023). It is also worth highlighting that this yellow-colored polyphenol, found primarily in the rhizome of *Curcuma longa* (L) and other *Curcuma* spp, is extremely used (for centuries) in the human diet as dye and seasoning (like curry), with an extensive range of nutraceutical properties very well documented in the literature.(A. Kumar et al., 2022; Sharifi-Rad et al., 2020)

Curcumin ($C_{21}H_{20}O_6$, **Figure 1**), presents a molecular weight of 368.39 g/mol and a melting point at 183°C.(Sharifi-Rad et al., 2020) This compound possesses keto-enol tautomerism depending on the pH (in acidic pH the ketone form is the dominant one (also in the cells), being the more stable enol form. Temperature also seems to influence this issue as higher temperatures favor the formation of the keto form. It is also worth highlighting that curcumin also presents cis-trans isomerism.(Bhatia et al., 2016; Slika & Patra, 2020) Curcumin is soluble in polar and nonpolar organic solvents and in alkali or extremely acidic solvents (like glacial acetic acid), being insoluble in water, neutral and acidic pH (however it is unstable in alkaline conditions).(Lestari & Indrayanto, 2014) Knowing the physicochemical characteristics of a component is crucial when the development of a nutraceutical is desired, since with the help of new technologies some factors such as poor solubility in water can be circumvented. Thus, this review article seeks to highlight all the steps that curcumin goes through for its activity as a nutraceutical: extraction, purification, absorption and activities, including the most recent studies of its association with nanotechnology.

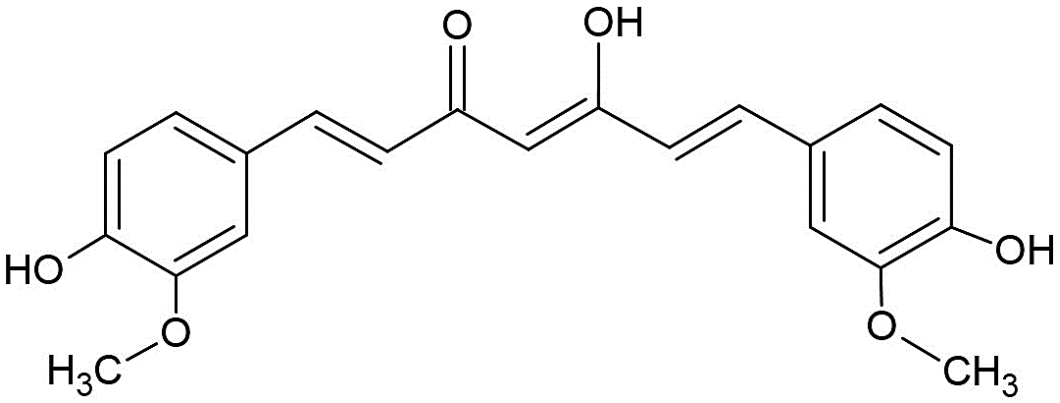

Figure 1. Curcumin chemical structure. Created with ACD/ ChemSketch.

2. Obtaining curcumin from food

The first factor to influence the obtaining of curcumin from its main source, *C. longa L* (turmeric), are the aspects related to this plant cultivation. Ideally, this plant adapts better to regions with a tropical and subtropical climate (e.g. the climate of India, its biggest producer). It is known that this geographical aspect of turmeric planting can directly influence the content of curcuminoids present in the plant.(Poudel et al., 2019) Another important point about cultivation is related to the level of sunlight that turmeric receives. According to the literature, the fact that the plantation is in the shade increases the yield of curcumin content. For this reason, in several plantations, this plant is intercropped with other crops.(Shannon et al., 2019) Furthermore, the use of organic fertilizers, a growing trend, has been shown to increase the quality of turmeric. The use of vermicompost, for example, has been associated with improved soil and increased curcumin yield and content.(Kadam & Kamble, 2020)

Although *C. longa* is the greatest source of curcumin in the human diet, as it is the most consumed, it is worth noting that different species of *Curcuma* vary in their curcumin content. *C. aromatica*, for example has shown to have a higher content of curcumin (1.2510%) than *C. longa* (0.8445%), *C. amada* (0.2121%), *C. caesia* (0.1368%) and *C. angustifolia* (0.0275%).(Kharade et al., 2017) The curcumin extraction process from the plant is an important step for its use as a nutraceutical, as it facilitates its consumption and increases its bioavailability it in the human body.(Carvalho et al., 2021) It is worth mentioning that in order to increase and allow better extraction, extraction must be preceded by the grinding of the rhizomes, for example with the help of a knives mill.(Paulucci et al., 2013)

The extraction process can occur by conventional techniques, such as solvent, soxhlet and maceration extractions.(K. Kumar et al., 2021; Priyadarsini, 2014) However, care must be taken during the extraction process since curcumin can undergo degradation by oxidation catalyzed by heat and

light.(Zielińska et al., 2020) Another limiting issue of those conventional methods is the solvent amount and toxicity. Although it is known that chlorinated solvents are capable of better extracting curcumin, ethanol seems to be the most preferable due its acceptability in the food industry.(Priyadarsini, 2014)

As a consequence of the negative points mentioned about conventional extraction methods, modern techniques that avoid exposing the plant to heat and that use smaller amounts of those organic solvents or even using less toxic solvents are preferable for this purpose, like ultrasound-assisted extraction, microwave-assisted extraction, enzyme-assisted extraction and supercritical fluid extraction.(Jiang et al., 2021) **Figure 2** summarizes the main characteristics of some conventional and modern extraction methods and **Table 1** highlights their advantages and disadvantages.

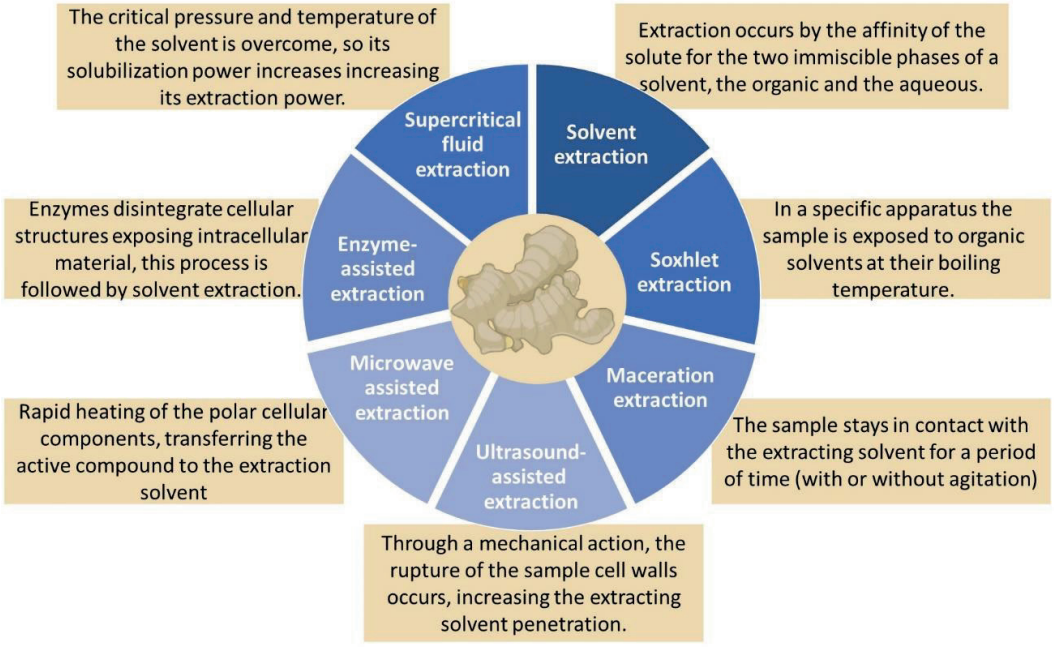

Figure 2. Main characteristics of some curcumin extraction methods. Created with BioRender.

Table 1: Main characteristics of some curcumin extraction methods.

Extraction method	Extraction temperature	Advantages	Disadvantages	References
Solvent extraction (Liquid-liquid extraction)	37 °C (ethanol:water)	Considered simple and practical (by the various solvent options).	Great amounts of organic solvents (toxic); Toxic residual impurities; Long time; degradation of many compounds.	(Durante et al., 2014; G. et al., 2023)
Soxhlet extraction	80 °C (ethanol:water)	Considered simple and efficient; low cost; do not requires an extract purification step.	Great amounts of organic solvents (toxic); Time-consuming; use of large amount of solvent; degradation of many compounds.	(Garcia-Vaquero et al., 2020)
Maceration extraction	Not necessary	Simple; low cost; can be performed without the use of temperatures.	Time consuming; lower extraction yield; requires an extract purification step	(Garcia-Vaquero et al., 2020; Nurhadi et al., 2020)
Ultrasound-assisted extraction	40 °C (ethanol)	Fast; higher yield and purity of the extract; more green (low energy and solvent consumption), possibility of reducing temperature.	Despite smaller amounts still uses organic solvents; low reproducibility and low power ultrasound delivered directly to the sample (both in the case of the bath).	(K. Kumar et al., 2021; Shirsath et al., 2021)
Microwave assisted extraction	Approximately 150 °C (castor oil)	More green (low energy and solvent consumption); extremely fast; multiple sample handling; high extraction yields; automation convenience;	Despite smaller amounts, still uses organic solvents; large samples or agglomerates need to go through a previous spraying step; If inadequate potency, (too high) can lead to low extraction yield and degradation.	(Hamid Nour et al., 2021; Suksaeree & Monton, 2024)
Enzyme-assisted extraction	32 °C (McIlvaine's buffer pH 4.5 + enzyme solution + distilled water)	Lower amount of organic solvents; use of low extraction temperatures; shorter time; complete exploration of plant material (greater specificity with the substrate, extracting bound forms, contained in the cell wall or vacuoles); higher yield.	Despite smaller amounts, still uses organic solvents; Cost (also from enzymes); since it destroys the cellular matrix it needs an additional step to separate and purify the final product; needs attention for conditions that can degrade enzymes; lower reuse of	(S. Das et al., 2021; Kurmudle et al., 2013)

			enzymes due to loss of catalytic activity after several uses.	
Supercritical fluid extraction (with carbon dioxide)	60 °C	No use of organic solvents so is a green method; use of near room temperatures; extract with high purity and quality; the gas used can be recycled	The high pressure required during the process leads to the need for safety requirements, which increases the cost.	(Nagavekar & Singhal, 2019)

After obtaining the extract, a concentration process, like lyophilization, spray-dryer, hot-air, far-infrared radiation and rotating evaporator, can be carried out in order to obtain a more stable, more bio-active final product. During the concentration process, the residual moisture of the product is removed, increasing its shelf life and reducing costs related to transport. It is also worth mentioning that the same precautions highlighted during extraction must be maintained in this subsequent step.(Carvalho et al., 2021) **Figure 3** highlights the main characteristics of the purification methods. (Charoenchai et al., 2020; Fernando & Amaratunga, 2022; Rodrigues et al., 2016)

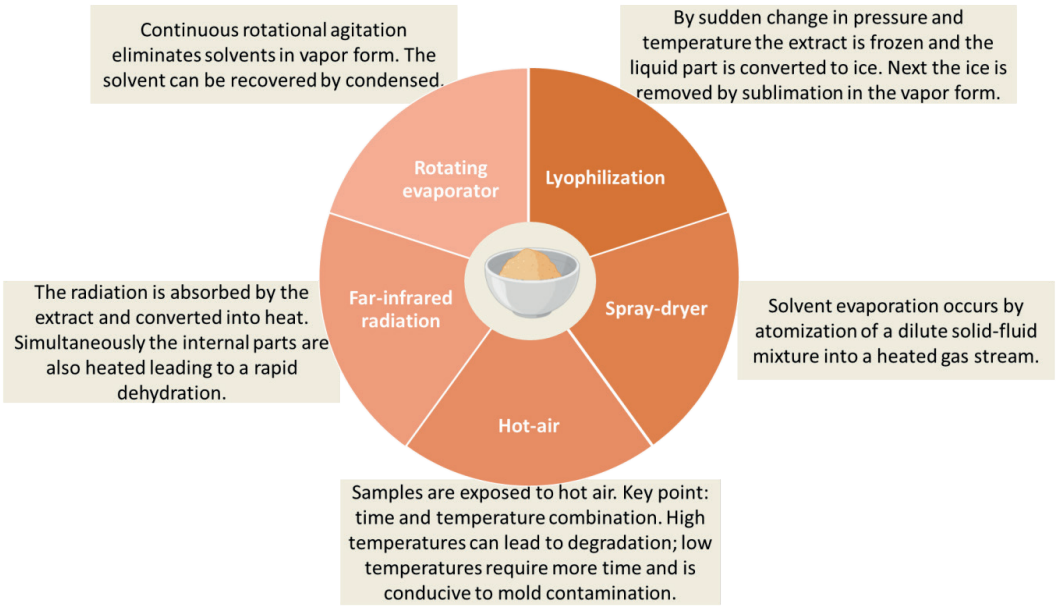

Figure 3. Main characteristics of some purification methods. Created with BioRender.

Despite being stored at low temperatures, the literature indicates that this drug is stable both at room temperature and at body temperature, which favors its use in therapy. However, at higher temperatures (greater than 55ºC) it can undergo degradation, which should be avoided in the extraction and concentration steps since it can alter the molecular structure of this active compound and lead to biodegradation and loss of nutraceutical properties.(Salem et al., 2014) For this reason, techniques that use lower temperatures for extract concentration, such as the evaporation route, are the most preferred and used.(Carvalho et al., 2021; Salem et al., 2014)

Another advantage of the concentration step is to make the sample ready for the next step, content quantification. This step is important in the production process of a product as it ensures that it meets the purity and quality standards necessary for its commercialization. It is performed by

analytical methods such as UV–Vis spectroscopy and fluorescence, thin layer chromatography, high-performance thin-layer chromatography, infrared spectroscopy, and high-performance liquid chromatography (HPLC).(Carolina Alves et al., 2019) Although there are several options for analytical techniques, chromatography is the most used one, with emphasis on HPLC. Through a bibliographic survey in SciFinder, performed by Carolina Alves and collaborators.(2019) the percentage of use of various analytical methods for curcumin quantification was evaluated, and the authors observed that 36% used HPLC, 19% used high-performance thin-layer chromatography, 14% used thin-layer chromatography, 12% used fluorescence spectroscopy and 12% used spectrophotometry (the other 7% were identified by the authors as "others"). **Table 2** shows the characteristics of curcumin extraction processes in samples from curcuma in articles published in 2023.

Table 2: Main characteristics of studies that addressed curcumin extraction in Curcuma samples in 2023.

Sample	Processing	Extraction method	Concentration method	Analytical method	Curcumin content	References
Dried turmeric	Grinded using motor	Soxhlet	Rotary evaporator	UV-Vis FT-IR Micro Raman CG-MS	-	(Deepa et al., 2023)
Fresh rhizomes of turmeric	High-pressure homogenization	Soxhlet	Rotary evaporator + three different types of drying: oven (O), vacuum (V) or freeze(F)	HPLC	0.139 mg mL^{-1} (O) 0.139mg mL^{-1} (V) 0.141 mg mL^{-1} (F)	(Vichakshana et al., 2023)
		Ultrasound-assisted			0.147 mg mL^{-1} (O) 0.133mg mL^{-1} (V) 0.143 mg mL^{-1} (F)	
	-	Soxhlet			0.132 mg mL^{-1} (O) 0.119mg mL^{-1} (V) 0.127 mg mL^{-1} (F)	
		Ultrasound-assisted			0.134 mg mL^{-1} (O) 0.173mg mL^{-1} (V) 0.128 mg mL^{-1} (F)	
Freshly harvested rhizomes	Water boiling + Solar drying	Solvent extraction	-	UV-Vis	5.57 mg g^{-1}	(G. et al., 2023)
	Water boiling + tray dryer				5.75 mg g^{-1}	
	Pressure cooking + Solar drying				5.88 mg g^{-1}	
	Pressure cooking + tray dryer				6.18 mg g^{-1}	
	Microwave heating + Solar drying				2.49 mg g^{-1}	

	Microwave heating + tray dryer				2.64 mg g^{-1}	
	Pressure-cooked + tray-dried	Ultrasound-assisted			6.18 - 7.801 mg g^{-1}	
Turmeric powder	-	Ultrasound	Filtration through Buchner funnel	UV-Vis	64.9 mg g^{-1} (optimal condition)	(X. Liu et al., 2023)

However, it is worth mentioning that depending on the purpose and extraction method used, it is necessary to carry out an additional purification step before the content quantification, in order to not only isolate curcumin from other curcuminoids, but also from others compounds present in the plant. Among these methods we can mention column chromatography, semi-preparative HPLC, high-speed counter-current chromatography, preparative supercritical fluid chromatography and crystallization.(Auychaipornlert et al., 2022; Jiang et al., 2021)

3. Ingestion and absorption

After obtaining a quality extract with a known curcumin content, it is ready to be consumed as a nutraceutical. The recommended daily dosage of curcumin is very relative, varying according to specific diets and therapeutic needs. It is estimated that adult Indians consume 80-200 mg of curcumin daily in their normal diet.(Qiu et al., 2016) It is worth mentioning that this component is considered safe by the Food and Drug Administration (FDA) and it is possible to observe studies addressing good tolerability and safety for doses in the range of 4,000 - 8,000 mg day^{-1}.(Hewlings & Kalman, 2017) After being ingested, a compound is released and solubilized in the gastrointestinal fluids in order to be absorbed by the small intestine cells and reach systemic circulation; however, due to its hydrophobic nature, curcumin has low solubility in these fluids, which limits its absorption.(Sabet et al., 2021) The low oral bioavailability of curcumin has been evidenced in several scientific studies.(Mahale et al., 2018; Schiborr et al., 2014)

The pharmacokinetics of turmeric intake was evaluated and four participants had an individual consumption of 3 g of turmeric within a food matrix, which according to the authors, is equivalent to 100 mg of curcumin intake. In only one participant curcumin was detected in the plasma (with a concentration of 3.2 nM) 2 h after food intake. However, in all four participants, plasma levels of curcumin metabolites, such as curcumin glucuronide and demethoxycurcumin glucuronide were observed, with a maximum concentration of 47.6 ± 28.5 nM and 1.9 ± 1.2 nM, respectively, after 30 minutes of feeding. This study also pointed to the possibility of existing a relationship between curcumin bioavailability and gender, once it was observed higher curcumin metabolites plasma levels in male participants (n = 3) compared to female ones (n = 1). The lower bioavailability of curcumin in women was related to higher levels of adipose tissue, which can hinder its absorption.(Mahale et al., 2018) However, extrapolating conclusions and generalizing based on this study can be complicated since the number of participants was small, especially regarding the women.

In another study, with a higher number of participants (13 women and 10 men), pointed to the lower bioavailability of curcumin in males. According to the authors the results can be related to the greater activity of hepatic drug efflux transporters (P-glycoprotein) and also due to the isoforms of

glucuronosyltransferase and sulfotransferase enzymes, which act in the biotransformation of this compound in men. Additionally, this study also compared the same dose, 500 mg of curcuminoids (containing 410 mg curcumin), in different curcumin formulations: native powder, micronized powder and liquid micelles. The authors concluded that both the micronized powder and the liquid micellar formulation significantly improved the oral bioavailability of this compound (without compromising its safety).(Schiborr et al., 2014)

While only 5 to 10% of curcumin absorption takes place in the small intestine, most (90 to 95%) takes place in the colon, due to its glycosylated form. After its absorption, its conversion into phenolic metabolites occurs, which via the portal vein reach the liver and undergo extensive metabolism through methylation, glucuronidation and sulfation reactions. From there, active metabolites are formed, which can enter the systemic circulation, reaching target cells and tissues, enabling its biological activity. The remaining metabolites are excreted in the urine and feces.(Shabbir et al., 2021) **Figure 4** summarizes curcumin process of absorption in the human body.

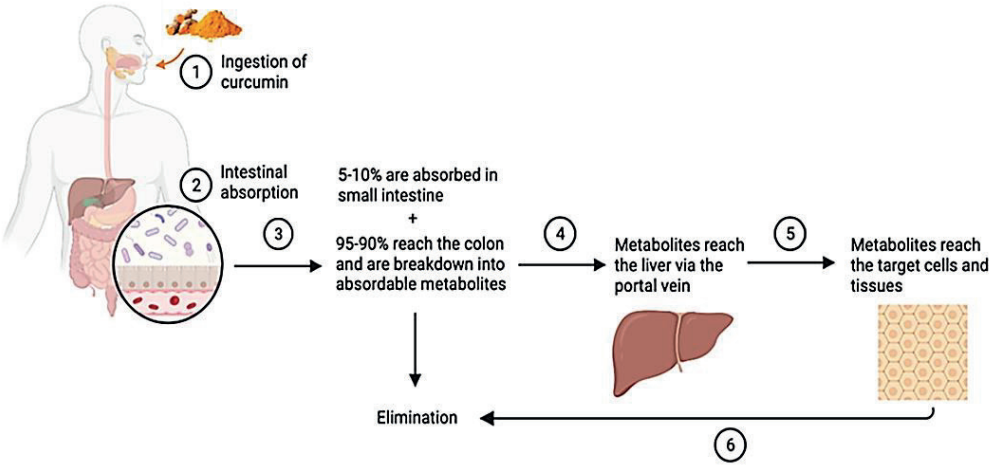

Figure 4. Steps that curcumin goes through from its ingestion to its elimination by the human body. Created with BioRender.

4. Biological properties of curcumin

In this topic, the different biological activities that curcumin has will be discussed in order to highlight the importance of this compound and the variety of therapeutic conditions in which it can be used. So, in addition to the text covering each of these activities in more detail, **Table 3** summarizes the studies mentioned in this topic.

Table 3: Main highlights of recent studies that address curcumin biological activity

Target	Range of dose	Method	Results remarks	References
Pseudomonas aeruginosa	6.75 mM	Planktonic	Cur+ 5 J/cm^2: reduction of 2.12 log10 Cur + 10 J/cm^2: reduction of 4.26 log10	(Abdulrahman et al., 2020)
		Biofilm	Cur without light: inhibition of 23% Cur + 5 J/cm^2: inhibition of 40% Cur + 10 J/cm^2: inhibition of 70%	
		Viability cells	Cur without light: viability of 91% Cur + 5 J/cm^2: viability of 78% Cur + 10 J/cm^2: viability of 71%	
		Reduction EPS	Cur without light: reduction of 32% Cur + 5 J/cm^2: reduction of 49% Cur + 10 J/cm^2: reduction of 94%	
Methicillin-Resistant *Staphylococcus aureus*	80 µg/mL^{-1} PDT and LED 110 mW/cm^2, 50 J/cm^2	Bacterial growth evaluation after PDT application	The group treated with PDT therapy decreased 2.12 Logs. Comparing the dark control with the PDT group, the difference was 2.03 Logs	(Ribeiro et al., 2022)
		Metabolic activity with Resazurin	The PDT group significantly reduced ($p<0.01$) when compared to the group treated only with Cur or LED, presenting 403.33 arbitrary fluorescence units for the LED group and 666.66 for the Cur group.	
		Production of ROS	PDT increased ROS production when compared to the group treated with LED or Cur alone ($p<0.01$).	
Helicobacter pylori	-	MIC	MIC: 16, 16 and 32 µg/mL^{-1} for compounds 1, 2, and 5, respectively.	(Han et al., 2006)
Bacillus subtilis	-	Hartree- Fock calculation	Affinity of the Cur to the receptor with up to −6.16 kcal/mol of energy	(Tripathy & Sahu, 2018)
Candida albicans	-	ESI-MS/MS and GCMS	Ergosterol reduction: Cur (23.12 µg/mL): No reduction Cur (92.5 µg/mL): 90% FLU: 48% Cur + FLU: 84%	(Sharma, 2012)

			Increase in phosphoglycerides Phosphatidyl glycerol: 48% Phosphatidyl choline: 17%	
			Sphingolipids reduction: Ceramide: 6x Inositol phosphoryl ceramide: 2x	
			Increase in ester intermediates of ergosterol biosynthesis: Episterol, fecosterol and lanosterol: 2-8x	
Aspergillus flavus	1-8 µg/mL	Germination and morphology	Inhibitory effects of turmeric EO on the spore germination: 17.01 to 85.47%. Morphology: Spores with rough walls, and depressions after 2 µL/mL treatment.	(Hu et al., 2017)
		Determination of ergosterol	Reduction: 14.80, 30.07, 38.95, 53.64 and 80.27%, respectively.	
		Antifungal effect of turmeric EO on mycelial growth	1, 2, 3, 4 and 8 µg/mL: 63.31, 71.15, 78.99, 91.03 and 93.41% of inhibition, respectively	
		Mitochondrial ATPase and dehydrogenases activity	Mitochondrial ATPase reduction (2-8 µg/mL): 29.1, 32.3, 42.7, and 74.6%, respectively. Dehydrogenases activity: 15.8, 42.2, 52.9, 71.4 and 84.7%, respectively.	
	4 µg/mL	Antifungal Efficacy of Turmeric EO During Corn Storage	Untreated corn: 74.3% of contaminated seeds Corn with treatment: 7.48% of contaminated seeds	
C. albicans	0-250 µg/mL	MIC	MIC_{80} = 250 µg/mL	(Y. S. Lee et al., 2022)
	125 µg/mL	Stress response	depletion pf Hps90 and efflux pump inhibition	
Human influenza virus PR8 (H1N1) and Avian influenza virus (H6N1)	0,10, 20 and 30 µM	Viral infections and curcumin treatment	Reduction of virus production in Madin-Darby canine kidney cells treated with Cur (reduction exceeding 90% at the highest concentration).	(Chen et al., 2010)
	30 µM	Plaque reduction assay	Simultaneously Cur addition the virus resulted in a more significant reduction in viral load	
	31.2 and	Haemagglutination inhibition test	Pretreatment with Cur prevented H1N1 and H6N1 virus from binding to chicken red blood cells	

	15.6 μM for Human and avian virus, respectively.			
Zika and Chikunguya virus	1- 100 mM and 1-10 μM	Surviving treatment	Dose-dependent decrease in viral titters from a concentration of 100 mM.	(Mounce et al., 2017)
	5 μM	Quantification of viral genomes via qRT-PCR and titers	Decrease in titers and genetic quantity of Zika virus	
		Infection and enumeration of viral titers	Cur inhibits Zika and Chikungunya viruses with pre-treatment of cells or treatment at the time of infection	
	1 μM to 1 mM	Infectivity of enveloped viruses	Both viruses showed > 99% loss of their infectivity at a dose of 1 mM	
		IC_{50} and EC_{50}	Zika: 1.90 μM	
			Chikungunya: 3.89 μM	
	1, 10, or 100 μM	Cell surface binding	Decrease in the binding of both viruses to the cell surface in a dose-dependent manner.	
HIV 1	20 – 120 μM	Tat protein degradation	Decrease in protein Tat, especially at concentrations >80 μM Regarding exposure time, the level of tat treated with Cur (80 μM) decreased over 8h Combined treatment of Cur (50 μM) + cycloheximide or Cur alone resulted in degradation of Tat protein (0-2.5h).	(Ali & Banerjea, 2016)
	0 – 80 μM	Tat protein activity	Change in Tat cDNA level after Cur treatment. Luciferase activity in Tat-transfected TZM-bl cells was 40 and 60% reduced after 20 and 40 μM, respectively.	
		Virion production	Decrease in the number of virions inside cells	
Taenia crassiceps	0 – 500 μM	Activity against *T. crassiceps*	100% inhibition of viability in 500 μM after 14h. LD_{50} of 240.05 μM. Cysticercu death obtained between 200 and 500 μM. 50% residual TGR activity in cysticercu exposed to 500 μM. 23x increase in ROS production	(Martínez-González et al., 2022)
	500 μM	Lethal effect / time	After 30 min: 70% mortality	

			After 120 min: 100% mortality After 30 min: 25x increase in ROS After 120 min: 23% reduction in TGR enzymatic activity	
	50 – 500 µM	Activity in the cysticercis integument	250 µM: Vacuolation of the integument. 500 µM: Drastic changes were observed	
	20 – 60 mM	Parasite load in mice	46% reduction in cysticerci number after maximum Cur treatment.	
Leishmania major	0 – 80 µM	Promastigote Cytotoxicity	LC50: 35 µM 20 µM: 75% survival 40 µM: 41.5% survival 60 µM: 25.3% survival 80 µM: 22 % survival	(Elamin et al., 2021)
		Apoptotic effect	20 µM: 24% 40 µM: 63% 60 µM: 72% 80 µM: 82.5%	
	80 µM	Proliferation inhibition	Control without treatment: time-dependent proliferation. Control with treatment: time-dependent decrease in proliferation (in 72h).	
		Effect on cell cycle by cytometry	Cur-dependent accumulation in the S phase of the cell cycle reaching after 16h (33%).	
Entamoeba histolytica	100 – 300 µM	Growth inhibition	100 µM: 48.4 % 200 µM: 52.7% 300 µM: 65.5%	(Rangel-Castañeda et al., 2018)
		Cellular viability	Trypan blue exclusion test after 6h: 100 µM: 37.1 % 200 µM: 39.3% 300 µM: 53.3%	
	100 + 5 µM of MTZ or 200 + 10 µM MTZ	Checkerboard: Dead cells	100 + 5 µM: 69.5% 200 + 10 µM: 87.25%	
	100 – 300 µM	Adhesion inhibition	After 12h 200 µM: 38.6% 300 µM: 64.9%	

			After 24h 300 µM: 78.8%	
		SEM	Trophozoites with spherical characteristics, formation of bubbles on the membranes surface and loss of locomotion structure. 100 µM: Membrane perforation and burst intracellular components. 200 µM: Total loss of cellular integrity. 300 µM: Cell disintegration.	
Plasmodium falciparum	0.5 – 50 µM	Drug sensitivity assays	5 µM: 50% inhibition (after 48h) 20 µM: 63% inhibition (after 48h) 35 µM: 70% inhibition (after 48h) 50 µM: 90% inhibition (after 48h)	(Chakrabarti et al., 2013)
	5 µM	Morphology	Presence of shrunken cells and aggregates concentrating at one end of the erythrocyte	
	5 and 20 µM	Action on microtubules	Spindle microtubules First cycle Control: 87.5% 5 µM: 31.76% 20 µM: 30.70% Subpellicular microtubules First cycle Control: 61.53% 5 µM: 53.57% 20 µM: 26.66% Spindle microtubules Second cycle Control: 90% 5 µM: 0% 20 µM: 7.14% Subpellicular microtubules Second cycle Control: 45.83% 5 µM: 0% 20 µM: 0%	

	Cur 1000 – 4000 nM Col 2000 – 8000 nM Pac 100 – 400 nM Vin 20 – 80 nM	Checkerboard	$FICI_{90}$ After 48h Cur + Col: ND Cur + Pac: 1.645 Cur + Vin: 1.640 $FICI_{90}$ After 96h Cur + Col: ND Cur + Pac: 1.036 Cur + Vin: 0.555	
Retinoblastoma	0-50 µM	Inhibition of cell proliferation	Cellules: SO-Rb50 and Y79 IC_{50} SO-Rb50: 38.4 µM IC_{50} Y79: 34.8 µM	(H. Wang et al., 2021)
	30 µM	Apoptosis	SO-Rb50: Control: <5% Cur: >10% Y79: Control: <5% Cur: >5% Inhibition of Bcl-2 Increase of pro-apoptotic proteins production (Bax and cleaved-caspase-3/9)	
		Transwell assay:	Reduction of migration and invasion of cells treated with Cur. Cur significantly regulated MMP2, RhoA, ROCK 1, and Vimentin proteins	
		JAK/STAT signaling	miR-99a was up-regulated in Cur-treated cell	
Osteosarcoma	2.5 – 10 µM	Inhibition of cell proliferation	Absorbance cells after 48h: MG-63 Control: 0.79 2.5 µM: 0.65 5 µM: 0.52 10 µM:0.38 HOS Control: 0.97 2.5 µM: 0.77 5 µM: 0.57 10 µM: 0.40	(Zhou et al., 2020)

		Absorbance cells after 72h: MG-63 Control: 1.37 2.5 µM: 1.15 5 µM: 0.78 10 µM: 0.37 HOS Control: 1.62 2.5 µM: 1.20 5 µM: 0.87 10 µM: 0.0.35
	Western blots	Increased Bax expression and decreased Bcl-2 levels
10 µM	Number of colonies	MG-63 (Colonies) Control: 31 ±4 Cur: 5 ± 2 HOS (Colonies) Control: 43 ± 3 Cur: 11 ± 2
	Flow cytometry: Apoptoses	MG-63 Control: 4.72 ± 0.8 Cur: 20.63% ± 3.67% HOS Control: 6.14 % ± 1.15% Cur:19.78% ± 1.64%
2.5 – 10 µM	Regulation of RECK expression	Decreased miR-21 expression. Control: 1.00 ± 0.16 2.5 µM: 0.59 ± 0.16 5 µM: 0.17 ± 0.01 10 µM: 0.11 ± 0.04 Increase RECK expression. Control: 1.00 ± 0.07 2.5 µM: 0.38 ± 0.11 5 µM: 0.25 ± 0.06 10 µM: 0.27 ± 0.11

	10 μM	Regulation of RECK expression via miR-21	miR-21 upregulated MG-63. Control: 1.00 ± 0.27 Cur: 22.31 ± 4.48 miR-21 upregulated HOS. Control: 1.00 ± 0.17 Cur: 7.70 ± 0.26 RECK downregulated MG-63. Control: 1.33 ± 0.21 Cur: 0.59 ± 0.22 RECK downregulated HOS. Control: 1.13 ± 0.39 Cur: 0.39 ± 0.19	
Acute monocytic leukemia	15 and 30 mg/Kg/day	Inhibition of cell proliferation	Reduction of tumor weight Control: 0.67g 15 mg/Kg: 0.47g (29.9% reduction) 30 mg/Kg: 0.35g (47.8% reduction)	(G. Zhu et al., 2020)
		Histology	Cur-treated group: massive damage to cancer cells, cytoplasmic condensation and nuclear pyknosis. Significant inhibition of SHI-1 cell proliferation with $p = 0.0668$ and $p = 0.0078$ for the group treated with 15 and 30 mg/kg, respectively.	
		Apoptosis induction	Significant increase in tumor cell apoptosis, especially in treatment with 30 mg/kg/day	
		MAPK alteration and NF-κB inhibition	Significant increase in p38 phosphorylation 15 mg/Kg: $p = 0.0479$ 30 mg/Kg: $p = 0.0059$ Significant increase in JNK 15 mg/Kg: $p = 0.0823$ 30 mg/Kg: $p = 0.0145$ Significant decrease in ERK1 phosphorylation 15 mg/Kg: $p = 0.774$ 30 mg/Kg: $p = 0.0475$ Significant decrease in ERK2 15 mg/Kg: $p = 0.662$	

			30 mg/Kg: *p = 0.0372* Decreased expression of the p-p65 protein 15 mg/Kg: *p = 0.048* 30 mg/Kg: *p = 0.0427*	
		Expression of MMP2, MMP9 and vimentin in SHI 1	Significant decrease of MMP9 15 mg/Kg: *p = 0.035* 30 mg/Kg: *p = 0.0215* Significant decrease of MMP2 15 mg/Kg: *p = 0.168* 30 mg/Kg: *p = 0.0081* Significant decrease of vimentin 15 mg/Kg: *p = 0.067* 30 mg/Kg: *p = 0.0013*	
Alzheimer's	150 mg/Kg	Spatial learning and memory deficits in vivo	Significant decrease in escape latency from day 3 to 5 in the training experiment. Cur increased platform crossing and time spent in the target quadrant and decreased travel distance. Possible synergistic effect between Cur and GW9662 (4 mg/Kg) in improving memory function.	(Z.-J. Liu et al., 2016)
		Protection of cholinergic neurons	Increase in ChAT enzyme levels after Cur treatment. Synergistic effect with coadministration of GW9662 (4 mg/Kg)	
		Neuroinflammatory response	Cur suppressed the production of toxic markers (TNF-α, IL-1β, COX-2 and NO). Decrease in neuroinflammation	
		NF-κB signaling pathway	Decreased IκB-α degradation and NF-κB p65 translocation Synergistic effect with coadministration of GW9662 (4 mg/Kg)	
		Activity of PPARγ	2x increase in PPARγ transcriptional activity along with a significant induction of PPARγ protein expression	
Parkison	0 – 16 μM	Astrocyte cell viability	Cytotoxicity only at the highest concentration (16 μM)	(Yu et al., 2016)
	8 μM	MPP-induced activation of primary astrocytes	MPP induced a reactive state in the astrocyte, however, this situation was reversed by Cur and attenuated the activation of astrocytes by MPP.	

		Pro-inflammatory cytokines	Pretreatment with cur reduced the production of TNF-α and IL-6.	
		ROS	Cur suppressed MPP-induced ROS production and increased MPP-suppressed GSH level.	
		NF-κB and TRL4 protein	MPP increased the level of NF-κB and IRF3, but was reduced in the presence of Cur. MPP increased TLR4 protein, however, Cur treatment decreased its amount.	
Huntington's disease	3 - 15 μM	Assessment of neurodegeneration	Treatment with Cur suppressed the degeneration of photoreceptor neurons in a dose-dependent manner, especially in the concentration of 10 μM	(Chongtham & Agrawal, 2016)
		Drosophila eye development	10 μM Cur, even at the early stage, resulted in Httex1p Q93-induced cytotoxicity, causing phenotypic changes such as rough eye with necrotic lesions and loss of pigmentation	
	5 - 15 μM	polyQ-mediated locomotor dysfunction	Cur improved the crawling ability of Httex1p Q93 and Q48 larvae in a dose-dependent manner as well as marked improvement in the crawling behavior of larvae at a dose of 10 μM Cur. Cur decreased the progressive loss of motor function in flies in a dose-dependent manner.	
	5 and 10 μM	PolyQ-induced cytotoxicity	Treatment with Cur reduced cell death by apoptosis in eye discs of larvae fed with 5 and 10 μM.	
Adults Who Recovered from SARS-CoV-2	500 mg	Inflammatory Biomarkers	Reduction of IL-6 ($\beta = -0.52$ and $p = 0.046$) and MCP-1 ($\beta = -0.12$, 95% and $p = 0.027$)	(Fessler et al., 2023)
Encephalomyelitis	100 mg/k-Kg + 0.4 mg/Kg of rGas6	EAE induction and treatment	Significantly attenuated the severity of EAE ($p < 0.001$)	(M. Sun et al., 2022)
		Histology	Decrease in inflammatory cells with $p < 0.05$	
		Inflammatory responses in EAE mice	Decreased serum levels of IL-6 and TNF-α and increased levels of IL-10 and TGF-β ($p < 0.01$)	
		Activation of microglia in EAE mice	Decreased protein levels of AXL and TMEM119	

	1 - 500 µM	Cur mitigated inflammatory responses that were stimulated by LPS in BV-2 cells	LPS + Cur decreased cell viability of BV2 at a concentration higher than 50 µM. LPS + Cur decreased the levels of TNF and IL-10	
	10,30 and 50 µM	AXL/JAK2/STAT3 signaling	Decrease in p-JAK2 and p-STAT3 protein levels with $p < 0.05$ when treated with Cur and rGas6 intervention. Inhibition of AXL, p-JAK2, and p-STAT3 in the spinal cord $p < 0.05$	
Metabolic syndrome	500 mg	Measurement of pro-inflammatory cytokines	Before treatment Cur/Placebo: TNF-α: 79.24±8.55 / 77.48±6.54 IL-6: 3.30±1.31 / 1.79±0.40 TGF-β: 4.60±1.37 / 5.87±1.15 MCP-1:131.52±14.91 / 130.54±20.41 After treatment Cur/Placebo: TNF-α: 63.02±8.18 / 78.90±8.17 IL-6:1.37±1.52 / 1.81±0.55 TGF-β: 2.49±0.99 / 5.49±1.05 MCP-1: 97.96±19.99 / 132.86±2.32±19.28	(Panahi et al., 2016)

Legend: Cur: Curcumin; EPS: Extracellular polymeric substances; PDT: Photodynamic Therapy; LED: Light Emitting Diode; MIC: Minimal inhibitory concentration; Compound 1: 3-(2-naphthyloxy)-4-oxo- 2-(trifluoromethyl)-4H-chromen-7-yl 3-chlorobenzoate; Compound 2: butyl 2-{[3- (2-naphthyloxy)-4-oxo-2-(trifluoromethyl)-4H-chromen-7-yl]oxy}propanoate; PDT: Antimicrobial photodynamic therapy; LED: Light Emitting Diode; ESI-MS/MS: Electron spray ionization tandem mass spectrometry-based lipid profiling; GCMS: Gas chromatography mass spectrometry; FLU: Fluconazole; EO: natural essential oil derived from turmeric (*Curcuma longa* L.); Hps90: heat shock protein 90; IC_{50}: 50% inhibitory concentrations; HIV 1: Human immunodeficiency virus; ROS: Reactive oxygen species; TGR: Thioredoxin-glutathione reductase; LD_{50}: Lethal dose; MTZ: Metronidazole; SEM: Scanning electron microscopy; ND: Not determined; Col: Colchicine; Pac: Paclitaxel; Vin: Vinblastine; SO-Rb50 and Y79: Human retinoblastoma cell line; Bcl2: Anti-apoptotic proteins; MG-63 and HOS: Human osteosarcoma cell lines; RECK: Reversion-inducing cysteine-rich protein with kazal motifs; miR: MicroRNAs; SHI 1: Acute monocytic leukemia; PPARγ: Peroxisome proliferator-activated receptor gamma; TNFα tumor necrosis factor-α; IL: Interleukins; GW9662: PPARγ inhibitor; NO: Nitric

oxide; COX: ChAT: Choline acetyltransferase; MPP: 1-methyl-4-phenylpyridinium ion; TRL4: toll-like receptor; ROS: Oxygen species; GSH: Antioxidant glutathione; PolyQ: Polyglutamine; Httex1p 93: mutant Htt with 93 glutamine residues; EAE: Experimental autoimmune encephalomyelitis; MCP-1: Monocyte chemoattractant protein; LPS: lipopolysaccharide; BV 2: murine BV-2 microglial cells; TNF-α: Tumor necrosis factor alpha; IL-6: interleukin 6; TGF-β: transforming growth factor beta; MCP-1: monocyte chemoattractant protein-1.

4.1. Antimicrobial activity

In the literature, it is possible to observe several mechanisms of antimicrobial action, like the inhibition of the quorum sensing process in biofilms. An essential factor in the formation of biofilms, quorum sensing is inhibited by the presence of curcumin. qRT-PCR studies with *Pseudomonas aeruginosa* demonstrated that 6.75 mM of this drug plus light doses of 5 and 10 J $(cm^2)^{-1}$downregulated quorum sensing genes, noting that this last mentioned dose of light is a more drastic form.(Abdulrahman et al., 2020)

Curcumin association with light (photodynamic therapy) also possesses another mechanism of action, the formation of reactive oxygen species (ROS), causing microorganisms to die. For example, in the study performed by Zhang *et al.*(J. Zhang et al., 2022) the sono-photodynamic sterilization technique (non-thermal sterilization technique with high penetration power) was evaluated using curcumin as a sono-photosensitizing agent, ultrasounic energy, and a blue Light Emitting Diode (LED) as the activating agent. It was observed that *Listeria monocytogenes* was adequately inactivated, and this fact was attributed to excessive production of ROS which led to cell deformation, protein degradation, membrane rupture, depolarization and leakage of cytoplasmic material, and apoptosis.

Still addressing the association of light and curcumin, Ribeiro *et al.*(2022) performed a study where, aiming to combat methicillin-resistant *Staphylococcus aureus* (MRSA) biofilm, curcumin was associated with LED light 450 nm, 110 mW $(cm^2)^{-1}$, 50 J $(cm^2)^{-1}$ for 455 s and it was observed that this association increased 109.33 units of fluorescence if compared with the control, while the uncombined curcumin and LED groups showed an increase of 2.67 and 65 units of fluorescence respectively.

A different antimicrobial mechanism also described involves shikimate pathway. This pathway is essential for the synthesis of microbial metabolites like aromatic amino acids, folic acid, and ubiquinone. *Helicobacter pylori* is an example of bacteria that uses the shikimate pathway, and by *in vitro* enzyme activity determination, it was observed that the presence of curcumin in the culture medium can inhibit *H. pylori* shikimate dehydrogenase in a dose-dependent manner. *H. pylori* shikimate dehydrogenase is an enzyme that catalyzes the NADPH dependent reduction of 3-dehydroshikimate to shikimate. It is worth noting that the shikimate pathway is responsible for the production of important metabolites for the microorganism, therefore the development of drugs that disrupt this pathway is an interesting strategy.(Han et al., 2006) Another important antimicrobial activity of curcumin reported in the literature is its action against FtsZ, a prokaryotic homologue of the eukaryotic cytoskeleton protein tubulin. This homologue is extremely important for bacteria since it acts in cell division and viability. Through an *in silico* test using the AutoDock 4.0 tool, it was

observed that curcumin has a high binding affinity with *Bacillus subtilis* FtsZ protein receptor, up to -6.16 kcal mol^{-1} of energy.(Tripathy & Sahu, 2018)

Inhibition of gene expression has also been evidenced. In addition to negatively inhibiting gene expression, curcumin acts by preventing the gene repair response, required in cases such as DNA damage. In other words, curcumin inhibits the SOS response.(Zheng et al., 2020) In fungi cells, like *Candida albicans*, ergosterol is one of the main components of the plasma and other intracellular organelles' membranes. Through electron spray ionization tandem mass spectrometry-based lipid profiling, it was observed by Sharma *et al.* (2012) that curcumin is capable of causing a drop in ergosterol levels and, consequently, accumulation of its biosynthetic precursors, preventing fungi growth. In addition to this direct damage, the accumulation of ergosterol biosynthetic precursors can increase ROS and yeast death. By RT-PCR, the authors were able to clarify that this reduction in ergosterol is due to curcumin targeting the ERG3 gene.

Effects on the microbial membrane are also reported. In *in vitro* fluorescence studies with 1,6-diphenyl-1,3,5-hexatriene carried out with *C. albicans* cells, it was observed that curcumin induces the rupture of the plasma membrane. Additionally with the aid of an ion-selective electrode meter, it was found that this rupture leads to potassium ion leakage from the cytosol which leads to dissipation in membrane potential.(W. Lee & Lee, 2014) Cell membrane disruption, inhibition of ergosterol synthesis, inhibition of cellular respiration, NADH oxidase, succinate dehydrogenase, and disruption of fungal cell endomembrane system, including the plasma membrane and mitochondria was also evidenced in *Aspergillus flavus* and *Fusarium graminearum* strains treated with curcumin.(Hu et al., 2017; Trigo-Gutierrez et al., 2021) Action against the efflux pump is also shown to be a mechanism of action for curcumin. In one study, using a HSP90-overexpressing *C. albicans* strain and a doxycycline-mediated HSP90 *C. albicans* strain, it was shown that curcumin triggered a decrease in heat shock protein 90 (Hsp90) in both *C. albicans* strains growth, affecting it at the post-transcriptional level. It was also observed that curcumin caused downregulation of HOG1 and CDR1, that impaired yeast growth, stress response, and CDR1 efflux pump activity.(Y. S. Lee et al., 2022)

The antiviral potential of curcumin is also discussed in the literature. In *in vitro* experiments carried out by Chen *et al.*(2010) with Madin-Darby canine kidney cells and influenza A virus, it was observed that the virus yield replication was reduced by around 95% after 24 h. The authors also evaluated the effect of curcumin at three possible moments related to the contact with the virus (before, during and after) and it was observed that simultaneous treatment was the best. Finally, a possible mechanism of action, haemagglutination inhibition, was studied with chicken erythrocytes, and it was observed that pre-treatment with curcumin was able to reduce the binding of the H1N1 virus to erythrocytes. Additionally, a lower concentration of curcumin was able to prevent this binding in

another subtype of the virus (H6N1). The authors further reinforced that this loss of activity of the influenza virus may be due to the interruption of the connection between the virus and its cellular receptor by virus envelope modification or preoccupying the binding site on haemagglutinin. In addition to influenza, curcumin has shown antiviral activity against different types of viruses, including emerging arboviruses (such as Chikungunya virus and Zika virus), hepatitis virus, human immunodeficiency virus (HIV), herpes simplex virus 2 (HSV-2) and human papillomavirus (HPV).(Praditya et al., 2019)

In one study, the activity of curcumin against enveloped viruses like Zika virus and Chikungunya was described. In an *in vitro* test carried out with HeLa and BHK-21 cells, it was observed that both viruses responded to anti-viral treatment, without interfering with cell viability. In direct treatment it was observed that curcumin activity was dependent on the dose and contact time between virus and drug (with the exception of the longest time studied, 72h, where viral titers became similar to untreated levels in the case of Zika virus). Different moments of treatment (before, during and after viral exposure) were also evaluated, and although both viruses were sensitive at any of the times evaluated, it was observed that the most effective times were before or at the time of infection. Both by qRT-PCR and western blot, it was observed that curcumin has no action against viral RNA or in the accumulation of proteins, therefore its activity against replication is prior to these processes, suggestively at the level of binding or entry.(Mounce et al., 2017)

Another study, with HEK-293T cells, pointed to the good antiviral activity of curcumin against HIV-1 by the decrease in the transactivation of the long terminal repeat (LTR) promoter mediated by Tat, an unfolded protein with important role in viral replication. By western blotting measures, Tat protein degradation rate was evidenced in the presence of curcumin in a dose and time dependent way through the proteasomal pathway.(Ali & Banerjea, 2016) There are also reports of curcumin activity against SARS-CoV-2 by inhibiting the SARS-CoV-2 3CL protease, an important molecule (highly conserved) that participates in viral replication. It is worth mentioning that more mechanisms are also described, such as direct interaction with viral surface proteins, disruption of the viral envelope and induction of an inflammatory process against the infection. Additionally, the presence of curcumin has been shown to protect against lethal pneumonia and acute respiratory distress syndrome by targeting NF-κB, inflammasome, IL-6 trans, and HMGB1 pathways.(Thimmulappa et al., 2021)

Finally, curcumin antiparasitic action is also reported in the literature. A study pointed that curcumin activity in the lethality of *Taenia crassiceps* cysticercus is related to oxidative stress in a dose-dependent form. By autooxidation, curcumin produces various unstable components to finally produce bicyclopentadione (a stable product). Oxidative stress causes partial inhibition of thioredoxin-glutathione reductase, most important enzyme involved in controlling parasite redox homeostasis.

Additionally, the intrinsic ability of curcumin-derived oxidative products generates ROS compromising cysticerci vitality. This study also evaluated the effect of curcumin on these parasites in an *in vivo* mice model and it was observed that the highest dose tested led to a decrease of 46 % of the parasite load.(Martínez-González et al., 2022)

Curcumin also seems to have a strong action in the cell cycle inactivation of the promastigote form of *Leishmania* species. By flow cytometry it was observed that the parasite death is caused by mitochondrial apoptosis (by the membrane failure), in a dose-dependent manner probably triggered by the regulation of Bcl-2, an anti-apoptotic effector. (Elamin et al., 2021) ROS production, cytosolic calcium elevation, phosphatidylserine exposure to the plasma membrane outer leaflet and DNA fragmentation in promastigotes of *L. donovan* can also be factors related to the antileishmanial activity of this drug.(R. Das et al., 2008)

Rangel-Castaneda *et al.*(2018) investigated its amebicide activity against *Entamoeba histolytica* trophozoites. Curcumin affected in a dose-dependent manner, not only the growth, but also the cell viability of these parasites. The highest curcumin concentration tested inhibited growth by 65.5% and allowed only 28.8% of trophozoites to remain viable. The results showed that the highest dose tested reduced adherence by 78.8%. Scanning electron microscopy images (SEM) showed morphological changes, damage to the parasitic membrane followed by loss of internal constituents, size changes, and parasites with loss of cellular integrity. Its antiparasitic action was also evidenced against *Plasmodium falciparum*. According to the Chakrabarti *et al*.(2013) in immunofluorescence studies carried out using a beta-tubulin antibody, curcumin activity was associated with its interaction with alpha-beta tubulin heterodimer interface, changing the microtubule morphology. The authors tested two curcumin concentrations and observed that this activity was dose dependent. **Figure 5** summarizes the mechanisms of action of curcumin against microorganisms covered in this topic.

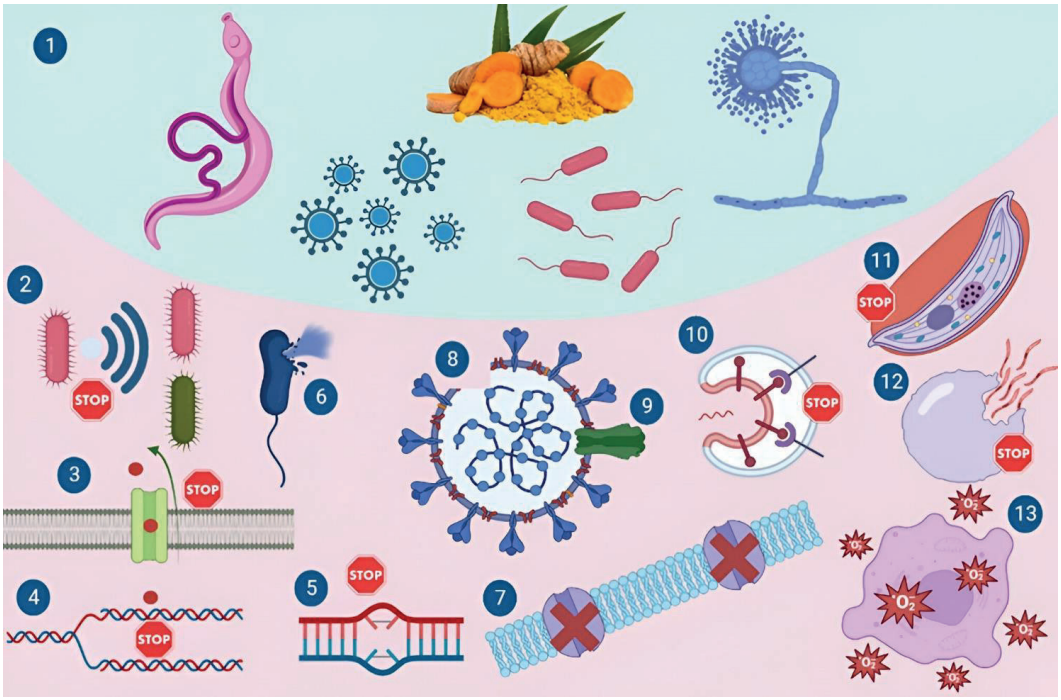

Figure 5. Main antimicrobial activities of curcumin. Created with BioRender. Legend: (**1**): Curcumin has biological activity against bacteria, fungi, virus and parasites; (**2**): inhibition of microbial signaling, as well as SOS response, the passage of drug resistance genetic information, and enzymatic signaling, among others. It can be between the same species or different species; (**3**): efflux pump inactivation; (**4**): inhibition of transcription and replication of genetic material; (**5**): inhibition of damaged DNA repair; (**6**): cell lysis and constituents loss; (**7**) synthesis inhibition or alteration of ergosterol in the fungal membrane, causing morphological imbalance and cell lysis. It can prevent the interaction of fungi with host cells, preventing infection; (**8**) Inhibition or alteration of the viral envelope with virus inactivation; (**9**) alteration of viral surface proteins, preventing the virus from infecting cells; (**10**): The alterations caused in items 8 and 9 cause viral inactivation and prevent new viruses from infecting host cells, fighting the infection; (**11**): acting on the cell cycle of parasites and blocking the formation of trophozoites, fighting infection; (**12**): blocking the parasitic cycle decreases the amount of trophozoites and prevents cells from being infected and (**13**): Increased ROS and oxidative stress.

4.2. Anticancer activity

The anticancer activity of curcumin is directly related to suppressing the initiation, progression, and metastasis of different cancer types, affecting carcinogenesis by acting on the angiogenesis and

tumor growth. This anticancer mechanism is mediated by the negative regulation of growth factors, transcription factors, protein kinases, inflammatory cytokines, and other oncogenic molecules important for the cancerous mass development. In view of the control of these oncogenic factors, the emergence of cancer cells and progression is disturbed and limited. This drug can act by inhibiting the phosphorylation of AKT in several cancer cell lines and, in this way, contributes to controlling the proliferation of cancer cells since its energy source is inactivated.(Hamzehzadeh et al., 2018)

Wang *et al.*(2020) aimed to investigate the anti-metastatic effect of curcumin in non-small cell lung cancer. Using a wound healing and transwell model, they evaluated cell migration and invasion, subsequently using real-time PCR they evaluated the involvement of miR-206 in these activities. It is worth mentioning that these molecules play a role in tumor suppression. It was observed that curcumin significantly inhibited cell invasion and migration due to overexpression of miR-206 and suppression of the PI3K/AKT/mTOR pathway.

The Janus kinase/JAK/STAT transducers pathway is responsible for the survival, proliferation and invasion of cancer cells. The expression of miR-99a has been reported in several cancers types, including bladder cancer, lung cancer, and liver cancer, among others. The anticancer potential of curcumin in this case is related to inhibiting cancer proliferation, invasion and migration, stimulating apoptosis, functioning in the upregulation of miR-99, and inhibiting the JAK/STAT signaling pathway. Furthermore, curcumin can inhibit the production of anti-apoptotic proteins (Bcl-2) and increase the production of pro-apoptotic proteins (Bax and cleavacaspasem-3/9). In this last case, the presence of curcumin provoked greater apoptosis of retinoblastoma cells. Furthermore, the same study reports a synergistic increase in the activity of antitumoral drugs associated with curcumin in thyroid cancer and stem cells.(H. Wang et al., 2021)

In order to determine the effect of curcumin on osteosarcoma, Zhou *et al.*(2020) studied the interference of different concentrations of this drug on cell proliferation and apoptosis (MG-63 and HOS) by flow cytometry. The authors evaluated the expression of miR-21 (promotes cell invasion and migration and is associated with poor prognosis of this type of cancer) and RECK (target of miR-21), in this type of cancer. It was observed by the authors that via miR-21, curcumin was able to positively regulate the expression of RECK, which consequently regulated Wnt/β-catenin signaling, inhibiting osteosarcoma.

Zhu *et al.*(2020) presented hopeful results in what would be a future therapy for the control of leukemias. The authors used an in vivo model of female BALB/c mice which received SHI-1 cells subcutaneously, which are an acute monocytic leukemia cell line. According to the authors, curcumin increased the level of apoptosis (**Figure 6A**) and decreased the invasion of SHI-1. Curcumin activated JNK and p38 while inhibited ERK and NF-κB signals, which caused a decrease in the amount of SHI-

1 tumor mass (**Figure 6B**). Furthermore, curcumin suppressed the metastatic potential of SHI-1 by down-regulating MMP9, MMP2 and vimentin expression. Finally, is worth highlighting that numerous other antitumor actions of curcumin are described in the literature, such as for: brain cancer (emphasis on glioblastoma multiform), breast cancer, colorectal cancer, cervical cancer, esophageal cancer, gastric cancer, nasopharyngeal cancer, oral cancer, ovarian cancer, pancreatic cancer, prostate cancer, renal cancer; skin cancer, and testicular cancer.(Alharbi et al., 2024; Arefnezhad et al., 2023; Atwan & Al-Ogaidi, 2024; Ganie et al., 2024; Hussein & Khaphi, 2023; W. Li et al., 2024; Ratan et al., 2023; Ryskalin et al., 2020; G. Wang et al., 2023; Xiao et al., 2024; B. Xu et al., 2023; Zhai et al., 2024; X. Zhang et al., 2023; T. Zhu et al., 2024) **Figure 7** summarizes some of the cancer types covered in this topic in which curcumin showed excellent activity.

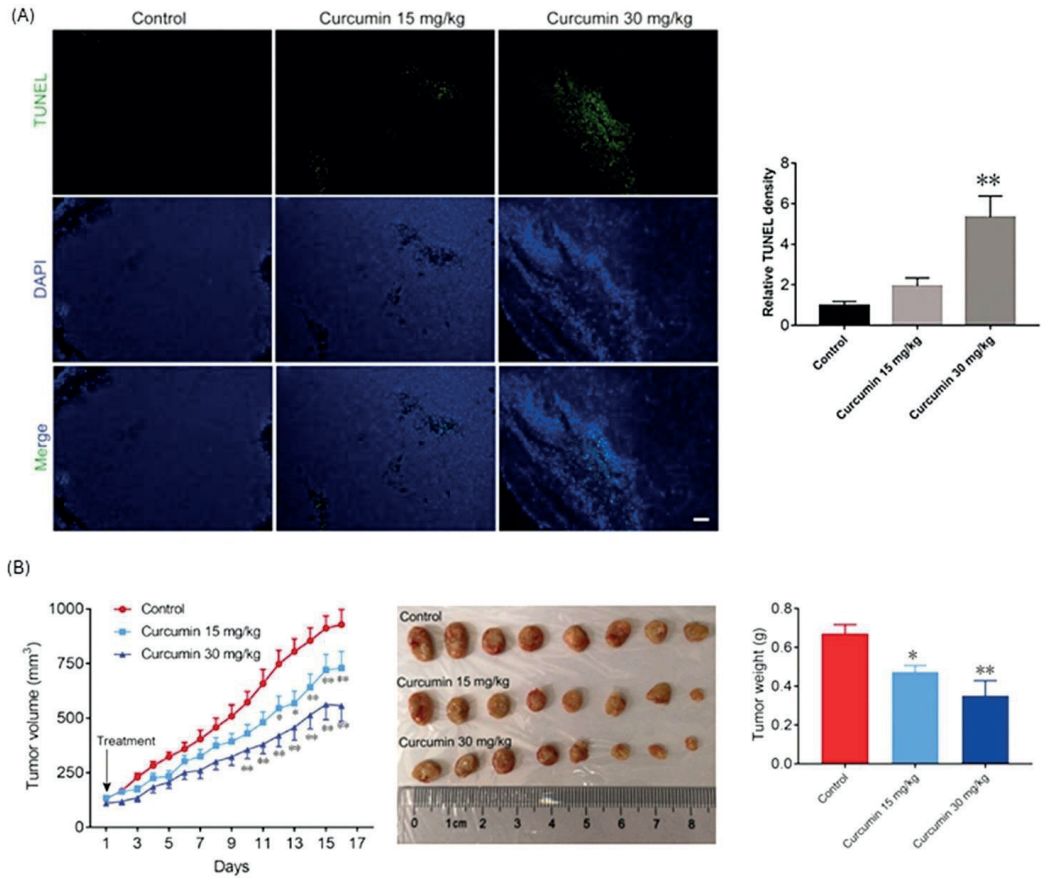

Figure 6. (A) Tumor sections stained by TUNEL showing that curcumin enhanced tumor apoptosis. (B) Curcumin reduced SHI-1 cells tumor growth *in vivo*. Reprinted with permission from (G. Zhu et al., 2020).

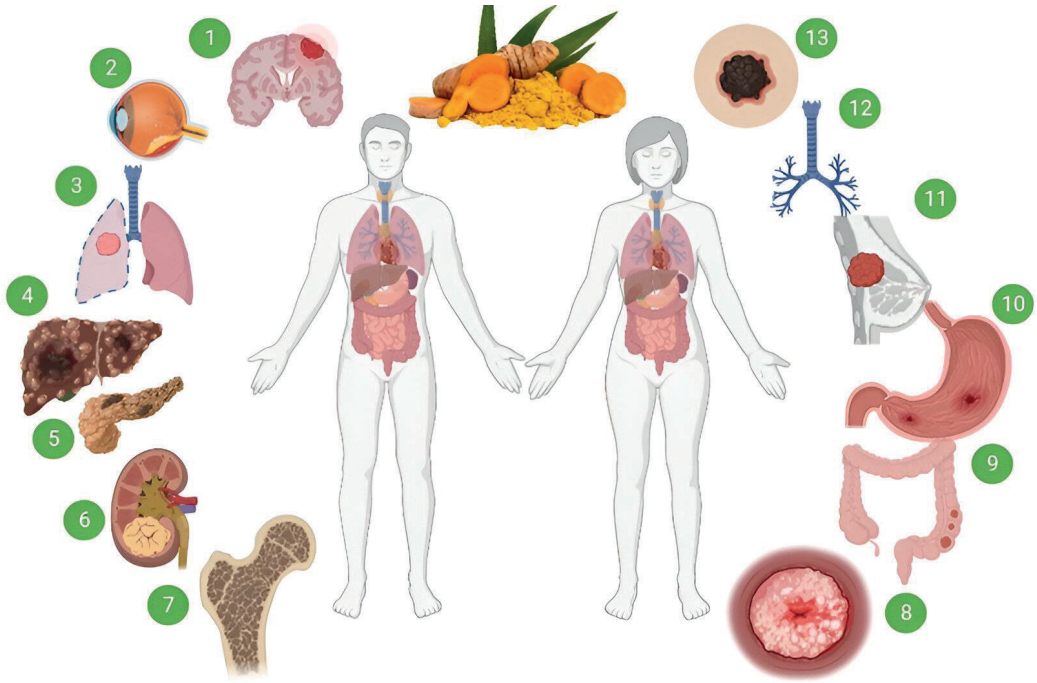

Figure 7. Types of cancer where curcumin has proven to be an excellent therapeutic agent: as well as brain anticancer activity (1); retinoblastoma (2); lung (3); hepatic (4); pancreatic (5); renal (6); osteosarcoma (7); cervical (8); intestinal (9); stomach (10); breast (11); tracheal/esophageal (12); skin (13); between others.

4.3. Activity in degenerative diseases

Neuroinflammation is a key factor in the development of Alzheimer's disease; curcumin potential action against this disease was studied *in vivo* by Liu *et al.*(2016) The authors used APP/PS1 transgenic mice with beta-amyloid-induced neuroinflammation in mixed neuronal and glial cultures. According to the *in vivo* assay, the authors observed memory deficits, indicated by more distant escape latency in tests containing the Morris water maze and accumulation of Aβ in the hippocampus. However, treatment with curcumin showed a significant decrease in escape latency from day 3 to day 5 in the training experiment. Furthermore, untreated mice showed decreased memory as this group showed a decrease in the number of platform crossings, increased travel distance, and time spent in the target quadrant. The curcumin-treated group showed an increase in the number of platform crossings and time spent in the target quadrant, while it showed a decrease in travel distance. Another important result was that curcumin protected cholinergic neurons, which prevents memory loss. It was

observed that curcumin was capable to inhibit the nuclear factor kappa B (NF-κB) signaling pathway, suggesting that this drug has an action in suppressing neuroinflammation. Finally, the results involving neural cells and glia showed that treatment with curcumin caused a decrease in inflammatory mediators, confirming the finding in the *in vivo* study where it was pointed out that curcumin is able to suppress neuroinflammation.

Another commonly diagnosed neurodegenerative pathology is Parkinson's disease, a slowly progressive multisystem disorder that affects the dopaminergic neurons of the substantia nigra pars compacta. Curcumin may contribute to the treatment of Parkinson's disease through the modulation of multiple transduction pathways. A study pointed to the interaction of curcumin in z-transcription proteins (STAT), growth factors and their receptors, cytokines, enzymes, and genes with cellular apoptosis functionality. This drug decreases the number of free radicals and helps to protect mitochondria, an important organ in cell homeostasis, preventing the disease progression.(Nebrisi, 2021)

According to Yu *et al.*(2016), astrocytes are associated with pro-inflammatory activity in the central nervous system, triggering Parkinson's disease. Therefore, the authors evaluated the protective potential of curcumin in primary astrocytes stimulated by the ion 1-methyl-4-phenylpyridinium-(MPP+-). According to the results, the presence of MPP+ caused the production of cytokines and ROS. However, cell wells treated with curcumin showed significantly lower levels of these cytokines and ROS. Curcumin also shows neuroprotective potential to regulate the BDNF and PI3k/Akt signaling pathways present in Parkinson's disease, slowing down the disease.(Jin et al., 2022) Additionally, other neuroprotective mechanisms of curcumin are been described, like antioxidant activity, reduction of nitric oxide and protecting brain cells from lipid peroxidation, prevention the formation of amyloid oligomers Aβ1-42, and disaggregation of formed fibrils, among others(Askarizadeh et al., 2020)

Huntington's disease is a progressive neural pathology, with a dominantly hereditary characteristic, caused by altered expansion of the polyglutamine repeat within the Huntingtin protein. A study pointed to the important role of curcumin in stopping the progression of Huntington's disease through a transgenic *Drosophila* model expressing Httex1p peptides Q93 and Q48. According to the results, treatment with curcumin did not cause harm to flies, acting as a protector against the cytotoxic effects of polyglutamine, the main cause of Huntington disease. The group that received food supplemented with curcumin showed an improvement in the control of neurodegeneration, progressive degeneration in the eyes, less alteration in motor function, and a decrease in ocular dysmorphology in transgenic *Drosophila* models.(Chongtham & Agrawal, 2016)

4.4. Anti-inflammatory activity

Finally, it is worth highlighting the anti-inflammatory activity of curcumin, considered one of its most powerful properties and often linked to other activities already mentioned above, interferes (synergistically) with some other types of target diseases. Curcumin has been shown to have a wide range of actions at the cellular level, such as expression of cytokines, enzymes, and regulation of transcription factor levels.(Aggarwal et al., 2024; Jamil et al., 2023) In a study, the anti-inflammatory potential of curcumin was evaluated in participants who were previously diagnosed with SARS-CoV-2. According to the clinical results, participants who received curcumin treatment (for 4 weeks) showed a reduction in pro-inflammatory IL-6 and monocyte chemoattractant protein (MCP-1) when compared to participants who received placebo treatment.(Fessler et al., 2023)

Sun *et al.*(M. Sun et al., 2022) evaluated the protective potential of curcumin against experimental autoimmune encephalomyelitis (EAE). According to the results, the presence of curcumin attenuated the severity of EAE in rats when compared to the control group. Furthermore, decreased serum levels of IL-6 and TNF-α (inflammatory cytokines) as well as increased IL-10 and TGF-β (protective cytokines) were reported in the group treated with curcumin and recombinant growth specific 6 (rGas6). So, curcumin treatment could inhibit the microglia-mediated inflammatory response by blocking the AXL/JAK2/STAT3 signaling pathway.

A study involving participants with metabolic syndrome showed that curcumin treatment decreased serum concentrations of TNF-α, IL-6, TGF-β, and MCP-1 (pro-inflammatory cytokines). In the group treated with placebo, the study showed that the values of IL-6, TNF-α, and MCP- remained unchanged at the end of the treatment. Therefore, comparing the group treated with curcumin and treated with placebo, the decrease was statistically significant ($p<0.001$).(Panahi et al., 2016)

5. Use of nanocarriers to improve curcumin solubility, stability and bioavailability

The potential pharmacological properties of curcumin have attracted great attention over the past years. Nonetheless, its clinical application is severely hampered by its extremely low-aqueous solubility (and instability) in physiological pH [13–17] (*i.e.*, 0.0004 mg ml^{-1} at pH 7.3).(Idoudi et al., 2022) Moreover, its low-cellular uptake, chemical instability, poor absorption, rapid metabolism, and clearance are responsible for its poor bioavailability, and suboptimal therapeutic effects.(Obeid et al., 2023)

Curcumin encapsulation in nanocarriers is an emerging solution to overcome these limitations. Nanoformulations enable the increase in solubility, the protection against the environment (hydrolysis inactivation), and the improvement of pharmacokinetic properties leading to an increase in cellular uptake rates and therapeutic efficiency at the site of action. Moreover, such formulations can also

reduce side effects and toxicity.(Gayathri et al., 2023) The characteristics of the nanoformulation, some of them shown in **Figure 8**, are responsible for their behavior inside the body. Despite their size, size distribution, and shape, factors like stiffness, porosity, topography, coating, and targeting molecules can control the responsiveness of the nanosystems and their biological effects.(Mitchell et al., 2021)

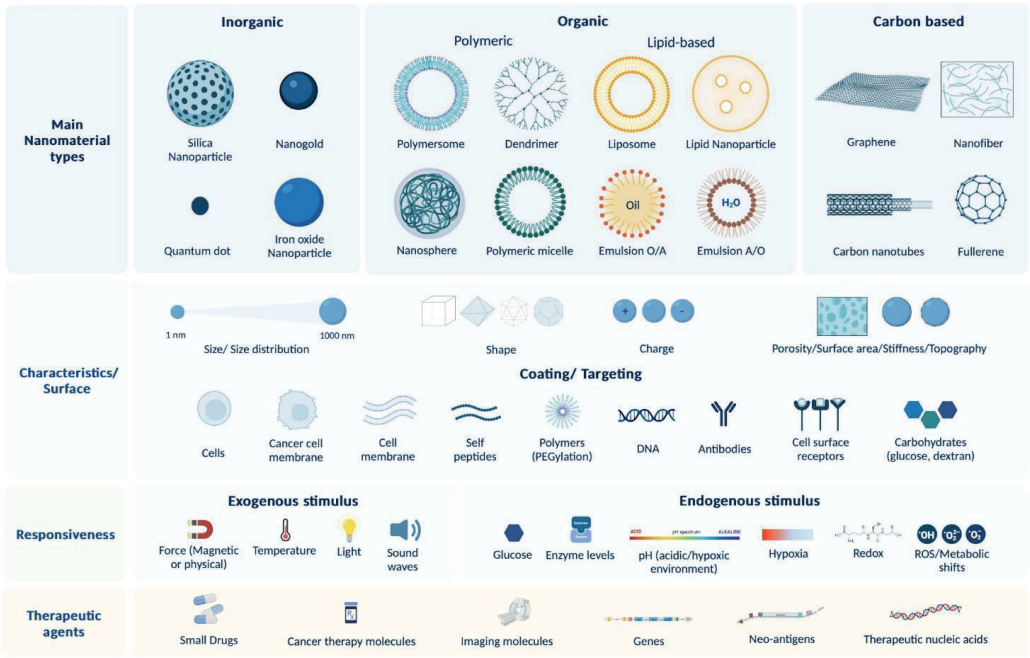

Figure 8. Classes, characteristics, surface, responsiveness and therapeutic agents of NPs: possible engineering to enhanced delivery of different nanosystems. Created with BioRender

Depending on the design, some formulations are targeted for long time circulation and retention in the body, while others have cellular delivery and intracellular release mechanisms. (Gayathri et al., 2023; Mitchell et al., 2021) Sustained release systems like poly-lactic-co-glycolic acid (PLGA) nanoparticles that undergo enzymatic hydrolysis to release the drug in a sustained manner, are capable of increasing curcumin retention in the body.(Sufi et al., 2020) Furthermore, negatively charged particles, like the solid lipid nanoparticles containing a novel curcumin derivative synthesized by Wei *et al.*(Wei et al., 2022), are prevented from combining with plasma proteins. This fact in addition to improving their stability, prolongs the circulation time in the human body. On the other hand, positively charged nanoparticles, such as amino functionalized MCM-41 (a type of mesoporous silica nanoparticle) loaded with curcumin, have the advantage of having greater cell uptake when compared

to negatively charged ones due to their electrostatic interaction with the cells.(Jambhrunkar et al., 2014) Finally, it is worth highlighting that nanoparticle functionalization can direct nanoformulations to cellular delivery. Medaglia *et al*.(Medaglia et al., 2024), for example, developed mesoporous silica nanoparticles loaded with curcumin and capped with polymyxin B. The work is based on the idea that in the presence of bacteria (especially Gram-negative) polymyxin B would unblock the mesopores by having greater interaction with the lipopolysaccharides present in the outer membrane of Gram-negative bacteria, thus releasing curcumin at the target site.

According to Joudeh and Linke(2022), NPs are generally categorized into four classes based on their composition: (1) inorganic NPs like silica, silver, copper, zinc, gold, iron, titanium oxide and quantum dots; (2) organic NPs like polymeric nanoparticles (PNPs) and nanospheres (solid matrix systems), nanocapsules (cavities surrounded by a polymeric membrane or shell) which are further divided into shapes (e.g., polymersomes, micelles, and dendrimers), and lipid-based NPs, namely liposomes, lipid NPs, and emulsions; (3) carbon-based nanomaterials like graphene, nanofibers, nanosphere, and fullerene; and (4) composite NPs (hybrids), which contain a combination of different nanomaterials. Each class is associated with numerous advantages and disadvantages regarding cargo, delivery, and patient response. **Table 4** describes the advantages and disadvantages of each of them.

Table 4: advantages and disadvantages of each nanoparticle type

Type	Advantages	Disadvantages	Reference
Inorganic	-Low toxicity; -Good biocompatibility; -Rich functionality; -Versatile; -Highly stable (especially when compared to organic nanoparticles); -Chemical inertness; -High cellular uptake; -Non-immunogenic response;	-Low cell transfer efficiency (which can be overcome with functionalization)	(Khalid et al., 2020; Paul & Sharma, 2010; Z. P. Xu et al., 2006)
Organic	-Not toxic; - Biocompatibility -Biodegradability;	-Low chemical stability; -Prone to microbial contamination; -Undesirable effects of the organic solvents used during its synthesis;	(Ijaz et al., 2020; Paul & Sharma, 2010)
Carbon-based	-Good thermal and electrical conductivity; -High-temperature resistance; -Versatile; -Chemical inertness; -Good biocompatibility; -Easy translocation across the cell membrane; -Low toxicity;	-Poor material toughness; -Poor dispersibility;	(Ijaz et al., 2020; Khalid et al., 2020; Wu & Mu, 2022)
Hybrids	-Combine interesting properties of more than one type of material;	-The synthesis process is often challenging (integration of incompatible materials)	(Khalid et al., 2020)

Nanoparticles can be produced using different methodologies mainly, physical, chemical, or biological.(Venkatas et al., 2022) Physical methods like sonication, membrane filtration, or ion exchange are characterized by a simple procedure and a sizable production. However, is a costly methodology since it requires plenty of energy consumption and specific equipment. Chemical methodologies are simple techniques that enable better control over NPs characteristics and tight size distribution. Condensation, oxidation, reduction, and electrochemical destruction are some examples.(Rai et al., 2015) These require external factors, for instance, temperature or pH, extended reaction time, and toxic materials. Biological or green methods are eco-friendly procedures that instead of using toxic chemicals use plant extracts, bacteria, viruses, or even fungi. This inexpensive approach is revolutionizing the creation of NPs.(Madani et al., 2022) Moreover, despite all the advantages there is still reduced knowledge about the control over particle size and shape, extraction of raw materials, and quality of final products.(Ying et al., 2022) It is also worth highlighting that a trend in the design and optimization of new formulations is the use artificial intelligence (AI) methods since they allow predicting their possible characteristics.(Khedri et al., 2022)

Tables relative to curcumin nanoformulations developed over the past years and clinical trials conducted on these formulations have been published elsewhere(Sharifi-Rad et al., 2020) In this review, we focused on the discussion of recent publications, since 2023, which are outlined in **Table 5**.

Table 5: Highlights of recent studies (from 2023) using nanotechnology to improve curcumin performance.

Type	Nanocarrier	General description	Nanomaterial characteristics remarks	Average diameter	Shape	Encapsulation efficiency	Method of production	Use	References
Inorganic nanoparticle	AgNPs	Cur–AgNPs	Strong antibacterial activity; huge surface area; cytotoxic effects (due chemical agents during synthesis)	40.71 ± 18 nm	Spherical	Not applicable	Reduction of AgNO3 with a solution containing hydroxypropyl-β-cyclodextrin and cur	Wound Dressing	(Aldakheel et al., 2023)
	ZnO Nanocomposite	Cur-ZnO nanocomposite	The nanoparticle material has been identified as a potential therapeutic agent for diabetes.	30±5 nm	Spherical	$8.1x10^{-6}$ mol l^{-1}	Mixture of Cur and ZnO solutions (for granulation and surface adsorption	Diabetes	(El-ghannam et al., 2023)
	Mesoporous glass NPs	SiO_2–CaO–P_2O_5 glass nanoparticles enriched with Zn^{2+} ions and loaded with Cur	Adjustable pore size shape and connectivity; biodegradability; capability load different compounds; control drug release; biological behavior can be improved	From 153 (±22) to 255 (±27)	Spherical	NA	Sol-gel method (microemul- sions of water, ethyl acetate (EA) and hexadecyltrimethylammo- nium bromide)	Bone regeneration	(Sánchez-Salcedo et al., 2023)
	AuNPs	Cur-coated AuNPs	Stable in physiologic solutions; good cellular uptake	22.2 ± 12.7 nm	Spherical	~230 μM (it as assumed that all Cur used corresponds to	Mixture of Cur solution with tetrachloroauric acid trihydrate solution (3	Antiparasitic (*Leishmania Major*)	(Amini et al., 2023)

						the amount in the NPs)	h stirring followed by 3 days to complete reaction)		
Organic Polymeric-based	Polymeric NPs	Cur-loaded chitosan NPs	Biodegradable; low toxicity; mucoadhesive; provide controlled release; prolong blood circulation; limit nonspecific uptake	20–30 nm	Semi-spherical	NA	Ionic gelation technique	Confronting reproductive toxicity	(Mohamed et al., 2023)
	Polymeric NPs	Cur-gelatin NPs	High specific surface area	272.19	Spherical	37.85%	Precipitation	Bacterially infected wounds	(Cai et al., 2023)
	Polymeric NPs	Cur-loaded in HPMC E15 and Poloxamer 407	Biocompatible; biodegradable; inert; mucoadhesive; sustained release ability; lubricant	170.2 nm	Spherical	90%	Precipitation (followed by submission to a high pressure homogenizer)	Dry eye disease	(Laddha et al., 2023)
	Core-shell	Intrinsic-protein aggregates (core) and Cur bounded with oleosome proteins (shell)	Reversible disassembly/reassembly properties; high stability, plasticity, and biocompatibility	NA	Putamen structure	81.24%	Disassembly and reassembly of oleosome proteins induced by guanidine hydrochloride	Carry Cur	(Y. Sun et al., 2023)
	Polymeric NPs	Cur-loaded PLGA embedded	Controlled drug delivery ability; biocompatible;	217.2 ± 5.2 nm	Spherical	69.98%	Emulsification-solvent diffu- sion method	Cell bioimaging	(R. Wang et al., 2023)

	in polyvinyl alcohol	biodegradable; increase cell uptake						
Polymeric NPs	Acetalated dextran Cur-loaded NPs coated with tanic acid	Biocompatible; pH-responsive; enhance biological responses; improve the delivery in the target site	321.1 ± 8.7 nm	Irregular and blunt spheres	40.7 ± 5.5%	Microfluidic-based nanoprecipitation	Tendinitis	(Molinaro et al., 2023)
Polymeric NPs	Core-shell PLLA/PLGA NPs loaded with Cur	Sustained release properties; host for different hydrophobic bioactive.	From 150 to 200 nm	Spherical with a rough surface	53–56%,	Membrane-assisted core-shell entrapment	Cur encapsulation	(Lamch, 2023)
Polymeric NPs	Lactoferrin, (−)-epigallocatechin gallate, and hyaluronic acid NPs with Cur	Improve cellular uptake	145 nm	Spherical	86%	pH-shift method	Improve bioavailability and bioactivity	(X. Li et al., 2023)
Polymeric NPs	Cur- Gum Arabic NPs	Reduced degradation in the gastric digestion phase	~500 nm	Spherical	0.51 µg/mg	Mixture of Cur and Gum Arabic solutions followed by rotary evaporation and freeze-drying	Improve stability and bioavailability	(Ai et al., 2023)
Polymeric NPs	Cur-Zein/caseinate-alginate NPs	Good stability against heat and high ionic strengths	177 nm	Spherical	83%	pH-shift method/electrostatic deposition method	Nutraceutical delivery	(Y. Huang et al., 2023)

	Core-shell	Cur-zein NPs (core) with carrageenan (a gelled polysaccharide as shell)	Biocompatible; safe; renewable; degradable; mucoadhesive; sustained release; limited resistance to acids	351.8 nm	Spherical	93.2%	Ultrasonication and magnetic stirring of a solution containing zein and Cur. This mixture were injected into ι-carrageenan under stirring, and finally solution of calcium chloride was injected into this mixture for cross-linking of the shell.	Cur encapsulation	(Ge et al., 2024)
	Biomolecule (pullulan)-based nanoparticle	Nano-cur	Solvent-free	≈ 31.63 nm	Spherical	59.19 % (conversion rate)	Microbial (*Aureobasidium pullulans*) fermentation	Report nanoparticle production and antioxidant activity	(Katiyar et al., 2024)
Organic Lipid-based	Liposome	Cur Nanoliposomal Delivery Systems	Biodegradable; biocompatible, safe; physical stability, protection in gastrointestinal milieu; enhanced cellular uptake; large scale production is a field that can be improved	From 224 to 345 nm	Spherical	From11.12 to 89.71%	Simil-microfluidic technology	Improve encapsulating capability of Cur	(Rahman et al., 2023)
	Liposome	Cur Nanoliposomal	Structure similar to cell membrane (favor drug	From 224 to 345 nm	Spherical	From11.12 to 89.71%	Simil-microfluidic technology	Improve encapsulating	(Piano et al., 2023)

	Delivery Systems	penetration); biocompatible; low toxicity and immunogenicity; controlled release; enhance drug intestinal absorption; continuous and large-scale production are fields to be improved					capability of Cur	
Liposome	Cur liposomes	Biocompatible; lubrication properties; facile preparation; traditional preparation methods are difficult to scale up	132.9 nm	Spherical	97.08%	Microfluidics, combined with Box-Behnken Design	Treatment of inflammatory osteolysis	(S. Huang et al., 2023)
Liposome	Soy phosphatidylcholine and hydrogenated SPC cur liposomes	Safe; no toxic; no immunogenic; biodegradable; biocompatible;	127.46 and 136.1 nm respectively	NA	72.88% and 62.12% respectively	Solvent evaporation method	Bladder cancer	(Gholami et al., 2023)
Liposome	Cur + Colistin liposome functionaliz	Able to co-encapsulate drugs; can fuse with cell membranes;	≈100 nm	Spherical	3.02% -3.55%	Thinfilm hydration method	Colistin resistance in bacterial infections	(Qin et al., 2023)

		ed with PEG	improve cellular uptake;						
Carbon based	Carbon quantum-dots	Green CQDs loaded with Cur	Extremely small size (less than 10 nm); low toxicity; excellent fluorescent nanomaterial; transmembrane carrier	3.07nm	Spherical	NA	Hydrothermal method	Improve the solubility and antioxidant performance of Cur	(Wen et al., 2023)
Hybrid	Carbon nanodot-chitosan NPs	Cur-carbon nanodot-decorated chitosan Nps	Facile preparation; low cytotoxicity; biocompatibility; biodegradability, mucoadhesive; pH-responsiveness	5,51 nm	Spherical with porous shape	NA	One-pot hydrothermal carbonization (to obtain Cur-carbon nanodot) and ionic gelation (to obtain chitosan NPs). Under stirring with the add both NPs was cross-linked with TPP	Hepatocellular Carcinoma	(Ilhan, 2023)
	Mixed lipid-polymer NPs	Phospholipid DMPC plus PDMAEMA-b-PLMA loaded with Cur	Safe; biocompatible; biodegradable; ease functionalization; structurally stable; no payload leakage; greater storage stability	≈ 100 nm	Spherical	99.8 % ± 4.1 %	Thin-film hydration method	Antibacterial therapy	(Naziris et al., 2023)
	Hybrid Graphene quantum-dots	Smart system based on magnetic	Targeted drug delivery; biocompatibility; low toxicity;	≈ 23 nm	N.A	N.A	One-step co-precipitation method	Multifunctional anticancer drug carrier	(Seyyedi Zadeh et al., 2023)

	GQDs-Fe_3O_4, functionalized by FA and loaded with Cur	photoluminescence capacity; stability	

Legend: Cur: curcumin; Silver nanoparticle (AgNPs) Silver nitrate ($AgNO_3$); Zinc oxide (ZnO); Gold nanoparticle (AuNPs); Hydroxypropyl Methylcellulose (HPMC); Poly(lactic acid−glycolic acid) (PLGA); Poly(L-lactide)/poly (lactide-co-glycolide) (PLLA/PLGA); Carbon quantum-dots (CQDs); tripolyphosphate pentasodium (TPP); Poly(2-(dimethylamino)ethyl methacrylate) (PDMAEMA); Poly(lauryl methacrylate) (PLMA); Graphene quantum-dots (GQDs); Iron oxide (FeO4); Formic acid (FA); Not available (NA).

5.1 Inorganic NPs

Based on non-carbon sources and metals, inorganic NPs stand out due to their distinctive optical and magnetic properties, large surface area, diversified surface chemistry, and controllable structures.(Q. Liu et al., 2021) In addition to incorporating curcumin into inorganic nanoparticles, it can be used as a green reagent in the synthesis of metallic nanoparticles like in the study carried out by Aldakeel *et al.*(2023) where curcumin was used as the reducing agent in the synthesis of silver nanoparticles. After, those nanoparticles were dispersed in a sodium alginate and gum arabic hydrogel in order to obtain a more biocompatible dressing for treating infections and wound healing. Curcumin-nanoparticles presented a size range between 20-70 nm by DLS and 40.71 nm by TEM, with a predominantly spherical morphology. The biological results showed that the developed nanoparticle have cytocompatibility in the three mammalian cell lines tested. Finally, the incorporated hydrogel showed substantial antibacterial activity against both gram-positive and gram-negative bacteria. In conclusion, the synthesis of curcumin-silver nanoparticle incorporated into the hydrogel was successful and environmentally friendly synthesized and therefore can be considered as a future therapy in the management of persistent wound infections.

5.2 Organic NPs

The research around organic NPs is increasing due to their biodegradability, non-toxicity, non-covalent intermolar character plus sensibility to heat, light temperature, and electromagnetic radiation.(Joudeh & Linke, 2022) Mohamed *et al.*(2023) developed a polymeric chitosan nanoparticle loaded with curcumin to control the reprotoxic potential of the pyrethroid fenpropathrin in rats. According to the characterization results, it was observed by FTIR that curcumin was incorporated into the nanoparticle due the presence of curcumin in the chitosan nanoparticle spectrum. The TEM images showed semi-spherical nanoparticles, ranging between 20-30 nm with interconnected structures. In contrast, the size of nanoparticles by DLS was 190 nm on average. The *in vivo* results showed that treatment with free curcumin and, mainly, curcumin incorporated into the chitosan nanoparticle had restorative effects on semen quality, sex hormone levels, antioxidant potential, and mRNA expression of target genes. Histological tests showed normality in the group treated with free and incorporated curcumin compared to the group treated with the pyrethroid fenpropathrin, which presented higher weight and smaller size. Furthermore, this better biological action was notably evidenced for loaded curcumin, which points to a promising protective therapy and control of reproductive toxicity.

With the aim of improving the bioavailability of curcumin, Ai *et al.*(2023) incorporated curcumin into a polymeric nanoparticle containing gum arabic. According to the DLS results, the

nanoparticles ranged from 457.4±7.1 to 470.1±6.3 nm. The PDI ranged from 0.10±0.04 to 0.23±0.05 and zeta potential results from −21.83 ± 0.32 to −19.33 ± 0.21. The encapsulation efficiency of curcumin decreased when the concentration increased, ranging from 6.37±0.04 to 0.86±0.01%. The FTIR results show that the -C–O–C-, -CH, –C=O groups may be related to the interaction of curcumin with gum arabic. According to the fluorescence tests, the presence of gum arabic provided greater solubility of curcumin in a medium containing water without alcohol. Another very important factor was that the nanoparticle increased the stability of curcumin against exposure to light. According to the results, the retention of free curcumin decreased to 27.4% after 5 h in contact with light. However, the curcumin content remained at 82% when found in the nanoparticle. Finally, the nanoparticle improved the bioavailability of curcumin in a simulated digestive process. According to the results, the amount of free and incorporated curcumin bioavailable in the simulated digestive system was 0.11 and 3.39 μg mL^{-1}, respectively. Furthermore, the authors changed the medium pH and observed that the bioavailable amount was lower, 2.82 μg mL^{-1}, suggesting that changes in pH may affect the bioavailability of the curcumin loaded into the nanoparticle containing gum arabic. In conclusion, gum arabic nanoparticles can be considered a promising system to improve the bioavailability of curcumin for application in salt-containing food systems.

Liposomes have also proven to be widely used to increase the bioavailability of curcumin. In pursuit of this, Gholami *et al.*(Gholami et al., 2023) developed liposomes based on soy phosphatidylcholine (SPC) and hydrogenated SPC (HSPC) with the therapeutic target of lung cancer cells. By DLS it was observed that the liposomes encapsulated with drug had a size of 127.46 and 136.1 nm respectively and both had zeta potential with a negative charge (-2.89 and -1.66 respectively). As for encapsulation efficiency, values of 72.88% and 62.12% were observed respectively. It is also worth highlighting that both formulations showed sustained release. Both formulations were stable during storage for a period of 14 weeks at 4°C. In accelerated stability tests carried out at different pH (several points from 3.5 to 12) the systems showed greater stability compared to the free drug. In *in vitro* cellular tests, it was observed that both formulations significantly increased cytotoxicity and cellular uptake in bladder carcinoma cells (HTB9).

Li *et al.*(2023) aimed to improve the dispersibility and stability of curcumin by its incorporating into nanoparticles containing (−)-epigallocatechin gallate, lactoferrin, and hyaluronic acid using the simple pH-shift method. DLS results showed that at pH between 6-7 the nanoparticles had sizes of 174.7 and 205.4 nm. The PDI was less than 0.25 with an electronegative charge. The TEM and SEM results pointed to a spherical morphology with uniform distribution, with an average diameter of less than 100nm. The encapsulation efficiency results showed that the lower the ratio of curcumin with lactoferrin and (−)-epigallocatechin gallate, the greater the loading capacity, ranging from 1.6 to

13.5%, and the encapsulation efficiency decreases from 90.9 to 66.8%. It is worth highlighting that the incorporation improved the stability of curcumin when exposed to light, storage, and temperature. In the *in vitro* studies it was observed that the bioavailability and absorption of curcumin by cells was better when incorporated into nanoparticles. Furthermore, incorporation improved redispersibility. Finally, biological tests indicate that incorporated curcumin showed a significantly better apoptosis rate in colorectal cancer cells when compared to free curcumin. It is therefore concluded that biopolymer nanoparticles can be used to improve the bioavailability and biological activity of this drug.

Rahman *et al.*(2023) developed and characterized solid lipid nanoparticles loaded with curcumin for lung cancer application. According to the characterization results, the nanoparticles had a size of 114.9 nm, PDI of 0.112, and zeta potential of -32.3 mV. However, when the nanoparticles were freeze-dried, the size was 119.5 nm, PDI was 0.124, and zeta potential was -34.6 mV. The encapsulation efficiency and loading capacity were 69.74 and 0.81%, respectively. Finally, TEM images showed that the nanoparticles loaded with curcumin had spherical shape and a smooth surface. The biological results involving cytotoxicity in lung cancer cells showed that the nanoparticle containing curcumin had a greater cellular uptake capacity (682.08 ± 6.33 ng μg^{-1}) compared to free curcumin (162.4 ± 4.2 ng μg^{-1}). Furthermore, the absorption of curcumin by cancer cells was greater when incorporated into nanoparticles. In conclusion, nanoparticles can be considered an efficient curcumin release system in the control of lung cancer, however, more studies need to be carried out to reinforce the results.

Finally, it is worth highlighting an example of co-encapsulation system with curcumin. In the study carried out by Qin *et al.*(Qin et al., 2023) by the checkerboard assay, it was observed that curcumin is capable of reversing bacterial resistance to colistin. Therefore, the authors developed a formulation composed by liposomes functionalized with poly(ethylene glycol) (PEG) and co-encapsulated with curcumin and colistin. The synthesized particles had a size of approximately 100 nm and a zeta potential of -7.6 mV. Through *in vitro* tests (with *Escherichia coli*), it was observed that when in the system, this drug combination was more efficient than when free. Furthermore, the system was also capable of improving the affinity of cystine - bacterial membrane, also improving curcumin cellular uptake leading to a decrease in the pump activity favoring the synergistic effect of the drugs. The effectiveness of this formulation was also demonstrated by an *in vivo* model of intestinal bacterial infection (in mice) with the same bacteria mentioned above.

5.3 Carbon-based NPs

As a result of their unique physical and chemical properties: regarding their structure, they can be obtained in various allotropic forms (depending on the carbon hybridization) like carbon nanotubes, graphite, graphitic carbon nitrate, diamond, among others; with respect to their high thermal conductivity (~ 5000 W m^{-1} K^{-1} for graphene for example) and electrical conductivity (fast heterogeneous electron transfer); their high mechanical strength; and their excellent optical activity.(Debnath & Srivastava, 2021; Madima et al., 2020) Carbon-based NPs have been used for an extensive range of applications, from drug delivery to bioimaging.(Maiti et al., 2019) Wen *et al.*(2023), in their study, used an environment-friendly method for the preparation of green tea carbon quantum dots (CQDs) loaded with curcumin. The system revealed light and salt solution stability plus excitation wavelength dependence. The microscopy results showed nanoparticles with good distribution, spacing, almost no agglomeration, and a spherical characteristic with average size of 3.07 nm. Additionally, the antibacterial performance of curcumin was preserved, and its antioxidant activity and solubility were enhanced, highlighting the potential of this formulation. In conclusion, the system resulted in a potent antioxidant and antibacterial agent from a natural source.

5.4 Hybrid NPs

Hybrid nanomaterials result from the conjugation between inorganic and/or organic materials. These synergistic advanced materials are characterized by distinctive versatility, particular performance, and properties.(Vargas-Bernal, 2020) Metal–organic frameworks (MOFs), for example, are hybrid materials that result from the coordination between metal clusters or ions and organic ligands. Its adjustable physical and chemical properties, controllable size distribution, sizeable surface area, and appropriate pore volume are responsible for superior drug loading compared to tradition nano-drug carriers.(Linnane et al., 2022)

Zadeh *et al.*(2023) synthesized a hybrid targeted multifunctional anticancer drug delivery system, GQDs conjugated with formic acid (FA) and loaded with curcumin (Cur/GQDs-Fe3O4-FA), **Figure 9**. According to TEM results, the nanoparticles had size of approximately 23 nm, spherical shape with aggregation in certain places. Despite enhancing the efficiency of curcumin, the carriers exhibited superparamagnetic behavior leading to dislocation to the tumor site when a magnetic field is applied. According to the cytotoxicity results, even at the highest concentration, the group treated with incorporated curcumin showed 95% cell viability. As for the anticancer potential, the viability of cancer cells treated with incorporated curcumin (80, 40 μg ml^{-1}) decreased with increasing concentration, reaching 2% cell viability. However, cell viability is higher for the group treated with incorporated curcumin. On the other hand, at low concentrations (5, 10, 20 μg mL^{-1}), the group treated

with incorporated curcumin has lower cell viability. Therefore, the multifunctional carrier containing curcumin could be a promising tool in anticancer therapy, including drug delivery systems.

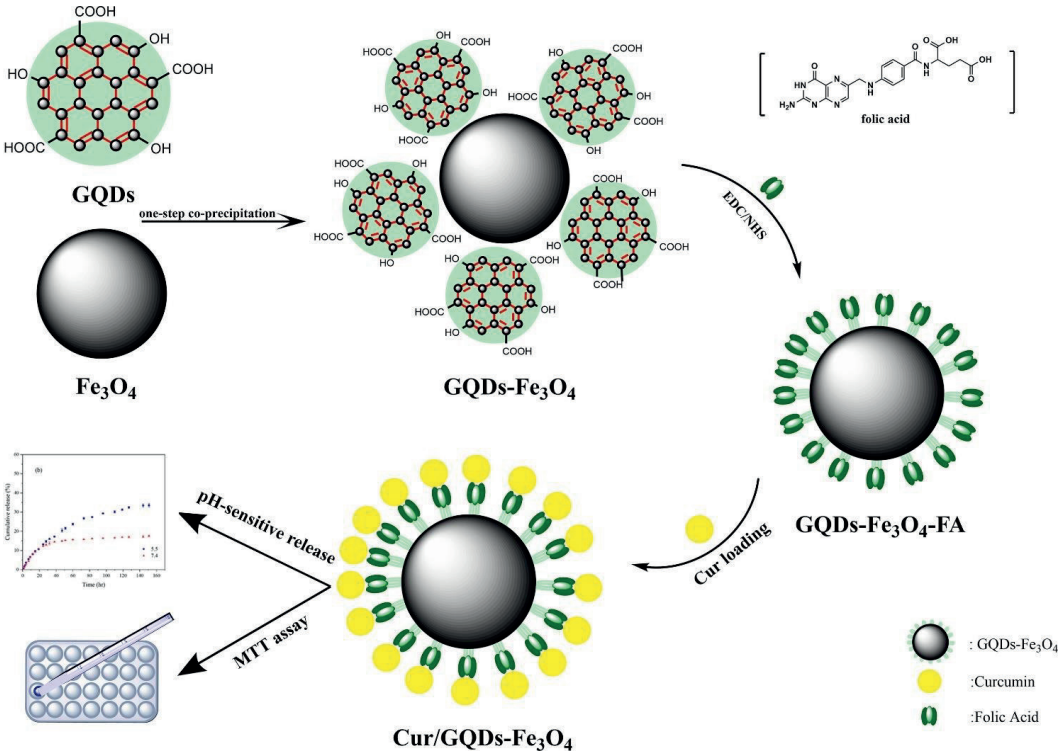

Figure 9. Representation of the developed hybrid particle. Reprinted with permission from (Seyyedi Zadeh et al., 2023)

6. Conclusions and future perspectives

Nutraceuticals are a class of food-derived products that have beneficial properties to the health and wellness of to the body. Curcumin is increasingly proving to be a powerful nutraceutical due to several benefits for human health, being evaluated against degenerative diseases, diabetes, liver diseases, cancer, and diseases of infectious origin. However, in order to obtain an isolated chemical substance that maintains its active biological properties, it is essential to know its physicochemical characteristics to preserve its activity both in the cultivation and extraction and purification phases. Nowadays, where environmental preservation is increasingly valued, it is worth highlighting that greener extraction methods, where fewer organic solvents are used, are preferable and are increasingly gaining ground.

Moreover, the use of nutraceuticals insoluble in aqueous solvents has the disadvantage of being poorly absorbed by the body. In addition to this issue, curcumin also has extensive catabolism and low chemical stability. In this sense, nanotechnology is a trend that has been observed as being the topic of research involving technologies which would be able to circumvent these limitations. However, it is worth highlighting that each type of nanocarrier (inorganic, organic, carbon-based, and hybrid) has its own characteristics and advantages. Furthermore, the choice of nanocarrier must be carefully evaluated and considered since its physico-chemical characteristics can control the responsiveness of the nanosystems and their biological effects. According to the survey here performed, it was possible to observe that curcumin associated with nanotechnology has been the topic of several studies in this year. This highlights that due to the therapeutic potential of this drug, the scientific community increasingly seeks to overcome its limitations through technology to provide patients the opportunity to enjoy the benefits of this "Indian solid gold", especially in pathologies that present difficulty in treatment, such as resistant infections and complicated-to-treat cancers.

7. Acknowledgements

The authors acknowledge the financial support from São Paulo Research Foundation (FAPESP- grant numbers: 19/26821-7; 22/02187-0 and 19/09831-9) and UMCG Research Funds. The authors also thank Dr Brandon W. Peterson for the help with the final text revision.

8. Declaration of interest

The authors declare no conflict of interest.

9. References

Abdulrahman, H., Misba, L., Ahmad, S., & Khan, A.U. (2020). Curcumin Induced Photodynamic Therapy Mediated Suppression of Quorum Sensing Pathway of Pseudomonas Aeruginosa: An Approach to Inhibit Biofilm in Vitro. *Photodiagnosis and Photodynamic Therapy, 30*, Article 101645. https://doi.org/10.1016/j.pdpdt.2019.101645

Aggarwal, D., Chaudhary, M., Bajaj, N., Sharma, D., Upadhyay, S. K., Garg, V. K., Abdulabbas, H. S., Tuli, H. S., & Rani, I. (2024). Anti-Inflammatory Potential of Curcumin: From Chemistry and Mechanistic Insight to Nanoformulations. *Current Bioactive Compounds, 20*(1). https://doi.org/10.2174/1573407219666230726164538

Ai, C., Zhao, C., Xiang, C., Zheng, Y., Zhong, S., Teng, H., & Chen. L. (2023). Gum Arabic as a Sole Wall Material for Constructing Nanoparticle to Enhance the Stability and Bioavailability of Curcumin. *Food Chemistry X*, *18*, Article 100724. https://doi.org/10.1016/j.fochx.2023.100724

Aldakheel, F.M., Mohsen, D., El Sayed, M.M., Fagir, M.H., & El Dein, D.K. (2023). Employing of Curcumin–Silver Nanoparticle-Incorporated Sodium Alginate-Co-Acacia Gum Film Hydrogels for Wound Dressing. *Gels, 9*(10), Article 780. https://doi.org/10.3390/gels9100780

Alharbi, H. M., Alqahtani, T., Alamri, A. H., Kumarasamy, V., Subramaniyan, V., & Babu, K. S. (2024). Nanotechnological synergy of mangiferin and curcumin in modulating PI3K/Akt/mTOR pathway: a novel front in ovarian cancer precision therapeutics. *Frontiers in Pharmacology, 14*. https://doi.org/10.3389/fphar.2023.1276209

Ali, A., & Banerjea, A.C. (2016). Curcumin Inhibits HIV-1 by Promoting Tat Protein Degradation. *Scientific Reports, 6*(1), Article 27539. https://doi.org/10.1038/srep27539

Alves, R. C., Fernandes, R. P., B. Fonseca-Santos, Victorelli, F. D., & Chorilli, M. (2019). A Critical Review of the Properties and Analytical Methods for the Determination of Curcumin in Biological and Pharmaceutical Matrices. *Critical Reviews in Analytical Chemistry, 49*(2), 138–149. https://doi.org/10.1080/10408347.2018.1489216

Amini, S.M., Hadighi, R., Najm, M., Alipour, M., Hasanpour, H., Vosoogh, M., Vosough, A., Hajizadeh, M. & Badirzadeh, A. (2023). The Therapeutic Effects of Curcumin-Coated Gold Nanoparticle Against Leishmania Major Causative Agent of Zoonotic Cutaneous Leishmaniasis (ZCL): An *In Vitro* and *In Vivo* Study. *Current Microbiology, 80*(4), Article 104. https://doi.org/10.1007/s00284-022-03172-1

Arefnezhad, R., Goleij, P., Heydari, N., Rezaei-Tazangi, F., & Motedayyen, H. (2023). Ameliorating Effects of Curcumin on Testicular Cancer. *Andrologia, 2023*, 1–7. https://doi.org/10.1155/2023/4558299

Askarizadeh, A., Barreto, G.E., Henney, N.C., Majeed, M., & Sahebkar, A. (2020). Neuroprotection by Curcumin: A Review on Brain Delivery Strategies. *International Journal of Pharmaceutics, 585*, Article 119476. https://doi.org/10.1016/j.ijpharm.2020.119476

Atwan, Q. S., & Al-Ogaidi, I. (2024). Improving the targeted delivery of curcumin to esophageal cancer cells via a novel formulation of biodegradable lecithin/chitosan nanoparticles with downregulated miR-20a and miR-21 expression. *Nanotechnology, 35*(13), 135103. https://doi.org/10.1088/1361-6528/ad15b9

Auychaipornlert, S., Lawanprasert, P.P., Piriyaprasarth, S., Sithisarn, P., & Mangmool. S. (2022). Design of Turmeric Rhizome Extract Nano-Formula for Delivery to Cancer Cells. *Molecules, 27*(3) Article 896. https://www.mdpi.com/1420-3049/27/3/896.

Bhatia, N. K., Kishor, S., Katyal, N., Gogoi, P., Narang, P., & Deep, S. (2016). Effect of pH and temperature on conformational equilibria and aggregation behaviour of curcumin in aqueous binary mixtures of ethanol. *RSC Advances, 6*(105), 103275–103288. https://doi.org/10.1039/C6RA24256A

Cai, X., He, Y., Cai, L., Zhan, J., Li, Q., Zhong, S., Hou, H., Wang, W., & Qiu, X. (2023). An Injectable Elastic Hydrogel Crosslinked with Curcumin–Gelatin Nanoparticles as a Multifunctional Dressing for the Rapid Repair of Bacterially Infected Wounds. *Biomaterials Science, 11*(9), 3227–3240. https://doi.org/10.1039/D2BM02126A

Carvalho, G.C., de Camargo, B.A.F., de Araújo, J.T.C., & Chorilli, M. (2021). Lycopene: From Tomato to Its Nutraceutical Use and Its Association with Nanotechnology. *Trends in Food Science & Technology*, *118*, 447–458. https://doi.org/10.1016/j.tifs.2021.10.015

Chakrabarti, R., Rawat, P.S., Cooke, B.M., Coppel, R.L. & Patankar, S. (2013). Cellular Effects of Curcumin on Plasmodium Falciparum Include Disruption of Microtubules. *PLoS ONE,* 8(3), Article e57302. https://doi.org/10.1371/journal.pone.0057302

Charoenchai, L., Monton, C., Luprasong, C., & Kraisintu, K. (2020). Pretreatment study of turmeric rhizomes and optimization of drying methods using microwave oven and hot air oven to obtain high quality of turmeric powder. *Journal of Current Science and Technology, 10*(1), 49–57.

Chen, D.-Y., Shien, J.-H., Tiley, L., Chiou, S.-S, Wang, S.-Y., Chang, T.-J., Lee, Y.-J., Chan, K.-W., & Hsu, W.-L. (2010). Curcumin Inhibits Influenza Virus Infection and Haemagglutination Activity. *Food Chemistry, 119*(4) 1346–1351. https://doi.org/10.1016/j.foodchem.2009.09.011

Chongtham, A., & Agrawal, N. (2016). Curcumin Modulates Cell Death and Is Protective in Huntington's Disease Model. *Scientific Reports, 6*(1), Article 18736. https://doi.org/10.1038/srep18736

Chopra, A.S., Lordan, R., Horbańczuk, O.K., Atanasov, A.G., Chopra, I., Horbańczuk, J.O., Jóźwik, A., Huang, L., Pirgozliev, V., Banach, M., & others (2022). The Current Use and Evolving Landscape of Nutraceuticals. *Pharmacological Research, 175*, Article 106001. https://linkinghub.elsevier.com/retrieve/pii/S1043661821005855.

Das, R., Roy, A., Dutta, N., & Majumder, H. K. (2008). Reactive oxygen species and imbalance of calcium homeostasis contributes to curcumin induced programmed cell death in Leishmania donovani. *Apoptosis, 13*(7), 867–882. https://doi.org/10.1007/s10495-008-0224-7

Das, S., Nadar, S.S., & Rathod, V.K. (2021). Integrated Strategies for Enzyme Assisted Extraction of Bioactive Molecules: A Review. *International Journal of Biological Macromolecules, 191*, 899–917. https://linkinghub.elsevier.com/retrieve/pii/S0141813021019814.

Debnath, S. K., & Srivastava, R. (2021). Drug Delivery With Carbon-Based Nanomaterials as Versatile Nanocarriers: Progress and Prospects. Frontiers in *Nanotechnology, 3*. https://doi.org/10.3389/fnano.2021.644564

Deepa, S., Madhu, S., Devasenan, S., Murali, G., Pancharatna, P.D., Maaza, M., Kaviyarasu, K., & Jeyaram, S. (2023). Extraction of Natural Pigment Curcumin from *Curcuma Longa*: Spectral, DFT, Third-Order Nonlinear Optical and Optical Limiting Study. *Journal of Fluorescence,*1-8. https://doi.org/10.1007/s10895-023-03421-x

Durante, M., Lenucci, M., & Mita, G. (2014). Supercritical Carbon Dioxide Extraction of Carotenoids from Pumpkin (Cucurbita Spp.): A Review. *International Journal of Molecular Sciences, 15*(4), 6725–6740. https://doi.org/10.3390/ijms15046725

Elamin, M., Al-Olayan, E., Abdel-Gaber, R., & Yehia. R.S., (2021). Anti-Proliferative and Apoptosis Induction Activities of Curcumin on Leishmania Major. *Revista Argentina de Microbiología, 53*(3), 240–247. https://doi.org/10.1016/j.ram.2020.08.004

El-ghannam, G., Sobeh, E.I., Korany, R.M.S., Saleh, H.M., & Elfeky, S.A. (2023). Pancreas Recovery in Diabetic Rats after Low Dose Curcumin@ZnO Nanoparticles Oral Treatment. *Nanomedicine Research Journal, 8*(2), 149–160. https://doi.org/10.22034/NMRJ.2023.02.004

Krishna, S.K. G., Sravanya, K., Pranuthi, & P., Thirumdas, R. (2023). Effect of Microwave Boiling and Ultrasound-Assisted Extraction on Curcumin from the Turmeric Rhizomes. *Food Science and Engineering, 4*(2)*,* 237–247. https://doi.org/10.37256/fse.4220233207

Fernando, A. J., & Amaratunga, S. (2022). Application of far-infrared radiation for sun-dried chili pepper (*Capsicum annum L.*): drying characteristics and color during roasting. *Journal of the Science of Food and Agriculture, 102*(9), 3781–3787. https://doi.org/10.1002/jsfa.11726

Fessler, S. N., Chang, Y., Liu, L., & Johnston, C. S. (2023). Curcumin Confers Anti-Inflammatory Effects in Adults Who Recovered from COVID-19 and Were Subsequently Vaccinated: A Randomized Controlled Trial. *Nutrients, 15*(7), 1548. https://doi.org/10.3390/nu15071548

Ganie, S. A., Naik, R. A., Dar, O. A., Rather, L. J., Assiri, M. A., & Li, Q. (2024). Design and fabrication of functionalized curdlan-curcumin delivery system to facilitate the therapeutic effects of curcumin on breast cancer. *International Journal of Biological Macromolecules, 267*, 131388. https://doi.org/10.1016/j.ijbiomac.2024.131388

Garcia-Vaquero, M., Rajauria, G., & Tiwari, B. (2020). Conventional Extraction Techniques: Solvent Extraction. In: Torres, M. D., Kraan, S., & Dominguez, H. (Eds.), *Sustainable Seaweed Technologies*: Cultivation, biorefinery, and applications (pp. 171–189). Elsevier. https://doi.org/10.1016/C2018-0-01462-0

Gayathri, K., Bhaskaran, M., Selvam, C., & Thilagavathi, R. (2023). Nano Formulation Approaches for Curcumin Delivery- a Review. *Journal of Drug Delivery Science and Technology, 82*, Article 104326. https://doi.org/10.1016/j.jddst.2023.104326

Ge, Q., Rong, S., Yin, C., McClements, D.J., Fu, Q., Li, Q., Han, Y., Liu, F., Wang, S., & Chen, S. (2024). Calcium Ions Induced ι-Carrageenan-Based Gel-Coating Deposited on Zein Nanoparticles for Encapsulating the Curcumin. *Food Chemistry, 434*, Article 137488. https://doi.org/10.1016/j.foodchem.2023.137488

Gholami, L., Momtazi-Borojeni, A. A., Malaekeh-Nikouei, B., Nikfar, B., Amanolahi, F., Mohammadi, A., & Kazemi Oskuee, R. (2023). Selective Cellular Uptake and Cytotoxicity of Curcumin-encapsulated SPC and HSPC Liposome Nanoparticles on Human Bladder Cancer Cells. *Current Pharmaceutical Design, 29*(13), 1046–1058. https://doi.org/10.2174/1381612829666230331084848

Hamzehzadeh, L., Atkin, S.L., Majeed, M., Butler, A.E., & Sahebkar, A. (2018). The Versatile Role of Curcumin in Cancer Prevention and Treatment: A Focus on PI3K/AKT Pathway. *Journal of Cellular Physiology, 233*(10) 6530–6537. https://doi.org/10.1002/jcp.26620

Han, C., Wang, L., Yu, K., Chen, L., Hu, L., Chen, K., Jiang, H., & Shen, X. (2006). Biochemical Characterization and Inhibitor Discovery of Shikimate Dehydrogenase from Helicobacter Pylori. *FEBS Journal, 273*(20), 4682–4692. https://onlinelibrary.wiley.com/doi/10.1111/j.1742-4658.2006.05469.x.

Hewlings, S., & Kalman, D. (2017). Curcumin: A Review of Its Effects on Human Health. *Foods, 6*(10), Article 92. https://doi.org/10.3390/foods6100092

Hu, Y., Zhang, J., Kong, W., Zhao, G., & Yang, M. (2017). Mechanisms of Antifungal and Anti-Aflatoxigenic Properties of Essential Oil Derived from Turmeric (Curcuma Longa L.) on Aspergillus Flavus. *Food Chemistry, 220*, 1–8. https://doi.org/10.1016/j.foodchem.2016.09.179

Huang, S., Xu, D., Zhang, L., Hao, L., Jia, Y., Zhang, X., Cheng, T., & Chen, J. (2023). Therapeutic Effects of Curcumin Liposomes and Nanocrystals on Inflammatory Osteolysis: *In Vitro* and *in Vivo* Comparative Study. *Pharmacological Research, 192*, Article 106778. https://doi.org/10.1016/j.phrs.2023.106778

Huang, Y., Zhan, Y., Luo, G., Zeng, Y., McClements, D.J., & Hu, K. (2023). Curcumin Encapsulated Zein/Caseinate-Alginate Nanoparticles: Release and Antioxidant Activity under in Vitro Simulated Gastrointestinal Digestion. *Current Research in Food Science, 6*, Article 100463. https://doi.org/10.1016/j.crfs.2023.100463

Hussein, H. A., & Khaphi, F. L. (2023). The Apoptotic Activity of Curcumin Against Oral Cancer Cells Without Affecting Normal Cells in Comparison to Paclitaxel Activity. *Applied Biochemistry and Biotechnology, 195*(8), 5019–5033. https://doi.org/10.1007/s12010-023-04454-5

Idoudi, S., Bedhiafi, T., Hijji, Y.M., & Billa, N. (2022). Curcumin and Derivatives in Nanoformulations with Therapeutic Potential on Colorectal Cancer. *AAPS PharmSciTech, 23*(5), Article 115. https://doi.org/10.1208/s12249-022-02268-y

Ijaz, I., Gilani, E., Nazir, A., & Bukhari, A. (2020). Detail review on chemical, physical and green synthesis, classification, characterizations and applications of nanoparticles. *Green Chemistry Letters and Reviews, 13*(3), 223–245. https://doi.org/10.1080/17518253.2020.1802517

Ilhan, H. (2023). Nanoarchitectonics of the Effects of Curcumin Carbon Dot-Decorated Chitosan Nanoparticles on Proliferation and Apoptosis-Related Gene Expressions in HepG2 Hepatocellular Carcinoma Cells. *ACS Omega, 8*(37), 33554–33563. https://doi.org/10.1021/acsomega.3c03405

Jambhrunkar, S., Qu, Z., Popat, A., Yang, J., Noonan, O., Acauan, L., Ahmad Nor, Y., Yu, C., & Karmakar, S. (2014). Effect of Surface Functionality of Silica Nanoparticles on Cellular Uptake and Cytotoxicity. *Molecular Pharmaceutics, 11*(10), 3642–3655. https://doi.org/10.1021/mp500385n

Jamil, S. N. H., Ali, A. H., Feroz, S. R., Lam, S. D., Agustar, H. K., Mohd Abd Razak, M. R., & Latip, J. (2023). Curcumin and Its Derivatives as Potential Antimalarial and Anti-Inflammatory Agents: A Review on Structure–Activity Relationship and Mechanism of Action. *Pharmaceuticals, 16*(4), 609. https://doi.org/10.3390/ph16040609

Jiang, T., Ghosh, R., & Charcosset, C. (2021). Extraction, Purification and Applications of Curcumin from Plant Materials-A Comprehensive Review. *Trends in Food Science & Technology, 112*, 419–430. https://linkinghub.elsevier.com/retrieve/pii/S0924224421002739.

Jin, T., Zhang, Y., Botchway, B.O.A., Zhang, J., Fan, R., Zhang, Y., & Liu, X. (2022). Curcumin Can Improve Parkinson's Disease via Activating BDNF/PI3k/Akt Signaling Pathways. *Food and Chemical Toxicology, 164*, Article 113091.

Joudeh, N., & Linke, D. (2022). Nanoparticle Classification, Physicochemical Properties, Characterization, and Applications: A Comprehensive Review for Biologists. *Journal of Nanobiotechnology, 20*(1), Article 262. https://doi.org/10.1186/s12951-022-01477-8

Kadam, J.H., & Kamble, B.M. (2020). Effect of Organic Manures on Growth, Yield and Quality of Turmeric (*Curcuma Longa L*). *Journal of Applied and Natural Science, 12*(2), 91–97. https://doi.org/10.31018/jans.vi.2249

Katiyar, S., Srivastava, N., & Choudhury, A. R. (2024). Microbial fermentation-based synthesis of nano-curcumin suggesting the role of pullulan in nano-formulation. *International Journal of Biological Macromolecules, 265*, 131088. https://doi.org/10.1016/j.ijbiomac.2024.131088

Khalid, K., Tan, X., Mohd Zaid, H. F., Tao, Y., Lye Chew, C., Chu, D.-T., Lam, M. K., Ho, Y.-C., Lim, J. W., & Chin Wei, L. (2020). Advanced in developmental organic and inorganic nanomaterial: a review. *Bioengineered, 11*(1), 328–355. https://doi.org/10.1080/21655979.2020.1736240

Kharade, S.S., Samal, K.C., & Rout, G.R. (2017). High Performance Thin Layer Chromatography Fingerprint Profile of Rhizome Extracts of Five Important Curcuma Species. *Proceedings of the National Academy of Sciences, India Section B: Biological Sciences, 87*(4), 1335–1341. https://doi.org/10.1007/s40011-016-0709-z

Khedri, M., Beheshtizadeh, N., Rostami, M., Sufali, A., Rezvantalab, S., Dahri, M., Maleki, R., Santos, H.A., & Shahbazi, M.-A. (2022). Artificial Intelligence Deep Exploration of Influential Parameters on Physicochemical Properties of Curcumin-Loaded Electrospun Nanofibers. *Advanced NanoBiomed Research, 2*(6), Article 2100143. https://doi.org/10.1002/anbr.202100143

Kumar, A., Hegde, M., Parama, D., & Kunnumakkara, A.B. (2022). Curcumin: The Golden Nutraceutical on the Road to Cancer Prevention and Therapeutics. A Clinical Perspective. *Critical Reviews™ in Oncogenesis, 27*(3), 33–63.https://doi.org/10.1615/CritRevOncog.2023045587

Kumar, K., Srivastav, S., & Sharanagat, V.S. (2021). Ultrasound Assisted Extraction (UAE) of Bioactive Compounds from Fruit and Vegetable Processing by-Products: A Review. *Ultrasonics Sonochemistry, 70*, Article 105325. https://doi.org/10.1016/j.ultsonch.2020.105325

Laddha, U.D., Chikhale, S.S., Dashputre, N.L., Gaikwad, S.S., Moravkar, K.K., & Kshirsagar, S.J. (2023). Development and in Vitro, Ex Vivo, in Vivo Investigation of Curcumin Loaded Nanoparticles in Management of Dry Eye Disease. *Journal of Drug Delivery Science and Technology, 87*, Article 104802. https://doi.org/10.1016/j.jddst.2023.104802

Lamch, Ł. (2023). Membrane-Assisted Core-Shell Entrapment Technique as a Powerful Tool for Curcumin Encapsulation. *Colloids and Surfaces A: Physicochemical and Engineering Aspects, 661*, Article 130938. https://doi.org/10.1016/j.colsurfa.2023.130938

Lee, W., & Lee, D.G. (2014). An Antifungal Mechanism of Curcumin Lies in Membrane-targeted Action within C*andida Albicans*. *IUBMB Life, 66*(11), 780–785. https://doi.org/10.1002/iub.1326

Lee, Y.S., Chen, X., Widiyanto, T.W., Orihara, K., Shibata, H., & Kajiwara, S. (2022). Curcumin Affects Function of Hsp90 and Drug Efflux Pump of *Candida Albicans*. *Frontiers in Cellular and Infection Microbiology, 12*. https://doi.org/10.3389/fcimb.2022.944611

Lestari, M.L.A.D., & Indrayanto, G. (2014). *Curcumin.* In Brittain, H. G. (Ed.), *Profiles of drug substances, excipients and related methodology* (pp. 113–204). Elsevier. https://doi.org/10.1016/B978-0-12-800173-8.00003-9

Li, W., Wang, F., Wang, X., Xu, W., Liu, F., Hu, R., & Li, S. (2024). Curcumin inhibits prostate cancer by upregulating miR-483-3p and inhibiting UBE2C. *Journal of Biochemical and Molecular Toxicology, 38*(2). https://doi.org/10.1002/jbt.23645

Li, X., He, Y., Zhang, S., Gu, Q., McClements, D.J., Chen, S., Liu, X., & Liu, F. (2023). Lactoferrin-Based Ternary Composite Nanoparticles with Enhanced Dispersibility and Stability for Curcumin Delivery. *ACS Applied Materials & Interfaces, 15*(14), 18166–18181. https://doi.org/10.1021/acsami.2c20816

Linnane, E., Haddad, S., Melle, F., Mei, Z., & Fairen-Jimenez, D. (2022). The Uptake of Metal–Organic Frameworks: A Journey into the Cell. *Chemical Society Reviews, 51*(14), 6065–6086. https://doi.org/10.1039/D0CS01414A

Liu, Q., Kim, Y., Im, G., Zhu, J., Wu, Y., Liu, Y., & Bhang, S.H. (2021). Inorganic Nanoparticles Applied as Functional Therapeutics. *Advanced Functional Materials* 31(12), Article 2008171. https://doi.org/10.1002/adfm.202008171

Liu, X., Wang, R., Wang, C., Li, W., Huang, Y., Li, Y., Wang, H., Peng, C., Hu, H., Wu, B., & Li, C. (2023). Graphene Oxide Assisted Solvent for Enhancing the Coupled Ultrasonic Extraction Process of Curcumin from *Curcuma Longa L*. *Separation Science and Technology,* 58(10), 1761–1772. https://doi.org/10.1080/01496395.2023.2215401

Liu, Z.-J., Li, Z.-H., Liu, L., Tang, W.-X., Wang, Y., Dong, M.-R., & Xiao, C. (2016). Curcumin Attenuates Beta-Amyloid-Induced Neuroinflammation via Activation of Peroxisome Proliferator-Activated Receptor-Gamma Function in a Rat Model of Alzheimer's Disease. *Frontiers in Pharmacology, 7*, Article 261. https://doi.org/10.3389/fphar.2016.00261

Madani, M., Hosny, S., Alshangiti, D.M., Nady, N., Alkhursani, S.A., Alkhaldi, H., Al-Gahtany, S.A., Ghobashy, M.M., & Gaber, G.A. (2022). Green Synthesis of Nanoparticles for Varied Applications: Green Renewable Resources and Energy-Efficient Synthetic Routes. *Nanotechnology Reviews, 11*(1), 731–759. https://doi.org/10.1515/ntrev-2022-0034

Madima, N., Mishra, S. B., Inamuddin, I., & Mishra, A. K. (2020). Carbon-based nanomaterials for remediation of organic and inorganic pollutants from wastewater. A review. *Environmental Chemistry Letters, 18*(4), 1169–1191. https://doi.org/10.1007/s10311-020-01001-0

Mahale, J., Singh, R., Howells, L.M., Britton, R.G., Khan, S.M., & K. Brown. (2018). Detection of Plasma Curcuminoids from Dietary Intake of Turmeric-Containing Food in Human Volunteers. *Molecular Nutrition & Food Research, 62*(16), Article 1800267. https://doi.org/10.1002/mnfr.201800267

Maiti, D., Tong, X., Mou, X., & Yang, K. (2019). Carbon-Based Nanomaterials for Biomedical Applications: A Recent Study. *Frontiers in Pharmacology, 9*, Article 1401. https://doi.org/10.3389/fphar.2018.01401

Martínez-González, J. J., Ríos-Morales, S.L., Guevara-Flores, A., Ramos-Godinez, M.P., López-Saavedra, A., Rendón, J.L., & Mena, I.P.A. (2022). Evaluating the Effect of Curcumin on the Metacestode of *Taenia Crassiceps*. *Experimental Parasitology, 239,* Article 108319. https://doi.org/10.1016/j.exppara.2022.108319

Medaglia, S., Otri, I., Bernardos, A., Marcos, M. D., Aznar, E., Sancenón, F., & Martínez-Máñez, R. (2024). Synergistic antimicrobial photodynamic therapy using gated mesoporous silica nanoparticles containing curcumin and polymyxin B. *International Journal of Pharmaceutics, 654*, 123947. https://doi.org/10.1016/j.ijpharm.2024.123947

Mitchell, M.J., Billingsley, M.M., Haley, R.M., Wechsler, M.E., Peppas, N.A., & Langer, R. (2021). Engineering Precision Nanoparticles for Drug Delivery. *Nature Reviews Drug Discovery, 20*(2), 101–124. https://doi.org/10.1038/s41573-020-0090-8

Mohamed, A.A.-R., Behairy, A., El-Hakim, Y.M.A., Metwally, M.M.M., Khamis, T., Abuzahrah, S.S., Abdelhamid, A.E., Alqahtani, S., Essawi, W.M., Alotaibi, B.S., & others (2023). Comparable Bio-Evaluation of Curcumin and Chitosan-Encapsulated Curcumin Nanoparticles against the Reprotoxic Potential of Fenpropathrin Pyrethroid in Rats: Genomic and Morphometric Prospectives. *Food and Chemical Toxicology, 179*, Article 113977. https://doi.org/10.1016/j.fct.2023.113977

Molinaro, G., Fontana, F., Tello, R.P., Wang, S., Cérda, S.L., Torrieri, G., Correia, A., Waris, E., Hirvonen, J.T. & others. (2023). *In Vitro* Study of the Anti-Inflammatory and Antifibrotic Activity of Tannic Acid-Coated Curcumin-Loaded Nanoparticles in Human Tenocytes. *ACS Applied Materials & Interfaces, 15*(19), 23012–23023. https://pubs.acs.org/doi/10.1021/acsami.3c05322.

Mounce, B.C., Cesaro, T., Carrau, L., Vallet, T., & Vignuzzi, M. (2017). Curcumin Inhibits Zika and Chikungunya Virus Infection by Inhibiting Cell Binding. *Antiviral Research, 142*, 148–157. https://doi.org/10.1016/j.antiviral.2017.03.014

Nagavekar, N., & Singhal, R.S. (2019). Supercritical Fluid Extraction of Curcuma Longa and Curcuma Amada Oleoresin: Optimization of Extraction Conditions, Extract Profiling, and Comparison of Bioactivities. *Industrial Crops and Products, 134*, 134–145. https://linkinghub.elsevier.com/retrieve/pii/S0926669019302274.

Naziris, N., Sekowski, S., Olchowik-Grabarek, E., Buczkowski, A., Balcerzak, Ł., Chrysostomou, V., Pispas, S., Małecka, M., Bryszewska, M., & Ionov, M. (2023). Biophysical Interactions of Mixed Lipid-Polymer Nanoparticles Incorporating Curcumin: Potential as Antibacterial Agent. *Biomaterials Advances, 144*, Article 213200. https://doi.org/10.1016/j.bioadv.2022.213200

Nebrisi, E.E. (2021). Neuroprotective Activities of Curcumin in Parkinson's Disease: A Review of the Literature. *International Journal of Molecular Sciences, 22*(20), Article 11248. https://doi.org/10.3390/ijms222011248

Nejatian, M., Darabzadeh, N., Bodbodak, S., Saberian, H., Rafiee, Z., Kharazmi, M.S., & Jafari, S.M. (2022). Practical Application of Nanoencapsulated Nutraceuticals in Real Food Products; a Systematic Review. *Advances in Colloid and Interface Science, 305*, Article 102690. https://linkinghub.elsevier.com/retrieve/pii/S0001868622000926.

Nour, A. H., Oluwaseun, A.R., Nour, A.H., Omer, M.S. & Ahmed, N. (2021). Microwave-Assisted Extraction of Bioactive Compounds (Review). In Churyumov, G. I. (Ed.), *Microwave Heating - Electromagnetic Fields Causing Thermal and Non-Thermal Effects*. IntechOpen. https://doi.org/10.5772/intechopen.96092

Nurhadi, B., Saputra, R. A., Setiawati, T. A., Husein, S. N., Faressi, F. R., Utari, C. D., Sukri, N., Kayaputri, I. L., & Setiasih, I. S. (2020). Comparison of Curcuma domestica and Curcuma xanthorrhiza oleoresins extracted using maceration, Soxhlet, and ultrasound-assisted extraction (UAE). *IOP Conference Series: Earth and Environmental Science, 443*(1), 012074. https://doi.org/10.1088/1755-1315/443/1/012074

Obeid, M.A., Alsaadi, M. & Aljabali, A.A. (2023). Recent Updates in Curcumin Delivery. *Journal of Liposome Research, 33*(1), 53–64. https://doi.org/10.1080/08982104.2022.2086567

Panahi, Y., Hosseini, M. S., Khalili, N., Naimi, E., Simental-Mendía, L. E., Majeed, M., & Sahebkar, A. (2016). Effects of curcumin on serum cytokine concentrations in subjects with metabolic syndrome: A post-hoc analysis of a randomized controlled trial. *Biomedicine & Pharmacotherapy, 82*, 578–582. https://doi.org/10.1016/j.biopha.2016.05.037

Paul, W., & Sharma, C. P. (2010). Inorganic nanoparticles for targeted drug delivery. *In Biointegration of Medical Implant Materials* (pp. 204–235). Elsevier. https://doi.org/10.1533/9781845699802.2.204

Paulucci, V.P., Couto, R.O., Teixeira, C.C.C., & Freitas, L.A.P. (2013). Optimization of the Extraction of Curcumin from Curcuma Longa Rhizomes. *Revista Brasileira de Farmacognosia*, *23*(1), 94–100. https://doi.org/10.1590/S0102-695X2012005000117

Piano, R., Caccavo, D., Lamberti, G., Remaut, K., Seynaeve, H. & Barba, A.A. (2023). A New Productive Approach and Formulative Optimization for Curcumin Nanoliposomal Delivery Systems. *Pharmaceutics, 15*(3), Article 959. https://doi.org/10.3390/pharmaceutics15030959

Poudel, A., Pandey, J., & Lee, H.-K. (2019). Geographical Discrimination in Curcuminoids Content of Turmeric Assessed by Rapid UPLC-DAD Validated Analytical Method. *Molecules, 24*(9), Article 1805. https://doi.org/10.3390/molecules24091805

Praditya, D., Kirchhoff, L., Brüning, J., Rachmawati, H., Steinmann, J., & Steinmann, E. (2019). Anti-Infective Properties of the Golden Spice Curcumin. *Frontiers in Microbiology, 10*, Article 912. https://doi.org/10.3389/fmicb.2019.00912.

Priyadarsini, K. (2014). The Chemistry of Curcumin: From Extraction to Therapeutic Agent. *Molecules 19*(12), 20091–20112. http://www.mdpi.com/1420-3049/19/12/20091.

Qin, C., Tang, N., Gan, Y., Zhao, H., Li, Y., Tian, G., Yang, Y. Y., Yuan, P., & Ding, X. (2023). Liposomes Co-Delivering Curcumin and Colistin to Overcome Colistin Resistance in Bacterial Infections. *Advanced Healthcare Materials, 12*(24). https://doi.org/10.1002/adhm.202202903

Qiu, P., Man, S., Li, J., Liu, J., Zhang, L., Yu, P., & Gao, W. (2016). Overdose Intake of Curcumin Initiates the Unbalanced State of Bodies. *Journal of Agricultural and Food Chemistry, 64*(13), 2765–2771. https://doi.org/10.1021/acs.jafc.6b00053

Rahman, M.A., Ali, A., Rahamathulla, M., Salam, S., Hani, U., Wahab, S., Warsi, M.H., Yusuf, M., Ali, A., Mittal, V., & Harwansh, R. K. (2023). Fabrication of Sustained Release Curcumin-Loaded Solid Lipid Nanoparticles (Cur-SLNs) as a Potential Drug Delivery System for the Treatment of Lung Cancer: Optimization of Formulation and In Vitro Biological Evaluation. *Polymers 15*(3), Article 542. https://doi.org/10.3390/polym15030542

Rai, M., Pandit, R., Gaikwad, S., Yadav, A., & Gade, A. (2015). Potential Applications of Curcumin and Curcumin Nanoparticles: From Traditional Therapeutics to Modern Nanomedicine. *Nanotechnology Reviews, 4*(2), 161–172. https://doi.org/10.1515/ntrev-2015-0001

Rangel-Castañeda, I.A., Hernández-Hernández, J.M., Pérez-Rangel, A., González-Pozos, S., Carranza-Rosales, P., Charles-Niño, C.L., Tapia-Pastrana, G., Ramírez-Herrera, M.A., & Castillo-Romero, A. (2018). Amoebicidal Activity of Curcumin on *Entamoeba Histolytica* Trophozoites. *Journal of Pharmacy and Pharmacology, 70*(3), 426–433. https://doi.org/10.1111/jphp.12867

Ratan, C., Arian, A. M., Rajendran, R., Jayakumar, R., Masson, M., & Mangalathillam, S. (2023). Nano-based formulations of curcumin: elucidating the potential benefits and future prospects in skin cancer. *Biomedical Materials, 18*(5), 052008. https://doi.org/10.1088/1748-605X/acf0af

Ribeiro, I.P., Pinto, J.G., Souza, B.M.N., Miñán, A.G., & Ferreira-Strixino, J. (2022). Antimicrobial Photodynamic Therapy with Curcumin on Methicillin-Resistant Staphylococcus Aureus Biofilm. *Photodiagnosis and Photodynamic Therapy, 37*, Article 102729. https://doi.org/10.1016/j.pdpdt.2022.102729

Rodrigues, F. A., Pimenta, V. de S. C., Braga, K. M. da S., & de Araújo, E. G. (2016). Obtenção de Extratos de Plantas do Cerrado. *Enciclopédia Biosfera, 13*(23), 870–887. https://doi.org/10.18677/Enciclopedia_Biosfera_2016_075

Ryskalin, L., Biagioni, F., Busceti, C. L., Lazzeri, G., Frati, A., & Fornai, F. (2020). The Multi-Faceted Effect of Curcumin in Glioblastoma from Rescuing Cell Clearance to Autophagy-Independent Effects. *Molecules, 25*(20), 4839. https://doi.org/10.3390/molecules25204839

Sabet, S., Rashidinejad, A., Melton, L.D., & McGillivray. D.J., (2021). Recent Advances to Improve Curcumin Oral Bioavailability. *Trends in Food Science & Technology, 110*, 253–266. https://doi.org/10.1016/j.tifs.2021.02.006

Salem, M., Rohani, S., & Gillies, E.R. (2014). Curcumin, a Promising Anti-Cancer Therapeutic: A Review of Its Chemical Properties, Bioactivity and Approaches to Cancer Cell Delivery. *RSC Advances, 4*(21), Article 10815. http://xlink.rsc.org/?DOI=c3ra46396f.

Sánchez-Salcedo, S., Heras, C., Lozano, D., Vallet-Regí, M., & Salinas, A.J. (2023). Nanodevices Based on Mesoporous Glass Nanoparticles Enhanced with Zinc and Curcumin to Fight Infection and Regenerate Bone. *Acta Biomaterialia, 166*, 655–669. https://doi.org/10.1016/j.actbio.2023.04.046

Schiborr, C., Kocher, A., Behnam, D., Jandasek, J., Toelstede, S., & Frank, J. (2014). The Oral Bioavailability of Curcumin from Micronized Powder and Liquid Micelles Is Significantly Increased in Healthy Humans and Differs between Sexes. *Molecular Nutrition & Food Research, 58*(3), 516–527. https://onlinelibrary.wiley.com/doi/10.1002/mnfr.201300724.

Schraufstätter, E., & Bernt, H. (1949). Antibacterial Action of Curcumin and Related Compounds. *Nature, 164*(4167), 456–457. https://doi.org/10.1038/164456a0

Shabbir, U., Rubab, M., Daliri, E.B.-M., Chelliah, R., Javed, A. & Oh, D.-H. (2021). Curcumin, Quercetin, Catechins and Metabolic Diseases: The Role of Gut Microbiota. *Nutrients, 13*(1), Article 206. https://doi.org/10.3390/nu13010206

Shannon, D.A., Santen, E., Salmasi, S.Z., Murray, T.J., Duong, L.T., Greenfield, J.T., Gonzales, T., & Foshee, W. (2019). Shade, Establishment Method, and Varietal Effects on Rhizome Yield and Curcumin Content in Turmeric in Alabama. *Crop Science, 59*(6), 2701–2710. https://onlinelibrary.wiley.com/doi/10.2135/cropsci2019.04.0262.

Sharifi-Rad, J., El Rayess, Y., Rizk, A.A., Sadaka, C., Zgheib, R., Zam, W., Sestito, S., Rapposelli, S., Neffe-Skocinska, K., Zielinska, D., & others. (2020). Turmeric and Its Major Compound Curcumin on Health: Bioactive Effects and Safety Profiles for Food, Pharmaceutical, Biotechnological and Medicinal Applications. *Frontiers in Pharmacology, 11*, Article 01021. https://doi.org/10.3389/fphar.2020.01021

Sharma, M. (2012). Lipidome Analysis Reveals Antifungal Polyphenol Curcumin Affects Membrane Lipid Homeostasis. *Frontiers in Bioscience, E4*(1), Article 1195. https://doi.org/10.2741/451

Shirsath, S. R., Sable, S. S., Gaikwad, S. G., & Gogate, P. R. (2021). Ultrasound assisted curcumin recovery from Curcuma aromatica: Understanding the effect of different operating parameters. *Chemical Engineering and Processing - Process Intensification, 169*, 108604. https://doi.org/10.1016/j.cep.2021.108604

Slika, L., & Patra, D. (2020). A short review on chemical properties, stability and nano-technological advances for curcumin delivery. *Expert Opinion on Drug Delivery, 17*(1), 61–75. https://doi.org/10.1080/17425247.2020.1702644

Sufi, S. A., Hoda, M., Pajaniradje, S., Mukherjee, V., Coumar, S. M., & Rajagopalan, R. (2020). Enhanced drug retention, sustained release, and anti-cancer potential of curcumin and indole-curcumin analog-loaded polysorbate 80-stabilizied PLGA nanoparticles in colon cancer cell line SW480. *International Journal of Pharmaceutics, 588*, 119738. https://doi.org/10.1016/j.ijpharm.2020.119738

Suksaeree, J., & Monton, C. (2024). Maximizing Curcuminoid Extraction from Curcuma aromatica Salisb. Rhizomes via Environmentally Friendly Microwave-Assisted Extraction Technique Using Full Factorial Design. International Journal of Food Science, 2024, 1–13. https://doi.org/10.1155/2024/4566123

Sun, M., Liu, N., Sun, J., Li, X., Wang, H., Zhang, W., Xie, Q., & Wang, M. (2022). Curcumin regulates anti-inflammatory responses by AXL/JAK2/STAT3 signaling pathway in experimental autoimmune encephalomyelitis. *Neuroscience Letters, 787*, 136821. https://doi.org/10.1016/j.neulet.2022.136821

Sun, Y., Zhong, M., Kang, M., Liao, Y., Wang, Z., Li, Y. & Qi, B. (2023). Novel Core-Shell Nanoparticles: Encapsulation and Delivery of Curcumin Using Guanidine Hydrochloride-Induced Oleosome Protein Self-Assembly. *LWT, 173*, Article 114352. https://doi.org/10.1016/j.lwt.2022.114352

Tang, C.-H. (2020). Nanocomplexation of Proteins with Curcumin: From Interaction to Nanoencapsulation (A Review). *Food Hydrocolloids, 109*, Article 106106. https://doi.org/10.1016/j.foodhyd.2020.106106

Thimmulappa, R.K., Mudnakudu-Nagaraju, K.K., Shivamallu, C., Subramaniam, K.J.T., Radhakrishnan, A., Bhojraj, S., & Kuppusamy, G. (2021). Antiviral and Immunomodulatory Activity of Curcumin: A Case for Prophylactic Therapy for COVID-19. *Heliyon, 7*(2), Article e06350. https://doi.org/10.1016/j.heliyon.2021.e06350

Trigo-Gutierrez, J.K., Vega-Chacón, Y., Soares, A.B., & Mima, E.G.O. (2021). Antimicrobial Activity of Curcumin in Nanoformulations: A Comprehensive Review. *International Journal of Molecular Sciences, 22*(13), Article 7130. https://doi.org/10.3390/ijms22137130

Tripathy, S., & Sahu, S.K. (2018). In-Silico Studies on Molecular Orbitals, Geometry Optimization and Molecular Docking of Curcumin as an Anti-Bacterial Drug Targets FtsZ Protein. *Journal of PeerScientist, 1*(2), Article e1000006.

Vargas-Bernal, R. (2020). Introductory Chapter: Hybrid Nanomaterials. In Vargas-Bernal, R., He, P., & Zhang, S. (Eds.), *Hybrid Nanomaterials - Flexible Electronics Materials*. IntechOpen.

Venkatas, J., Daniels, A., & Singh, M. (2022). The Potential of Curcumin-Capped Nanoparticle Synthesis in Cancer Therapy: A Green Synthesis Approach. IntechOpen. https://doi.org/10.5772/intechopen.92012

Vichakshana, G.A.D., Foo, S.C., & Choo, W.S. (2023). Impact of High-Pressure Homogenization Pretreatment on Recovery of Curcumin from Turmeric by Different Combinations of Extraction and Drying Methods. *Innovative Food Science & Emerging Technologies, 83*, Article 103249. https://doi.org/10.1016/j.ifset.2022.103249

Wang, G., Zhu, J., Wang, Z., Xu, Z., Shi, Y., & Luo, L. (2023). Curcumin Increases Radiosensitivity of Radioresistant Nasopharyngeal Cancer. *Discovery Medicine, 35*(176), 418. https://doi.org/10.24976/Discov.Med.202335176.42

Wang, H., Zhang, K., Liu, J., Yang, J., Tian, Y., Yang, C., Li, Y., Shao, M., Su, W., & Song, N. (2021). Curcumin Regulates Cancer Progression: Focus on NcRNAs and Molecular Signaling Pathways. *Frontiers in Oncology, 11,* Article 660712. https://doi.org/10.3389/fonc.2021.660712

Wang, N., Feng, T., Liu, X., & Liu, Q. (2020). Curcumin Inhibits Migration and Invasion of Non-Small Cell Lung Cancer Cells through up-Regulation of MiR-206 and Suppression of PI3K/AKT/MTOR Signaling Pathway. *Acta Pharmaceutica, 70*(3), 399–409. https://doi.org/10.2478/acph-2020-0029

Wang, R., Zou, L., Yi, Z., Zhang, Z., Zhao, M., & Shi, S. (2023). PLGA Nanoparticles Loaded with Curcumin Produced Luminescence for Cell Bioimaging. *International Journal of Pharmaceutics, 639*, Article 122944. https://doi.org/10.1016/j.ijpharm.2023.122944

Wei, Y., Li, K., Zhao, W., He, Y., Shen, H., Yuan, J., Pi, C., Zhang, X., Zeng, M., Fu, S., Song, X., Lee, R. J., & Zhao, L. (2022). The Effects of a Novel Curcumin Derivative Loaded Long-Circulating Solid Lipid Nanoparticle on the MHCC-97H Liver Cancer Cells and Pharmacokinetic Behavior. *International Journal of Nanomedicine, 17*, 2225–2241. https://doi.org/10.2147/IJN.S363237

Wen, F., Li, P., Zhang, Y., Zhong, H., Yan, H., & Su, W. (2023). Preparation, Characterization of Green Tea Carbon Quantum Dots/Curcumin Antioxidant and Antibacterial Nanocomposites. *Journal of Molecular Structure, 1273*, Article 134247. https://doi.org/10.1016/j.molstruc.2022.134247

Wu, H., & Mu, W. (2022). Application prospects and opportunities of inorganic nanomaterials for enzyme immobilization in the food-processing industry. *Current Opinion in Food Science, 47*, 100909. https://doi.org/10.1016/j.cofs.2022.100909

Xiao, Y., Guo, G., Wang, H., Peng, B., Lin, Y., Qu, G., Li, B., Jiang, Z., Zhang, F., Wu, J., & Liang, M. (2024). Curcumin/L-OHP co-loaded HAP for cGAS-STING pathway activation to enhance the natural immune response in colorectal cancer. *Bioengineering & Translational Medicine, 9*(1). https://doi.org/10.1002/btm2.10610

Xu, B., Yuan, C., & Zhang, J. (2023). Curcumin Inhibits Proliferation of Renal Cell Carcinoma in vitro and in vivo by Regulating miR-148/ADAMTS18 through Suppressing Autophagy. *Chinese Journal of Integrative Medicine, 29*(8), 699–706. https://doi.org/10.1007/s11655-022-3690-9

Xu, Z. P., Zeng, Q. H., Lu, G. Q., & Yu, A. B. (2006). Inorganic nanoparticles as carriers for efficient cellular delivery. *Chemical Engineering Science, 61*(3), 1027–1040. https://doi.org/10.1016/j.ces.2005.06.019

Ying, S., Guan, Z., Ofoegbu, P.C., Clubb, P., Rico, C., He, F., & Hong, J. (2022). Green Synthesis of Nanoparticles: Current Developments and Limitations. *Environmental Technology & Innovation, 26*, Article 102336. https://doi.org/10.1016/j.eti.2022.102336

Yu, S., Wang, X., He, X., Wang, Y., Gao, S., Ren, L., & Shi, Y. (2016). Curcumin Exerts Anti-Inflammatory and Antioxidative Properties in 1-Methyl-4-Phenylpyridinium Ion (MPP+)-Stimulated Mesencephalic Astrocytes by Interference with TLR4 and Downstream Signaling Pathway. *Cell Stress and Chaperones, 21*(4), 697–705. https://doi.org/10.1007/s12192-016-0695-3

Zadeh, E.S., Ghanbari, N., Salehi, Z., Derakhti, S., Amoabediny, G., Akbari, M., & Tokmedash, A.M. (2023). Smart PH-Responsive Magnetic Graphene Quantum Dots Nanocarriers for Anticancer Drug Delivery of Curcumin. Materials Chemistry and Physics, 297, Article 127336. https://doi.org/10.1016/j.matchemphys.2023.127336

Zhai, L.-L., Li, W.-B., Chen, L.-J., Wang, W., Ju, T.-F., & Yin, D.-L. (2024). Curcumin inhibits the invasion and migration of pancreatic cancer cells by upregulating TFPI-2 to regulate ERK- and JNK-mediated epithelial–mesenchymal transition. *European Journal of Nutrition, 63*(2), 639–651. https://doi.org/10.1007/s00394-023-03296-5

Zhang, J., Zheng, P., Li, J., Yang, Y., Zeng, S., Qiu, J., & Lin, S. (2022). Curcumin-Mediated Sono-Photodynamic Treatment Inactivates Listeria monocytogenes via ROS-Induced Physical Disruption and Oxidative Damage. *Foods, 11*(6), 808. https://doi.org/10.3390/foods11060808

Zhang, X., Zhu, L., Wang, X., Zhang, H., Wang, L., & Xia, L. (2023). Basic research on curcumin in cervical cancer: Progress and perspectives. *Biomedicine & Pharmacotherapy, 162*, 114590. https://doi.org/10.1016/j.biopha.2023.114590

Zheng, D., Huang, C., Huang, H., Zhao, Y., Khan, M.R.U., Zhao, H. & Huang, L. (2020). Antibacterial Mechanism of Curcumin: A Review. *Chemistry & Biodiversity, 17*(8), Article e2000171. https://onlinelibrary.wiley.com/doi/10.1002/cbdv.202000171.

Zhou, L., Lu, Y., Liu, J., Long, S., Liu, H., Zhang, J., & Zhang, T. (2020). The Role of MiR-21/RECK in the Inhibition of Osteosarcoma by Curcumin. *Molecular and Cellular Probes, 51*, Article 101534. https://doi.org/10.1016/j.mcp.2020.101534

Zhu, G., Shen, Q., Jiang, H., Ji, O., Zhu, L., & Zhang, L. (2020). Curcumin Inhibited the Growth and Invasion of Human Monocytic Leukaemia SHI-1 Cells *in Vivo* by Altering MAPK and MMP Signalling. *Pharmaceutical Biology, 58*(1), 25–34. https://doi.org/10.1080/13880209.2019.1701042

Zhu, T., Liang, D., Zhang, Q., Sun, W., & Shen, X. (2024). Curcumin-encapsulated fish gelatin-based microparticles from microfluidic electrospray for postoperative gastric cancer treatment. *International Journal of Biological Macromolecules, 254*, 127763. https://doi.org/10.1016/j.ijbiomac.2023.127763

Zielińska, A., Alves, H., Marques, V., Durazzo, A., Lucarini, M., Alves, T.F., Morsink, M., Willemen, N., Eder, P., Chaud, M., & others. (2020). Properties, Extraction Methods, and Delivery Systems for Curcumin as a Natural Source of Beneficial Health Effects. *Medicina, 56*(7), Article 336. https://doi.org/10.3390/medicina56070336

CHAPTER 11

Nano-in-nano particles dual-loaded with curcumin and benzydamine hydrochloride for the treatment of vulvovaginal candidiasis: from development to biological application *in vitro* and *in vivo*

Gabriela Corrêa Carvalho, Maria Nolasco Viseu Domingues, Gabriel Davi Marena, Ermei Mäkilä, Jiachen Li, Gésinda Geertsema-Doornbusch, Cleverton Roberto de Andrade, Marc C. A. Stuart, Mohammad-Ali Shahbazi, Ione Corrêa, Brandon W. Peterson, Jarno Salonen, Helena F. Florindo, Taís Maria Bauab, Marlus Chorilli*, Hélder A. Santos*

Under review in Small

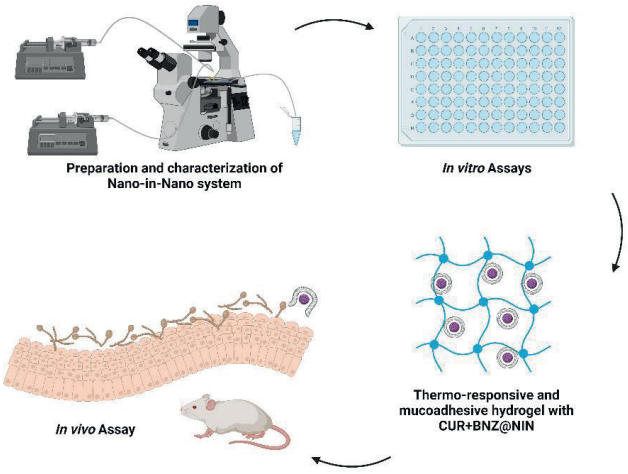

Abstract

Vulvovaginal candidiasis represents a public health challenge due to its reports of high incidence and recurrences. These are caused by host-related factors like compromised immune system, or pathogen-related factors, such as resistance to antifungal agents, making this medical problem desirable to develop new therapeutic options. In this context, natural origin substances like curcumin, are increasingly treatment alternatives. However, some curcumin properties limit its therapeutic application, such as insolubility in aqueous solvents, which leads to low bioavailability. Nevertheless, the association of nanotechnology and drugs of plant origin proves to be a promising alternative to overcome the reported drawbacks. Despite being caused by a fungus, patients suffer significantly from the inflammation resulting from this disease, thus this study aimed to develop a hybrid carrier nanoformulation by microfluidics loaded with two drugs, benzydamine hydrochloride (anti-inflammatory drug) and curcumin (antifungal). Transmission electron cryomicroscopy combined with energy dispersive X-ray analysis confirmed that the nanoparticle was properly developed. Through *in vitro* biological studies, it was possible to observe that, in addition to being safe, the encapsulation of both drugs in the nanocarrier drastically reduced their cytotoxicity. Finally, although the final nanoformulation did not show anti-fungal *in vitro* activity, the *in vivo* study indicated to anti-fungal and anti-inflammatory therapeutic potential.

1. Introduction

Vulvovaginal candidiasis (VVC) is an infection in the vulva region caused by the fungus *Candida* sp., which is considered a public health problem since it is the second leading cause of vaginitis. While there is a lack of updated global prevalence data for this disease, its prevalence can be observed through studies carried out in specific countries, like 18% in Brazil (Carvalho, de Oliveira, et al., 2021), 33% in sub–Saharan Africa (Mushi et al., 2022) 22.8% in Taiwan and 15.5 and 14% in Belgium on summer and winter respectively (Donders et al., 2022). Despite the wide range of available drugs, literature reports highlight ineffective treatments attributed to fungus resistance to several drugs used in therapy. Those ineffective treatments may result in complications, such as pelvic abscess, pelvic inflammatory disease, infertility and miscarriage, underscoring the clinical importance of studying new therapeutic options (Araujo et al., 2020; Barbedo et al., 2010; Jane et al., 2019; Marchaim et al., 2012). In this context, an increasing amount of research is being done in order to overcome this resistance issue. For example new strategies associating drugs already well established in therapeutics, such as sponges chitosan-based sponges containing clotrimazole (Martins et al., 2023) and stimuli-responsive *in situ* miconazole nitrate spray gel (Hsin et al., 2023). As well as exploring others active molecules, like ibrexafungerp (Sucher et al., 2022) and natural products(Hassan et al., 2021). Plant-based alternatives, such as curcumin (CUR), have been gaining increasing attention. This compound, a yellow polyphenol and hydrophobic bioactive extracted from the *Curcuma longa L* rhizome, has several pharmacological properties, including anti-inflammatory and antifungal actions, especially against *Candida* sp. (Molinaro et al., 2023; Obeid et al., 2023; Santezi et al., 2021). This drug was selected here since several studies in the literature pointed to its therapeutic efficiency against Candida infections, specially VVC (Cacaci et al., 2023; Pozharani et al., 2023; Rodero et al., 2018).

Although antifungals of natural origin are considered efficient to overcome the limitations, such as resistance and adverse effects of conventional therapy, it may not be sufficient in the case of symptomatic patients. This is because, in addition to the infection, these patients also present the recruitment of polymorphonuclear leukocytes in the vaginal lumen, causing acute symptoms. Therefore, the association of antifungals and anti-inflammatory drugs is an interesting strategy for the treatment of symptomatic patients (Felix et al., 2019; Yano et al., 2017). However, CUR is insoluble in aqueous solvents, which leads to low bioavailability, hindering its use in therapy (Alves et al., 2019; Shi & Maguer, 2000). The association of nanotechnology with drugs of plant origin with low solubility in aqueous media proves to be a promising alternative (de Lima et al., 2020; Carvalho et al., 2020; dos Santos et al., 2019).

In addition to CUR, it is worth mentioning benzydamine hydrochloride (BNZ), a synthetic nonsteroidal anti-inflammatory drug (Cheng et al., 2023; Sugiarto et al., 2020). This drug is widely

used for topical applications, and it is possible to observe several articles in the literature where it was used to treat VVC. Furthermore, it is the active component of several formulations marketed worldwide for the treatment of gynecological conditions. In addition to this activity, BNZ also has well-documented antifungal activity, which makes it an ideal drug for VVC treatment (Boselli et al., 2012; di Stefano et al., 2020; Sugiarto et al., 2020).

Among the various systems used for drug delivery, lipid-based ones like liposomes can be highlighted, as it is one of the most widely used systems in the world. This popularity is attributed to advantages like excellent biocompatibility, customizable size, easy surface modulation, drug protection from degradability, ability to control the release of incorporated drugs, and high retention of drug loads retention at the action site (Duong et al., 2023; Wu et al., 2022; Zhang & Huang, 2020). This type of system consists of spherical vesicles containing one or more lipid bilayers. Since it has hydrophobic and hydrophilic properties, it exhibit versatility to incorporate both, hydrophobic (inside the lipid bilayer) and hydrophilic molecules (in the core) (Mitchell et al., 2021).

A second system that is also considered promising and also needs to be highlighted is mesoporous silica nanoparticle (MSNs). These nanoparticles stands out due to their desirable properties, such as large surface area, high chemical and thermal stabilities, tunable particle diameter and pore structure, free hydroxyl groups for functionalization, biodegradability, biocompatibility, low toxicity, and easy elimination from organisms, are being widely applied for biomedicine purposes. (Carvalho et al., et al., 2020; Lérida-Viso et al., 2023; Sábio et al., 2023) Although there is a considerable amount of research involving MSNs, only one formulation has been approved by the Food and Drug Administration (FDA) for clinical trials to date. In this sense, hybrid nanoparticles, with lipids and natural polymers for example, have been considered an alternative to bring this type of material closer to its application in therapy as those materials make silica a more biomolecule-friendly and stable, in addition to provide a barrier against premature release and increase its circulation time in the body. (Dumontel et al., 2023; Noureddine et al., 2023)

Thus, aiming to design a novel hybrid nano-in-nano (NIN) formulation, which would allow controlled and prolonged antifungal and anti-inflammatory action of CUR and BNZ, a hybrid nanoparticle system was proposed. The strategy was to incorporate one drug into the lipid bilayer of the liposome and the other into the MSNs, which would be encapsulated in the core of this liposome. Additionally, considering the challenge of a smart administration, it is worth mentioning that semi-solid formulations are difficult to apply in the vagina, and that liquids cause discomfort as they can quickly disperse from the application site. Taking into account the aforementioned, thermo-responsive and mucoadhesive hydrogels are an interesting alternative, since they are liquid at room temperature

and gel at body temperature, bypassing these limitations (Arpa et al., 2023; Carvalho et al., 2021; Khan et al., 2023).

In the present work, we sought to develop and evaluate a NIN system incorporated with CUR and BNZ, one in each part of the nanoparticle (MSN and lipid bilayer) dispersed in thermoresponsive hydrogels and evaluate its antifungal and anti-inflammatory biological activity, *in vitro* and *in vivo*, against VVC.

2. Material and methods

2.1. Mesoporous silica nanoparticles synthesis and characterization

MSNs were synthesized according to Carvalho et al., (2022) with some modifications. Firstly, 0.61 g of cetyltrimethylammonium bromide (CTAB) (Sigma-Aldrich®) and 180 mL of distilled water were added in a round bottom flask and kept under stirring at 60 °C for 30 min. Then, 55.8 mL of octane (Fisher Scientific), 105 µL of styrene (Fisher Scientific) (previously washed three times in 2.5 M NaOH), 0.14 g of L-Lysine (Fisher Scientific), 6.42 mL of tetraethyl orthosilicate (TEOS) (Sigma-Aldrich®), 0.20 g of sodium dihydrochloride 2,2'-Azobis(2-methylproprylnamide) (AIBA) (Fisher Scientific), were added. After, with the help of a needle, nitrogen was immersed in the mixture for approximately 30 min, then the needle was lifted but kept inside the flask throughout the reaction time (3 h). It is worth noting that during this period the magnetic stirring and the temperature of 60°C were maintained.

After, the suspension was transferred to a separatory funnel for phase separation overnight (room temperature). Then, the suspension phase was collected and centrifuged (Sorvall Discovery™ 90SE, Kendro Laboratory Products) at 21,000 rpm for 15 min, the precipitate was washed 5 times with distilled water and ethanol. At the end of the washes, the precipitate was suspended in 60 mL of methanol. Sequentially, the particles were subjected to an acid reflux step, for this 15 mL of chloroform and 1.5 mL of hydrochloric acid were added and kept under reflux with magnetic stirring at 60 °C for a period of 6 h. Then, the resultant solution was centrifuged at 21,000 rpm for 15 min, the precipitate was washed 5 times with distilled water and ethanol. (Carvalho et al., 2022) Lastly, the precipitate was dispersed in 4-(2-hydroxyethyl)-1-piperazineethanesulfonic acid (Hepes) buffer (pH 7.4) (Sigma-Aldrich®) and kept under refrigeration (1 – 4 ºC).

In order to evaluate the MSN formation hydrodynamic size, polydispersity index (PDI) and zeta potential were evaluated by dynamic light scattering (DLS) (ZEN3600, Malvern Panalytical Ltd.,) using HEPES buffer (pH 7.4) as the dispersant. Additionally, Fourier-transform infrared spectroscopy (FTIR) Golden Gate™ Single Reflection Diamond attenuated total reflectance (ATR) System (AgilentTechnologies Cary 670 and sliding wear tester TR-17), thermogravimetric (TG) (PerkinElmer

TGA-7) (using a synthetic air purge; measure program done stepwise using 10°C/min heating ramp with 25 min isothermal segments at 35 and 120 °C) and nitrogen sorption analysis (at 196 °C in a Micromeritics 3Flex 3500) using the Brunauer–Emmett–Teller (BET) method to calculate the surface area. Pore volume was estimated as the total adsorbed amount at a relative pressure of $p/p_0 = 0.97$ while pore size distribution was calculated with MicroActive v5.01 software (Micromeritics Corp.) using density functional theory, assuming cylindrical pores with kernel model for oxide surfaces. Prior to analysis the sample was degassed at 120 °C under high vacuum. Finally, TEM (TalosF200i operating at 80 KeV with a Ceta 16M camara) was also carried out.

2.2. Preparation and characterization of the hybrid system

A cylindrical borosilicate glass capillary (WPI®) (external diameter of 1000 μm) was tapered at one of its ends with the aid of a micropipette puller (P-1000 Sutter Instrument®). Then it was polished until an internal diameter of 100 μm. (Cerdá et al., 2023; Känkänen et al., 2023; J. P. Martins et al., 2018) It was then inserted into a cylindrical borosilicate glass capillary, (internal diameter of 1.1 mm). Dispensing needles (McMaster-carr) were fixed at the beginning of each capillary to facilitate the entry of inner and outer fluids (**Figure 1A-D**). The inner fluid was composed of MSN (2 mg/mL) outer composed by egg yolk phosphatidylcholine (E80 ©Lipoid and soybean phosphatidylcholine (S100 ©Lipoid) solubilized in ethanol (10 mg/mL each). It is worth noting that the microfluidics system consisted of two syringe pumps (PHD Ultra™ Harvard Apparatus) and a microscope (Leica DM IL LED) (Arduino et al., 2021; Liu et al., 2022; Tramontano et al., 2023). Regarding the flow several attempts were made (1:7; 1:10; 1:5; 1:2.5; 9:1; 7:1) (Martins et al., 2018; Zhang et al., 2023). It is worth noting that the samples were collected in a solution containing 1% poloxamer in deionized water. Formulations with a PDI close to or below 0.2 in DLS analyses (using deionized water as the dispersant) were further characterized by transmission electron microscopy (TEM). Additionally, to confirm the formation of the hybrid nanoparticle transmission electron cryomicroscopy (CryoTEM (Tecnai T20 - FEI, Eindhoven the Netherlands with an Us400 slow scan CCD camara and operating at 200 keV) and energy dispersive X-ray (EDX) (X-max 80T SDD detector, Oxford instruments) analyzes were performed.

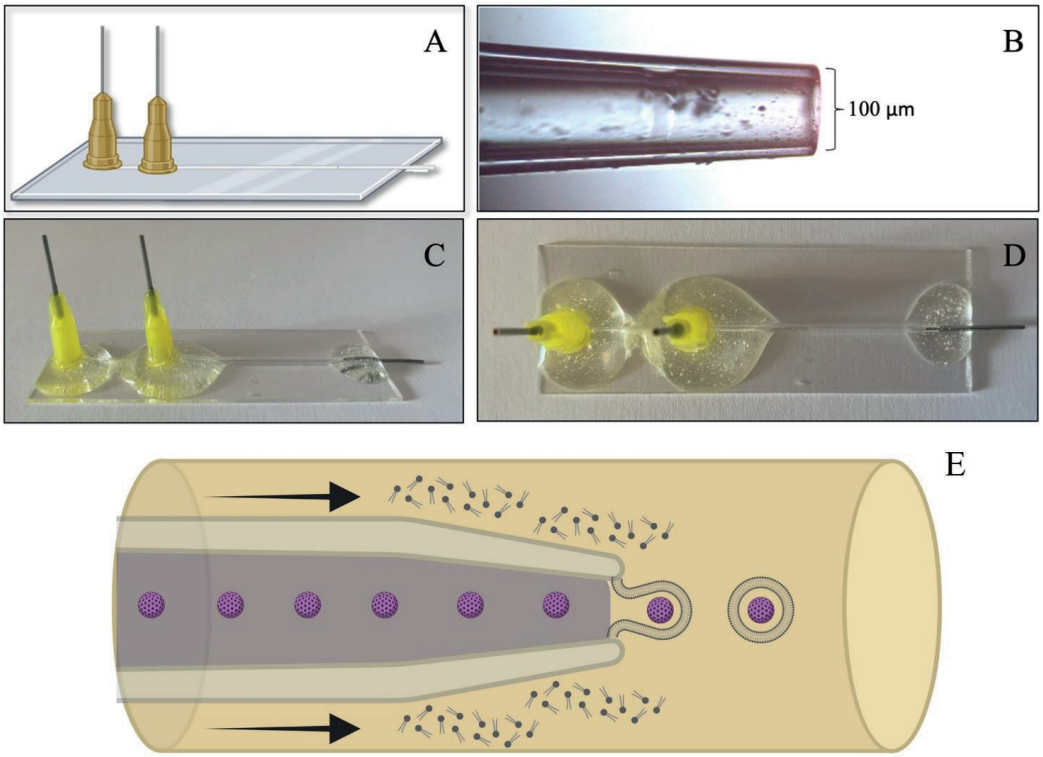

Figure 1. Microfluidics microchip used for the hybrid nanoparticle synthesis. (A) Graphic representation; (B) Microscope image of the inner capillary with 100 µm diameter; (C) Side view of the microfluidics chip; (D) Top view of the microfluidics chip; (E) Schematic hypothesis of the hybrid nanoparticle system assembly by the co-flow microfluidics system. The hybrid nanoparticle consists of CUR-loaded MSN encapsulated into a BNZ-loaded lipid-bilayer. Legend: CUR: curcumin; BNZ: benzydamine hydrochloride; MSN: mesoporous silica nanoparticle.

2.3. *In vitro* synergism assay (checkerboard)

The Supporting Information and **Figure S1** describe this methodology in detail, Briefly, for this assay, two 96-well microplates were used. One of them with CUR (Pharmaceutical Secondary Standard from Supelco®) in the concentration range: 1000–7.8125 µg/mL), and the other with BNZ (analytical standard from Sigma-Aldrich®) in the concentration range: 1000–12.625 µg/mL). Concentration of 1×10^3 yeasts/mL of *C. albicans* FMB-01 (clinical strain resistant to azoles provided by the Medical School of São Paulo State University; Ethical Assessment: 55758222.6.0000.5411) was used as the inoculum. The results were analyzed according to the fractional inhibitory concentration index (FICI), if FICI ≤ 0.5 the drugs combination have a synergism effect, if FICI > 0.5

- 4.0 the drugs combination has a neutral effect and if FICI > 4.0 the drugs combination has an antagonistic effect (CLSI, 2017; LaFayette et al., 2010).

2.4. Drugs encapsulation

Prior to the drug encapsulation stage in the hybrid nanoparticle system, there was a need to develop and validate a high-performance liquid chromatography (HPLC) (Agilent, 1260 infinity II) analytical method with a C18 column (Sulpelco® 15 cm × 4.6 mm, 5 µm) in order to allow the separation and detection of both drugs, CUR and BNZ. Regarding the development of the HPLC method, the best condition observed was the gradient of 70:30 acetonitrile and 0.2% phosphoric acid in water 0.9 mL/min over 1.5 min, change in the flow to 1.5 mL/min over 0.5 min and change of mobile phase composition to 80:20. The best detection wavelength was 230 nm (Kundu & Nithiyanantham, 2013; Molinaro et al., 2023). In **Figure S2** it is possible to observe the HPLC chromatogram, the first peak corresponds to the BNZ and the second corresponds to CUR.

After, the drugs were encapsulated. Firstly, CUR was loaded into MSN, and for this, 2.5 mg/mL of the drug was dissolved in 750 µL of ethanol and kept stirring at 8 ºC. Next, 250 µL of MSN (20 mg/mL in HEPES buffer) was added, and the solution was kept shaking for 24 h. Next, the nanoparticles were collected, centrifuged at 14000 rpm for 15 min and the precipitate was resuspended in a basic ethanolic solution and maintained under magnetic stirring for 24 h to destroy the MSN. After this period, it was centrifuged under the same conditions mentioned above and the supernatant was read in HPLC.

For BNZ encapsulation into the lipid layer, 1 mg/mL of the drug was dissolved in an ethanolic solution containing the lipids, then the hybrid nanoparticle system was synthesized as described in *Section 2.2*. To evaluate the amount of incorporated drug, 1 mL of nano-in-nano (NIN) was centrifuged (Eppendorf 5417r) at 3000 rpm for 5 min and the precipitate was resuspended in 500 µL of chloroform in order to destroy the lipid layer of the particle. The solution was filtered and analyzed in HPLC. Finally, after evaluating the amount of drug incorporated separately, the simultaneous incorporation was evaluated, and for this, immediately after CUR encapsulation in the MSN, the NIN was prepared with the other drug, and the amount of both drugs encapsulation was performed in both methods mentioned above. The loading degree (LD) was calculated according to Martins et al. (2022). The hybrid nanoparticle system formation after the drugs' encapsulation was evaluated by both TEM and Cryo-TEM.

2.5. *In vitro* drug release

To have a preview of developed nanosystem behavior, a preliminary release study was performed on a shaker incubator equipment, which allowed the samples (CUR and BNZ dual loaded in the nano-in-nano (CUR+BNZ@NIN) and CUR+BNZ, in triplicate) to remain during the entire assay at 37 ± 0.5 °C under constant stirring of 150 rpm. (Rodero et al., 2018) For this study, the sink conditions were respected. (United States Pharmacopeia, 2020) To mimic the vaginal environment, the acceptor medium contained simulated vaginal fluid (Biochemazone™), 2% tween 80 and 5% propanol, with a pH of 4.5, compatible with the human vaginal one (Marques et al., 2011; United States Pharmacopeia, 2020). Samples aliquots (200 µL) were collected at multiple times points (10 min; 30 min; 1 h; 2 h; 3 h; 6 h; 12 h; 24 h, 36 h, 48 h, 60h, 72 h 84 h and 96 h), additionally, at each collection point the same volume of acceptor medium was replaced. The drug content in the aliquots was quantified by the validated HPLC method, as described above. Additionally, the samples collected at times 0, 3 h, 6 h, 24 h e 48 h were evaluated for its size by DLS and morphology by TEM (CM12, Philips Eindhoven, operating at 120keV with an Us400 slow scan CCD camara). For the TEM the samples were negatively stained with phosphotungstic acid (PTA) 1% in water (Martins et al., 2018).

2.6. Storage stability assessment

In order to determine the time range that a formulation will be ideal for use in the laboratory and also to make a correlation with its shelf-life, samples were prepared, (day 0) and analyzed by DLS regarding its size, PDI and zeta potential. The samples were then stored in a refrigerator and analyzed every 15 days. It is worth noting that shortly before DLS analysis, the samples were centrifuged at 3000 rpm for 5 min and the precipitate was resuspended in 1 mL of deionized water. In parallel, statistical analysis (two-way ANOVA with Tukey's multiple comparisons) in the software GraphPad Prism® was carried out in order to determine significant changes in the evaluated parameters. Finally, using Cryo-TEM, at a time point of choice that they were not stable, the difference in the nanosystem morphology was evaluated.

2.7. *In vitro* cytotoxicity evaluation

Normal Human Dermal Fibroblasts (NHDF) were maintained in culture in Dulbecco's Modified Eagle's Media (high glucose) (Gibco®) containing 10% fetal bovine serum and 1% Pen-Strep (Gibco®).(Duraccio et al., 2019; Perlíková et al., 2021) Prior to the test, the cells were harvested with trypsin-ethylenediaminetetraacetic acid (EDTA)-phosphate buffer solution (Gibco®) and diluted at a density of 1.5×10^5 cells/mL. Then, the cells were seeded in a 96-well (0.2 mL per well) and left to

attach for 24 h. After the attachment, the medium was discarded, and the cells were washed with 200 µL of PBS pH 7.4. Next, the cells were exposed to the controls (9% Triton X-100 solution (Boom) as positive control and cell media as negative control), CUR+ BNZ @NIN (concentration range 1–0.031 mg/mL) and free drugs (in concentrations corresponding to the drug amount present in the formulation dilutions, for CUR and BNZ respectively: 400–12.5 µg/mL and 50-1.6 µg/mL). Then, the plate was incubated for 24 and 48 h at 37 °C in 5% of CO_2 and 95% relative humidity. In order to quantify the number of viable cells CellTiter-Glo™ (©Promega corporation) assay was performed. The experiment was performed in triplicate (Heikkilä et al., 2010; Imlimthan et al., 2020; Tahir et al., 2019).

2.8. Evaluation of antifungal activity *in vitro*

For the determination of the CUR+ BNZ @NIN minimum inhibitory concentration (MIC) two *C. albicans* strains were used, ATCC 18804 and FMB-01. In addition to the main nanosystem, CUR incorporated in MSN (CUR@MSN), BNZ loaded in the NIN (BNZ@NIN) and NIN (without drug) were also analyzed as controls. Since all formulations had the same amount of the respective drug present, the CUR and BNZ range evaluated was 596.25–4.65 µg/mL and 63.75–0.5 µg/mL. Prior the test, both strains were cultivated in 2 mL of Sabouraud Dextrose Broth (SDB) (Difco-Becton) and incubated at 37 ºC for 48 h, then, a suspension corresponding to 0.5 on the McFarland scale were confirmed by cells count in a Neubauer chamber (*ca*. 1×10^6 cells/mL) were prepared. In order to have a inoculum with 5.0×10^3 cells/mL two consecutive dilutions were made (1:100 and 1:20) (CLSI, 2017).

After, in a 96-well microplate 100 µL of Roswell Park Memorial Institute (RPMI 1640) medium with pH 7.0–7.2) was added in each well. Then the samples were added in the first-row wells and a serial dilution in the 8 subsequent wells were performed. Then, 100 µL of the inoculum were also added. It is worth mentioning that sterility and growth controls were also performed (CLSI, 2017). The microplate was incubated at 37 °C for 48 h. Finally, 20 µL of 2% triphenyltetrazolium chloride (TTC) (Sigma-Aldrich®) solution were added and after an incubation of 2h at 37 °C a visual reading were performed (lack of fungi growth remain colorless and growth turn the solution pink).

2.9. Thermo-responsive and mucoadhesive hydrogel containing CUR+BNZ@NIN development, characterization and *in vitro* release test

Chitosan (1%) (Sigma-Aldrich®) and poloxamer 407 (Sigma-Aldrich®) were used to confer mucoadhesive and thermo-responsive characteristics, respectively, to the hydrogel (Araujo et al., 2021; Carvalho et al., 2021). Various poloxamer percentages were tested (15, 16.5, 17, 18, 19, 20, 25%) with

the same manufacturing methodology. Initially, deionized water with 1% acetic acid was kept under magnetic stirring in an ice bath for 2 min. Then, chitosan was added and kept in magnetic stirring for another 40 min. After obtaining a homogeneous viscous substance, poloxamer was added gradually under magnetic stirring with the aid of manual stirring until a homogeneous solution was obtained. Subsequently, it was kept overnight in an ice bath. (Ribeiro et al., 2022) To manufacture the hydrogel containing the nanosystem (CUR+ BNZ@NIN@HG), a volume of 5mL of CUR+BNZ@NIN was centrifuged at 3000 rpm for 5 min and then the precipitate was resuspended with 1mL of hydrogel. A rheometer (Anton Paar MCR 92) was used to characterize the hydrogel with and without the nanosystem concerning its gelation point, viscosity *versus* temperature, frequency sweep (at 37 ºC) and linear viscoelastic range (at 37 ºC) (Abbaszadeh et al., 2023; Ahmadian et al., 2021; Carvalho et al., 2023). Additionally, a texture analyzer (Brookfield CT3) was used to evaluate the injectability of the final hydrogel (with and without CUR+BNZ@NIN) with the aid of a vaginal applicator, temperatures of 25 and 37 ºC were tested (Abbaszadeh et al., 2023; Carvalho et al., 2023).

For the *in vitro* release test, some changes to the methodology carried out in item 2.5 were made. The experiment was performed in a 12-well microplate, while the acceptor media was added to the microplate well, the sample was added to cell culture inserts. The stirring speed was changed to 100 RPM. The samples analyzed were the NIN@hydrogel containing both drugs and the hydrogel with the combination of both free drugs.

2.10. Antifungal and anti-inflammatory activity evaluation in *in vivo* mice model

Female BALB/c mice had 8 to 10 weeks weighing around 20 to 25 g were used. The animals were kept in cages at appropriate temperature, with ventilation, 12-h light/dark cycle with water and food available. In order to assist in the induction of the disease, the mice received 0.1 mL of estradiol solution (2 mg/day) intraperitoneally twice in week two. (Carrara et al., 2010; Kalo-Klein & Witkin, 1989) Vaginal infections were induced by intravaginal application of 20 µL of a *C. albicans* suspension containing 2.5×10^8 cells/mL. In the post-infection period, a dose of estradiol (Sigma-Aldrich®) (alternate days) was administered (also intraperitoneally) to maintain the pseudo-estrus state. In order to evaluate the formulation antifungal activity, vaginal washes were carried out with PBS 6 h before treatment, part of the collected volume was sown in Sabouraud Dextrose Agar with chloramphenicol (Difco-Becton). The plates were incubated at 37 ± 0.5 ºC for 48 h, and the colony count was expressed in CFU/mL. The experimental protocol design is summarized in **Figure S3** with a total treatment period of seven days (Toledo et al., 2020; Rodero et al., 2018). It is worth highlighting that the experimental groups for the *in vivo* were carefully selected to obtain the smallest number of groups

that included all the necessary comparisons (**Table S1**), with the smallest number of animals (sample calculation carried out in the software "Power & Sample Size Calculator"). "

As for dosage, 25 µg of BNZ (1 time the combined MIC_9 value) and 239 µg of CUR (12 times the combined MIC_9 value obtained in the checkerboard assay performed in this study) were administered per application. It is worth noting that all formulations were applied at the same dosage, adjusting the final volume in order to standardize the same drug concentration. For the commercial drug Clotrimazole, Medley®, one of the recommended medications by the Center of Disease Control and Prevention (CDC) for VVC treatment, was the one of choice (Workowski et al., 2021). The recommendation in the medicine leaflet was followed, adjusting dosage according to the animal's weight.

Immediately after the euthanasia, the animals were shaved in the vaginal region and through a longitudinal cut in the infra-abdominal region, the vulva and vagina of all animals were collected (and preserved in 4% formaldehyde for 7 days) for histopathological analysis. After this period, a macroscopic analysis was performed to identify the anatomical parts, which were sectioned longitudinally and included in paraffin. After, 4 µM sections were obtained, stained in periodic acid-Schiff (PAS) and blindly evaluated by an experienced pathologist, previously calibrated. The analyses were performed at two different times with a minimum interval of 1 week between them. Light microscope (Carl Zeiss, Primo Star, Germany) was used at 100, 200, and × 400 magnifications.

Firstly, candidiasis was analyzed in two ways, first distribution classification as absent (0); focal (1), multifocal (2) and diffuse (3) and evaluated semi-quantitatively (fungal burden) in the absence of fungi (0), up to five fungal elements per section (standard: 5 mm punch) (1), from six fungal elements per section to five per field at high magnification (×400) (2), from 6 to 50 per field at high magnification (3) and more than 50 per field at high magnification (4) (Quintella et al., 2011). In addition, other parameters were evaluated, such as spongiosis (absent (0), focal (1), multifocal (2) and diffuse (3)), and presence (1) and absence (0) of atrophy, acanthosis, hyperkeratosis and sawtooth projections. After tabulating the data, two-way ANOVA with multiple comparisons was the test of choice for statistical analysis, which was carried out in the software GraphPad Prism®. This *in vivo* experiment was approved by the School of Pharmaceutical Sciences of São Paulo State University; Ethical accreditation number: 02.00082.2019.

3. Results and discussion

3.1. MSN synthesis and characterization

According to the DLS analysis, the MSNs had an average hydrodynamic size of 140.8 nm, with a PDI of 0.213 and zeta potential of -23.4 mV, indicating good size distribution, and charge, similar to

previous reports (Baghirov et al., 2016; Patra et al., 2016; Prabhakar et al., 2013; Şen Karaman et al., 2018).

In order to confirm that the silica matrix had been formed, FTIR analysis was first performed. In **Figure 2** it is possible to observe bands in the regions of 800 and 1085 cm^{-1} corresponding to symmetrical and asymmetrical axial stretching of Si-O-Si respectively, which is characteristic of the silica matrix. Furthermore, the band around 960 cm^{-1} can be attributed to an axial Si-OH stretching, which can be due to the silanols groups available on the surface and inside the MSN pores (Carvalho et al., 2022; Ruan et al., 2019; Sun et al., 2019).

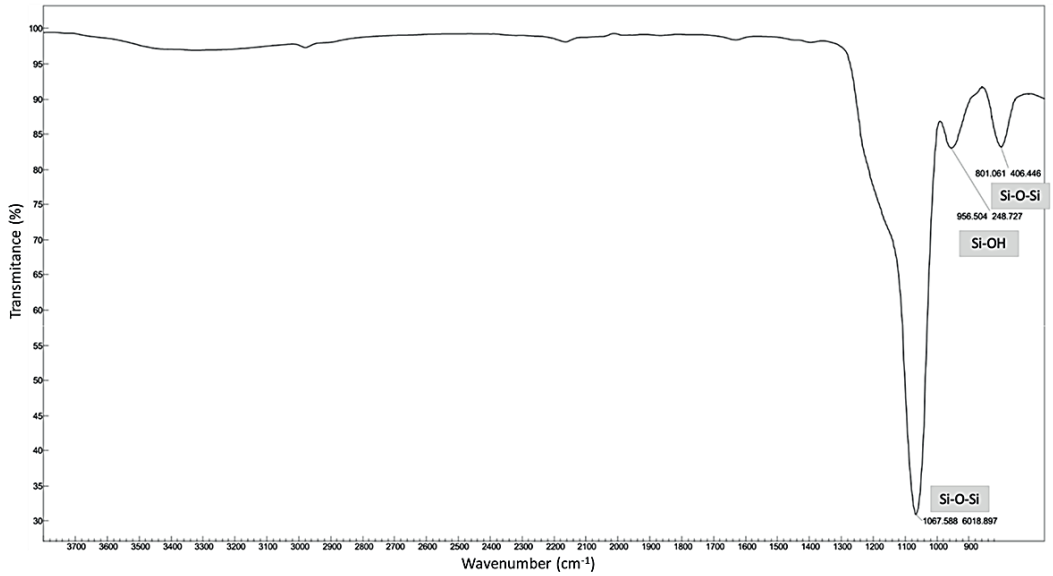

Figure 2. Bare MSN characterization: FTIR spectrum.

Subsequently, in order to verify whether the acid reflux process was capable of removing the organic matter (making the pores free for drug incorporation), a stepwise TG analysis was carried out. **Figure 3A** represents the TG graph of weight *versus* temperature (**Figure S4** represents the TG weight *versus* temperature *versus* time graph). It is possible to observe that initially there is a weight loss (9.2 wt% loss of the initial weight) related to humidity and water bound in two stages. The first one is due to the weakly adsorbed water from the environment that was almost completely removed at 35 °C, while the second one is due the hydrogen-bonded water removed at 120 °C (Maturi et al., 2019). Subsequently, small weight loss (approximately 0.72%) starting at 495 °C, is possibly due to the remaining residue of the pore templating agent or other organic impurities left from the synthesis process (Liou, 2004; Maturi et al., 2019).

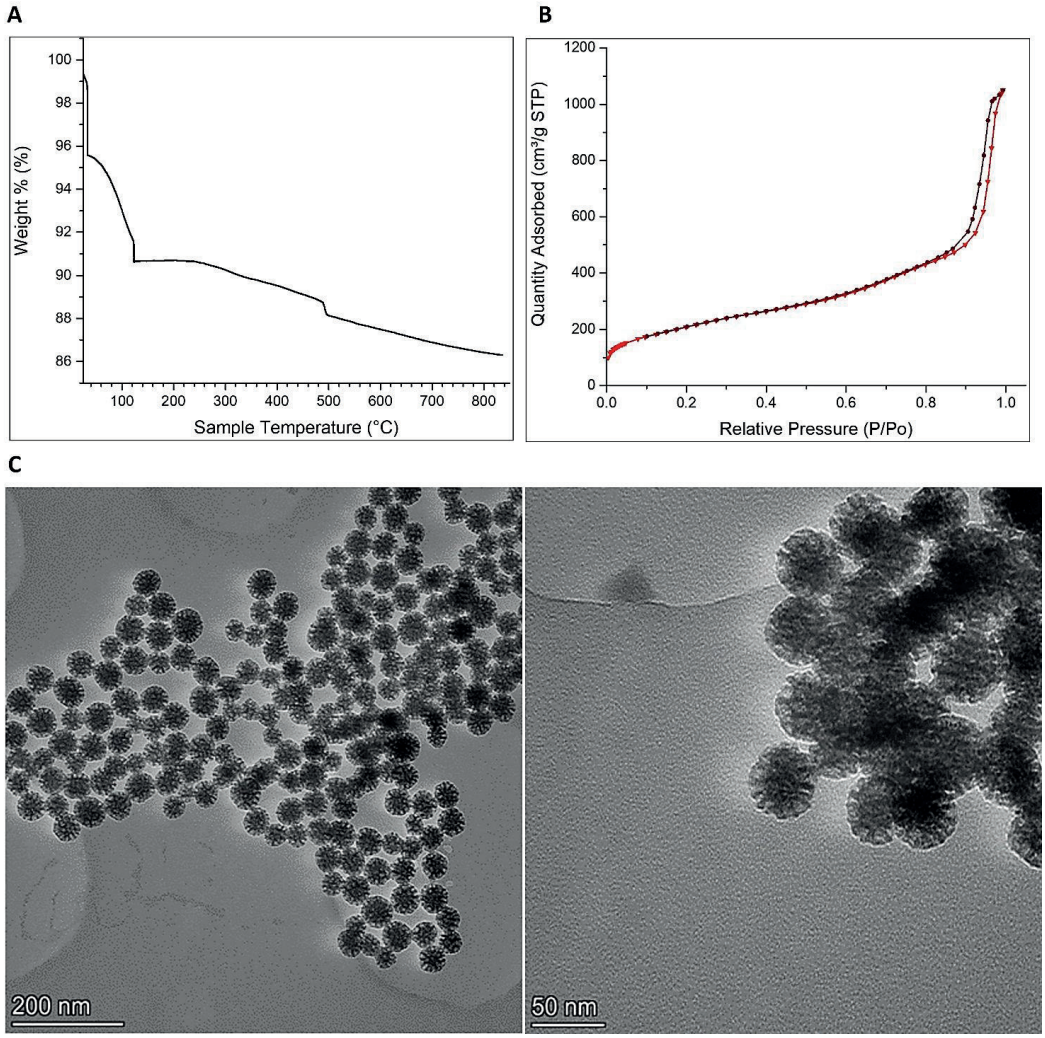

Figure 3. Bare MSN characterization. (A) TGA weight loss curve; (B) BET adsorption-desorption isotherm graph; (C) TEM micrographs.

Surface area and pore size distribution were analyzed by nitrogen sorption measurement. It was observed that the nanoparticles obtained have a specific surface area of 762 m^2/g and an estimated pore volume of 1.58 cm^3/g, with a type IV adsorption-desorption isotherm, as shown in **Figure 3B** (Thommes et al., 2015). Pore size distribution calculation shows 2 to 4 nm cylindrical pores, as well as some 7 nm pores. Finally, the samples were characterized by TEM and **Figure 3C** shows that the MSNs have a spherical shape, with ~50 nm in size and structures suggestive of mesopores, which reinforces the BET findings described above.

3.2. Hybrid nanoparticle system development and characterization

The formation of the NIN was possible with the flow condition of 9 and 1 mL/h for the inner and outer phases, respectively. **Figures 4A and 4B** compare the CryoTEM images of pure MSN and NIN, where it is possible to observe the lipid nanoparticle surrounding the MSN. It is also possible to observe that the nanoparticles are homogeneous, which indicates the obtention of monodisperse hybrid nanoparticles. The presence of the lipid coating was further confirmed with EDX. The obtained spectra from the area shown in **Figure 4C** indicates the presence of phosphorus from the phosphatidylcholine in the NIN system.

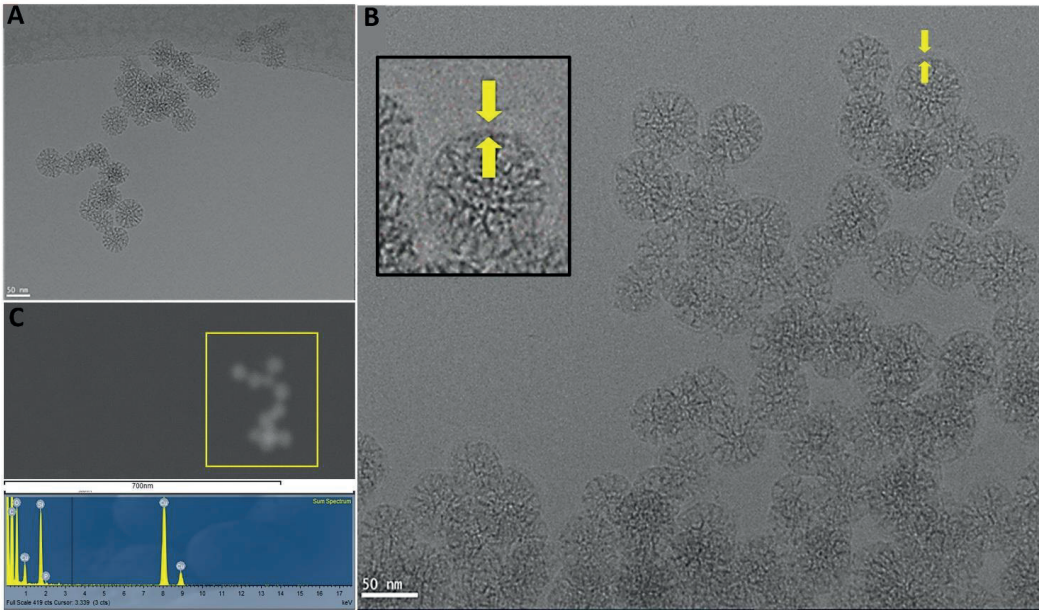

Figure 4. Nano-in-nano characterization results. Cryo-TEM images of the MSN (A) and the nano-in-nano (yellow arrows indicate the lipid-bilayer) (B); EDX analysis of the elemental composition of the nano-in-nano (C).

From the Cryo-TEM images it is also possible to observe that after the lipid coverage the nanoparticles maintained their spherical shape but increased in size, from 50 nm to *ca*. 70 nm. By DLS, an increase in the average hydrodynamic diameter was also observed, from 140.8 (MSN) to 208.8 nm (NIN). Furthermore, a change in zeta potential was also noted, from -23.4 to -5.31 mV. The zwitterionic character of the phosphatidylcholine group present in both lipids gives to the nanoparticles a charge a closer to neutral (Ingebrigtsen et al., 2017; Trapani et al., 2013).

3.3. *In vitro* synergism assay (checkerboard)

Although both drugs have antifungal activity, it is of paramount importance to predict the behavior of both drugs when combined, in order to verify whether this association is desirable. Through calculations, a synergistic relationship between the drugs was observed, in addition, the drugs combination minimal inhibitory concentration (MIC_{90}) value was 19.5 µg/mL for CUR with 23.4 µg/mL for BNZ (**Table 1**). In **Figure S5** it is possible to observe the surface graph of all combinations.

Table 1 Checkerboard microdilution assay to evaluate curcumin and benzydamine hydrochloride combination effect against a resistant *C. albicans* strain.

Drug	MIC_{90} alone	MIC_{90} combined
CUR	62.5 µg/mL	19.5 µg/mL
BNZ	125.0 µg/mL	23.4 µg/mL

Legend: CUR: curcumin; BNZ: benzydamine hydrochloride; MIC_{90}: minimal inhibitory concentration

3.4. Drugs encapsulation

In addition to the LD%, **Table 2** shows the amount of each drug, in mg/mL, loaded into the particle (based on the amount detected by HPLC). Highlighting this value is important once it allows a parallel with the amount of drug necessary to have the antifungal activity, based on checkerboard results (**Table 1**). The fact that the incorporated value per mL is at least 1 time the combined MIC makes this a promising system.

Table 2. CUR and BNZ co-loading amounts and LD% in the hybrid nanoparticle system.

System	CUR		BNZ	
	Loading amount (µg/mL)	LD%	Loading amount (µg/mL)	LD%
CUR@MSN	158	16.3	-	-
BNZ@LP	-	-	69	6.7
CUR+BNZ@NIN	477	22	51	2.5

Legend: CUR: curcumin; BNZ: benzydamine hydrochloride; MSN: mesoporous silica nanoparticle; LP: lipid lawyer of the NIN; NIN: hybrid nanoparticle

3.5. *In vitro* drug release

Figure 5A shows the release profile for both, free BNZ and BNZ-loaded into NIN, around 60%. Despite being considered a water-soluble drug, the solubility of BNZ is not high, as reported

elsewhere (Ali et al., 2018). However, there is a consensus that it is better solubilized in ethanol than in water (Çolak, 2016; Pilicheva et al., 2022; Sharma et al., 2017).

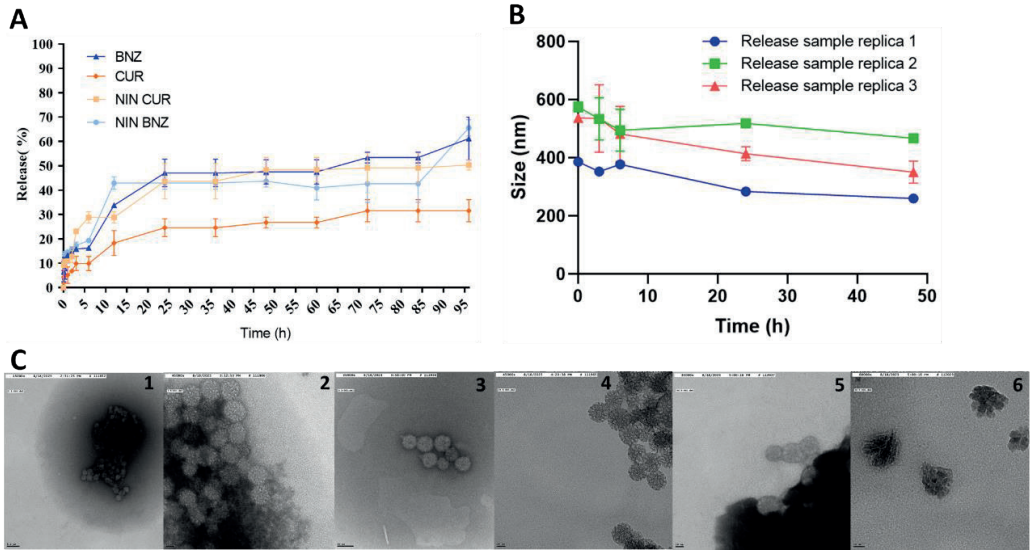

Figure 5. Results from the drug release tests of CUR and BNZ from dual-loaded CUR+BNZ@NIN@HG compared to CUR+BNZ@HG performed in simulated vaginal fluid under agitation at 150 RPM at 37 ºC. Data are represented as the mean of a triplicate. (A) Drug release profiles; (B) Release samples replicas size change according to DLS measurements; (C) TEM images of the release samples replicas at time 0 (1), 3h (2), 6h (3), 24 (4), and 48h (5 and 6). Legend: CUR: curcumin; BNZ: benzydamine hydrochloride; NIN: hybrid nanoparticle; HG: hydrogel.

For CUR, it is possible to observe that its incorporation into the NIN increased the solubility of this drug, as a higher percentage of release was observed (50.3% in NIN and 31.5% for free drug), which is desirable since this drug is hydrophobic and the issue of its insolubility in aqueous solvent is a limiting factor for its application in therapy. It is worth highlighting that this not so high percentage of release is in line with previous studies in the literature (Daryasari et al., 2016; Hartono et al., 2016; Liu et al., 2022).

Figure 5B represents the triplicate DLS size reading of the three samples (replicas) used for the release assay. It is possible to observe that the three samples showed the same pattern, which is consistent with the release results, which shows a release plateau after 24 h (**Figure 5A**). It is worth mentioning that the measured size was higher than the DLS of the NIN in deionized water (**Figure**

5B), probably due to the content of the simulated vaginal fluid which could have led to protein corona formation (Pareek et al., 2018; Pino et al., 2014).

Regarding the TEM of the samples collected during the drug release tests, it is possible to observe the formed NIN at time 0 (**Figure 5C-1**). However, at time 3h (**Figure 5C-2**) they appear less stained at the edge (which indicates a smaller lipid layer). Additionally, at the edges of the aggregate it is possible to observe a morphology destruction, which may be caused by the lipid being destroyed. It is worth mentioning that black dots were observed (drug crystals). At 6h (**Figure 5C-3**), it is difficult to observe the nanoparticle pores, which may indicate degradation, which seems to be more drastic at 24 and 48 h (**Figure 5C-4, 5C-5 and 5C-6**) (Möller & Bein, 2019; Noureddine et al., 2023; Wei et al., 2023). This monitoring of NIN morphology carried out by TEM suggest that during the drug release tests, most likely, the lipid layer was disrupted, which enabled the drugs to be release from the nanohybrid. Moreover, the lipid disintegration and the MSN degradation aspect of the MSN over time in the simulated vaginal fluid point to their biodegradable behavior, which is desirable during the development of a new formulation (Cheng et al., 2022; Martins et al., 2022).

3.6. Storage stability assessment

Stability assessment is an important tool during the development of a drug as it predicts its behavior during storage. Regarding the size, no statistically significant difference was observed between times 0 and 30 days (**Figure 6A**). In the following times (from 45 days onwards), a statistically significant difference (p value <0.0001) was observed when compared with time 0, suggesting loss of stability. It is worth noting that no statistically significant difference was observed for the other parameters. In view of the zeta potential result, we hypothesize that the stability loss after 30 days is due to the lipid nanoparticle layer disintegration; MSN without this lipid coating has a is highly negative zeta potential (-23.4 mV), but after its encapsulation by the lipids, a hybrid nanoparticle with zeta potential close to neutrality (-5.31 mV) was obtained, therefore, the remaining MSN would be more negative than the hybrid particle. To confirm this issue, TEM analysis was carried out in the 60-day sample. As it can be seen in **Figure 6B**, the amount of NIN present is lower compared to **Figure 4B**, supporting the abovementioned hypothesis.

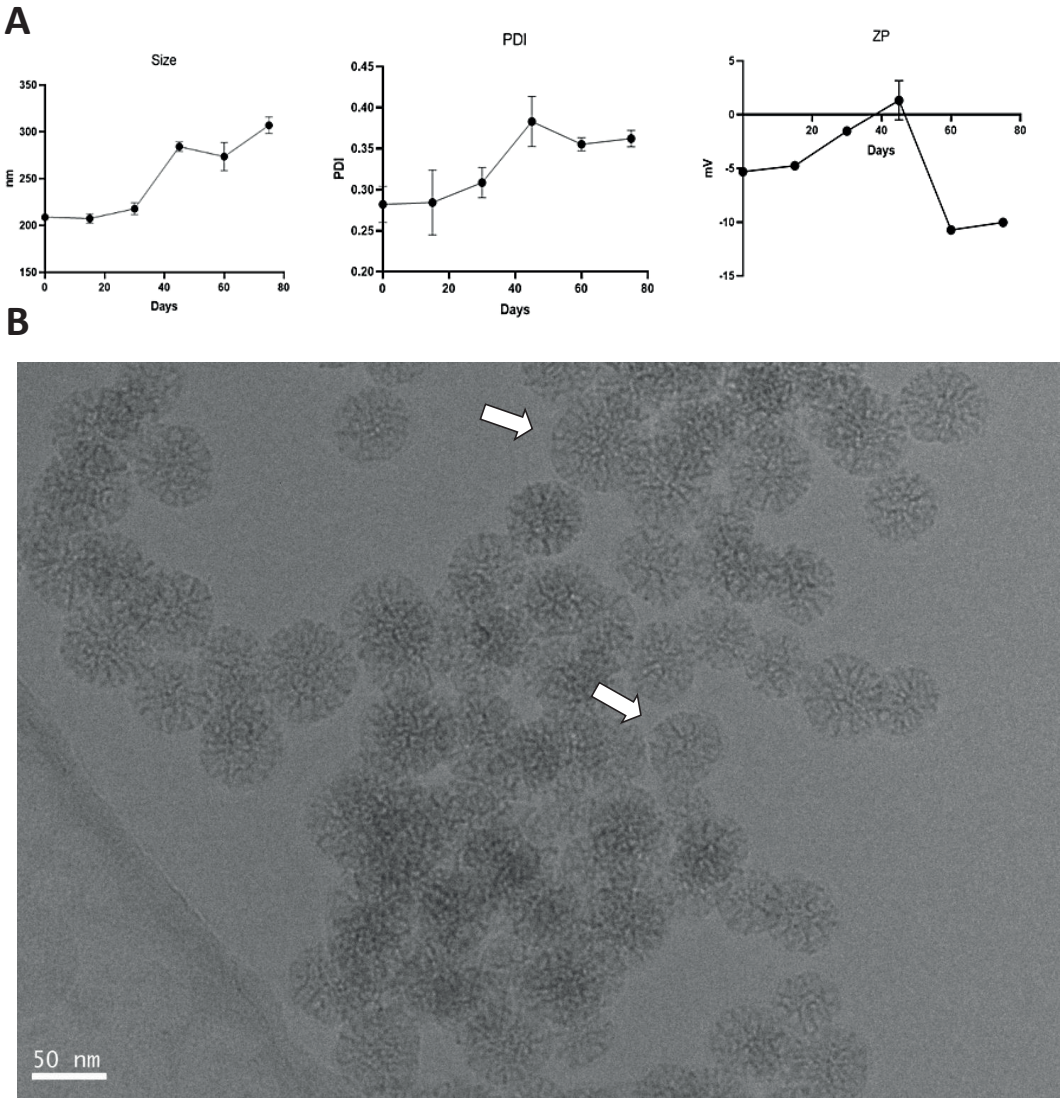

Figure 6. CUR+BNZ@NIN stability assessment (A) tracking by DLS for 75 days after synthesis; (B) Cryo-TEM image after 60 days of synthesis (white arrows indicate the lipid-bilayer). Legend: CUR: curcumin; BNZ: benzydamine hydrochloride; NIN: hybrid nanoparticle.

3.7. *In vitro* cytotoxicity evaluation

Figure 7 shows that the four highest doses tested of the free drugs showed cytotoxicity for NHDF cells; however, when loaded into the NIN nanosystem, no cytotoxicity was observed at any of the concentrations tested, demonstrating that the drug-loaded NIN system bypassed the cytotoxicity limitation of the drugs combination, which is desirable in terms of applying this formulation in therapy.

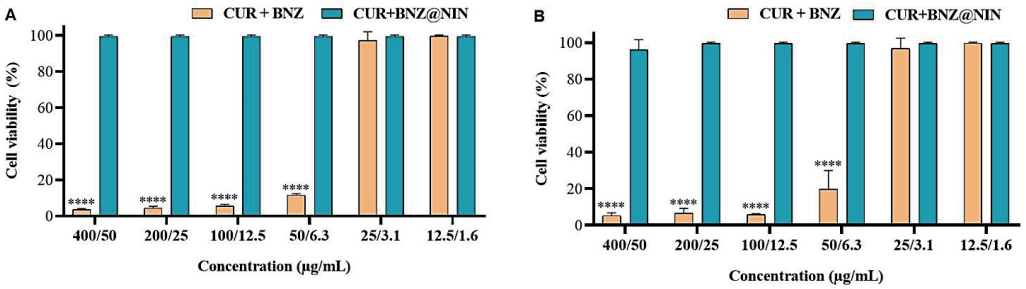

Figure 7. Cytotoxicity evaluation of CUR+BNZ versus CUR+BNZ@NIN in NHDF cells at 24 h (A) and 48 h (B), using the CellTiter-Glo™ assay. Concentrations of 400, 200, 100, 50, 25 and 12.5 µg/mL of CUR and 50, 25, 12.5, 6.3, 3.1 and 1.6 µg/mL of BNZ were analyzed of both samples. The results are the mean of a triplicate and were analyzed by two-way ANOVA (****$p<0.0001$). Legend: CUR: curcumin; BNZ: benzydamine hydrochloride; NIN: hybrid nanoparticle;

3.8. Evaluation of antifungal activity *in vitro*

Although the Clinical and Laboratory Standards Institute (CLSI) (CLSI, 2017) recommends 48 h of incubation, it was decided to additionally test an incubation time of 72 h to guarantee adequate time for antifungal activity, since the incorporated drug would have a barrier to overcome, meaning the drug would have to first be released from the nanocarrier and then be available to carry out the activity. For the American Type Culture Collection (ATCC) strain, it was observed that no formulation showed activity at the tested concentrations, neither at 48h nor at 72h. However, for the clinical strain, the highest concentration of CUR@MSN tested, 596.25 µg/mL, was MIC_{50} in 48h. The other conditions tested showed no activity.

Even though CUR+BNZ@NIN did not show activity in this *in vitro* study, it was decided to continue the development of this formulation since although *in vitro* tests are used to predict the behavior of a formulation during its application *in vivo*, it is possible to observe in the literature that this is not always the case. For example, in a study whose objective was the development of a nanoemulsion containing micafungin against *C. auris* infection, it was observed that although free micafungin presented excellent activity (MIC of 0.062 mg/mL) when incorporated into the nanoemulsion, no activity was observed. However, in the antifungal *in vivo* assay with *Galleria mellonella* it was observed that in addition to having extremely superior activity to the free drug (greater reduction in the counting forming units (CFU) number) the nanoemulsion incorporated with the drug was also able to completely eradicate the infection on the second day of treatment (Marena et al., 2023). In a study performed elsewhere (Jebril et al., 2020), it was observed that lower doses of

silver nanoparticles showed low percentages of fungal inhibition (less than 20%); however, in the *in vivo* test, a better activity was observed.

3.9. Thermo-responsive and mucoadhesive hydrogel containing CUR+BNZ@NIN development, characterization and *in vitro* drug release test

From the formulations developed, the best one contained 19% poloxamer, since when associated with NIN it has a gelation point of *ca.* 33 ºC (**Figure 8A**), within the range considered ideal for thermosensitive hydrogels for topical application (26 to 34 ºC) (Arpa et al., 2023; Kolawole & Cook, 2023). Without NIN, the observed gelation value decreases (**Figure 8B**), a behavior that has already been reported in the literature; however, the point of choice was based on the final formulation NIN@hydrogel (Arpa et al., 2023). However, in **Figure S6** it is possible to observe the gelation graph of the other attempts. According to the literature, to be considered viscous, a substance must have a viscosity greater than 1000 mPas (Bothner & Wik, 1987). **Figures 8C and 8D**, at temperatures of 30 ºC and 25 ºC, NIN@hydrogel and the pure hydrogel, respectively, present this viscosity, which agrees with the gelation data.

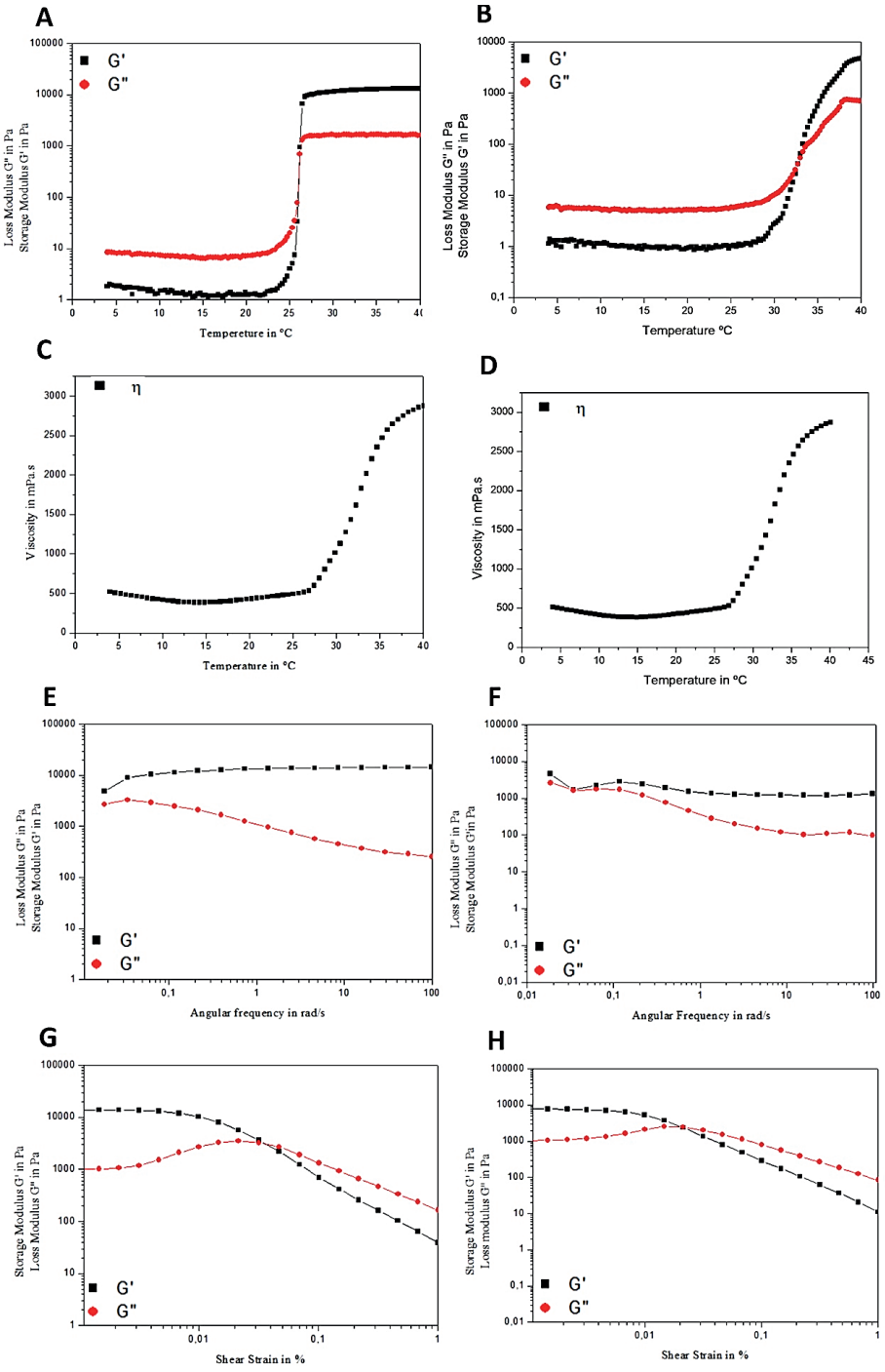

Figure 8. Rheology results of the prepared hydrogel. (A) Hydrogel gelation analysis; (B) NIN@HG gelation analysis; (C) Hydrogel viscosity *versus* temperature analysis; (D) NIN@HG viscosity *versus*

temperature analysis; (E) Hydrogel frequency sweep analysis; (F) NIN@HG frequency sweep analysis; (G) Hydrogel linear viscoelastic range analysis; (H) NIN@HG linear viscoelastic range analysis. Legend: NIN: hybrid nanoparticle; HG: hydrogel.

In **Figures 8E** and **8F** it is possible to observe the frequency sweep, it is worth noting that the lower angular frequencies observed indicates a solid-like substance. Additionally, the fact of the almost crossover observed in the NIN@hydrogel graph indicates that it is stickier than the pure hydrogel, probably due to the fact that the temperature influences on the its viscosity (Adejokun & Dodou, 2019; Block et al., 2011). Finally, the linear viscoelastic region determination allowed an immediate distinction to be made between gels and entanglement networks, and it is possible to observe in **Figures 8G** and **8H** that both presented this region up to 0.1%, as the storage modules were drastically greater than loss modules (Rosalina & Bhattacharya, 2002). Regarding the injectability test carried out with vaginal applicators on a texture analyzer, it was observed that at both temperatures tested, 37 ºC and 25 ºC, the force required to inject is low, around 1 N for the free hydrogel and between 0 and 1 for NIN@ hydrogel.

After the physical characterization, *in vitro* drug release tests were carried out, and the drug release profiles obtained with the samples dispersed in hydrogel (**Figure 9**) were compared with those without the hydrogel (**Figure 5A**). It is possible to observe that CUR showed a similar pattern, however, the solubility of the BNZ increased significantly in both samples, loaded and free. This may be due to the presence of poloxamer in the formulation. For example, in a previous study of hydrogel formulations with poloxamer and chitosan containing BNZ, it was observed that the formulation containing only poloxamer was the one with the highest percentage of release (100% in 6 h), which is in accordance with what was observed in this study (Tuğcu-Demiröz, 2017). Other studies in the literature have shown that after dispersion in hydrogels, BNZ shows 100% release (Karavana et al., 2009). In another study, where two percentages of poloxamer were compared (18 and 20%), although not statistically significant different (p>0.05), the authors also highlighted that the increase in poloxamer 407 concentration reflected an increase in BNZ release (Arpa et al., 2023). A possible hypothesis for this fact would be that the mixture of polymers present in the hydrogel can affect the crystallinity of this drug, increasing its solubility (Mehravaran et al., 2022).

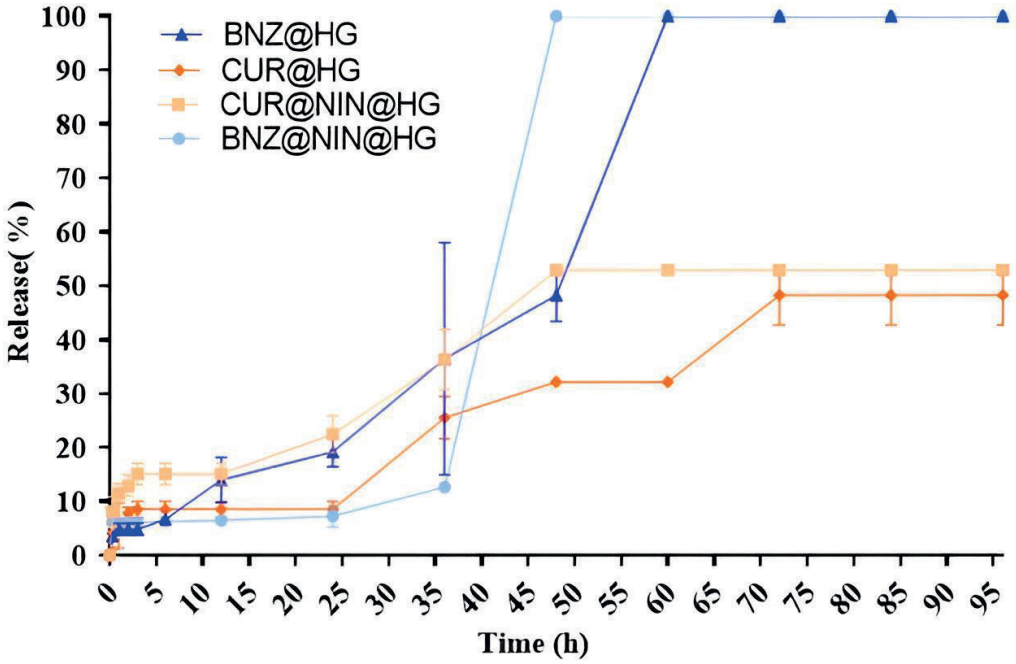

Figure 9. Release profile of CUR and BNZ from dual-loaded CUR+BNZ@NIN@HG compared to CUR+BNZ@HG in simulated vaginal fluid kept under agitation at 100 rpm at 37 ºC. Data are represented as the mean of a triplicate. Legend: CUR: curcumin; BNZ: benzydamine hydrochloride; NIN: hybrid nanoparticle; HG: hydrogel.

3.10. Antifungal and anti-inflammatory activity evaluation in *in vivo* mice model

BALB/c mice were chosen as they have a better response to polymorphonuclear cells, which have been shown to act directly to combat this type of fungal infection in humans (Czechowicz et al., 2022; Nippe et al., 2011; Tacchini-Cottier et al., 2000). To monitor the effect of the three doses administered to the animals in the statistical analysis the log CFU/mL value of each post-treatment sample was compared with the respective log CFU/mL value after infection (before starting the treatment) and it was observed that only the BNZ@NIN group did not show statistically significant differences (p value 0.0921), showing that this sample prevented fungal load to increase. In all other groups, this increase was statistically significant differences (p value <0.0001), except in the negative infection control group.

According to the candidiasis distribution in the vaginal epithelium, in histopathological analysis (main results summarized in **Table 3** and **Figure 10A**), it was observed that the combination of the two drugs was the most effective treatment in reducing the fungal amount, highlighting the

potential of this combination for the treatment of this disease. Another factor that reinforces this observation is its greater efficiency compared to the commercial control. However, in semi-quantitative candidiasis analysis (fungal burden) it is important to highlight that CUR@MSN showed better results both in this parameter and in the *in vitro* study (*Section 3.8*). It was observed that CUR+BNZ@NIN, BNZ@NIN and the commercial formulation were the second-best treatment options, which indicates that they presented similar therapeutic efficiencies. It is also important to highlight that in the groups treated with CUR+BNZ@HG, CUR and BNZ, a high increase in the scale points was observed, and in the case of BNZ, statistically significant differences (p value of 0.0203) were observed when compared with the infection control; showing that the incorporation of the drugs in the NIN increased their therapeutic potential. When incorporated in the hydrogel, the NIN nanosystem was not as efficacy as the non-incorporated one; however, the efficacy was still superior when compared to the free drugs groups (p value of >0.9999 in both cases).

Table 3. Main results of the histopathological analysis performed with the vulva and vagina stained with periodic acid-Schiff.

Group	Parameter in scoring units			
	Candidiasis		Spongiosis	Sawtooth projections
	Distribution	Fungal burden		
Negative for infection	0.000	0.000	0.000	0.000
Positive for infection	1.285	1.428	1.142	0.714
CUR+BNZ@NIN@HG	1.166	1.500	0.666	0.571
CUR+BNZ@NIN	1.571	1.166	0.666	0.714
CUR+BNZ@HG	1.166	2.00	2.000	0.857
BNZ@NIN	0.857	1.166	2.000	0.714
CUR@MSN	1.000	1.000	1.428	1.000
CUR+BNZ	0.666	1.142	0.857	0.571
CUR	1.000	2.000	1.333	1.000
BNZ	1.666	2.667	0.500	1.000
Commercial formulation	0.833	1.166	0.500	0.500

Legend: CUR: curcumin; BNZ: benzydamine hydrochloride; NIN: hybrid nanoparticle; HG: hydrogel; commercial formulation: clotrimazole.

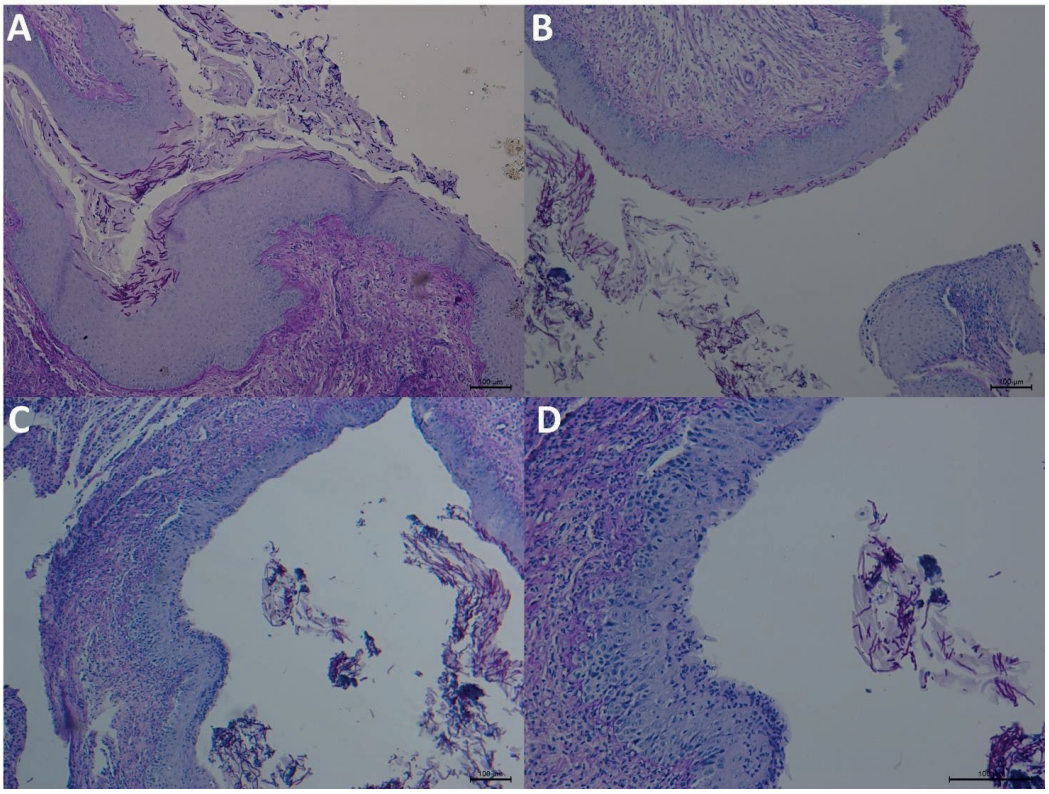

Figure 10. Histopathological sections of vulva and vagina stained with periodic acid-Schiff, scale bars correspond to 100µm (A) Candidiasis and tissue desquamation with fungi; (B) Epithelium with "sawtooth projections"; (C) Spongiosis (20×); (D) Spongiosis (40×).

One of the characteristic symptoms of the inflammation present in VVC is itching and redness (like in eczematous dermatitis), in histopathological analysis it reflects in epidermis infiltration with polymorphonuclear cells characterizing spongiosis (**Figure 10C** and **10D**) (Arya & Naureen, 2023; Tanei & Hasegawa, 2022). In this study, the presence of infection, although not statistically significant different ($p = 0.050$), was shown to increase the amount of spongiosis (**Table 3**). When comparing the infection control group with other groups, it was observed that mice treated with CUR+BNZ@NIN@HG, CUR+BNZ@NIN, CUR+BNZ and commercial drug showed, although not statistically significant different ($p = 0.9815$, 0.9815, 0.9998 and 0.8298, respectively), an expressive reduction in the spongiosis amount. This confirms the already well-established fact that the use of BNZ in the treatment of VVC is an interesting option. It is worth highlighting that it is common to observe residual inflammatory infiltrates in treated groups of VVC in *in vivo* model (Araújo et al., 2013). In

parallel, a correlation analysis was carried out between candidiasis-fungal burden and spongiosis, and the CUR+BNZ@NIN group were the only treatment group that showed a statistically significant difference (*p* value of 0.0161), which indicates that the decrease in spongiosis observed in the CUR+BNZ@NIN group is directly connected to the decrease in fungal load caused by this same group. Another parameter that is worth highlighting is the sawtooth projections (**Figure 10B**), which is very common in histological findings of inflammatory diseases (Gaudiano et al., 2017; Navas-Alfaro et al., 2003; Pathave et al., 2022). It is formed from a corrosive action of the inflammatory infiltrate on the epithelium, leading to disorganization of the basal layer (Navas-Alfaro et al., 2003). These three parameters combined (fungal burden, spongiosis and sawtooth projections) suggest the therapeutic potential of CUR+BNZ@NIN@HG and its therapeutic equivalence with the commercial formulation.

This itching characteristic of VVC leads the patient to scratch or rub in the hope of relieving this uncomfortable symptom. However, this act can lead to tissue hyperkeratosis, which corresponds to keratinization of the affected area (Burrows et al., 2008; Nyirjesy, 2002). In this study, hyperkeratosis showed no statistically significant difference (*p* value of >0.9999), between the control groups; this can be attributed to the increase in keratinization observed with the complete resolution of the skin rash, considering a seven-day therapeutic regimen, this time may have been enough to improve symptoms and infection resolution, but not enough for mucosal keratinization (Tuoni et al., 2023). Furthermore, the inflamed tissue may have lesions, which as they progress to chronicity, become thicker due to hyperplasia of the epithelium (acanthosis). This parameter is generally mild or absent when there is spongiosis or inflammation, probably this may be the reason why this parameter was not relevant for this study during data analysis (negative and positive control groups for infection presented very close values). It is worth highlighting that acanthosis generally occurs in areas with the presence of fungal hyphae and its occurrence is related to the clinical progression to vulvar carcinoma (de Bernardis et al., 2002; Mahalingam et al., 2022; Nascimento et al., 2004; Pichardo-Geisinger, 2017). Finally, atrophy is a common histopathological finding during VVC as it is a consequence of the decrease in estrogen levels (Ruaa et al., 2021). However, in this study, changes in this parameter were unremarkable probable due to the estradiol doses administered during the trial, a key step for the establishment of vaginal infection *in vivo* (Carrara et al., 2010; Kalo-Klein & Witkin, 1989).

4. Conclusion

In this study, we reported the development of a hybrid nanoparticle dual-loaded with CUR and BNZ to combat not only the *Candida* infection but also to relieve the inflammation symptoms caused by the invasion of this fungus' pseudo-hyphae in the vaginal mucosa. In order to develop a hybrid nanoparticle composed by MSN inside a liposome in a reproducible manufacturing way a new

microfluidics approach was optimized as an innovative and efficient solution. Through *in vitro* cytotoxicity studies, it was possible to determine that in addition to being safe, the drugs-loading in the nanoparticle drastically reduced their toxicity. In addition, despite the checkerboard microdilution assay pointed to how promising the antifungal activity of these drugs combination is against resistant *C. albicans* strains, after the loading in the hybrid nanoparticle no activity was observed *in vitro*. However, the histology performed in the *in vivo* study pointed to CUR+BNZ@NIN antifungal and anti-inflammatory therapeutic potential. Ultimately, this study offers new possibilities for the development of silica-based hybrid nanoparticles by microfluidics and at the same time highlights the potential combination of CUR and BNZ for the treatment of VVC.

5. Acknowledgments

The authors acknowledge São Paulo Research Foundation (FAPESP- grant numbers: 22/02187-0, 19/26821-7 and 19/09831-9), and UMCG Research Funds for the financial support.

6. References

Abbaszadeh, S., Eskandari, M.R., Nosrati-Siahmazgi, V., Musaie, K., Mehrabi, S., Tang, R., Jafari, M.R., Xiao, B., Hosseinpour Sarmadi, V., Haghi, F., & others. (2023). A photoactive injectable antibacterial hydrogel to support chemo-immunotherapeutic effect of antigenic cell membrane and sorafenib by near-infrared light mediated tumor ablation. *Materials Today Bio*, *19*, Article 100609. https://doi.org/10.1016/j.mtbio.2023.100609

Adejokun, D.A., & Dodou, K. (2019). Quantitative Sensory Interpretation of Rheological Parameters of a Cream Formulation. *Cosmetics*, *7*(1), Article 2. https://doi.org/10.3390/cosmetics7010002

Ahmadian, Z., Correia, A., Hasany, M., Figueiredo, P., Dobakhti, F., Eskandari, M.R., Hosseini, S.H., Abiri, R., Khorshid, S., Hirvonen, J., & others. (2021). A Hydrogen-Bonded Extracellular Matrix-Mimicking Bactericidal Hydrogel with Radical Scavenging and Hemostatic Function for pH-Responsive Wound Healing Acceleration. *Advanced Healthcare Materials*, *10*(3), Article 2001122. https://doi.org/10.1002/adhm.202001122

Ali, A., Wahlgren, M., Pedersen, L., & Engblom, J. (2018). Will a water gradient in oral mucosa affect transbuccal drug absorption? *Journal of Drug Delivery Science and Technology*, *48*, 338–345. https://doi.org/10.1016/j.jddst.2018.10.004

Alves, R.C., Perosa Fernandes, R., Fonseca-Santos, B., Victorelli, F.D., & Chorilli, M. (2019). A Critical Review of the Properties and Analytical Methods for the Determination of Curcumin in Biological and Pharmaceutical Matrices. *Critical Reviews in Analytical Chemistry*, *49*(2), 138–149. https://doi.org/10.1080/10408347.2018.1489216

Araujo, V.H.S., de Souza, M.P.C., Carvalho, G.C., Duarte, J.L., & Chorilli, M. (2021). Chitosan-based systems aimed at local application for vaginal infections. *Carbohydrate Polymers*, *261*, Article 117919. https://doi.org/10.1016/j.carbpol.2021.117919

Araujo, V.H.S., Duarte, J.L., Carvalho, G.C., Silvestre, A.L.P., Fonseca-Santos, B., Marena, G.D., Ribeiro, T.C., Ramos, M.A.S., Bauab, T. M., & Chorilli, M. (2020). Nanosystems against candidiasis: a review of studies performed over the last two decades. *Critical Reviews in Microbiology*, *46*(5), 508-547. https://doi.org/10.1080/1040841X.2020.1803208

Arduino, I., Liu, Z., Rahikkala, A., Figueiredo, P., Correia, A., Cutrignelli, A., Denora, N., & Santos, H.A. (2021). Preparation of cetyl palmitate-based PEGylated solid lipid nanoparticles by microfluidic technique. *Acta Biomaterialia*, *121*, 566–578. https://doi.org/10.1016/j.actbio.2020.12.024

Arpa, M.D., Kesmen, E.E., & Biltekin, S.N. (2023). Novel Sprayable Thermosensitive Benzydamine Hydrogels for Topical Application: Development, Characterization, and In Vitro Biological Activities. *AAPS PharmSciTech*, *24*(8), Article 214. https://doi.org/10.1208/s12249-023-02674-w

Baghirov, H., Karaman, D., Viitala, T., Duchanoy, A., Lou, Y. R., Mamaeva, V., Pryazhnikov, E., Khiroug, L., De Lange Davies, C., Sahlgren, C., & Rosenholm, J. M. (2016). Feasibility study of the permeability and uptake of mesoporous silica nanoparticles across the blood-brain barrier. *PLoS ONE*, *11*(8), 1–22. https://doi.org/10.1371/journal.pone.0160705

Barbedo, L.S., Sgarbi, D.B.G. (2010). Candidíase. *DST J Bras Doenças Sex Transm*, *22*, 22–38.

Block, C., Watzeels, N., Rahier, H., Van Mele, B., & Van Assche, G. (2011). Rheology of nanocomposites. *Journal of Thermal Analysis and Calorimetry*, *105*(2), 731–736. https://doi.org/10.1007/s10973-011-1417-9

Boselli, F., Petrella, E., Campedelli, A., Muzi, M., Rullo, V., Ascione, L., Papa, R., & Saponati, G. (2012). Efficacy and Tolerability of Fitostimoline (Vaginal Cream, Ovules, and Vaginal Washing) and of Benzydamine Hydrochloride (Tantum Rosa Vaginal Cream and Vaginal Washing) in the Topical Treatment of Symptoms of Bacterial Vaginosis. *ISRN Obstetrics and Gynecology*, *2012*, 1–5. https://doi.org/10.5402/2012/183403

Bothner, H., & Wik, O. (1987). Rheology of Hyaluronate. *Acta Oto-Laryngologica*, *104*(sup442), 25–30. https://doi.org/10.3109/00016488709102834

Burrows, L.J., Shaw, H.A., & Goldstein, A.T. (2008). The Vulvar Dermatoses. *The Journal of Sexual Medicine*, *5*(2), 276–283. https://doi.org/10.1111/j.1743-6109.2007.00703.x

Cacaci, M., Squitieri, D., Palmieri, V., Torelli, R., Perini, G., Campolo, M., Di Vito, M., Papi, M., Posteraro, B., Sanguinetti, M., & Bugli, F. (2023). Curcumin-Functionalized Graphene Oxide Strongly Prevents Candida parapsilosis Adhesion and Biofilm Formation. *Pharmaceuticals*, *16*(2), Article 275. https://doi.org/10.3390/ph16020275

Carrara, M.A., Donatti, L., Damke, E., Svidizinski, T.I.E., Consolaro, M.E.L., & Batista, M.R. (2010). A New Model of Vaginal Infection by Candida albicans in Rats. *Mycopathologia*, *170*(5), 331–338. https://doi.org/10.1007/s11046-010-9326-1

Carvalho, G.C., Araujo, V.H.S., Fonseca-Santos, B., de Araújo, J.T.C., de Souza, M.P.C., Duarte, J.L., & Chorilli, M. (2021). Highlights in poloxamer-based drug delivery systems as strategy at local application for vaginal infections. *International Journal of Pharmaceutics*, *602*, Article 120635. https://doi.org/10.1016/j.ijpharm.2021.120635

Carvalho, G.C., de Oliveira, R.A P., Araujo, V.H.S., Sábio, R.M., de Carvalho, L.R., Bauab, T.M., Corrêa, I., & Chorilli, M. (2021). Prevalence of vulvovaginal candidiasis in Brazil: A systematic review. *Medical Mycology, 59(10), 946–957.* https://doi.org/10.1093/mmy/myab034

Carvalho, G.C., Marena, G.D., Leonardi, G.R., Sábio, R.M., Corrêa, I., Chorilli, M., & Bauab, T.M. (2022). Lycopene, Mesoporous Silica Nanoparticles and Their Association: A Possible Alternative against Vulvovaginal Candidiasis? *Molecules*, *27*(23), Article 8558. https://doi.org/10.3390/molecules27238558

Carvalho, G.C., Sábio, R.M., & Chorilli, M. (2020). An Overview of Properties and Analytical Methods for Lycopene in Organic Nanocarriers. *Critical Reviews in Analytical Chemistry*, 51(7), 67-86. https://doi.org/10.1080/10408347.2020.1763774

Carvalho, G.C., Sábio, R.M., de Cássia Ribeiro, T., Monteiro, A.S., Pereira, D.V., Ribeiro, S.J.L., & Chorilli, M. (2020). Highlights in Mesoporous Silica Nanoparticles as a Multifunctional Controlled Drug Delivery Nanoplatform for Infectious Diseases Treatment. *Pharmaceutical Research*, *37*(10), Article 191. https://doi.org/10.1007/s11095-020-02917-6

Carvalho, T., Bártolo, R., Pedro, S.N., Valente, B.F.A., Pinto, R.J.B., Vilela, C., Shahbazi, M.-A., Santos, H.A., & Freire, C.S.R. (2023). Injectable Nanocomposite Hydrogels of Gelatin-Hyaluronic Acid Reinforced with Hybrid Lysozyme Nanofibrils-Gold Nanoparticles for the Regeneration of Damaged Myocardium. *ACS Applied Materials & Interfaces*, *15*(21), 25860–25872. https://doi.org/10.1021/acsami.3c03874

Cerdá, S.L., Fontana, F., Wang, S., Correia, A., Molinaro, G., Tello, R.P., Hirvonen, J., Celia, C., Barreto, G., & Santos, H.A. (2023). Development of siRNA and Budesonide Dual-Loaded Hybrid Lipid–Polymer Nanoparticles by Microfluidics Technology as a Platform for Dual Drug Delivery to Macrophages: An In Vitro Mechanistic Study. *Advanced Therapeutics*, *6*(8), Article 2300048. https://doi.org/10.1002/adtp.202300048

Cheng, G., Li, X., Li, Z., Zhao, K., & Zhu, G. (2023). Deep eutectic solvent-imprinted polymer based on magnetic UiO-66-NH2 for fast and selective removal of benzydamine hydrochloride in environmental samples. *Journal of Molecular Liquids*, *375*, Article 121343. https://doi.org/10.1016/j.molliq.2023.121343

Cheng, R., Jiang, L., Gao, H., Liu, Z., Mäkilä, E., Wang, S., Saiding, Q., Xiang, L., Tang, X., Shi, M., & others. (2022). A pH-Responsive Cluster Metal–Organic Framework Nanoparticle for Enhanced Tumor Accumulation and Antitumor Effect. *Advanced Materials*, *34*(42), Article 2203915. https://doi.org/10.1002/adma.202203915

CLSI. (2017). *M27: reference method for broth dilution antifungal susceptibility testing of yeasts* (4th ed). Clinical and Laboratory Standards Institute.

Çolak, Ş. (2016). Investigation of radiosterilization of Benzydamine Hydrochloride by electron spin resonance spectroscopy. *Radiation Physics and Chemistry*, *127*, 204–209. https://doi.org/10.1016/j.radphyschem.2016.07.004

Czechowicz, P., Nowicka, J., & Gościniak, G. (2022). Virulence Factors of Candida spp. and Host Immune Response Important in the Pathogenesis of Vulvovaginal Candidiasis. *International Journal of Molecular Sciences*, *23*(11), Article 5895. https://doi.org/10.3390/ijms23115895

Daryasari, M.P., Akhgar, M.R., Mamashli, F., Bigdeli, B., & Khoobi, M. (2016). Chitosan-folate coated mesoporous silica nanoparticles as a smart and pH-sensitive system for curcumin delivery. *RSC Advances*, *6*(107), 105578–105588. https://doi.org/10.1039/C6RA23182A

de Bernardis, F., Boccanera, M., Calderone, R., & Chilar, R. (2002). Mucosal infection and immunity in candidiasis. *Mycology Series*, *14*, 461–482.

de Freitas Araújo, M.G., Pacífico, M., Vilegas, W., Dos Santos, L.C., Icely, P.A., Miró, M.S., Scarpa, M.V.C., Bauab, T.M., & Sotomayor, C. E. (2013). Evaluation of Syngonanthus nitens (Bong.) Ruhl. extract as antifungal and in treatment of vulvovaginal candidiasis. *Medical Mycology*, *51*(7), 673–682. https://doi.org/10.3109/13693786.2013.795294

de Lima, L., A.S. Ramos, M., Toledo, L. G. de, Rodero, C. F., Hilário, F., dos Santos, L. C., Chorilli, M., & Bauab, T. M. (2020). Syngonanthus nitens (Bong.) Ruhland Derivatives Loaded into a Lipid Nanoemulsion for Enhanced Antifungal Activity Against Candida parapsilosis. *Current Pharmaceutical Design*, *26*(14), 1556–1565. https://doi.org/10.2174/1381612826666200317131041

di Stefano, A.F.D., Radicioni, M. M., Vaccani, A., Caccia, G., Focanti, F., Salvatori, E., Pelacchi, F., Picollo, R., Rosignoli, M. T., Olivieri, S., & others. (2020). Phase I Study in Healthy Women of a Novel Antimycotic Vaginal Ovule Combining Econazole and Benzydamine. *Infectious Diseases in Obstetrics and Gynecology*, *2020*, 1–11. https://doi.org/10.1155/2020/7201840

Donders, G.G.G., Ruban, K., Donders, F., & Reybrouck, R. (2022). Lab-Based Retrospective 10-Year Analysis Shows Seasonal Variation of Vaginal Candida Infection Rates in Belgium. *Journal of Clinical Medicine*, *11*(3), Article 574. https://doi.org/10.3390/jcm11030574

dos Santos, R., Aparecido, M., da Silva, P.B., de Toledo, L.G., Oda, F.B., da Silva, I. C., dos Santos, L.C., dos Santos, A.G., de Almeida, M.T.G., Pavan, F.R., & Bauab, T.M. (2019). Intravaginal Delivery of Syngonanthus nitens (Bong.) Ruhland Fraction Based on a Nanoemulsion System Applied to Vulvovaginal Candidiasis Treatment. *Journal of Biomedical Nanotechnology*, *15*(5), 1072–1089. https://doi.org/10.1166/jbn.2019.2750

Dumontel, B., Conejo-Rodríguez, V., Vallet-Regí, M., & Manzano, M. (2023). Natural Biopolymers as Smart Coating Materials of Mesoporous Silica Nanoparticles for Drug Delivery. *Pharmaceutics*, *15*(2), Article 447. https://doi.org/10.3390/pharmaceutics15020447

Duong, V.-A., Nguyen, T.-T.-L., & Maeng, H.-J. (2023). Recent Advances in Intranasal Liposomes for Drug, Gene, and Vaccine Delivery. *Pharmaceutics*, *15*(1), Article 207. https://doi.org/10.3390/pharmaceutics15010207

Duraccio, D., Strongone, V., Malucelli, G., Auriemma, F., de Rosa, C., Mussano, F.D., Genova, T., & Faga, M.G. (2019). The role of alumina-zirconia loading on the mechanical and biological properties of UHMWPE for biomedical applications. *Composites Part B: Engineering*, *164*, 800–808. https://doi.org/10.1016/j.compositesb.2019.01.097

Felix, T.C., de Brito Röder, D.V.D., & Pedroso, R.S. (2019). Alternative and complementary therapies for vulvovaginal candidiasis. *Folia Microbiologica*, *64*(2), 133–141. https://doi.org/10.1007/s12223-018-0652-x

Gaudiano, C., Tadolini, M., Busato, F., Vanino, E., Pucci, S., Corcioni, B., & Golfieri, R. (2017). Multidetector CT urography in urogenital tuberculosis: use of reformatted images for the assessment of the radiological findings. A pictorial essay. *Abdominal Radiology*, *42*(9), 2314–2324. https://doi.org/10.1007/s00261-017-1129-0

Hartono, S.B., Hadisoewignyo, L., Yang, Y., Meka, A.K., Antaresti, & Yu, C. (2016). Amine functionalized cubic mesoporous silica nanoparticles as an oral delivery system for curcumin bioavailability enhancement. *Nanotechnology*, *27*(50), Article 505605. https://doi.org/10.1088/0957-4484/27/50/505605

Hassan, N., Firdaus, S., Padhi, S., Ali, A., & Iqbal, Z. (2021). Investigating natural antibiofilm components: a new therapeutic perspective against candidal vulvovaginitis. *Medical Hypotheses*, *148*, Article 110515. https://doi.org/10.1016/j.mehy.2021.110515

Heikkilä, T., Santos, H. A., Kumar, N., Murzin, D. Y., Salonen, J., Laaksonen, T., Peltonen, L., Hirvonen, J., & Lehto, V.-P. (2010). Cytotoxicity study of ordered mesoporous silica MCM-41 and SBA-15 microparticles on Caco-2 cells. *European Journal of Pharmaceutics and Biopharmaceutics*, *74*(3), 483–494. https://doi.org/10.1016/j.ejpb.2009.12.006

Hsin, Y.K., Thangarajoo, T., Choudhury, H., Pandey, M., Meng, L.W., & Gorain, B. (2023). Stimuli-Responsive in situ Spray Gel of Miconazole Nitrate for Vaginal Candidiasis. *Journal of Pharmaceutical Sciences*, *112*(2), 562–572. https://doi.org/10.1016/j.xphs.2022.09.002

Imlimthan, S., Correia, A., Figueiredo, P., Lintinen, K., Balasubramanian, V., Airaksinen, A.J., Kostiainen, M.A., Santos, H.A., & Sarparanta, M. (2020). Systematic in vitro biocompatibility studies of multimodal cellulose nanocrystal and lignin nanoparticles. *Journal of Biomedical Materials Research Part A*, *108*(3), 770–783. https://doi.org/10.1002/jbm.a.36856

Ingebrigtsen, S.G., Didriksen, A., Johannessen, M., Škalko-Basnet, N., & Holsæter, A.M. (2017). Old drug, new wrapping − A possible comeback for chloramphenicol? *International Journal of Pharmaceutics*, *526*(1–2), 538–546. https://doi.org/10.1016/j.ijpharm.2017.05.025

Jane, W.J., Iramiot, J.S., & Kalule, J.B. (2019). Prevalence and Antifungal Susceptibility patterns of Candida Isolated on CHROMagarTMCandida at a Tertiary Referral Hospital, Eastern Uganda. *Microbiology Research Journal International*, *28(6)*, 1–6. https://doi.org/10.9734/mrji/2019/v28i630151

Jebril, S., Khanfir Ben Jenana, R., & Dridi, C. (2020). Green synthesis of silver nanoparticles using Melia azedarach leaf extract and their antifungal activities: In vitro and in vivo. *Materials Chemistry and Physics*, *248*, Article 122898. https://doi.org/10.1016/j.matchemphys.2020.122898

Kalo-Klein, A., & Witkin, S.S. (1989). *Candida albicans*: Cellular immune system interactions during different stages of the menstrual cycle. *American Journal of Obstetrics and Gynecology*, *161*(5), 1132–1136. https://doi.org/10.1016/0002-9378(89)90649-2

Känkänen, V., Fernandes, M., Liu, Z., Seitsonen, J., Hirvonen, S.-P., Ruokolainen, J., Pinto, J.F., Hirvonen, J., Balasubramanian, V., & Santos, H.A. (2023). Microfluidic preparation and optimization of sorafenib-loaded poly(ethylene glycol-block-caprolactone) nanoparticles for cancer therapy applications. *Journal of Colloid and Interface Science*, *633*, 383–395. https://doi.org/10.1016/j.jcis.2022.11.124

Karaman, D.S., Patrignani, G., Rosqvist, E., Smått, J.-H., Orłowska, A., Mustafa, R., Preis, M., & Rosenholm, J.M. (2018). Mesoporous silica nanoparticles facilitating the dissolution of poorly soluble drugs in orodispersible films. *European Journal of Pharmaceutical Sciences*, *122*, 152–159. https://doi.org/10.1016/j.ejps.2018.06.027

Karavana,Y.H., S., Güneri, P., & Ertan, G. (2009). Benzydamine hydrochloride buccal bioadhesive gels designed for oral ulcers: Preparation, rheological, textural, mucoadhesive and release properties. *Pharmaceutical Development and Technology*, *14*(6), 623–631. https://doi.org/10.3109/10837450902882351

Khan, B., Arbab, A., Khan, S., Fatima, H., Bibi, I., Chowdhry, N.P., Ansari, A.Q., Ursani, A. A., Kumar, S., Hussain, J., & Abdullah, S. (2023). Recent progress in thermosensitive hydrogels and their applications in drug delivery area. *MedComm – Biomaterials and Applications*, *2*(3), Article e55. https://doi.org/10.1002/mba2.55

Kolawole, O.M., & Cook, M.T. (2023). In situ gelling drug delivery systems for topical drug delivery. *European Journal of Pharmaceutics and Biopharmaceutics*, *184*, 36–49. https://doi.org/10.1016/j.ejpb.2023.01.007

Kundu, S., & Nithiyanantham, U. (2013). In situ formation of curcumin stabilized shape-selective Ag nanostructures in aqueous solution and their pronounced SERS activity. *RSC Advances*, *3*(47), 25278-25290. https://doi.org/10.1039/c3ra44471f

LaFayette, S.L., Collins, C., Zaas, A.K., Schell, W.A., Betancourt-Quiroz, M., Gunatilaka, A.A.L., Perfect, J.R., & Cowen, L.E. (2010). PKC Signaling Regulates Drug Resistance of the Fungal Pathogen Candida albicans via Circuitry Comprised of Mkc1, Calcineurin, and Hsp90. *PLoS Pathogens*, *6*(8), Article e1001069. https://doi.org/10.1371/journal.ppat.1001069

Lérida-Viso, A., Estepa-Fernández, A., García-Fernández, A., Martí-Centelles, V., & Martínez-Máñez, R. (2023). Biosafety of mesoporous silica nanoparticles; towards clinical translation. *Advanced Drug Delivery Reviews*, *201*, Article 115049. https://doi.org/10.1016/j.addr.2023.115049

Liou, T.-H. (2004). Evolution of chemistry and morphology during the carbonization and combustion of rice husk. *Carbon*, *42*(4), 785–794.

https://doi.org/10.1016/j.carbon.2004.01.050

Liu, C., Jiang, F., Xing, Z., Fan, L., Li, Y., Wang, S., Ling, J., & Ouyang, X.-K. (2022). Efficient Delivery of Curcumin by Alginate Oligosaccharide Coated Aminated Mesoporous Silica Nanoparticles and In Vitro Anticancer Activity against Colon Cancer Cells. *Pharmaceutics*, *14*(6), Article 1166. https://doi.org/10.3390/pharmaceutics14061166

Liu, Z., Lian, W., Long, Q., Cheng, R., Torrieri, G., Zhang, B., Koivuniemi, A., Mahmoudzadeh, M., Bunker, A., Gao, H., & others. (2022). Promoting Cardiac Repair through Simple Engineering of Nanoparticles with Exclusive Targeting Capability toward Myocardial Reperfusion Injury by Thermal Resistant Microfluidic Platform. *Advanced Functional Materials*, *32*(36), Article 2204666. https://doi.org/10.1002/adfm.202204666

Mahalingam, S.S., Jayaraman, S., & Pandiyan, P. (2022). Fungal Colonization and Infections—Interactions with Other Human Diseases. *Pathogens*, *11*(2), Article 212. https://doi.org/10.3390/pathogens11020212

Marchaim, D., Lemanek, L., Bheemreddy, S., Kaye, K.S., & Sobel, J.D. (2012). Fluconazole-resistant *Candida albicans* vulvovaginitis. *Obstetrics & Gynecology*, *120*(6), 1407–1414. http://10.1097/AOG.0b013e31827307b2

Marena, G.D., Carvalho, G.C., dos Santos Ramos, M.A., Chorilli, M., & Bauab, T.M. (2023). Anti- *Candida auris* activity in vitro and in vivo of micafungin loaded nanoemulsions. *Medical Mycology*, *61*(7), Article myac090. https://doi.org/10.1093/mmy/myac090

Marques, M.R.C., Loebenberg, R. & Almukainzi, M. (2011). Simulated biological fluids with possible application in dissolution testing. *Dissolution Technol*, *18*(3), 15–28.

Martins, F., Morgado, D.L., Sarmento, B., de Camargo, E.R., & das Neves, J. (2023). Chitosan-based sponges containing clotrimazole for the topical management of vulvovaginal candidiasis. *International Journal of Pharmaceutics*, *647*, Article 123508. https://doi.org/10.1016/j.ijpharm.2023.123508

Martins, J.P., Figueiredo, P., Wang, S., Espo, E., Celi, E., Martins, B., Kemell, M., Moslova, K., Mäkilä, E., Salonen, J., & others. (2022). Neonatal Fc receptor-targeted lignin-encapsulated porous silicon nanoparticles for enhanced cellular interactions and insulin permeation across the intestinal epithelium. *Bioactive Materials*, *9*, 299–315. https://doi.org/10.1016/j.bioactmat.2021.08.007

Martins, J.P., Liu, D., Fontana, F., Ferreira, M.P.A., Correia, A., Valentino, S., Kemell, M., Moslova, K., Mäkilä, E., Salonen, J., & others. (2018). Microfluidic Nanoassembly of Bioengineered Chitosan-Modified FcRn-Targeted Porous Silicon Nanoparticles @ Hypromellose Acetate Succinate for Oral Delivery of Antidiabetic Peptides. *ACS Applied Materials & Interfaces*, *10*(51), 44354–44367. https://doi.org/10.1021/acsami.8b20821

Maturi, F.E., Sábio, R.M., Silva, R.R., Lahoud, M.G., Meneguin, A.B., Valente, G.T., Caface, R.A., Leite, I.S., Inada, N.M., & Ribeiro, S.J.L. (2019). Luminescent Mesoporous Silica Nanohybrid Based on Drug Derivative Terbium Complex. *Materials*, *12*(6), Article 933. https://doi.org/10.3390/ma12060933

Mehravaran, M., Haeri, A., Rabbani, S., Mortazavi, S.A., & Torshabi, M. (2022). Preparation and characterization of benzydamine hydrochloride-loaded lyophilized mucoadhesive wafers for the treatment of oral mucositis. *Journal of Drug Delivery Science and Technology*, *78*, Article 103944. https://doi.org/10.1016/j.jddst.2022.103944

Mitchell, M.J., Billingsley, M.M., Haley, R.M., Wechsler, M.E., Peppas, N.A., & Langer, R. (2021). Engineering precision nanoparticles for drug delivery. *Nature Reviews Drug Discovery*, *20*(2), 101–124. https://doi.org/10.1038/s41573-020-0090-8

Molinaro, G., Fontana, F., Tello, R.P., Wang, S., Cérda, S.L., Torrieri, G., Correia, A., Waris, E., Hirvonen, J.T., Barreto, G., & Santos, H.A. (2023). In Vitro Study of the Anti-inflammatory and Antifibrotic Activity of Tannic Acid-Coated Curcumin-Loaded Nanoparticles in Human Tenocytes. *ACS Applied Materials & Interfaces*, *15*(19), 23012–23023. https://doi.org/10.1021/acsami.3c05322

Möller, K., & Bein, T. (2019). Degradable Drug Carriers: Vanishing Mesoporous Silica Nanoparticles. *Chemistry of Materials*, *31*(12), 4364–4378. https://doi.org/10.1021/acs.chemmater.9b00221

Mushi, M. F., Olum, R., & Bongomin, F. (2022). Prevalence, antifungal susceptibility and etiology of vulvovaginal candidiasis in sub–Saharan Africa: a systematic review with meta-analysis and meta-regression. *Medical Mycology*, *60*(7), Article myac037. https://doi.org/10.1093/mmy/myac037

Nascimento, A.F., Granter, S.R., Cviko, A., Yuan, L., Hecht, J.L., & Crum, C.P. (2004). Vulvar acanthosis with altered differentiation: a precursor to verrucous carcinoma? *The American Journal of Surgical Pathology*, *28*(5), 638–643.

Navas-Alfaro, S.E., Fonseca, E.C. da, Guzmán-Silva, M.A., & Rochael, M.C. (2003). Análise histopatológica comparativa entre líquen plano oral e cutâneo. *Jornal Brasileiro de Patologia e Medicina Laboratorial*, *39*(4). https://doi.org/10.1590/S1676-24442003000400013

Nippe, N., Varga, G., Holzinger, D., Löffler, B., Medina, E., Becker, K., Roth, J., Ehrchen, J.M., & Sunderkötter, C. (2011). Subcutaneous Infection with S. aureus in Mice Reveals Association of Resistance with Influx of Neutrophils and Th2 Response. *Journal of Investigative Dermatology*, *131*(1), 125–132. https://doi.org/10.1038/jid.2010.282

Noureddine, A., Maestas-Olguin, A., Tang, L., Corman-Hijar, J.I., Olewine, M., Krawchuck, J.A., Ebode, J. T., Edeh, C., Dang, C., Negrete, O.A., & others. (2023). Future of Mesoporous Silica Nanoparticles in Nanomedicine: Protocol for Reproducible Synthesis, Characterization, Lipid Coating, and Loading of Therapeutics (Chemotherapeutic, Proteins, siRNA and mRNA). *ACS Nano*, *17*(17), 16308–16325. https://doi.org/10.1021/acsnano.3c07621

Nyirjesy, P. (2002). Lichen sclerosus and other conditions mimicking vulvovaginal candidiasis. *Current Infectious Disease Reports*, *4*(6), 520–524. https://doi.org/10.1007/s11908-002-0039-6

Obeid, M.A., Alsaadi, M., & Aljabali, A.A. (2023). Recent updates in curcumin delivery. *Journal of Liposome Research*, *33*(1), 53–64. https://doi.org/10.1080/08982104.2022.2086567

Pareek, V., Bhargava, A., Bhanot, V., Gupta, R., Jain, N., & Panwar, J. (2018). Formation and Characterization of Protein Corona Around Nanoparticles:

A Review. *Journal of Nanoscience and Nanotechnology*, *18*(10), 6653–6670. https://doi.org/10.1166/jnn.2018.15766

Pathave, H., Nikam, V., Dongre, A., & Khopkar, U. (2022). A retrospective study of skin biopsies of 184 cutaneous lichen planus patients. *Turkish Journal of Dermatology*, *16*(2), 38-43. https://doi.org/10.4103/tjd.tjd_116_21

Patra, D., Şen Karaman, D., Desai, D., El Khoury, E., & Rosenholm, J.M. (2016). Preparation of curcumin loaded mesoporous silica nanoparticles: Determining polarizability inside the mesopores. *Materials Research Bulletin*, *84*, 267–272. https://doi.org/10.1016/j.materresbull.2016.08.012

Perlíková, P., Krajczyk, A., Doleželová, E., Slapničková, M., Milisavljevic, N., Slavětínská, L.P., Tloušt'ová, E., Gurská, S., Džubák, P., Hajdúch, M., & others. (2021). Synthesis and Antitrypanosomal Activity of 6-Substituted 7-Methyl-7-deazapurine Nucleosides. *ACS Infectious Diseases*, *7*(4), 917–926. https://doi.org/10.1021/acsinfecdis.1c00062

Pichardo-Geisinger, R. (2017). Atopic and Contact Dermatitis of the Vulva. *Obstetrics and Gynecology Clinics of North America*, *44*(3), 371–378. https://doi.org/10.1016/j.ogc.2017.05.003

Pilicheva, B., Uzunova, Y., & Marudova, M. (2022). Polyelectrolyte Multilayer Films as a Potential Buccal Platform for Drug Delivery. *Polymers*, *14*(4), Article 734. https://doi.org/10.3390/polym14040734

Pino, P. del, Pelaz, B., Zhang, Q., Maffre, P., Nienhaus, G.U., & Parak, W.J. (2014). Protein corona formation around nanoparticles – from the past to the future. *Mater. Horiz.*, *1*(3), 301–313. https://doi.org/10.1039/C3MH00106G

Pozharani, L.B., Baloglu, E., Suer, K., Guler, E., Burgaz, E.V., & Kunter, I. (2023). Development and optimization of in-situ gels for vaginal delivery of metronidazole and curcumin via box-behnken design: *In vitro* characterization and anti-trichomonas activity. *Journal of Drug Delivery Science and Technology*, *86*, Article 104739. https://doi.org/10.1016/j.jddst.2023.104739

Prabhakar, N., Näreoja, T., von Haartman, E., Karaman, D.Ş., Jiang, H., Koho, S., Dolenko, T.A., Hänninen, P.E., Vlasov, D.I., Ralchenko, V.G., & others. (2013). Core–shell designs of photoluminescent nanodiamonds with porous silica coatings for bioimaging and drug delivery II: application. *Nanoscale*, *5*(9), 3713-3722. https://doi.org/10.1039/c3nr33926b

Quintella, L.P., Passos, S.R.L., Vale, A.C.F., Galhardo, M.C.G., Barros, M.B.L., Cuzzi, T., Reis, R.S., Carvalho, M.H.G.F., Zappa, M. B., & Schubach, A.O. (2011). Histopathology of cutaneous sporotrichosis in Rio de Janeiro: a series of 119 consecutive cases. *Journal of Cutaneous Pathology*, *38*(1), 25–32. https://doi.org/10.1111/j.1600-0560.2010.01626.x

Arya, N.R. & Naureen, B.R. (2023). Candidiasis. *StatPearls*. https://www.ncbi.nlm.nih.gov/books/NBK560624/

Ribeiro, T. de C., Sábio, R.M., Luiz, M.T., de Souza, L.C., Fonseca-Santos, B., da Silva, L.C.C., Fantini, M.C.A., Planeta, C.S., & Chorilli, M. (2022). Curcumin-Loaded Mesoporous Silica Nanoparticles Dispersed in Thermo-Responsive Hydrogel as Potential Alzheimer Disease Therapy. *Pharmaceutics*, *14*(9), Article 1976. https://doi.org/10.3390/pharmaceutics14091976

Rodero, C.F., Calixto, G.M.F., dos Santos, K., Sato, M.R., Ramos, M. S., Miró, M.S., Rodríguez, E., Vigezzi, C., Bauab, T.M., Sotomayor, C.E., & Chorilli, M. (2018). Curcumin-loaded liquid crystalline systems for controlled drug release and improved treatment of vulvovaginal candidiasis. *Molecular Pharmaceutics*, *15*(10), 4491–4504. https://doi.org/10.1021/acs.molpharmaceut.8b00507

Rosalina, I., & Bhattacharya, M. (2002). Dynamic rheological measurements and analysis of starch gels. *Carbohydrate Polymers*, *48*(2), 191–202. https://doi.org/10.1016/S0144-8617(01)00235-1

Ruaa, K.M., ALsailawi, H.A., Abdulrasool, M.M., Mudhafar, M., Mays, A.D., & Bashi, A.M. (2021). A Review Study on the Effects of Estrogen Level on Vaginal Candida spp. of Women with Estrogen-Related Receptor Breast Cancer. *Journal of Life Sciences*, *15*(1), 30-40. https://doi.org/10.17265/1934-7391/2021.01.002

Ruan, L., Chen, W., Wang, R., Lu, J., & Zink, J.I. (2019). Magnetically Stimulated Drug Release Using Nanoparticles Capped by Self-Assembling Peptides. *ACS Applied Materials & Interfaces*, *11*(47), 43835–43842. https://doi.org/10.1021/acsami.9b13614

Sábio, R.M., Carvalho, G.C., Li, J., Chorilli, M., & Santos, H.A. (2023). Advanced porous materials for antimicrobial treatment. *Nano Select,* 1-20. https://doi.org/10.1002/nano.202300114

Santezi, C., Reina, B.D., de Annunzio, S.R., Calixto, G., Chorilli, M., & Dovigo, L.N. (2021). Photodynamic potential of curcumin in bioadhesive formulations: Optical characteristics and antimicrobial effect against biofilms. *Photodiagnosis and Photodynamic Therapy*, *35*, Article 102416. https://doi.org/10.1016/j.pdpdt.2021.102416

Sharma, D., Singh, R., & Garg, R. (2017). Development and validation of stability indicating UV spectro-photometric method for the estimation of benzydamine hydrochloride in bulk and in pharmaceutical dosage form: a novel analytical technique for conducting in-vitro quality control tests. *International Journal Of Pharmaceutical Sciences And Research*, *9*(2), 678–686. http://dx.doi.org/10.13040/IJPSR.0975-8232.9(2).678-86

Shi, J., & Maguer, M.L. (2000). Lycopene in tomatoes: chemical and physical properties affected by food processing. *Critical Reviews in Food Science and Nutrition*, *40*(1), 1–42. https://doi.org/10.1080/10408690091189275

Sucher, A.J., Thai, A., Tran, C., Mantena, N., Noronha, A., & Chahine, E.B. (2022). Ibrexafungerp: A new triterpenoid antifungal. *American Journal of Health-System Pharmacy*, *79*(24), 2208–2221. https://doi.org/10.1093/ajhp/zxac256

Sugiarto, A., Kapuangan, C., Tantri, A.R., & Chrisnata, V. (2020). Effectivity of benzydamine hydrochloride gargle to reduce propofol consumption in endoscopic retrograde cholangiopancreatography procedure: a randomized controlled trial. *BMC Anesthesiology*, *20*(1), Article 123. https://doi.org/10.1186/s12871-020-00996-x

Sun, K., Ding, T., Xing, Y., Mo, D., Zhang, J., & Rosenholm, J.M. (2019). Hybrid mesoporous nanorods with deeply grooved lateral faces toward cytosolic drug delivery. *Biomaterials Science*, *7*(12), 5301–5311. https://doi.org/10.1039/C9BM01251F

Tacchini-Cottier, F., Zweifel, C., Belkaid, Y., Mukankundiye, C., Vasei, M., Launois, P., Milon, G., & Louis, J.A. (2000). An Immunomodulatory

Function for Neutrophils During the Induction of a CD4+ Th2 Response in BALB/c Mice Infected with Leishmania major. *The Journal of Immunology*, *165*(5), 2628–2636. https://doi.org/10.4049/jimmunol.165.5.2628

Tahir, N., Madni, A., Correia, A., Rehman, M., Balasubramanian, V., Khan, M.M., & Santos, H.A. (2019). Lipid-polymer hybrid nanoparticles for controlled delivery of hydrophilic and lipophilic doxorubicin for breast cancer therapy. *International Journal of Nanomedicine*, *14*, 4961–4974. https://doi.org/10.2147/IJN.S209325

Tanei, R., & Hasegawa, Y. (2022). Immunological Pathomechanisms of Spongiotic Dermatitis in Skin Lesions of Atopic Dermatitis. *International Journal of Molecular Sciences*, *23*(12), Article 6682. https://doi.org/10.3390/ijms23126682

Thommes, M., Kaneko, K., Neimark, A.V., Olivier, J.P., Rodriguez-Reinoso, F., Rouquerol, J., & Sing, K. S. W. (2015). Physisorption of gases, with special reference to the evaluation of surface area and pore size distribution (IUPAC Technical Report). *Pure and Applied Chemistry*, *87*(9–10), 1051–1069. https://doi.org/10.1515/pac-2014-1117

Toledo, L.G., Ramos, M.A. S., Silva, P.B., Rodero, C. F., Gomes, V.S., Silva, A.S., Pavan, F. R., da Silva, I. C., Oda, F.B., Flumignan, D. L., & others. (2020). Improved in vitro and in vivo Anti-*Candida albicans* Activity of Cymbopogon nardus Essential Oil by Its Incorporation into a Microemulsion System. *International Journal of Nanomedicine*, *15*, 10481–10497. https://doi.org/10.2147/IJN.S275258

Tramontano, C., Martins, J.P., de Stefano, L., Kemell, M., Correia, A., Terracciano, M., Borbone, N., Rea, I., & Santos, H.A. (2023). Microfluidic-Assisted Production of Gastro-Resistant Active-Targeted Diatomite Nanoparticles for the Local Release of Galunisertib in Metastatic Colorectal Cancer Cells. *Advanced Healthcare Materials*, *12*(6), Article 2202672. https://doi.org/10.1002/adhm.202202672

Trapani, A., Di Gioia, S., Ditaranto, N., Cioffi, N., Goycoolea, F.M., Carbone, A., Garcia-Fuentes, M., Conese, M., & Alonso, M.J. (2013). Systemic heparin delivery by the pulmonary route using chitosan and glycol chitosan nanoparticles. *International Journal of Pharmaceutics*, *447*(1–2), 115–123. https://doi.org/10.1016/j.ijpharm.2013.02.035

Tuğcu-Demiröz, F. (2017). Development of in situ poloxamer-chitosan hydrogels for vaginal drug delivery of benzydamine hydrochloride: Textural, mucoadhesive and in vitro release properties. *Marmara Pharmaceutical Journal*, *21*(4), 762–770. https://doi.org/10.12991/mpj.2017.3

Tuoni, C., Mazzatenta, C., & Filippi, L. (2023). Congenital Cutaneous Candidiasis with Nail Involvement. *The Journal of Pediatrics*, *260*, Article 113470. https://doi.org/10.1016/j.jpeds.2023.113470

United States Pharmacopeia. (2020). *<1092> The Dissolution Procedure: Development and Validation.* 43. ed. Rockville: The United States Pharmacopeia Convention.

Wei, M., Shen, X., Fan, X., Li, J., & Bai, J. (2023). PD-L1 aptamer-functionalized degradable hafnium oxide nanoparticles for near infrared-II diagnostic imaging and radiosensitization. *Frontiers in Bioengineering and Biotechnology*, *11, Article 1224339*. https://doi.org/10.3389/fbioe.2023.1224339

Workowski, K. A., Bachmann, L.H., Chan, P.A., Johnston, C.M., Muzny, C.A., Park, I., Reno, H., Zenilman, J.M., & Bolan, G.A. (2021). Sexually Transmitted Infections Treatment Guidelines, 2021. *MMWR. Recommendations and Reports : Morbidity and Mortality Weekly Report. Recommendations and Reports*, *70*(4), 1–187. https://doi.org/10.15585/mmwr.rr7004a1

Wu, Y., Li, Y., Zou, Y., Rao, W., Gai, Y., Xue, J., Wu, L., Qu, X., Liu, Y., Xu, G., & others. (2022). A multi-mode triboelectric nanogenerator for energy harvesting and biomedical monitoring. *Nano Energy*, *92*, Article 106715. https://doi.org/10.1016/j.nanoen.2021.106715

Yano, J., Noverr, M.C., & Fidel, P.L. (2017). Vaginal Heparan Sulfate Linked to Neutrophil Dysfunction in the Acute Inflammatory Response Associated with Experimental Vulvovaginal Candidiasis. *MBio*, *8*(2), Article e00211-17. https://doi.org/10.1128/mBio.00211-17

Zhang, P., Liu, Y., Feng, G., Li, C., Zhou, J., Du, C., Bai, Y., Hu, S., Huang, T., Wang, G., & others. (2023). Controlled Interfacial Polymer Self-assembly Coordinates Ultrahigh Drug Loading and Zero-Order Release in Particles Prepared under Continuous Flow. *Advanced Materials*, *35*(22), Article 2211254. https://doi.org/10.1002/adma.202211254

Zhang, Y., & Huang, L. (2020). Liposomal delivery system. In Chung, E. J., Leon, L., & Rinaldi, C. (Eds.), *Nanoparticles for Biomedical Applications: Fundamental Concepts, Biological Interactions and Clinical Applications* (pp. 145–152). Elsevier. https://doi.org/10.1016/B978-0-12-816662-8.00010-2

Supplementary experimental description

1. *In vitro* synergism assay (checkerboard)

For this assay, two 96-well microplates, named A and B, were needed. Plate A with curcumin (CUR) (Pharmaceutical Secondary Standard from Supelco®) in the concentration range: 1000−7.8125 µg/mL), and plate B with benzydamine hydrochloride (BNZ) (analytical standard from Sigma-Aldrich®) in the concentration range: 1000−12.625 µg/mL). Initially, 50 µL of Roswell Park Memorial Institute (RPMI 1640) (Sigma-Aldrich®) culture medium was added to all wells of the microplate A in columns 2 to 10 (lines A-H). Then, to this plate A 50 µL of drug 1 was added to column 1 followed by serial dilution (50 µL) from column 1 to column 9 (**Figure S4**). In microplate B, 100 µL of RPMI 1640 was added in all wells of lines B to H. Then, to this plate B 100 µL of drug 2 was added in line A (columns 1 to 10), followed by serial dilution (100 µL) from line A to line G (Figure S1). Next, 50 µL of drug 2 (Plate B) was transferred to the respective wells of the microplate containing drug 1 (Plate A). It is worth highlighting that line H (columns 1-9) and column 10 (rows A-G) represent CUR and BNZ alone, respectively.

After, *C. albicans* (100 µL) was added to all wells of columns 1 to 11 (final concentration of $1x10^3$ yeasts/mL). The microplate was incubated at 37°C for 48 h. Columns 11 (A – D) and 11 (E – H) represent the growth and sterility controls of the culture medium, respectively. After 48h, 100 µL of 2,3-bis(2-methoxy-4-nitro-5-sulfophenyl)-5-[carbonyl(phenylamino)]-2H-tetrazolium-hydroxide (XTT at 0.005g/10mL) (Sigma-Aldrich®) was added and the plate was incubated for 2 h. After incubation, spectrophotometric reading was performed at 492 nm to assess metabolic activity. The experiment was performed in triplicate The results are analyzed according to the fractional inhibitory concentration index (FICI), as defined by FICI= (MICA + MICB), where MICA is the minimum inhibitory concentration (MIC) of CUR combined/MIC of CUR alone and MICB is the MIC of BNZ combined/MIC of BNZ alone. If FICI ≤ 0.5 the drugs combination have a synergism effect, if FICI > 0.5 - 4.0 the drugs combination has a neutral effect and if FICI > 4.0 the drugs combination has an antagonistic effect (CLSI, 2017; LaFayette et al., 2010).

Supplementary Figures and Tables

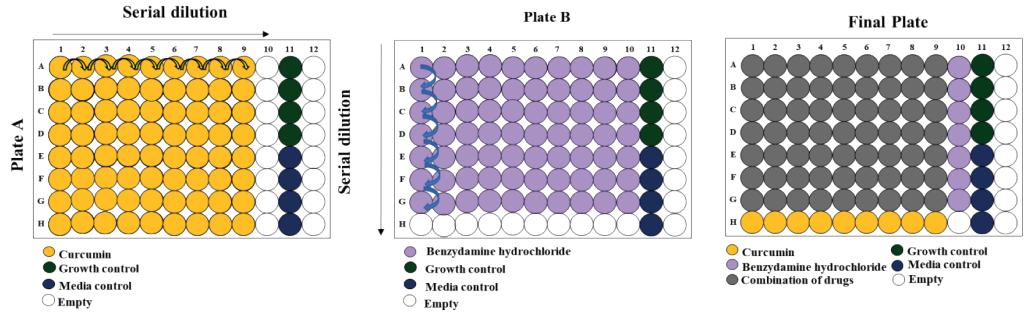

Figure S1. Schematization of the checkerboard microdilution assay performed to evaluate curcumin and benzydamine hydrochloride association effect against a resistant *C. albicans* strain.

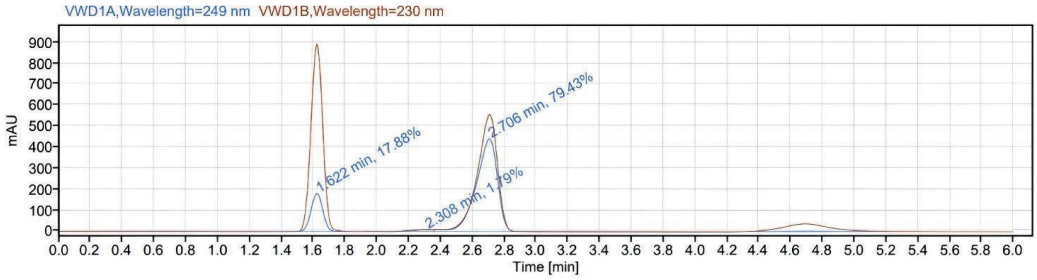

Figure S2. HPLC chromatogram obtained with a gradient of 70:30 acetonitrile and 0.2% phosphoric acid in water 0.9 mL/min over 1.5 min, change in the flow to 1.5 mL/min over 0.5 min and change of mobile phase composition to 80:20.

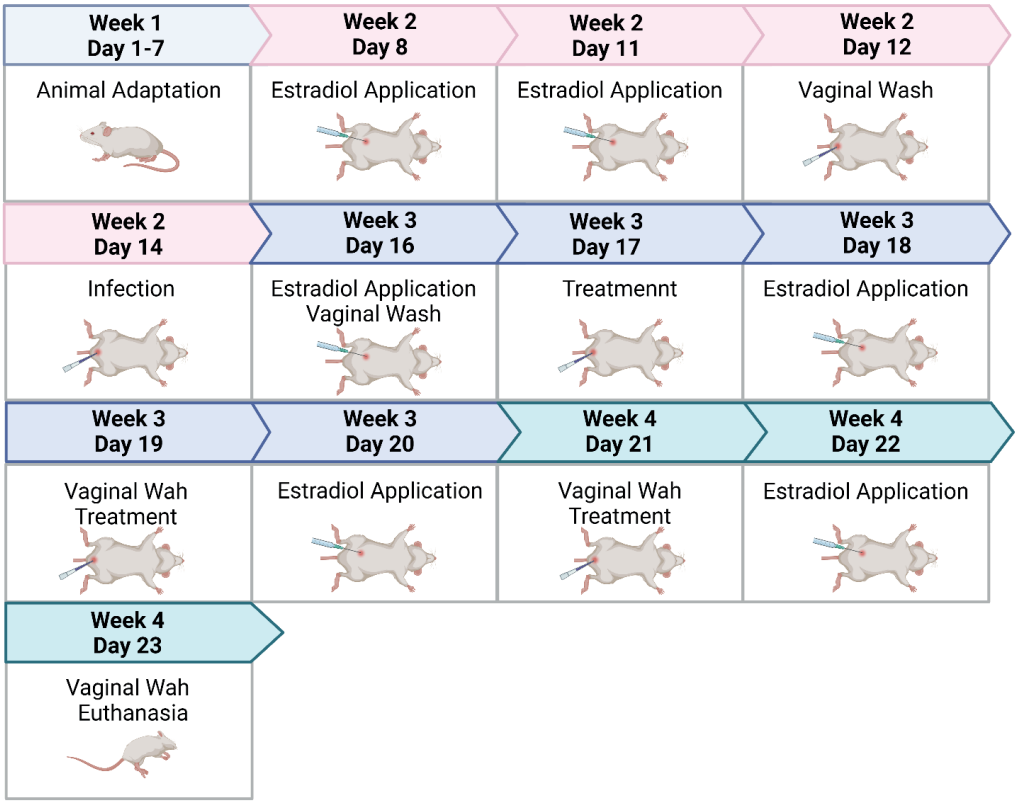

Figure S3. Schematic representation of the *in vivo* drugs testing protocol model with female BALB/c mice for VVC treatment.

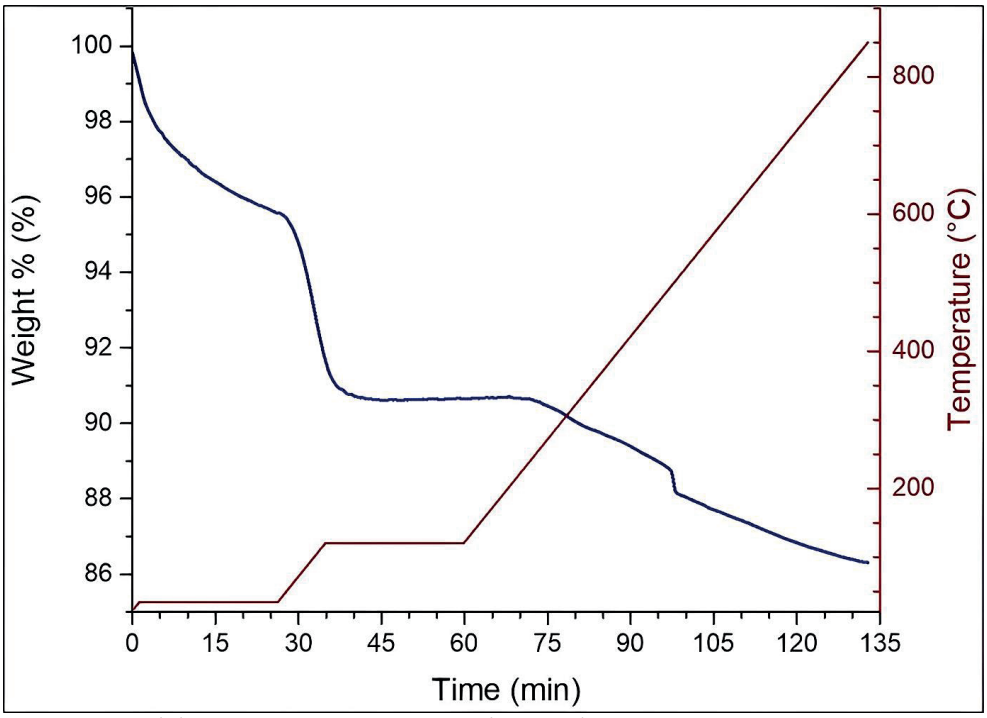

Figure S4. TG weight *versus* temperature *versus* time graph

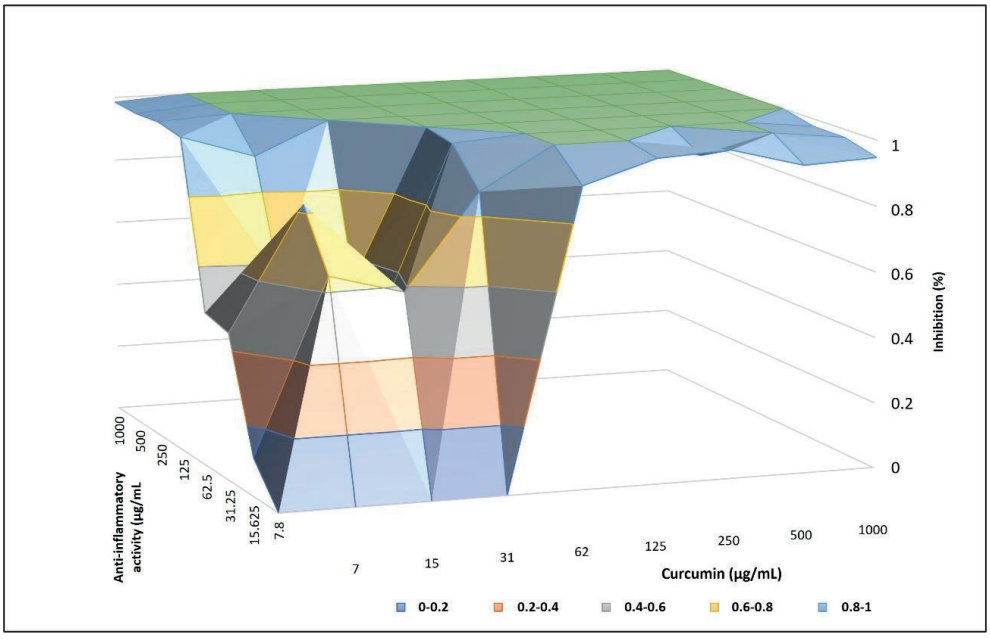

Figure S5. Surface graph of the results of all combinations tested in the checkerboard assay

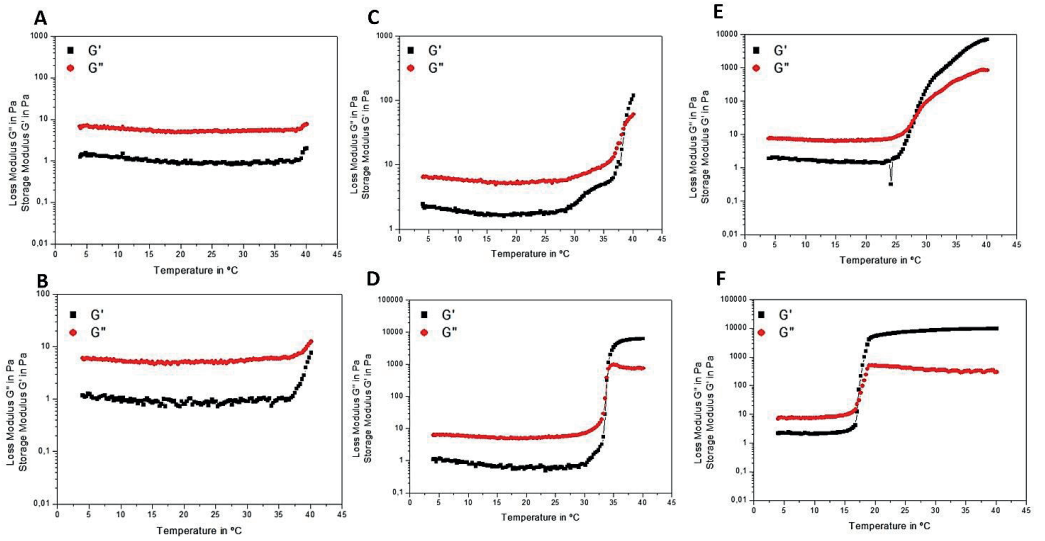

Figure S6. Gelation analysis results of CUR+BNZ@NIN dispersed in hydrogel with different percentages of poloxamer: (A) 15%; (B) 16.5%; (C) 17%, (D) 18%; (E) 20; (F) 25%.

Table S1. Experimental groups tested in the *in vivo* assay model with female BALB/c mice for VVC treatment.

Experimental group	Sample	Animals number
Group 1	Negative for infection	7
Group 2	Positive for infection	7
Group 3	CUR+BNZ@NIN@HG	7
Group 4	CUR+BNZ@NIN	7
Group 5	CUR+BNZ@HG	7
Group 6	BNZ@NIN	7
Group 7	CUR@MSN	7
Group 8	CUR+BNZ	7
Group 9	CUR	7
Group 10	BNZ	7
Group 11	NIN	7
Group 12	HG	7
Group 13	Drugs solvent	7
Group 14	Commercial formulation	7

Legend: CUR: curcumin; BNZ: benzydamine hydrochloride; NIN: hybrid nanoparticle; HG: hydrogel; commercial formulation: clotrimazole.

References

CLSI. (2017). *M27: reference method for broth dilution antifungal susceptibility testing of yeasts* (4th ed.). Clinical and Laboratory Standards Institute.

LaFayette, S. L., Collins, C., Zaas, A. K., Schell, W. A., Betancourt-Quiroz, M., Gunatilaka, A. A. L., Perfect, J. R., & Cowen, L. E. (2010). PKC Signaling Regulates Drug Resistance of the Fungal Pathogen *Candida albicans* via Circuitry Comprised of Mkc1, Calcineurin, and Hsp90. *PLoS Pathogens, 6*(8), *Article* e1001069. https://doi.org/10.1371/journal.ppat.1001069

CHAPTER 12

Highlights in poloxamer-based drug delivery systems as strategy at local application for vaginal infections

Gabriela Corrêa Carvalho, Victor Hugo Sousa Araujo, Bruno Fonseca-Santos, Jennifer Thayanne Cavalcante de Araújo, Maurício Palmeira Chaves de Souza, Jonatas Lobato Duarte, Marlus Chorilli*

International Journal of Pharmaceutics, v. 602, n.1, 120635, pp. 1-13 2021

Reprinted with permission in accordance with the journal's author's rights policy - Elsevier.

Abstract

Infectious diseases related to the vagina include diseases caused by the imbalance of the vaginal flora and by sexually transmitted infections. Some of these present themselves as a public health problem due to the lack of efficient treatment that leads to their complete cure, and others due to the growing resistance to drugs used in therapy. In this sense, new treatment strategies are desirable, with vaginal administration rout being a great choice since can bypass first-pass metabolism and decrease drug interactions and adverse effects. However, it is worth highlighting limitations related to patient's discomfort at application time. Thereby, the use of poloxamer-based drug delivery systems is desirable due its stimuli-sensitive characteristic. Therefore, the present review reports a brief overview of poloxamer properties, biological behavior and advances in poloxamer applications in controlled drug release systems for infectious diseases related to the vagina treatment and prevention.

1. Introduction

When developing a formulation it is essential to take into account aspects related to the disease and the desired effect for the appropriate administration route of choice, a fundamental step towards drug therapy success (Sábio et al., 2021). When the formulation under development is for a disease related to the vagina treatment or prevention the vaginal route is the best choice because it is a potential site for local drug delivery (Veazey et al., 2003; Wong et al., 2014).

Although being considered alternative, the vaginal route is practical and well-established (dos Santos et al., 2020; Jalalvandi et al., 2020). As there are no cells with metabolic enzymes, this route has the advantage of circumventing the first pass effect, common in oral route, which allows the use of lower dosages of drugs, avoiding side effects incidence. It is also noteworthy that this route is desirable due to the large superficial area of the vaginal region, excellent blood supply, dense and homogeneous vascularization and high permeability of the mucosa, mainly for low molecular weight drugs (de Araújo et al., 2019; Ensign et al., 2014; Rohan & Sassi, 2009; Sharifzadeh et al., 2020).

Despite the fact that most medicines available on the market are in the form of solid water-based gels, in the field of research the use of new drug delivery strategies has been increasingly gaining ground (Rohan & Sassi, 2009). Solid water-based gels formulations have several disadvantages, among them can be highlighted patient's difficulty in administering these gels, reporting "mess", because as this type of formulation has low retention in the vaginal lumen it causes drug leakage. A fact that cannot only decrease patient's adherence to treatment but also decrease its effectiveness (Garg et al., 2005; Rohan & Sassi, 2009). It is also noteworthy that factors inherent to the application site, such as vaginal physiology and anatomy as well as the presence of secretion and vaginal fluids renewal also decrease the time that the formulation remains at the application site, which also compromises the treatment efficiency (dos Santos et al., 2020).

In this sense, the use of polymers in the development of nanotechnology and hydrogels surrounding formulation has been gaining great prominence. Of these promising polymers, poloxamer stands out due its stimuli-sensitive characteristic, desirable for vaginal application (dos Santos et al., 2020; Leyva-Gómez et al., 2018; Wong et al., 2014; Zarrintaj et al., 2020). Therefore, the present review reports a brief overview of poloxamer properties, biological behavior and advances in poloxamer applications in controlled drug release systems for infectious diseases related to the vagina treatment and prevention.

2. Poloxamer

2.1. General aspects

Poloxamer, also known as Pluronic®, Lutrol® and Synperonic®, are a non-ionic synthetic triblock copolymer formed by a hydrophobic central chain of poly (propylene oxide) embedded between two poly (ethylene oxide) chains with hydrophilic character. The synthesis of this polymer occurs by anionic sequential polymerization in the presence of sodium and potassium hydroxide (activators) (Bodratti & Alexandridis, 2018; Giuliano et al., 2020; Ruel-Gariepy & Leroux, 2004; Zarrintaj et al., 2020). First the opening of the ethylene oxide and propylene oxide ring occurs, with the poly(p-phenylene oxide) (PPO) units being formed first and then the Poly(ethylene oxide) (PEO) unit is polymerized to them (Herzberger et al., 2016).

The Pluronic nomenclature shows the physical state of this polymer by the letter that precedes the number, they are L, P or F to which they indicate liquid, paste and flake respectively (Zarrintaj et al., 2020). This copolymer is white, tasteless and odorless, with free flowing properties. As for solubility, its amphiphilic characteristic makes it soluble in both, polar and non-polar solvents (Chowdhury et al., 2017). There are more than 30 poloxamer agents with molecular weights varying from 1,100 to 14,000 (Ruel-Gariepy & Leroux, 2004). Although they have the same chemical structure, what differs between them is its molecular weight due to the variation in its quantity of poly (propylene oxide) and poly (ethylene oxide) units. It is worth noting that the more the amount of poly ethylene oxide units in the molecule, the greater its solubility in water and the lower its molecular weight. (Kabanov et al., 2002; Schmolka, 1977). Thus, each type of poloxamer has a different hydrophilic-lipophilic balance (HLB), a fundamental parameter when choosing the most appropriate type of poloxamer for a given formulation because it indicates whether it is solubilized in water or oil. The lower the value and HLB the lower its solubility in water (Gadhave, 2014; Zarrintaj et al., 2020).

Poloxamer has a reversible thermo-responsive sol-to-gel transition, which induces the formation of a solid gel from a solution, a property that is widely explored in the drug development area since the 50's (Abdeltawab et al., 2020; Chowdhury et al., 2017; dos Santos et al., 2020; Zarrintaj et al., 2020). This thermodynamic characteristic is due to the fact that this material behaves like an unstructured low molecular solution at low temperature and self-assemble into spherical micelles (micellization) as the temperature increases and the critical micellar temperature (CMT) (or temperature or Krafft point) is reached, due to copolymers aggregation (**Figure 1**) (Chowdhury et al., 2017; Zarrintaj et al., 2020). Another important factor for this process is the critical micelle concentration (CMC), as it represents the appropriate copolymers concentration for the micelles formation, being CMC inversely proportional to the number of PPO units and to CMT, (Alexandridis et al., 1994; Giuliano et al., 2018). Being considered linear the relationship between the logarithm of the poloxamer concentration and the sol-gel transfer temperature, relationship observed in polymers with the same proportion of PEO and PPO units (Vadnere et al., 1984). The micellization process

occurs because the PEO units are swollen due to hydration, remaining on the micelle outside, while the PPO units are dehydrated being on the inside of the spherical micelle formed (Gratieri et al., 2010; Kabanov et al., 2002). These spheres are formed due to a hard sphere crystallization, that is, due an orderly packaging (Mortensen & Brown, 1993).

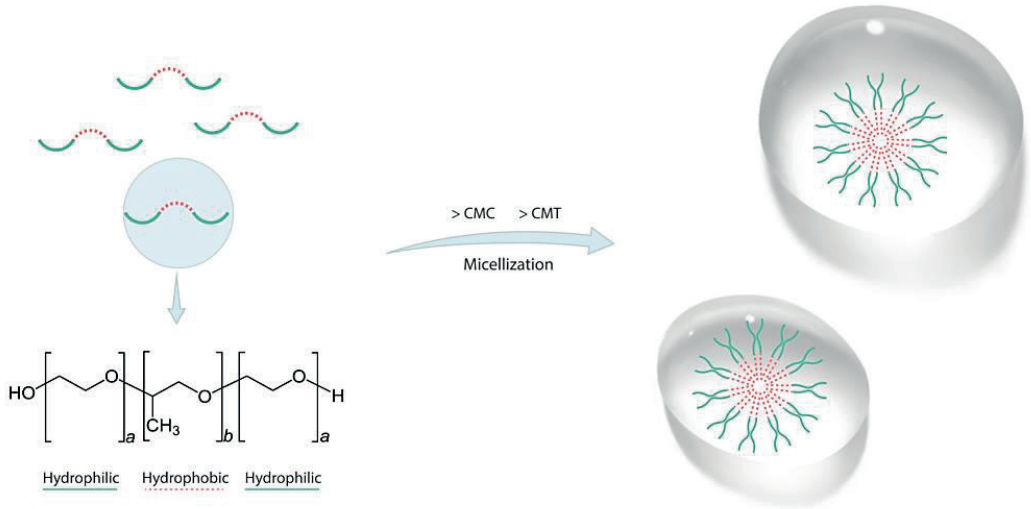

Figure 1: Schematic representation of poloxamer micellization process in solution. Legend: Critical micellar temperature (CMT); Critical micelle concentration (CMC).

This complex behavior is a consequence of the amphiphilic characteristic of this polymer. Its flow varies from Newtonian, at sufficiently low temperatures, to viscoelastic, at higher temperatures, through desolvation mechanism. The increase in temperature induces dehydration and changes in the hydrophobic chain's conformation, while desolvation mechanism makes the polymer chains closer, increasing the chains friction, the number of interactions between them and entanglement in the polymeric network, causing an increase in the solution viscosity. It is worth noting that at temperatures above the gel point its rheological behavior is unstable (Jalaal et al., 2017; Miller & Drabik, 1984; Tung, 1994; Vadnere et al., 1984; Vandenhaute et al., 2014). It is worth noting that the values of CMT and CMC vary according to poloxamer type, as it is dependent on the number of PEO and PPO units, (Alexandridis et al., 1994; Fakhari et al., 2017; Giuliano et al., 2018). As there are different types of poloxamer, the physico-chemical characteristics differ from one to the other, **Table 1** highlights main characteristics of some types of poloxamer used in the pharmaceutical area.

Table 1: Main characteristics of some types of poloxamer used in the pharmaceutical area.

Poloxamer type	Trade name	Molar mass	Poly (propylene oxide): poly (ethylene oxide) rate	CMC/CMT	Hydrophilic-lipophilic balance	References
101	Pluronic® L-31	1100 g mol^{-1}	18.0:4.0	2.0×10^{-2} mol L^{-1}/ -9.7 kJ mol^{-1}	3.2	(Krupka & Exner, 2011; Lopes & Loh, 1998)
124	Pluronic® L-44	2200 g mol^{-1}	22.8:20.0	3.6×10^{-3} mol L^{-1}/ 37°C	16	(Batrakova et al., 1999; Chowdhury et al., 2017)
181	Pluronic® L-61	2000 g mol^{-1}	31.0:4.5	1.1 x 10^{-4} mol L^{-1}/ 37°C	3	(Batrakova et al., 1999; Suliman et al., 2014)
182	Pluronic® L-62	2500 g mol^{-1}	34.5:11.4	4.0 x 10^{-4} mol L^{-1}/ 37°C	7	(Batrakova et al., 1999; Katakam & Banga, 1997)
188	Pluronic ® F-68	8400 g mol^{-1}	29.0:152.7	4.8 x 10^{-4} mol L^{-1}/ 37°C	29	(Batrakova et al., 1999; Giuliano et al., 2018)
235	Pluronic ® P-85	4600 g mol^{-1}	39.7:52.3	6.5 x 10^{-5} mol L^{-1}/ 37°C	16	(Batrakova et al., 1999; Vasconcelos et al., 2017)
238	Pluronic ® F-88	11400 g mol^{-1}	39.3:207.8	2.5 x 10^{-4} mol L^{-1}/ 37°C	28	(Batrakova et al., 1999; Visentin et al., 2012)
331	Pluronic ® L-101	3800 g mol^{-1}	58.9:8.6	2.1 x 10^{-6} mol L^{-1}/ 37°C	1	(Batrakova et al., 1999; Rudt & Müller, 1993)
335	Pluronic ® P-105	6500 g mol^{-1}	56.03: 73.86	6.2 x 10^{-6} mol L^{-1}/ 37°C	15	(Shubhra et al., 2014)
338	Pluronic ® F-108	14600 g mol^{-1}	50.3:265.4	2.2 x 10^{-5} mol L^{-1}/ 37°C	27	(Batrakova et al., 1999; Meng et al., 2020)
403	Pluronic ® P-123	5750 g mol^{-1}	69.4:39.2	4.4 x 10^{-6} mol L^{-1}/ 37°C	8	(Batrakova et al., 1999; Akkari et al., 2016)
407	Pluronic® F127	12600 g mol^{-1}	65.2:200.4	2.8 x 10^{-6} mol L^{-1}/ 37°C	22	(Batrakova et al., 1999; Giuliano et al., 2020)

2.2. Poloxamer biological behavior: biocompatibility, biodistribution, biodegradability and clearance

The available toxicology data indicate that poloxamers have 50% lethal dose (LD_{50}) less than 5 $g.kg^{-1}$ based on oral and dermal exposure. Radiolabeled-poloxamers have been investigated concerning absorption, distribution, metabolization, and excretion on rats and dogs followed by intravenous (IV) and oral administration (Chemicals, 1996; Rodgers et al., 1984; Wang & Stern, 1975; Willcox et al., 1978). The primary excretion route is renal and a minor excretion is biliary. After 24 hours post IV administration, poloxamer polymer was found in organs of dogs, particularly in liver, lungs and muscles (Willcox et al., 1978). Another study reinforces that poloxamer has a quick depuration by the renal route and it was found in the urine of rats, however in plasma it was not found (Port et al., 1978).

Acute and subchronic toxicity of poloxamers has been related in the literature. Studies related to acute toxicity of Poloxamers 124, 182, 188, and 235 were carried out in albino rats; liquid forms were administered in the range of 1-15 $mg.kg^{-1}$, and poloxamer 188 was dissolved into corn oil and administered from 2 to 15 $mg.kg^{-1}$. At low doses (not shown) no symptoms were signed, but with an increase of dose, the animals exhibited mild sedation. The necropsy of died rats revealed lungs edema, as well as, stomach distention, engorgement of the lungs and intestines vascular dilation. for Poloxamers 124, 182, 188, and 235 oral LD_{50} values obtained were 5, 5.5, >15, and >34.6 g/kg, respectively (Leaf, 1967). Poloxamer 188, at doses of 500 and 1000 $mg.kg^{-1}$, demonstrated ability to induct pulmonary foam cells, additionally at the dose levels of 100 – 1000 $mg.kg^{-1}$ induced degenerative changes in kidneys proximal tubules. The test was performed in rats and chemicals were administered by intravenous route (Magnusson et al., 1986).

The effect of intramuscular injections of poloxamers was evaluated. Poloxamers 238, 335, 403, and 407 were administered at 0.25 $g.mL^{-1}$ in saline to rabbits. Single and multiple doses were performed, blood samples were collected and creatine kinase was assayed. Poloxamers 335 and 403 were able to increase the enzyme levels 4.6 and 9.1 times compared to saline injection. On the other hand, Poloxamers 238 and 407 induced creatine kinase levels comparable to saline. When administrated in the multiple-dose, the animals was killed and the results was similar to single-dose; there were high levels of enzyme in the blood, and they were proportional to poloxamers lipophilicity grade (Johnston & Miller, 1985).

Poloxamers 181 and 407 were evaluated as vehicles by administration in IV route in rats. Because of its use as vehicles, no information of mass was provided. At high dose, in acute toxicity, pulmonary edema and hypervolemia were observed. In subacute test the animals showed weight gain, appetite suppression, and increase in the spleen, liver and adrenal weight. Acute toxicity was carried out in

Beagles dogs and although no deaths was observed clinical signs like tachycardia and vomiting were noted (Alakhov et al., 1999).

Poloxamer 407 was tested on the acute toxicity at dose of 5 $g.kg^{-1}$ by intraperitoneal (IP) injections, within 8 weeks the mice died. Lower doses (< 5 $g.kg^{-1}$) exhibited no deaths. Doses of 25 or 50 mg were administered by i.p. route and the biomarkers were monitored in blood, as alanine aminotransaminase (ALT), blood urea nitrogen, cholesterol and triglycerides. No changes in ALT levels were noticed, however, the levels of blood urea nitrogen were slightly lower for tested groups when compared to controls animals' group. On the third day, levels of cholesterol and triglycerides in blood were slightly lower than the control group. Yet, on the eighth day, the triglycerides levels were slightly higher in both test groups (Li et al., 1998).

Remark was made that Poloxamer 407 injection (≤ 27.5 $mg.kg^{-1}$) did not induce hyperlipidemia nor altered other blood biomarkers in habits. However, poloxamer induced dose-dependent hyperlipidemia in rabbits (Blonder et al., 1999). Johnston and collaborators (1993) evaluated the potential toxicity of poloxamer 407 at 0.3 $g.kg^{-1}$ and 1.0 $g.kg^{-1}$ in rats by multiple-dose. At 4 days of administration of 0.3 $g.kg^{-1}$, an increase in monocytes number was observed, and the dose of 1.0 $g.kg^{-1}$ led to distinct splenomegaly and loss of weight.

Short-term toxicity also was evaluated to poloxamers and the rate of mortality in rats was assessed for Poloxamers 182, 235 and 338 was 51%, 20%, and 15%, respectively, the deaths were caused by inanition. Poloxamers 182 and 235 lead increase of liver in female, whereas male adrenal was enlarged for Poloxamer 338. Additionally, Poloxamer 188 was administered by I.V. route (0.5 $g.\ kg^{-1}$), by 5 days per week for 7 weeks. No adverse reactions and changes in blood, urine and necropsy examinations was observed (Leaf, 1967).

The exposition of Poloxamers 188 and 331 was carried out by Comai and Sullivan (1980), the dietary fat absorption and fecal-fat elimination were determined. Poloxamer 331 led to an increase in fecal-fat elimination, which was dose-dependent. No observation was noticed to Poloxamers 188. Values of cholesterol, triglycerides and glucose were similar in the groups. Poloxamer at 3% lead to a decrease in liver weight of animals.

Poloxamer 101 was inhaled and rats were exposed to 97 mg/m^3 by 6 h per day for 5 days a week during 2 weeks. As positive control ethylene oxide/propylene oxide copolymer was used and after 3 expositions the rats died (9 of 10), the necropsy revealed consolidation, congestion and red discoloration of the lungs. For Poloxamer 101, all rats survived the 10 exposures and no toxicity signs were noted. Slight alveolitis only was observed after 2 weeks of poloxamer exposure (Ulrich et al., 1992).

A subchronic toxicology study of Poloxamer 188 administration in rats at 3% and 5% by weight in food was performed. During the experimentation, 3% and 5% groups showed animals deaths, being 2 and 14 animals died (45 rats per groups), respectively. The authors attributed these deaths to inanition and infections. No findings of toxicological aspects were found in the necropsy evaluation. Dogs were also exposed to 50 mg and 100 $mg.kg^{-1}$ and no changes in blood and urine analysis were observed when compared to the control group. On 90-day exposure, rats and dogs were exposed to Poloxamers331, 235, and 338 and no deaths was attributable to this exposure in any groups. Slight transient diarrhea was observed in rats from the 5.0 $mg.kg^{-1}$ group (Leaf, 1967).

Palmer and collaborators (1998) described the chronic administration (IP) of Poloxamer 407 in mice (0.5 g/kg every third day by 300 days). This study reported increase in plasma triglyceride and cholesterol levels and atherosclerotic lesions formation (Palmer et al., 1998) due to oxidation of circulating lipids (Johnston et al., 2003). Intake of hydroxymethylglutaryl-CoA (HMG-CoA) reductase inhibitors, atorvastatin, with a dose of 20 mg/kg/day was able to reduce not only the plasma cholesterol and triglycerides levels, but also regressed atherosclerotic lesions induced by poloxamer 407 administration in C57BL/6 mice (Johnston et al., 2000).

Poloxamer 188 was evaluated on blood hemolysis in mice, rats, hamsters and rabbits. Concentrations ranging of 4 -10% were tested and no hemolysis were noticed at 4% (Lowe et al., 1995), as well as, Poloxamer 188 was related to accelerating thrombolysis (Hunter et al., 1990). On the other hand, Poloxamer 407 was able to reduce the hemolytic potential of amphiphilic drugs (Feitosa et al., 2019).

In human, clinical trials were performed to evaluate safety. Poloxamer 188 was investigated in a double-blind crossover study with 10 male subjects and, at the end of the study, the authors suggest a smaller intestinal transit time and a small degree of loose bowel action (Connaughton & McCarthy, 1982). The use of Poloxamer 188 was well-tolerated, except by the increase of serum creatinine levels. Preexisting renal dysfunction plays a role in the increase of creatinine in patients (O'Keefe et al., 1996).

Dermal sensibilization is a test to evaluate allergic response to a product, excipients or drugs. Using animal models, Poloxamer 188 was assessed using dogs, rabbits, and guinea pigs. The polymer was applied 10 times (1 times/ day) and at 14 days no erythema was found and no sensitization was evidenced. Rabbits skin were evaluated on microscopy and histological analysis, and no alterations on the epidermis was noted (Leaf, 1967).

Leaf (1967) evaluated a paste based on Poloxamer 188 on 10 volunteers, the formulation was applied to the forearm every other day (total of 10 applications). Skin irritation was not observed. The past was applied again after 14 days and no skin sensitization evidence was observed in any of the volunteers.

2.3. Poloxamer use in drug delivery systems

Poloxamer use is approved by FDA and listed as pharmaceutical excipient in the United States and European Pharmacopoeias (Russo & Villa, 2019). Due to its temperature-dependent self-assembly characteristic poloxamer can be used in the development of new therapeutic strategies, highlighting those involving nanoparticles and hydrogel (Chowdhury et al., 2017; dos Santos et al., 2020; Yapar & Ýnal, 2013; Zarrintaj et al., 2020). This strategy is desirable mainly when the objective of the formulation under development is to stabilize or increase the solubility of an active ingredient improving not only its bioavailability and therapeutic efficacy but also patient compliance (Bodratti & Alexandridis, 2018). The amphiphilic nature of this polymer allows drug carrying due to its self-assembly in micelles (with size between 10-100 nm), being its use desirable for carrying both hydrophobic and hydrophilic drugs (Wu et al., 2015; Zarrintaj et al., 2020). It is also noteworthy that this polymer is an excellent surfactants for nanoemulsion synthesis (Zarrintaj et al., 2020).

The use of polymers in nanoparticles synthesis is desirable because they provide bioadhesion, assist in controlled release and facilitate penetration into the mucosa (Leyva-Gómez et al., 2018). In the study by Das et al., (2010) it is possible to observe that the use of Poloxamer 407 in the synthesis of a nanoparticle increases the solubility of poorly aqueous soluble drugs, such as curcumin, in the other components used for the synthesis, increasing its encapsulation efficiency (EE).

In a study carried out by Zhao and collaborators (2013), Poloxamer 235 was combined to a liposome membrane to enable the controlled release of an embedded fat-soluble drug, as the poloxamer is able to cause transient holes in the nanoparticle membrane, providing greater permeability to the incorporated drug. The use of poloxamer-based coating on nanopaticles allows it to penetrate deeply in mucus gel layer regions in the mucosa as it has the ability to change the viscosity of the mucus by reducing its barrier effect, increasing its permeation through interaction with the body's lipid membranes (Leyva-Gómez et al., 2018; Sonvico et al., 2018).

Its use as a component of hydrogel is due to its attractive reversible thermosensitive activity that enable its administration in liquid form and subsequent gelation at vaginal temperature (37 °C), forming a highly viscous gel (Britton, 2018; Giuliano et al., 2020; Leyva-Gómez et al., 2018; Wong et al., 2014; Zarrintaj et al., 2020). Hydrogel can be defined as a system consisting of two- or multi-component with a three-dimensional polymer chains network dispersed in a liquid, which completes the space between the macromolecules (interstice). When the liquid is water, this gel is called a hydrogel (Ahmed, 2015; Frade et al., 2018). This viscous gel is able to bypass complaints from patients regarding conventional formulations application as it increases the mucoadhesiveness and vaginal retention duration time. Another advantage of using this type of gel is its association with nanoparticles, this association enables nanoparticles non-aggregation and increases nanosystem

capacity of controlling the drug release (dos Santos et al., 2020; Garg et al., 2005; Rohan & Sassi, 2009; Wong et al., 2014). It is worth mentioning that the Poloxamer 407 and 188 stands out for this purpose, as they present this inverse thermosensitivity (Leyva-Gómez et al., 2018; Patel et al., 2009; Zarrintaj et al., 2020).

The mucus present on vaginal epithelial cells is resistant and able to adhere to particles, preventing their penetration. In the case of drug-carrying nanoparticles it is necessary that they pass through this mucus layer to reach the vaginal epithelial cells (Cone, 2009). Poloxamer thermoresponsible gels allow nanosystem mucus penetration, promoting its cellular absorption. The use of this type of gel allows nanosystem to be captured by the vaginal epithelium due the increase of macromolecules in the mucus, causing a wide mucus mesh, which results in greater penetration through it. In HeLa cells it was observed that this time was 30 minutes (counting from nanoparticle release from the gel) (Wong et al., 2014). In this way, poloxamer mucoadhesive properties are desirable for vaginal application not only because it enables a good drug concentration *in situ* for a prolonged period of time, but also due the decrease in the drug dose and adverse effects. Being, therefore, a very promising strategy in the field of controlled drug release by vaginal application (de Araújo et al., 2021; dos Santos et al., 2020; Giuliano et al., 2018).

In addition to the poloxamer it is important to mention another polymer of its family, the poloxamines, or Tetronic® as they are also known. They differs from poloxamer in terms of its chemical structure, as it consists of a tetrafunctional copolymer block formed by a central ethylenediamine group that connects four units of poly (ethylene oxide) - poly (propylene oxide) (Moghimi & Hunter, 2000). Like poloxamer, this type of polymer also has gelling capacity through the formation of micelles. Its micellization process dependents on factors such as concentration, temperature and pH. Due to its solubilization and sustained release of poorly water-soluble drugs capacity, biocompatibility, pH-responsive and thermogelling characteristic its use has been more and more desirable in drug delivery area, both as hydrogels or nanoparticles component (Cho et al., 2012; Moghimi & Hunter, 2000; Pillai et al., 2020; Puig-Rigall et al., 2021; Rey-Rico et al., 2011).

Additionally, studies involving cyclodextrin polymers, mainly those formed by the combination of this cyclic oligosaccharides with poloxamer or poloxamine, called polyrotaxane, are very promising in both, hydrogels and nanoparticles preparation due to the micelles formed by them (**Figure 2**) (He et al., 2012; Higashi et al., 2013; Larrañeta & Isasi, 2014; Tang et al., 2020). These types of compounds are formed by one or more cyclodextrin units, the macrolide, and one or more linear polymers units, the axis, in which macrolide crosses the axis, which due its bulky molecules at the ends, causes the macrolide retention. Its use is desirable because they have both, the characteristics

of cavity structure of a cyclodextrins, and the characteristics of the polymer used (Farias et al., 2020; Higashi et al., 2013; Tang et al., 2020).

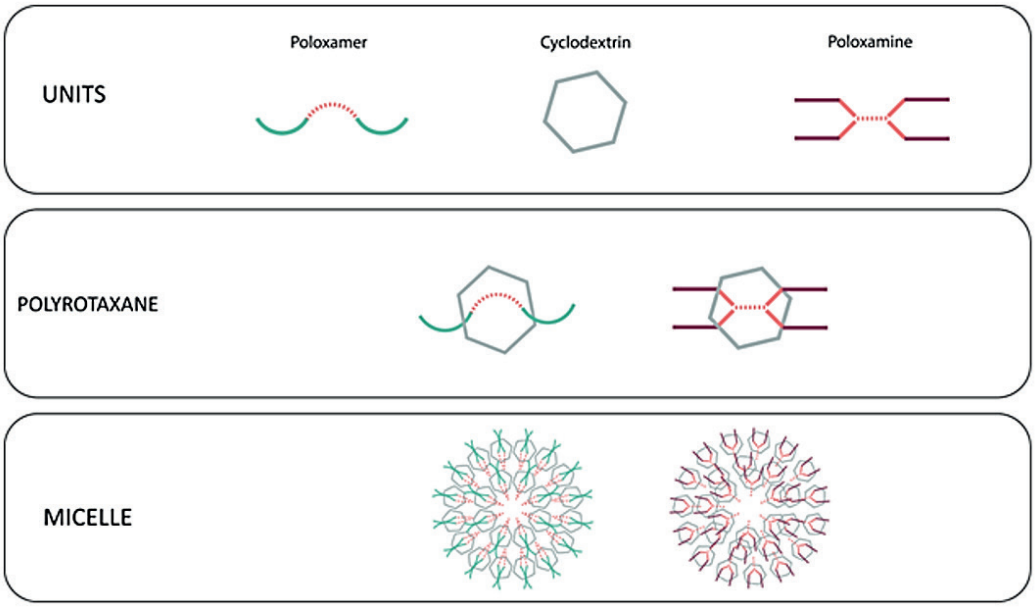

Figure 2: schematic representation of the polyrotaxane and its forming units, as well as the micelles that they can originate.

3. Poloxamer-based vaginal systems application in infectious diseases related to vagina

Infectious diseases are those caused by bacteria, fungi, viruses or parasites that have the ability to be transmitted from one person to another directly or indirectly (WHO, 2021). The vagina is a gateway to both, systemic and local infectious diseases (vaginal infectious diseases) (da Silva et al., 2014; HIV.gov., 2019; Palmeira-de-Oliveira et al., 2015). As a systemic disease related to the vagina it can be cited the human T cell lymphotropic virus (HTLV), acquired immunodeficiency syndrome (AIDS), and syphilis, all sexually transmitted infections (U.S. Department of Health & Human Services, 2019; WHO, 2017).

AIDS is caused by the attack of the human immunodeficiency virus (HIV) in the immune system. It is worth noting that although three decades have passed since the epidemic, this virus continues to worry global health authorities due to the high number of infected people, around 38 million. Although this disease has treatment it is based on the use of antiretrovirals, which besides just leading to undetectable viral load it has several adverse effects and possibility of resistance (Cojocaru et al., 2020; Cunha-Reis et al., 2016; U.S. Department of Health & Human Services, 2019; Singh et al., 2017).

Therefore, even today, the development of an effective treatment for this disease is still a world priority (Kaseke et al., 2021). HTLV, also STI caused by virus, has between five and 10 million infected individuals worldwide (CdA et al., 2021). This virus subtype I is related to severe neurological and degenerative diseases, such as myelopathy/tropical spastic paraparesis, and hematological diseases, such as leukemia and adult human T-cell lymphoma (Rolon & Yao, 2020).

Syphilis, caused by the bacteria *Treponema pallidum*, is also an STI (WHO, 2017). Despite being an easy disease to be diagnosed and treated it is a serious worldwide public health problem because, in addition to being endemic in low-income countries, it has increasing prevalence levels in high-income countries (Kojima & Klausner, 2018; Santos et al., 2020). Despite genital lesions are the first symptoms, this disease is characterized by latency periods, systemic dissemination and progression to acute complications, which if left untreated lead to serious complications (Avelleira & Bottino, 2006; Mathur et al., 2019).

Although infectious vaginal diseases are not associated with high mortality rates, in addition to being prevalent, especially in women of reproductive age, they lead patients to high levels of anxiety and reduced quality of life (Palmeira-de-Oliveira et al., 2015). Infectious vaginal diseases can occur due to an imbalance of the vaginal flora or due to sexual transmission (Li et al., 2019; Ramyadevi et al., 2016). The vagina has several microbial communities composing its flora, such as *Lactobacilli* sp. and *Candida* sp., when in balance the vaginal flora represents a defense mechanism (Ameen et al., 2017; Ferrer, 2000). Internal and external factors such as stress, hormonal variations, immunosuppression, diabetes and use of antibiotics, can lead to imbalance, favoring the occurrence of infections such as vulvovaginal candidiasis (VVC) and bacterial vaginosis (Toledo et al., 2020; Li et al., 2019; Mtibaa et al., 2017; Sangamithra et al., 2013).

Bacterial vaginosis (BV) is the most common disease caused by the imbalance of the vaginal flora, being *Gardnerella vaginalis* the most frequently isolated etiological agent. Its main symptoms are increased vaginal pH, bad smell and vaginal itching (Bautista et al., 2016; Bekasiak et al., 2020; Hay, 2017; Kenyon et al., 2013). Additionally it can also be observed an increase in vaginal enzyme activity, alteration in fluids composition, increase in viscosity and the formation of bacterial biofilms, which alters the absorption of drugs (Leyva-Gómez et al., 2019). The great concern about this infection is the fact that it favors the appearance of others etiologic agents like HIV, herpes simplex virus (HSV)-2, *Neisseria gonorrhoeae*, *Trichomonas vaginalis*, and *Chlamydia trachomatis*. It is also noteworthy that BV is closely related to the presence of anaerobic bacteria, which damage the vaginal epithelium and facilitate contamination by human papillomavirus (HPV) (Coudray & Madhivanan, 2020; Kenyon et al., 2013).

C. trachomatis is the cause of the most prevalent bacterial STI. Although this disease is asymptomatic in most cases, if untreated it can lead to infertility, pelvic inflammatory disease, chronic pelvic pain, ectopic pregnancy, abortions, low birth weight, postpartum endometritis and transmission to the newborn (Haggerty et al., 2010; Kiguen et al., 2019). Gonorrhea, also a STI caused by bacteria, has been considered a public health threat due to the *N. gonorrhoeae*, its causative agent, increasing incidence of resistance (Ma et al., 2020a, 2020b). Although most infections are genital, it can also occur in the pharynx and the rectum and anus. This disease varies from asymptomatic, the most common form, to the occurrence of acute salpingitis, a serious complication since it is one of the main causes of female infertility (Hook & Kirkcaldy, 2018; Penna et al., 2000).

VVC, the second cause of vaginitis, is caused by the imbalance of the vaginal flora, this disease is related to the inflammation caused by *Candida* spp. (Bonifácio et al., 2015; Ramos et al., 2016; Gonçalves et al., 2016; Rodero et al., 2018; Sangamithra et al., 2013). About 70-75% of women will develop this disease at some point in their life, what is not desirable because it can affect patient's work performance and social sphere due to pain and great discomfort causes by it. In cases of immunocompromised patients, VVC can lead to serious systemic infections, what is worrying (Ascioglu et al., 2002; Donders & Sobel, 2017). This fungi virulence factors, like biofilm formation, hyphae formation, adhesion, protease excretion and phenotypic exchange, mediated this disease pathogenesis (Nett, 2018; Rodríguez-Cerdeira et al., 2019; Tamura et al., 2007).

For viral diseases that affect the vagina, HPV and HSV can be mentioned (Usyk et al., 2020). HPV is the most common STI pathogen in adult women, being de cause of benign genital lesions, the condyloma. Is worth highlighting that a small percentage of infected women develop cervical precancer and cancer (Sarier et al., 2020; Usyk et al., 2020). Genital herpes, STI with more than 400 million infected worldwide, is caused by HSV type 1 (HSV-1) and type 2 (HSV-2), being the last one the most common. Infection by this virus last a lifetime and can trigger from an acute and recurrent vesiculoucerative disease to erosions on the vulva, labia, vagina and cervix, with 8-10 days of duration (Bernstein, 2020; Bhatta et al., 2018).

Parasitic diseases are also a public health problem due to the millions of deaths caused each year (Edrissian et al., 2016; Hobbs et al., 2019; Momčilović et al., 2019). Trichomoniasis, vaginal scabies and oxyuriasis stands out as diseases related to vagina, among which trichomoniasis besides being the most common, is also the most prevalent non-viral STI in the world (Ahmed & Yesmin, 2008; Kissinger et al., 2018; Palmeira-de-Oliveira et al., 2015; Secor et al., 2014; Shaw et al., 2019). Caused by the adhesion of *T. vaginalis*, this disease is mostly asymptomatic. When symptomatic, it presents symptoms like itching, vaginal odor, purulent discharge, vaginal irritation, vulvar erythema, dysuria and pelvic pain. Complications include endometritis, adnexitis, pyosalpinx, cervical dysplasia,

infertility and premature birth and low birth weight (Daugherty et al., 2019; Fichorova, 2009; Khurana & Singh, 2018; Kissinger et al., 2018; Margarita et al., 2019; Shaw et al., 2019; Vilela & Benchimol, 2011).

VB, gonorrhea, *C. trachomatis,* VVC and *T. vaginalis* in addition to being infectious vaginal diseases, they have a problem in relation to resistance to drugs commonly used in their therapy (Alessio & Nyirjesy, 2019; dos Santos et al., 2020; Ma et al., 2020a; Mestrovic & Ljubin-Sternak, 2018; Tomás et al., 2020). It is also noteworthy that other diseases, such as HPV and HSV, lack treatment for the complete cure (Garland & Steben, 2014; Sarier et al., 2020). In this sense, the development of topic formulations using thermoresponsive bioadhesive strategies are interesting in order to improve the treatment and prevention of infectious vaginal diseases providing greater local concentration of drugs, less drug interaction and adverse effects. Being the use of nanotechnology and new active ingredients, such as plant extracts and probiotics desirable in order to circumvent the growing problem of resistance to drugs (Palmeira-de-Oliveira et al., 2015; Rohan & Sassi, 2009). **Table 2** describes main aspects of formulation development in articles published in the last 10 years that used poloxamer as a component of nanosystems or thermoresponsive hydrogels in the prevention or treatment of infectious diseases through the vaginal route.

Table 2: Main aspects of formulation development in articles published in the last 10 years using poloxamer as a component of drug delivery systems in the prevention or treatment of infectious diseases through the vaginal route.

Microorganism	Poloxamer Type	Delivery System Type based on poloxamer	Active ingredient	Assay	References
Niesseria gonnorea	Poloxamer 407	Thermosensitive hydrogel	*Lactobacillus crispatus*	*In vitro*	(Gnaman et al., 2020)
HIV	Poloxamer 407 and poloxamer 188	Solid Lipid nanoparticles and gel	Dolutegravir sodium	*Ex vivo*	(Anjum & Lakshmi, 2020)
Escherichia coli and *Staphylococcus aureus*	Poloxamer 407 Poloxamer 188	Thermosensitive hydrogel	Curcumin	*In vivo* and *in vitro*	(Zhang et al., 2019)
Candida spp.	Poloxamer 407	Lipid nanoparticle	*Astronium urundeuva* leaves extract and fluconazole	*In vitro*	(Bonifácio et al., 2019)
Candida albicans	Poloxamer 407	Gel-flakes	Ketoconazole	*In vitro and In vivo*	(Ellah et al., 2019)
HIV	Poloxamer 407	Hydrogel	Theaflavin and nifeviroc or Nile red	*In vitro* and *in vivo*	(Tian et al., 2019)
Trichomonas vaginalis	Poloxamer P407	Hydrogel	-	*In vitro*	(Malli et al., 2019)
C. albicans	Poloxamer 407 and Poloxamer 188	Thermoresponsive gel	Amphotericin B	*In vitro and In vivo*	(Ci et al., 2018)
HIV	Poloxamer 407	Gel	Tenofovir	*In vitro*	(Timur et al., 2018)
E. coli, S. aureus and *Pseudomonas aeruginosa.*	Poloxamer 407 Poloxamer 188	Expansible thermal gelling foam aerosol	Silver nanoparticles	*In vitro* and *in vivo*	(Mei et al., 2017)
T. vaginalis	Poloxamer 407	Hydrogel	metronidazole	*In vitro* and *ex vivo*	(Malli et al., 2017)
HIV	Poloxamer 407	Polymeric nanoparticles	Efavirenz and Tenofovir	*In vitro* and *in vivo*	(Cunha-Reis et al., 2016)
HIV	Poloxamer 407	Polymeric nanoparticles	Tenofovir	*In vitro* and *in vivo*	(Machado et al., 2016)
HSV	Poloxamer 407	Polymer nanoparticles and in situ gel	Acyclovir	*In vitro*, *in vivo*, and *ex vivo*	(Ramyadevi et al., 2016)
C. albicans	Poloxamer 407	Liquid crystal precursor	Curcumin	*In vitro*	(Salmazi et al., 2015)

HIV	Poloxamer 407 and Poloxamer 338	Polymeric nanoparticles, thermosensitive gel and nanosuspension	Rilpivirine	*In vitro* and *in vivo*	(Kovarova et al., 2015)
HIV	Poloxamer 407 and Poloxamer 188	Hydrogel	M48U1 peptide	*In vitro*	(Bouchemal et al., 2015)
T. vaginalis	Poloxamer 407 and Poloxamer 188	Hydrogel	-	*In vitro and Ex vivo*	(Pradines et al., 2015)
S. aureus and *E. coli*	Poloxamer 407	Mucoadhesive and thermally sensitive gel	Amoxicillin	*In vitro*	(Rossi et al., 2014)
HSV and HIV	Poloxamer 407	Bioadhesive gel	Acyclovir and tenofovir	*In vitro* and *in vivo*	(Shankar & Alt, 2014)
Candida spp.	Poloxamer 407	Thermoresponsive hydrogel	Propolis extractive solution	*In vitro*	(Pereira et al., 2013)
HIV	Poloxamer 338	Polymeric nanoparticles	Dapivirine	*In vitro* and *ex vivo*	(das Neves et al., 2013)
HIV	Poloxamer 407	Hydrogel	M48U1 peptide	*In vitro*	(Bouchemal et al., 2013)
HIV	Poloxamer 407 and Poloxamer 188	Polymeric nanoparticles and thermosensitive hydrogel	Raltegravir and efavirenz	*In vitro*	(Date et al., 2012)
HIV	Poloxamer 407	pH-responsive Polymeric nanoparticles	Tenofovir or tenofovir disoproxil fumarate	*In vitro*	(Zhang et al., 2011)

3.1. Application of gel and hydrogel, based on poloxamer, in infectious diseases related to the vagina

Recently, Gnaman and collaborators (2020) studied the effect of poloxamer hydrogel for *Lactobacillus crispatus* delivery for vaginal protection against *N. gonnorea*. It was shown that *L. crispatus* could be used not only to inhibit *N. gonorrhoeae* infection and BV treatment, but also as a vaginal suppository for healthy women with recurrent urinary tract infections history (Czaja et al., 2007; Hemmerling et al., 2010). In this study the researches produced a thermosensitive hydrogel containing 21.5% of Poloxamer 407, 1% of sodium alginate and 9 $\log_{10}$ colony forming units (CFU) of *L. crispatus* per gel sample (5 g). The hydrogel preparation was not deleterious for lactobacillus and the rheological behavior, inherent to poloxamer, was suitable for vaginal application. The hydrogel was able to be a potential probiotic for *N. gonorrhoeae* inhibition. The developed formulation proved to be an important way to prevent vaginal bacteria disease. Aspects related to the number and frequency of applications must be investigated, aiming the best performance of the developed system (N'Guessan Gnaman et al., 2020). Additionally, other probiotics and bioactive molecules can be veiculated in these type of system for vaginal protection against bacterial infections.

In this subjective, Zhang and collaborators (2019) used poloxamer hydrogel to veiculate curcumin solid dispersions for local treatment of injured vaginal bacterial infection and for vaginal wound healing improvement. Curcumin (diferuloylmethane) is the main natural polyphenol found in *Curcuma longa* rhizome (Alves et al., 2019; Hewlings & Kalman, 2017). It has an array of biological activities such as anti-inflammatory, antioxidant, anti-tumor, anticoagulant and immunomodulatory (Maheshwari et al., 2006; Victorelli et al., 2021). The hydrogel was prepared using Poloxamer 407 and Poloxamer 188 (6:1, w/w) dissolved in water with subsequent curcumin solid dispersions addition. Curcumin-loaded hydrogels showed suitability for application and associated physiological gelation behavior. High therapeutic efficiency was observed after topical application in injured vaginal bacterial infection, such as relief in inflammation and vaginal wound healing improvement, when compared to lincomycin/lidocaine gel, both commercial products. Remark was made that antibacterial activity *in vivo* was better than *in vitro*, which can be attributed to the recuperation of the vaginal microenvironment and to the improvement of Lactobacillus intravaginal growth in *in vivo* experiments (Zhang et al., 2019).

In a study conducted by Rossi and collaborators (2014), mucoadhesive and thermally sensitive gels containing amoxicillin trihydrate at 2% w/w, based in chitosan lactate + Poloxamer 407, was compared with hydrogels based in chitosan lactate + glycerolphosphate for vaginal mucositis treatment. Chitosan is a mucoadhesive biopolymer that has lots of biological properties, such as wound healing properties on human fibroblasts and antibacterial activity against *Staphylococcus aureus* and

Escherichia coli (Dutta, 2016; Hirano, 1996; Kim, 2018). Glycerolphosphate induces chitosan thermogelation by hydrophobic interactions that are potentiated by the temperature increase (Rossi et al., 2014). As a result of both gels comparison, it was observed that were capable to be in gel form at physiological temperature and to have a consistency that allow easy application and good distribution in the vaginal mucosa at room temperature. The poloxamer based gels gelled in the temperature of 37ºC, under high shear stress, superior to flow characteristics. Under low shear stress, and when mixed with simulated vaginal fluid, they formed a stronger and more elastic gel. However, it was less mucoadhesive than the one containing glycerolphosphate. In fact, the mucus adhesion properties are responsible for greater contact of the drug with the site of action, making the system more effective. Nevertheless, both formulations were characterized by antimicrobial properties against the two bacteria, *S. aureus* and *E. coli,* and presented 45% release of the drug loaded after a period of 3 h. When compared with poloxamer pure hydrogels, all results obtained by polymeric mixture were superior. In this way, it is possible to confirm that double strategy is more effective than a single strategy (Rossi et al., 2014). Thus, it is reasonable to conclude that hydrogels with mucoadhesiveness and thermically response can be used in many vaginal diseases.

Ci and collaborators (2018) developed a thermoresponsive gel for dispersing nanoparticles with 246.8 ± 8.0 nm containing amphotericin B, with 100% of EE, which, in turn to demonstrated greater anti-candida potential *in vivo* than commercially available tablets containing the same drug, as well as significant mucoadhesive capacity and retention time. Also using poloxamer as a hydrogel component, Ellah and collaborators (2019) dispersed ketoconazole gel-flakes in order to increase its mucoadhesion, which in turn demonstrated liquid characteristics in the application moment and rapid transformation into gel after exposure to 37 °C, vaginal temperature. Additionally, the clinical study carried out by the authors demonstrated a significant improvement in the symptoms described by the patients, as well as efficiency in the eradication of *Candida albicans*, showing the potential of the developed product.

In order to properly explore the antimicrobial and anti-inflammatory potential of propolis for the treatment of VVC, Pereira and collaborators (2013) developed mucoadhesive systems in order to increase the formulation residence time in the vaginal mucosa. The authors evaluated different physical properties of the developed system composed by Poloxamer 407 and Carbopol 934P, such as temperature of gelation, mucoadhesion, adhesion and rheological properties, which demonstrated that the increase in mucoadhesion is proportional to the increase in Poloxamer 407 concentration. The antifungal activity of propolis, dispersed in the mucoadhesive matrix, was evaluated *in vitro* in strains of *C. albicans*, *Candida parapsilosis, Candida glabrata*, *Candida tropicalis*. It is worth mentioning that the developed formulation showed activity against all the mentioned strains, from 46.02 mg/mL to 50.99 mg/mL.

HIV infection can be easily associated in cases of chronic HSV-2 infection, so Shankar and collaborators (2014) developed a bioadhesive gel based on Poloxamer 407 and polycarbophil USP with loaded-acyclovir and tenofovir, aiming the protection against HSV- 2 and HIV. The formulation demonstrated protection of Vero cells against HSV-2 strains *in vitro.* Additionally in the *in vivo* trial it was observed an increased survival (21 days) in BALB/c mice infected intravaginally with HSV-2 when compared to the vehicle (8 days). It was also found that SR-2P was not a potential vaginal irritant after 10 days of treatment in Sprague Dawley rabbits and rats, with absence of histopathological changes, similar to carboxymethylcellulose, the control vehicle. Therefore, the developed formulation can be a candidate for safe intravaginal formulations against vaginal viral infections.

Timur and collaborators (2018) developed tenofovir-loaded chitosan nanoparticles incorporated into Poloxamer 407 thermosensitive vaginal gel. The nanoparticles showed a high particle size of 545.1 nm, sustained release at pH 5.5 and into gel presented gelation at 26.6 ºC and less mucoadhesion. All isolated formulations without drug were considered safe for vaginal administration in the cytotoxicity assay against L929 cells. Considering that, the thermosensitive formulation containing antiretroviral can be an alternative for controlled release system in the HIV prevention.

Bouchemal and collaborators (2013) developed poloxamer-based hydrogels containing a peptide synthesized with p-(cyclohexylmethyloxy) phenylalanine residue, denominated M48U1, which has high affinity for binding to gp120, as an anti-HIV-1 microbicide. Two types of poloxamer (Poloxamer 407 and Poloxamer 188) were used to develop the hydrogels, combined with hydroxypropyl methylcellulose (HPMC). The formulation demonstrated non-toxicity *in vitro* and sustained release in simulated vaginal fluid (SVF). In the vaginal mucosa permeation test, in macaque (*Macaca fascicularis*), it was found that the peptide does not cross the mucosa. In another study by Bouchemal and collaborators (2015), it was found that the hydrogel (Poloxamer 407-HPMC M48U1-loaded) showed inhibition of HIV-1 gag p24 and did not show cytotoxicity against HeLa, Caco-2/TC7, HT29/MTX, and peripheral blood mononuclear cells (PBMCs) cells. Therefore, both studies suggested that HPMC collaborates to improve mucoadhesion and the active ingredient concentration available in hydrogels after 24 h (around 25%) may contribute to the protection against HIV diffusion through the vaginal mucosa. However, *in vivo* tests are necessary to prove the preventive effect of the formulation.

Another thermosensitive hydrogel was developed with nanosized layered double hydroxides and Poloxamer 407. It was loaded with theaflavin, nifeviroc, or Nile red, a hydrophobic drug that was the model drug chosen for some assays. The theaflavin/Nile red hydrogel presented a good compatibility with the vaginal mucosa, showed sustained drugs release in the plasma and retention in

rabbit's vaginal tissue. As for nifeviroc, it was released from the hydrogel and was able to compete with HIV for C-C chemokine receptor type 5, preventing viral replication. Thus, thermosensitive hydrogel can be a good vehicle for hydrophilic or hydrophobic anti-HIV drugs, capable of providing sustained release and reaching the bloodstream, in addition to accumulating in the vaginal tissue for localized action (Tian et al., 2019).

A poloxamer hydrogel (Poloxamer 407) containing chitosan-coated Poly(isobutylcyanoacrylate) nanoparticles with the diameter in the range of 185-210 nm and zeta potential of +34.3-+40.4 mV, presented anti-*Trichomonas vaginalis* activity similar to metronidazole, with no histotoxicity in vaginal pig mucosa (Pradines et al., 2015). A chitosan/poloxamer hydrogel (Poloxamer 407) carrying metronidazole (MTZ) presented a decrease in *T. vaginalis* viability, showing a reduction in MTZ absorption in pig vaginal mucosa compared to MTZ solution (Malli et al., 2017). It has been demonstrated that poloxamer hydrogel (Poloxamer 407) can block *T. vaginalis* motility and act as a barrier against this vaginal infection (Malli et al., 2019).

3.2. Application of nanoparticles, based on poloxamer, in infectious diseases related to the vagina

In the study conducted by Bonifácio and collaborators (2019), poloxamer was used in the composition of nanostructured lipid systems containing *Astronium urundeuva* leaves extract in order to increase the bioadhesion of these nanosystems. The antifungal potential was evaluated *in vitro* against *C. albicans* and *C. glabrata*, demonstrating synergistic activity of the extract with fluconazole, with the ability to inhibit biofilm formation.

In another study using poloxamer 407 as the surfactant in nanoparticle synthesis, with an average diameter of 275 nm, with the aim of encapsulate efavirenz. These nanoparticles were incorporated in a polymeric film containing tenofovir, considered non-cytotoxic (HeLa cells) and showed a retention around 80% in the genital tract, being able to reach uterine regions in mice. Improved pharmacokinetics was also observed without changes in genital mucosa or cytokines/chemokines. The film demonstrated efficiency in the combination of drugs, being potentially safe as anti-HIV vaginal delivery system, showing greater retention in the genital region. However, long-term studies are necessary to confirm its safety in intravaginal application (Cunha-Reis et al., 2016).

Machado and collaborators (2016) also used nanoparticles-in-film technology to release tenofovir from nanoparticles containing Poloxamer 407, used as a surfactant, for intravaginal application. The nanoparticles had a mean diameter of 127 nm and showed less cytotoxicity *in vitro* against HEC-1-A, CaSki, and HeLa cells than the control containing mucosal irritating agent, nonoxynol-9, as well as on CD-1 mice without changes after intravaginal treatment. Therefore,

considered safe in *in vivo* model, the developed system can be used in pre-exposure prophylaxis against HIV.

The prodrug tenofovir disoproxil fumarate, or tenofovir, were encapsulated in nanoparticles using poloxamer P407 as surfactant. The particle size of the formulations was between 200 and 300 nm, with sustained release in simulant human semen fluid, and considered non-cytotoxicity up to 10 mg/mL for End1/E6E7 and Vk2/E6E7 cells with non-cytotoxicity up to 10 mg/mL for these cells and *L. crispatus*. These nanoparticles can be used as an alternative to nanosystems for intravaginal release carrying anti-HIV drugs (Zhang et al., 2011).

Dapivirine was incorporated into nanoparticles coated with Poloxamer 338 NF [triblock copolymer of poly (ethylene oxide), poly (propylene oxide)] that presented particle size less than 200 nm and sustained release in SVF media. This formulation demonstrated HIV-1 inhibition in TZM-bl cells and a reduction in *in vitro* toxicity in CaSki and Vk2/E6E7 cells and *ex vivo* in porcine vaginal mucosa tissue, maintaining tissue integrity. In addition, less permeability was found in both monolayer and mucosal tissue tests when compared with free dapivirine. This factor can influence the reduction of the systemic exposure of the drug and consequently lead to less toxicity. Complementary, *in vivo* studies should be performed to prove the anti-HIV effect of poloxamer surface-modified dapivirine-loaded nanoparticles (das Neves et al., 2013).

3.3. Application of nanoparticle, based on poloxamer, dispersed in hydrogel or gel, also based on poloxamer, in infectious diseases related to the vagina

Kovarova and collaborators (2015) evaluated thermosensitive vaginal gel based on mixture of poloxamers (Poloxamer 407 and Poloxamer 188) containing rilpivirine-loaded nanoparticles, using Poloxamer 407 as the surfactant. The nanoparticles showed a small particle size (66.0 nm) and HIV-1 inhibitory action *in vitro*. In *in vivo* assay, performed in humanized BLT mice, the developed formulation was administered intravaginally and it was found that they can remain for up to 24 h and reach the target HIV cells, making viral RNA detectable in only 50% of the animals that were treated 24 h before exposure. The rilpivirine long-acting was also loaded in Poloxamer 338 nanosuspensions and showed sustained plasma levels for up to 28 days after a single dose administrated intramuscularly and demonstrated effective protection when administered to BLT mice 1 week before vaginal infection with HIV-1, verified by the absence of RNA and viral DNA. Therefore, formulations administered via intravaginal or intramuscular can be used as prophylaxis against HIV infection.

Aiming a local drug release and reduction of adverse effects, the dolutegravir sodium-loaded solid lipid nanoparticles gel, using Poloxamers 407 or 188 as the surfactant, and Poloxamers 407 for the gel. The developed system had particle size of 455.7 nm. The formulation containing Poloxamer

407 showed greater release *in vitro* and sustained manner of dolutegravir sodium than the formulation with Poloxamer 188, being chosen for the *ex vivo* assay. In goat vaginal tissue, the gel showed a permeation and deposition 16-fold greater in vaginal tissue than free dolutegravir sodium. In conclusion, the formulation showed sustained release with high drug deposition in vaginal tissue being its use desirable in cases of pre-exposure prophylaxis (Anjum & Lakshmi, 2020).

Two polymers' blends were used in the synthesis of two different nanoparticles containing acyclovir and *in situ* gelling system, with Poloxamer 407 as the surfactant, for HSV-2 treatment. One named AN-1 was composed by polyvinyl pyrrolidine (PVP)/ethyl cellulose (EC), and the other, AN-2, by PVP/Eudragit RSPO. AN-1 and AN-2 presented particle size of 403 and 99 nm. Both formulations were incorporated into a Poloxamer gel. The *in situ* gel containing AN-1 showed greater permeation through the vaginal mucosa of goats suggesting that smaller particles can permeate more easily. It was also observed good viability in vaginal epithelial cells at a concentration of 250 μg/mL when compared with free acyclovir at the same concentration. Poloxamer gel containing AN-1 had a sustained release, capable of reaching higher plasma levels in concentration 10 times lower, in addition to being retained in the vaginal mucosa for local action, which can be desired in HSV-2 infections (Ramyadevi et al., 2016).

Date and collaborators (2012) developed poloxamers-based thermosensitive vaginal gel containing efavirenz/raltegravir-loaded nanoparticles, with poloxamer used as the surfactant. The nanoparticles demonstrated a particle size of 81.8 nm, the vaginal gel showed gelation around 30 ºC. The nanosystem into the thermosensitive vaginal gel, showed the capacity of release and absorption by HeLa in *in vitro* tests. The gel containing nanoparticles with antiretrovirals showed good thermosensitive characteristics for vaginal release, with potential for prophylaxis of heterosexual HIV transmission.

3.4. Application of others type of systems, based on poloxamer, in infectious diseases related to the vagina

In antibacterial application, a foam aerosol based on thermal transformation was designed to improve the formulation penetration efficiency and to extend the retention time. The expansible thermal gelling foam aerosol (ETGFA) containing Poloxamer 407/108 thermal sensitive matrix, silver nanoparticle (commercially obtained), adhesive agent and propellant, was optimized by Mei and collaborators (2017). ETGFA showed foam expansion and was able to deliver silver nanoparticles to the deep vaginal rugae. The thermal sensitive gelation process provided longer drug retention time in vaginal canal associated to adhesive strength and viscoelasticity. In i*n vitro* drug release and bacteria inhibitory tests it was indicated that the drug incorporation into ETGFA formulation achieved

comparable drug release behavior of the commercial gel, Asimi®, although with enhanced antimicrobial effects against *E. coli*, *S. aureus*, *Pseudomonas aeruginosa* (Mei et al., 2017).
Salmazi and collaborators (2015) developed liquid crystal precursors to better explore the anti-candida potential of curcumin for the treatment of CVV. Liquid crystal precursors originate the liquid crystal in contact with the vaginal mucus, a system with high mucoadhesive power and with the ability to remain in the vaginal mucosa (Araujo et al., 2020). In this study, the authors observed that the compound precursors Procetyl® AWS, oleic acid, chitosan and Poloxamer 407 were able to form liquid crystal in contact with artificial vaginal mucus, demonstrating high mucoadhesiveness in mucosal vaginal porcine. In i*n vitro* studies with *C. albicans* it was demonstrated that the system optimized curcumin activity sixteen times more against a standard strain and was two times more potent against a clinical strain than its solution (Salmazi et al., 2015).

4. Conclusion and future perspectives

Although the literature brings reports of poloxamer toxicity, no *in vivo* or clinical studies reporting the cutaneous toxicity of this polymer were observed, being therefore considered biocompatible in topical applications. Among poloxamer physical chemical properties stands out its reversible thermoresponsiveness, which makes this polymer liquid at room temperature and with the consistency of gel at body temperature, bypassing patient complaints about vaginal application. Additionally, it also provides mucoadhesiveness, which is attractive in the case of new strategies for the treatment and prevention of infectious diseases related to the vagina due to the longer duration of the formulation's local permanence, which consequently causes an increase in therapeutic efficacy. Additionally, when used as a component of a nanoparticle it assists in the controlled drug release and facilitate the penetration into the mucosa, increasing the effectiveness of the system.

The articles found in the literature show that hydrogels based on poloxamer is the most frequent application of this polymer for the treatment or prevention of infectious diseases. Remark was made that infection prevention strategies were only observed for viruses, which is desirable and important in the case of sexually transmitted diseases. It is worth noting that for bacteria and parasites, no articles were found involving the use of poloxamer in the nanoparticle's synthesis, which makes room for future works.

5. Acknowledgments

This work was supported by the Coordenação de Aperfeiçoamento de Pessoal de Nível Superior – Brasil (CAPES) [Finance Code 001] and by Sao Paulo Research Foundation (FAPESP, Brazil) grant number 2019/25125-7. The authors are grateful to the financial support provided by National Council

for Scientific and Technological Development (CNPq, Brazil) Grant number 408244/2018-6. This study is part of the National Institute of Science and Technology in Pharmaceutical Nanotechnology: a transdisciplinary approach INCT-NANOFARMA, which is supported by FAPESP, Grant number 2014/50928-2, and by CNPq, Brazil Grant number 465687/2014-8.

6. References

Abd Ellah, N. H., Abdel-Aleem, J.A., Abdo, M. N., Abou-Ghadir, O.F., Zahran, K.M., & Hetta, H.F. (2019). Efficacy of ketoconazole gel-flakes in treatment of vaginal candidiasis: Formulation, in vitro and clinical evaluation. *International Journal of Pharmaceutics*, *567*, Article 118472. https://doi.org/10.1016/j.ijpharm.2019.118472

Abdeltawab, H., Svirskis, D., & Sharma, M. (2020). Formulation strategies to modulate drug release from poloxamer based in situ gelling systems. *Expert Opinion on Drug Delivery*, *17*(4), 495–509. https://doi.org/10.1080/17425247.2020.1731469

Ahmed, E.M. (2015). Hydrogel: Preparation, characterization, and applications: A review. *Journal of Advanced Research*, *6*(2), 105–121. https://doi.org/10.1016/j.jare.2013.07.006

Ahmed, R., & Yesmin, K. (2008). Menstrual hygiene: breaking the silence. In Wicken, J., Verhagen, J., Sijbesma, C., Silva, C., & Ryan, P. (Eds.), *Beyond Construction: Use by All. A Collection of Case Studies from Sanitation and Hygiene Promotion Practitioners in South Asia.* (pp. 283-287). *WaterAid*.

Akkari, A.C.S., Campos, E.V.R., Keppler, A.F., Fraceto, L.F., de Paula, E., Tófoli, G. R., & de Araujo, D.R. (2016). Budesonide-hydroxypropyl-β-cyclodextrin inclusion complex in binary poloxamer 407/403 system for ulcerative colitis treatment: A physico-chemical study from micelles to hydrogels. *Colloids and Surfaces B: Biointerfaces*, *138*, 138–147. https://doi.org/10.1016/j.colsurfb.2015.11.048

Alakhov, V., Klinski, E., Li, S., Pietrzynski, G., Venne, A., Batrakova, E., Bronitch, T., & Kabanov, A. (1999). Block copolymer-based formulation of doxorubicin. From cell screen to clinical trials. *Colloids and Surfaces B: Biointerfaces*, *16*(1–4), 113–134. https://doi.org/10.1016/S0927-7765(99)00064-8

Alessio, C., & Nyirjesy, P. (2019). Management of Resistant Trichomoniasis. *Current Infectious Disease Reports*, *21*(9), Article 31. https://doi.org/10.1007/s11908-019-0687-4

Alexandridis, P., Holzwarth, J. F., & Hatton, T. A. (1994). Micellization of poly (ethylene oxide)-poly (propylene oxide)-poly (ethylene oxide) triblock copolymers in aqueous solutions: thermodynamics of copolymer association. *Macromolecules*, *27*(9), 2414–2425.

Alves, R.C., Fernandes, R.P, Fonseca-Santos, B., Victorelli, F.D., & Chorilli, M. (2019). A critical review of the properties and analytical methods for the determination of curcumin in biological and pharmaceutical matrices. *Critical Reviews in Analytical Chemistry*, *49*(2), 138–149. https://doi.org/10.1080/10408347.2018.1489216

Ameen, F., Moslem, M., Tami, M.A., Al-Ajlan, H., & Al-Qahtani, N. (2017). Identification of Candida species in vaginal flora using conventional and molecular methods. *Journal de Mycologie Medicale, 27*(3), 364-368. https://doi.org/10.1016/j.mycmed.2017.04.105

Anjum, R., & Lakshmi, P.K. (2020). Dolutegravir sodium loaded solid lipid nanoparticles: A vaginal drug delivery system for pre-exposure prophylaxis of HIV. *Journal of Research in Pharmacy*, *24*(4), 552–561. https://doi.org/10.35333/jrp.2020.203

Araujo, V.H.S., Duarte, J.L., Carvalho, G.C., Silvestre, A.L.P., Fonseca-Santos, B., Marena, G.D., Ribeiro, T. de C., dos Santos Ramos, M.A., Bauab, T.M., & Chorilli, M. (2020). Nanosystems against candidiasis: a review of studies performed over the last two decades. *Critical Reviews in Microbiology*, *46*(5), 508-547. https://doi.org/10.1080/1040841X.2020.1803208

Ascioglu, S., Rex, J.H., de Pauw, B., Bennett, J.E., Bille, J., Crokaert, F., Denning, D. W., Donnelly, J.P., Edwards, J.E., Erjavec, Z., & othets. (2002). Defining Opportunistic Invasive Fungal Infections in Immunocompromised Patients with Cancer and Hematopoietic Stem Cell Transplants: An International Consensus. *Clinical Infectious Diseases*, *34*(1), 7–14. https://doi.org/10.1086/323335

Avelleira, J.C.R., & Bottino, G. (2006). Sífilis: diagnóstico, tratamento e controle Syphilis: diagnosis, treatment and control. *An Bras Dermatol*, *81*(2), 111–126. https://doi.org/10.1590/S0365-05962006000200002

Batrakova, E., Lee, S., Li, S., Venne, A., Alakhov, V., & Kabanov, A. (1999). Fundamental relationships between the composition of pluronic block copolymers and their hypersensitization effect in MDR cancer cells. *Pharmaceutical Research*, *16*(9), 1373–1379. https://doi.org/10.1023/A:1018942823676

Bautista, C.T., Wurapa, E., Sateren, W.B., Morris, S., Hollingsworth, B., & Sanchez, J. L. (2016). Bacterial vaginosis: a synthesis of the literature on etiology, prevalence, risk factors, and relationship with chlamydia and gonorrhea infections. *Military Medical Research*, *3*(1), Article 4. https://doi.org/10.1186/s40779-016-0074-5

Bekasiak, A., Dammann, F., & Nader, C. (2020). A Rare Cause of a Scrotal Abscess due to the Symbiotic Infection of Gardnerella vaginalis and Prevotella bivia in an Adult Male. *Pathogens*, *9*(2), Article 93. https://doi.org/10.3390/pathogens9020093

Bernstein, D.I. (2020). Use of the Guinea pig model of genital herpes to evaluate vaccines and antivirals: Review. *Antiviral Research*, *180*, Article 104821. https://doi.org/10.1016/j.antiviral.2020.104821

Bhatta, A. K., Keyal, U., Liu, Y., & Gellen, E. (2018). Vertical transmission of herpes simplex virus: an update. *JDDG: Journal Der Deutschen*

Dermatologischen Gesellschaft, *16*(6), 685–692. https://doi.org/10.1111/ddg.13529

Blonder, J.M., Baird, L., Fulfs, J.C., & Rosenthal, G.J. (1999). Dose-dependent hyperlipidemia in rabbits following administration of poloxamer 407 gel. *Life Sciences*, *65*(21), PL261–PL266. https://doi.org/10.1016/S0024-3205(99)00495-6

Bodratti, A., & Alexandridis, P. (2018). Formulation of Poloxamers for Drug Delivery. *Journal of Functional Biomaterials*, *9*(1), Article 11. https://doi.org/10.3390/jfb9010011

Bonifácio, B. V., Ramos, M. A.S., da Silva, P. B., Negri, K.M.S., Lopes, É.O., de Souza, L.P., Vilegas, W., Pavan, F.R., Chorilli, M., & Bauab, T.M. (2015). Nanostructured lipid system as a strategy to improve the anti-*Candida albicans* activity of Astronium sp. *International Journal of Nanomedicine*, *10*, Article 5081. https://doi.org/10.2147/IJN.S79684

Bonifácio, B.V., Vila, T.V.M., Masiero, I.F., da Silva, P.B., da Silva, I.C., Lopes, É.O., Ramos, M. A.S., de Souza, L. P., Vilegas, W., Pavan, F. R., & others. (2019). Antifungal Activity of a Hydroethanolic Extract From Astronium urundeuva Leaves Against Candida albicans and Candida glabrata. *Frontiers in Microbiology*, *10,* Article 2642. https://doi.org/10.3389/fmicb.2019.02642

Bouchemal, K., Aka-Any-Grah, A., Dereuddre-Bosquet, N., Martin, L., Lievin-Le-Moal, V., Le Grand, R., Nicolas, V., Gibellini, D., Lembo, D., Poüs, C., & others. (2015). Thermosensitive and mucoadhesive pluronic-hydroxypropylmethylcellulose hydrogel containing the mini-CD4 M48U1 is a promising efficient barrier against HIV diffusion through macaque cervicovaginal mucus. *Antimicrobial Agents and Chemotherapy*, *59*(4), 2215–2222. https://doi.org/10.1128/AAC.03503-14

Bouchemal, K., Frelichowska, J., Martin, L., Lievin-Le Moal, V., Le Grand, R., Dereuddre-Bosquet, N., Djabourov, M., Aka-Any-Grah, A., Koffi, A., & Ponchel, G. (2013). Note on the formulation of thermosensitive and mucoadhesive vaginal hydrogels containing the miniCD4 M48U1 as anti-HIV-1 microbicide. *International Journal of Pharmaceutics*, *454*(2), 649–652. https://doi.org/10.1016/j.ijpharm.2013.02.055

Britton, E. (2018). *Effects of Hofmeister Ions on Gelation of Gelatin and Pluronic Hydrogels*. IdeaExchange@UAkron https://ideaexchange.uakron.edu/honors_research_projects/697/

Chemicals, BASF Performance. (1996). Pluronic and Tetronic Surfactants. *BASF Corp*.

Cho, E., Lee, J.S., & Webb, K. (2012). Formulation and characterization of poloxamine-based hydrogels as tissue sealants. *Acta Biomaterialia*, *8*(6), 2223–2232. https://doi.org/10.1016/j.actbio.2012.03.003

Chowdhury, P., Nagesh, P.K.B., Kumar, S., Jaggi, M., Chauhan, S.C., & Yallapu, M.M. (2017). *Pluronic Nanotechnology for Overcoming Drug Resistance,* 207–237. https://doi.org/10.1007/978-981-10-5864-6_9

Ci, T., Yuan, L., Bao, X., Hou, Y., Wu, H., Sun, H., Cao, D., & Ke, X. (2018). Development and anti-Candida evaluation of the vaginal delivery system of amphotericin B nanosuspension-loaded thermogel. *Journal of Drug Targeting*, *26*(9), 829–839. https://doi.org/10.1080/1061186X.2018.1434660

Cojocaru, F.D., Botezat, D., Gardikiotis, I., Uritu, C.M., Dodi, G., Trandafir, L., Rezus, C., Rezus, E., Tamba, B.I., & Mihai, C.T. (2020). Nanomaterials designed for antiviral drug delivery transport across biological barriers. *Pharmaceutics*, *12*(2), 1–34. https://doi.org/10.3390/pharmaceutics12020171

Comai, K., & Sullivan, A.C. (1980). Antiobesity activity of pluronic L-101. *International Journal of Obesity*, *4*(1), 33–42.

Cone, R.A. (2009). Barrier properties of mucus. *Advanced Drug Delivery Reviews*, *61*(2), 75–85. https://doi.org/10.1016/j.addr.2008.09.008

Connaughton, J., & McCarthy, C.F. (1982). Comparison of combination of ispaghula/poloxamer 188 and placebo on gastrointestinal transit time. *Irish Medical Journal*, *75*(3), 93–94.

Coudray, M.S., & Madhivanan, P. (2020). Bacterial vaginosis—A brief synopsis of the literature. *European Journal of Obstetrics & Gynecology and Reproductive Biology*, *245*, 143–148. https://doi.org/10.1016/j.ejogrb.2019.12.035

Cunha-Reis, C., Machado, A., Barreiros, L., Araújo, F., Nunes, R., Seabra, V., Ferreira, D., Segundo, M.A., Sarmento, B., & das Neves, J. (2016). Nanoparticles-in-film for the combined vaginal delivery of anti-HIV microbicide drugs. *Journal of Controlled Release*, *243*, 43–53. https://doi.org/10.1016/j.jconrel.2016.09.020

Czaja, C.A., Stapleton, A. E., Yarova-Yarovaya, Y., & Stamm, W.E. (2007). Phase I Trial of a Lactobacillus crispatus Vaginal Suppository for Prevention of Recurrent Urinary Tract Infection in Women. *Infectious Diseases in Obstetrics and Gynecology*, *2007*, 1–8. https://doi.org/10.1155/2007/35387

da Silva, P.B., dos Santos, M.A.R., Bonifácio, B.V., Negri, K.M.S., Sato, M.R., Bauab, T.M., & Chorilli, M. (2014). Nanotechnological strategies for vaginal administration of drugs—A review. *Journal of Biomedical Nanotechnology*, *10*(9), 2218–2243. https://doi.org/10.1166/jbn.2014.1890

das Neves, J., Araújo, F., Andrade, F., Michiels, J., Ariën, K.K., Vanham, G., Amiji, M., Bahia, M.F., & Sarmento, B. (2013). In vitro and Ex Vivo evaluation of polymeric nanoparticles for vaginal and rectal delivery of the anti-HIV drug dapivirine. *Molecular Pharmaceutics*, *10*(7), 2793–2807. https://doi.org/10.1021/mp4002365

Das, R.K., Kasoju, N., & Bora, U. (2010). Encapsulation of curcumin in alginate-chitosan-pluronic composite nanoparticles for delivery to cancer cells. *Nanomedicine: Nanotechnology, Biology and Medicine*, *6*(1), 153–160. https://doi.org/10.1016/j.nano.2009.05.009

Date, A.A., Shibata, A., Goede, M., Sanford, B., La Bruzzo, K., Belshan, M., & Destache, C. J. (2012). Development and evaluation of a thermosensitive vaginal gel containing raltegravir+efavirenz loaded nanoparticles for HIV prophylaxis. *Antiviral Research*, *96*(3), 430–436. https://doi.org/10.1016/j.antiviral.2012.09.015

Daugherty, M., Glynn, K., & Byler, T. (2019). Prevalence of Trichomonas vaginalis Infection Among US Males, 2013--2016. *Clinical Infectious Diseases*, *68*(3), 460–465. https://doi.org/10.1093/cid/ciy499

de Araújo, P.R., Calixto, G.M.F., Araújo, V.H.S., Sato, M.R., Rodero, C.F., Oshiro-Junior, J.A., Bauab, T.M., & Chorilli, M. (2021). In vivo study of hypericin-loaded poloxamer-based mucoadhesive in situ gelling liquid crystalline precursor system in a mice model of vulvovaginal candidiasis. *Medical Mycology, 59*(8), 821-827. https://doi.org/10.1093/mmy/myab006

de Araújo, P.R., Calixto, G.M.F., da Silva, I.C., Zago, L. H.P., Junior, J. A.O., Pavan, F.R., Ribeiro, A.O., Fontana, C.R., & Chorilli, M. (2019). Mucoadhesive In Situ Gelling Liquid Crystalline Precursor System to Improve the Vaginal Administration of Drugs. *AAPS PharmSciTech*, *20*(6), Article 225. https://doi.org/10.1208/s12249-019-1439-3

Donders, G.G.G., & Sobel, J.D. (2017). *Candida vulvovaginitis : A store with a buttery and a show window*. Mycoses, *60*(2), 70–72. https://doi.org/10.1111/myc.12572

dos Santos, A.M., Carvalho, S.G., Araujo, V.H.S., Carvalho, G.C., Gremião, M.P.D., & Chorilli, M. (2020). Recent advances in hydrogels as strategy for drug delivery intended to vaginal infections. *International Journal of Pharmaceutics*, *590*, Article 119867. https://doi.org/10.1016/j.ijpharm.2020.119867

Dutta, P. K. (Ed.). (2016). *Chitin and Chitosan for Regenerative Medicine*. Springer India. https://doi.org/10.1007/978-81-322-2511-9

Edrissian, G.H., Rokni, M.B., Mohebali, M., Nateghpour, M., Mowlavi, G., & Bahadori, M. (2016). History of medical parasitology and parasitic infections in Iran. *Archives of Iranian Medicine*, 19(8), 601-607.

Ensign, L.M., Cone, R., & Hanes, J. (2014). Nanoparticle-based drug delivery to the vagina: A review. *Journal of Controlled Release*, *190*, 500–514. https://doi.org/10.1016/j.jconrel.2014.04.033

Fakhari, A., Corcoran, M., & Schwarz, A. (2017). Thermogelling properties of purified poloxamer 407. *Heliyon*, *3*(8), Article e00390. https://doi.org/10.1016/j.heliyon.2017.e00390

Farias, F., Orlando, T., Salbego, P., & Martins, M. (2020). Rotaxanos – interações intercomponentes e movimentos moleculares. *Química Nova, 44*(1), Article 76-85. https://doi.org/10.21577/0100-4042.20170623

Feitosa, V.A., Almeida, V.C. de, Malheiros, B., Castro, R.D. de, Barbosa, L.R.S., Cerize, N.N.P., & Rangel-Yagui, C.O. (2019). Polymeric micelles of pluronic F127 reduce hemolytic potential of amphiphilic drugs. *Colloids and Surfaces B: Biointerfaces*, *180*, 177–185. https://doi.org/10.1016/j.colsurfb.2019.04.045

Ferrer, J. (2000). Vaginal candidosis: epidemiological and etiological factors. *International Journal of Gynecology & Obstetrics*, *71*, 21–27. https://doi.org/10.1016/S0020-7292(00)00350-7

Fichorova, R.N. (2009). Impact of *T. vaginalis* infection on innate immune responses and reproductive outcome. *Journal of Reproductive Immunology*, *83*(1–2), 185–189. https://doi.org/10.1016/j.jri.2009.08.007

Frade, M., de Annunzio, S., Calixto, G., Victorelli, F., Chorilli, M., & Fontana, C. (2018). Assessment of Chitosan-Based Hydrogel and Photodynamic Inactivation against Propionibacterium acnes. *Molecules*, *23*(2), Article 473. https://doi.org/10.3390/molecules23020473

Gadhave, A. (2014). Determination of hydrophilic-lipophilic balance value. *Int. J. Sci. Res*, *3*(4), 573–575.

Garg, S., Vermani, K., Garg, A., Anderson, R.A., Rencher, W.B., & Zaneveld, L.J.D. (2005). Development and Characterization of Bioadhesive Vaginal Films of Sodium Polystyrene Sulfonate (PSS), a Novel Contraceptive Antimicrobial Agent. *Pharmaceutical Research*, *22*(4), 584–595. https://doi.org/10.1007/s11095-005-2490-1

Garland, S.M., & Steben, M. (2014). Genital herpes. *Best Practice & Research Clinical Obstetrics & Gynaecology*, *28*(7), 1098–1110. https://doi.org/10.1016/j.bpobgyn.2014.07.015

Giuliano, E., Paolino, D., Cristiano, M.C., Fresta, M., & Cosco, D. (2020). Rutin-Loaded Poloxamer 407-Based Hydrogels for In Situ Administration: Stability Profiles and Rheological Properties. *Nanomaterials*, *10*(6), Article 1069. https://doi.org/10.3390/nano10061069

Giuliano, E., Paolino, D., Fresta, M., & Cosco, D. (2018). Mucosal Applications of Poloxamer 407-Based Hydrogels: An Overview. *Pharmaceutics*, *10*(3), Article 159. https://doi.org/10.3390/pharmaceutics10030159

Gonçalves, B., Ferreira, C., Alves, C. T., Henriques, M., Azeredo, J., & Silva, S. (2016). Vulvovaginal candidiasis: Epidemiology, microbiology and risk factors. *Critical Reviews in Microbiology*, *42*(6), 905–927. https://doi.org/10.3109/1040841X.2015.1091805

Gratieri, T., Gelfuso, G.M., Rocha, E.M., Sarmento, V.H., de Freitas, O., & Lopez, R.F.V. (2010). A poloxamer/chitosan in situ forming gel with prolonged retention time for ocular delivery. *European Journal of Pharmaceutics and Biopharmaceutics*, *75*(2), 186–193. https://doi.org/10.1016/j.ejpb.2010.02.011

Haggerty, C.L., Gottlieb, S.L., Taylor, B.D., Low, N., Xu, F., & Ness, R.B. (2010). Risk of Sequelae after Chlamydia trachomatis Genital Infection in Women. *The Journal of Infectious Diseases*, *201*(S2), 134–155. https://doi.org/10.1086/652395

Hay, P. (2017). Bacterial vaginosis. *F1000Research*, *6*, Article 1761. https://doi.org/10.12688/f1000research.11417.1

He, B., Liu, Lai, Li, Wang, Chang, & Gu, Z. (2012). Supramolecular nanoparticles generated by the self-assembly of polyrotaxanes for antitumor drug delivery. *International Journal of Nanomedicine*, *2021*(7), 5249-5258. https://doi.org/10.2147/IJN.S33649

Hemmerling, A., Harrison, W., Schroeder, A., Park, J., Korn, A., Shiboski, S., Foster-Rosales, A., & Cohen, C.R. (2010). Phase 2a Study Assessing Colonization Efficiency, Safety, and Acceptability of Lactobacillus crispatus CTV-05 in Women With Bacterial Vaginosis. *Sexually Transmitted Diseases*, *37*(12), 745–750. https://doi.org/10.1097/OLQ.0b013e3181e50026

Herzberger, J., Niederer, K., Pohlit, H., Seiwert, J., Worm, M., Wurm, F. R., & Frey, H. (2016). Polymerization of Ethylene Oxide, Propylene Oxide, and Other Alkylene Oxides: Synthesis, Novel Polymer Architectures, and Bioconjugation. *Chemical Reviews*, *116*(4), 2170–2243.

https://doi.org/10.1021/acs.chemrev.5b00441

Hewlings, S., & Kalman, D. (2017). Curcumin: A Review of Its Effects on Human Health. *Foods*, *6*(10), Article 92. https://doi.org/10.3390/foods6100092

Higashi, T., Motoyama, K., & Arima, H. (2013). Cyclodextrin-Based Polyrotaxanes and Polypseudorotaxanes as Drug Delivery Carriers. *Journal of Drug Delivery Science and Technology*, *23*(6), 523–529. https://doi.org/10.1016/S1773-2247(13)50080-3

Hirano, S. (1996). Chitin Biotechnology Applications. *Biotechnology annual review,* 2, 237-258. https://doi.org/10.1016/S1387-2656(08)70012-7

Hobbs, E.C., Trevisan, C., Johansen, M.V., Dorny, P., & Gabriël, S. (2019). Value of electronic educational media in combatting parasitic diseases. *Trends in Parasitology*, *35*(3), 173–176. https://doi.org/10.1016/j.pt.2018.10.001

Hook, E.W., & Kirkcaldy, R.D. (2018). A Brief History of Evolving Diagnostics and Therapy for Gonorrhea: Lessons Learned. *Clinical Infectious Diseases*, *67*(8), 1294–1299. https://doi.org/10.1093/cid/ciy271

Hunter, R.L., Bennett, B., & Check, I.J. (1990). The effect of poloxamer 188 on the rate of in vitro thrombolysis mediated by t-PA and streptokinase. *Fibrinolysis*, *4*(2), 117–123. https://doi.org/10.1016/0268-9499(90)90007-7

Jalaal, M., Cottrell, G., Balmforth, N., & Stoeber, B. (2017). On the rheology of Pluronic F127 aqueous solutions. *Journal of Rheology*, *61*(1), 139–146. https://doi.org/10.1122/1.4971992

Jalalvandi, E., Jafari, H., Amorim, C.A., Petri, D.F.S., Nie, L., & Shavandi, A. (2020). Vaginal Administration of Contraceptives. *Scientia Pharmaceutica*, *89*(1), Article 3. https://doi.org/10.3390/scipharm89010003

Johnston, T.P., Baker, J.C., Hall, D., Jamal, S., Palmer, W.K., & Emeson, E.E. (2000). Regression of poloxamer 407-induced atherosclerotic lesions in C57BL/6 mice using atorvastatin. *Atherosclerosis*, *149*(2), 303–313. https://doi.org/10.1016/S0021-9150(99)00339-1

Johnston, T.P., Beris, H., Wout, Z.G., & Kennedy, J.L. (1993). Effects on splenic, hepatic, hematological, and growth parameters following high-dose poloxamer 407 administration to rats. *International Journal of Pharmaceutics*, *100*(1–3), 279–284. https://doi.org/10.1016/0378-5173(93)90103-M

Johnston, T.P., Li, Y., Jamal, A.S., Stechschulte, D.J., & Dileepan, K.N. (2003). Poloxamer 407-induced atherosclerosis in mice appears to be due to lipid derangements and not due to its direct effects on endothelial cells and macrophages. *Mediators of Inflammation*, *12*(3), 147–155. https://doi.org/10.1080/0962935031000134860

Johnston, T.P., & Miller, S.C. (1985). Toxicological evaluation of poloxamer vehicles for intramuscular use. *PDA Journal of Pharmaceutical Science and Technology*, *39*(2), 83–89.

Kabanov, A.V, Batrakova, E.V, & Alakhov, V.Y. (2002). Pluronic® block copolymers for overcoming drug resistance in cancer. *Advanced Drug Delivery Reviews*, *54*(5), 759–779. https://doi.org/10.1016/S0169-409X(02)00047-9

Kaseke, C., Tano-Menka, R., Senjobe, F., & Gaiha, G.D. (2021). The Emerging Role for CTL Epitope Specificity in HIV Cure Efforts. *The Journal of Infectious Diseases*, *223*(Supplement_1), S32–S37. https://doi.org/10.1093/infdis/jiaa333

Katakam, M., & Banga, A.K. (1997). Use of Poloxamer Polymers to Stabilize Recombinant Human Growth Hormone Against Various Processing Stresses. *Pharmaceutical Development and Technology*, *2*(2), 143–149. https://doi.org/10.3109/10837459709022619

Kenyon, C., Colebunders, R., & Crucitti, T. (2013). The global epidemiology of bacterial vaginosis: a systematic review. *American Journal of Obstetrics and Gynecology*, *209*(6), 505–523. https://doi.org/10.1016/j.ajog.2013.05.006

Khurana, S., & Singh, S. (2018). Human Trichomoniasis. In Singh, P. P. (Ed.), *Infectious Diseases and Your Health* (pp. 99–111). Springer.

Kiguen, A.X., Marramá, M., Ruiz, S., Estofan, P., Venezuela, R.F., Mosmann, J.P., Monetti, M.S., Rivero, V., & Cuffini, C.G. (2019). Prevalence, risk factors and molecular characterization of Chlamydia trachomatis in pregnant women from Córdoba, Argentina: A prospective study. *Plos One*, *14*(5), Article e0217245. https://doi.org/10.1371/journal.pone.0217245

Kim, S. (2018). Competitive Biological Activities of Chitosan and Its Derivatives: Antimicrobial, Antioxidant, Anticancer, and Anti-Inflammatory Activities. *International Journal of Polymer Science*, *2018*, 1–13. https://doi.org/10.1155/2018/1708172

Kissinger, P., Muzny, C.A., Mena, L.A., Lillis, R.A., Schwebke, J.R., Beauchamps, L., Taylor, S.N., Schmidt, N., Myers, L., Augostini, P., & others. (2018). Single-dose versus 7-day-dose metronidazole for the treatment of trichomoniasis in women: an open-label, randomised controlled trial. *The Lancet Infectious Diseases*, *18*(11), 1251–1259. https://doi.org/10.1016/S1473-3099(18)30423-7

Kojima, N., & Klausner, J.D. (2018). An Update on the Global Epidemiology of Syphilis. *Current Epidemiology Reports*, *5*(1), 24–38. https://doi.org/10.1007/s40471-018-0138-z

Kovarova, M., Council, O.D., Date, A.A., Long, J.M., Nochii, T., Belshan, M., Shibata, A., Vincent, H., Baker, C.E., Thayer, W.O., & others. (2015). Nanoformulations of Rilpivirine for Topical Pericoital and Systemic Coitus-Independent Administration Efficiently Prevent HIV Transmission. *PLoS Pathogens*, *11*(8), 1–19. https://doi.org/10.1371/journal.ppat.1005075

Krupka, T.M., & Exner, A.A. (2011). Structural parameters governing activity of Pluronic triblock copolymers in hyperthermia cancer therapy. *International Journal of Hyperthermia*, *27*(7), 663–671. https://doi.org/10.3109/02656736.2011.599828

Larrañeta, E., & Isasi, J.R. (2014). Non-covalent hydrogels of cyclodextrins and poloxamines for the controlled release of proteins. *Carbohydrate Polymers*, *102*, 674–681. https://doi.org/10.1016/j.carbpol.2013.11.002

Leaf, C.W. (1967). Toxicology of some non-ionic surfactants. *Soap Chem Spec*, Article *43*, 48.

Leyva-Gómez, G., Prado-Audelo, M.L., Ortega-Peña, S., Mendoza-Muñoz, N., Urbán-Morlán, Z., González-Torres, M., González-Del Carmen, M.,

Figueroa-González, G., Reyes-Hernández, O.D., & Cortés, H. (2019). Modifications in Vaginal Microbiota and Their Influence on Drug Release: Challenges and Opportunities. *Pharmaceutics*, *11*(5), Article 217. https://doi.org/10.3390/pharmaceutics11050217

Leyva-Gómez, G., Piñón-Segundo, E., Mendoza-Muñoz, N., Zambrano-Zaragoza, M., Mendoza-Elvira, S., & Quintanar-Guerrero, D. (2018). Approaches in Polymeric Nanoparticles for Vaginal Drug Delivery: A Review of the State of the Art. *International Journal of Molecular Sciences*, *19*(6), Article 1549. https://doi.org/10.3390/ijms19061549

Li, B., Wang, Y., Ling, C., & Wang, W. (1998). Acute Toxicity Test of a New Pharmaceutical Adjuvant─ Poloxamer 407. *China Pharmacy*, 3.

Li, T., Liu, Z.-H., Li, K., & Bai, H.-H. (2019). Evaluation of the vaginal microbiome in clinical diagnosis and management of vaginal infectious diseases. *Chinese Medical Journal*, *132*(9), Article 1100.https://doi.org/10.1097/CM9.0000000000000211

Lopes, J.R., & Loh, W. (1998). Investigation of self-assembly and Micelle polarity for a wide range of ethylene oxide- propylene oxide- ethylene oxide block copolymers in water. *Langmuir*, *14*(4), 750–756. https://doi.org/10.1021/la9709655

Lowe, K.C., Furmidge, B.A., & Thomas, S. (1995). Haemolytic Properties of Pluronic Surfactants and Effects of Purification. *Artificial Cells, Blood Substitutes, and Biotechnology*, *23*(1), 135–139. https://doi.org/10.3109/10731199509117673

Ma, K.C., Mortimer, T.D., Duckett, M. A., Hicks, A.L., Wheeler, N.E., Sánchez-Busó, L., & Grad, Y.H. (2020a). Increased power from conditional bacterial genome-wide association identifies macrolide resistance mutations in Neisseria gonorrhoeae. *Nature Communications*, *11*(1), Article 5374. https://doi.org/10.1038/s41467-020-19250-6

Ma, K.C., Mortimer, T.D., Hicks, A.L., Wheeler, N.E., Sánchez-Busó, L., Golparian, D., Taiaroa, G., Rubin, D.H.F., Wang, Y., Williamson, D.A., & others. (2020b). Adaptation to the cervical environment is associated with increased antibiotic susceptibility in Neisseria gonorrhoeae. *Nature Communications*, *11*(1), Article 4126. https://doi.org/10.1038/s41467-020-17980-1

Machado, A., Cunha-Reis, C., Araújo, F., Nunes, R., Seabra, V., Ferreira, D., das Neves, J., & Sarmento, B. (2016). Development and in vivo safety assessment of tenofovir-loaded nanoparticles-in-film as a novel vaginal microbicide delivery system. *Acta Biomaterialia*, *44*, 332–340. https://doi.org/10.1016/j.actbio.2016.08.018

Magnusson, G., Olsson, T., & Nyberg, J.-A. (1986). Toxicity of pluronic F-68. *Toxicology Letters*, *30*(3), 203–207. https://doi.org/10.1016/0378-4274(86)90156-6

Maheshwari, R.K., Singh, A.K., Gaddipati, J., & Srimal, R.C. (2006). Multiple biological activities of curcumin: A short review. *Life Sciences*, *78*(18), 2081–2087. https://doi.org/10.1016/j.lfs.2005.12.007

Malli, S., Bories, C., Pradines, B., Loiseau, P.M., Ponchel, G., & Bouchemal, K. (2017). In situ forming pluronic® F127/chitosan hydrogel limits metronidazole transmucosal absorption. *European Journal of Pharmaceutics and Biopharmaceutics*, *112*, 143–147. https://doi.org/10.1016/j.ejpb.2016.11.024

Malli, S., Loiseau, P.M., & Bouchemal, K. (2019). Trichomonas vaginalis Motility Is Blocked by Drug-Free Thermosensitive Hydrogel. *ACS Infectious Diseases,* 6(1), 114-123. https://doi.org/10.1021/acsinfecdis.9b00243

Maneschy, C.A., M., Barile, K.A., JAd, C., Palmeira, M., & Amaral, C.E. (2021). Epidemiological and Molecular Profile of Blood Donors Infected With HTLV-1/2 in the State of Pará, Northern Brazil. *Brazilian Journal of Microbiology*, 52, 2001-2006. https://doi.org/10.1007/s42770-021-00609-w

Margarita, V., Marongiu, A., Diaz, N., Dessí, D., Fiori, P. L., & Rappelli, P. (2019). Prevalence of double-stranded RNA virus in Trichomonas vaginalis isolated in Italy and association with the symbiont Mycoplasma hominis. *Parasitology Research*, *118*(12), 3565–3570. https://doi.org/10.1007/s00436-019-06469-6

Mathur, M., Acharya, P., Karki, A., Shah, J., & KC, N. (2019). Dermoscopic clues in the skin lesions of secondary syphilis. *Clinical Case Reports*, *7*(3), 431–434. https://doi.org/10.1002/ccr3.1999

Mei, L., Chen, J., Yu, S., Huang, Y., Xie, Y., Wang, H., Pan, X., & Wu, C. (2017). Expansible thermal gelling foam aerosol for vaginal drug delivery. *Drug Delivery*, *24*(1), 1325–1337. https://doi.org/10.1080/10717544.2017.1375575

Meng, F., Kwon, S., Wang, J., & Yeo, Y. (2020). Immunoactive drug carriers in cancer therapy. In Park, K. (Ed.), *Biomaterials for Cancer Therapeutics: Evolution and innovation* (pp. 53–94). Elsevier. https://doi.org/10.1016/B978-0-08-102983-1.00003-X

Mestrovic, T., & Ljubin-Sternak, S. (2018). Molecular mechanisms of Chlamydia trachomatis resistance to antimicrobial drugs. *Front Biosci*, *23*, 656–670. https://doi.org/10.2741/4611

Miller, S.C., & Drabik, B.R. (1984). Rheological properties of poloxamer vehicles. *International Journal of Pharmaceutics*, *18*(3), 269–276. https://doi.org/10.1016/0378-5173(84)90142-X

Moghimi, S.M., & Hunter, A.C. (2000). Poloxamers and poloxamines in nanoparticle engineering and experimental medicine. *Trends in Biotechnology*, *18*(10), 412–420. https://doi.org/10.1016/S0167-7799(00)01485-2

Momčilović, S., Cantacessi, C., Arsić-Arsenijević, V., Otranto, D., & Tasić-Otašević, S. (2019). Rapid diagnosis of parasitic diseases: current scenario and future needs. *Clinical Microbiology and Infection*, *25*(3), 290–309. https://doi.org/10.1016/j.cmi.2018.04.028

Mortensen, K., & Brown, W.Y.N. (1993). Poly (ethylene oxide)-poly (propylene oxide)-poly (ethylene oxide) triblock copolymers in aqueous solution. The influence of relative block size. *Macromolecules*, *26*(16), 4128–4135.

Mtibaa, L., Fakhfakh, N., Kallel, A., Belhadj, S., Belhaj Salah, N., Bada, N., & Kallel, K. (2017). Vulvovaginal candidiasis: Etiology, symptomatology and risk factors. *Journal de Mycologie Médicale*, *27*(2), 153–158. https://doi.org/10.1016/j.mycmed.2017.01.003

N'Guessan Gnaman, K.C., Bouttier, S., Yeo, A., Any-Grah, A.A.S.A., Geiger, S., Huang, N., Nicolas, V., Villebrun, S., Faye-Kette, H., Ponchel, G., &

others. (2020). Characterization and in vitro evaluation of a vaginal gel containing Lactobacillus crispatus for the prevention of gonorrhea. *International Journal of Pharmaceutics*, *588*, Article 119733. https://doi.org/10.1016/j.ijpharm.2020.119733

National Institutes of Health. (2007). *Understanding emerging and re-emerging infectious diseases*. Biological Sciences Curriculum Study. NIH Curriculum Supplement Series. National Institutes of Health, Bethesda, MD.

Nett, J. E. (2018). Special issue: Candida and candidiasis. *Journal of Fungi*, *4*(3), 4–6. https://doi.org/10.3390/jof4030074

O'Keefe, J.H., Grines, C. L., DeWood, M.A., Schaer, G.L., Browne, K., Magorien, R. D., Kalbfleisch, J.M., Fletcher, W.O., Bateman, T.M., & Gibbons, R.J. (1996). Poloxamer-188 as an adjunct to primary percutaneous transluminal coronary angioplasty for acute myocardial infarction. *The American Journal of Cardiology*, *78*(7), 747–750. https://doi.org/10.1016/S0002-9149(96)00414-6

Palmeira-de-Oliveira, R., Palmeira-de-Oliveira, A., & Martinez-de-Oliveira, J. (2015). New strategies for local treatment of vaginal infections. *Advanced Drug Delivery Reviews*, *92*, 105–122. https://doi.org/10.1016/j.addr.2015.06.008

Palmer, W.K., Emeson, E.E., & Johnston, T.P. (1998). Poloxamer 407-induced atherogenesis in the C57BL/6 mouse. *Atherosclerosis*, *136*(1), 115–123. https://doi.org/10.1016/S0021-9150(97)00193-7

Patel, H.R., Patel, R.P. & Patel, M.M. (2009). Poloxamers: A pharmaceutical excipients with therapeutic behaviors. *International Journal of PharmTech Research*, *1*(2), 299–303.

Penna, G.O., Hajjar, L.A., & Braz, T.M. (2000). Gonorrhea. *Revista Da Sociedade Brasileira de Medicina Tropical*, *33*(5), 451–464. https://doi.org/10.1590/S0037-86822000000500007

Pereira, R.R. de A., Godoy, J.S.R., Svidzinski, T.I.S., & Bruschi, M.L. (2013). Preparation and Characterization of Mucoadhesive Thermoresponsive Systems Containing Propolis for the Treatment of Vulvovaginal Candidiasis. *Journal of Pharmaceutical Sciences*, *102*(7), 2271–2280. https://doi.org/10.1002/jps

Pillai, S.A., Sharma, A.K., Desai, S.M., Sheth, U., Bahadur, A., Ray, D., Aswal, V.K., & Kumar, S. (2020). Characterization and application of mixed micellar assemblies of PEO-PPO star block copolymers for solubilization of hydrophobic anticancer drug and in vitro release. *Journal of Molecular Liquids*, *313*, Article 113543. https://doi.org/10.1016/j.molliq.2020.113543

Port, C.D., Garvin, P.J., & Ganote, C.E. (1978). The effect of Pluronic F-38 (Polyoxamer 108) administered intravenously to rats. *Toxicology and Applied Pharmacology*, *44*(2), 401–411. https://doi.org/10.1016/0041-008X(78)90200-4

Pradines, B., Bories, C., Vauthier, C., Ponchel, G., Loiseau, P.M., & Bouchemal, K. (2015). Drug-free chitosan coated poly (isobutylcyanoacrylate) nanoparticles are active against Trichomonas vaginalis and non-toxic towards pig vaginal mucosa. *Pharmaceutical Research*, *32*(4), 1229–1236. https://doi.org/10.1007/s11095-014-1528-7

Puig-Rigall, J., Blanco-Prieto, M.J., Aydillo, C., Radulescu, A., Molero-Vilchez, D., Dreiss, C.A., & González-Gaitano, G. (2021). Poloxamine/D-α-Tocopheryl polyethylene glycol succinate (TPGS) mixed micelles and gels: Morphology, loading capacity and skin drug permeability. *Journal of Molecular Liquids*, *324*, Article 114930. https://doi.org/10.1016/j.molliq.2020.114930

Ramyadevi, D., Rajan, K.S., Vedhahari, B.N., Ruckmani, K., & Subramanian, N. (2016). Heterogeneous polymer composite nanoparticles loaded in situ gel for controlled release intra-vaginal therapy of genital herpes. *Colloids and Surfaces B: Biointerfaces*, *146*, 260–270. https://doi.org/10.1016/j.colsurfb.2016.06.022

Ramos, M.S., Toledo, L., Calixto, G., Bonifácio, B., Araújo, M.F., dos Santos, L., de Almeida, M., Chorilli, M., & Bauab, T. (2016). Syngonanthus nitens Bong. (Rhul.)-Loaded Nanostructured System for Vulvovaginal Candidiasis Treatment. *International Journal of Molecular Sciences*, *17*(8), Article 1368. https://doi.org/10.3390/ijms17081368

Rey-Rico, A., Silva, M., Couceiro, J., Concheiro, A., & Alvarez-Lorenzo, C. (2011). Osteogenic efficiency of in situ gelling poloxamine systems with and without bone morphogenetic protein-2. *Eur Cell Mater*, *21*(4), 317–340. https://doi.org/: 10.22203/eCM.v021a24

Rodero, C.F., Calixto, G.M.F., dos Santos, K., Sato, M.R., Ramos, M.S., Miró, M. S., Rodríguez, E., Vigezzi, C., Bauab, T.M., Sotomayor, C.E., & Chorilli, M. (2018). Curcumin-loaded liquid crystalline systems for controlled drug release and improved treatment of vulvovaginal candidiasis. *Molecular Pharmaceutics*, *15*(10), 4491–4504. https://doi.org/10.1021/acs.molpharmaceut.8b00507

Rodgers, J.B., Friday, S., & Bochenek, W.J. (1984). Absorption and excretion of the hydrophobic surfactant, 14C-poloxalene 2930, in the rat. *Drug Metabolism and Disposition*, *12*(5), 631–634.

Rodríguez-Cerdeira, C., Gregorio, M.C., Molares-Vila, A., López-Barcenas, A., Fabbrocini, G., Bardhi, B., Sinani, A., Sánchez-Blanco, E., Arenas-Guzmán, R., & Hernandez-Castro, R. (2019). Biofilms and vulvovaginal candidiasis. *Colloids and Surfaces B: Biointerfaces*, *174*(May 2018), 110–125. https://doi.org/10.1016/j.colsurfb.2018.11.011

Rohan, L.C., & Sassi, A.B. (2009). Vaginal Drug Delivery Systems for HIV Prevention. *The AAPS Journal*, *11*(1), 78-87. https://doi.org/10.1208/s12248-009-9082-7

Rolon, R.M.M., & Yao, J.D.C. (2020). Laboratory Diagnosis of HTLV-1-Associated Myelopathy. *Clinical Microbiology Newsletter*, *42*(16), 129–134. https://doi.org/10.1016/j.clinmicnews.2020.07.004

Rossi, S., Ferrari, F., Bonferoni, M.C., Sandri, G., Faccendini, A., Puccio, A., & Caramella, C. (2014). Comparison of poloxamer- and chitosan-based thermally sensitive gels for the treatment of vaginal mucositis. *Drug Development and Industrial Pharmacy*, *40*(3), 352–360. https://doi.org/10.3109/03639045.2012.762654

Rudt, S., & Müller, R.H. (1993). In vitro phagocytosis assay of nano- and microparticles by chemiluminescence. II. Effect of surface modification by coating of particles with poloxamer on the phagocytic uptake. *Journal of Controlled Release*, *25*(1–2), 51–59. https://doi.org/10.1016/0168-3659(93)90094-L

Ruel-Gariepy, E., & Leroux, J.-C. (2004). In situ-forming hydrogels—review of temperature-sensitive systems. *European Journal of Pharmaceutics and Biopharmaceutics*, *58*(2), 409–426. https://doi.org/10.1016/j.ejpb.2004.03.019

Russo, E., & Villa, C. (2019). Poloxamer Hydrogels for Biomedical Applications. *Pharmaceutics*, *11*(12), Article 671. https://doi.org/10.3390/pharmaceutics11120671

Sábio, R. M., Meneguin, A. B., Santos, A.M., Monteiro, A.S., & Chorilli, M. (2021). Exploiting mesoporous silica nanoparticles as versatile drug carriers for several routes of administration. *Microporous and Mesoporous Materials*, *312*, Article 110774. https://doi.org/10.1016/j.micromeso.2020.110774

Salmazi, R., Calixto, G., Bernegossi, J., Ramos, M.A.S., Bauab, T.M., & Chorilli, M. (2015). A curcumin-loaded liquid crystal precursor mucoadhesive system for the treatment of vaginal candidiasis. *International Journal of Nanomedicine*, *10*, Article 4815. https://doi.org/10.2147/IJN.S82385

Sangamithra, V., Verma, R., Sengottuvelu, S., & Sumathi, R. (2013). Candida infections of the genitourinary tract. *Research Journal of Pharmacy and Technology*, *6*(10), 1111–1115.

Santos, M.M., Lopes, A.K.B., Roncalli, A.G., & Lima, K.C. de. (2020). Trends of syphilis in Brazil: A growth portrait of the treponemic epidemic. *Plos One*, *15*(4), Article e0231029. https://doi.org/10.1371/journal.pone.0231029

Sarier, M., Ceyhan, A.M., Sepin, N., Ozel, E., Inal, M.M., Kukul, E., & Soylu, A. (2020). HPV infection in urology practice. *International Urology and Nephrology*, *52*(1), 1–8. https://doi.org/10.1007/s11255-019-02302-2

Schmolka, I.R. (1977). A review of block polymer surfactants. *Journal of the American Oil Chemists' Society*, *54*(3), 110–116. https://doi.org/10.1007/BF02894385

Secor, W.E., Meites, E., Starr, M.C., & Workowski, K.A. (2014). Neglected parasitic infections in the United States: trichomoniasis. *The American Journal of Tropical Medicine and Hygiene*, *90*(5), 800–804. https://doi.org/10.4269/ajtmh.13-0723

Shankar, G.N., & Alt, C. (2014). Prophylactic treatment with a novel bioadhesive gel formulation containing aciclovir and tenofovir protects from HSV-2 infection. *Journal of Antimicrobial Chemotherapy*, *69*(12), 3282–3293. https://doi.org/10.1093/jac/dku318

Sharifzadeh, G., Hezaveh, H., Muhamad, I.I., Hashim, S., & Khairuddin, N. (2020). Montmorillonite-based polyacrylamide hydrogel rings for controlled vaginal drug delivery. *Materials Science and Engineering: C*, *110*, 110609. https://doi.org/10.1016/j.msec.2019.110609

Shaw, M.K., Porterfield, H.S., Favaloro, S., Dehon, P.M., Van Der Pol, B., Quayle, A. J., & McGowin, C.L. (2019). Prevalence and cervical organism burden among Louisiana women with Trichomonas vaginalis infections. *PloS One*, *14*(6), Article e0217041. https://doi.org/10.1371/journal.pone.0217041

Shubhra, Q.T.H., Tóth, J., Gyenis, J., & Feczkó, T. (2014). Poloxamers for surface modification of hydrophobic drug carriers and their effects on drug delivery. *Polymer Reviews*, *54*(1), 112–138. https://doi.org/10.1080/15583724.2013.862544

Singh, L., Kruger, H.G., Maguire, G.E.M., Govender, T., & Parboosing, R. (2017). The role of nanotechnology in the treatment of viral infections. *Therapeutic Advances in Infectious Disease*, *4*(4), 105–131. https://doi.org/10.1177/2049936117713593

Sonvico, F., Clementino, A., Buttini, F., Colombo, G., Pescina, S., Stanisçuaski Guterres, S., Raffin Pohlmann, A., & Nicoli, S. (2018). Surface-Modified Nanocarriers for Nose-to-Brain Delivery: From Bioadhesion to Targeting. *Pharmaceutics*, *10*(1), Article 34. https://doi.org/10.3390/pharmaceutics10010034

Suliman, A.S., Anderson, R.J., & Elkordy, A.A. (2014). Norfloxacin as a model hydrophobic drug with unique release from liquisolid formulations prepared with PEG200 and Synperonic PE/L-61 non-volatile liquid vehicles. *Powder Technology*, *257*, 156–167. https://doi.org/10.1016/j.powtec.2014.02.048

Tamura, N.K., Negri, M.F.N., Bonassoli, L.A., & Svidzinski, T.I.E. (2007). Virulence factors for Candida spp recovered from intravascular catheters and hospital workers' hands. *Revista Da Sociedade Brasileira de Medicina Tropical*, *40*(1), 91–93. https://doi.org/S0037-86822007000100021

Tang, W., Zou, C., Da, C., Cao, Y., & Peng, H. (2020). A review on the recent development of cyclodextrin-based materials used in oilfield applications. *Carbohydrate Polymers*, *240*, Article 116321. https://doi.org/10.1016/j.carbpol.2020.116321

Tian, W., Han, S., Huang, X., Han, M., Cao, J., Liang, Y., & Sun, Y. (2019). LDH hybrid thermosensitive hydrogel for intravaginal delivery of anti-HIV drugs. *Artificial Cells, Nanomedicine and Biotechnology*, *47*(1), 1234–1240. https://doi.org/10.1080/21691401.2019.1596935

Timur, S.S., Şahin, A., Aytekin, E., Öztürk, N., Polat, K.H., Tezel, N., Gürsoy, R.N., & Çalış, S. (2018). Design and in vitro evaluation of tenofovir-loaded vaginal gels for the prevention of HIV infections. *Pharmaceutical Development and Technology*, *23*(3), 301–310. https://doi.org/10.1080/10837450.2017.1329835

Toledo, L.G., Ramos, M.A.S., Silva, P.B., Rodero, C.F., Gomes, V.S., Silva, A.N., Pavan, F. R., da Silva, I.C., Oda, F.B., Flumignan, D.L., & others. (2020). Improved in vitro and in vivo Anti-Candida albicans Activity of Cymbopogon nardus Essential Oil by Its Incorporation into a Microemulsion System. *International Journal of Nanomedicine*, *Volume 15*, 10481–10497. https://doi.org/10.2147/IJN.S275258

Tomás, M., Palmeira-de-Oliveira, A., Simões, S., Martinez-de-Oliveira, J., & Palmeira-de-Oliveira, R. (2020). Bacterial vaginosis: Standard treatments and alternative strategies. *International Journal of Pharmaceutics*, *587*, Article 119659. https://doi.org/10.1016/j.ijpharm.2020.119659

Tung, I.-C. (1994). Rheological behavior of poloxamer 407 aqueous solutions during sol-gel and dehydration processes. *International Journal of Pharmaceutics*, *107*(2), 85–90. https://doi.org/10.1016/0378-5173(94)90445-6

Ulrich, C.E., Geil, R.G., Tyler, T.R., & Kennedy, G.L. (1992). Two-week aerosol inhalation study in rats of ethylene oxide/propylene oxide copolymers. *Drug and Chemical Toxicology*, *15*(1), 15–31. https://doi.org/10.3109/01480549209035170

U.S. Department of Health & Human Services (2019). *The global HIV/AIDS epidemic*. HIV.gov. https://www.hiv.gov/hiv-basics/overview/data-and-trends/global-statistics

Usyk, M., Zolnik, C.P., Castle, P.E., Porras, C., Herrero, R., Gradissimo, A., Gonzalez, P., Safaeian, M., Schiffman, M., & Burk, R.D. (2020). Cervicovaginal microbiome and natural history of HPV in a longitudinal study. *Plos Pathogens*, *16*(3), Article e1008376. https://doi.org/10.1371/journal.ppat.1008376

Vadnere, M., Amidon, G., Lindenbaum, S., & Haslam, J. (1984). Thermodynamic studies on the gel-sol transition of some pluronic polyols. *International Journal of Pharmaceutics*, *22*(2–3), 207–218. https://doi.org/10.1016/0378-5173(84)90022-X

Vandenhaute, M., Schelfhout, J., Van Vlierberghe, S., Mendes, E., & Dubruel, P. (2014). Cross-linkable, thermo-responsive Pluronic® building blocks for biomedical applications: Synthesis and physico-chemical evaluation. *European Polymer Journal*, *53*, 126–138. https://doi.org/10.1016/j.eurpolymj.2014.01.016

Vasconcelos, T., Marques, S., & Sarmento, B. (2017). The biopharmaceutical classification system of excipients. *Therapeutic Delivery*, *8*(2), 65–78. https://doi.org/10.4155/tde-2016-0067

Veazey, R.S., Shattock, R.J., Pope, M., Kirijan, J.C., Jones, J., Hu, Q., Ketas, T., Marx, P.A., Klasse, P.J., Burton, D.R., & Moore, J.P. (2003). Prevention of virus transmission to macaque monkeys by a vaginally applied monoclonal antibody to HIV-1 gp120. *Nature Medicine*, *9*(3), 343–346. https://doi.org/10.1038/nm833

Victorelli, F.D., Calixto, G.M.F., dos Santos, K.C., Buzzá, H.H., & Chorilli, M. (2021). Curcumin-loaded Polyethyleneimine and chitosan polymer-based Mucoadhesive liquid crystalline systems as a potential platform in the treatment of cervical Cancer. *Journal of Molecular Liquids*, *325*, Article 115080. https://doi.org/10.1016/j.molliq.2020.115080

Vilela, R.C., & Benchimol, M. (2011). Interaction of *Trichomonas vaginalis* and *Tritrichomonas foetus* with keratin: an important role in parasite infection. *Memorias Do Instituto Oswaldo Cruz*, *106*(6), 701–704. https://doi.org/10.1590/S0074-02762011000600009

Visentin, A., Rodríguez-Rojo, S., Navarrete, A., Maestri, D., & Cocero, M.J. (2012). Precipitation and encapsulation of rosemary antioxidants by supercritical antisolvent process. *Journal of Food Engineering*, *109*(1), 9–15. https://doi.org/10.1016/j.jfoodeng.2011.10.015

Wang, Z.-Y.J.O., & Stern, I.J. (1975). Disposition in rats of a polyoxypropylene-polyoxyethylene copolymer used in plasma fractionation. *Drug Metabolism and Disposition*, *3*(6), 536–542.

WHO. (2021). *Infectious diseases*. World Health Organization. http://www.emro.who.int/health-topics/infectious-diseases/index.html

WHO (2017). *WHO guideline on syphilis screening and treatment for pregnant women*. World Health Organization. https://www.who.int/publications/i/item/9789241550093

Willcox, M.L., Newman, M.M., & Paton, B.C. (1978). A study of labeled pluronic F-68 after intravenous injection into the dog. *Journal of Surgical Research*, *25*(4), 349–356. https://doi.org/10.1016/0022-4804(78)90130-0

Wong, T.W., Dhanawat, M., & Rathbone, M.J. (2014). Vaginal drug delivery: strategies and concerns in polymeric nanoparticle development. *Expert Opinion on Drug Delivery*, *11*(9), 1419–1434. https://doi.org/10.1517/17425247.2014.924499

Wu, X., Ge, J., Zhu, J., Zhang, Y., Yong, Y., & Liu, Z. (2015). A general method for synthesizing enzyme–polymer conjugates in reverse emulsions using Pluronic as a reactive surfactant. *Chemical Communications*, *51*(47), 9674–9677. https://doi.org/10.1039/C5CC01776A

Yapar, E., & Ýnal, Ö. (2013). Poly(ethylene oxide)–Poly(propylene oxide)-Based Copolymers for Transdermal Drug Delivery: An Overview. *Tropical Journal of Pharmaceutical Research*, *11*(5), 855-866. https://doi.org/10.4314/tjpr.v11i5.20

Zarrintaj, P., Ramsey, J.D., Samadi, A., Atoufi, Z., Yazdi, M.K., Ganjali, M.R., Amirabad, L.M., Zangene, E., Farokhi, M., Formela, K., & others. (2020). Poloxamer: A versatile tri-block copolymer for biomedical applications. *Acta Biomaterialia*, *110*, 37–67. https://doi.org/10.1016/j.actbio.2020.04.028

Zhang, M., Zhuang, B., Du, G., Han, G., & Jin, Y. (2019). Curcumin solid dispersion-loaded in situ hydrogels for local treatment of injured vaginal bacterial infection and improvement of vaginal wound healing. *Journal of Pharmacy and Pharmacology*, *71*(7), 1044–1054. https://doi.org/10.1111/jphp.13088

Zhang, T., Sturgis, T.F., & Youan, B.B.C. (2011). PH-responsive nanoparticles releasing tenofovir intended for the prevention of HIV transmission. *European Journal of Pharmaceutics and Biopharmaceutics*, *79*(3), 526–536. https://doi.org/10.1016/j.ejpb.2011.06.007

CHAPTER 13

General discussion

Although it is generally known in the literature that VVC is a worldwide prevalent disease, the lack of numbers makes it difficult to establish public health action plans to combat and prevent this disease, mainly because despite not being considered a sexually transmitted disease, it can be transmitted in this way (Balakrishnan et al., 2022; Martínez-García et al., 2023). Even though the systematic review with meta-analysis discussed in **Chapter 2** showed a prevalence of 18% in Brazil, when comparing this value with other countries official data or studies published in the literature, like the Netherlands (19.2 per 1000 inhabitants),), Granada in Spain (14.6%), Cameroon (54%) and sub–Saharan Africa (33%) it is suggested that this calculated value is underestimated since Brazil is a tropical country, climate conducive to fungal infections (Dou et al., 2015; Dutch Institute for Research in Health Care, 2022; Martínez-García et al., 2023; Mushi et al., 2022; Nsongmayi & Ambe, 2023). In addition to point to the lack of epidemiological data in Brazil, this chapter also pointed to the lack of homogeneity when comparing the different Brazilian regions, which shows to be related to public funds distribution, especially for health and research.

Beyond to this missing information, still little is known about *C. auris* in the literature, a new candida strain, covered in detail in **Chapter 3**. Despite not being prevalent as a VVC etiological agent, clinical cases can be observed in the literature (Krishnasamy et al., 2021; Kumar et al., 2015; Mesini et al., 2021). The biggest worrying issue regarding this strain is the fact that it is multi-resistant, difficult to treat and has high rates of contagion (Chowdhary et al., 2023). However, as previously mentioned, to carried out plans to contain a disease it is of crucial importance to widely understood about it by the scientific society. Searching for an alternative treatment for VVC caused by drug-resistant strains, lycopene initially showed to be desirable due to the various studies previously published in the literature that highlighted its antifungal and anti-inflammatory potential, as addressed in **Chapters 4 and 5**. However, free lycopene did not show both activities, as observed in **Chapter 8** and **Appendix 1**.

Since the combination of a drug with nanotechnology, in addition to being motivated to increase solubility, protection in terms of stability and the possibility of controlled release, is also desirable for increasing the efficiency, its association with lycopene was saw as an attractive strategy (Araújo et al., 2015; Araujo et al., 2020). Through the **Chapters 4 and 5**, it was possible to see that, although a growing trend, there are still few studies involving the association of lycopene with nanotechnology, and no studies associating lycopene with inorganic nanoparticles were found. Among the various options of inorganic nanoparticles, MSN stands out, due not only to its desirable characteristics but also to its growing application for the treatment of infectious diseases, as discussed in **Chapter 6**.

Despite not having presented good activity, lycopene-loaded MSN did not present toxicity in *vivo* (**Chapter 8**), what makes it an interesting system to be tested for other pathologies. It is worth

highlighting that this toxicity test was also motivated by the presence of the CTAB residue, observed in the FTIR spectrum. In this sense, careful observation was carried out both in this toxicity assay and in the minimum inhibitory concentration assay in order to assess whether this residue was sufficient to cause toxicity in eukaryotic or prokaryotic cells, since as CTAB is derived from quaternary ammonium it is capable of imparting toxicity to nanoparticles, as discussed in detail in **Chapter 9**. However, it was observed that the remaining residue was not sufficient to cause toxicity in any of the conditions studied.

Chapter 7 pointed to another advantage of this nanosystem: lycopene protection from thermal degradation (observed by DSC). This chapter also addressed the initial pharmacotechnical development of this nanosystem such as the development of an analytical method for lycopene quantification. Although the method developed was not green, due to the presence of chloroform, which is toxic not only to humans but also to the environment, it proved to be efficient for quantifying this drug (Funari et al., 2023). Additionally, a parallel of encapsulation efficiency and loading degree by HPLC and TGA was tried. However, it was the limitation of the study since no correlation was observed. This is probably due to the fact that this comparison was made with an indirect method (quantification of the unincorporated supernatant by HPLC) and a direct method (quantification of incorporated lycopene by TGA).

Once the main objective of this thesis was the development of a formulation for the treatment VVC caused by resistant strain and because this first one did not show activity, a second strategy was chosen, now using curcumin, a molecule also of natural origin with several biological properties, as discussed in **Chapter 10**. However, curcumin also present limitations for its use in therapy, such as low aqueous solubility. Although this molecule has both antifungal and anti-inflammatory activity, it was decided to combine it with another drug already widely used in therapy, benzydamine hydrochloride (Molinaro et al., 2023; Rodero et al., 2018; Tuğcu-Demiröz et al., 2021). In this context, the nanotechnology was used not only to increase the aqueous solubility of curcumin but also as an intelligent tool for the association of these two drugs (**Chapter 11**).

Microfluidics was an essential implement for the synthesis of this second therapeutic option as it enabled the synthesis of a hybrid nanoparticle in a reproducible way (Martins & Santos, 2023). As for biological activity, despite not having shown *in vitro* activity, the *in vivo* study pointed to the potential of this formulation both for reducing the fungal load and for reducing inflammatory symptoms, especially bearing in mind that the clinical strain used is highly resistant. For the future, perhaps if a higher dosage of this system is tested the better the results will be. Finally, although the thermoresponsive hydrogel has not influenced a major therapeutic improvement, the idea of its use continues to be attractive due to the ease of use by the patient as it is easier to apply and, once applied,

it does not leak to the outside, not causing discomfort for the patient, among other advantages mentioned in **Chapter 12**.

In short, to achieve the main objective of this thesis, which is the development of a therapeutic hope for society, pre-clinical stages of development of a new medicine were carried out. Several stages of literature study were performed in order to have scientific basis for choosing the best and unprecedented strategies. Although the physicochemical development was successfully carried out, free and incorporated lycopene did not show the desired activity expected, which was overcome by replacing this drug with the association of curcumin with benzydamine hydrochloride, which represents an unprecedented and promising strategy. However, a platform capable of incorporating both drugs was desirable, therefore, continuing with the choice of MSN, its association with a lipid-bilayer proved to be an interesting alternative for increasing its biocompatibility. Finally, to the best of our knowledge, the use of microfluidics in synthesis of this hybrid nanoparticle confers the innovative potential of the carrier proposed here.

References

Araújo, F., Shrestha, N., Granja, P.L., Hirvonen, J., Santos, H.A., & Sarmento, B. (2015). Safety and toxicity concerns of orally delivered nanoparticles as drug carriers. *Expert Opinion on Drug Metabolism & Toxicology*, *11*(3), 381–393. https://doi.org/10.1517/17425255.2015.992781

Araujo, V.H.S., Duarte, J.L., Carvalho, G.C., Silvestre, A.L.P., Fonseca-Santos, B., Marena, G.D., Ribeiro, T. de C., Ramos, M. A.S., Bauab, T.M., & Chorilli, M. (2020). Nanosystems against candidiasis: a review of studies performed over the last two decades. *Critical Reviews in Microbiology*, *46*(5), 508–547. https://doi.org/10.1080/1040841X.2020.1803208

Balakrishnan, S.N., Yamang, H., Lorenz, M.C., Chew, S.Y., & Than, L.T.L. (2022). Role of Vaginal Mucosa, Host Immunity and Microbiota in Vulvovaginal Candidiasis. *Pathogens*, *11*(6), Article 618. https://doi.org/10.3390/pathogens11060618

Chowdhary, A., Jain, K., & Chauhan, N. (2023). *Candida auris* Genetics and Emergence. *Annual Review of Microbiology*, *77*(1), 583–602. https://doi.org/10.1146/annurev-micro-032521-015858

Dou, N., Li, W., Zhou, E., Wang, C., Xiao, Z., & Zhou, H. (2015). Risk factors for candida infection of the genital tract in the tropics. *African Health Sciences*, *14*(4), 835-839. https://doi.org/10.4314/ahs.v14i4.10

Dutch Institute for Research in Health Care. (2022). *Jaarcijfers aandoeningen - Huisartsenregistraties*. Nivel. https://www.nivel.nl/nl/nivel-zorgregistraties-eerste-lijn/cijfers-over-aandoeningen/jaarcijfers-aandoeningen-huisartsenregistraties

Funari, C.S., Rinaldo, D., Bolzani, V.S., & Verpoorte, R. (2023). Reaction of the Phytochemistry Community to Green Chemistry: Insights Obtained Since 1990. *Journal of Natural Products*, *86*(2), 440–459. https://doi.org/10.1021/acs.jnatprod.2c00501

Krishnasamy, L., Senthilganesh, J., Saikumar, C., & Nithyanand, P. (2021). Biofilm-forming fluconazole-resistant Candida auris causing vulvovaginal candidiasis in an immunocompetent patient: A case report. *Asian Pacific Journal of Tropical Medicine*, *14*(2), 94-96. https://doi.org/10.4103/1995-7645.306768

Kumar, D., Banerjee, T., Pratap, C.B., & Tilak, R. (2015). Itraconazole-resistant Candida auris with phospholipase, proteinase and hemolysin activity from a case of vulvovaginitis. *The Journal of Infection in Developing Countries*, *9*(4), 435–437. https://doi.org/10.3855/jidc.4582

Martínez-García, E., Martínez-Martínez, J.C., Martín-Salvador, A., González-García, A., Pérez-Morente, M.Á., Álvarez-Serrano, M.A., & García-García, I. (2023). Epidemiological Profile of Patients with Vulvovaginal Candidiasis from a Sexually Transmitted Infection Clinic in Southern Spain. *Pathogens*, *12*(6), Article 756. https://doi.org/10.3390/pathogens12060756

Martins, J.P., & Santos, H.A. (2023). Microfluidics as a Tool for the Synthesis of Advanced Drug Delivery Systems. In Lamprou, D. (Ed.), *Nano- and Microfabrication Techniques in Drug Delivery: Recent Developments and Future Prospects* (pp. 321–364). Springer International Publishing. https://doi.org/10.1007/978-3-031-26908-0_13

Mesini, A., Saffioti, C., Mariani, M., Florio, A., Medici, C., Moscatelli, A., & Castagnola, E. (2021). First Case of Candida auris Colonization in a Preterm, Extremely Low-Birth-Weight Newborn after Vaginal Delivery. *Journal of Fungi*, *7*(8), Article 649. https://doi.org/10.3390/jof7080649

Molinaro, G., Fontana, F., Tello, R.P., Wang, S., Cérda, S.L., Torrieri, G., Correia, A., Waris, E., Hirvonen, J.T., Barreto, G., & A. Santos, H. (2023). In Vitro Study of the Anti-inflammatory and Antifibrotic Activity of Tannic Acid-Coated Curcumin-Loaded Nanoparticles in Human Tenocytes. *ACS Applied Materials & Interfaces*, *15*(19), 23012–23023. https://doi.org/10.1021/acsami.3c05322

Mushi, M.F., Olum, R., & Bongomin, F. (2022). Prevalence, antifungal susceptibility and etiology of vulvovaginal candidiasis in sub–Saharan Africa: a systematic review with meta-analysis and meta-regression. *Medical Mycology*, *60*(7), Article myac037. https://doi.org/10.1093/mmy/myac037

Nsongmayi, E.D., & Ambe, N.F. (2023). Vulvovaginal candidiasis in patients attending the Buea Regional Hospital-Cameroon: Prevalence and risk factors. *Journal of Public Health and Community Medicine*, 1(1), 13-20. https://doi.org/10.5455/JPHCM.20230731123555

Rodero, C.F., Calixto, G.M.F., dos Santos, K., Sato, M.R., Ramos, M.S., Miró, M. S., Rodríguez, E., Vigezzi, C., Bauab, T.M., Sotomayor, C.E., & others. (2018). Curcumin-loaded liquid crystalline systems for controlled drug release and improved treatment of vulvovaginal candidiasis. *Molecular Pharmaceutics*, *15*(10), 4491–4504. https://doi.org/10.1021/acs.molpharmaceut.8b00507

Tuğcu-Demiröz, F., Saar, S., Kara, A. A., Yıldız, A., Tunçel, E., & Acartürk, F. (2021). Development and characterization of chitosan nanoparticles loaded nanofiber hybrid system for vaginal controlled release of benzydamine. *European Journal of Pharmaceutical Sciences*, *161*, Article 105801. https://doi.org/10.1016/j.ejps.2021.105801

CHAPTER 14

Conclusions and future perspectives

This thesis sought to develop a formulation that would be considered an interesting alternative to the growing issue of resistance to antimicrobials currently available in therapy. Although the first alternative chosen, LYC@MSN, did not present the desired *in vitro* antifungal and anti-inflammatory activity, showing that it is not suitable for VVC treatment, the *in vivo* toxicity studies carried out here made it clear that both, the free drug and its association with MSN, are non-toxic therapeutic options that could be tested for pathologies that require a pro-inflammatory drug for their treatment.

However, in order to reach the thesis proposal, more literature research was carried out to develop the ideal formulation. Curcumin has been observed to hold therapeutic promise for treating *C. albicans* infections. However, in order to enhance its activity, the association of two drugs with complementary activities, such as anti-inflammatory, in a system that allowed dual loading was seen as a proposal to be better explored. The combination between curcumin and benzydamine hydrochloride has proven to be extremely synergistic and can also be applied to other pathologies caused by *C. albicans* or even be tested for other types of fungal infections. The hybrid nanosystem developed here using microfluidics proved to be suitable and reproducible and can be applied to other types of pathologies where combinations of drugs are desirable.

Although this second formulation developed, hybrid nanoparticles dual-loaded with curcumin and benzydamine hydrochloride, proved to be promising and safe for the treatment of this disease the scientific society should not reduce efforts to provide even greater well-being to the society, as not every formulation reaches clinical application, the greater the number of research for the development of promising formulations, the greater the chance of one reaching clinical practice.

ABSTRACT

This thesis sought to develop a formulation for the treatment of vulvovaginal candidiasis (VVC) caused by a resistant strain combining products of natural origin and nanotechnology. However, to reach the ideal formulation several steps were necessary. After presenting the thesis theme (**Chapter 1**), it was started with the estimated calculation of the prevalence of this disease in Brazil through a systematic review of the literature with meta-analysis, **Chapter 2**, in order to fill this gap since there is a lack of official data in the country. Next, when it comes to resistant strains of Candida, *C. auris* needs to be mentioned, since in addition to its resistance problems, mentioned in **Chapter 3**, it was also the cause of cases of vaginal infections.

Next, in **Chapters 4** and **5**, the physical-chemical and biological characteristics of lycopene were presented, a molecule considered promising in the literature. Since no studies were found in the literature associating this product of natural origin with inorganic nanoparticles, in **Chapter 6** issues inherent to the application of mesoporous silica nanoparticles (MSN), the nanoparticle of choice for this thesis, were addressed for the treatment of infectious diseases. In the two subsequent **Chapters**, **7** and **8**, the pharmacotechnical development of lycopene incorporated into MSN, its antifungal activity and toxicity in an *in vivo* model of *Galleria Mellonella* larvae were studied. In view of the organic matter residues of cetyltrimethylammonium bromide observed in the FTIR analyzes in **Chapter 9**, the general aspects of this surfactant and its toxicity in prokaryotic and eukaryotic cells were discussed in detail.

Since lycopene did not present antifungal (neither free nor incorporated) and anti-inflammatory activity (**Appendix 1**), the focus of the study turned on another natural product also considered promising, curcumin, whose physicochemical and biological characteristics were addressed in detail in **Chapter 10**. For this new strategy, this drug was combined in a hybrid nanoparticle with benzydamine hydrochloride, an anti-inflammatory with antifungal activity widely used for the treatment of vaginal pathologies. The pharmacotechnological development and evaluation of its biological activity *in vitro* and *in vivo* was covered in detail in **Chapter 11**. Finally, in **Chapter 12** the thermoresponsive behavior of poloxamer was discussed, a behavior that was explored for the application of the nanosystem *in vivo* in the previous chapter.

Keywords:1. Nanoparticles. 2. Candidiasis - Vulvovaginal. 3. Curcumin. 4. Drug resistance - Fungal. 5. Hydrogels.

RESUMO

Nesta tese buscou-se o desenvolvimento de uma formulação para o tratamento de candidíase vulvovaginal (CVV) causada por cepa resistente associando produtos de origem natural e nanotecnologia. Entretanto, para se chegar na formulação ideal vários degraus foram necessários. Após a apresentação da temática da tese (**Capítulo 1**) iniciou-se com o cálculo estimado da prevalência desta doença no Brasil por meio de uma revisão sistemática da literatura com meta-análise, **Capítulo 2**, a fim de suprir esta lacuna uma vez que faltam dados oficiais no país. Na sequência, em se tratando se cepas resistentes de Candida a *C. auris* não poderia não ter sido mencionada, uma vez que além de seus problemas de resistência, mencionados no **Capítulo 3**, ainda foi a causa de casos de infecções vaginais.

Na sequência, nos **Capítulos 4 e 5** foi apresentado as características físico-química e biológica do licopeno, uma molécula dita como promissora pela literatura. Uma vez que não foi encontrado estudos na literatura associando este produto de origem natural com nanopartículas inorgânicas, no **Capítulo 6** foi abordado questões inerentes a aplicação da nanopartícula de sílica mesoporosa (NSM), nanopartícula de escolha desta tese, para o tratamento de doenças infecciosas. Nos dois **Capítulos** subsequentes, **7 e 8** o desenvolvimento farmacotécnico do licopeno incorporado na NSM, sua atividade antifúngica e toxicidade em modelo *in vivo* de larvas de *Galleria Mellonella* foram estudados. Em vista dos resíduos de matéria orgânica de brometo de cetiltrimetilamônio observados nas análises de FTIR no **Capítulo 9** foi abordado em detalhes sobre os aspectos gerais deste surfactante e sua toxicidade em células procarióticas e eucarióticas.

Uma vez que o licopeno não apresentou atividade antifúngica (nem livre nem incorporado) e anti-inflamatória (**Anexo 1**) o foco do estudo recaiu sobre outro produto natural também considerado promissor, a curcumina, sujas características físico-químicas e biológicas foram abordadas em detalhes no **Capítulo 10**. Para esta nova estratégia, este fármaco foi combinado em uma nanopartícula hibrida com o cloridrato de benzidamina, um anti-inflamatório com atividade antifúngica muito utilizado para o tratamento de patologias vaginais. O desenvolvimento farmacotecnológico e a avaliação de sua atividade biológica *in vitro* e *in vivo* foi abordada em detalhes no **Capítulo 11**. Por fim, no **Capítulo 12** foi abordado sobre o comportamento termorresponsivo do poloxamer, comportamento este explorado para a aplicação do nanosistema *in vivo* no capítulo anterior.

Palavras-chave: 1. Nanopartículas. 2. Candidíase - Vulvovaginal. 3. Curcumina. 4. Resistência a medicamentos - Fúngico. 5. Hidrogéis.

SAMENVATTING

Dit proefschrift beoogde een nieuwe behandeling te ontwikkelen voor vulvovaginale candidiasis (VVC) veroorzaakt door een resistente stam, waarbij natuurlijke producten werden gecombineerd met nanotechnologie. Verschillende stappen waren nodig om tot de ideale samenstelling te komen. Na de introductie (**Hoofdstuk 1**) werd in **Hoofdstuk 2** de prevalentie van deze ziekte in Brazilië geschat, middels een systematisch literatuuronderzoek met meta-analyse. Dit was nodig vanwege het gebrek aan officiële gegevens in het land. Resistente Candida-stammen, met name *C. auris*, die naast resistentieproblemen ook vaginale infecties kan veroorzaken werden besproken in **Hoofdstuk 3**.

Hoofdstukken 4 en **5** beschreven de fysisch-chemische en biologische eigenschappen van lycopeen, volgens de literatuur een veelbelovend molecuul. Omdat er geen literatuurstudies werden gevonden die dit natuurlijke product combineerden met anorganische nanodeeltjes, besprak **Hoofdstuk 6** mesoporeuze silica nanodeeltjes (MSN) - de nanodeeltjeskeuze voor dit proefschrift - in relatie tot de behandeling van infectieziekten. **Hoofdstukken 7** en **8** bestudeerden de farmaceutische ontwikkeling van in MSN opgenomen lycopeen, evenals de anti-schimmelwerking en toxiciteit in een *in vivo* model met *Galleria Mellonella*-larven. Gezien de waargenomen organische resten van cetyltrimethylammoniumbromide (CTAB) in de FTIR-analyses in **Hoofdstuk 9**, werden de algemene aspecten van deze oppervlakteactieve stof en de toxiciteit in prokaryotische en eukaryotische cellen uitvoerig besproken.

Aangezien lycopeen geen anti-schimmelwerking (vrij of opgenomen) en ontstekingsremmende activiteit vertoonde (**Appendix 1**), verschoof de focus van de studie naar een ander veelbelovend natuurlijk product, curcumine, waarvan de fysisch-chemische en biologische kenmerken uitgebreid werden behandeld in **Hoofdstuk 10**. Voor deze nieuwe strategie werd dit geneesmiddel gecombineerd in een hybride nanodeeltje met benzydaminehydrochloride, een ontstekingsremmer met anti-schimmelwerking die veel wordt gebruikt voor de behandeling van vaginale aandoeningen. De farmaceutische ontwikkeling en evaluatie van de biologische werking *in vitro* en *in vivo* werden in detail behandeld in **Hoofdstuk 11**. Tot slot belichtte **Hoofdstuk 12** het thermoresponsieve gedrag van poloxameer, dat in het vorige hoofdstuk werd onderzocht voor de toepassing van het nanosysteem *in vivo*.

Trefwoorden:1. Nanodeeltjes. 2. Candidiasis - Vulvovaginaal; 3. Curcumine. 4. Geneesmiddelenresistentic - Schimmel; 5. Hydrogels

APPENDIX 1

Assessment of anti-inflammatory activity using bone marrow-derived macrophages

1. Methodology

For this experiment, a C57BL/6 male mice was used. After the animal was euthanized, the skin of the lower limbs was removed and the main muscles at the base were cut to expose the hip joint to enable the femur to be cut (**Figure 1A**). Next, the Achilles tendon was cut and the muscles around the tibia were removed. Then the main muscles around the femur were removed (**Figure 1B**) and the leg was cut at the knee joint (by torsion). Before removing the fibula, the main muscles surrounding the tibia were removed (**Figure 1C**). The epiphyses of the femur and tibia were then removed to allow access to the bone marrow with a 23G needle. The inner parts of the bones were slowly washed with 2-3 ml of PBS to remove the bone marrow (**Figure 1D**) (Toda et al., 2021).

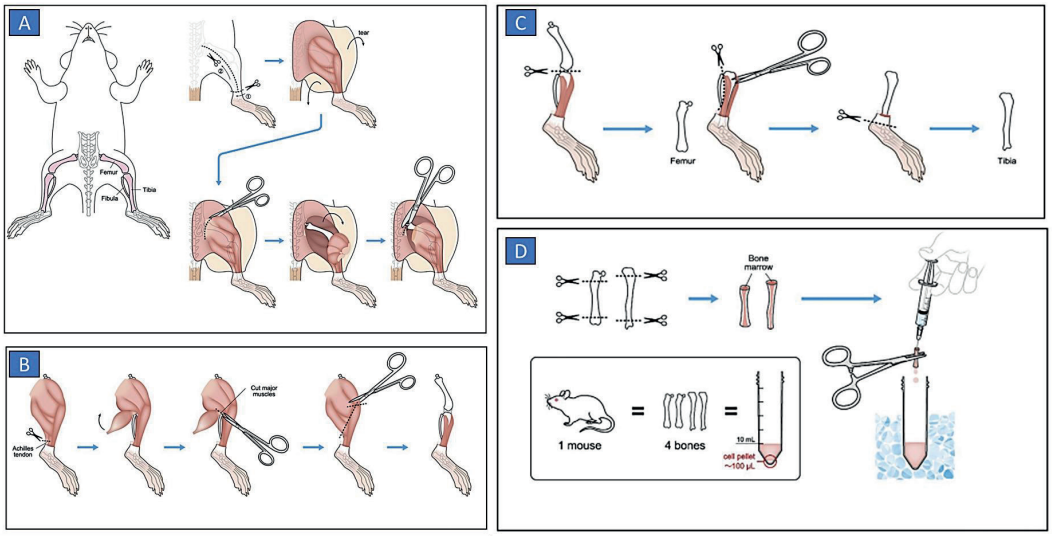

Figure 1: Collection process of bone marrow from mice leg. Reprinted with permission from Toda et al., 2021.

Next, the cells were centrifuged at 350 RCF for 5 min at 23°C, the supernatant was discarded, and the pellet was reconstituted with blood cell lysing buffer and incubated at room temperature for 1-2 min. Next, 9 mL of cold PBS were added and the cells were counted. As many red cells were still observed, the above procedure was repeated. The cell pellet obtained was then resuspended in 1 mL of RPMI 1640 supplemented with 10% of FBS and 1% Penicillin/Streptomycin (Pen/Strep). Next, the cells were plated in petri dishes at a concentration of $2x10^6$ cells/plate and incubated at 37°C for 3 days (day 0). On day 3 the medium was exchanged for a fresh medium (same composition as previously mentioned). On day 5, part of the plates was added with 100 ng/mL of lipopolysaccharide

(LPS, Sigma-Aldrich®, USA) and 10 ng/mL of gamma interferon (IFN-γ, PeproTech, UK) in order to differentiate the M0 macrophages into M1. On day 6, in the remaining plates (maintained in M0) only the medium was replaced. Finally, on day 7, the cells were detached from the plate with a solution of 5mM EDTA and cold PBS, it is worth highlighting that the entire process was carried out in an ice bath. Next, the cells were centrifuged and counted, 10^5 cells were added per well of 12-well plates. After 8 h of incubation at 37ºC, LYC at different concentrations (5uM; 2.5uM and 1.25uM) was added. In the control plates (M0 and M1) medium were added (Figueiredo et al., 2021; Gao et al., 2023).

After 2.5 days of incubation, the cells were detached from the plate in an ice bath with cold PBS and 5 mM EDTA, and the contents of each well were transferred to tubes. Next, 0.1 uL of Fc receptor binding reagent was added per tube and incubated for 10 min at room temperature. Then, the primary antibody was added (1,25 uL of the CD86 one and 0,25 uL of the CD206), next the tubes were incubated for 20 min in the dark. After this period, the samples were washed with 2mL of staining buffer and centrifuged at 300 g for 5 min at 4 ºC. The supernatant was discarded and then the fluorescent-conjugated secondary antibody was added (0,025 uL/100 uL for the CD86 and 0,0125 uL/100 uL for the CD206) and incubated for 20 min in the dark. The washing and centrifugation step was repeated as mentioned previously and then the pellet was resuspended in 0.5 mL of cell staining buffer. Finally, flow cytometric analysis was performed. The experiment was performed in triplicate (BioLegend, 2023; Diagnostics, 2023; Figueiredo et al., 2021).

2. Result and discussion

As the intention of this study was to evaluate the anti-inflammatory activity of LYC M0 macrophages were maintained in contact with LPS in order to cause an inflammation of the cells. When an inflammation is occurring greater quantity of M1 macrophages (stained by anti-mouse CD86) is observed. From a drug with anti-inflammatory activity, it is expected that a greater quantity of M2 macrophages (stained by the anti-mouse CD206) will be observed since the polarization of macrophages from inflammatory to anti-inflammatory would occur (Figueiredo et al., 2021; Shahbazi et al., 2018). As can be seen in **Figure 2**, contradicting some articles in the literature, LYC showed dose-dependent pro-inflammatory activity, since the higher the concentration of the drug, the more inflamed the cells (Cha et al., 2017; Hazewindus et al., 2012; Mozos et al., 2018). However, it is worth mentioning that it is possible to observe few studies in the literature reporting its pro-inflammatory activity (Palozza et al., 2011).

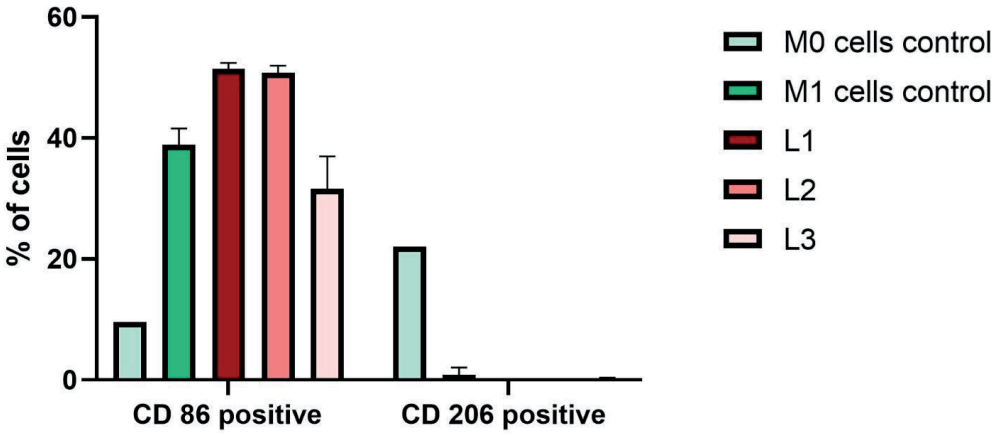

Figure 2: Percentage of positive cells by dye type. Legend: L1: 5uM of lycopene; L2: 2.5uM of lycopene; L3: 1.25uM of lycopene

3. References

BioLegend. (2023). *Technical protocols*. https://www.biolegend.com/protocols/cell-surface-flow-cytometry-staining-protocol/4283/

Cha, J. H., Kim, W. K., Ha, A. W., Kim, M. H., & Chang, M. J. (2017). Anti-inflammatory effect of lycopene in SW480 human colorectal cancer cells. *Nutrition Research and Practice*, *11*(2), 90-96. https://doi.org/10.4162/nrp.2017.11.2.90

Diagnostics, C. (2023). *Flow Cytometry Protocol: Cell Surface Marker Staining*. Creative Diagnostics. https://www.creative-diagnostics.com/flow-cytometry-protocol-cell-surface-marker-staining.htm

Figueiredo, P., Lepland, A., Scodeller, P., Fontana, F., Torrieri, G., Tiboni, M., Shahbazi, M., Casettari, L., Kostiainen, M.A., Hirvonen, J., & others. (2021). Peptide-guided resiquimod-loaded lignin nanoparticles convert tumor-associated macrophages from M2 to M1 phenotype for enhanced chemotherapy. *Acta Biomaterialia*, *133*, 231–243. https://doi.org/10.1016/j.actbio.2020.09.038

Gao, H., Wang, S., Long, Q., Cheng, R., Lian, W., Koivuniemi, A., Ma, M., Zhang, B., Hirvonen, J., Deng, X., & others. (2023). Rational design of a polysaccharide-based viral mimicry nanocomplex for potent gene silencing in inflammatory tissues. *Journal of Controlled Release*, *357*, 120–132. https://doi.org/10.1016/j.jconrel.2023.03.037

Hazewindus, M., Haenen, G.R.M.M., Weseler, A.R., & Bast, A. (2012). The anti-inflammatory effect of lycopene complements the antioxidant action of ascorbic acid and α-tocopherol. *Food Chemistry*, *132*(2), 954–958. https://doi.org/10.1016/j.foodchem.2011.11.075

Mozos, I., Stoian, D., Caraba, A., Malainer, C., Horbańczuk, J.O., & Atanasov, A.G. (2018). Lycopene and Vascular Health. *Frontiers in Pharmacology*, *9*, Article 521. https://doi.org/10.3389/fphar.2018.00521

Palozza, P., Simone, R., Catalano, A., Monego, G., Barini, A., Mele, M.C., Parrone, N., Trombino, S., Picci, N., & Ranelletti, F.O. (2011). Lycopene prevention of oxysterol-induced proinflammatory cytokine cascade in human macrophages: inhibition of NF-κB nuclear binding and increase in PPARγ expression. *The Journal of Nutritional Biochemistry*, *22*(3), 259–268. https://doi.org/10.1016/j.jnutbio.2010.02.003

Shahbazi, M.-A., Sedighi, M., Bauleth-Ramos, T., Kant, K., Correia, A., Poursina, N., Sarmento, B., Hirvonen, J., & Santos, H.A. (2018). Targeted Reinforcement of Macrophage Reprogramming Toward M2 Polarization by IL-4-Loaded Hyaluronic Acid Particles. *ACS Omega*, *3*(12), 18444–18455. https://doi.org/10.1021/acsomega.8b03182

Toda, G., Yamauchi, T., Kadowaki, T., & Ueki, K. (2021). Preparation and culture of bone marrow-derived macrophages from mice for functional analysis. *STAR Protocols*, *2*(1), Article 100246. https://doi.org/10.1016/j.xpro.2020.100246

ACKNOWLEDGMENTS

My contact with the academic area began in my first year of life, although I don't remember, I was there, in some way, encouraging **my mother (prof. Dr. Ione Corrêa)** in her PhD defense. Since early, this contact with science, always listening and learning about the infection impact on human life, led me down to this path.

When I talk about my journey I need to mention **Prof. Dr. Marco Antonio Utrera Martines**, who accepted a 17-year-old girl with a great desire to learn about research in his laboratory. In sequence, **Prof. Dr. Luciana Miyagusku**, comes like a mother, always encouraging and supporting me (even today). Another professor who was, and still is, very important to who I am is **Prof. Dr. Terezinha de Jesus Andreoli Pinto**, who with an incalculable generosity taught me her special way of thinking about science and passed to me her research critical sense, in addition to giving me the title of master and specialist in quality control.

Then, feeling ready for the biggest challenge of my life, until now, **Prof. Dr. Marlus Chorilli** came into my scientific life. Prof. Marlus accepted me into his research group with a challenging project and thanks to his sweet way to ask for manuscripts, which were essential for this thesis, made my Curriculum Vitae extremely competitive, with which I was even able to win an award. Prof. Marlus always supported me in finding a way out of difficult moments during the execution of this thesis, teaching that always we need to face the difficulties with a smile on the face. Thanks to him that I got the much-desired scholarship from São Paulo Research Foundation (FAPESP), which provided the research internship scholarship abroad with which I was able to be included in **Prof. Dr. Hélder Almeida Santos** research group. Prof. Hélder, the one responsible for the possibility of the double degree, welcomed me as a member of his scientific family, providing not only scientific meetings, in which I could learn from his wonderful way of thinking about science, but also moments of relaxation (like the incredible afternoon at Laser tag) to get closer to each other, as a family. Prof. Hélder showed me the true meaning of dedication and commitment.

My thanks also go to my co-supervisors. **Prof. Dr. Tais Maria Bauab** was always willing to help and even providing support when everything seemed lost, because, as she says, "*negative results are also interesting results*". I would also like to thank **Dr. Brandon W. Peterson** and **Dr. Rafael Miguel Sábio** for always being readily available to help and advice.

In addition to my supervisors, I would like to highlight my immense gratitude to my Paranymphs. Arriving in a different country, with a challenging project, can be scary but you two were always there, from the beginning, giving me all the support and encouragement I needed. **Gésinda**

Geertsema-Doornbusch is a person with a huge heart, I was lucky to have her as a partner in many experiments, she never spared efforts to help me with whatever I needed to achieve all my goals. She was always there giving me advice or comforting hugs when I needed it. From this partnership a beautiful friendship emerged, I will never forget you! Just like Gésinda, **Jiachen Li** was also there, perhaps the fact that he had already worked with mesoporous silica nanoparticle brought us together at the beginning, but it was his choice to stay and always be by my side for whatever I needed. His humility during scientific discussions and his happiness in being able to help others are admirable. Thank you for being an "big brother" to me in the Santos Lab family, thank you for always being there to support and advise me.

In addition, I would like to thank the support and collaboration of several people with whom I had the pleasure of sharing this journey, this work was only possible due to their collaboration and support:

- **To all the co-authors of this thesis**, your collaboration was essential in the development of this work, especially **Prof. Dr. Ione Corrêa** (my mother), from Botucatu Faculty of Medicine – UNESP, for teaching me how to do a systematic review and **Prof. Dr. Cleverton Roberto de Andrade** from Araraquara Dental School – UNESP, for teaching me how to prepare and analyze the histology slides.
- **To all the technicians** from the Department of Biomaterials & Biomedical Technology at UMCG, each one of them helped and supported me during my stay in Santos Lab, especially **Gésinda Geertsema-Doornbusch** and **Marja Slomp**, who always did everything they could to help me.
- **To all my laboratory colleagues at UNESP** (both in pharmacotechnics and physiology of microorganisms laboratory), especially **Gabriel Davi Marena**, **Leidiana Rocha dos Reis, Maurício Palmeira Chaves de Souza**, **Tais de Cassia Ribeiro** and **Victor Hugo Sousa Araujo** for such enriching discussions. In addition to the discussions, **Gabriel** was always by my side, being my partner in several experiments, supporting me and all my decisions (even when we were far away). Giving me his hug in so many moments of despair and understanding myself as I am. My eternal gratitude to you, my love!
- **To all my laboratory colleagues at Santos Lab** (UMCG), You all welcomed me with open arms, always willing to help me in both experiments and discussions, I am very grateful to each one of you. I would like to express my special thanks to **Jiachen Li**, **Maria Margarida Dias Carmona Lobita, Micaela Gaspar Gonçalves Fernandes** and **Soraia Filipa Tavares Pinto.**
- **To all the Department of Biomaterials & Biomedical Technology (UMCG) members,** who

always treated me with great kindness and were always willing to help me. I would like to express a special thanks to **Dr. Laís Ribovski,** as she has already gone through the same trajectory I am facing now, her advice has always helped me a lot. We could have just been office mates, but our conversations always brought me comfort, as if even far from home I was somehow close feeling loved and embraced. Thank you very much for your friendship!

- To all my family, especially my grandmother **Regina Batista Corrêa**. Sometimes all we need is to see a smile on the face of the one we love.
- To all my friends, especially **Fernanda Havik de Oliveira**, for the support to face this journey.

INSTITUTIONAL ACKNOWLEDGMENTS

To the **School of Pharmaceutical Sciences of the São Paulo State University (UNESP)** and the **Postgraduate Program in Pharmaceutical Sciences**, for the opportunity to perform the PhD course and for accept the double degree.

To **São Paulo Research Foundation** for financing the project in Brazil (grant number 19/26821-7) and abroad (grant number 22/02187-0). This study was financed in part by the **Coordenação de Aperfeiçoamento de Pessoal de Nível Superior** - Brasil (CAPES) - Finance Code 001.

To the **Department of Biomaterials & Biomedical Technology at University Medical Center Groningen (UMCG)** and the **University of Groningen**, for the opportunity to perform the double degree PhD and to the **UMCG research founds**.

To the **qualification exam board**, **Prof. Dr. Felipe Rebello Lourenço** and **Prof. Dr. Marco Antonio Utrera Martines**, for their suggestions.

To the **Clinical Hospital of the Botucatu Medical School – UNESP** (especially to **Dr. Suelen de Souza Assunpção Nishio)**, for providing the clinical strain.

To the **Experimental Research Unit (UNIPEX) Botucatu Medical School – UNESP** (especially to **Paulo Cesar Georgete** and **José Carlos Georgete**) for the Training in Laboratory Animal Management.

To the **Library of the Botucatu Medical School – UNESP** (especially **Marluci Betini** and **Nivaldete Costa Fernandes Cruz**) for always being very helpful, instructive and for welcoming me so well.

To the **Distance Education Center (NEaD) of the Botucatu Medical School – UNESP** (especially **Maria Clara Ribeiro Maciel** and **Dr. Ana Silvia Sartori Barraviera Seabra Ferreira)** for the receptiveness and help in transforming the idea of the cover illustration into reality.

ABOUT THE AUTHOR

Gabriela Corrêa Carvalho was born on May 3, 1994, in the city of Botucatu, State of São Paulo - Brazil. Throughout her school life she studied at La Salle School (a Catholic school), however, she completed an exchange student program in the United States of America where she studied for 6 months at Foothill High School in Henderson, Nevada. In 2011 she finished her studies and passed on the entrance exam to study Pharmacy at the Federal University of Mato Grosso do Sul, so in the beginning of 2012 she moved to Campo Grande, State of Mato Grosso do Sul - Brazil.

As she always liked the academic area, following her mother's example, during her first year of graduation (2012), she did a scientific initiation developing the project "*Mesoporous silica in a controlled drug release system*", under the guidance of Prof. Dr. Marco Antonio Utrera Martines, where she had her first contact with mesoporous silica nanoparticles. In the following year (2013), she received a scholarship from the Institutional Scientific Initiation Scholarship Program (PIBIC) of the National Council for Scientific and Technological Development (CNPq) to work on the same project.

Due to her interest in quality control and microbiology, in 2014 she was again awarded with a PIBIC scholarship, but this time to develop the project "*Good Practices in Human Milk Selection and Handling at Campo Grande University Hospital*" under the guidance of Prof. Dr. Luciana Miyagusku. In 2015 she continued to develop this project, however as a voluntary PIBIC, once during this year Gabriela received a scholarship from the University to be a monitor in the Food Microbiology discipline on the Undergraduate course of Food Technology, assisting in both theoretical and practical classes.

After completing her degree in pharmacy (2017), Gabriela competed in the selection process for a master's degree in Pharmaceuticals and Medicines at the University of São Paulo, which she began working on in the same year (therefore moving to São Paulo capital - Brazil) on her project entitled "*Alternative methods in monitoring the microbiological quality of treated water for dialysis*" with a CNPq scholarship and under the supervision of Prof. Dr. Terezinha de Jesus Andreoli Pinto. At the same time, from 2018 to 2019 she completed a Specialization in Quality of Related Pharmaceutical Products and Cosmetics, also at the University of São Paulo and also under the supervision of Prof. Dr. Terezinha.

Finally, right after finishing the master's degree and specialization (2019) Gabriela began her PhD in Pharmaceutical Sciences at the São Paulo State University under the guidance of Prof. Dr. Marlus Chorilli, with the project initially titled "*Evaluation of the potential of lycopene incorporated into mesoporous silica nanoparticles dispersed in thermoresponsive hydrogels in the treatment of vulvovaginal candidiasis* " with a scholarship from the Coordination for the Improvement of Higher Education Personnel (CAPES), moving therefore to the city of Araraquara, also in the state of São Paulo - Brazil. Gabriela subsequently applied and was awarded a scholarship from the São Paulo Research Foundation (FAPESP).

In 2022 Gabriela was invited (as a guest lecture) to teach the discipline “Quality Management and Assurance” offered to students enrolled in the undergraduate Pharmacy Course (full-time and evening courses) in the Pharmaceutical Sciences at the São Paulo State University. Also in this year, she applied for a research internship scholarship abroad, also from FAPESP, with which she was able to do part of her PhD under Prof. Dr. Hélder A. Santos supervision at the University Medical Center Groningen, moving to Groningen - Netherlands, for approximately 1 year. During this period Gabriela applied for a double degree, which was approved. Due to the promising results of his research carried out at the University Medical Center Groningen, FAPESP authorized the change of the thesis title to “*Nano-in-nano containing curcumin and benzydamine hydrochloride for the treatment of vulvovaginal candidiasis: from development to biological application in vitro and in vivo*”, which made it possible to finalize the project and carry out the *in vivo* tests upon her return to Brazil.

In 2023 Gabriela received the best student award from the Association of Pharmacy Professionals at the 12th Annual International Convention & 6th Indo-Australian conference based on her academic curriculum. In addition to this award, Gabriela got the second place for the best oral presentation award of the work entitled: “*Physicochemical characterization of a lycopene-loaded mesoporous silica nanoparticle formulation*”, one of the chapters of this thesis, at the same event. Also in 2023, Gabriela received an honorable mention from the president of the Regional Pharmacy Council of the State of São Paulo for the relevant services provided to the pharmaceutical profession in the State of São Paulo as a volunteer member of the youth technical work group.

List of publications

1- **Carvalho, G.C.,** Marena, G.D., Nascimento, A.L.C.S., Camargo, B.A.F., Sábio, R.M., Lourenço, F.R., Santos, H.A., Chorilli, M. (2024). *Nano Select 1*. https://doi.org/10.1002/nano.202300131

2- Marena, G.D., **Carvalho, G.C.,** Ruiz-Gaitán, A., Onisto, G.S., Bugalho, B.C.M., Genezini, L.M.V., Santos, M.O.D., Blanco, A.L., Chorilli, M., Bauab, T.M. (2024). Potential Activity of Micafungin and Amphotericin B Co-Encapsulated in Nanoemulsion against Systemic *Candida auris* Infection in a Mice Model. *Journal of Fungi 10*, Article 253. https://doi.org/ 10.3390/jof10040253

3- Sábio, R.M., **Carvalho, G.C.**, Li, J., Chorilli, M., Santos, H. A. (2023). Advanced porous materials for antimicrobial treatment, *Nano Select*, *1*, 1-20. https://doi.org/10.1002/nano.202300114

4- Marena, G.D., **Carvalho, G.C.**, dos Santos Ramos, M.A., Chorilli, M., Bauab, T.M. (2023). Anti- *Candida auris* activity *in vitro* and *in vivo* of micafungin loaded nanoemulsions. *Medical Mycology, 61*(7), Article myac090. https://doi.org/10.1093/mmy/myac090

5- Marena, G.D., Ruiz-Gaitán, A., Garcia-Bustos, V., Tormo-Mas, M.Á., Pérez-Royo, J.M., López, A., Bernarbe, P., Ruiz, M.D.P., Zaragoza M.L., Saez, C.V., Mansilla, A.A., Gómez, E.V., **Carvalho, G.C.,** Bauab, T.M., Chorilli, M., Pemán, J. (2023) Nanoemulsion Increases the Antifungal Activity of Amphotericin B against Four *Candida auris* Clades: *In Vitro* and *In Vivo* Assays. *Microorganisms*, *11*, Article 1626. https://doi.org/10.3390/microorganisms11071626

6- **Carvalho, G. C.,** Marena, G. D., Leonardi, G. R., Sábio, R. M., Corrêa, I., Chorilli, M., Bauab, T. M. (2022). Lycopene, Mesoporous Silica Nanoparticles and Their Association: A Possible Alternative against Vulvovaginal Candidiasis? *Molecules, 27*(23), Article 8558. https://doi.org/10.3390/molecules27238558

7- **Carvalho, G. C.,** Marena, G. D., Karnopp, J. C. F., Jorge, J., Sábio, R. M., Martines, M. A. U., Bauab, T. M., Chorilli, M. (2022). Cetyltrimethylammonium bromide in the synthesis of mesoporous silica nanoparticles: General aspects and in vitro toxicity. *Advances in Colloid and Interface Science, 307*, Article 102746. https://doi.org/10.1016/j.cis.2022.102746

8- Marena, G.D*****, **Carvalho, G.C.*,** Monazzi, L.G.S., Lima, T.M, Almeida, M.T.G, Silva, J.L.M., Fortunato, G.C., Araujo, V.H.S., Venancio, D.C.V., Chang, M.R., Chorilli, M. (2022). Infection caused by *Candida auris*: state of the art, *Mycosphere, 13*, 820-861. https://doi.org/ 10.5943/mycosphere/13/1/10 (***** shared first authorship)

9- Camargo B. A.F., Fonseca-Santos, B., Carvalho, G.S., **Carvalho, G.C.**, FILIPPO, L.D., Araújo, V.H.S., Duarte, J.L.; Silvestre, A.L.P., Bauab, T.M.; Chorilli, M. (2022). Functionalized lipid-based drug delivery nanosystems for the treatment of human infectious diseases. *Critical Reviews in Microbiology*, *1*, 1-17. https://doi.org/10.1080/1040841X.2022.2047007

10- Marena, G.D., Ramos, M.A. dos S., **Carvalho, G.C.**, de Lima, L.C., Nascimento, A.L.C.S., Sábio, R.M., Rodero, C.F., Spósito, L., Bauab, T.M., Chorilli, M. (2022). Development and characterization of an amphotericin B - loaded nanoemulsion applied to *Candida auris* biofilms control. *Journal of Drug Delivery Science and Technology, 74*, Article 103566. https://doi.org/10.1016/j.jddst.2022.103566

11- Ribeiro, T.C., Sábio, R.M., **Carvalho, G.C.,** Fonseca-Santos, B., Chorilli, M. (2022) Exploiting mesoporous silica, silver and gold nanoparticles for neurodegenerative diseases treatment. *International Journal of Pharmaceutics, 624*, Article 121978. https://doi.org/10.1016/j.ijpharm.2022.121978

12- Marena, G.D., Ramos, M.A.S., **Carvalho, G.C.,** Junior, J.A.P., Resende, F.A., Corrêa, I., Ono, G.Y.B.; Araujo, V.H.S., Camargo, B.A.F., Bauab, T.M., Chorilli, M. (2022) Natural product-based nanomedicine applied to fungal infection treatment: A review of the last 4-years. *Phytotherapy Research, 1*, 1-36. https://doi.org/10.1002/ptr.7460

13- **Carvalho, G.C.,** Dua, K., GUPTA, G., Bugno, A., Pinto, T.J.A. (2022) Reflection about the hemodialysis water microbiological quality in Brazil. *Brazilian Journal of Pharmaceutical Sciences, 615*, Article 121518. https://doi.org/10.1590/s2175-97902022e19235

14- **Carvalho, G.C.,** Sábio, R.M., Pinto, T.J.A., Spósito, L., Chorilli, M. (2022). An overview of the use of central venous catheters impregnated with drugs or with inorganic nanoparticles as a strategy in preventing infections. *International Journal of Pharmaceutics, 615*, Article 121518. https://doi.org/10.1016/j.ijpharm.2022.121518

15- Luiz, M.T., Dutra, J.A.P., Ribeiro, T.C., **Carvalho, G.C.,** Sábio, R.M., Marchetti, J.M., Chorilli, M. (2022). Folic acid-modified curcumin-loaded liposomes for breast cancer therapy. *Colloids and Surfaces A: Physicochemical and Engineering Aspects, 645*, Article 128935. https://doi.org/10.1016/j.colsurfa.2022.128935

16- **Carvalho, G.C.,** de Camargo, B.A.F., de Araújo, J.T.C., Chorilli, M. (2021). Lycopene: From tomato to its nutraceutical use and its association with nanotechnology. *Trends in Food Science & Technology, 118*, 447–458. https://doi.org/10.1016/j.tifs.2021.10.015

17- Araujo, V.H.S., Fernandes, L., **Carvalho, G.C.,** Reis, L., Scarpa, M.V.C., Chorilli, M. (2021). Validation of an Innovative Analytical Method for Simultaneous Quantification of Curcumin and Fluconazole using HPLC from Nanostructured Lipid Carriers. *Journal of Separation Science*, 1-10. https://doi.org/10.1002/jssc.202100514

18- **Carvalho, G.C.,** de Oliveira, R.A.P., Araujo, V.H.S., Sábio, R.M., de Carvalho, L.R., Bauab, T.M., Corrêa, I., Chorilli, M. (2021). Prevalence of vulvovaginal candidiasis in Brazil: A systematic review. *Medical Mycology, 59*(10), 946–957. https://doi.org/10.1093/mmy/myab034

19- Araujo, V.H.S., de Souza, M.P.C., **Carvalho, G.C.,** Duarte, J.L., & Chorilli, M. (2021). Chitosan-based systems aimed at local application for vaginal infections. *Carbohydrate Polymers, 261*, Article 117919. https://doi.org/10.1016/j.carbpol.2021.117919

20- **Carvalho, G.C.,** Araujo, V.H.S., Fonseca-Santos, B., de Araújo, J.T.C., de Souza, M.P.C., Duarte, J.L., Chorilli, M. (2021). Highlights in poloxamer-based drug delivery systems as strategy at local application for vaginal infections. *International Journal of Pharmaceutics, 602*, Article 120635. https://doi.org/10.1016/j.ijpharm.2021.120635

21- de Souza, M.P.C., Camargo, B.A.F., Spósito, L., Fortunato, G.C., **Carvalho, G.C.,** Marena, G.D., Meneguin, A.B., Bauab, T.M., Chorilli, M. (2021). Highlighting the use of micro and nanoparticles based-drug delivery systems for the treatment of *Helicobacter pylori* infections. *Critical Reviews in Microbiology, 47*(4), 1–26. https://doi.org/10.1080/1040841X.2021.1895721

22- Araújo, J,T.C., Duarte, J.L., Filippo, L.D., Araújo, V.H.S., **Carvalho, G.C.**, Chorilli, M. (2021). Nanosystem functionalization strategies for prostate cancer treatment: a review. *Journal of Drug Targeting*, 1-14. https://doi.org/10.1080/1061186X.2021.1892121

23- **Carvalho, G.C.,** Sábio, R.M., Chorilli, M. (2020). An Overview of Properties and Analytical Methods for Lycopene in Organic Nanocarriers. *Critical Reviews in Analytical Chemistry*, 1–13. https://doi.org/10.1080/10408347.2020.1763774

24- **Carvalho, G. C.,** Sábio, R. M., de Cássia Ribeiro, T., Monteiro, A. S., Pereira, D. V., Ribeiro, S. J. L., & Chorilli, M. (2020). Highlights in Mesoporous Silica Nanoparticles as a Multifunctional Controlled Drug Delivery Nanoplatform for Infectious Diseases Treatment. *Pharmaceutical Research, 37*(10), 1–30. https://doi.org/10.1007/s11095-020-02917-6

25- **Carvalho, G.C**., Bugno, A., Almodovar, A.A.B., Silva, F.P.L., Pinto, T.J.A. (2020). Validation of an alternative method and its applicability on water treated for dialysis and dialysate analysis. *Brazilian Journal of Nephrology*, *42*(2). https://doi.org/10.1590/2175-8239-JBN-2019-0203

26- Araujo, V.H.S., Duarte, J.L., **Carvalho, G.C.,** Silvestre, A.L.P., Fonseca-Santos, B., Marena, G.D., Ribeiro, T.C., Ramos, M.A.S., Bauab, T.M., Chorilli, M. (2020). Nanosystems against candidiasis: a review of studies performed over the last two decades. *Critical Reviews in Microbiology, 46*(5), 508–547. https://doi.org/10.1080/1040841X.2020.1803208

27- Riccio, B.V., Spósito, L., **Carvalho, G.C**., Ferrari, P.C., Chorilli, M. (2020) Resveratrol isoforms and conjugates: A review from biosynthesis in plants to elimination from the human body. *Archiv der Pharmazie*, Article e2000146. https://doi.org/10.1002/ardp.202000146

28- dos Santos, A.M., Carvalho, S.G., Araujo, V.H.S., **Carvalho, G.C.,** Gremião, M.P.D., Chorilli, M. (2020). Recent advances in hydrogels as strategy for drug delivery intended to vaginal infections. *International Journal of Pharmaceutics, 590*, Article 119867. https://doi.org/10.1016/j.ijpharm.2020.119867

29- Ogusuko, C.S., Chadi, P.F., Oliveira, R.A.P., **Carvalho, G.C**., Corrêa, I. (2020). Coqueluche na infância: Revisão Integrativa da doença. *Journal of Epidemiology and Infection Control*, *10*(3), 1-19. https://doi.org/10.17058/jeic.v10i3.14291 (in Portuguese).

30- Chadi, P.F., Orso, L.F., Silva, A.L., Oliveira, R.A.P., **Carvalho, G.C**., Corrêa, I. (2019). Avaliação da ficha de coqueluche dos casos positivos em dois municípios do interior paulista. *Revista de Saúde Digital e Tecnologias Educacionais, 4*(2), 20-34. (in Portuguese)

31- Prata, R.A., Simão, E. P. C., Chadi, P. F., Tavares, A.L.G., Benedetti, N.A., Orso, L.F., Caldeira, S.M., **Carvalho, G.C**., Corrêa, I. (2016). Higienização de unidade móvel de saúde. *Vigilância Sanitária em Debate: Sociedade, Ciência e Tecnologia, 4*, 51 - 55. https://doi.org/10.3395/2317-269x.00683 (in Portuguese)

32- Chadi, P.F., Braz, A.C.G., **Carvalho, G.C**., Prata, R.A., Correa, I. (2014). Avaliação dos procedimentos de higienização dos brinquedos infantis e das brinquedotecas nacionais. *Revista da Universidade Vale do Rio Verde, 12*, 296 – 305. http://dx.doi.org/10.5892/ruvrd.v12i2.1728 (in Portuguese)

Accepted: 1 article as first author.

Submitted: 1 article as first author; 2 as co-author; co-author of 1 book chapter.